

AIR QUALITY MODELING

Theories, Methodologies,
Computational Techniques, and
Available Databases and Software

Volume IV - Advances and Updates

Editor

Paolo Zannetti

Chapter Authors

Charisios Achillas
Roberto Bellasio
Roberto Bianconi
Peter Builtjes
Luca Delle Monache
John Douros
Evangelia Fragkou
Emilia Georgieva
Michael Johnson

Stephen L. Kerrin
Bryan Matthews
Paul C.H. Miller
Nicolas Moussiopoulos
Robert Paine
Thomas J. Rappolt
Steven D. Reynolds
Zbigniew Sorbjan
Milton E. Teske

Cristiane Thé
Jesse Thé
Harold W. Thistle
Silvia Trini Castelli
Christos Vlachokostas
Robert J. Yamartino
Paolo Zannetti

Published by
The EnviroComp Institute
Air & Waste Management Association

EnviroComp
The EnviroComp Institute

 AIR & WASTE MANAGEMENT
ASSOCIATION

AIR QUALITY MODELING

Theories, Methodologies, Computational Techniques,
and Available Databases and Software

Volume IV – Advances and Updates

Blank Page

Dedicated to my nephew, Carlo, and nieces, Roberta and Giovanna

PZ

Blank Page

AIR QUALITY MODELING
Theories, Methodologies, Computational Techniques,
and Available Databases and Software
Volume IV – Advances and Updates

Editor

Paolo Zannetti

Chapter Authors

Charisios Achillas, Roberto Bellasio, Roberto Bianconi, Peter Builtjes,
Luca Delle Monache, John Douros, Evangelia Fragkou, Emilia Georgieva,
Michael Johnson, Stephen L. Kerrin, Bryan Matthews, Paul C.H. Miller,
Nicolas Moussiopoulos, Robert Paine, Thomas J. Rappolt, Steven D. Reynolds,
Zbigniew Sorbjan, Milton E. Teske, Cristiane Thé, Jesse Thé, Harold W. Thistle,
Silvia Trini Castelli, Christos Vlachokostas, Robert J. Yamartino, Paolo Zannetti

Published by

The EnviroComp Institute
Air & Waste Management Association



AIR & WASTE MANAGEMENT
ASSOCIATION

◆
SINCE 1907

EnviroComp
The EnviroComp Institute

Copyright © 2010 The EnviroComp Institute and Air & Waste Management Association. All rights reserved.

Notice regarding copyrights: Chapter authors retain copyrights to their original materials. All requests for permission to reproduce chapter material should be directed to the appropriate author(s); all other requests should be directed to the Air & Waste Management Association, One Gateway Center, 3rd Floor, 420 Ft. Duquesne Blvd., Pittsburgh, PA 15222-1435, USA.

ISBN 978-1-9334740-9-0 (CD-ROM version)

Printed in the United States of America.

Copies of this CD-ROM may be purchased by visiting the EnviroComp Institute site at <http://envirocomp.org/books/aqm.html>, the Air & Waste Management Association's online library at <http://www.awma.org>, or by contacting the A&WMA directly at 1-800-270-3444 or 1-412-232-3444 (please reference A&WMA Order Code OTHP-28-CD).

This book is also available from the A&WMA in hard copy format: Order Code OTHP-28 (ISBN 978-1-9334740-8-3).

For updates, additional information, and online discussion regarding this book series, please visit <http://envirocomp.org/books/aqm.html>.

Table of Contents – Volume IV¹

	<u>Preface</u>	<u>xi</u>
	<u>About the Editor</u>	<u>xiii</u>
	<u>About the Publishers</u>	<u>xiii</u>
	<u>About the Chapter Authors</u>	<u>xiv</u>
<u>1</u>	<u>The Problem – Air Pollution</u>	<u>1</u>
	1 <u>Our Natural Environment</u>	<u>1</u>
	2 <u>Air Pollution, Some Definitions</u>	<u>3</u>
	3 <u>Primary and Secondary Pollutants</u>	<u>5</u>
	4 <u>A Short History of Air Pollution Modeling</u>	<u>6</u>
	5 <u>Air Pollution Modeling Guidelines</u>	<u>13</u>
<u>2</u>	<u>The Tool – Mathematical Modeling</u>	<u>21</u>
	1 <u>Why Air Quality Modeling</u>	<u>21</u>
	2 <u>Modeling Categorized</u>	<u>23</u>
	3 <u>Modeling the Atmosphere</u>	<u>29</u>
	4 <u>Modeling Alternatives</u>	<u>31</u>
	5 <u>Spatial and Temporal Scales</u>	<u>33</u>
	6 <u>Spatial and Temporal Resolution</u>	<u>34</u>
	7 <u>Uncertainty: Bias, Imprecision, and Variability</u>	<u>35</u>
	8 <u>Evaluation of Model Performance</u>	<u>37</u>
	9 <u>Data Needs</u>	<u>40</u>
	10 <u>Uses of Models</u>	<u>42</u>
<u>3</u>	<u>Emission Modeling and Inventory</u>	<u>47</u>
<u>4</u>	<u>Air Pollution Meteorology</u>	<u>49</u>
<u>5</u>	<u>Meteorological Modeling</u>	<u>51</u>
<u>5D</u>	<u>Recent Advances in the Similarity Theory of the Stable Boundary Layer</u>	<u>53</u>
	1 <u>Introduction</u>	<u>53</u>
	2 <u>Scaling Systems</u>	<u>54</u>
	3 <u>Empirical Verification</u>	<u>59</u>
	4 <u>Structure of Stable Turbulence</u>	<u>64</u>

¹ The table of contents for Volumes I, II and III can be found in this book on pages [467](#), [471](#) and [475](#), respectively.

<u>5E</u>	<u>Coupling Meteorological and Air Quality Models</u>	<u>73</u>
1	<u>Introduction</u>	<u>73</u>
2	<u>Meteorological Data</u>	<u>75</u>
3	<u>The Coupling</u>	<u>80</u>
4	<u>Examples of Coupling Processors</u>	<u>83</u>
5	<u>Sources of Data over the Internet</u>	<u>99</u>
<u>6</u>	<u>Plume Rise</u>	<u>107</u>
<u>7</u>	<u>Gaussian Plume Models</u>	<u>109</u>
<u>8</u>	<u>Gaussian Puff Modeling</u>	<u>111</u>
<u>9</u>	<u>Special Applications of Gaussian Models</u>	<u>113</u>
1	<u>Some Mathematical Properties of the Gaussian and Their Practical Implications</u>	<u>114</u>
2	<u>Gaussian Applications</u>	<u>118</u>
3	<u>Gaussian Regulatory Model Improvements</u>	<u>125</u>
<u>10</u>	<u>Eulerian Dispersion Models</u>	<u>131</u>
<u>11</u>	<u>Lagrangian Particle Models</u>	<u>133</u>
<u>12</u>	<u>Atmospheric Transformations</u>	<u>135</u>
<u>13</u>	<u>Deposition Phenomena</u>	<u>137</u>
<u>13A</u>	<u>Modeling of Pesticide Application, Deposition and Drift</u>	<u>139</u>
1	<u>Introduction</u>	<u>140</u>
2	<u>Sprayer Types</u>	<u>142</u>
3	<u>Ground Application</u>	<u>143</u>
4	<u>Aerial Application</u>	<u>147</u>
5	<u>Conclusions</u>	<u>155</u>
<u>14</u>	<u>Indoor Air Pollution Modeling</u>	<u>161</u>
<u>15</u>	<u>Modeling of Adverse Effects</u>	<u>163</u>
<u>15E</u>	<u>Ecological Risk Assessment for Air Toxics</u>	<u>165</u>
1	<u>Introduction</u>	<u>166</u>
2	<u>Site Characterization</u>	<u>169</u>
3	<u>Air Dispersion Modeling for Ecological Risk Assessment</u>	<u>188</u>
4	<u>Estimation of COPC Concentrations in Media</u>	<u>205</u>
5	<u>Ecological Risk Problem Formulation</u>	<u>232</u>
6	<u>Risk Analysis</u>	<u>257</u>
7	<u>Risk Characterization</u>	<u>278</u>
	<u>Conversion Factors</u>	<u>295</u>
	<u>List of Acronyms</u>	<u>295</u>
	<u>List of Variables</u>	<u>298</u>
	<u>Definitions</u>	<u>301</u>

<u>15F</u>	<u>Combined Assessment of Health Impacts and Emission Abatement Strategies</u>	<u>303</u>
1	<u>Introduction</u>	<u>304</u>
2	<u>Air Quality and Health: The Issue</u>	<u>305</u>
3	<u>Methodological Framework</u>	<u>306</u>
4	<u>Health Impact Assessment</u>	<u>308</u>
5	<u>Cost – Benefit Analysis</u>	<u>310</u>
6	<u>Uncertainties and Research Needs</u>	<u>311</u>
7	<u>Summary and Conclusions</u>	<u>312</u>
<u>16</u>	<u>Statistical Modeling</u>	<u>317</u>
<u>16C</u>	<u>Ensemble-Based Air Quality Predictions</u>	<u>319</u>
1	<u>Introduction</u>	<u>319</u>
2	<u>Ensemble Designs</u>	<u>322</u>
3	<u>Ensemble-Based Deterministic Predictions</u>	<u>332</u>
4	<u>Ensemble-Based Probabilistic Predictions</u>	<u>334</u>
5	<u>Spread-Skill Relationship</u>	<u>338</u>
6	<u>Post-Processing and Calibration</u>	<u>339</u>
7	<u>Ensembles Economic Values</u>	<u>341</u>
<u>17</u>	<u>Evaluation of Air Pollution Models</u>	<u>349</u>
<u>18</u>	<u>Regulatory Modeling</u>	<u>351</u>
<u>19</u>	<u>Case Studies</u>	<u>353</u>
<u>19A</u>	<u>Case Studies: Multi-Scale Air Pollution and Meteorological Modeling</u>	<u>355</u>
1	<u>Introduction</u>	<u>355</u>
2	<u>Case Studies</u>	<u>358</u>
<u>20</u>	<u>The Future of Air Pollution Modeling</u>	<u>371</u>
<u>21</u>	<u>Active Groups in Air Pollution Modeling</u>	<u>373</u>
1	<u>Introduction</u>	<u>374</u>
2	<u>Model Developers’ Groups</u>	<u>376</u>
3	<u>Model Users’ Groups</u>	<u>424</u>
<u>22</u>	<u>Available Software</u>	<u>435</u>
<u>23</u>	<u>Available Databases</u>	<u>437</u>
<u>24</u>	<u>Physical Modeling of Air Pollution</u>	<u>439</u>

<u>25</u>	<u>Measurement of Atmospheric Dispersion Using Gaseous Tracers</u>	<u>441</u>
1	<u>Introduction to Atmospheric Tracer Studies</u>	<u>441</u>
2	<u>Historical Perspective and Application of Atmospheric Tracers</u>	<u>442</u>
3	<u>Typical Components of a Tracer Study</u>	<u>443</u>
4	<u>Quality Assurance</u>	<u>452</u>
5	<u>Data Management Techniques for Tracer Studies</u>	<u>454</u>
6	<u>Applying Tracer Data to Validation of Model Performance</u>	<u>454</u>
<u>26</u>	<u>Air Quality Modeling: Pre-Processing and Post-Processing</u>	<u>459</u>
<u>27</u>	<u>Air Quality Modeling Resources on the Web – An Update</u>	<u>461</u>
1	<u>Introduction</u>	<u>461</u>
2	<u>Regulatory Issues</u>	<u>462</u>
3	<u>Books</u>	<u>463</u>
4	<u>Available Software</u>	<u>463</u>
5	<u>Dispersion Models</u>	<u>464</u>
6	<u>Photochemical Models</u>	<u>464</u>
7	<u>Receptor Models</u>	<u>465</u>
8	<u>Air Quality Forecast and Resources</u>	<u>465</u>
9	<u>Visibility Modeling</u>	<u>466</u>
10	<u>Courses Online</u>	<u>466</u>
	<u>Table of Contents – Volume I</u>	<u>467</u>
	<u>Table of Contents – Volume II</u>	<u>471</u>
	<u>Table of Contents – Volume III</u>	<u>475</u>
	<u>Authors’/Contributors’ Index for Volumes I – IV</u>	<u>479</u>
	<u>Subject Index for Volumes I – IV</u>	<u>483</u>

Preface

This is the fourth and final volume of our book series on Air Quality Modeling jointly published by the EnviroComp Institute and the Air & Waste Management Association (A&WMA). The series provides environmental scientists, engineers, researchers, and students with a uniquely comprehensive and organized body of information in virtually all aspects of computer simulation of air pollution and related atmospheric phenomena.

This series was initially designed to provide an update and expansion to my 1990 book on Air Pollution Modeling². All volumes in this series are available in both a traditional book format and an electronic format (CD-ROM). The electronic version is not a simple digital copy of the printed files, but includes additional material, such as active Internet pointers, videos, and computer animations. Moreover, the CD-ROM material can be quickly and easily searched by keywords. The book series also has its own Web page, <http://envirocomp.org/books/aqm.html> which readers are encouraged to visit for additional information.

Volume I took an in-depth look at the fundamentals of modeling, from a review of air pollution meteorology, to an introduction to Gaussian plume models; from a discussion of plume rise formulations, to a review of Eulerian grid models. Volume II addressed more advanced topics, such as Lagrangian modeling, chemical transformations in the atmosphere, and indoor air pollution modeling. Volume III presented special air quality issues, such as emission modeling, mesoscale meteorology, computational fluid dynamics for microscale flows, Gaussian plume and puff models, odor modeling, greenhouse gases and global climate change, and modeling pre-processors and post-processors.

This final Volume IV updates some chapters presented in previous volumes and provides discussion of new topics, including the coupling of meteorological and air quality modeling; the modeling of pesticide application, deposition and drift; ecological risk assessment from air toxics; health impacts and emission abatement strategies; ensemble predictions and data assimilation; and tracer studies.

As a whole, the four volumes now provide a unique and comprehensive description of all technical topics related to air quality modeling.

I want to express my sincere thanks to the chapter authors for their competence, dedication, and patience in the production of this final volume. Thanks are also

² Zannetti, P. (1990): Air Pollution Modeling – Theories, Computational Methods, and Available Software. Computational Mechanics Publications, Southampton, and Van Nostrand Reinhold, New York. 450pp.

<http://www.amazon.ca/Pollution-Modeling-Theories-Computational-Available/dp/0442308051>

This book is now out of print but can be freely downloaded at:

<http://www.envirocomp.com/pops/airpollution.html>

due to A&WMA Publications for their help and support in the preparation of the entire book series. Sincere appreciation is again extended to Scott Cragin who, as with previous volumes, provided extremely valuable editorial and organizational assistance throughout the entire book production cycle.

Paolo Zannetti
Fremont, California
August 2010

About the Editor

Dr. Paolo Zannetti is the President of the EnviroComp Institute and EnviroComp Consulting, Inc. in Fremont, California. He received a Doctoral Degree in Physics from the University of Padova (Italy) and a QEP Certification from the Institute of Professional Environmental Practice (IPEP). He has managed a vast range of environmental projects throughout his professional career. With a specialization in air pollution and environmental modeling and software, Dr. Zannetti's experience has covered research and development studies, teaching, consulting, modeling software development, project management, editorial activities, and expert testimony. In addition to authoring in 1990 the first comprehensive textbook on this topic (*Air Pollution Modeling — Theories, Computational Methods and Available Software*), Dr. Zannetti has authored more than 250 publications, primarily for peer-reviewed journals and conference proceedings.

For more information, visit <http://www.envirocomp.com/people1/zannetti.html>.

About the Publishers

The EnviroComp Institute

The International Institute of Environmental Sciences and Environmental Computing (EnviroComp) is a nonprofit, Internet-based institute and software laboratory dedicated to the study of environmental sciences and pollution phenomena. Founded in 1996, the EnviroComp Institute also promotes the publication of a unique, new-generation series of environmental books in electronic format. For more information, visit the institute's Web site at <http://www.envirocomp.org>.

The Air & Waste Management Association

The Air & Waste Management Association (A&WMA) is a nonprofit, nonpartisan professional organization that provides information, training, and networking opportunities to thousands of environmental professionals around the world. A&WMA was founded in 1907 and is headquartered in Pittsburgh, Pennsylvania. For more information, visit the association's Web site at <http://www.awma.org>.

About the Chapter Authors/Contributors for Volumes I-IV ([Additional information](#) is provided in the CD-ROM version)

Achillas

Dr. Charisios Achillas
Dipl. Mechanical Engineer
Laboratory of Heat Transfer and
Environmental Engineering
School of Engineering
Aristotle University Thessaloniki
Box 483, 54124 Thessaloniki,
GREECE

Phone: +30 2310 996092
+30 2310 996011(secretariat)
Fax: +30 2310 996012
Email: achillas@aix.meng.auth.gr
Work site: <http://aix.meng.auth.gr>

Anfossi

Dr. Domenico Anfossi
CNR - ISAC, Sezione di Torino
Corso Fiume 4
I-10133 – Torino
ITALY

Phone: +39 011 6606376
Phone direct: +39 011 3839826
Fax: +39 011 6600364
Email: anfossi@to.infn.it or
d.anfossi@isac.cnr.it
Work site: <http://www.isac.cnr.it/>

Bellasio

Roberto Bellasio
Partner, Enviroware – Environmental
Consulting
Via Dante, 142
20049 Concorezzo (MB)
ITALY

Phone: +39.039.6203636
Phone direct: +39.039.6203229
Email: rbellasio@enviroware.com
Work site: <http://www.enviroware.com>

Bianconi

Dott. Roberto Bianconi
Enviroware srl
via Dante, 142
20049 Concorezzo (MB)
ITALY

Phone: +39 039 620 3636
Email: rbianconi@enviroware.com
Work site: <http://www.enviroware.com>

Builtjes

Prof. Dr. Peter Builtjes
Department of Climate
Air and Sustainability
Netherlands Organisation for
Applied Scientific Research, TNO
Princetonlaan 6
3584 CB Utrecht
THE NETHERLANDS

Phone: +31 088 866 20
Fax: +31 088 866 2044
Email: peter.builtjes@tno.nl
Work site: [http://www.tno.nl/groep.cfm?
context=markten&content=
producten&laag1=186&item
id=157&Taal=2](http://www.tno.nl/groep.cfm?context=markten&content=producten&laag1=186&itemid=157&Taal=2)
Personal site: [http://www.lotos-
euros.nl/team/peter/peter.htm](http://www.lotos-euros.nl/team/peter/peter.htm)

Buono

Maureen E. Buono
Malcolm Pirnie, Inc.
104 Corporate Park Drive
White Plains, NY 11102
USA

Byun

Dr. Daewon W. Byun
Professor
312 Science & Research Bldg. 1
Geoscience Department
University of Houston
Houston, Texas 77204-5007
USA

Email: dwbyun@math.uh.edu

Canepa

Elisa Canepa, PhD
CNR-ISMAR
Via De Marini 6
I-16149 Genova
ITALY

Phone: +39 010 6475 432
Fax: +39 010 6475 400
Email: elisa.canepa@ismar.cnr.it
Personal email: canepae@libero.it
Work site: http://www.ismar.cnr.it/index_html

Carrington

David B. Carrington, Ph.D.
Los Alamos National Laboratory
Theoretical Division
T-3 Fluid Dynamics and
Solid Mechanics Group
P.O. Box 1663
MS-B216
Los Alamos, NM 87545
USA

Phone: (505) 667-3569
Email: dcarring@lanl.gov

Chow

Judith C. Chow, Sc.D.
Department of Atmospheric Sciences
Desert Research Institute
University of Nevada, Reno
2215 Raggio Parkway
Reno, NV 89512
USA

Phone direct: (775) 674-7050
Fax: (775) 674-7009
Email: judith.chow@dri.edu
Work site: <http://www.das.dri.edu/>
Personal site: <http://www.dri.edu/People/judyc/>

Cochran

Mr. Brad Cochran
Sr. Associate, CPP, Inc.
1415 Blue Spruce Drive
Fort Collins, CO 80524
USA

Phone: (970) 221-3371
Fax: (970) 221-3124
Email: bcochran@cppwind.com
Work site: www.cppwind.com

Daly

Aaron Daly
EnviroComp Consulting, Inc.
2298 Ocaso Camino
Fremont, CA 94539
USA

Phone: (408) 893-1874
Fax: (408) 351-8400
Email: daly@envirocomp.com
Work site: <http://www.envirocomp.com>

Degrazia

Dr. Gervásio A. Degrazia
Universidade Federal de Santa Maria
Departamento de Física
97105900 Santa Maria – RS
BRASIL

Phone: +55 55 2208616
+55 55 2208032
Email: degrazia@ccne.ufsm.br

Delle Monache

Dr. Luca Delle Monache, M.S., Ph.D.
Research Applications Laboratory
National Center for Atmospheric Research
PO Box 3000
Boulder, CO 80307-3000
USA

Phone: (303) 497-2736
Fax: (303) 497-8386
Work site: <http://www.ral.ucar.edu>
Personal site: <http://www.rap.ucar.edu/staff/lucadm-staff.php>

Diosey

Phyllis G. Diosey
Malcolm Pirnie, Inc.
104 Corporate Park Drive
White Plains, NY 11102
USA

Phone: (914) 641-2646
Fax: (914) 641-2645
Email: pdiosey@pirnie.com
Work site: <http://www.pirnie.com>

Douros

Mr. John Douros, MSc
Laboratory of Heat Transfer and
Environmental Engineering
School of Engineering
Aristotle University Thessaloniki
Box 483, 54124 Thessaloniki,
GREECE

Phone: +30 2310 996054
+30 2310 996011(secretariat)
Fax: +30 2310 996012
Email: jdouros@aix.meng.auth.gr
Work site: <http://aix.meng.auth.gr>

Eastman

Joseph L. Eastman, Ph.D.
Research Faculty
UMBC/GEST
Hydrological Sciences Branch
NASA/GSFC Code 974
Building 33, Room A322
Greenbelt, MD 20771
USA

Phone: (410) 279-9702
Fax: (301) 614-5808
Email: eastman@hsb.gsfc.nasa.gov or
jleastman@comcast.net
Work site: <http://gest.umbc.edu/directory.html>

Ferrero

Prof. Enrico Ferrero, Ph.D.
Dipartimento di Scienze e
Tecnologie Avanzate
Universita' del Piemonte Orientale
"A. Avogadro"
Viale Teresa Michel, 11
15121 Alessandria
ITALY

Phone: +39 0131 360 151
Fax: +39 0131 360 199
Email: enrico.ferrero@mfn.unipmn.it
Work site: <http://dista.unipmn.it/>
Personal site: <http://people.unipmn.it/ferrero/>

Finzi

Prof. Giovanna Finzi
Dipartimento di Ingegneria
dell'Informazione
Università degli Studi di Brescia
Via Branze 38, 25123 Brescia
ITALY

Phone: +39 030 371 5459
Fax: +39 030 380014
Email: finzi@ing.unibs.it
Personal site: <http://www.ing.unibs.it/~finzi/index.html>

Fragkou

Dr. Evangelia Fragkou, Ph.D.
Laboratory of Heat Transfer and
Environmental Engineering
Dept. of Mechanical Engineering
Box 483
Aristotle University of Thessaloniki
54 124, Thessaloniki
GREECE

Phone: +30 2310 996060
Fax: +30 2310 996012
Email: lia@aix.meng.auth.gr
Work site: <http://aix.meng.auth.gr/lhtee/>

Freedman

Frank R. Freedman, Ph.D.
The EnviroComp Institute
2298 Ocaso Camino
Fremont, CA 94539
USA

Phone: (408) 291-0933
Email: freedman@air-basics.com
Website: freedman@air-basics.com

Georgieva

Dr. Emilia Georgieva
European Commission – DG JRC
Institute for Environment and
Sustainability
Via E. Fermi, 2749 (TP 441)
21027 Ispra (VA)
ITALY

Phone: +39 0332 783060
Fax: +39 0332 785236
Email: emilia.georgieva@jrc.ec.europa.eu
Work site: <http://ies.jrc.ec.europa.eu/>

González Barras

Prof. Dr. Rosa M. González Barras
Department of Geophysics and
Meteorology
Faculty of Physics, Complutense
University of Madrid (UCM)
Ciudad Universitaria
28040 Madrid
SPAIN

Phone: +34 91 394 4513
Fax: +34 91 394 4798
Email: rgbarras@fis.ucm.es
Work site: <http://www.ucm.es/info/Geofis/>

Hibberd

Dr. Mark Hibberd
CSIRO Atmospheric Research
PMB1
Aspendale VIC 3195
AUSTRALIA

Phone: +61 3 9239 4400
Phone direct: +61 3 9239 4545
Fax: +61 3 9239 4444
Email: mark.hibberd@csiro.au
Work site: <http://www.dar.csiro.au>
Personal site: <http://www.dar.csiro.au/profile/hibberd.html>

Hurley

Dr. Peter Hurley
CSIRO Atmospheric Research
PMB1
Aspendale VIC 3195
AUSTRALIA

Phone: +61 3 9239 4400
Phone direct: +61 3 9239 4547
Fax: +61 3 9239 4444
Email: peter.hurley@csiro.au
Work site: <http://www.dar.csiro.au>
Personal site: <http://www.dar.csiro.au/profile/hurley.html>

Irwin

John S. Irwin, CCM
John S. Irwin and Associates
1900 Pony Run Road
Raleigh, NC 27615-7415
USA

Phone: (919) 541-5682
Email: jsirwinetal@nc.rr.com
Work site: <http://www.jsirwin.com>

Johnson

Mr. Michael A. Johnson, B.Sc.
Lakes Environmental Software, Inc.
6-60 Bathurst Drive
Waterloo, Ontario N2T 1T3
CANADA

Phone: (519) 746 5995
Fax: (519) 746 0793
Email: mike.johnson@weblakes.com
Work site: <http://www.weblakes.com>

Keen

Prof. Cecil S. Keen
Atmospheric Sciences / Geography
(c/o Box 2)
Minnesota State University
Mankato, MN 56002-8400
USA

Phone: (507) 389-5169
Fax: (507) 345-1283
Email: cecil.keen@mnsu.edu
Work site: <http://www.mnsu.edu/weather>

Kerrin

Stephen L. Kerrin
Project Director 2
SCS Engineers, Inc.
970 Los Vallecitos Blvd. Suite 100
San Marcos, CA 92009
USA

Phone: (760) 744-9611 ext 107
Email: skerrin@scsengineers.com

Lacser

Avraham Lacser, Ph.D.
Israel Institute for Biological Research
(IIBR)
POB 19
NESS ZIONA 74100
ISRAEL

Phone: +972 8 9381488
Fax: +972 8 9401404
Email: lacser@iibr.gov.il
Work site: <http://www.iibr.gov.il>

Lee

Russell Lee
RF Lee Consulting
825-C Merrimon Avenue, # 385
Asheville, NC 28804
USA

Phone: (704) 562-6772
Email: Russell.Lee@RFLee.com
Work site: <http://www.RFLee.com>

Luhar

Dr. Ashok Luhar
Centre for Australian Weather and Climate
Research
CSIRO Marine and Atmospheric Research
Private Bag No. 1
Aspendale VIC 3195
AUSTRALIA

Phone: +61 3 9239 4400
Fax: +61 3 9239 4444
Email: ashok.luhar@csiro.au
Work site: <http://www.cmar.csiro.au>
<http://www.cawcr.gov.au>

Lyons

Walter A. Lyons, Ph.D., CCM
FORENSIC METEOROLOGY
ASSOCIATES, Inc. (FMA)
46050 Weld County Road 13
Fort Collins, CO 80524
USA

Phone: (800) 854-7219
Fax: (970) 482-8627
Email: walyons@frii.com
Work site: <http://www.forensic-weather.com>

Matthews

Bryan D. Matthews
Lakes Environmental Software
1333 W. McDermott
Suite 200
Allen, TX 75013
USA

Phone: (469) 519-1093
Fax: (469) 519-1094
Email: bryan.matthews@weblakes.com
Work site: www.weblakes.com/

McAlpine

J.D. McAlpine
Meteorologist
Envirometrics, Inc.
4128 Burke Ave N
Seattle, WA 98103
USA

Phone: (206) 633-4456
Email: jdmac6@gmail.com
Work site: www.envirometrics.com

Michelsen

Dr. Hope Michelsen
Combustion Research Facility
Sandia National Labs
P. O. Box 969; MS 9055
Livermore, CA 94551
USA

Phone direct: (925) 294-2335
Fax: (925) 294-2276
Email: hamiche@sandia.gov
Work site: <http://www.ca.sandia.gov/CRF/>

Miller

Dr. Paul Miller
Silsoe Spray Applications Unit
(part of The Arable Group)
Wrest Park
Silsoe
Bedford
MK45 4HP
UNITED KINGDOM

Phone: +44 1525 862995 ext 100
Fax: +44 1525 862583
Email: paul.miller@theablegroup.com
Work site: <http://www.niab.com/>
[http://www.niab.com/pages/id/270/
Silsoe_Spray_Applications_Unit](http://www.niab.com/pages/id/270/Silsoe_Spray_Applications_Unit)

Moon

Dennis A. Moon, Ph.D.
Chief Scientist
WindLogics, Inc.
201 NW 4th St.
Grand Rapids, MN 55744
USA

Phone: (651) 556-4281
Email: dmoon@WindLogics.com
Work site: <http://www.WindLogics.com>

Moussiopoulos

Prof. Dr.-Ing. habil. Nicolas
Moussiopoulos
Laboratory of Heat Transfer and
Environmental Engineering
Dept. of Mechanical Engineering
Aristotle University
Box 483, University Campus
54124 Thessaloniki
GREECE

Phone: +30 2310 996011
Fax: +30 2310 996012
Email: moussio@eng.auth.gr
Work site: <http://aix.meng.auth.gr>

Nelson

Thomas E. Nelson
FMA Research, Inc.
Yucca Ridge Field Station
46050 Weld County Road
Fort Collins, CO 80524
USA

Email: tnelson@frii.com

Nunnari

Prof. Giuseppe Nunnari
Dipartimento di Ingegneria, Elettrica,
Elettronica e dei Sistemi
Viale A. Doria, 6
95125 Catania
ITALY

Phone: +39 095 738 2306
Fax: +39 095 330793
Email: gunnari@diees.unict.it
Work sites: [http://www.dees.unict.it/
users/gunnari/](http://www.dees.unict.it/users/gunnari/)
<http://www.diees.unict.it>
Group site: <http://www.scg.dees.unict.it/>

Oettl

Dr. Dietmar Oettl
Air Quality Department Styria
Landhausgasse 7
8010 Graz
AUSTRIA

Phone: +43 316 877 3327
Email: dietmar.oettl@stmk.gv.at
Work site: www.umwelt.steiermark.at

Paine

Robert Paine, CCM, QEP
AECOM
2 Technology Park Drive
Westford, MA 01886
USA

Phone: (978) 589-3164
Fax: (978) 589-3374
Email: bob.paine@aecom.com
Work site: <http://www.aecom.com/>

Pepper

Dr. Darrell W. Pepper
Professor and Director, NCACM
Department of Mechanical Engineering
University of Nevada Las Vegas
4505 Maryland Parkway
Las Vegas, NV 89154-4027
USA

Phone: (702) 895-1056
Fax: (702) 895-0498
Cell: (702) 528-7213
Email: dwpepper@nscee.edu
Work site: www.ncacm.unlv.edu

Pérez

Dr. Juan L. Pérez
Environmental Software and Modelling
Group
Computer Science School
Technical University of Madrid (UPM)
Campus de Montegancedo
Boadilla del Monte
28660 Madrid
SPAIN

Phone: +34 91 336 7465
Fax: +34 91 336 7412
Email: jlperez@fi.upm.es
Work site: <http://artico.lma.fi.upm.es>

Petersen

Ronald L. Petersen, CCM
Vice President, CPP, Inc.
1415 Blue Spruce Drive
Fort Collins, CO 80524
USA

Phone: (970) 221 3371
Fax: (970) 221 3124
Email: rpetersen@cppwind.com
Work site: www.cppwind.com

Physick

Dr. William Physick
CSIRO Atmospheric Research
PMB1
Aspendale VIC 3195
AUSTRALIA

Phone: +61 3 9239 4400
Phone direct: +61 3 9239 4636
Fax: +61 3 9239 4444
Email: bill.physick@csiro.au
Work site: <http://www.dar.csiro.au>
Personal site: <http://www.dar.csiro.au/profile/physick.html>

Pun

Dr. Betty K. Pun
Air Quality Division
Atmospheric and
Environmental Research, Inc
2682 Bishop Drive, Suite 120
San Ramon, CA 94583
USA

Phone: (925) 244-7125
Fax: (925) 244 7129
Email: pun@aer.com
Work site: <http://www.aer.com>

Rappolt

Thomas J. Rappolt
Vice President and
SCS Tracer Office Director
SCS Engineers, Inc.
970 Los Vallecitos Blvd. Suite 100
San Marcos, CA 92009
USA

Phone: (760) 744-9611 ext 107
Email: trappolt@scsengineers.com

Reynolds

Steven D. Reynolds, PhD
Envair
12 Palm Ave
San Rafael, CA 94901
USA

Phone: (415) 457-6955
Fax: (415) 457-6955
Email: steve@sreynolds.com

Richter

Dr. Richard O. Richter, P.E.
Exponent, Inc.
320 Goddard, Suite 200
Irvine, CA 92612
USA

Phone: (949) 341-6015
Fax: (949) 341-6059
Email: rrichter@exponent.com
Work site: <http://www.exponent.com>

Roth³

Philip M. Roth, Ph.D.

Ruby

Michael Ruby, Ph.D., P.E.
President
Envirometrics, Inc.
4128 Burke Ave N
Seattle WA 98103
USA

Phone: (206) 633-4456
Email: mruby@envirometrics.com
Work site: www.envirometrics.com

³ Deceased. See page 639 of Volume II.

San José

Prof. Dr. Roberto San José
Environmental Software and
Modelling Group
Computer Science School
Technical University of Madrid (UPM)
Campus de Montegancedo
Boadilla del Monte
28660 Madrid
SPAIN

Phone: +34 91 336 7465
Fax: +34 91 336 7412
Email: roberto@fi.upm.es
Work site: <http://artico.lma.fi.upm.es>

Sarma

Dr. Ananthakrishna Sarma
Senior Research Scientist
Center for Atmospheric Physics
SAIC, MS T2-3-1
1710 SAIC Dr.
McLean, VA 22102
USA

Phone: (703) 676-7017
Cell: (703) 589-0847
Fax: (703) 676-5509
Email: sarmaa@saic.com
Work site: <http://vortex.saic.com>

Seigneur

Dr. Christian Seigneur
Cerea (Atmospheric Environment Center)
Joint Laboratory École des Ponts Paris
Tech / EDF R&D
Université Paris-Est
77455 Marne la Vallée Cedex 2
FRANCE

Phone direct: +33 (0)1 64 15 21 41
Fax: +33 (0)1 64 15 21 70
Email: seigneur@cerea.enpc.fr
Work site: <http://cerea.enpc.fr>

Sheehan

Dr. Patrick J. Sheehan
Exponent, Inc.
1970 Broadway, Suite 250
Oakland, CA 94612
USA

Phone: (510) 208-2008
Fax: (510) 208-2039
Email: psheehan@exponent.com
Work site: <http://www.exponent.com>

Solomon

Douglas Solomon
US EPA - Emission Inventory and
Analysis Group
USA

Phone: (919) 541-4132
Fax: (919) 685-3185
Email: solomon.douglas@epa.gov

Sorbjan

Prof. Zbigniew Sorbjan, Ph.D., D.Sc.
(1) Department of Physics
Marquette University
P.O. Box 1881
Milwaukee, WI 53201
USA
(2) Institute of Geophysics
Polish Academy of Sciences
ul. Księcia Janusza 64
01-452 Warsaw
POLAND

Phone: +01 414 332 0561
Fax: +01 414 288-3989
Email: zbigniew.sorbjan@mu.edu
Work site: (1) <http://www.marquette.edu/>
(2) <http://www.igf.edu.pl/en/>
Personal site: <http://academic.mu.edu/sorbjan/>

Teske

Dr. Milton E. Teske, Ph.D.
Continuum Dynamics, Inc.
34 Lexington Avenue
Ewing, NJ 08618
USA

Phone: 609-538-0444 ext 109
Fax: 609-538-0464
Email: milt@continuum-dynamics.com
Work site: <http://www.continuum-dynamics.com>

Thé, C.

Cristiane L. Thé, M.A.Sc.
Director
Lakes Environmental Software
60 Bathurst Drive, Unit 6
Waterloo, Ontario
N2V 2A9
CANADA

Phone: (519) 746-5995
Fax: (519) 746-0793
Email: cris.the@weblakes.com
Work site: <http://www.WEBLAKES.com>

Thé, J.

Jesse Thé, Ph.D. P.Eng.
President
Lakes Environmental Software
60 Bathurst Drive, Unit 6
Waterloo, Ontario
N2V 2A9
CANADA

Phone: (519) 746-5995
Fax: (519) 746-0793
Email: Jesse.the@weblakes.com
Work site: <http://www.WEBLAKES.com>

Thistle

Harold W. Thistle, Ph.D.
Forest Health Technology Enterprise Team
Forest Health Protection
USDA Forest Service
180 Canfield St.
Morgantown, WV 26505
USA

Phone: (304) 285-1574
Fax: (304) 285-1564
Email: hthistle@fs.fed.us

Tourlou

Dr. Eng. Paraskevi-Maria Tourlou
Hellenic Ministry of Transport and
Communications
Land Transport Safety Directorate
Anastaseos 2 & Tsigante str.
GR-10191 Papagos, Athens
GREECE

Phone: +30 210 6508468 and 2310 996011
Fax: +30 210 6508493 and 2310 996012
Email: evelina@aix.meng.auth.gr
Work site: <http://aix.meng.auth.gr/lhtee/>

Trini Castelli

Dr. Silvia Trini Castelli
Institute of Atmospheric Sciences and
Climate – ISAC
Italian National Research Council – CNR
Corso Fiume, 4
I-10133 Torino
ITALY

Phone: +39 011 3839828
Fax: +39 011 6600364
Email: S.TriniCastelli@isac.cnr.it
Work site: <http://www.isac.cnr.it>
Personal site: <http://www.isac.cnr.it/~turboto/TriniCastelli-CV-new.htm>

van Dop

Dr. Han van Dop
Institute for Marine and
Atmospheric Research Utrecht
Utrecht University
P.O. Box 80.005
3508 TA Utrecht
THE NETHERLANDS

Phone: +31 30 253 3154
Fax: +31 30 254 3163
Email: h.vandop@phys.uu.nl
Personal site: <http://www.phys.uu.nl/~dop/>

Venkatram

Akula Venkatram, Ph.D.
Professor of Mechanical Engineering
UC Riverside
A343 Bourns Hall
Riverside, CA 92521
USA

Phone: (909) 787-2195
Fax: (909) 787-2899
Email: venky@engr.ucr.edu
Personal sites: <http://www.engr.ucr.edu/mechanical/people/venkatram.html>
<http://www.engr.ucr.edu/~venky/>

Vlachokostas

Dr. Christos Vlachokostas –
Dipl. Mechanical Engineer
Laboratory of Heat Transfer and
Environmental Engineering
School of Engineering
Aristotle University Thessaloniki
Box 483, 54124 Thessaloniki,
GREECE

Phone: +30 2310 996092
+30 2310 996011(secretariat)
Fax: +30 2310 996012
Email: vlahoco@aix.meng.auth.gr
Work site: <http://aix.meng.auth.gr>

Watson

John G. Watson, Ph.D.
Department of Atmospheric Sciences
Desert Research Institute
University of Nevada, Reno
2215 Raggio Parkway
Reno, NV 89512
USA

Phone direct: (775) 674-7046
Fax: (775) 674-7009
Email: john.watson@dri.edu
Work site: <http://www.das.dri.edu/>
Personal site: <http://www.dri.edu/People/johnw/>

Yamartino

Robert J. Yamartino, Ph.D.
Integrals Unlimited
509 Chandler's Wharf
Portland, ME 04101
USA

Phone: (207) 780-0594
Cell: (207) 233-4565
Email: rjy@maine.rr.com

Zannetti

Dr. Paolo Zannetti, QEP
President, EnviroComp Consulting, Inc.
and
The EnviroComp Institute
2298 Ocaso Camino
Fremont, CA 94539
USA

Phone: (510) 490-3438
Fax: (510) 490-3357
Email: zannetti@envirocomp.com
Work site: <http://www.envirocomp.com> and
<http://www.envirocomp.org>
Personal site: [http://www.envirocomp.com/
people1/zannetti.html](http://www.envirocomp.com/people1/zannetti.html)

Builtjes, P. and R. Paine 2010. *The Problem – Air Pollution*. Chapter 1 of *AIR QUALITY MODELING - Theories, Methodologies, Computational Techniques, and Available Databases and Software. Vol. IV – Advances and Updates* (P. Zannetti, Editor). Published by The EnviroComp Institute (<http://www.envirocomp.org>) and the Air & Waste Management Association (<http://www.awma.org>).

Chapter 1

The Problem – Air Pollution

Peter Builtjes⁽¹⁾ and Robert Paine⁽²⁾

⁽¹⁾ *TNO Environment and Geosciences, P.O. Box 80015, 3508 TA Utrecht (The Netherlands)*

peter.builtjes@tno.nl

⁽²⁾ *AECOM Environment, 2 Technology Park Drive, Westford, MA 01886 (USA)*

bob.paine@aecom.com

Abstract: An introduction is given about general aspects of air pollution. In addition, an overview is presented about the history of air pollution modeling.

Key words: Air pollution, Air pollution regulations, Air pollution modeling.

1 Our Natural Environment

Air pollution can be seen as the result of emissions of man-made, anthropogenic trace gases and particles into our environment.

The chemical composition of the current atmosphere differs considerably from the chemical composition of the natural atmosphere, as it existed in pre-industrial times. This means that, at the moment, nowhere on earth is there natural air, which could also be considered clean air. Our atmosphere is polluted everywhere, which means that the chemical composition differs from the pre-industrial situation.

The chemical composition of the natural atmosphere has shown gradual changes as long as the earth has existed. Life started on earth, in the oceans in fact, in an atmosphere that hardly contained any oxygen, only about 0.015% against the current level of about 21%. The atmosphere at that moment contained nearly 99% CO₂, some N₂, and only traces of H₂O and O₂. Because of the low oxygen level, no

stratospheric ozone layer could have been formed. So, the surface of the earth received all the UV-B radiation that is captured these days by the ozone layer. This also explains why life had to start in the oceans, at about 10 m below sea level - a depth where the UV-B radiation was substantially lower.

At first, life on earth, which started about 3 billion years ago, was plant-like and with the aid of photosynthesis-produced oxygen. This way, the oxygen level slowly increased in the atmosphere. This increase in oxygen contributed to the development of a stratospheric ozone layer, making life on the surface of the earth possible, about 400 million years ago. Although fluctuations may have occurred, for example in the oxygen level, with possible maximum values up to 23%, the overall chemical composition of the natural atmosphere, as far as we know, has been relatively stable over the last 10 million years.

The chemical composition of the pre-industrial/natural global averaged atmosphere is shown in table 1:

Table 1. The chemical composition of the natural atmosphere.

	Gas	% by volume	ppm	ppm by the year 2000
Nitrogen	N ₂	78.1		
Oxygen	O ₂	20.9		
Argon	Ar	0.92		
Neon	Ne		18.2	
Helium	He		5.2	
Krypton	Kr		1.14	
Xenon	Xe		0.09	
Carbon dioxide	CO ₂		280.0	360.0
Methane	CH ₄		0.750	1.75
Nitrous oxide	N ₂ O		0.270	0.310

The composition given in table 1 is that of the dry atmosphere. H₂O-vapor has a concentration fluctuating between 40 ppm and 40,000 ppm (4%).

The ecosystem “life” created the chemical composition of the atmosphere in which this ecosystem can exist, i.e., a chemical composition in which life can sustain. The chemical composition with its high oxygen level is not in chemical equilibrium, but this non-equilibrium state can be maintained by life itself.

Based on this fact, James Lovelock developed the Gaia-theory (Gaia, the Greek goddess of the earth), [Lovelock (1972, 1979)]. In short, his theory states that the earth, including the atmosphere, is a 'living', homeostatic organism. In contrast, the surrounding planets where there is no life, Venus and Mars, have a completely different chemical composition, which is in chemical equilibrium (their atmosphere contains about 99% CO₂, some N₂, and nearly no O₂ and H₂O).

In other words, our atmosphere is a very special one, and we should handle it with care.

2 Air Pollution, Some Definitions

There are several conceivable approaches to define air pollution. For example, the change in the global, chemical composition of the pre-industrial atmosphere, as given in Table 1, and which is due to human influence, can be called air pollution; all man-made, anthropogenic emissions into the air can be considered air pollution. So air pollution - but at a very local scale, not detectable at a global scale - did not start until mankind started 'to play with fire'.

The global increase in the concentrations of CO₂, CH₄ and N₂O (shown in Table 1), all greenhouse gases, could, and should be called 'air pollution' in the broad sense, even though these species are not toxic for human beings and the ecosystem.

Another approach is to distinguish between the emissions of safe, non-toxic, and harmful compounds, and only consider the last as air pollution. This distinction, however, has two clear drawbacks. About 1940 and even much later, manmade emissions of CFCs were considered safe because they are inert in the troposphere. However, the decrease of the stratospheric ozone layer has taught us differently. In the same way, CO₂ emissions are safe in the sense that they are not toxic, but their increase leads – most likely – to a climate change, which in turn will be harmful to large parts of the ecosystem.

The second drawback is that natural emissions can also be harmful, such as emissions of dioxine caused by a forest fire as a result of lightning.

One anthropogenic influence that has actually decreased “natural” emissions is the human intervention to prevent the widespread extent of wildland fires that used to exist prior to the 20th century (Barry, 2007). In the past century, substantial efforts were initiated, at least in the United States, to curtail the extent of natural fires due to the encroachment of human population in formerly remote areas. Recently, it has been realized that this human intervention has led to adverse effects such as the buildup of low-level brush that has led to more extensive fires that are harder to control. In addition, the benefits of wildland fires to maintain the ecosystem in its natural state have been compromised. One way to return closer to the level of natural wildfire emissions that existed in pre-industrial times is to conduct prescribed burning under controlled conditions to minimize the harmful effects of wildland fires while maximizing their benefits. Even so, the extent of “natural” emissions from pre-industrial fires will likely never be realized again because as population continues to encroach upon forested areas, there will be human intervention to restrict wildfires that would never have occurred in previous centuries.

Next to anthropogenic emissions, it is possible to distinguish between natural emissions and biogenic emissions.

Natural emissions should be defined as emissions caused by the non-living world, such as volcanic emissions, sea-salt emissions, and natural fires.

Biogenic emissions are emissions resulting from the ecosystem, like VOC-emissions from forests, and CH₄-emissions from swamps. In principle, natural and biogenic emissions lead to the chemical composition of the pre-industrial, natural atmosphere.

The philosophical question [whether manmade emissions should also be considered as biogenic, because man is part of the ecosystem] can be retorted by the distinction that mankind, by making fires, creates anthropogenic emissions.

Although the distinction in these three categories: anthropogenic, natural, and biogenic could be useful, quite a number of intermediate emissions exist. Examples are the NO-emissions by soil bacteria, which is a function of the earlier deposited nitrogen on the soil due to anthropogenic emissions of N-compounds or earlier deposited manure containing nitrogen. There is the question of whether or not VOC-emissions are due to planting or not planting of trees, and whether or not dust-emissions are the consequence of paving or not paving sandy roads. These are such intermediate emissions, biogenic or natural, but with a clear human influence.

Although anthropogenic emissions started when man learned to make fire, and the air quality, especially the concentrations of fine particles, surpassed air quality guidelines in and around the cave dwellings of the Neanderthal man, the impact of air pollution has been of a local character for a long time.

In Europe, elevation of concentration levels occurred for the first time in the middle ages, resulting in the first laws on air pollution that were often focused on odor nuisance around local factories. Also, burning coal for heating and cooking led to air pollution, until well into the last century. London for example, was 'famous' for its fog. Subsequently, the industrial revolution involved a tremendous increase in the use of fossil fuel for thermally-generated power to run factories and later to supply electrical power and as a consequence of industrial emissions from smelters, petrochemical plants, pulp mills, etc. Consequently, as from about 1850, a number of gases started to increase in concentration, like the gases mentioned in Table 1 - CO₂, CH₄ and N₂O – and in addition, for example, sulfate aerosols.

It should be emphasized here that air pollution in the strict sense ('toxic') and global (climate) change are interrelated phenomena. Directly, because they often have the same emission sources, and more indirectly because species like tropospheric ozone and aerosols play a role both in local and regional air quality, as well as in climate change.

3 Primary and Secondary Pollutants

The main, primary – i.e., directly emitted – gaseous pollutants are the following:

- Carbon compounds, e.g. CO₂, CO, CH₄, the VOC's (volatile organic compounds)
- Nitrogen compounds, e.g. N₂O, NO, NH₃
- Sulfur compounds, e.g. SO₂, H₂S
- Halogen compounds, e.g. chlorides, fluorides, bromides

The main, primary particle pollutants are the following:

- Particles smaller than 2.5 μm in diameter. Included are the Aitken nuclei, particles smaller than 0.1 μm in diameter, which grow rather fast by coagulation to larger particles. The chemical composition of these primary particles is, to a large extent, carbon but also heavy metals as iron, zinc, copper, etc., will also be contained in these particles.
- Particles with a diameter from 2.5 to 10 μm. These larger particles are often composed of sea salt and dust.

Most air pollutants, except the halogen compounds, will be chemically transformed in the troposphere by the OH-radical. The OH-radical is formed in the troposphere by photo-dissociation of O₃, and subsequent reaction of oxygen with H₂O-vapor to OH (Levy, 1971). The OH-radical reacts not with N₂, O₂, H₂O, CO₂, but with other compounds as CO, CH₄, H₂, NO, NO₂, SO₂, NH₃. The OH-radical can be seen as the cleansing agent of the atmosphere, since it transforms primary air pollutants into secondary pollutants, which are subsequently removed from the atmosphere by dry and wet deposition. In this way the OH-radical determines the atmospheric residence time of most compounds in the atmosphere.

The main, secondary – i.e., formed in the atmosphere – gaseous pollutants are:

- NO₂ and HNO₃ formed from NO
- O₃ formed through photochemical reactions

The main, secondary particles are:

- Sulfate aerosols formed from SO₂, and Nitrate aerosols formed from NO₂ followed by the reaction with NH₃ to form ammonium (bi) sulfate and ammonium nitrate.
- Organic aerosols formed from gaseous organic compounds.

These secondary particles consist mainly of small particles with a diameter less than 2.5 μm.

4 A Short History of Air Pollution Modeling

Air pollution modeling is an attempt to describe the causal relation between emissions, atmospheric concentrations, and deposition. Air pollution measurements give quantitative information about concentrations and deposition, but they can only give the levels at specific locations. In principle, air pollution modeling can give a more complete and consistent description, including an analysis of the causes - emissions sources, meteorological processes, physical and chemical transformations - that have led to these concentrations/deposition.

Air pollution models play an important role in science, because of their capability to assess the importance of the relevant processes. Air pollution models are the only method that quantifies the relationship between emissions and concentrations/depositions, including the consequences of future scenarios and the determination of the effectiveness of abatement strategies.

The concentrations of species in the atmosphere are determined by transport and diffusion. This means that in considering the history of air pollution modeling, some remarks should be made concerning transport and diffusion. Transport phenomena, characterized by the mean velocity of the fluid, have been measured and studied for centuries. For example, the average wind was studied for sailing purposes. The study of diffusion (turbulent motion) is more recent. Although turbulent motions have been observed from the moment people looked at rivers and streams, one could mention Reynolds' paper in 1895 as the scientific starting point for the formulation of the famous criterion for laminar-to-turbulent flow transition in pipes.

One of the first articles in which turbulence in the atmosphere is mentioned, was published by Taylor (1915). In later years, he developed the 'Taylor-theory of turbulent diffusion', Taylor (1921). In this theory, it is shown that the diffusion from a point source can only be described with a constant eddy diffusivity, K , for travel times, which are much larger than the turbulent integral time scale, the so-called diffusion limit. For smaller time-scales the effective turbulent diffusivity is proportional to the travel time.

Until about 1950, a number of studies were performed on the subject of diffusion in the atmosphere (Richardson and Proctor, 1925; Sutton, 1932; Bosanquet, 1936; Church, 1949; Thomas et al., 1949; Inoue, 1950; Batchelor, 1950). Already, the paper by Richardson considered long-range aspects; up to over 80 km. Bosanquet is one of the first who published about the impact of chimney plumes. A paper by Chamberlain (1953) already considered the deposition of aerosols.

4.1 Modeling of Point Sources

The study of the dispersion from low and high level point sources, especially experimental, was a major topic shortly after 1955. Papers on this subject

appeared by Smith (1957), Gifford (1957 a, b), Hay and Pasquill (1957), Record and Cramer (1958) and Haugen (1959) both devoted to the Prairie grass experiment, Stewart et al. (1958), Monin (1955, 1959), Ogura (1959). Perhaps the first paper on this subject was by Roberts (1923).

The publication by Pasquill ‘Atmospheric Diffusion’, which appeared in 1962, was a major milestone in summarizing the work performed until that moment. It illustrates that air pollution modeling around the beginning of the sixties was focused on local dispersion phenomena, mainly from point sources with SO₂ as major component in the application studies.

The Gaussian plume model was formulated, in which the horizontal and vertical spread of the plume was determined experimentally. Tables appeared with the famous Pasquill-Gifford sigma-values in the horizontal and vertical direction, and as a function of the atmospheric stability ranging from very stable, class F, up to very unstable, class A. The experimental sigma values are in their functions with distance from the source in reasonable agreement with the Taylor-theory. The differences are caused by the fact that the Taylor-theory holds for homogeneous turbulence, which is not the case in the atmosphere.

In the sixties, the studies concerning dispersion from a point source continued and were broadening in scope. Major studies were performed by Högstrom (1964), Turner (1964), Briggs (1965) - the famous plume-rise formulas -, Moore (1967), Klug (1968). The use and application of the Gaussian plume model spread over the whole globe, and became a standard technique in every industrial country to calculate the stack height required for permits, see for example Beryland (1975) who published a standard work in Russian. The Gaussian plume model concept was soon applied also to line and area-sources. Gradually, the importance of the mixing height was realized (Holzworth, 1967, Deardorff, 1970, 1972) and its major influence on the magnitude of ground level concentrations.

The basic concepts of predicting ground-level concentrations from stack emissions involved the variables listed below.

- Wind direction determines the trajectory of the emissions. Complications with this variable are that the wind direction varies with height and location, especially in stable conditions when the atmosphere is not well mixed. It is also well known that the validity of straight-line Gaussian plume models are limited to the degree of the wind persistence and other meteorological variables as a function of plume travel time.
- Wind speed affects both the plume rise of buoyant emissions (by affecting the rate of ambient air entrainment and source effects such as building and stack downwash) and the dilution of the emissions with ambient air. It is also well known that wind speeds generally increase with height due to frictional effects near the ground, but there can be challenges in simulating the vertical and horizontal changes of wind speed, similar to the wind direction challenges.

- The ambient temperature affects the rise of buoyant plumes in that the entrainment of ambient air into plumes will reduce their buoyancy with time. “Final” plume rise is considered to be reached when the vertical velocity associated with plume buoyancy is comparable to vertical wind fluctuations in the atmosphere.
- The stability of the atmosphere was, in the early era of Gaussian models, expressed as classes that ranged from 1 (very unstable) through 4 (neutral) and to 7 (very stable). The discrete stability classes were determined through several methods, including the Turner (1964) method based upon wind speed, solar elevation, and cloud cover, as well as alternative methods described in the United States Environmental Protection Agency (USEPA) document, *Meteorological Monitoring Guidance for Regulatory Modeling Applications* (2000). These alternative methods involve use of site-specific turbulence and wind data, as well as solar radiation, wind speed, and vertical temperature difference data. The specification of a stability class allowed Gaussian dispersion models to assign rates of plume dispersion in the vertical and horizontal, as well as to determine plume rise formulas.
- The mixing height is the height above the surface through which relatively vigorous mixing occurs. Early Gaussian dispersion models only considered limits to mixing in convective conditions, as defined by the height of a temperature inversion aloft. This variable was used in Gaussian models to determine a depth within which an emitted plume was trapped and into which it would eventually mix thoroughly after sufficient travel time. However, plumes emitted above the mixed layer height could be assumed not to be entrained within the mixed layer, and therefore not affect ground-level pollutant concentrations.

In addition to these plume modeling concepts, atmospheric scientists (e.g., Turner, 1969 and Pasquill, 1976) categorized six types of plume behavior visible under various conditions of stable and unstable conditions. The plume types were referred to as “looping”, “coning”, fanning”, “lofting”, “fumigation”, and “trapping”. Early Gaussian dispersion models were designed to simulate these effects through appropriate combinations of the variables described above as incorporated into dispersion modeling schemes. A review of the air pollution modeling papers published in the sixties and seventies indicates that these papers appear to be mainly written by meteorologists, specialized in boundary layer meteorology and atmospheric turbulence. These studies focused often on the effect of atmospheric stability on plume spread. During the next decade, besides research on local dispersion (for a good overview, see Nieuwstadt and van Dop, 1982), the spatial scale of air pollution modeling increased substantially.

In the period after 1980 to the present time (2009), additional enhancements were made to steady-state Gaussian models. Major developments in an improved understanding of the planetary boundary layer (PBL) began in the 1970s, as described by Venkatram (1978, 1980), Wyngaard (1988), Izumi (1971), Dyer

(1979), van Ulden and Holtslag (1985), Businger (1973), Panofsky et al. (1977, 1984), and Kaimal et al. (1976). One milestone involved numerical simulations by investigators Deardorff and Willis (see 1975, 1978, and 1981 papers), revealing the convective boundary layer's (CBL's) vertical structure and important turbulence scales. Insights into dispersion followed from laboratory experiments, numerical simulations, and field observations (Briggs 1973, 1984, and 1988; Lamb 1982; Weil 1988a,b). For the stable boundary layer (SBL), advancements occurred more slowly. However, a sound theoretical/experimental framework for surface layer dispersion and approaches for elevated sources existed by the mid-1980s (Briggs 1988; Venkatram 1988).

Advances in Gaussian models using stability classes were made in the USA with the Rough Terrain Diffusion Model (Paine and Egan, 1987), improvements in the Industrial Source Complex Model (USEPA, 1995a,b), and AUSPLUME in Australia (EPA Victoria, 2004).

The changes to the earlier straight-line Gaussian models brought about by application of the considerable research noted above were as follows, as described by Weil, 1985):

- Discrete stability classes were replaced by continuous functions of similarity scaling parameters such as the friction velocity (u_*), the convective velocity scale (w_*), and the Monin-Obukhov length (L).
- Variables such as wind direction and speed, temperature, and turbulence were scaled with height using available on-site measurements and enhanced with boundary-layer concepts.
- Mixing heights were generalized into both convective and mechanical (shear-induced) components.
- Source effects such as building downwash were improved with developments such as the PRIME model (Schulman et al., 2000).
- Plume interactions with terrain were advanced with the concept of the dividing streamline height in models such as CTDMPLUS (Perry et al., 1989; Perry, 1992).

Starting in the 1980s, researchers began to apply this information to applied dispersion models. These included eddy-diffusion techniques for surface releases, statistical theory and PBL scaling for dispersion parameter estimation, and a new probability density function (PDF) approach for the CBL. Much of this work was reviewed and promoted in workshops (Weil, 1985), revised texts (Pasquill and Smith, 1983), and in short courses and monographs (Nieuwstadt and van Dop, 1982; Venkatram and Wyngaard, 1988). By the mid- to late 1980s, new applied dispersion models had been developed, including the Power Plant Siting Program (PPSP) model (Weil and Brower, 1984), Second-Order Closure Integrated Puff (SCIPUFF) (Sykes et al., 1998), Operationelle Meteorologiske Luftkvalitetsmodeller (OML) (Berkowicz et al., 1986), Hybrid Plume Dispersion Model (HPDM) (Hanna and Paine, 1989), Multiple Source Dispersion Algorithm Using On-Site Turbulence Data (TUPOS) (Turner et al., 1986), and the Complex Terrain Dispersion Model Plus

Algorithms for Unstable Situations (CTDMPLUS) (Perry et al. 1989); later, the Advanced Dispersion Modeling System (ADMS), developed in the United Kingdom (Carruthers et al. 1992; CERC, 2004), was added as well.

In February 1991, the U.S. Environmental Protection Agency (USEPA) in conjunction with the American Meteorological Society (AMS) formed the AMS and EPA Regulatory Model (AERMOD) Improvement Committee (AERMIC), with the purpose of incorporating scientific advances from the 1970s and 1980s into a state-of-the-art Gaussian dispersion model for regulatory applications. AERMIC's early efforts are described by Weil (1992). To improve PBL parameterizations, other concerns such as plume interaction with terrain, surface releases, building downwash (PRIME model; Schulman et al., 2000), and urban dispersion were addressed. These efforts resulted in AERMOD (Cimorelli et al., 2005 and Perry et al., 2005), which was adopted as a recommended short-range dispersion model by the USEPA in late 2005.

4.2 Air Pollution Modeling at Urban and Larger Scales

Shortly after 1970, scientists began to realize that air pollution was not only a local phenomenon. It became clear - firstly in Europe - that the SO₂ and NO_x emissions from tall stacks could lead to acidification at large distances from the sources. It also became clear - firstly in the US - that ozone was a problem in urbanized and industrialized areas. And so it was obvious that these situations could not be tackled by simple Gaussian-plume type modeling.

Two different modeling approaches were followed, Lagrangian modeling and Eulerian modeling. In Lagrangian modeling, an air parcel is followed along a trajectory, and is assumed to keep its identity during its path. In Eulerian modeling, the area under investigation is divided into grid cells, both in vertical and horizontal directions.

Lagrangian modeling, directed at the description of long-range transport of sulfur, began with studies by Rohde (1972, 1974), Eliassen and Saltbones (1975) and Fisher (1975). The work by Eliassen was the start for the well-known EMEP-trajectory model which has been used over the years to calculate trans-boundary air pollution of acidifying species and later, photo-oxidants. Lagrangian modeling is often used to cover longer periods of time, up to years.

The simulation of long-range transport as well as short-range transport in complex wind situations from individual sources was improved with the development of Lagrangian puff models such as CALPUFF (users guide - Scire et al., 2000) and the Second-Order Closure Integrated Puff (SCIPUFF) (Sykes et al., 1998; Santos et al., 2000). These models have a meteorological pre-processor as well as a dispersion module, and were specifically suited for the transport and dispersion of individual stack emissions for long distances. These models treat source emissions as being broken up into a series of puff releases. The puffs are

advected throughout the modeling domain by the wind fields generated using the meteorological preprocessor (or supplied directly from mesoscale modeling output, such as MM5). Concentrations at user-specified receptors are computed by adding the contributions of all of the puffs currently in the modeling domain during each model time step (which can be a fraction of an hour). Puffs are grown and diluted using various dispersion formulas, and can be broken into smaller puffs if they become large and are subject to significant shears.

These models are useful for long-range transport issues as well as near-field impacts in special situations such as:

- Complex flows/dispersion effects
- Coastal zones
- Complex terrain
- Inhomogeneity in surface conditions/dispersion rates
- Plume fumigation, inversion breakup
- Calm and near-calm wind conditions.

Eulerian modeling began with studies by Reynolds et al. (1973) for ozone in urbanized areas, with Shir and Shieh (1974) for SO₂ in urban areas, and Egan et al. (1976) and Carmichael and Peters (1979) for regional scale sulfur. From the modeling studies by Reynolds on the Los Angeles basin, the well-known Urban Airshed Model-UAM originated. Eulerian modeling, in these years, was used only for specific episodes of a few days.

So in general, Lagrangian modeling was mostly performed in Europe, over large distances and longer time-periods, and focused primarily on SO₂. Eulerian grid modeling was predominantly applied in the US, over urban areas and restricted to episodic conditions, and focused primarily on O₃. Also hybrid approaches were studied, as well as particle-in-cell methods (Sklarew et al., 1971). Early papers on both Eulerian and Lagrangian modeling are by Friedlander and Seinfeld (1969), Eschenroeder and Martinez (1970) and Liu and Seinfeld (1974).

A comprehensive overview of long-range transport modeling in the seventies was presented by Johnson (1980).

Recent advances in “whole atmosphere models” have produced state-of-the-art photochemical models capable of simulating ozone, regional haze, and fine particulate impacts of thousands of sources distributed over large regions. These models include CMAQ (Byun and Ching, 1999), CAMx (Morris et al., 2004), and TAPM (Hurley, 2005). Similar to the Lagrangian models mentioned above, these models employ a meteorological pre-processor. They also require extensive emissions preprocessing in order to appropriately characterize the numerous chemical constituents used in the model. The models employ advanced gas phase chemistry mechanisms in its computations. They also generally have sophisticated post-processors and graphical user interfaces to facilitate display and interpretation of the modeling results.

The next, obvious step in scale is global modeling of earth's troposphere. The first global models were 2-D models, in which the global troposphere was averaged in the longitudinal direction (see Isaksen and Rohde, 1978). The first, 3-D, global models were developed by Peters and Jouvanis (1979) (see also Zimmermann, 1988).

In the period after 2000, operational weather prediction models were linked with integrated models such as HYSPLIT (ARL, 2009). As noted by the model documentation, the HYSPLIT (HYbrid Single-Particle Lagrangian Integrated Trajectory) model is a complete system for computing simple air parcel trajectories to complex dispersion and deposition simulations. The dispersion of a pollutant is calculated by assuming either puff or particle dispersion. The model's default configuration assumes a puff distribution in the horizontal and particle dispersion in the vertical direction. In this way, the greater accuracy of the vertical dispersion parameterization of the particle model is combined with the advantage of having an ever-expanding number of particles represent the pollutant distribution.

In general, Lagrangian particle models are like Lagrangian puff models except that they treat emissions as numerous particles that are moved in time by a mean wind and a random (Monte Carlo) turbulent component. The concentration in a model grid box is determined by counting the number of particles that are in the box at any given time.

There are other modeling approaches used for specialized applications. A partial list is provided below.

- Dispersion models suitable for heavy gas releases are needed to account for near-field slumping and spreading of accidental releases of a heavy gas. The alternative model area at USEPA's web site at www.epa.gov/scram001 lists some of these models.
- Computational fluid dynamics (CFD) models incorporate complex wind flow models with very small grid sizes (on the order of 1 m) and small time steps (on the order of 1 s) so that small-scale turbulence effects can be resolved by the model. They are useful for complex flows with complicated structures that are not readily accommodated by larger-scale routine models. The models are highly computer intensive and are generally limited to case studies rather than extensive time simulations.
- Wind tunnel models are also useful for studying complex geometries that are not amenable to conventional modeling approaches. Although many controlled experiments can be conducted by this technique, it is difficult to simulate stable or unstable boundary layers in a wind tunnel. In addition, artificial boundary conditions are required due to the finite size of the wind tunnel.

5 Air Pollution Modeling Guidelines

Many countries have their unique ambient standards and have issued guidelines for approved modeling procedures. These standards and modeling guidelines are subject to change. The bulleted items below provide selected web sites for information as of early 2010.

- World Bank International Finance Corporation environmental guidelines are available at:
<http://www.ifc.org/ifcext/sustainability.nsf/Content/EnvironmentalGuidelines>.
- United States modeling guidance: www.epa.gov/scram001. This site also has a link to individual state websites. It also lists alternative models, some of which were developed in other countries.
- United States national ambient air quality standards: <http://www.epa.gov/ttn/naaqs/>
- Canadian air quality standards are available at <http://www.hc-sc.gc.ca/ewh-semt/air/out-ext/reg-eng.php>. Modeling guidance is issued by individual provinces (e.g., Ontario, Alberta, and British Columbia).
- Mexican air quality standards are compared to USA standards at http://www.epa.gov/ttn/catc1/cica/airq_e.html.
- European air quality standards are provided at <http://ec.europa.eu/environment/air/quality/standards.htm>. Databases on European emissions and monitoring are available through <http://www.eea.europa.eu/themes/air>.
- Various European countries use different dispersion modeling approaches. However, “Guidance on the use of models for the European air quality Directive” issued by the Forum for Air Quality Modelling in Europe (FAIRMODE) is meant to “provide a harmonised focus for modelling activities that are relevant to the Air Quality Directive”. This document is available at:
http://fairmode.europa.eu/fo1404948/Model_guidance_document_v5_1a.pdf/download.
- Australia’s air quality and emission standards are available at <http://www.environment.gov.au/atmosphere/airquality/standards.html>. Individual Australian states have established their own modeling procedures, which are available on their respective web sites.
- New Zealand has a guideline for atmospheric dispersion modeling available at <http://www.mfe.govt.nz/publications/air/atmospheric-dispersion-modelling-jun04/html/page11.html>.

References

Air Resources Laboratory, 2009, HYSPLIT - Hybrid Single Particle Lagrangian Integrated Trajectory Model. <http://ready.arl.noaa.gov/HYSPLIT.php>.

Barry, A., 2007, Forest Policy Up in Smoke: Fire Suppression in the United States. Property and Environment Research Center. Available at:
www.perc.org/pdf/Forest%20Policy%20Up%20in%20Smoke.pdf.

- Batchelor, G.K., 1950, The application of the similarity theory of turbulence to atmospheric diffusion. *Quart. J.R.Met.Soc.* 76:133.
- Berkowicz, R., J. R. Olesen, et al., 1986, The Danish Gaussian air pollution model (OLM): Description, test and sensitivity analysis, in view of regulatory applications. *Air Pollution Modeling and Its Application*. V. C. De Wispelaire, F. A. Schiermeier and N. V. Gillani. New York, Plenum: 453-481.
- Beryland, M.Y., 1975, Contemporary problems of atmospheric diffusion and pollution of the atmosphere. Gidrometezdat, Leningrad, translated into English by NERC, USEPA.
- Bosanquet, C.H., and Pearson, J.L., 1936, The spread of smoke and gases from chimneys. *Trans. Faraday Soc.* 32:1249.
- Briggs, G.A., 1965, A plume rise model compared with observations. *J.Air Poll. Control Association* 15:433.
- Briggs, G. A., 1973, Diffusion estimation for small emissions. Air Resources Atmospheric Turbulence and Diffusion Laboratory, Environmental Research Laboratory, NOAA, 1973 Annual Rep. ATDL-79, 59 pp.
- Briggs, G.A., 1984, Plume rise and buoyancy effects. *Atmospheric Science and Power Production*, D. Randerson, Ed. U.S. Department of Energy, 327–366.
- Briggs, G.A., 1988, Analysis of diffusion field experiments. *Lectures on Air Pollution Modeling*, A. Venkatram and J. C. Wyngaard, Eds., Amer. Meteor. Soc., 63–117.
- Businger, J. A., 1973, Turbulent transfer in the atmospheric surface layer. *Workshop on Micrometeorology*, D. A. Haugen, Ed., Amer. Meteor. Soc., 67–100.
- Byun, D.W. and J.K.S. Ching, 1999, Science Algorithms of the EPA Models-3 Community Multiscale Air Quality (CMAQ) Modelling System, U.S. Environmental Protection Agency, Research Triangle Park, NC. EPA/600/R-99/030.
- Carmichael, G.R., and Peters, L.K., 1979, Numerical simulation of the regional transport of SO₂ and sulfate in the eastern United States. *Proc. 4th Symp. on turbulence, diffusion and air pollution*, AMS 337.
- Carruthers, D.J., R.J. Holroyd, J.C.R. Hunt, W.S. Weng, A.G. Robins, D.D. Apsley, D.J. Thomson, and F.B. Smith, 1992, UK-ADMS – a New Approach to Modelling Dispersion in the Earth's Atmospheric Boundary Layer. In *Proceedings of the Workshop: Objectives for Next Generation of Practical Short-Range Atmospheric Dispersion Models*, May 6-8, 1992, Riso, Denmark, pp. 143-146. (1992)
- CERC, 2004, *ADMS 3 User Guide: Version 3.2*, Cambridge Environmental Research Consultants, Ltd. (available at <http://www.cerc.co.uk/software/pubs/ADMS%203%20User%20Guide.pdf>)
- Chamberlain, A.C., 1953, 'Aspects of travel and deposition of aerosol and vapour clouds' A.E.R.E., HP/R 1261, H.M.S.O.
- Church, P.E., 1949, Dilution of waste stack gases in the atmosphere. *Ind.Eng. Chem.* 41:2753.
- Cimorelli, A.J., S.G. Perry, A. Venkatram, J.C. Weil, R.J. Paine, R.B. Wilson, R.F. Lee, W.D. Peters, and R.W. Brode, 2005, AERMOD: A Dispersion Model for Industrial Source Applications. Part I: General Model Formulation and Boundary Layer Characterization'. *Journal of Applied Meteorology*, 44, 682-693. American Meteorological Society, Boston, MA.

- Deardorff, J.W., 1970, Convective velocity and temperature scales for the unstable planetary boundary layer and for Rayleigh convection. *J. Atm. Sci.* 27, 1211-1213.
- Deardorff, J.W., 1972, Numerical investigation of neutral and unstable planetary boundary layers. *J. Atmos. Sci.*, 29, 91–115.
- Deardorff, J.W., and Willis, G.E., 1975, A parameterization of diffusion into the mixed layer. *J. Appl. Met.* 14:1451.
- Dyer, A. J., 1974, A review of flux-profile relationships. *Bound.-Layer Meteor.*, 7, 363–372.
- Egan, B.A., Rao, K.S., and Bass, A., 1976, A three dimensional advective-diffusive model for long-range sulfate transport and transformation. *7th ITM*, 697, Airlie House.
- Eliassen, A., and Saltbones, J., 1975, Decay and transformation rates of SO₂ as estimated from emission data, trajectories and measured air concentrations. *Atm. Env.* 9:425.
- EPA Victoria, 2004, AUSPLUME Gaussian Plume Dispersion Model: Technical User Manual. Environment Protection Authority of Victoria, Australia.
- Eschenroeder, A.Q. and J.R. Martinez, 1970, “Mathematical Modeling of Photochemical Smog”, American Institute Aeronautics and Astronautics (Proceedings), Eight Aerospace Sciences Meeting, New York, Jan 19-21.
- Fisher, B.E.A., 1975, The long-range transport of sulfur dioxide. *Atm.Env.* 9,: 1063.
- Friedlander, S.K. and J.H. Seinfeld, 1969, A Dynamic Model of Photochemical Smog. *Environ. Science Technol.*, 3, 1175.
- Gifford, F.A., 1957a, Relative atmospheric diffusion of smoke plumes. *J. Met.* 14:410.
- Gifford, F.A., 1957b, Further data on relative atmospheric diffusion. *J. Met.* 14:475.
- Hanna, S.R. and R.J. Paine, 1989, Hybrid Plume Dispersion Model (HPDM) Development and Evaluation. *J. Appl. Meteor.*, 28, 206-224.
- Haugen, D.A., 1959, Project Prairie Grass, a field programme in diffusion. *Geographical research paper* 59, vol III, G.R.D.A.F.C., Bedford, Mass.
- Hay, J.S., and Pasquill, F., 1957, Diffusion from a fixed source at a height of a few hundred feet in the atmosphere. *J. Fluid Mech.* 2:299.
- Hicks, B. B., 1985, Behavior of turbulent statistics in the convective boundary layer. *J. Climate Appl. Meteor.*, 24, 607–614.
- Högstrom, U., 1964, An experimental study on atmospheric diffusion. *Tellus*, 16:205.
- Holzworth, G.C., 1967, Mixing depth, wind speed and air pollution potential for selected locations in the U.S.A. *J.Appl.Met.* 6:1039.
- Hurley, P. 2005, The Air Pollution Model (TAPM) Version 3. User Manual. CSIRO Atmospheric Research Internal Paper No. 31 (available at http://www.cmar.csiro.au/eprint/open/hurley_2005e.pdf).
- Inoue, E., 1950, On the turbulent diffusion in the atmosphere. *J.Met.Soc.* Japan, 28:13.

- Isaksen, I.S.A., and Rohde, H., 1978, A two-dimensional model for the global distribution of gases and aerosol particles in the troposphere. *Rep. AC-47*, Dep. of Meteor. Univ Stockholm, Sweden.
- Izumi, Y., 1971, Kansas 1968 Field Program data report. Air Force Cambridge Research Laboratory, No. 379, AFCRL-72-0041, 79 pp.
- Johnson, W.B., 1980, Interregional exchange of air pollution: model types and applications. *10 th ITM*, 3, Amsterdam.
- Kaimal, J. C., J. C. Wyngaard, D. A. Haugen, O. R. Cote, Y. Izumi, S. J. Caughey, and C. J. Readings, 1976, Turbulence structure in the convective boundary layer. *J. Atmos. Sci.*, 33, 2152–2169.
- Lamb, R.G. and J.H. Seinfeld, 1973, Mathematical modeling of urban air pollution - General theory. *Envir. Sci. Technol.*, 7, 253-261.
- Lamb, R. G., 1982, Diffusion in the convective boundary layer. *Atmospheric Turbulence and Air Pollution Modelling*, F. T. M. Nieuwstadt and H. van Dop, editors, D. Reidel.
- Levy, H., 1971, Normal atmosphere: large radical and formaldehyde concentrations predicted. *Science*, 173:141.
- Liu, M.K. and J.H. Seinfeld, 1974, On the Validity of Grid and Trajectory Models of Urban Air Pollution, *Atmos. Environ.*, 9, 555-574.
- Lovelock, J.E., 1972, Gaia as seen through the atmosphere. *Atm. Env.* 6, 579.
- Lovelock, J.E., 1979. Gaia, a new look at life on earth. Oxford Univ. Press.
- Monin, A.S., 1955, The equation of turbulent diffusion. *Dokl. Akad. Naak.*, 105, 256.
- Monin, A.S., 1959, Smoke propagation in the surface layer of the atmosphere. *Atmospheric diffusion and air pollution*, ed. Frenkiel and Sheppard, advances in *Geophysics*, 6:331, Academic Press.
- Moore, D.J., 1967, Physical aspects of plume models. *Atm.Env.* 1:411.
- Morris, R., G. Yarwood, C. Emery, and B. Koo, 2004, Development and Application of the CAMx Regional One-Atmospheric Model to Treat Ozone, Particulate and Visibility, Air Toxics, and Mercury. Presented at the 97th Annual Meeting and Exhibition of the Air & Waste Management Association, Indianapolis, IN USA.
- New Zealand Ministry for the Environment, 2004, Good Practice Guide for Atmospheric Dispersion Modelling, Reference No. ME522, (available at <http://www.mfe.govt.nz/publications/air/atmospheric-dispersion-modelling-jun04/index.html>).
- Ogura, Y., 1959, Diffusion from a continuous source in relation to a finite observation interval. *Atmospheric diffusion and air pollution*, ed. Frenkiel and Sheppard, advances in *Geophysics* 6,149, Academic Press.
- Paine, R.J. and B.A. Egan, 1987, User's Guide to the Rough Terrain Diffusion Model (RTDM), (Rev. 3.20). NTIS # PB88-171467/REB. U.S. Environmental Protection Agency, Research Triangle Park, NC.
- Panofsky, H. A., and J. A. Dutton, 1984, *Atmospheric Turbulence: Models and Methods for Engineering Applications*. John Wiley and Sons, 417 pp.

Panofsky, H. A., H. Tennekes, D. H. Lenschow, and J. C. Wyngaard, 1977, The characteristics of turbulent velocity components in the surface layer under convective conditions. *Bound.-Layer Meteor.*, 11, 355–361.

Pasquill, F., 1962, Atmospheric diffusion. *Van Nostrand*, New York.

Pasquill, F., 1976, Atmospheric dispersion parameters in Gaussian plume modeling—Part III: Possible requirements for change in the Turner's Workbook values. U.S. Environmental Protection Agency Rep. EPA-600/4-76-030B, 53 pp.

Pasquill, F., and F. R. Smith, 1983, Atmospheric Diffusion. John Wiley and Sons, 440 pp.

Perry, S.G., D.J. Burns, L.H. Adams, R.J. Paine, M.G. Dennis, M.T. Mills, D.J. Strimaitis, R.J. Yamartino, and E.M. Insley, 1989, User's Guide to the Complex Terrain Dispersion Model Plus Algorithms for Unstable Situations (CTDMPLUS) Volume I: Model Description and User Instructions. EPA-600/8-89-041. U.S. Environmental Protection Agency, Research Triangle Park, NC (NTIS PB89-181424). (1989)

Perry, S. G., 1992, CTDMPLUS: A dispersion model for sources near complex topography. Part I: Technical formulations. *J. Appl. Meteor.*, 31, 633–645.

Perry, S.G., A. Cimorelli, J. C. Weil, A. Venkatram, R. J. Paine, R. B. Wilson, R. F. Lee, and W. D. Peters, 2005, AERMOD: A dispersion model for industrial source applications. Part II: Model performance against seventeen field-study databases. *J. Appl. Meteor.*, 44, 694–708.

Peters, L.K., and Jouvani, A.A., 1979, Numerical simulation of the transport and chemistry of CH₄ and CO in the troposphere. *Atm.Env.* 13:1443.

Record, F.A., and Cramer, H.E., 1958, Preliminary analysis of Project Prairie grass diffusion measurements. *J.Air Poll.Cont.Ass.*, 8:240.

Reynolds, S., Roth, P., and Seinfeld, J., 1973, Mathematical modeling of photochemical air pollution. *Atm.Env.*, 7.

Reynolds, O., 1895, On the dynamical theory of incompressible viscous fluids and the determination of the criterion. *Phil. Transactions of the Royal Soc. of London.* series A, 186:123.

Richardson, L.F., and Proctor, D., 1925, Diffusion over distances ranging from 3 to 86 km. *Memoirs of the R.Met. Soc.*, vol 1:1.

Roberts, O.F.T., 1923, The theoretical scattering of smoke in a turbulent atmosphere. *Proc. Roy. Soc. A*, 104, 640.

Rohde, H., 1972, A study of the sulfur budget for the atmosphere over northern Europe. *Tellus*, 24:128.

Rohde, H., 1974, Some aspects of the use of air trajectories for the computation of large scale dispersion and fallout patterns. *Adv. in Geophysics*, 18B: 95, Academic Press.

Santos, L., R. I. Sykes, P. Karamchandani, C. Seigneur, F. Lurmann, R. Arndt, and N. Kumar, 2000, Second-Order closure integrated puff (SCIPUFF) model with gas and aqueous phase chemistry and aerosols - Paper 6.8. Preprints, 11th Joint Conference on the Applications of Air Pollution Meteorology with the A&WMA, American Meteorological Society, Boston, MA.

Schulman, L. L., D. G. Strimaitis, and J. S. Scire, 2000, Development and evaluation of the PRIME plume rise and building downwash model. *J. Air Waste Manage. Assoc.*, 50, 378–390.

Scire, J.S., D.G. Strimaitis, and R.J. Yamartino, 2000, A User's Guide for the CALPUFF Dispersion Model (Version 5) available through <http://www.epa.gov/scram001>.

Shir, C.C. and L.J. Shieh, 1974, A generalized urban air pollution model and its application to the study of SO₂-distribution in the St. Louis Metropolitan area, *J. Appl. Met.* 19, 185-204.

Sklarew, R.C. et al., 1971, A particle-in-cell method for numerical solution of the atmospheric diffusion equation and application to air pollution problems; Systems, Science and Software. Ca-Reg 35R-844, Vol I.

Smith, F.B., 1957, The diffusion of smoke from a continuous elevated point source into a turbulent atmosphere. *J.Fluid Mech.*, 2:49.

Stewart, N.G. et al., 1958, The atmospheric diffusion of gases discharged from the chimney of the Harwell Pile. *Int J.Air Poll.* 1:87.

Sutton, O.G., 1932, A theory of eddy diffusion in the atmosphere. *Proc. Roy. Soc. A*, 135:143.

Sykes, R.I., S.F. Parker, D.S. Henn, C.P. Cerasoli and L.P. Santos, 1998, PC-SCIPUFF Version 1.2. PD Technical Documentation. ARAP Report No. 718. Titan Corporation, Titan Research & Technology Division, ARAP Group, Princeton, NJ.

Taylor, G.I., 1915, Eddy motion in the atmosphere. *Phil. Transactions of the Royal Soc. of London.* Series A, 215:1.

Taylor, G.I., 1921, Diffusion by continuous movements. *Proc. London Math. Soc.*, 20:196.

Thomas, M.D., et al., 1949, Dispersion of gases from tall stacks. *Ind. and En. Chemistry*, 41:2409.

Turner, D.B., 1964, A diffusion model for an urban area. *J.Appl. Met.* 3:83.

Turner, D.B., 1969, Workbook of Atmospheric Dispersion Estimates. PHS Publication No. 999 AP-26. U.S. Department of Health, Education, and Welfare, Public Health Service, Cincinnati, OH (NTIS No. PB-191482).

Turner, D. B., T. Chico, and J. Catalano, 1986, TUPOS—A multiple source Gaussian dispersion algorithm using on-site turbulence data. U.S. Environmental Protection Agency Rep. EPA/600/8-86/010, 39 pp.

U.S. Environmental Protection Agency, 1995a, User instructions. Vol. 1, User's Guide for the Industrial Source Complex (ISC3) Dispersion Models (revised), Environmental Protection Agency Rep. EPA-454/b-95-003a, 390 pp.

U. S. Environmental Protection Agency 1995b, User's guide for the Industrial Source Complex (ISC3) dispersion models. Volume II: Description of model algorithms. EPA-454/B-95-003b, 120 pp. [NTIS PB95-222758.]

U. S. Environmental Protection Agency, 2000, Meteorological Monitoring Guidance for Regulatory Modeling Applications (MMGRMA). EPA-454/R-99-005.

van Ulden, A. P., and A. A. M. Holtslag, 1985, Estimation of atmospheric boundary layer parameters for diffusion applications. *J. Climate Appl. Meteor.*, 24, 1196–1207.

Venkatram, A., 1978, Estimating the convective velocity scale for diffusion applications. *Bound.-Layer Meteor.*, 15, 447–452.

- Venkatram, A., 1980, Estimating the Monin-Obukhov length in the stable boundary layer for dispersion calculations. *Bound.-Layer Meteor.*, 19, 481–485.
- Venkatram, A. 1988, Dispersion in the stable boundary layer. *Lectures on Air Pollution Modeling*, A. Venkatram and J. C. Wyngaard, Eds., Amer. Meteor. Soc., 229–265.
- Venkatram, A., 1992, Vertical dispersion of ground-level releases in the surface boundary layer. *Atmos. Environ.*, 26A, 947–949.
- Venkatram, A., and J. C. Wyngaard, Eds., 1988, *Lectures on Air Pollution Modeling*. Amer. Meteor. Soc., 390 pp.
- Venkatram, A., D. G. Strimaitis, and D. Dicristofaro, 1984, A semiempirical model to estimate vertical dispersion of elevated releases in the stable boundary layer. *Atmos. Environ.*, 18, 923–928.
- Warneck, P., 1988, Chemistry of the natural atmosphere, *Int. Geoph. Series*, 41, Academic Press.
- Weil, J.C., 1985, Updating applied diffusion models. *J. Clim. and App. Meteor.*, 24(11), 1111–1130.
- Weil, J. C., 1985, Updating applied diffusion models. *J. Clim. and App. Meteor.*, 24, 1111–1130.
- Weil, J.C., 1988a, Dispersion in the convective boundary layer. *Lectures on Air Pollution Modeling*, A. Venkatram and J. C. Wyngaard, Eds., Amer. Meteor. Soc., 167–227.
- Weil, J.C., 1988b, Plume rise. *Lectures in Air Pollution Modeling*, A. Venkatram and J. C. Wyngaard, Eds., Amer. Meteor. Soc., 119–162.
- Weil, J. C., 1992, Updating the ISC model through AERMIC. Preprints, 85th Annual Meeting of Air and Waste Management Association, Air and Waste Management Association, Pittsburgh, PA.
- Weil, J.C., and R. P. Brower, 1984, An updated gaussian plume model for tall stacks. *J. Air Pollut. Control Assoc.*, 34, 818–827.
- Willis, G. E., and J. W. Deardorff, 1981, A laboratory study of dispersion in the middle of the convectively mixed layer. *Atmos. Environ.*, 15, 109–117.
- Willis and Deardorff, 1978, A laboratory study of dispersion from elevated source within a modeled convection mixed layer, *Atmos. Environ.* 12, 1305–1311.
- Wyngaard, J. C., 1988, Structure of the PBL. *Lectures on Air Pollution Modeling*, A. Venkatram and J. C. Wyngaard, Eds., Amer. Meteor. Soc., 9–57.
- Zimmermann, P.H., 1988, Moguntia: a handy global tracer model, *17th ITM*. 593, Cambridge.

BRANKLEY PARK

Reynolds, S. D. and R. Paine 2010. *The Tool – Mathematical Modeling*. Chapter 2 of *AIR QUALITY MODELING - Theories, Methodologies, Computational Techniques, and Available Databases and Software. Vol. IV - Advances and Updates* (P. Zannetti, Editor). Published by The EnviroComp Institute (<http://www.envirocomp.org/>) and the Air & Waste Management Association (<http://www.awma.org/>).

Chapter 2

The Tool – Mathematical Modeling

Steven D. Reynolds ^{(1),3} and Robert Paine ⁽²⁾

⁽¹⁾ *Envair*

San Rafael, California, USA

steve@sreynolds.com

⁽²⁾ *AECOM, Westford, Massachusetts, USA*

bob.paine@aecom.com

Abstract: This chapter addresses modeling background – needs and concepts - and definitions in a brief survey. Topics include uses of models (regulatory compliance and resolution of litigation), categorization of model by general type (Gaussian and grid-based), general governing equations, categories of model inputs, types of solutions of equations, alternative model formulations, spatial and temporal scales addressed and resolutions adopted, types of uncertainty of concern, experience and current and proposed approaches to evaluation of model performance, and data needs.

Key Words: Gaussian model, Lagrangian puff model, photochemical models, grid-based models, air quality modeling, simulation models, emissions modeling, dispersion modeling, chemical transformation, regulatory application, resolution, uncertainty, model performance evaluation, data needs.

1 Why Air Quality Modeling

Understanding the relationship between primary pollutant emissions and air quality, represented by the ambient concentrations of atmospheric pollutants, is essential to developing emissions control strategies. The better this understanding is achieved, the more effective will be the strategies and the greater the opportunity for minimizing control costs while maintaining an acceptably low risk of exceeding an ambient standard, such as the United States National Ambient Air

³ Philip M. Roth (deceased) and Steven Reynolds prepared the original Chapter 2 for Vol. I of this book series. This manuscript was subsequently revised to include updated information provided by Robert Paine.

Quality Standards (NAAQS). US federal ambient standards exist for 8 pollutants and pollutant groups: CO, SO₂, NO₂, ozone, fine particles, particles less than 10 microns in diameter (PM₁₀), total suspended particles (TSP) and lead. As noted in Chapter 1, many countries have adopted similar air quality standards for these pollutants, although the form and level of the standards may differ from the US NAAQS. In addition, many states in the US and countries throughout the world have adopted acceptable ambient levels for air toxics compounds. In the United States, these ambient levels are documented on state web sites that are accessible from links at www.epa.gov/scram001. In some cases, the emissions-ambient concentration (e/ac) relationship is reasonably straightforward: linear, proportional, and scalable. In others it is extremely complex: nonlinear, controlled either by a number of key chemical reactions or by mixing rates, and necessitating an understanding of a range of dynamic phenomena, such as deposition rates and emissions of biogenic species.

Air quality simulation models (AQSMs) provide a means for relating emissions and air quality. They range in form from quite simple to extremely complex. Many types have been developed during the past three decades. However, three have emerged as the main types in use: (a) the Gaussian model, for use in simulating dynamic plumes in the near field, (b) the Lagrangian puff model (a variant of the Gaussian model applied to puffs) for use in simulating single source transport and simplified chemistry over travel distances of several hundred kilometers, and (c) the grid-based photochemical AQSM, for use originally in simulating ambient ozone concentrations, and more recently for aerosols, SO₂ and its reaction products, and other reactive pollutants for a large inventory of sources over long distances. The framework of the grid-based model, omitting chemistry, can also be used to simulate nonreactive pollutant concentration fields.

The main premises in adopting models for use are that:

- They will serve as reasonably accurate estimators of air quality for any selected combinations of emissions
- The time, cost, and staffing requirements that attend their use will be commensurate with the need, and
- If the accuracy of estimates falls short, the model deficiencies will be correctable within the availability of the resources or at least understood and accounted for.

Presuming that a suitable model is available, it may see a number of uses:

- Regulatory planning and analysis, such as the preparation of federal and state implementation plans (FIPs and SIPs)
- Estimation of uncertainties through sensitivity analysis
- Planning for the conduct of field studies, and
- Identification of research and development needs

The most common and most critical use of these techniques in the United States is modeling to support FIP and SIP preparation, as well as for New Source Review.

Generally, planners attempt to ensure that recommendations for emissions controls are consistent with emissions control requirements formulated through modeling that demonstrates compliance with ambient air quality standards. Consequently, participants in the planning process have an interest in models being as accurate as possible. Oftentimes, then, their focus is on improving simulation accuracy, evaluating model performance, conducting sensitivity studies and uncertainty analyses, and simulating alternative emissions control scenarios. If these steps can be conducted with satisfaction, the planner's job is greatly facilitated.

In June 2010, the United States Environmental Protection Agency established⁴ a new 1-hour SO₂ NAAQS. Part of the implementation of this new standard involves a departure from past practice: dispersion models are to be used to determine compliance with the standard in place of monitors in most cases. This places more importance on the accuracy of models to simulate realistic concentrations, and this issue is discussed at more length later in this chapter.

2 Modeling Categorized

2.1 Applications of Models

Air quality simulation models are employed in a wide variety of applications, most of which are associated with local, state or federal regulatory requirements in the United States and many other countries.

2.1.1 Dispersion Modeling

The principal focus of dispersion modeling, especially for nonreactive pollutants, is estimation of ambient concentrations of primary pollutants that have been dispersed in the atmosphere through turbulent diffusion. Strictly speaking, this modeling category applies to pollutants that do not undergo atmospheric chemical transformation. However, it also applies for pollutants for which simple assumptions are incorporated to mirror mass depletion due to chemical transformation, such as linear decay terms, as well as deposition.

Models in use for modeling nonreactive pollutants include:

- The Gaussian formula in one of its many manifestations. This formula represents the first of the commonly used models, and is applied primarily to plumes, both individual and multiple. If circumstances permit, it may also be applied to groups or aggregations of sources. Also, the Gaussian formula can be written in a form to simulate the dispersion of individual puffs, instead of plumes. In the United States, AERMOD (Cimorelli et al., 2005) is an example of a model in wide use for these types of applications.

⁴ <http://www.epa.gov/ttnnaqs/standards/so2/ft/20100622.pdf>

CALPUFF (Scire et al., 2000) is a Lagrangian puff model using Gaussian puff formulations that is used for long-range transport modeling of single sources as well as short-range modeling of complex flows.

- The approximate solution of the governing equation of mass conservation, which includes a simplifying assumption that relates turbulent fluxes, $\langle u'c' \rangle$, to concentration gradients, $\partial c / \partial x_i$, through the adoption of an eddy diffusivity, K_i ,

$$\langle u'c' \rangle = -K_i \left(\partial c / \partial x_i \right) \quad (1)$$

This equation is commonly applied for more widely or uniformly distributed pollutants such as carbon monoxide (CO), where large individual plumes are not dominant.

- An approximate solution of the governing equations of mass conservation in a coordinate system that moves with the average wind velocity – the so-called “trajectory model”. The solutions in the fixed and moving coordinate systems are related. They differ in that certain assumptions are made for the trajectory model that do not apply for the “gridded model”, notably neglect of horizontal wind shear, horizontal turbulent diffusion, and vertical advective transport (Liu and Seinfeld, 1974). Also, acceptance of the trajectory model implies that parcel integrity is reasonably maintained for the length of time of the model simulation. However, some advanced trajectory models such as HYSPLIT (Air Resources Laboratory, 2009) include dispersion modules to mitigate the limitations of a trajectory model.
- The solution of the governing equation of mass – usually in parallel with the governing equation of momentum – using more rigorous and complex procedures, and thus avoiding the application of K-theory. Such models tend to be research models, in development, computing-intensive, and one-of-a-kind. They are not in common use.

2.1.2 Modeling of Chemical Transformations⁵

By far, the most common approach for modeling complex chemical transformations is through use of coupled mass balance equations incorporating K-theory, one for each pollutant that is being modeled. In the United States, CMAQ (Byun and Ching, 1999) and CAMx (Morris et al., 2004) are commonly used for these applications. Virtually all models now in use for estimating tropospheric ozone concentrations and the concentrations of secondary fine particles are based on these equations, with differences among models being in the submodels or modules for one or more dynamic processes, such as transport,

⁵ See also: Pun, B.K. et al. 2005. Atmospheric Transformations. Chapter 12 of AIR QUALITY MODELING – Theories, Methodologies, Computational Techniques, and Available Databases and Software. Vol. II – Advanced Topics (P. Zannetti, Editor). Published by The EnviroComp Institute (<http://www.envirocomp.org/>) and the Air & Waste Management Association (<http://www.awma.org/>).

chemistry, and deposition, and in the numerical integration procedure. These models are used for SIP and FIP preparation, regional planning, and other regulatory applications.

Trajectory models are also used in special applications. However, each assumption noted earlier still must be considered; in most situations encountered they will not all apply.

2.1.3 Modeling of Pollutant Deposition⁶

Generally, the same family of models, based on the governing equation of mass conservation, is used to estimate deposition fluxes as a function of location, and integrated over time, the accumulation of deposited material. Use of the “non-reactive” form of the model, incorporating simplifying assumptions, allows for calculation over longer simulated times at reasonable computational times. Deposition calculations, less common than the calculation of ambient concentrations, are of interest for estimation of:

- Acidic deposition and acid loadings over a seasonal period
- Ecosystem impacts of air pollutants, such as deposition of nitrogen compounds onto sensitive watersheds, and
- Contributions to accumulation of pollutants in lakes and subsequent eutrophication

The sub-models or modules that address deposition can vary greatly in formulation, rigor, and level of detail. In the past, several of the simulation models in use incorporated rather primitive treatments of deposition. More recently, improved algorithms have been developed and included in models. Nevertheless, considerable uncertainty attends deposition estimates due to the lack of evaluation databases and uncertainty in the specification of some of the model input parameters.

2.1.4 Modeling of Adverse Impacts

The objective of modeling “impacts”, in contrast to ambient concentrations, is to examine more directly certain selected effects. An example mentioned earlier is the estimation of acidic fluxes. Health effects of pollution are, of course, a major issue as far as adverse impacts are concerned.

Visibility degradation also falls under the heading of “impacts”, as does ecosystem loading. In the United States, use of a Lagrangian puff model such as CALPUFF for modeling the long-range effects of individual sources with

⁶ See also: San José, R. et al. 2005. Deposition Phenomena. Chapter 13 of AIR QUALITY MODELING - Theories, Methodologies, Computational Techniques, and Available Databases and Software. Vol. II – Advanced Topics (P. Zannetti, Editor). Published by The EnviroComp Institute (<http://www.envirocomp.org/>) and the Air & Waste Management Association (<http://www.awma.org/>).

simplified chemistry serves as the most common approach for such analyses, incorporating those modifications or additions needed to address the specific effect. For example, in the case of visibility degradation (an adverse effect of pollution, in the sense that visibility impairment does not allow a full enjoyment of vistas, especially in high sensitive areas, such as National Parks), a post-calculation algorithm is included to convert estimated concentrations into a measure of visibility impairment. This general category of modeling is experiencing increasing use because the range of issues now being examined in the regulatory arena is broadening.

Note that for all modeling applications, spatial extent is a key attribute. Early applications tended to be limited to urban or metropolitan scale. Today, regional scale is of primary concern because of the recognition that pollutant problems are not confined to a local area, but can extend for many hundreds of miles and include a number of emissions centers. Modeling outlined here applies in principle at local to regional – and in some cases – subcontinental scales. Fortunately, substantial advances in computing power and efficient algorithms for numerical computation and display of modeling results have facilitated the expansion of the scope of what is possible for regional modeling.

2.2 Estimating Inputs to Air Quality Simulation Models

Three major categories of information are required to formulate inputs to models: air quality, emissions, and meteorology. Consequently, it is appropriate to think in terms of *a modeling system*, as depicted in Figure 1 and not only an air quality model. Emissions and meteorological information, as well as boundary and initial conditions, must be supplied to the air quality model, as shown by the flows in the figure. The output concentrations are often used as input to specialized post-processors that provide graphical displays, source culpability analyses, computation of visibility impacts (as mentioned above), etc.

Boundary and initial conditions are needed to drive models based on conservation of mass. Boundary conditions are generally difficult to estimate, data are sparse, and often no independent means of estimation exists. The two primary approaches to estimation include acquisition of data at the inflow boundaries, both upwind and overhead, and estimation using a model of much broader spatial scale but coarser spatial resolution.

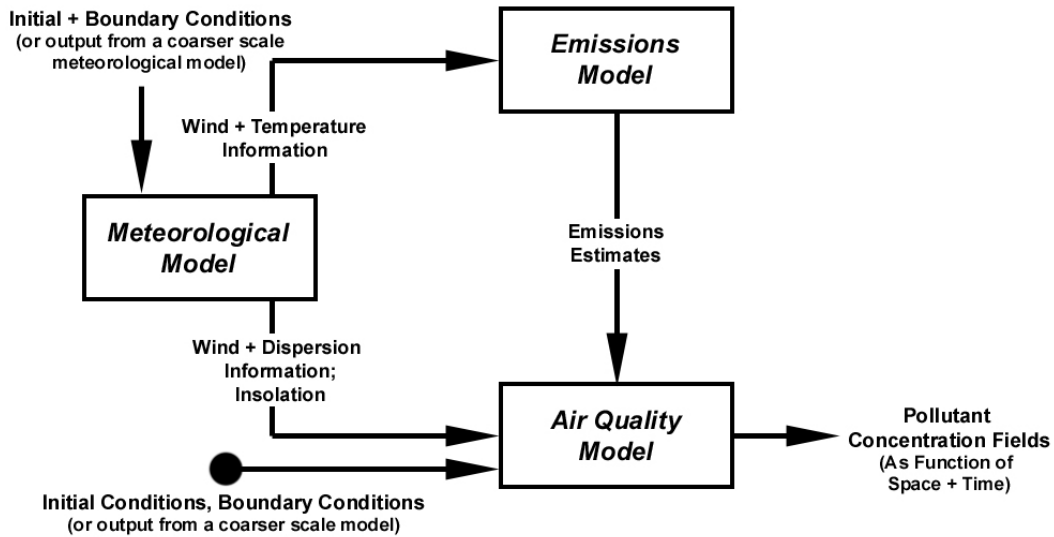


Figure 1. The Air Quality Modeling System.

Emissions are estimated using a wide array of options, from hand-counts and bookkeeping to sophisticated modeling. Where possible, computer-based emissions models and management of emissions data are used – to insure uniformity of procedure, reduce error rates, greatly enhance data handling, and increase the rate at which estimation is conducted. Even for a given geographical application, a wide range of approaches to emissions estimation – for the different emissions categories – might be adopted.

In the early stages of air quality modeling, simple approaches to estimation of meteorological variables were prevalent – from hand-prepared wind maps to the use of straightforward diagnostic models, the latter including parameterized treatments of key variables. These models were generally limited to the consideration of meteorological data at a single station, which is most commonly the case for Gaussian models. More recently, prognostic models have been widely accepted for use. These models are based on solving the equations of conservation of mass, energy, and momentum and produce as output 3-dimensional gridded meteorological fields for each hour (or even for sub-hour periods). They have proven to be quite helpful and an excellent complement to the use of air quality models based on the equations of mass conservation.

2.3 Categories of Air Quality Models Primarily in Use

The primary models (and modeling systems) in use today are those based on the numerical integration of the equations of conservation of mass and those based on the Gaussian formula, the latter for a range of source configurations and extensions of the basic equation.

2.3.1 Numerical Solution of the Equations of Conservation of Mass

The governing equations of conservation of mass are given by:

$$\frac{\partial c_i}{\partial t} + u_x \frac{\partial c_i}{\partial x} + u_y \frac{\partial c_i}{\partial y} + u_z \frac{\partial c_i}{\partial z} = \frac{\partial}{\partial x} \left(K_x \frac{\partial c_i}{\partial x} \right) + \frac{\partial}{\partial y} \left(K_y \frac{\partial c_i}{\partial y} \right) + \frac{\partial}{\partial z} \left(K_z \frac{\partial c_i}{\partial z} \right) + R_i(c_1, c_2, \dots, c_n) + E_i(x, y, z, t) - S_i(x, y, z, t) \quad (2)$$

where: u_x, u_y, u_z = velocity
 c_i = concentration of i^{th} species
 R_i = chemical generation rate of species i
 E_i = emissions flux
 S_i = removal flux

Emissions, meteorological, and air quality fields are provided as inputs, and the equations are integrated forward numerically in time to produce pollutant concentration fields.

Note that in special circumstances the simpler trajectory solution may apply. However, even advanced trajectory models such as HYSPLIT are not currently accepted for general use for regulatory applications in the USA without a project-specific demonstration. However, these models are useful for computing trajectories, especially with links to archived or predicted databases of gridded meteorological data such as those available to HYSPLIT.

2.3.2 Gaussian Models

The basic Gaussian equation,

$$c(x, y, z) = \frac{q}{2\pi \bar{u} \sigma_y \sigma_z} \exp\left(-\frac{y^2}{2\sigma_y^2}\right) \cdot \left[\exp\left(-\frac{(z-h)^2}{2\sigma_z^2}\right) + \exp\left(-\frac{(z+h)^2}{2\sigma_z^2}\right) \right] \quad (3)$$

where: q = source strength
 h = stack height
 σ_y, σ_z = lateral and vertical dispersion coefficients

is a solution to the equation of mass conservation where conditions are steady state ($\partial c / \partial t = 0$), velocity \bar{u} is constant, and diffusion in the x-direction can be neglected. [See Seinfeld and Pandis, 1998, section 18-1 to 18-2, for a full derivation.] Many variants of the Gaussian plume and puff formulas exist; formulas for individual sources are summarized in Seinfeld and Pandis, section

18-3. AERMOD introduces a skewed distribution to the vertical dispersion in convective conditions, for example. These models also have specialized approaches for dealing with source effects such as building downwash (the PRIME model, Schulman et al., 2000). CALPUFF is a widely used Lagrangian puff model that has adapted the Gaussian model to a puff-tracking approach.

These two approaches to modeling dominate applications today and have done so for the past two decades. Consequently, these formulations and supporting emissions and meteorological modeling will receive the preponderance of attention in this book.

3 Modeling the Atmosphere

3.1 Deterministic Modeling and Stochastic Processes

The atmosphere is stochastic; transport and dispersion exhibit random behavior. Thus, for a given set of parameters – temperature profiles, average wind velocity, solar radiation, and surface roughness – different manifestations might occur in the atmosphere, purely dependent on random events. In addition, Gaussian models rely upon single-station input data for modeling of plume impacts over a large area that is often heterogeneous. Consequently, model outputs should, in principle, be expressed as distributions that display the random character of the variables of interest. In fact, most models in use are deterministic; they display the average behavior of the spectrum of random outcomes that might occur. A few, such as SCIPUFF (Santos et al., 2000) provide estimates of the concentration uncertainty in addition to the expected mean concentration value. In general, those using models or their results should be aware of this aspect of their formulation.

3.2 Modeling Representative Conditions vs. A Long-Term Time Record

Typically, modeling is conducted for average conditions or for a limited period of time, sometimes termed “an episode”. A great deal can be learned from such an exercise, and the results themselves are generally useful. However, atmospheric and man-made conditions, such as wind fields and traffic intensity, vary, and can vary in many ways and combinations.

Modeling longer periods of time provides a means for examining a range of outcomes, but does so at additional cost, use of staff time, and level of detail. In the past modeling was largely confined to shorter intervals – from one day to a few days. More recently, especially with advances in computational power, parallel processing, and numerical algorithm efficiencies; investigators have demonstrated the use of models – even the more complex models - for one or more annual periods. With attention being given to longer averaging periods in

the formulation of new ambient air quality standards, the application of models for longer periods is critical.

3.3 Using Models Instead of Monitors to Demonstrate Compliance with Ambient Standards

Ambient monitoring data has been the traditional, long-established benchmark used by the USEPA to determine compliance with the NAAQS and dispersion modeling has been used primarily to evaluate the impact of proposed sources. However, the USEPA has concerns with relying only upon monitoring data to evaluate current air quality in terms of compliance with the 1-hour SO₂ NAAQS, and instead favors the use of dispersion modeling. The following reasons are identified in their final rule⁷ that establishes the 1-hour SO₂ NAAQS:

- It would take considerable time to design and implement new monitoring networks.
- Ambient monitoring is resource-intensive, and even with many more monitors; the coverage around each major SO₂ source may not be adequate to determine the peak impacts.
- A reliance upon modeling rather than monitoring is a “technically appropriate, efficient, and readily available method for assessing short-term ambient SO₂ concentrations in areas with large point sources.”
- Due to the generally localized impacts of SO₂, USEPA has not historically considered monitoring alone to be an adequate, nor the most appropriate, tool to identify all maximum concentrations of SO₂. In the case of SO₂, USEPA further believes that monitoring is not the most cost-efficient method for identifying all areas of maximum concentrations.

The use of modeling in past compliance assessments has been very limited. Modeling practices such as those described in USEPA’s guidance for modeling the peak emissions for all hours and using peak regional background concentrations are mostly suited to future sources, rather than existing sources. These modeling procedures could lead to large overestimates in the actual concentrations, which are what monitors would provide. The use of modeling rather than monitoring should focus upon the “gold standard” of matching the actual concentrations that a monitor would measure at each model receptor point. This means modeling realistic source and background conditions.

Although refined models such as AERMOD have shown good performance for predicting short-term concentrations, this performance is subject to the following best practices if monitored compliance is replaced with modeled compliance:

- Actual hourly emissions concurrent with meteorological data used in the modeling analysis should be used. Use of peak emission rates for all hours of the analysis will likely result in indications of false violations of the NAAQS.

⁷ <http://www.epa.gov/ttnnaqs/standards/so2/fr/20100622.pdf>

- Actual stack heights should be used as input to the models.
- Modeling of background sources should follow the same approach – use of actual hourly emissions should be used.
- Inclusion of regional monitoring concentrations should be done on an hourly basis concurrent with the hourly emissions for sources being modeled and the hourly meteorology used in the modeling. Use of multiple monitors with the highest value for each hour not included in the hourly average is one approach to prevent double counting of modeled and monitored concentrations.

4 Modeling Alternatives

While grid models and Gaussian models provide a means for simulating a broad range of atmospheric processes, alternative modeling approaches may prove as or more useful in supporting particular avenues of research and analysis. For example, box models play a central role in air chemistry research studies. Receptor models provide direct *emissions-air quality* relationships using basic source information and measured ambient pollutant concentrations. In recognition of the stochastic character of the atmosphere, limited efforts have been devoted to developing suitable statistical models. Although each of these approaches has a limited range of applicability, they provide insight into certain aspects of air pollution phenomena and in some cases may serve to corroborate or place in question the results obtained from comprehensive simulation models.

4.1 Box Models

A box model is a mathematical representation of pollutant dynamics that take place in a well-mixed volume of air. In general, these models provide very limited representations of atmospheric transport phenomena. However, they are well suited to supporting atmospheric chemistry research studies. For example, a smog chamber is a stirred vessel that employs natural light or ultraviolet lamps to study the chemical transformations of precursors in forming ozone and other photochemical reaction products under controlled laboratory conditions. Fresh precursors may be added to the chamber to simulate basic characteristics of actual diurnal emissions patterns that occur in urban or rural areas. Since chamber-specific wall effects may be important, they need to be characterized and simulated in the box model. Typically, the governing equations of a box model are a set of coupled, nonlinear, stiff ordinary differential equations derived from a chemical kinetics mechanism that are solved using suitable numerical solution procedures.

4.2 Receptor Models⁸

Receptor models are based on statistical analyses of ambient pollutant measurements and pertinent emissions information. They are of particular value in situations where detailed knowledge of actual emissions rates is subject to significant uncertainties. For example, receptor models provide an important means for apportioning measured values of certain types of primary particulates. Establishing such relationships using a source-oriented model is much more problematic given the large uncertainties in emissions estimates for fugitive sources of particulates.

Receptor models can be grouped into three major categories (Seigneur, 2001): (1) models that apportion primary PM using source information, (2) models that apportion primary PM without using source information, and (3) models that apportion primary and secondary PM. In each of these categories, there exist some well-established techniques as well as some recent emerging techniques. For example, the chemical mass balance approach has been applied to PM₁₀ problems throughout the western U.S. with generally good success (PM₁₀ is defined as particulate matter – PM – made of particles less than 10 μm in diameter). New methods of factor analysis can also be employed in areas where source profiles are not available. The reliability of receptor models for PM_{2.5} is quite different since the majority of the fine particle mass is due to secondary particle formation (PM_{2.5} is defined as particulate matter – PM – made of particles less than 2.5 μm in diameter). The ability of these models to provide quantitative apportionment of the measured aerosol mass to the pertinent sources is more uncertain. In regulatory applications, a key issue is the ability of these models to adequately represent source-receptor relationships associated with nonlinear chemical reaction phenomena that lead to secondary fine particle formation.

4.3 Statistical Models⁹

Statistical models provide estimates of concentration levels as a function of some combination of space, time, meteorological, emissions and other pertinent variables. These relationships are derived using various regressions, statistical and analysis techniques. Since these relationships are derived from available measurements, their range of applicability is limited to the conditions under which the data were collected. Nonlinear relationships between reactive precursors and

⁸ See also: Watson, J.G. and J.C. Chow 2005. *Receptor Models*. Chapter 16B of *AIR QUALITY MODELING - Theories, Methodologies, Computational Techniques, and Available Databases and Software. Vol. II – Advanced Topics* (P. Zannetti, Editor). Published by The EnviroComp Institute (<http://www.envirocomp.org/>) and the Air & Waste Management Association (<http://www.awma.org/>).

⁹ See also: Finzi, G. and G. Nunnari 2005. *Air Quality Forecast and Alarm Systems*. Chapter 16A of *AIR QUALITY MODELING - Theories, Methodologies, Computational Techniques, and Available Databases and Software. Vol. II – Advanced Topics* (P. Zannetti, Editor). Published by The EnviroComp Institute (<http://www.envirocomp.org/>) and the Air & Waste Management Association (<http://www.awma.org/>).

secondary pollutants are particularly difficult to accurately represent in such models. To date, limited effort is being devoted to the development of statistical models largely because of their constrained range of applicability, the lack of physical characterizations in the model, and, often, a limited database. Models using “fuzzy logic” that depend upon a study of past events are sometimes used in ozone forecasting (see, for example, Sen et al., 2009).

4.4 Lagrangian Particle Models¹⁰

Lagrangian particle models – often referred to as Monte Carlo models – simulate atmospheric diffusion by tracking the movement of thousands of fictitious particles representing air pollution. Particles move according to average wind and turbulence parameters and include semi-random pseudo-velocities calculated using a computer-based random-number generator. These models apply well for unreactive pollutants, but revert to a gridded formulation for reactive systems, with various imposed limitations. Their use is becoming more common, particularly for unreactive species, though regulatory applications are still rare.

4.5 Other Specialized Models

Other modeling approaches are used for specialized applications. One of these is a set of dispersion models for heavy gas releases, as described in Chapter 1. Other such specialized models include computational fluid dynamics models and wind tunnel models. These two types of models are used to simulate complex flows, often around complicated structures for situations that are not well accommodated by larger-scale routine models.

5 Spatial and Temporal Scales

Models are typically applied to study impacts of individual sources, multiple-source industrial facilities, metropolitan areas, or larger regional areas up to subcontinental scale. The spatial scales of concern can range from up to a few tens of kilometers for large industrial point sources, to a few hundred kilometers for individual urban areas, to a few thousand kilometers for larger regional areas comprised of several metropolitan areas. When applying models to regional-scale domains, consideration must be given to the spatial scale of important atmospheric phenomena that ultimately contributes to regional air quality problems. Nested grid capabilities, an important feature of contemporary regional models, allow them to resolve important phenomena and concentration gradients in areas of the domain where significant sources are present.

¹⁰ See also: Anfossi, D. and W. Physick 2005. Lagrangian Particle Models. Chapter 11 of AIR QUALITY MODELING – Theories, Methodologies, Computational Techniques, and Available Databases and Software. Vol. II – Advanced Topics (P. Zannetti, Editor). Published by The EnviroComp Institute (<http://www.envirocomp.org/>) and the Air & Waste Management Association (<http://www.awma.org/>).

The time scales of concern are related to ambient air quality standards, which have averaging times ranging from one hour to one year. In Gaussian model regulatory applications in the US, simulations using up to five years of meteorological data may be carried out to develop estimates of peak concentrations with averaging times ranging from one hour to one year. In photochemical model regulatory applications in the US, simulations of annual periods have become more common with computational and numerical algorithm advances.

Models are formulated to represent key phenomena on the spatial and temporal scales of interest. For example, localized urban models typically do not provide sufficient treatment of upper air dynamics and, therefore, are generally not applicable to regions of the order of several hundreds of kilometers where vertical transport in the free troposphere, up to several kilometers above ground, may be important. Air quality models that include a detailed treatment of chemistry may be limited in their applications sub-annual periods because of the computational costs associated with the numerical integration of the chemical kinetic equations. Models that use a simplified treatment of atmospheric chemistry can be applied to longer time periods (e.g., one year or more) without prohibitive computational costs. The ability to simulate long time periods is generally obtained at the expense of some accuracy (since the treatment of chemistry is less accurate in long-term models). Another approach for estimating annual-average concentrations is to apply an episodic model for several typical meteorological scenarios and to reconstruct a full year by combining these scenarios with appropriate weighting factors. This approach involves making approximations with the representativeness of the meteorology, whereas the use of a long-term model involves making approximations with the chemistry.

6 Spatial and Temporal Resolution

Short-term Gaussian plume models are typically applied using hourly meteorological data spanning a period of up to five years. However, recent versions of CALPUFF have allowed the input of sub-hourly meteorological and emissions data to characterize better temporal resolution for these input parameters. However, most models provide hourly concentration estimates at any user-specified point downwind of the source. However, because these models are based on steady-state assumptions, they cannot truly resolve concentration fluctuations and their applicability is effectively limited to a 1-hour travel distance.

Grid-based models provide concentration estimates that are spatially averaged over the volume of a grid cell, whose size may range from 1 to 40 km or more in the horizontal directions and from ten meters to several hundred meters in the vertical direction. Contemporary grid models employ nested grids with relatively fine spatial resolution in dense and/or heterogeneous source areas (such as cities

where significant spatial gradients may exist in the concentration field) and relatively coarse resolution in rural areas (where spatial gradients are much smaller). Use of nested grids is largely motivated by a desire to optimize the computational time required to perform a simulation.

The ability to provide variable vertical resolution can also be important. In general, relatively fine vertical resolution is used near the ground where large vertical gradients in the concentration field are likely to occur because of the near proximity of most sources. Concentration gradients aloft are often much smaller, allowing the use of coarser vertical grid resolution. In establishing the vertical grid structure, careful consideration must be given to the spatial features of elevated stable layers aloft and the possible need to adequately resolve elevated plumes from large point sources. If such plumes are not adequately resolved, they may be subject to significant averaging errors. In addition, the timing and location of plume fumigation to the ground may be in error. For nitrogen oxides (NO_x) plumes, this can have a significant effect on VOC/ NO_x in the areas where plume fumigation is predicted to occur (or not occur) and can also have a profound influence on the relative effectiveness of VOC versus NO_x controls on ozone formation in such areas. (VOC stands for volatile organic compounds, for example, reactive, non-methane hydrocarbons)

7 Uncertainty: Bias, Imprecision, and Variability

Uncertainty attends all elements of the modeling enterprise: accuracy and precision of the supporting and test data bases, the model-generated emissions and meteorological fields, initial and boundary conditions, and at the end of the sequence, air quality modeling and the results of interest. Variability also accompanies meteorological and biogenic emissions variables (natural variability) and activities that derive from human behavior, such as traffic loading (man-derived variability). As should be apparent, the contributions of uncertainty to modeling results are broadly-based, and the results of modeling are quite susceptible to errors. Modelers, of course, attempt to reduce error levels as effectively as possible, but uncertainties will persist, as many sources of uncertainty are outside the modeler's range of influence. Notable among these are errors in inputs, particularly emissions-related, and variability of all types. Model outputs may range widely in their sensitivity to uncertainties. Where they are insensitive, errors or variability may be of only casual concern; where sensitivity is high, errors particularly may be a major issue. See Morgan and Henrion (1990) and Hanna (1993) for detailed introduction to and treatment of uncertainty in air quality modeling.

Typically, little attempt is made to estimate quantitatively the bias or error in model output. While it may be important to know model bias and error, and it may be of particular interest to the decision-maker, it may be quite difficult or

impossible to calculate. In these circumstances, modelers sometimes use “best judgment” to estimate errors; however, this cannot be expected to be reliable.

An example of how the uncertainty of several input model variables can be evaluated at once is illustrated by Irwin and Hanna (2005). In this study, a Monte Carlo (MC) probabilistic uncertainty analysis was applied to releases from 26 field study experiments. In the MC probabilistic uncertainty procedure, the modeling system was run to simulate 100 years of hourly concentrations that were altered for random choices of variations in the input parameters. The resulting geometric standard deviations in the reported predicted concentrations were then analyzed.

As noted by Irwin and Hanna, the Gaussian dispersion model provides a smoothed view of reality. Irwin and Lee (1996) analyzed the Prairie Grass data, as well as additional tracer data from the Kincaid power plant, which had a 183-m stack with a typical buoyant plume rise on the order of 200 m. They concluded that the scatter in the concentration values about the ensemble average Gaussian lateral profile could be characterized for both experimental data sets as having a log-normal distribution with a geometric standard deviation on the order of 2.

The SCIPUFF model (Santos et al., 2000) explicitly solves for the fluctuations in concentration internal to the plume. Typically, the relative fluctuation (standard deviation divided by the mean) is simulated to be about 2 on the plume centerline, and is larger towards the edges of the plume.

In the absence of such studies, sensitivities of the model results to uncertainties in the model inputs are often estimated. They generally provide information on the response of the output to uncertainties in inputs, under the assumption that the model is basically correctly formulated and the inputs are sound. If there is error in the model or inputs, the results of sensitivity analyses may be derivatively tainted.

Efforts are being made to introduce more sophisticated approaches to uncertainty analysis into modeling. For example, Yang, Wilkinson, and Russell (1997) have developed techniques for facilitating the conduct of sensitivity analysis through use of the direct decoupled method. However, if there is an unknown error in the model or inputs, no sensitivity analysis will properly address its presence. Rather, an attempt must be made to detect its presence, determine the cause or causes and the importance of the error (if feasible) and, as appropriate, correct, mitigate, or eliminate the problem and repeat the modeling and sensitivity analysis.

8 Evaluation of Model Performance¹¹

Model performance evaluation (MPE) is the process of testing a model's ability to estimate accurately observed measures of air quality over a range of meteorological, emissions, and air quality conditions. When conducted thoughtfully and thoroughly, the process focuses and directs the continuing cycle of model development, data collection, model testing, diagnostic analysis, refinement, and retesting. Far too often in the past this process has been foreshortened in order to "validate" the model with readily available data so that its use in regulatory decision-making could be justified. Obviously, serious inquiry into the model's adequacy or reliability is difficult if not impossible in such a situation.

The performance of Gaussian models has been the subject of numerous studies. Typically, an inert tracer gas is released from a source and measured at various downwind locations. Assessments of model performance rely on comparisons of calculated and measured concentration levels. Routine application of these models in a regulatory setting generally does not involve any performance evaluation due to the time and expense involved, and because approved models are considered by reviewing agencies to be generally applicable (although this is typically considered on a case-by-case basis). At best, the models are applied using site-specific meteorological data.

In contrast, there is a long history of MPE for photochemical models involving the comparison of observed and estimated concentrations of ozone and, to a lesser extent, other pollutant species. The principal comparisons included temporal comparisons of differences between observation and estimation for individual monitoring sites, spatial comparisons of differences, as shown through deficit-enhancement maps, and a range of statistics, including regional and subregional average bias, gross error, and differences in area-wide maximum ozone concentrations, independent of time and location.

The focus of all these types of comparisons has been on ozone. Although NO_x and VOC comparisons have been carried out for some time, no requirement or informal rule was ever developed stipulating that NO_x or VOC estimates correspond at any prescribed level. Furthermore, no standard practice for judging model performance has evolved. Traditionally, the EPA guideline model (Urban Airshed Model) (EPA, 1990) was accepted for use in control strategy assessment when average discrepancies (e.g., gross errors) for ozone were of the order of 35% or less, and inaccuracy or bias is "not large" (i.e., ± 5 -15% according to EPA's definition) (EPA, 1991). Often, however, it was determined that models

¹¹ See also: Canepa, E. and J. Irwin 2005. Evaluation of Air Pollution Models. Chapter 17 of AIR QUALITY MODELING - Theories, Methodologies, Computational Techniques, and Available Databases and Software. Vol. II – Advanced Topics (P. Zannetti, Editor). Published by The EnviroComp Institute (<http://www.envirocomp.org/>) and the Air & Waste Management Association (<http://www.awma.org/>).

passing these arbitrary performance criteria contained significant flaws, commonly in the form of internal, compensating errors that compromised the overall reliability of the entire modeling demonstration. To accommodate inevitable modeling errors, photochemical models are often used to determine the *relative change* in the levels of ozone or fine particulate matter rather than the absolute value. For example, in order to determine the effect of emission controls, photochemical models will be run for the controlled (future) and uncontrolled (current) cases, and the ratio of the results are applied to the current ozone concentrations to estimate the future concentrations. The United States EPA has provided guidance for conducting regional and photochemical modeling simulations in a 2007 guidance document, “Guidance on the Use of Models and Other Analyses for Demonstrating Attainment of Air Quality Goals for Ozone, PM_{2.5}, and Regional Haze”.

While in many scientific disciplines "hands-off" testing of models is required, a different tradition evolved in the evaluation of grid-based photochemical models. The improvement of model performance is an integral part of MPE. In cases in which differences between observations and estimates are unacceptably large, the modeler is expected (allowed) to carry out a diagnostic analysis, identify the potential causes of the discrepancies, suggest and make changes in model formulation or processing of input data, and repeat model testing. Thus, evaluation and improvement make up an iterative sequence and, in fact, they are inextricably coupled. Evolving from this philosophy is the common practice of undertaking model performance improvement activities with each modeling episode separately.

A key limitation in MPE to date has been the generally inadequate level of stressfulness to which models have been subjected in testing. Three main outcomes of testing are possible: A model performs inadequately and is so judged, a model performs well and is so judged, or a model appears to perform adequately but is, in fact, significantly flawed. To ensure during testing that a model reveals its flaw(s), it must be adequately "stressed," that is, subjected to testing that is designed to reveal and even highlight or amplify inherent inadequacies.

Because testing has not been properly implemented, flawed models containing compensatory errors internally have been historically accepted for use. A notable instance is the long-standing use of underestimates of VOC emissions as input to the Urban Airshed Model (UAM), previously used in the United States for photochemical modeling. Modelers had either directly or inadvertently compensated for these underestimates by introducing offsetting bias into the model. In one instance, modelers compensated for suspected underestimation of the emissions inventory by artificially elevating the boundary conditions (on the top and sides). In another study, a "lid" was placed on the vertical velocity in the UAM to prevent or reduce the loss of surface ozone to layers aloft and thus improve model performance. In a third case, meteorological inputs were

"beneficially altered" to advect the high ozone cloud directly toward the peak ozone monitoring station. These types of input modifications no doubt changed the source-receptor emissions characteristics of the air basins and had unknown effects on the reliability of the emissions control strategies. In these and other situations, the changes were asserted to be "within the range of experimental or scientific uncertainty."

Several scientists, motivated by a number of objectives, have proffered recommendations for improvements to the MPE process. They include improving the process, adequately stressing models, improving the quality of available databases, standardizing the practice, and demystifying the practice through clearer communication. Indeed, guidelines have been developed (Reynolds, Roth, and Tesche, 1994; ASTM, 2000; Chang and Hanna, 2004) for providing a sound context for performance evaluation, establishing a common understanding of the process, and ensuring that evaluation efforts are properly formulated and reasonably complete. Elements of such a comprehensive and satisfactory model evaluation process include:

- (a) Evaluating the scientific formulation of the model through a thorough review process
- (b) Assessing the fidelity of the computer code to the scientific formulation, governing equations, and numerical solution process
- (c) Evaluating the predictive performance of individual process modules and preprocessor models (e.g., emissions and meteorological)
- (d) Evaluating the predictive performance of the full model
- (e) Conducting sensitivity analyses
- (f) Carrying out corroborative analyses
- (g) Carrying out comparative modeling, and
- (h) Implementing a quality assurance activity.

All of these activities should be carried out in accordance with the procedures prescribed in an application-specific MPE protocol.

Obviously, the effort suggested above is considerably greater than that customarily devoted to MPE. However, air quality models are being viewed as essential tools in the development of emissions control plans. The costs of controls are sufficiently high that society will wish assurance that imposed controls would be effective in reducing air pollution levels. It is thus vital that the overall planning process includes sufficient time and resources for conducting thorough evaluations of model performance. In addition, there is likely to be a significantly increased demand for the collection of suitable emissions, meteorological, and air quality data to support MPE. The comprehensive evaluation of model performance should be considered essential to the overall air quality management program for an area.

9 Data Needs

AQSMs require various types of emissions, meteorological, air quality, and geophysical data. Model inputs may be assembled directly from suitable data sources or may be generated through use of other preprocessor models (e.g., emissions or prognostic meteorological modeling systems). The availability of appropriate data to derive model inputs, to evaluate model performance, and to diagnose and rectify model performance problems is crucial to the successful application of an air quality model.

9.1 Gaussian Models

Gaussian models are typically applied using one to five years of on-site surface meteorological data, including wind speed and direction, temperature, relative humidity, standard deviation of the horizontal wind direction, and rainfall. Upper air meteorological data are employed to estimate hourly mixing height estimates. Some models require estimates of other boundary layer parameters. Geophysical data include estimates of terrain height at source and receptor locations as well as land use. Tracer release experiments with suitable downwind measurements might be carried out to provide a database for evaluating model performance, although this is typically not carried out in routine applications of Gaussian models.

Lagrangian puff models require more extensive input data such as three-dimensional meteorological fields with accompanying two-dimensional databases for land use and terrain.

9.2 Photochemical Grid Models

Photochemical grid models are mostly used for ozone simulations and require several data sets for input preparation and model evaluation: air quality, meteorological, emissions, and geophysical. Such models require a complete specification of the spatial and temporal variations of key atmospheric phenomena. Unfortunately, the available data needed to derive such estimates fall far short of what is desired.

A typical air quality data set with which to evaluate model performance consists of hourly surface measurements of ozone and oxides of nitrogen (NO_x) derived from monitoring stations operated by air regulatory agencies, usually located in or immediately downwind of urban areas. Those monitoring sites located in rural areas are often in the general proximity of commercial or industrial sources. Very little routine NO/NO_x monitoring is conducted at true rural sites, nor is there routine collection of total or speciated volatile organic compounds (VOC) data. No routine monitoring of ozone or precursors aloft is conducted. Data are rarely available for direct specification of pollutant concentrations on upwind boundaries of the modeling domain.

Photochemical grid models require a complete specification of the temporal and spatial variations of key meteorological variables, such as wind velocity, temperature, and cloud cover. The National Weather Service collects surface weather data supplemented by twice-daily radiosonde soundings at various locations throughout the country. These data supplemented with the surface meteorological data gathered at the air monitoring stations constitute the typical meteorological database available for developing meteorological inputs to photochemical grid models.

Photochemical grid models also require a complete specification of gridded, temporally resolved emissions estimates for all chemical species. Emissions data are normally assembled by air regulatory agencies with varying quality, representativeness, and reliability, often influenced by the ozone National Ambient Air Quality standards - NAAQS - attainment status of the particular area. (A region in the US is defined as an attainment region if air pollution measurements indicate the NAAQS are not exceeded). An emission modeling system may be needed to provide an effective means to organize, manipulate, and process emissions data for a large modeling domain.

Geophysical data are needed for specifying gridded terrain and land use inputs. Various federal agencies maintain geophysical data bases for topography, land use/land cover, population, employment, and so on that are used in various ways to develop the inputs needed by photochemical modeling systems.

In a few nonattainment areas, such as the northeast US, special field measurement studies have been performed to provide a better characterization and understanding of meteorological and air quality conditions than is otherwise provided by routine surface monitoring. Typically, these programs are carried out over a limited time period and consist of intensive monitoring of aloft meteorological and air quality conditions via instrument aircraft and remote sounding devices, enhanced surface monitoring of ozone and precursor species (sometimes including VOCs) in urban and rural sites, tracer-diffusion studies for model evaluation, and intensive, focused collection of emissions data from key source categories such as power plants, on-road motor vehicles, and targeted area sources. Though useful, these studies are very costly, capture a fraction of aerometric conditions associated with ozone exceedances, and have decreasing utility to support modeling as time passes.

Occasionally, major field studies are designed and implemented in parallel with integrated model development, testing and refinement activities. The SARMAP (Demassa, 1996) study in central California was a noteworthy example. Here, models were used to assist in the design of an intensive emissions, air quality, and meteorological data collection activity, supplemented with many research-grade investigations into specific processes: dry deposition and turbulence, biogenic emissions from various plant species, on-road motor vehicle driving patterns, boundary layer transport dynamics, and so on. Though very costly, these

programs provide a solid basis for further model development as well as the opportunity for testing of individual process modules in the overall modeling system.

10 Uses of Models

Several uses of models have been listed earlier, ranging from the practical to the research-oriented. In this section we discuss two practical arenas of application: regulatory compliance and resolution of litigation.

10.1 Regulatory Compliance

Today models are commonly used in planning to estimate if a geographical area:

- That now exceeds a specified standard will attain the standard if certain prescribed emissions reductions are implemented
- Now in attainment will remain so due to the favorable offsetting effects of growth and emissions controls, and
- Now in attainment is likely to exceed a standard due to the effects of growth and insufficient emissions control

As noted, these modeling activities are often included under the general umbrella of SIP and FIP preparation. A comprehensive process might include:

- Detailed planning and protocol preparation
- Conduct of a field program to obtain data needed for many purposes, including the preparation of model inputs and the evaluation of model performance
- Independent programs for quality assurance and control
- Archiving and error-checking for the complete data base, including emissions
- Adaptation and testing of a model system selected for use, including air quality, emissions, and meteorological models
- Iterative improvement of model performance consistent with good scientific practice until a specified standard of performance is met
- Conduct of sensitivity studies, to better understand the system being modeled
- Control strategy analysis, and
- Estimation and analysis of uncertainties and risks

Funding needed for such efforts may range from a \$2-5M to \$25M or more. If a comprehensive field program is included, that component alone may cost from \$3M to \$15M or more. The total elapsed time required ranges from 4 to 6 years or more. Clearly, such commitments are substantial.

While grid-based photochemical modeling offers the best opportunity for long range planning for the attainment and maintenance of secondary air pollutant standards, its potential may be limited in one or more of the following ways:

- Components of an ambient air quality and meteorological data base may be sparse, inaccurate, or lacking
- Funding to conduct a comprehensive study may be inadequate
- Staff to conduct the work may be available for only a portion of the time needed, or may be unacceptably inexperienced in modeling
- The calendar time available may be inadequate, and/or
- Model performance may be inadequate and not easily correctable

See Roth, Tesche and Reynolds (1998), for an evaluation of regulatory modeling efforts conducted during the 1990-95 period. In recent years, the USEPA has held annual modeling workshops and has posted the presentations made at these workshops to keep the modeling user community updated on current modeling guidance and performance. Ongoing updates to USEPA modeling guidance are available at www.epa.gov/scram001.

Section 3.3 has a discussion of how models can be applied to replace monitors to demonstrate compliance with ambient standards. As noted in the discussion, it is important to supply models with realistic (hourly) emissions input data in order to replicate what would be measured at a monitor. If such modeling is done on a widespread basis (there are about 2000 major SO₂ sources in the United States), then there would be a substantial effort involved in the preparation of the emissions data, which would involve compiling hourly data for many stacks.

10.2 Resolution of Litigation¹²

Environmental litigation has been steadily increasing over the last four decades, especially in relation to accidental releases of chemicals into the environment. This phenomenon is particularly noticeable in the United States (US). However, this trend is also affecting European countries and courts that deal with international issues. The parties and their attorneys involved in litigation need expert witnesses such as scientists, engineers, medical doctors, etc., in order to comprehend various cases and help define litigation strategy, producing accurate and convincing written reports as well as providing expert testimony to judges and juries.

In the past, experts hired for litigation cases were required to provide opinions and subsequently support them with published citations, professional experience, and simple “pen-and-paper” calculations. Today computer simulations are used in virtually all-technical fields. For example, in air pollution, computer simulation models have been used in the US since the early 1970s as “regulatory tools”, i.e.,

¹² Section written by P. Zannetti
EnviroComp Consulting, Inc. Fremont, California, USA. (<http://www.envirocomp.com>).

official tools recommended by regulatory agencies to simulate the concentration impact of emissions of chemicals into the atmosphere. But the same “regulatory” models, or similar tools, can also be used to simulate the past, e.g., to simulate an accidental release from an industrial facility. Accidental releases in the US are often litigated in court, whereas experts are hired in order to perform a reconstruction of the incidents. Today, these experts commonly use simulation models to estimate the concentration impact in the neighboring areas downwind from the release. The use of computer simulation models is clearly necessary in accidental release cases (as well as in many other environmental litigation cases, e.g., groundwater contamination). The formidable task for attorneys on both sides is to understand as much as possible about modeling techniques and be able to present or criticize the results of those models in court.

If modeling is to be used in a litigation case, the expert witness must make several important choices. First of all, does the case warrant the use of a complex computer model? Should perhaps a simple model be chosen? Which model will be easier to explain to a jury? In one case, for example, the expert may use a computer model developed and recommended by the US Environmental Protection Agency (EPA). In another scenario, the expert might use a “research prototype” code developed at a university or a national laboratory. In yet another case, the expert might utilize a model recently developed, or even a model (or a set of calculations) expressly developed for the case at hand. The expert should bear in mind that each choice has advantages and disadvantages. Clearly, models that are widely used by other scientists and recommended by regulatory agencies can be perceived as more reliable than others. However, in litigation, an expert witness has ample latitude in selecting the tools that are most appropriate for the case. Whatever tool is chosen, the expert witness must be able to persuasively present it as reliable, peer-reviewed science whose results can be trusted. In all cases, the expert witness must feel comfortable in the ability to justify results and opinions to a non-technical audience under an often-hostile cross-examination. For additional information on the subject of the use of air pollution models in litigation cases, see Zannetti (2001).

References

Air Resources Laboratory, 2009, HYSPLIT - Hybrid Single Particle Lagrangian Integrated Trajectory Model. <http://ready.arl.noaa.gov/HYSPLIT.php>.

American Society for Testing and Materials, 2000, Standard Guide for Statistical Evaluation of Atmospheric Dispersion Model Performance (D 6589), (Available at <http://www.astm.org>), 100 Barr Harbor Drive, PO Box C700, West Conshohocken, PA 19428, 17 pages.

Byun, D.W. and J.K.S. Ching, 1999, Science Algorithms of the EPA Models-3 Community Multiscale Air Quality (CMAQ) Modelling System, U.S. Environmental Protection Agency, Research Triangle Park, NC. EPA/600/R-99/030.

Chang, J.C. and S.R. Hanna, 2004, Air Quality Model Performance Evaluation, *Meteorol. Atmos. Phys.* 87, 167–196.

Cimorelli, A.J., S.G. Perry, A. Venkatram, J.C. Weil, R.J. Paine, R.B. Wilson, R.F. Lee, W.D. Peters, and R.W. Brode, 2005, AERMOD: A Dispersion Model for Industrial Source Applications. Part I: General Model Formulation and Boundary Layer Characterization'. *Journal of Applied Meteorology*, 44, 682-693. American Meteorological Society, Boston, MA.

DeMassa, J. et al., 1996, "Performance Evaluation of SAQM in Central California and Attainment Demonstration for the 3-6 August 1990 Ozone Episode." California Air Resources Board, Sacramento, CA, 1996.

Hanna, S.R., 1993. Uncertainties in Air Quality Model Prediction. *Boundary-Layer Meteorology*, 62: 3-20.

Irwin, J. S. and R. F. Lee, 1996. Comparative evaluation of two air quality models: Within-regime evaluation statistic. *Int. J. Environ. Pollut.*, 8: 346–355.

Irwin, J. S. and S. R. Hanna, 2005. Characterizing uncertainty in plume dispersion models. *Int. J. Environ. Pollut.*, 25: 6–24.

Liu, M. K., and Seinfeld, J. H., 1974, On the Validity of Grid and Trajectory Models of Urban Air Pollution. *Atmos. Environ.*, 9, pp. 555-574.

Morgan, M. G., and Henrion, M., 1990, Uncertainty: A Guide to Dealing with Uncertainty in Quantitative Risk and Policy Analysis. Cambridge Univ. Press.

Morris, R., G. Yarwood, C. Emery, and B. Koo, 2004, Development and Application of the CAMx Regional One-Atmospheric Model to Treat Ozone, Particulate and Visibility, Air Toxics, and Mercury. Presented at the 97th Annual Meeting and Exhibition of the Air & Waste Management Association, Indianapolis, IN USA.

Reynolds, S. D., Roth, P. M. and Tesche, T. W., 1994, A Process for Stressful Evaluation of Photochemical Model Performance. Envair, San Rafael, CA.

Roth, P. M., Tesche, T. W. and Reynolds, S. D., 1998, A Critical Review of Regulatory Air Quality Modeling for Tropospheric Ozone. North American Research Strategy for Tropospheric Ozone (NARSTO), Research Triangle Park, NC.

Santos, L., R. I. Sykes, P. Karamchandani, C. Seigneur, F. Lurmann, R. Arndt, and N. Kumar, 2000, Second-Order closure integrated puff (SCIPUFF) model with gas and aqueous phase chemistry and aerosols - Paper 6.8. Preprints, 11th Joint Conference on the Applications of Air Pollution Meteorology with the A&WMA, American Meteorological Society, Boston, MA.

Schulman, L. L., D. G. Strimaitis, and J. S. Scire, 2000, Development and evaluation of the PRIME plume rise and building downwash model. *J. Air Waste Manage. Assoc.*, 50, 378–390.

Scire, J.S., D.G. Strimaitis, and R.J. Yamartino, 2000, A User's Guide for the CALPUFF Dispersion Model (Version 5). Available through <http://www.epa.gov/scram001>.

Seigneur, C., 2001, Current Status of Air Quality Models for Particulate Matter. *Journal of the Air & Waste Management Association*, 51, pp. 1508-1521.

Seinfeld, J. H. and Pandis, S. N., 1998, Atmospheric Chemistry and Physics. Wiley-Interscience.

Sen, Z, A. Altunkaynak, and, K. Alp, 2009, Contour diagram fuzzy model for maximum surface ozone prediction, Expert Systems with Applications, Volume 36, Issue 3, Part 2, April 2009, Pages 6389-6402, ISSN 0957-4174, DOI: 10.1016/j.eswa.2008.07.050.

(<http://www.sciencedirect.com/science/article/B6V03-4T1Y3PX9/2/3983d721634c65015e7746ea557d9bdf>).

U.S. Environmental Protection Agency, 1990, “User’s Guide for the Urban Airshed Model-Volume I: User’s Manual for UAM (CBIV).” U.S. Environmental Protection Agency, EPA-450/4-90-007a, Research Triangle Park, NC.

U.S. Environmental Protection Agency, 1991, “Guideline for Regulatory Application of the Urban Airshed Model,” EPA-450/4-91-013, Office of Air Quality Planning and Standards, Research Triangle Park, NC.

U. S. Environmental Protection Agency, 2007, Guidance on the Use of Models and Other Analyses for Demonstrating Attainment of Air Quality Goals for Ozone, PM2.5, and Regional Haze. April 2007. EPA - 454/B-07-002.

Yang, Y.J., Wilkinson, J.G., and Russell, A.G., 1997, Fast Direct Sensitivity Analysis of Multidimensional Photochemical Models. *Environ. Sci. Technol.*, 31, 2859-2868.

Zannetti, P., 2001, Environmental Litigation – Air Pollution Models and Modelers in Court (Invited Paper). Air Pollution 2001, Ninth International Conference on Modeling, Monitoring, and Management of Air Pollution, 12-14 Sept 2001, Ancona, Italy, Wessex Institute of Technology, Ashurst, Southampton, U.K.

Chapter 3

Emission Modeling and Inventory

A comprehensive chapter on “Emission Modeling and Inventory” was presented in Volume III of this book series. The abstract of this chapter is reprinted below:

Emissions Inventory (EI) has rapidly evolved from an art to a science. More complex emissions estimates techniques have been developed in the past decade, even against reduction in investment in the same period. More accurate industrial and regional emissions inventory are under development every year, with coordination by various regulatory agencies, such as state, tribal, and the USEPA. There are 3 main factors for increased emissions inventory accuracy, which are listed below:

- 1. Improved and expanded regulatory requirements*
- 2. Better emissions inventory models and methods*
- 3. Accumulated experiences in conducting emissions inventory*

This Chapter will describe existing approaches to creating emissions inventories.

For additional information, the reader can visit:

- Emissions Factors & AP 42, *Compilation of Air Pollutant Emission Factors*
<http://www.epa.gov/ttn/chief/ap42/index.html>
- United Kingdom's emission factor database
<http://www.naei.org.uk/emissions/index.php>
- European Environment Agency's 2005 Emission Inventory Guidebook
<http://www.eea.europa.eu/publications/EMEP CORIN AIR4>
- California ARB EMISSION INVENTORY MODELS
<http://www.arb.ca.gov/html/soft.htm>

- National Emissions Inventory (NEI) Air Pollutant Emissions Trends Data
<http://www.epa.gov/ttnchie1/trends/>

Chapter 4

Air Pollution Meteorology

A chapter on “Air Pollution Meteorology” was presented in Volume I of this book series. The abstract is reprinted below.

The primary object of this chapter is to introduce meteorological fundamentals related to the transport of air pollutants in the atmosphere. The material contained in the chapter is divided into two sections. Section 1 is very basic and mostly related to atmospheric flows in larger scales. It discusses forms of atmospheric motions, weather systems, forces, and clouds. The material contained in Section 2 is more detailed and focused on processes in the atmospheric boundary layer. Turbulence, mixing and diffusion in this layer are examined and explained. Various regimes, such as stable flows, free and forced convection, in cloudless and cloud-topped mixed layers are discussed. Their mathematical and physical description is also reviewed, including similarity theories and mixed layer models.

For additional information, the reader can visit:

- SI:409 Basic Air Pollution Meteorology Course
http://yosemite.epa.gov/oaqps/eogtrain.nsf/DisplayView/SI_409_0-5?OpenDocument
- Air Quality Meteorology Course
<http://www.shodor.org/metweb/>

BRANK
P
2000

Chapter 5

Meteorological Modeling

A brief introduction to the topic “Meteorological Modeling” was presented in Volume I of this book series.

Chapter 5B – Large-Eddy Simulations of the Atmospheric Boundary Layer was included in Volume II. The abstract is reprinted below.

In this Chapter, the large-eddy simulation technique is described. The presented material consists of two parts. In the first one, technical issues including filtering, subgrid modeling, and numerical integration, are discussed. In the second part, simulations of typical prototypes of the atmospheric boundary layer are presented, including convective, neutral, stable, and cloud-topped cases.

In Volume III we presented two chapters:

5A – Meteorological Modeling for Air Quality Applications. The abstract is reprinted below.

The phrase “meteorological modeling” (or synonymously “atmospheric modeling” and “numerical weather prediction”) refers to the numerical representation of the atmosphere and its processes. This chapter describes the various processes that are usually included in numerical models that are relevant to air quality applications. Due to the mathematical complexities of many of these processes, parameterizations are used to simplify the numerical models. Many different parameterizations exist for these processes, and representative examples are presented.

5C – Computational Fluid Dynamics of Microscale Meteorological Flows for Air Quality Applications. The abstract is reprinted below.

There is an ever-increasing need to simulate airflow at the micro-meteorological scale for environmental applications. Dispersion of pollutants around buildings and pedestrian level wind-speeds are two applications that concern environmental planners. Wind tunnels are still the main tool used, but computational methods are becoming more popular as a way to address these issues. Computational Fluid Dynamics (CFD) simulations are being used more often to model the surface layer of the atmosphere for environmental application. The use of CFD in this field is still experimental in nature and inherent weaknesses are apparent, but advances in computing and simulation methods are continually driving it towards becoming a reliable tool for predicting local air quality and other environmental conditions.

This review addresses today's common method of simulating the atmospheric surface layer in an urban environment using CFD. The features of the surface layer that are important for flow modeling are discussed as well as different methods for applying them in CFD. Different turbulence models and techniques for simulating the surface layer in CFD are reviewed as well. Current guidelines and processes for conducting a project are also described and discussed.

This chapter is intended for environmental scientists or engineers as an overview of the basics of CFD and its application to the surface layer of the atmosphere so that one can know how to conduct or evaluate a CFD analysis for compliance with industry best practices.

In this Volume IV, we include:

5D – Recent Advances in the Similarity Theory of the Stable Boundary Layer

5E – Coupling Meteorological and Air Quality Models

Sorbjan, Z., 2010. *Recent Advances in the Similarity Theory of the Stable Boundary Layer*. Chapter 5D of *AIR QUALITY MODELING - Theories, Methodologies, Computational Techniques, and Available Databases and Software. Vol. IV – Advances and Updates* (P. Zannetti, Editor). Published by The EnviroComp Institute (<http://www.envirocomp.org/>) and the Air & Waste Management Association (<http://www.awma.org/>).

Chapter 5D

Recent Advances in the Similarity Theory of the Stable Boundary Layer

Zbigniew Sorbjan ^{(1) (2)}

⁽¹⁾ *Department of Physics, Marquette University, Milwaukee (USA)*
zbigniew.sorbjan@mu.edu

⁽²⁾ *Institute of Geophysics, Polish Academy of Sciences, Warsaw (Poland)*
sorbjan@igf.edu.pl

Abstract: The gradient-based scaling system for the stably stratified boundary layer is introduced and examined by using data collected during the SHEBA field program in the Arctic. The resulting similarity functions for fluxes and variances are expressed in an analytical form, which is practically unaffected by self-correlation. The flux Richardson number R_f is found to be proportional to the Richardson number R_i , with the proportionality coefficient varying slightly with stability, from 1.11 to 1.47. The Prandtl number decreases from 0.9 in nearly-neutral conditions, down to 0.7 for larger values of R_i . The budget of the turbulent kinetic energy indicates that for $R_i > 0.7$, turbulence must be non-stationary and decaying, or sporadic. Turbulence within the stably stratified boundary layer is classified into four regimes: “nearly-neutral”, “weakly-stable”, “very-stable”, and “extremely-stable”.

Key Words: gradient-based scaling, SHEBA data, similarity theory, stable boundary layer.

1 Introduction

Observations collected during recent years in the stable boundary layer challenge many classical concepts and indicate that the structure of the stable regime is more complex than previously anticipated (e.g., Sorbjan and Balsley, 2008). Stable turbulence survives at Richardson numbers exceeding the critical value $Ri_{cr}=1/4$ (e.g., Galperin et al. 2007). It can have either a continuous or intermittent character (e.g., Coulter and Doran 2002; Van de Wiel et al. 2003)

within weakly stable or very stable regimes (e.g., Oyha et al. 1997, Mahrt 1998). The weakly stable case is usually associated with strong turbulence, significant wind shear, clouds, continuous turbulence near the surface, and sub-critical values of the Richardson number. In contrast, the very stable regime is defined by a lesser wind shear, clear skies, supercritical values of the Richardson number, and weak turbulence. It may assume an "upside-down" character (Mahrt 1999), with the strongest turbulence at the top of the surface inversion layer, where it is generated by vertical shear on the underside of the lower-level jet stream (Newsom and Banta 2003; Banta 2008; Cuxart, 2008).

Weak turbulence in very stable conditions limits the validity of the Monin-Obukhov similarity, regarded as the major tool for understanding near-surface turbulence (e.g., Sorbjan 2006a; 2006b). The similarity predictions for gradients are formally valid only in sub-critical cases. Similarity functions cannot be accurately estimated during very stable stratification due to the uncertainty introduced by small values of fluxes, and also due to serious self-correlation errors (Klipp and Mahrt 2004; Baas et al 2006). The attempts to resolve the problem are often executed by arbitrarily extending the validity of the similarity approach into the supercritical region, despite a large scatter of observational points.

The primary purpose of this chapter is to examine the self-similar structure of the stably stratified boundary layer using novel gradient-based similarity formulation and data collected during the SHEBA field program (1997/1998) in the Arctic.

2 Scaling Systems

2.1 Governing Parameters

Let us consider the most basic dependence between fluxes and gradients. According to the classic K-theory, the turbulent kinematic fluxes of momentum τ (modulus) and temperature H in the horizontally homogeneous flow can be expressed in terms of the mean wind shear $S = \sqrt{(dU/dz)^2 + (dV/dz)^2}$ and the (virtual) potential temperature gradient $\Gamma = d\Theta/dz$ (Sorbjan, 2010, Sorbjan and Grachev, 2010):

$$\tau = K_m S \quad (1a)$$

$$H = -K_h \Gamma \quad (1b)$$

where U and V are components of the wind vector, and the eddy viscosity K_m and diffusivity K_h can be written in the form:

$$K_m = (\kappa z)^2 S f_m(Ri) \quad (2a)$$

$$K_h = (\kappa z)^2 S f_h(Ri) \quad (2b)$$

Above, $\kappa = 0.4$ is the von Karman constant, z is the height, f_m and f_h are empirical functions of the Richardson number, defined as $Ri = N^2/S^2$, where $N = \sqrt{\beta\Gamma}$ is the Brunt-Väisälä frequency, $\beta = g/T_o$ is the buoyancy parameter, g is the gravity acceleration, and T_o is the reference temperature. Equation (2a) follows from an expressions for the eddy diffusivity $K_m = l^2 S$ of Prandtl (1932) and the mixing length $l = \kappa z / (1 + \kappa z / l_\infty)$ of Blackadar (1962), with the ratio z / l_∞ assumed to be dependent on the Richardson number. The eddy diffusivity K_h is defined analogously.

When the empirical functions f_m, f_h , are specified, the system (1) - (2) is closed. It describes the relationship between the fluxes τ, H and parameters S, Γ, b, z . We will not attempt to find the solution of the system (1) - (2). Instead, some general conclusions will be derived by employing the approach of the dimensional analysis (e.g., Barenblatt, 1996).

A simple analysis of (1) - (2) indicates that the choice of the similarity scales for the set of 6 variables: $\{\tau, H, S, \Gamma, z, b\}$, with 3 independent units, [m], [s], [K], is not unique and can be performed in a number of ways. Generally, any 3 dimensionally independent parameters in the above list can be selected to build a system of three scales for length, temperature, and velocity. Below, we will consider scaling systems, based on the following choice of the parameters:

$$\{\tau, H, b\} \quad (3a)$$

$$\{z, \Gamma, b\} \quad (3b)$$

The scales derived from the first set of parameters will be referred to as “flux-based scaling”, while the remaining sets will be called “gradient-based scaling” systems. It should be mentioned that other “gradient-based scaling” systems could also be proposed in the stable regime. For example, one could augment the system (1)-(3) by the equations for vertical velocity and temperature variances σ_w, σ_θ , and consider $\{\sigma_w, \Gamma, b\}$, $\{\sigma_\theta, \Gamma, b\}$, or $\{\varepsilon, \Gamma, b\}$ as governing parameters, where ε the dissipation rate (Sorbjan and Balsley 2008).

2.2 The Flux-Based Scaling

Historically, the first scaling system for the atmospheric boundary layer was proposed by Monin and Obukhov (1954), who employed (3a), with the surface

values of fluxes τ_o , H_o , to construct 3 scales for length $L_* = -\tau_o^{3/2} / (\kappa\beta H_o)$, temperature $T_* = -H_o / u_*$, and velocity $u_* = \sqrt{\tau_o}$. Based on a dimensional analysis, Monin and Obukhov concluded that the non-dimensional products of statistical moments X in the surface layer (such as σ_w , σ_θ , S , Γ), and the flux-based scales, are universal functions φ_x of a single dimensionless parameter z/L_* :

$$\frac{X}{u_*^a T_*^b L_*^c} = \varphi_x(z/L_*) \quad (4)$$

where the exponents a , b , c are chosen in such a way that φ_x is dimensionless. The above result conveys the so-called “self-similarity”, a property, which manifests itself in the reduction of the number of independent dimensionless variables in comparison to the number of dimensional ones (e.g., Barenblatt, 1996). Self-similarity substantially simplifies the description of phenomena and their experimental, analytical and computational analysis.

By using second-order closure equations, Nieuwstadt (1984) demonstrated that the assumption of the constancy of fluxes with height is not necessary, so that the scales in the stable boundary layer can be height dependent (local):

$$U_*(z) = \sqrt{\tau} \quad (5a)$$

$$\vartheta_*(z) = -\frac{H}{U_*} \quad (5b)$$

$$\Lambda_*(z) = -\frac{\tau^{3/2}}{\kappa\beta H} \quad (5c)$$

where capital letters are used to mark the local scales.

Sorbjan (e.g., 1986a; 1986b; 1986c; 1988) argued that the functional form of universal similarity functions of the argument z/L_* and z/Λ_* is identical in stable conditions, $\varphi_x(z/L_*) = \varphi_x(z/\Lambda_*)$. As a result:

$$\frac{\kappa z}{U_*} S = \varphi_m(z/\Lambda_*) \quad (6a)$$

$$\frac{\kappa z}{\vartheta_*} \Gamma = \varphi_h(z/\Lambda_*) \quad (6b)$$

Applying a definition of the Richardson number yields

$$Ri = \frac{z}{\Lambda^*} \frac{\varphi_h(z/\Lambda^*)}{\varphi_m^2(z/\Lambda^*)} \quad (7)$$

Equation (7) shows that Ri is a function of z/Λ^* . This fact allows us to rewrite (6) in the equivalent form:

$$\frac{\kappa z}{U_*} S = \psi_m(Ri) \quad (8a)$$

$$\frac{\kappa z}{g_*} \Gamma = \psi_h(Ri) \quad (8b)$$

where ψ_m , ψ_h are the universal similarity functions of the Richardson number. The same result can be formally obtained based on (1) - (2), with $\psi_m \sim 1/f_m^{1/2}$, $\psi_h \sim f_m^{1/2}/f_h$. Thus we can conclude that the K theory formulation (1) - (2) is equivalent to the Monin-Obukhov similarity approach.

In neutral conditions, the parameters z/L^* and Ri are nearly zero, which implies that values of similarity functions are constant. Specifically, $\varphi_m(0)=1$ and $\varphi_h(0) = Pr_o$, where Pr_o is a constant referred to as the neutral value of the Prandtl number. When the temperature gradient Γ is sufficiently large, turbulence is expected to be local and independent on the distance from the underlying surface (the “z-less regime”). A dimensional analysis leads to a conclusion that the similarity functions in this case are linear, $\varphi_m \sim \varphi_h \sim z/\Lambda^*$. As thermal stratification increases, the parameter $z/\Lambda^* = \kappa z \beta g_*/U_*^2$ tends to $0/0$. Consequently, the similarity functions become singular, and strongly impacted by self-correlation.

2.3 The Gradient-Based Scaling

An alternative similarity scaling can be introduced by using (3b), which involves the temperature gradient Γ , the buoyancy parameter β and height z (Sorbjan 2010):

$$U_s = k z N \quad (9a)$$

$$T_s = k z \Gamma \quad (9b)$$

$$L_s = k z \quad (9c)$$

where k the von Karman constant was added for convenience. As before, we will consider only cases when the Brunt-Väisälä frequency N is sufficiently large.

Employing (10), we will obtain from (1) - (2):

$$\frac{\tau}{U_s^2} = G_t(Ri) \quad (10a)$$

$$-\frac{H}{U_s T_s} = G_h(Ri) \quad (10b)$$

where $G_t \sim f_m / Ri$, $G_h = f_h / Ri^{1/2}$.

The above results can be generalized by stating that the non-dimensional products of statistical moments X in the surface layer and the above scales must be universal functions of a single dimensionless parameter Ri :

$$\frac{X}{U_s^a T_s^b L_s^c} = G_x(Ri) \quad (11)$$

Note that the temperature gradient G appears on both sides of (11), within the similarity scales and in the definition of the Richardson number. This fact implies self-correlation, due to the relative errors in the evaluation of Γ . One can expect, however, that such errors are relatively small when the temperature gradient is sufficiently large, and thus the self-correlations effects related to G are not serious.

Applying (11) to the standard deviations of the vertical velocity and temperature yields:

$$\frac{\sigma_w}{U_s} = G_w(Ri) \quad (12a)$$

$$\frac{\sigma_\theta}{T_s} = G_\theta(Ri) \quad (12b)$$

Using (2), (5), (8) and (9) one can also obtain the relationship between the Monin-Obukhov and gradient-based functions:

$$G_t = \frac{1}{Ri \psi_m^2} \quad (13a)$$

$$G_h = \frac{1}{Ri^{1/2} \psi_m \psi_h} \quad (13b)$$

Even though the gradient-based scaling system is formally equivalent to the Monin-Obukhov similarity approach in the stable case, there exists, however, an essential difference. The flux-based approach employs fluxes as external

(specified) parameters. As a result, the practical application of the flux-based expressions requires inverting the similarity laws, and calculating surface fluxes from the provided (measured) values of gradients in the surface layer. This procedure is ill posed in very stable conditions, because the fluxes are small. Moreover, the practical application of the local similarity formulation (5) requires that fluxes are known a priori as functions of height, which is often difficult to accomplish. Within the gradient-based formulation, the gradients play the role of external parameters, which does not imply singularities.

3 Empirical Verification

3.1 Data

Sorbjan (2010) and Sorbjan and Grachev (2010) verified the similarity functions formulated in the previous section by employing data collected during the SHEBA experiment. The experiment took place over the Arctic pack ice, drifting in the Beaufort Gyre to the north of Alaska (latitude from 74°N to 81°N) from October 1997 through September 1998 (Andreas et al. 1999; 2003; 2006; Persson et al. 2002; Grachev et al. 2005; 2007a; 2007b; 2008). The sub-polar localization offered a number of advantages, especially due to the stationarity of weather conditions, and the lack of contamination by drainage or strong advective flows. Except for rare periods, instruments ran almost continuously for 11 months and produced well over 6000 hours of useful data, covering a wide range of stability conditions.

Turbulent and mean meteorological data during SHEBA were obtained on the 20-m main tower (Grachev et al. 2005). Observations were continuously collected at five levels, located at 2.2 m, 3.2 m, 5.1 m, 8.9 m, and 18.2 or 14 m above the surface. The variances and covariances at each level were based on one-hour averaging, and derived through frequency integration of spectra and cospectra. To prevent a possible flux loss caused by inadequate frequency responses and sensor separations, a prerequisite that the wind velocity $U > 1 \text{ m s}^{-1}$ has been imposed on the data. Data for the first level, which reflected a relatively large scatter due to local surface effects, were not considered. In addition, data with a temperature difference between the air at median level and the snow surface less than 0.5 C were excluded to avoid the large uncertainty in determining the sensible heat flux. Vertical gradients of the mean wind speed and the potential temperature were obtained by fitting a second-order polynomial through the 1-hr profiles followed by an evaluation of the derivative with respect to z for levels 1–5.

The data points presented below are based on a bin-averaging of the individual one-hour data at levels 2, 3, 4, and 5. For this purpose, data were first sorted into bins for the Richardson number Ri as the sorting parameter. Then the mean values of relevant parameters were computed for each bin (e.g., Grachev et al 2008).

A special prerequisite was applied on the data to limit the influence of outliers on the bin-averaging. It had the following form: $0.5Ri_e < Ri < 2Ri_e$, where the value of the Richardson number Ri_e is estimated based on an equation analogous to (7), for the analytical form of the Monin-Obukhov similarity functions φ_h and φ_m of z/L^* , obtained by Grachev et al. (2007a) and Grachev et al. (2008). If the actual value of a Richardson number Ri was not in the range defined by Ri_e , the data point was rejected.

3.2 Empirical Similarity Functions

The dependence of the dimensionless fluxes, $G_t = \tau/U_s^2$ and $G_h = -H/(U_s T_s)$ on the Richardson number Ri is shown in Figure 1. The vertical lines with horizontal bars represent the confidence intervals, obtained by adding/subtracting the standard deviation to/from the mean values evaluated at level 3. Because the ordinate is logarithmic, the confidence intervals are asymmetric. The dimensionless moments $G_w = \sigma_w/U_s$ and $G_\theta = \sigma_\theta/T_s$ are depicted in Figure 2. A clustering of data points in Figures 1 and 2 is caused by the fact that the Richardson number Ri is a sorting parameter on levels 2-5.

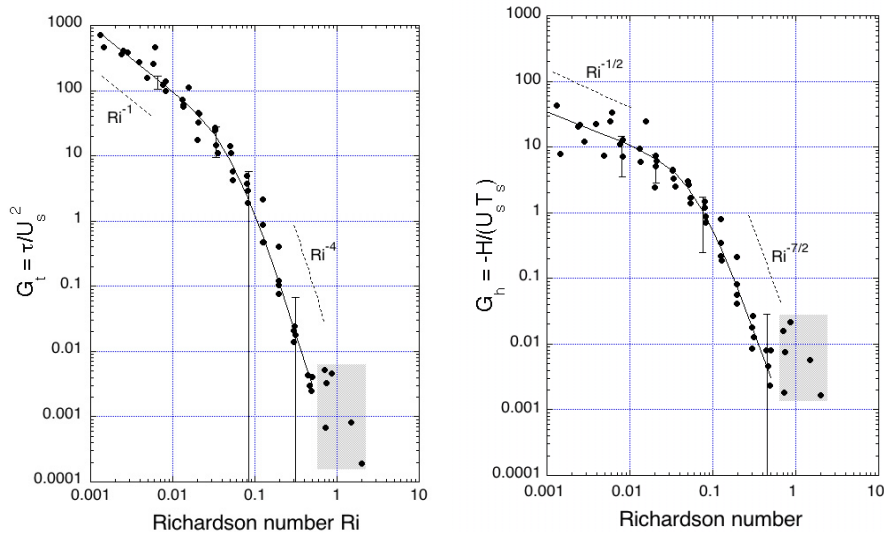


Figure 1. Dependence of the bin-averaged values of the dimensionless: (a) momentum flux $G_t = \tau/U_s^2$, (b) heat flux $G_h = -H/(U_s T_s)$, on the Richardson number Ri . The solid lines are plotted based on Equations 16a and 16b. The vertical lines represent the confidence intervals evaluated at level 5. The shaded box marks data points within the “extremely-stable” domain.

It can be noticed that the scatter of data points in Figure 1b is larger than in Figure 1a. This effect can be associated with thermal inhomogeneity around the observational site (e.g., Kukharets and Tsvang 1998; Tsvang et al 1998). The ice floe around the main tower was multi-year pack ice with varying degrees of thickness and a surface composed of ice of a different type and salinity, snow of a different depth and age, melt-ponds, and even leads (e.g., Sorbjan and Grachev, 2010). These surface patches were characterized by different albedo, thermal capacity and conductivity and, therefore, by different temperatures. Andreas et al. (1998) reported analogous behavior for humidity statistics over a surface with vegetation that was patchy at meter scales.

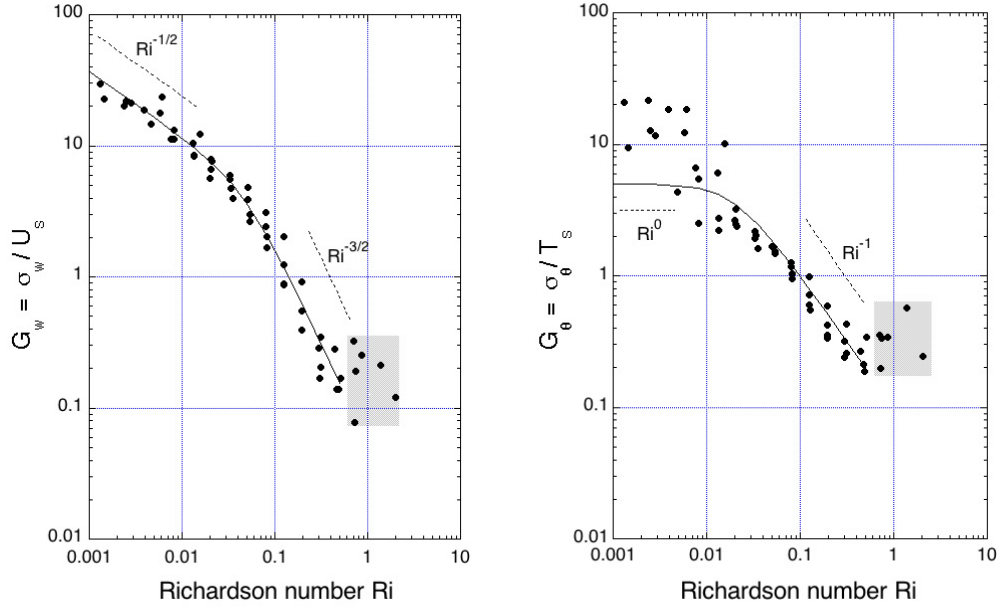


Figure 2. Dependence of the bin-averaged values of the dimensionless standard deviations for: (a) vertical velocity $G_w = \sigma_w / U_s$, (b) temperature $G_\theta = \sigma_\theta / T_s$, on the Richardson number Ri . The solid lines are plotted based on Equations 16c and 16d. The shaded box marks data points within the “extremely-stable” domain.

In order to further evaluate the presented results, let us first notice that in nearly-neutral conditions, $\tau \sim (\kappa z S)^2$, $\sigma_w \sim \kappa z S$, and also that $H \sim (\kappa z)^2 S N^2 / \beta$, $\sigma_\theta \sim \kappa z N^2 / \beta$. Thus, we can conclude that in nearly-neutral conditions

$$G_t \sim Ri^{-1} \quad (14a)$$

$$G_h \sim Ri^{-1/2} \quad (14b)$$

$$G_w \sim Ri^{-1/2} \quad (14c)$$

$$G_\theta \sim Ri^0 \quad (14d)$$

Figures 1a, b and 2a confirm the above predictions for $Ri < 0.01$. The values of the dimensionless temperature variance G_q , in Figure 2b, are larger than expected in the nearly-neutral range. This fact implies that values of the temperature variance are underestimated in nearly-neutral conditions.

In the supercritical range in Figures 1 and 2, the values of the similarity functions fall off in a coherent fashion for the increasing values of Ri . This indicates the presence of a self-similar regime in very stable conditions. The dimensional analysis and the system (1)-(2), however, do not allow the formulation of any constructive similarity prediction. Therefore, we will assume, based on the presented empirical evidence, that the similarity functions obey the following power laws:

$$G_t \sim Ri^{-4} \quad (15a)$$

$$G_h \sim Ri^{-7/2} \quad (15b)$$

$$G_w \sim Ri^{-3/2} \quad (15c)$$

$$G_\theta \sim Ri^{-1} \quad (15d)$$

valid approximately in the range $0.1 < Ri < 0.7$. Above this range, the values of similarity functions are incoherent and scattered. Such behaviour indicates a lack of any general similarity laws for larger values of Ri . Consequently, we will limit our analysis to the range of $Ri < 0.7$, and disregard the domain marked by the shaded boxes in Figures 1-2, and also in the remaining figures.

Taking (14) and (15) into consideration, we will adopt the following approximations of the similarity functions:

$$G_t \equiv \frac{\tau}{U_s^2} = \frac{1}{Ri(1 + 300Ri^2)^{3/2}} \quad (16a)$$

$$G_h \equiv -\frac{H}{U_s T_s} = \frac{1}{0.9 Ri^{1/2} (1 + 250Ri^2)^{3/2}} \quad (16b)$$

$$G_w \equiv \frac{\sigma_w}{U_s} = \frac{1}{0.85 Ri^{1/2} (1 + 450Ri^2)^{1/2}} \quad (16c)$$

$$G_\theta \equiv \frac{\sigma_\theta}{T_s} = \frac{5}{(1 + 2500Ri^2)^{1/2}} \quad (16d)$$

The above equations are represented in Figures 1 and 2 by solid curves. The agreement of the curves with data points is generally good.

Using (13a, b) and (16a, b), we will also obtain:

$$\psi_m \equiv \frac{\kappa z}{U_*} S = \frac{1}{Ri^{1/2} G_t^{1/2}} = (1 + 300Ri^2)^{3/4} \quad (17a)$$

$$\psi_h \equiv \frac{\kappa z}{g_*} \Gamma = \frac{G_t^{1/2}}{G_h} = 0.9 \frac{(1 + 250Ri^2)^{3/2}}{(1 + 300Ri^2)^{3/4}} \quad (17b)$$

in the range $Ri < 0.7$.

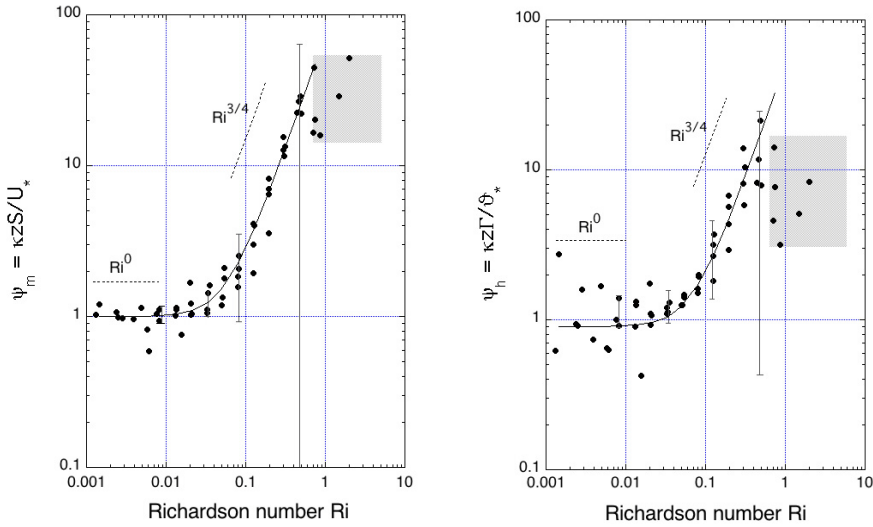


Figure 3. Dependence of the bin-averaged values of the flux-based similarity functions, (a) ψ_m , and (b) ψ_h , on the Richardson number Ri . The solid curves are described by Equations 17a, and 17b. The vertical lines represent the confidence intervals evaluated at level 5. The shaded box marks the “extremely-stable” domain.

The values of the similarity functions ψ_m , ψ_h , defined by (8), are plotted in Figure 3. Data points in the figure agree with curves defined by expressions (17), except for the outliers in the shaded box, which are highly scattered. The scatter of data points for ψ_h is larger than for ψ_m , which could be associated with the effects of thermal inhomogeneity around the observational site.

4 Structure of Stable Turbulence

Let us now consider the flux Richardson number, defined as $Rf = -\beta H / (\tau S)$. Employing (16a, b) we obtain:

$$Rf = \frac{G_h}{G_t} Ri^{1/2} = \frac{Ri (1 + 300Ri^2)^{3/2}}{0.9 (1 + 250Ri^2)^{3/2}} \quad (18)$$

in the range $Ri < 0.7$. The above expression is depicted in Figure 4 as a solid curve. In accordance with (18), $Rf = 1.11 Ri$ in nearly-neutral conditions and $Rf = 1.46 Ri$ for large values of Ri . Consequently, the curve in the figure differs only slightly from a straight line.

Taking into consideration that $Rf \equiv Ri / Pr$ and by using (18), we also receive:

$$Pr = 0.9 \frac{(1 + 250Ri^2)^{3/2}}{(1 + 300Ri^2)^{3/2}} \quad (19)$$

in the range $Ri < 0.7$. The above expression is shown in Figure 5 as a solid curve.

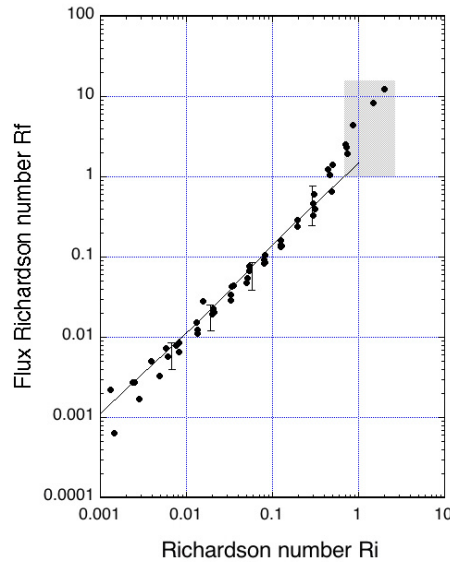


Figure 4. Dependence of the bin-averaged values of the flux Richardson number Rf on the gradient Richardson number Ri . The solid line is plotted based on Equation 18. The vertical lines represent the confidence intervals evaluated at level 5. The shaded box marks data points within the “extremely-stable” domain.

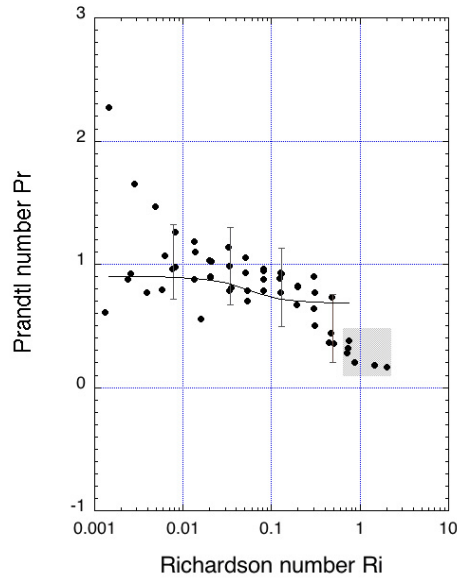


Figure 5. Dependence of the bin-averaged values of the Prandtl number Pr , on the Richardson number Ri . The solid line is plotted based on Equation 19. The vertical lines represent the confidence intervals for evaluated at level 5. The shaded box marks the “extremely-stable” domain.

Equation (19) indicates that the Prandtl number is equal to 0.9 in nearly-neutral conditions and to 0.7 for larger values of Ri . The scatter of the data points is large, which does not permit a precise evaluation of the Prandtl number. When all displayed data points are considered, the resulting mean value of the Prandtl number is 0.83, the median is equal to 0.85, and the standard deviation is 0.36.

The resulting neutral value 0.9 is larger than the value $Pr_o = 0.74$ of Businger (1973), than the neutral limit of 0.8 proposed by Churchill (2002), and than the value 0.85, obtained by Kader and Yaglom (1990). According to Ohya (2001), Grachev et al. (2007b), Esau and Grachev (2007), Zilitinkevich et al. (2008), Anderson (2009), the Prandtl number increases with Ri in supercritical conditions. A detailed analysis of Grachev et al. (2007b) implies, however, that such a result is spurious. When the special prerequisite limiting the influence of outliers on the bin-averaging, discussed in Section 3.1, is not imposed, the resulting SHEBA points indeed show that Pr increases with the increasing values of Ri . With the prerequisite applied, however, the Prandtl number decreases slightly, as shown in Figure 2 (Sorbjan and Grachev, 2009).

Note, that the steady-state, turbulent energy budget can also be expressed in the following form (e.g., Sorbjan, 1989):

$$K_m S^2 (1 - Rf) = \varepsilon \quad (20)$$

Since the dissipation rate ε is positive-definite, the above equation allows us to conclude that the steady state, which results from a balance of shear production and buoyant-dissipative destruction, takes place only for $Rf < 1$. Figure 5 indicates that $Rf = 1$ at $Ri = 0.7$. Thus, at the Richardson number Ri exceeding the value $Ri_s = 0.7$, which is larger than the critical value $Ri_{cr} = 0.25$ indicated by the linear stability evaluation (Miles 1961), the steady-state turbulence would not be present. In other words, at $Ri > Ri_s$, turbulence is non-stationary and decaying or sporadic. The inequality $Ri < Ri_{cr} = 0.25$, is a sufficient condition for the presence of steady-state turbulence, i.e., if satisfied, it guarantees that steady-state turbulence exists. The inequality $Ri < Ri_s = 0.7$ is a necessary condition for the presence of steady-state turbulence, i.e., it must be satisfied for steady-state turbulence to take place. This conclusion generally coincides with Abarbanel et al. (1984), who found, based on non-linear stability analysis, that the transition from turbulence to laminar flow takes place at $Ri = 1$. A similar conclusion was reached by Cheng et al (2002) and Fernando (2003).

Figure 6 shows the dependence between the Richardson number Ri and the stability parameter z/Λ_* . The plot was obtained by employing z/Λ_* as a sorting parameter for SHEBA data. As a result, the number of SHEBA data points differs from those in previous figures. The values in the figure generally agree with the results of Yagüe et al (2006). The figure shows, for example, that at $z/\Lambda_* \approx 4$, Ri is about 0.25, which coincides with the results of Businger et al. (1967) and Dyer (1974), and disagrees with Holtslag and De Bruin (1988) and Beljaars and Holtslag (1991), who obtained that the corresponding value of Ri is much higher, and in the range of 0.7 - 0.9.

The solid curve in Figure 6 is derived from the following equation:

$$\frac{z}{\Lambda_*} = Ri \frac{\psi_m^2}{\psi_h} = \frac{Ri (1 + 300Ri^2)^{9/4}}{0.9 (1 + 250Ri^2)^{3/2}} \quad (21)$$

which was obtained by using (7) and (17). It can be noted that the above expression is not affected by self-correlation. The equation indicates that the critical value $Ri_s = 0.7$ corresponds to the value $z/\Lambda_* \approx 50$.

Figure 6 shows an agreement between the solid curve and the data points for $z/\Lambda_* < 1$, and a disagreement for very stable conditions, when $z/\Lambda_* > 1$. We interpret this discrepancy as a result of using the stable parameter z/Λ_* as a sorting parameter and relatively large errors in evaluation of z/Λ_* in very stable conditions.

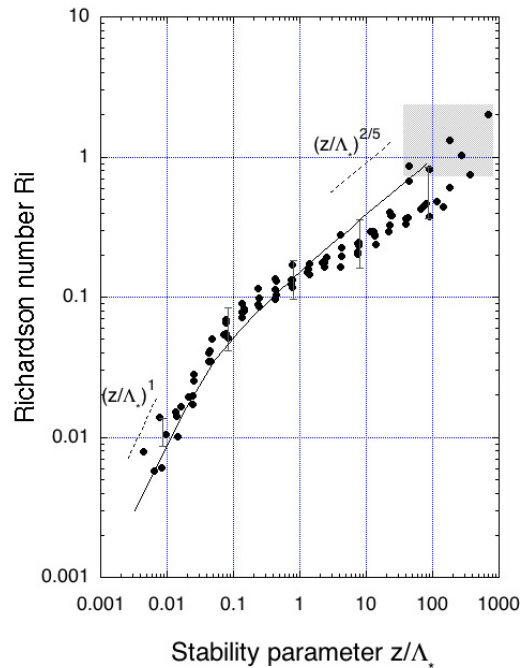


Figure 6. Dependence of the bin-averaged values of the gradient Richardson number Ri and the dimensionless height z / Λ_* . The solid line is based on Equation 21. The vertical lines represent the confidence intervals evaluated at level 5. The shaded box marks the “extremely-stable” domain.

Referring to Figure 6, we will identify four stable regimes, which can be present within the stable boundary layer. They can be named: “nearly-neutral”, “weakly-stable”, “very-stable”, and “extremely-stable”. In the “nearly-neutral” regime ($0 < z / \Lambda_* < 0.02$, or $0 < Ri < 0.02$), the dimensionless gradients ψ_m and ψ_h are nearly constant. The “weakly-stable” regime ($0.02 < z / \Lambda_* < 0.6$, or $0.02 < Ri < 0.12$) is the transition between “nearly-neutral” and “very-stable” conditions. In the “very-stable” regime ($0.6 < z / \Lambda_* < 50$, or $0.12 < Ri < 0.7$), the dimensionless gradients ψ_m and ψ_h are exponential. The presence of any scaling laws in “extremely-stable” conditions, when $z / \Lambda_* > 50$ and $Ri > 0.7$, is doubtful (e.g., Cheng et al., 2005), since turbulence in this case can be impacted by local influences, such as surface non-heterogeneity, or propagating gravity waves. The specified above regimes are controlled by local stability parameters and can generally occur at any height within the stably stratified boundary layer.

Acknowledgements

The author's appreciation is directed to Dr. A.A. Grachev of CIRES/NOAA for providing the processed SHEBA data and for evaluation of the confidence intervals. The work has been partly supported by the Central and Eastern Europe Climate Change Impact and Vulnerability

Assessment Project (CECILIA) financed by UE 6.FP, Contract GOCE 037005 to Warsaw University of Technology, Warsaw, Poland, and also by the National Science Foundation grant ATM-0938293.

References

Abarbanel HD, Holm DD, Mardsen JE, Ratiu T. 1984. Richardson number criterion for the nonlinear stability of three-dimensional stratified flow. *Physical Review Letters*. **52**: 2352-2355

Anderson PS. 2009. Measurement of Prandtl number as function of Richardson number avoiding self-correlation. *Boundary-Layer Meteorol*, 131: 345–362

Andreas EL, Hill RJ, Gosz JR, Moore D.I., Otto WD, and Sarma AD. 1998. Statistics of surface-layer turbulence over terrain with metre-scale heterogeneity, *Boundary-Layer Meteorol*, 86: 379-408

Andreas EL, Fairall CW., Guest PS., and Persson POG. 1999. An Overview of the SHEBA Atmospheric Surface Flux Program, 13th Symposium on Boundary Layers and Turbulence. Dallas, TX, Amer Meteorol Soc, Proceedings, 550–555

Andreas EL, Fairall CW, Grachev AA, Guest PS, Horst TW, Jordan RE, and Persson POG. 2003. Turbulent transfer coefficients and roughness lengths over sea ice: the SHEBA results. Seventh Conference on Polar Meteorology and Oceanography and Joint Symposium on High-Latitude Climate Variations, American Meteorological Society. 12–16 May 2003, Hyannis, Massachusetts, AMS Preprint CD-ROM

Andreas EL, Claffey KJ, Jordan RE, Fairall CW, Guest PS, Persson POG, Grachev AA. 2006. Evaluations of the von Kármán Constant in the Atmospheric Surface Layer. *J Fluid Mech*, 559: 117-149

Baas P, Steeneveld GJ, van de Wiel BJH, Holtslag AAM. 2006. Exploring Self-Correlation in Flux–Gradient Relationships for Stably Stratified Conditions. *J Atmos Sci*, 63: 3045–3054

Banta, RM, 2008, Stable-boundary-layer regimes from the perspective of the low-level jet. *Acta Geophys*. **56**: 58-87

Barenblatt GI. 1996. *Scaling, self-similarity laws, and intermediate asymptotes*. Cambridge Texts in Applied Mathematics 14, Cambridge University Press, 380 pp.

Beljaars ACM, Holtslag AAM. 1991. Flux parameterization over land surfaces for atmospheric models. *J Appl Meteor*, 30: 327-341

Blackadar, AK. 1962. The vertical distribution of wind and turbulent exchange in neutral atmosphere. *J Geoph Res*, 67: 3095-3103

Businger JA. 1973. Turbulent transfer in the atmospheric surface layer, Chapter 2 in: Workshop on Micrometeorology. Ed.: DA Haugen. Amer Meteorol Soc, 67-10

Businger JA, Miyake M, Dyer AJ, Bradley F. 1967. On the direct determination of the turbulent heat flux near the ground. *J Appl Meteor*, 6: 1025-1032

Cheng Y, Canuto VM, Howard AM. 2002. An improved model for the turbulent PBL. *J. Atmos. Sci*. **59**: 1550-1565.

- Churchill SW. 2002. A reinterpretation of the turbulent Prandtl number. *Ind Eng Chem Res*, 41: 6393-6401
- Coulter RL, Doran JC. 2002. Spatial and Temporal Occurrences of Intermittent Turbulence During CASES-99. *Boundary-Layer Meteorol*, 105: 329-349
- Cuxart J. 2008. Nocturnal basin low-level jets: an integrated study, *Acta Geophys*, 56: 100-113
- Dyer AJ. 1974. A review of flux profile relationship. *Boundary-Layer Meteorol*, 7: 363-372
- Esau I, Grachev A. 2007. Turbulent Prandtl Number in Stably Stratified Atmospheric Boundary Layer: Intercomparison between LES and SHEBA Data. *e-WindEng*, 006: 01-17
- Fernando HJS. 2003. Turbulent patches in stratified shear flow. *Physics of Fluids*. **15**: 3164-3169
- Galperin, B, Sukoriansky, S, and Anderson, PS. 2007. On the critical Richardson number in stably stratified turbulence, *Atmos Sci Letters*, ASL.153
- Grachev AA, Fairall CW., Persson POG, Andreas EL, and Guest PS. 2005. Stable boundary-layer scaling regimes: The SHEBA data, *Boundary-Layer Meteorol*, 116: 201-235
- Grachev AA, Andreas EL, Fairall CW, Guest PS, Persson POG .2007a. SHEBA Flux profile relationships in the stable atmospheric boundary layer', *Boundary-Layer Meteorol*, 124, 315 - 333
- Grachev AA, Andreas EL, Fairall CW, Guest PS, Persson POG .2007b. On the turbulent Prandtl Number in the Stable Atmospheric Boundary Layer, *Boundary-Layer Meteorol*, 125: 329 - 341
- Grachev AA, Andreas EL, Fairall CW, Guest PS, Persson POG .2008. Turbulent measurements in the stable atmospheric boundary layer during SHEBA: ten years after, *Acta Geophys*, 56: 142-166
- Holtslag AAM and De Bruin FTM. 1988. Applied modeling of night-time surface energy balance over land. *J Appl Meteor*, 27: 689-704
- Kader BA, Yaglom AM. 1990. Mean fields and fluctuation moments in unstably stratified turbulent boundary layers, *J Fluid Mech*, 212: 637-662
- Klipp, CL, Mahrt L. 2004. Flux-gradient relationship, self-correlation and intermittency in the stable boundary layer, *Quart J Roy Meteorol Soc*, 130: 2087-2103
- Kukharets VP, Tsvang LR. 1998. Atmospheric Turbulence characteristics over a Temperature-Inhomogeneous Land Surface. Part I: Statistical characteristics of small-scale spatial inhomogeneities of land surface temperature. *Boundary-Layer Meteorol*. 86: 89-101
- Mahrt, L. 1998. Stratified atmospheric boundary layers. *Boundary-Layer Meteorol*, 90: 375-396
- Mahrt L. 1999. Stratified atmospheric boundary layers. *Boundary-Layer Meteorol*, 90: 375-296
- Monin AS, Obukhov AM. 1954. Basic laws of turbulence mixing in the surface layer of the atmosphere. *Trudy Geof. Inst. AN SSSR*, 24: 163-187
- Newsom KR, Banta RM. 2003. Shear-flow instability in the stable nocturnal boundary layer as observed by Doppler lidar during CASES-99. *J Atmos Sci*, 60: 16-33
- Nieuwstadt FTM. 1984. The turbulent structure of the stable, nocturnal boundary layer. *J Atmos Sci*, 41: 2202-2216

- Oyha YD, Neff E, Meroney EN. 1997. Turbulence structure in a stratified boundary layer under stable conditions. *Boundary-Layer Meteorol*, 83: 139-161
- Oyha YD. 2001. Wind tunnel study of atmospheric stable boundary layers over a rough surface. *Boundary-Layer Meteorol*, 98: 57-82
- Persson POG, Fairall CW, Andreas EL, Guest PS, Perovich DK. 2002. Measurements near the atmospheric surface flux group tower at SHEBA: Near-surface conditions and surface energy budget. *J Geophys Res*, 107, 8045, doi: 10.1029/2000JC000705
- Prandtl, L. 1932 *Meteorologische Anwendungen der Stromungslehre*. *Beitr Phys Atmosph*, 19: 188-202.
- Sorbjan Z. 1986a. On similarity in the atmospheric boundary layer. *Boundary-Layer Meteorol*, 34: 377 - 397
- Sorbjan Z. 1986b. On the vertical distribution of passive species in the atmospheric boundary layer. *Boundary-Layer Meteorol*, 35: 73-81
- Sorbjan Z. 1986c. Local similarity of spectral and cospectral characteristics in the stable-continuous boundary layer. *Boundary-Layer Meteorol*, 35: 257-275
- Sorbjan Z. 1988. Structure of the stably-stratified boundary layer during the Sesame-1979 experiment. *Boundary-Layer Meteorol*, 44: 255-260
- Sorbjan, Z. 1989. *Structure of the Atmospheric Boundary Layer*. Prentice-Hall, 316 pp.
- Sorbjan, Z. 2006a. Local structure of turbulence in stably-stratified boundary layers. *J Atmos Sci*, 63: 526-537
- Sorbjan Z. 2006b. Comments on "Flux-gradient relationship, self-correlation and intermittency in the stable boundary layer". *Quart J Roy Meteorol Soc*, B, 617, 132: 1371-1373
- Sorbjan Z, Balsley BB .2008. Microstructure of turbulence in the nocturnal boundary layer. *Boundary-Layer Meteorol*, 129: 191-210
- Sorbjan Z .2010. Scaling and similarity laws in the stable boundary layer. Submitted to *Quart J Roy Meteorol Soc*.
- Sorbjan Z, Grachev AA. 2010. An evaluation of the flux-gradient relationship in the stable boundary layer. Accepted to *Boundary-Layer Meteorol*.
- Tsvang LR, Kukharets VP, Perepelkin VG. 1998. Atmospheric turbulence characteristics over a temperature-inhomogeneous Land Surface. Part II: The effect of small-scale inhomogeneities of surface temperature on some characteristics of the atmospheric surface layer, *Boundary-Layer Meteorol*, 86: 103-124
- Van de Wiel BJH, Moene A, Hartogenesis G, De Bruin HA, and Holtslag AAM. 2003. Intermittent turbulence in the stable boundary layer over land. Part III. A classification for observations during CASES-99. *J Atmos Sci*, 60: 2509-2522
- Yagüe C, Viana S, Maqueda G, Redondo JM. 2006. Influence of stability on the flux-profile relationships for wind speed, φ_m , and temperature, φ_h , for the stable atmospheric boundary layer. *Nonlin Processes Geophys*, 13: 185-203

Zilitinkevich S, Elperin T, Kleorin N, Rogachevskii I, Esau I, Mauritsen T, Miles M. 2008. Turbulence energetics in stably stratified geophysical flows: strong and weak mixing regimes. *Quart J Roy Meteorol Soc*, 134, 793-799

BRAND
PAPER

Bellasio R. and R. Bianconi 2010. *Coupling Meteorological and Air Quality Models*. Chapter 5E of *AIR QUALITY MODELING - Theories, Methodologies, Computational Techniques, and Available Databases and Software. Vol. IV – Advances and Updates* (P. Zannetti, Editor). Published by The EnviroComp Institute (<http://www.envirocomp.org/>) and the Air & Waste Management Association (<http://www.awma.org/>).

Chapter 5E

Coupling Meteorological and Air Quality Models

Roberto Bellasio and Roberto Bianconi

Enviroware srl, via Dante 142, 20049 Concorezzo (MB) (Italy)
info@enviroware.com , <http://www.enviroware.com>

Abstract: Current computational and storage capabilities allow running highly complex computer codes in very short times over large domains with high time resolution over long periods. This computational power has stemmed a series of new developments in the creation of three-dimensional air quality models that are integrated into a meteorological model (online modeling) or can make use of most widely used meteorological models (offline modeling). This chapter presents the main features of meteorological models and the relevant aspects that need to be considered when setting up some software for offline coupling.

Key Words: meteorological models, air quality models, offline coupling, meteorological input.

1 Introduction

Air quality models (AQMs) are computer codes that solve numerically or implement analytical solutions to the conservation equations for pollutant masses. They are a necessary tool for evaluating and predict air quality at different scales in space and time.

The dispersion of pollutants in the atmosphere is strongly influenced by meteorological conditions that, in turn, can be observed or estimated. While there are conditions where meteorology does not change significantly over the domain of interest, in several applications it is important to account for the variations of

meteorological variables in space and time. These latter cases are where using a meteorological model is a need.

In general, the model complexity that should guarantee the more precise accounting of the physics (and chemistry) of atmospheric processes comes at a higher cost of meteorological input complexity. For this reason it is important to select the right type of air quality model depending on the problem that is faced.

In fact, the great success of simpler analytical models, such as the Gaussian one, is also due to the limited set of meteorological variables needed and their homogeneity. For example, it is sufficient to only have a single measurement of the average wind speed and direction and an estimate of atmospheric stability in terms of Pasquill-Gifford class, to compute with acceptable precision the concentration close to the source of an inert pollutant emitted from a non-buoyant source. This applies when the atmospheric stability is neutral or stable so that the planetary boundary layer height does not play a main role in first approximation.

There are, however, many situations where more measurements must be used and fed into a meteorological model that can compute three-dimensional fields of meteorological variables over a large area. These meteorological data can then drive complex non-stationary and non-homogeneous dispersion models.

Air quality and meteorology modeling were traditionally separated prior to the 1970's (Zhang, 2008). The three-dimensional chemical transport models until that time were driven by either measured or analyzed meteorological fields at a time resolution of 1–6 h from a mesoscale meteorological model on urban/regional scales, or by outputs at a much coarser time resolution (e.g., 6-h or longer) from a global circulation model (GCM). This technique is referred to as *offline coupling* or *offline modeling*. Offline modeling refers to when there is no feedback from the atmospheric chemistry in the CTM to the meteorological simulations, as would occur with the impacts of particulate matter on radiation, clouds, and precipitation. This absence of feedback is the main disadvantage, together with the large amount of data exchange, of the offline modeling, because it may result in a loss of important process information that occurs at a time scale smaller than that of the outputs from the offline meteorology models. Such feedbacks, on the other hand, can be simulated in *fully-coupled online models*, without space and time interpolation of meteorological fields but commonly with higher computational costs.

Both offline and online models are actively used in current regional and global models. Offline models are frequently used in ensembles, operational forecasting and sensitivity simulations. Online models are increasingly used for applications in which the feedbacks become important (e.g., locations with high frequencies of clouds and large aerosol loadings) and when the local scale wind and circulation systems change quickly. For online models, the coupled meteorology-air quality

modeling is essential for accurate model simulations (e.g., real-time operational forecasting or simulating the impact of future climate change on air quality).

This chapter deals with offline modeling. Some examples of online-coupled modeling are described by Zhang (2008). In this chapter, meteorological models are discussed, presenting for both diagnostic and prognostic, which are the relevant features. Also discussed are the advantages and disadvantages of their use compared to the other models. The discussion then focuses on the coupling, pointing out the relevant aspects to be tackled whereupon examples of couplings are then introduced. At the end of this chapter we provide some useful resources of geophysical and meteorological data located on the Internet.

2 Meteorological Data

Meteorology is a primary factor affecting actual and simulated air quality, therefore it is very important to measure and assess it in a reliable way. In a limited number of situations, meteorological observations can be used directly as input to AQMs. Instead, meteorological measurements are generally used as input to meteorological models, integrated when necessary with parameterizations of processes that are not measured.

2.1 Meteorological Observations

The simplest interfacing between meteorology and AQMs are based on the direct use of measurements. This is typically limited to Gaussian models.

Meteorological observations can be made at ground level and aloft. They are either routinely made (e.g. meteorological and air quality stations, airports) or on the spot for specific needs (e.g. measuring campaigns). While measurements at ground are generally available with hourly resolution, measurements aloft are made in general up to two times per day (at main airports).

Most meteorological measurements carried out at surface level (typically 10 m AGL for wind and 2 m AGL for temperature) give information about wind speed and direction, temperature, relative humidity, precipitation and pressure. Some also include net radiation and cloud cover (this last especially at airports). Sonic anemometers, which can take measurements with very fine temporal resolution (20 Hz or better and are therefore suited for turbulence and heat exchange measurements), are not so diffuse in routine meteorological stations. These hourly routine meteorological observations are almost always carried out at a single level above the ground, and therefore the vertical profile of the variables is missed.

Routine measurements aloft are made with rawinsondes that measure wind speed and direction, temperature, relative humidity and pressure. Other measurements that include turbulence are made with SODARs.

These measurements at surface and aloft are often enough to characterize the meteorological conditions for applying simpler dispersion models. In fact, starting from a limited set of observed parameters (wind speed, temperature, cloud cover and land use) it is possible to apply some schemes that define the structure of the surface layer.

The characterization obtained, however, is site-specific and it is only valid close to the location where measurements are taken. When an evaluation of a wider area is required, especially when measurements show clearly that observations within the area significantly differ; it is necessary to rely on a meteorological model.

2.2 Meteorological Models

There are many situations where the use of a meteorological model must be preferred to the use of meteorological measurements. This is when the meteorological conditions are not homogeneous over the domain of interest, for example in presence of complex terrain as well as on coastal areas.

The resulting complex wind circulation affects the transport and diffusion of pollutants and recirculation patterns can develop. Also, the extent of the mixing layer can change abruptly, especially at coastal sites where a thermal internal boundary layer (TIBL) develops. These features are not described by point measurements.

At a bare minimum, in order for models to catch these circulation features it is necessary that they adequately describe the terrain elevation and the land use with sufficient accuracy. This is generally obtained with small enough grid cells.

As pointed out in Brode and Anderson (2008), it is important to recognize that while a 3D meteorological model can generate spatially varying three dimensional wind fields, this does not guarantee that the wind fields generated by said model will provide a more appropriate treatment of plume transport and dispersion. This also does not necessarily result in an improved estimate of concentrations compared to a dispersion model based on single meteorological station measurements.

Meteorological models can be broadly divided into diagnostic and prognostic categories and in these terms they are described hereafter.

Diagnostic meteorological models reconstruct the three-dimensional wind and temperature field over domains extending up to thousands of square kilometers. They are called diagnostic because they try to reconstruct a dynamically consistent wind field starting from “observations” at surface and aloft. These observations are either real measurements or data coming from another meteorological model output at a larger scale. The consistency is often found by

applying the continuity equation in order to estimate the vertical wind components starting from the horizontal ones and imposing the conservation of mass (minimization of divergence).

These models start from sparse values at ground level of meteorological variables including at least wind speed and direction, temperature and cloud cover. The input also includes upper air data (height above ground, wind speed and direction, temperature). Diagnostic models also use as input, the terrain height and the land use for each cell of their regularly gridded computational domain.

Typically an initial guess wind field is adjusted for kinematic effects of terrain, slope flows, and terrain blocking effects to produce a first wind field estimate. Then an objective analysis procedure is used to introduce observational data into the previous step wind field to produce a final wind field, also based on mass conservation. Measured winds contribute to grid points where the wind is reconstructed with a weight that decreases with distance.

Diagnostic models include micrometeorological modules for the computation of the sensible heat flux, the Monin-Obukhov length and the velocity scales in the planetary boundary layer. These variables are used to compute the height of the planetary boundary layer and the turbulent dispersion coefficients for the dispersion models.

Diagnostic models can also receive as input relative humidity and precipitation rate values from sparse points and interpolate them to the regular output grid.

Prognostic (or dynamical) meteorological models are based on the complete solution of all the equations for the hydrodynamic flow. This set of equations is numerically solved after the introduction of some simplifications. The most important simplification is perhaps the one, which distinguishes the models in hydrostatic and non-hydrostatic. Hydrostatic models are those in which the vertical equation of motion contains only gravity and the vertical pressure gradient while the vertical acceleration is ignored (vertical acceleration is maintained in non hydrostatic models). The hydrostatic assumption is acceptable at scales greater than about 10 km, while it is not acceptable at smaller scales. Prognostic models have the advantage to be able, in theory, to predict all the meteorological fields, even at small scales, independently from the set of measures (which is instead fundamental for diagnostic models). This strength is also a weak point for prognostic models because after a simulation has started, during the simulation, there is no more comparison with the measurements; therefore possible numerical errors cannot be solved. The Four Dimensional Data Assimilation (FDDA) technique has been recently introduced in some prognostic models to use observations in order to correct possible prediction errors.

Prognostic models solve the conservation equations in Eulerian framework and they can be applied at any scale in space and time. They require a proper

initialization and the correct description of boundary conditions for the whole duration of the simulation.

Prognostic models include the calculation of the PBL evolution as well as all the description of convective precipitation, distribution of atmospheric water vapor content and cloud physics.

The higher complexity of prognostic models comes at a computational cost that might not be convenient for some air quality applications that require results in relatively short time periods.

2.3 Comparison of Diagnostic and Prognostic Model Features

Both diagnostic and prognostic meteorological models have some important favorable characteristics, one compared to the other. Considering diagnostic models, since they are "reinitialized" by the measures at each hour, there is no accumulation of errors as the time evolves. On the other hand, since they need observations that are carried out at hourly intervals (when not at longer times), their time resolution can be not less than 1 hour.

Diagnostic meteorological models are easier to get acquainted with and less consuming in terms of computational times and input/output data storage. This is particularly important in air quality studies. In fact, air quality legislation establishes limits that often require the analysis of the hourly concentrations for at least one full year. The European legislation, for example, in order to protect the human health, establishes that the 1-hour average concentration of NO₂ must not exceed 200 µg/m³ more than 18 times in one year. This means that AQMs, in order to be useful planning tools, must be capable of estimating the 1-hour pollutant(s) concentration for a whole year over a fine grid mesh. Therefore the input meteorological variables to AQMs must be available at least with the same space and time resolution, and must be reliable.

The capability to obtain the 3D meteorological fields for one or more years with hourly time resolution and fine grids (e.g. 250 m) is of fundamental importance in obtaining the statistics of interest from the AQMs.

Moreover, the fact that these models directly use as input, the meteorological observations guarantees that the model output will almost reproduce the input at the same location. This is particularly important when a measurement is available close to an emission source of interest because it guarantees that the initial dispersion is based on the observed values.

Diagnostic models however have some limitations. These are mainly the limited physics they describe and the fact that they do not have prediction capabilities. In fact they can only run with past observations or using the output of a prognostic model as a provider of forecast meteorological input.

A generic limitation of all the gridded models is related to their ability to simulate terrain generated wind fields (Brode and Anderson, 2008). This ability is limited by the horizontal resolution of terrain and land use data on the model grid. For example, a river valley that is about 1 kilometer wide from peak to peak and about 500 meters deep would not be adequately resolved by a 250-meter grid spacing. This is because a single grid cell could span the entire valley wall from ridge top to river level, such that the slopes of the valley walls represented by gridded terrain elevations could be highly reduced. This effect significantly affects the gravity driven slope flows and other diagnostic wind field adjustments.

Also, diagnostic models do not compute turbulence and can only provide some parameters that can be used as input for parameterizations that were found from the analysis of datasets of observations and are reported in literature.

The prognostic wind fields in some cases have the advantage to better represent regional flows and certain aspects of sea breeze circulations along with slope/valley circulations where dynamical consistency is required.

Also, they can incorporate the dispersion equations for one or more species, and this allows accounting for feedback effects that pollutants can have on meteorology. An example of this is the attenuation of solar radiation due to the presence of particulate matter with variable size.

The complexity and more exhaustive description of the involved physical processes make these models more prone to numerical errors. Also this requires a large set of input parameters and data that might be more difficult to collect and store as opposed to the requirements for diagnostic models.

Some pros and cons of diagnostic and prognostic models are summarized in the following table.

Table 1. Pros and Cons of diagnostic and prognostic models.

	PROS	CONS
DIAGNOSTIC	<ul style="list-style-type: none"> - no error propagation - fast computer codes meteo input and output are locally consistent 	<ul style="list-style-type: none"> - high frequency of input data - reduced set of equations - no predictive capabilities - turbulence of wind not computed limited capability of producing effects that were not observed
PROGNOSTIC	<ul style="list-style-type: none"> - prognostic capabilities - computation of turbulence - more complete description of physical processes - possibility to integrate a dispersion model (online modeling) 	<ul style="list-style-type: none"> - heavier computational costs - propagation of errors unless complex FDDA is incorporated

The choice of a diagnostic or a prognostic model is not straightforward. For example, Hu et al. (2010) predicted the PM_{2.5} concentrations for the California Regional Particulate Air Quality Study (CRPAQS) using the CIT/UID (Kleeman and Cass, 2001) air quality model run. Plus, using meteorological output from a diagnostic objective analysis method and the output of the prognostic WRF model (Skamarock et al., 2008) initialized with that analysis and, as a third option, integrated with four-dimensional data assimilation (FDDA).

The results using the diagnostic analysis as meteorological input were superior to those of the prognostic model alone. When the FDDA was used it gave better results than the diagnostic input configuration.

Seaman (2000) describes a number of features of the meteorological models for air quality applications.

3 The Coupling

As discussed before, while the online modeling has a number of advantages, the offline modeling offers the possibility to use one of the state-of-the-art meteorological models with any given air quality model. Also, an offline coupling is necessary when the time-space domain of the application of the air quality model is smaller than that of the meteorological model.

Due to all the differences among meteorological models as well as among air quality models, it is necessary - for offline modeling - to develop some ad-hoc software that can transfer the meteorological output to the air quality model, completing the required information that is missing with some computed fields.

The common issues that must be considered when coupling a meteorological three-dimensional model with an air quality model include:

- Data format conversion
- Effects of boundaries
- Sub-domain selection
- Interpolation in horizontal and vertical directions
- Coordinate system conversion
- Conversion of classification schemes
- Conversion of units
- Calculation of additional parameters
- Integration with additional observations

Models can have standard formats for their input/output files (e.g. GRIB, NetCDF, GDAS) but often they have a proprietary format that requires one to incorporate in the coupling code the routines that can decode the meteorological model output and make the *data format conversion* required by the air quality model.

While this is a mere software task, all other issues are not limited to the development of a generally complex software, but they involve a number of considerations on the physics of the models and the scope of the application.

Meteorological models are all based on an Eulerian formulation. They solve the conservation equations and boundary effects thus affect them. This is especially true for mass conservation. For this reason it is always a good choice to locate the domain of the dispersion model within the domain of the meteorological model, so that no information is missing and the boundary effects that may be present in the meteorological model output do not influence the extracted meteorological fields. The need for an appropriate *sub-domain extraction* holds for both the horizontal and the vertical direction: the top of dispersion model must be well below the top of the meteorological model.

The horizontal and vertical cell sizes might not match the sizes of the dispersion model. For this reason it may be necessary to apply an *interpolation in horizontal and vertical directions* to obtain the meteorological model output at different locations in space.

Along the *horizontal*, since the domain of the dispersion model is smaller than the meteorological model domain, there might be cases where the coordinate systems are different. For example, coordinates are in longitude/latitude degrees for the meteorological model (where the distance between adjacent grid points is not

conserved) and the coordinates are in metric for the dispersion model. Moreover, meteorological models running at large scale, as in case of regional models that may cover a portion of an entire continent or more, generally use longitude and latitude coordinates. Since there are a number of existing projections, the coupling software should be able in such cases to make a *coordinate system conversion*.

The interpolation along the *vertical* can be more complex than for the horizontal: there are in fact many vertical coordinate systems that are not necessarily based on the height above some reference but they can be expressed in terms of pressure. This means that the vertical coordinate system can even be time variable at a given location (mass coordinates), as for example in the case of the meteorological model WRF.

For this reason it is important that the coupler, in the case of an Eulerian air quality model, can guarantee the mass conservation. This is especially important in presence of complex terrain. Usually conservation is obtained with the adjustment of vertical velocity with numerical schemes of different complexity that can even be incorporated in the air quality model (Hu and Odman, 2008).

Interpolations along the vertical may also require that the profile of height dependence of variables is known. There are in fact several variables that do not have a linear-with-height profile. For example, the mixing ratio or the vertical potential temperature in the PBL during typical daytime conditions are almost uniformly distributed along the vertical in the bulk of the mixed layer, but their profile is different in the surface layer and in the entrainment zone at the top (e.g. Stull, 1988). This might require that the coupling software incorporate some equations that allow estimating the elevation of the mixing layer and some parameters that allow identifying the stability conditions (e.g. Monin-Obukhov length, Richardson bulk number, etc.).

Both the meteorological and the dispersion model may use some input data that are described in terms of classes with corresponding values for one or more parameters. One clear example is the land use type, which is categorized in a number of discrete classes, each of them characterized by a specific value of albedo, roughness length, Bowen ratio, leaf area index (LAI) and others. If any of these parameters is used by the air quality model, it might be necessary to perform a *conversion of classification schemes* to assign the land use classes of the meteorological model to those that are in use in the air quality model. This conversion may include some modification to one or more of the parameters so that they are consistent with the classification that is in use in the air quality model.

Care must be given to *units* in use by the models, so that the values are always properly converted, if needed.

In some cases it is necessary to implement the *calculation of additional parameters*. In fact, depending on the meteorological model, there are many variables that might not be computed or produced in output. For example when coupling an air quality model such as AERMOD that bases the diffusion schemes on the scaling parameters of the boundary layer to a meteorological model as WRF, it is necessary to compute from available output fields some variables as convective scale velocity and mechanical mixing height that are then used for the calculation of the vertical and lateral turbulent fluctuations (Kesarkar et al., 2007). The available output from the meteorological model drives the choice of the approach. For example the calculation of turbulent fluctuations for AERMOD using MM5 or the Eta model (Black, 1994) can go through parameterizations based on the turbulent kinetic energy (Isakov et al., 2007).

Depending on the application of the air quality model and the processes implemented, it is sometimes useful to include in the coupler the *integration with additional observations* as well as the incorporation of datasets that are not included in the meteorological model output. For example this is the case of clouds information that can be acquired from satellite imaging and used in the air quality model in wet deposition and photolysis calculations.

4 Examples of Coupling Processors

The general concepts of the previous paragraph are discussed here in specific context, with description of software couplers that are commonly used.

Air Quality Models (AQMs) require different meteorological input variables depending on their type. Simple Gaussian models require basically only the horizontal components of wind field (wind speed and wind direction), mixing height, Pasquill-Gifford stability classes and temperature for plume rise calculation. Advanced Gaussian models are capable of estimating dry and wet deposition, and for this purpose they require additional meteorological data such as precipitation, mechanical and convective scale velocities (u_* and w_*) and a few others. Moreover Gaussian models require the meteorological variables for a single point, which must (should) be representative for the whole simulation domain.

A broad distinction among more complex air quality models is generally made on the reference frame used to develop the equations that describe the fate of pollutants. There are two different approaches, the Eulerian and the Lagrangian one. The Eulerian framework is fixed and the equations are expressed in terms of fluxes while the Lagrangian one is linked to each portion of fluid considered and moves with it.

The Eulerian gridded approach is based on the mass conservation of the species under the assumption that velocity and temperature of the fluid are not influenced

by the concentration of the pollutant, so that the mass balance equation is not coupled to the energy and momentum conservation equations. The calculation domain is made of computational volumes within which all the conservation equations are numerically solved. The basic equations of the Eulerian gridded models are reported, for example, in Zannetti (1990) and Seinfeld and Pandis (1998).

Eulerian and Lagrangian numerical models require additional meteorological variables, such as the vertical wind component and the Monin Obukhov length to describe turbulence (in place of the Pasquill Gifford Classes). These variables must be available for a 3-D domain.

Very complex AQMs, capable of predicting the formation of secondary pollutants, both in gas and aerosol phase, require even more variables such as the solar actinic flux and the water vapor mixing ratio.

4.1 MM5CAMX and WRF-CAMX Processors

The Comprehensive Air quality Model with extensions (CAMx) is a publicly available open-source computer modeling system for the integrated assessment of gaseous and particulate air pollution (<http://www.camx.com>). CAMx is designed to simulate air quality over many geographic scales, treat a wide variety of inert and chemically active pollutants (ozone, inorganic and organic PM_{2.5}/PM₁₀, mercury and toxics), provide source-receptor sensitivity and process analyses, and be computationally efficient along with easy to use.

The meteorological inputs needed by CAMx are 3-dimensional gridded fields of: horizontal wind components, temperature, pressure, water vapor, vertical diffusivity, clouds and rainfall; which should be generated by self-consistent meteorological models (MM5, WRF, RAMS, etc.).

The MM5 mesoscale model of PSU/NCAR (<http://www.mmm.ucar.edu/mm5/>) is a limited-area, non-hydrostatic, terrain-following sigma-coordinate model designed to simulate or predict mesoscale atmospheric circulation. The model is supported by several pre- and post-processing programs, which are referred to collectively as the MM5 modeling system.

MM5 can be used for a broad spectrum of theoretical and real-time studies, including applications of both predictive simulation and four-dimensional data assimilation to monsoons, hurricanes and cyclones. On the smaller meso-beta and meso-gamma scales (2-200 km), MM5 can be used for studies involving mesoscale convective systems, fronts, land-sea breezes, mountain-valley circulations and urban heat islands.

The Weather Research and Forecasting (WRF) model (<http://wrf-model.org>) is a NWP and atmospheric simulation system designed for both research and operational applications. The model is suitable for a broad span of applications across scales ranging from large-eddy to global simulations, and can be configured for both research and operational applications.

The development of WRF has been a collaborative effort among the National Center for Atmospheric Research's (NCAR) Mesoscale and Microscale Meteorology (MMM) Division, the National Oceanic and Atmospheric Administration's (NOAA) National Centers for Environmental Prediction (NCEP) and Earth System Research Laboratory (ESRL), the Department of Defense's Air Force Weather Agency (AFWA) and Naval Research Laboratory (NRL), the Center for Analysis and Prediction of Storms (CAPS) at the University of Oklahoma and the Federal Aviation Administration (FAA) with the participation of university scientists.

WRF is maintained and supported as a community model to facilitate wide use internationally, for research, operations, and teaching. There are thousands of WRF users around the World.

The WRF software framework provides the infrastructure that accommodates the dynamics solvers, physics packages that interface with the solvers and programs for initialization (WRF-Var and WRF-Chem).

There are two dynamics solvers in the WRF software framework: the Advanced Research WRF (ARW) solver (originally referred to as the Eulerian mass or "em" solver) developed primarily at NCAR, and the NMM (Non-hydrostatic Mesoscale Model) solver developed at NCEP. The software framework includes also the WRF-Chem model, which provides capabilities for air chemistry modeling.

An Arakawa C horizontal grid characterizes the WRF model along with terrain-following hydrostatic-pressure vertical coordinates.

One of the activities in coupling meteorology models and CTM is to interpolate the variables on the same grid scheme. For example, MM5 data are on an Arakawa B grid with flip of i, j indices from standard configuration, while CAMx data are on an Arakawa C grid. These two Arakawa grid schemes are graphically illustrated in Figure 1 where scalars are calculated at the center of the grid cells in both schemes, while the difference is the position where wind components are calculated. Considering WRF, both WRF and CAMx data are calculated on Arakawa C grids.

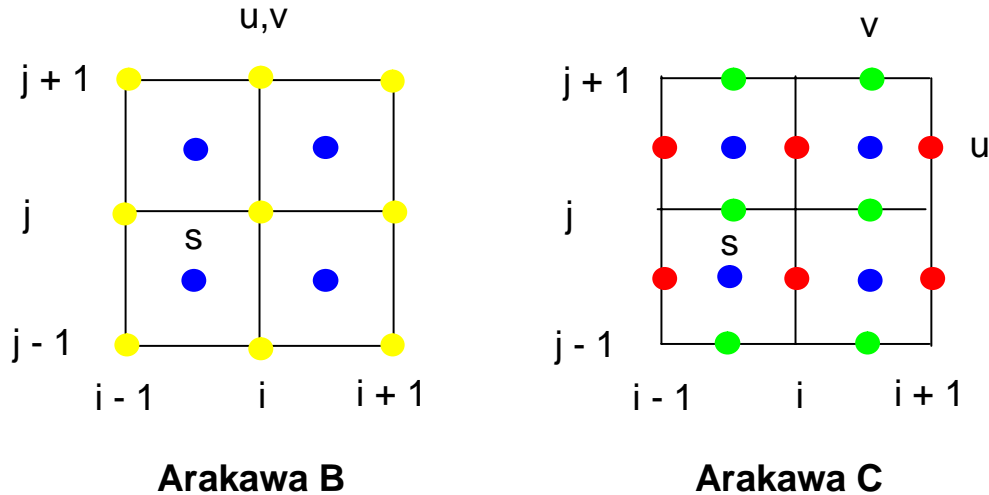


Figure 1. A simple graphical illustration of the Arakawa B (left) and the Arakawa C (right) horizontal grids. Scalars are in the center of the grids for both schemes (blue circles); u and v wind components are at the corners of the grids in Arakawa B (yellow circles); u and v components are at the center of the vertical and horizontal grid faces respectively in Arakawa C (red and green circles respectively).

The two CAMx processors contain three different interpolation routines: INTERP_CART, INTERP_GEO and INTERP_LCP, which are called accordingly to the coordinates projection used. INTERP_CART and INTERP_GEO basically carry out the same operations: rotate wind direction if needed, interpolate wind and all the other variables from the MM5 Arakawa B or WRF Arakawa C to cell centers on the CAMx grid, and finally vertically aggregate the variables from the MM5 sigma-p coordinate system to the CAMx vertical coordinate system. INTERP_LCP is used when the CAMx domain is a small window of the meteorology domain, this routine horizontally interpolates from the MM5 Arakawa B or WRF Arakawa C to the CAMx grid.

After the variables interpolation, the vertical dispersion coefficient must be calculated. This procedure can be done using three routines based on the O'Brian (1970) methodology (KVCALC_OB70), the CMAQ ACM2 methodology (KVCALC_ACM2) described by Pleim (1997), and the TKE methodology (KV_TKE) employed in RAMS (Mellor and Yamada, 1974/1982; Helfand and Labraga, 1988).

After these processes, followed by operations on cloud fields, water contents, cells with snow, topography and renormalization of land use, output files with CAMx format are produced.

4.2 CMAQ Meteorology-Chemistry Interface Processor (MCIP)

The Community Multiscale Air Quality modeling system (Byun and Schere, 2006), best known as CMAQ (<http://www.cmaq-model.org>) simulates atmospheric processes and air quality (including gas-phase chemistry, heterogeneous chemistry, particulate matter, and airborne toxic pollutants) over a broad range of spatial and temporal scales using a comprehensive computational framework based on first-principles solutions. The CMAQ modeling system is considered to be the state-of-the-science for Eulerian air quality modeling. It is widely used for a variety of retrospective, forecasting, regulatory, climate, atmospheric process-level and emissions control applications. CMAQ is used by local, state, and national government agencies, at academic institutions and in private industry.

MCIP uses MM5 or WRF-ARW output files to create netCDF based input meteorology for the emissions model and the CCTM. The CMAQ CTM uses Arakawa C horizontal staggering (Figure 1), where the horizontal wind components are on perpendicular cell faces and all other prognostic fields are defined at the cell centers. MCIP performs the following functions (Otte and Pleim, 2010):

- Extracts meteorological model output for the CTM horizontal grid domain. MM5 data are on an Arakawa B grid; therefore there is a difference in the physical locations of the wind components between the MM5 and CMAQ. Interpolating the raw MM5 wind components in MCIP from the cell corners to the cell faces is necessary to use them in CMAQ. On the contrary both WRF-ARW and CMAQ use an Arakawa C-staggered horizontal grid, so horizontal interpolation is in principle not required. Since the plume rise calculations in the emissions processor still expect wind components on the cell corners regardless of the input meteorological model, wind components are interpolated to the Arakawa B grid to satisfy this requirement (Otte and Pleim, 2010).
- Processes all required meteorological fields for the CTM and the emissions model.
- Collapses meteorological model fields, if coarser vertical resolution data are desired for the CTM. MCIP uses mass-weighted averaging on higher vertical-resolution meteorological model output.
- Optionally computes surface and planetary boundary layer (PBL) fields using output from the meteorological model.
- Computes dry-deposition velocities for important gaseous species using the surface and PBL parameters. MCIP can compute dry deposition using two methods: the RADM dry deposition method (Wesely, 1989) calculates deposition velocities of 13 chemical species using friction velocities and aerodynamic resistances. Inputs required for this method include temperature, humidity, and horizontal wind component profiles. The surface exchange aerodynamic method (Pleim et al., 2001) uses

surface resistance, canopy resistance, and stomatal resistance to compute dry deposition velocities.

- Computes cloud top, cloud base, liquid water content, and cloud coverage for cumuliform clouds using simple convective schemes.
- Outputs meteorological/geophysical files in the I/O API format, which is standard within the Models-3 framework.

Appel et al. (2010) presented a comparison of the operational performances of two CMAQ simulations that utilize input data from MM5 and WRF meteorological models. Two sets of CMAQ model simulations were performed for January and August 2006, one set utilized MM5 meteorology (MM5-CMAQ) and the other utilized WRF meteorology (WRF-CMAQ), while all other model inputs and options were kept the same. The results of the simulations have shown some differences, which are primarily caused by the differences in the calculation of wind speed, planetary boundary layer height, cloud cover and friction velocity in the MM5 and WRF model simulations. Differences in the calculation of vegetation fraction and several other parameters result in smaller differences in the predicted CMAQ model concentrations.

4.3 The CALMET Meteorological Processor of CALPUFF

CALPUFF (Scire et al., 2000b) is a multi-layer, multi-species non-steady-state puff dispersion modeling system that simulates the effects of time- and space-varying meteorological conditions on pollutant transport, transformation, and removal. CALPUFF is intended for use on scales from tens of meters from a source to hundreds of kilometers. It includes algorithms for near-field effects such as stack tip downwash, building downwash, transitional buoyant and momentum plume rise, rain cap effects, partial plume penetration, subgrid scale terrain and coastal interactions effects and terrain impingement. It also has longer range effects such as pollutant removal due to wet scavenging and dry deposition, chemical transformation, vertical wind shear effects, overwater transport, plume fumigation and visibility effects of particulate matter concentrations.

CALPUFF is appropriate for long-range transport (source-receptor distances of 50 to several hundred kilometers) of emissions from point, volume, area, and line sources. The meteorological input data should be fully characterized with time- and space-varying three-dimensional wind and meteorological conditions using CALMET. CALPUFF may also be used on a case-by-case basis when the model is more appropriate for the specific application. The purpose of choosing a modeling system like CALPUFF is to fully treat stagnation, wind reversals, and time and space variations of meteorological conditions on transport and dispersion.

Beside the 3-D meteorological fields developed by the CALMET diagnostic meteorological model, CALPUFF can use single station meteorological data stored in format used by other dispersion models (ISC3ST, AUSPLUME,

CTDMPLUS). However single station meteorological files do not allow CALPUFF to take advantage of its capabilities to treat spatially varying meteorological fields.

CALPUFF produces files of hourly concentrations of ambient concentrations for each modeled species, wet deposition fluxes, dry deposition fluxes, and for visibility applications and extinction coefficients.

CALMET (Scire et al., 2000a) is a diagnostic meteorological model that reconstructs the 3-D wind and temperature fields starting from meteorological measurements, orography and land use data. Besides the wind and temperature fields, CALMET determines the 2-D fields of micro meteorological variables needed to carry out dispersion simulations (mixing height, Monin-Obukhov length, friction velocity, convective velocity and others). CALMET uses a terrain following vertical coordinate system. The vertical wind component w is defined at the vertical cell faces, while the other variables are defined at grid centers.

The boundary layer module of CALMET allows for calculating 2D gridded fields of surface friction velocity, convective velocity scale, Monin-Obukhov length, mixing height and Pasquill-Gifford-Turner (PGT) stability classes.

CALMET adopts two different boundary layer algorithms for applications overland and overwater. The energy balance method of Holtslag and van Ulden (1983) is used over land surfaces to calculate the sensible heat flux, the surface friction velocity, the Monin-Obukhov length and the convective velocity scale. The mixing layer height is then calculated starting from the computed sensible heat flux and the temperature radiosoundings (Carson, 1973; Maul, 1980). The boundary layer parameters overwater are calculated using a different algorithm, which also requires the air-sea temperature difference.

The boundary layer parameters calculated by CALMET are used in CALPUFF to determine the horizontal and vertical dispersion coefficients of a puff. Different algorithms are used according to the stability conditions and to the position of the puff within the planetary boundary layer (Weil, 1985; Briggs, 1985; Panofsky et al., 1977; Hicks, 1985; Arya, 1984; Nieustadt, 1984).

The flow diagram of the CALMET model is illustrated in Figure 2. The diagnostic wind field module uses a two-step approach for the computation of the wind field. In the first step an initial guess wind field is adjusted for kinematic effects of terrain, slope flows and terrain blocking effects to produce a Step 1 wind field. The second step consists of an objective analysis procedure to introduce observational data into the Step 1 wind field to produce a final wind field. CALMET can optionally use the output of prognostic meteorological models such as MM5 in three different ways:

- As a replacement for the initial guess field,
- As a replacement for the Step 1 field,
- As pseudo observations in the objective analysis procedure.

The prognostic wind fields in some cases have the advantage of better representing regional flows and certain aspects of sea breeze circulations and slope/valley circulations.

CALMET needs meteorological observations at surface and upper air data. At surface the following variables are needed with hourly resolution: wind speed, wind direction, temperature, cloud cover, ceiling height, surface pressure, relative humidity and precipitation rate. The upper air data, needed at least twice daily, must contain for each vertical level: wind speed, wind direction, temperature, pressure and height.

The output of the CALMET model is directly interfaced with dispersion models such as CALPUFF (Lagrangian puff model), CALGRID (Eulerian photochemical model) and KSP (Lagrangian particle model).

Brode and Anderson (2008) critical review of the CALPUFF application in near fields pointed out some important issues about CALMET. These limitations are largely due to its inability to ensure dynamical consistency in the simulated wind field. An example of the potential importance of this limitation is given by the phenomenon of drainage flows that often occur in valley situations under light-wind stable conditions. The three-dimensional structure of gravity-driven wind fields within a valley is very complex. These wind fields are often associated with complex thermal structures within the valley that develop as cold air drains down from the ridge tops and accumulate within the valley. A transition from down-slope to down-valley flows will typically develop over time and with distance from the ridge, creating significant lateral and vertical gradients of wind and temperature. CALMET is not able to simulate the thermal structures within the valley that are associated with these complex flows. The three-dimensional temperature fields computed within CALMET are based on either available upper air soundings and surface measurements or gridded prognostic model inputs, depending on user-specified options. The three-dimensional temperature fields are not adjusted to reflect the influence of these drainage flows. As a consequence, for example, the lapse rate used to compute plume rise in CALPUFF would not reflect the stable stratification generated by drainage flows. Therefore CALPUFF would overestimate the plume height for buoyant releases and underestimate the ground-level concentrations.

Reducing the horizontal grid resolution could face some of the CALMET issues. However this would increase the computational burden, unless the overall domain size is decreased, which could limit the applicability of the results by excluding important synoptic or mesoscale features that influence the complex winds. Recent studies have shown significant sensitivity to grid resolution, with some

evidence of a possible bias toward lower concentrations as grid resolution increases.

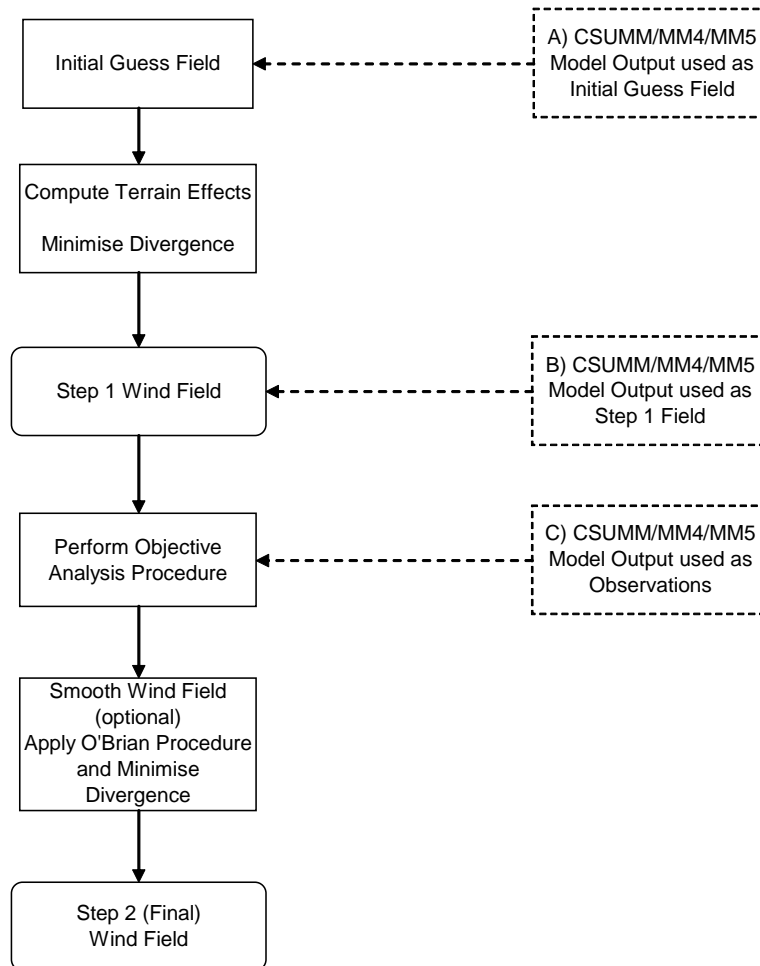


Figure 2. Flow diagram of the CALMET model.

Finally, CALMET does not include algorithms to account for the differential heating that occurs during the daytime as the sun heats one side of the valley wall while the other side is shaded, which generate complex cross-valley circulations. These circulation patterns will vary depending upon the orientation of the valley and solar elevation angle (based on time of day and season), and may significantly affect plume transport plus dispersion depending on the location of the source relative to the valley orientation. Some new algorithms for calculating the solar radiation over sloping surfaces and improving the temperature interpolation considering different terrain heights have been introduced in a modified version of CALMET that is not publicly available (Bellasio et al., 2005).

4.4 CALMET and LAPMOD

The basic assumption of Lagrangian particle models is that the mass of pollutant is divided in a number of particles moving within the atmospheric fluid with the same velocity of the fluid itself. This velocity is made by the sum of a mean vector (the mean wind) and a fluctuation around the mean. The trajectory of each particle describing a portion of the mass of the pollutant is reconstructed by evaluating the position of the particle at discrete time intervals:

$$\bar{x}_{t+dt} = \bar{x}_t + \bar{u} dt$$

$$\bar{u} = u_{mean} + \bar{u}'$$

The mean wind is estimated from measurements or from a meteorological model. The fluctuation of the wind velocity has a distribution with zero mean and it is estimated using a meteorological model, or through parameterizations coming from observation campaigns. The time evolution of this stochastic variable is a first-order Markov process and it is described by the non-linear Langevin equation:

$$d\bar{u}' = a(\bar{u}', \bar{x}, t)dt + b(\bar{x}, t)dW$$

where a is the deterministic acceleration and dW is a random forcing from a normal distribution with dt standard deviation.

When coupling a Lagrangian particle model with some meteorological model output most of the issues to be considered are the same faced with Eulerian air quality models. The main specific issue for Lagrangian particle models is the definition of the distribution of the probability function for the wind velocity fluctuations.

LAPMOD is a new Lagrangian particle dispersion model evolved from the model PLPM (Vitali et al., 2006). It is a full three-dimensional model capable of simulating the release of multiple sources with different shapes (point, line, area, volume) with arbitrary emission rates of multiple substances, including radionuclides. LAPMOD accounts for buoyant point sources as well as linear decay of radionuclides and includes the algorithms for dry and wet deposition.

The meteorological input for LAPMOD is provided by CALMET. LAPMOD can directly read the binary output file of CALMET to acquire the three-dimensional fields of wind and temperature as well as the two-dimensional fields of friction velocity, convective velocity, Monin-Obukhov length and boundary layer height. Some input fields to CALMET (directly input or estimated internally from landuse classification) are also transferred to LAPMOD: terrain elevation, leaf area index, roughness length and precipitation.

The relevant part of the coupling (that is implemented internally into the LAPMOD code) is the calculation of the higher moments of the distribution of the wind velocity. There are several schemes for this task. An effective one, implemented in LAPMOD, is based on the first 4 moments of the distribution of the probability density function of the Eulerian turbulent velocity, under the assumption that it has a quadratic form (Franzese et al., 1999):

$$a = \alpha w^2 + \beta w + \gamma$$

Routine meteorological measurements do not provide higher moments of the distribution of the wind fluctuations. At the same time, these are not standard output variables from meteorological models and for this reason they need to be incorporated in the software that prepares the meteorological input.

For this reason it is necessary to rely on parameterizations available in literature. A possible set of these, the one implemented in LAPMOD, is given hereafter, where the following variables are used:

$Ri = L / z_i$	bulk Richardson number (-)
L	Monin-Obukhov length (m)
z_i	boundary layer height (m)
C_0	Kolmogorov universal constant ($m^{-1}s^{3/2}$)
ε	eddy dissipation rate (m^2s^{-3})

Vertical Component

a and b coefficients in convective conditions ($Ri < -1$)

$$\alpha(z) = \frac{(1/3) \overline{\partial w^3 / \partial z} - \overline{w^3} / 2 \overline{w^2} \left[\overline{\partial w^3 / \partial z} - C_0 \varepsilon(z) \right] - \overline{w^2} \overline{\partial w^2 / \partial z}}{\left(\overline{w^4} - \overline{w^3}^2 \right) / \left(\overline{w^2} - \overline{w^2}^2 \right)}$$

$$\beta(z) = \frac{1}{2 \overline{w^2}} \left[\frac{\overline{\partial w^3}}{\partial z} - 2 \overline{w^3} \alpha(z) - C_0 \varepsilon(z) \right]$$

$$\gamma(z) = \frac{\overline{\partial w^2}}{\partial z} - \overline{w^2} \alpha(z)$$

$$a = \alpha w^2 + \beta w + \gamma$$

$$b = C_0 \varepsilon$$

For the moments of the distribution (overbar terms above) there are several parameterizations available in literature coming from observations. For example (Hanna et al., 1982a; Franzese et al., 1999):

$$\frac{\overline{w^2}}{w_*^2} = a_1 + a_2 \left(\frac{z}{z_i} \right)^{2/3} \left(1 - \frac{z}{z_i} \right)^{4/3}$$

$$\frac{\overline{w^3}}{w_*^3} = a_3 + \left(\frac{z}{z_i} \right) \left(1 - \frac{z}{z_i} \right)^2$$

$$\overline{w^4} = 3.5 \overline{w^2}^2$$

$$\varepsilon = 0.4 \frac{w_*^3}{z_i}$$

Where a_1 , a_2 and a_3 are fitting parameters.

a and b coefficients in stable and neutral conditions ($Ri \geq -1$)

$$\alpha(z) = 0.5 \frac{1}{(\overline{w^2})^2} \frac{\partial (\overline{w^2})^2}{\partial z} = \frac{1}{(\overline{w^2})} \frac{\partial \overline{w^2}}{\partial z}$$

$$\beta(z) = -\frac{1}{T_L}$$

$$\gamma(z) = 0.5 \frac{\partial (\overline{w^2})^2}{\partial z} = \overline{w^2} \frac{\partial \overline{w^2}}{\partial z}$$

$$b(z) = \overline{w^2} \sqrt{\frac{2}{T_L}}$$

Horizontal Components*Any stability condition*

$$a = \alpha w^2 + \beta w + \gamma$$

with:

$$\alpha = 0$$

$$\beta(z) = -\frac{1}{T_L}$$

$$\gamma = 0$$

$$b(z) = \sigma \sqrt{\frac{2}{T_L}}$$

where σ is the alongwind (U) or crosswind (V) standard deviation of the distribution of the wind speed fluctuations along those directions and T_{LU} and T_{LV} are the corresponding Lagrangian times.

Convective conditions

$$T_{LU} = T_{LV} = 0.15 \frac{z_i}{\sigma_V}$$

$$\sigma_V = u_* \left(12 - 0.5 \frac{z_i}{L} \right)^{\frac{1}{3}}$$

Neutral conditions

$$\sigma_U = 2u_* \exp\left(1 - \frac{z}{z_i}\right) \quad \sigma_V = \sigma_W = 1.3u_* \exp\left(-\frac{2fz}{u_*}\right)$$

$$T_{LU} = T_{LV} = T_{LW} = -\frac{0.5z}{\sigma_W \left(1 + 15 \frac{fz}{u_*}\right)}$$

Stable conditions

$$\sigma_U = 2u_* \left(1 - \frac{z}{z_i}\right) \quad \sigma_V = \sigma_W = 1.3u_* \left(1 - \frac{z}{z_i}\right)$$

$$T_{LU} = 0.15 \frac{z_i}{\sigma_U} \sqrt{\frac{z}{z_i}} \quad T_{LV} = 0.07 \frac{z_i}{\sigma_V} \sqrt{\frac{z}{z_i}} \quad T_{LW} = 0.10 \frac{z_i}{\sigma_W} \left(\frac{z}{z_i} \right)^{0.8}$$

The scaling parameters that appear in these equations can be computed, for example, with the scheme of Holtslag and Van Ulden (1983).

Alternatively, prognostic models can directly provide the standard deviations of the wind components, the planetary boundary layer height and the eddy dissipation rate so that these can be used in the above equations.

4.5 FLEXPART and the ECMWF Data

FLEXPART (e.g. Stohl et al., 2005) is a Lagrangian particle dispersion model designed for calculating the long-range and mesoscale dispersion of air pollutants.

The ECMWF meteorological fields on a latitude/longitude grid feed the FLEXPART model. The first action that must be done on the meteorological files is their transformation from the Gridded Binary (GRIB) format.

The model needs five three-dimensional fields: horizontal and vertical wind components, temperature and specific humidity. The meteorological input data are located on ECMWF model levels, which are defined by a hybrid coordinate system η . These coordinates are then converted into pressure coordinates.

The two-dimensional meteorological fields needed by the model are: surface pressure, total cloud cover, 10 m horizontal wind components, 2 m temperature and dew point temperature, large scale and convective precipitation, sensible heat flux, east/west and north/south surface stress.

Starting from the surface stress and the air density, FLEXPART determines the friction velocity u^* . If surface stress and sensible heat flux are not available, the friction velocity, the Monin-Obukhov length and other scaling parameters are calculated using the Berkowicz and Prahm method (1982). The mixing layer height is calculated according to Vogelesang and Holtslag (1996) methodology.

Once calculated for each ECMWF point (0.5 or 0.25 degree) and time (6 hours), the mixing layer height must be adequately processed in order to consider spatial and temporal variations on scales not resolved by the ECMWF model. These scales play an important role in determining the thickness of the layer over which a tracer is effectively mixed (Stohl et al., 2005). The height of the convective mixing layer reaches its maximum value in the afternoon before a much shallower stable mixing layer forms. If, for example, meteorological data are available at 12:00 and 18:00, the simple linear interpolation of the mixing height calculated for these two times might result in overestimation of the calculated concentration for tracers released at the surface shortly before the breakdown of the convective

mixing layer. A similar problem is also encountered for spatial variations of mixing layer due to complex topography and variability in land use or soil wetness. In order to consider these problems, FLEXPART adopts an “envelope” mixing height obtained from the mixing height calculated at each point, the standard deviation of the ECMWF model subgrid topography, the wind speed at height of the original mixing layer, and the Brunt-Vaisala frequency.

The boundary layer parameters calculated as explained above are then used for calculating the standard deviations of the wind speed components and the Lagrangian times by means of the Hanna (1982b) parameterization scheme, modified accordingly to Ryall and Maryon (1997) for the standard deviation of the vertical wind component.

4.6 Measurements and Gaussian Models

Gaussian models are widely described in literature (e.g. Zannetti, 1990; Seinfeld and Pandis, 1998). Well-known advanced Gaussian models are ISC3 and AERMOD. Most of these models require meteorological variables at surface (e.g. 10 m AGL) and at a single point. An exception is AERMOD, which also can take into account variables that are measured at upper levels. The surface meteorological variables needed by Gaussian models are essentially wind speed and direction, temperature, stability conditions and height of the mixing layer.

Measurements carried out at surface must be vertically extrapolated in order to determine their values at the heights of the sources. This operation is usually done within the dispersion model using algorithms based on the scaling properties of the planetary boundary layer. A more precise indication would come from upper air measurements, but these are costly and not always available, especially for long periods with high temporal frequency of measurement (e.g. rawinsondes or SODAR).

When a reliable and representative meteorological station is available close to the source, its data must be used to produce the model input file. Rarely the meteorological monitoring stations have information about cloud cover, which is fundamental information. Cloud covers can be obtained from METAR data, which are available from the most important airports. Cloud cover, solar radiation and wind speed allow determination of the Pasquill Gifford stability class (e.g. Zannetti, 1990). The mixing layer height at each hour can be estimated starting from the surface radiation budget (e.g. Hostlag and van Ulden, 1983). The surface radiation budget also allows acquisition of the friction velocity u^* , the Monin-Obukhov length L and other scaling parameters.

Under stable conditions the mixing height can be estimated with diagnostic equations, which depend only from u^* and L . Under neutral conditions the mixing height depends only from the mechanical turbulence, which means u^* (e.g. Zilitinkevich, 1972; Zilitinkevich, 1989). During daytime unstable conditions the

mixing height must be estimated by means of prognostic equations as, for example, the one proposed by Batchvarova and Grining (1991). An exhaustive review of the equations needed to estimate the mixing height is given in (Seibert et al., 2000).

One of the main problems when using dispersion models that are fed by a single meteorological station is that the meteorological station closest to the dispersion domain is often tenths of km far away. Such a station therefore might not be representative for the area. A possible approach to overcome the problem could be the use of a 3-D prognostic or a diagnostic meteorological model for determining the meteorological field over a wide domain, then the extraction of the variables from a single model grid close to the sources of interest. This approach would also solve the problem of possible missing data present in a single meteorological station, because the model would fill the gaps. Moreover, for dispersion models that require both surface and upper air variables, such as AERMOD, this approach has the advantage that all the variables would refer to the same point (grid). Some variables needed by the atmospheric dispersion model (Monin-Obukhov length, friction velocity, convective velocity, etc.) might be calculated by specific routines, if not directly available from the dispersion model. The US-EPA, for example, is planning to develop specific processors, for using AERMOD starting from the MM5 prognostic models (US-EPA 9th Modeling Conference Presentations). The US-EPA is also planning to develop some processors to use CALPUFF starting from MM5 or WRF, therefore bypassing the use of the CALMET diagnostic meteorological model. An example of methodology for the application of AERMOD with incomplete input data has been presented by Turtos et al. (2010).

4.7 Other Couplers

Apart from those already cited, there are several software packages that were developed for coupling meteorological and dispersion models. On a global scale, a recent example of interesting coupling (Flemming et al., 2010) is the one between the ECMWF's integrated forecast system (IFS) and the global chemistry and transport models (CTMs) MOCAGE (Josse et al., 2004; Bousserez et al., 2007), MOZART-3 (Kinnison et al., 2007) and TM5 (Krol et al., 2005). This is a special type of coupling, since the resulting modeling system has the IFS taking care of the transport of the reactive gases and one of the CTMs providing the chemical transformations based on the meteorological predictions of the IFS. The system however includes a feedback so that the changes of concentration of the chemical species are assimilated by the IFS itself.

Apart from the availability of the meteorological input for each of these models, an additional advantage of the coupling of the same meteorological input with more CTM models is that these can be used to produce ensemble forecasts of air quality isolating the variability within the chemistry and transport part of the system.

5 Sources of Data over the Internet

One of the most difficult tasks in running air quality models is to find all the input data needed. Generally the number of input data increases with the model complexity. This paragraph contains some hints about Internet sites, which contain useful data for the whole World. Once downloaded from Internet, the data cannot be used as they are but they need to be processed in order to find possible gaps, missing values or to average them on the model grid mesh. Scripting languages, such as Perl, are very useful and powerful in this phase.

5.1 Land Cover

Land cover data are important for meteorological and AQ models for many reasons. For example, because they are related to the roughness length and to deposition velocity of some pollutants they are also needed during emission inventories.

At the European level, the land cover data can be obtained from the CORINE land cover project, which is part of the CORINE program and is intended to provide consistent localized geographical information on the land cover of the Member States of the European Community. Two useful Internet sites to browse these data are:

<http://www.eea.europa.eu/publications/COR0-landcover>

<http://image2000.jrc.ec.europa.eu/>

Global land cover data are available from the University of Maryland Department of Geography (<http://glcf.umiacs.umd.edu/data/landcover>). Imagery from the AVHRR satellites acquired between 1981 and 1994 were analyzed to distinguish fourteen land cover classes (Hansen et al., 2000). The land cover data are available at three spatial scales: 1 degree, 8 kilometer and 1 kilometer pixel resolutions.

5.2 Orography

The Shuttle Radar Topography Mission (SRTM) obtained elevation data on a near-global scale to generate the most complete high-resolution digital topographic database of Earth. SRTM consisted of a specially modified radar system that flew onboard the Space Shuttle Endeavour during an 11-day mission in February of 2000. SRTM is an international project spearheaded by the National Geospatial-Intelligence Agency (NGA), NASA, the Italian Space Agency (ASI) and the German Aerospace Center (DLR). There are three resolution outputs available, including 1-kilometer and 90-meter resolutions for the world and a 30-meter resolution for the US. The SRTM data are available from <http://glcf.umiacs.umd.edu/data/srtm>.

Orography data are also available from the National Geophysical Data Center of NOAA at this address:

<http://www.ngdc.noaa.gov/cgi-bin/mgg/ff/nph-ewform.pl/mgg/topo/customdatacd>

5.3 Meteorology

Meteorological data at upper levels are available from two different Internet sites of NOAA:

The Integrated Global Radiosonde Archive (IGRA) consists of radiosonde and pilot balloon observations at over 1,500 globally distributed stations (<http://www.ncdc.noaa.gov/oa/climate/igra/index.php>). Observations are available for standard, surface, tropopause and significant levels for many variables, among which are: wind direction and speed, pressure, temperature, geopotential height and dew point. The period of record varies from station to station, with many starting from 1970.

The Radiosonde Observation (RAOB) Internet site (<http://www.esrl.noaa.gov/raobs/>) allows the download of upper air meteorological data by specifying the time interval, the wind units and selecting the stations by their WMO code, by country or by coordinates.

Other meteorological data at surface and at upper levels are the GDAS (Global Data Assimilation System), which is one of the operational systems of the National Weather Service's National Centers for Environmental Prediction (NCEP). These data are available at <http://www.arl.noaa.gov/gdas1.php> with 1-degree space resolution and 3-hour time resolution.

Surface data are available from many Internet sites as METAR data, which is a weather format predominantly used by pilots as a part of fulfilling a pre-flight weather briefing. Meteorologists also use aggregated METAR information to assist in weather forecasting. METAR data are available at many points of the World, practically at all the main airports. The METAR phrase is not so clear at first glance for non-expert people. For example the string

KFDW 110215Z AUTO 06016G21KT 7SM -DZ OVC003 17/17 A3001 RMK AO1

indicates a report issued by the airport with ICAO code KFWD (Fort Worth, TX) at 02:15 UTC of day 11 of some month (month and year are not specified). At such hour both temperature and dew point are 17°C (62.6°F), there is a solid overcast at 300ft, a light drizzle is present, visibility is 7 statute miles, wind speed is 16 knots and wind direction is 60 degrees. A wind gust of 21 knots has also been observed. It is clear that METAR strings must be automatically processed by software before they can be used in AQ models. One of the possible sources of METAR data is <http://weather.noaa.gov/weather/metar.shtml>.

Acronyms

- AFWA – Department of Defense’s Air Force Weather Agency
- AGL – above ground level
- AQM – air quality model
- CAPS – Center for Analysis and Prediction of Storms
- CRPAQS – California Regional Particulate Air Quality Study
- CTM – chemical transport model
- ECMWF – European Centre for Medium Range Weather Forecasting
- ESRL – Earth System Research Laboratory
- FAA – Federal Aviation Administration
- FDDA – Four Dimensional Data Assimilation
- GCM – global circulation model
- GDAS – global data assimilation system
- GRIB – gridded binary
- LAI – leaf area index
- METAR – METeorological Aerodrome Report
- NCAR – National Center for Atmospheric Research
- NCEP – National Centers for Environmental Prediction
- NOAA – National Oceanic and Atmospheric Administration
- NRL – Naval Research Laboratory
- NWP – numerical weather prediction
- PBL – planetary boundary layer
- PSU – Penn State University
- TIBL – thermal internal boundary layer
- SODAR – SOnic Detection And Ranging

References

Appel K. W., S. J. Roselle, R. C. Gilliam, and J. E. Pleim. Sensitivity of the Community Multiscale Air Quality (CMAQ) model v4.7 results for the eastern United States to MM5 and WRF meteorological drivers. *Geosci. Model Dev.*, 3, 169–188, 2010

Arya S.P.S. (1984) Parametric relations for the atmospheric boundary layer. *Boundary Layer Meteorology*, 30, 57-73.

Batcharova, E., Gryning, S. E., 1991. Applied model for the growth of the daytime mixed layer. *Boundary Layer Meteorology*, 56, 261-274.

Bellasio R., G. Maffei, J. Scire, M.G. Longoni, R. Bianconi and N. Quaranta (2005) Algorithms to account for topographic shading effects and surface temperature dependence on terrain elevation in diagnostic meteorological models. *Boundary-Layer Meteorology*, 114: 595-614.

Berkowicz, R. and Prahm, L. P.: Evaluation of the profile method for estimation of surface fluxes of momentum and heat, *Atmos. Environ.*, 16, 2809–2819, 1982.

Black T. (1994) The new NMC mesoscale eta model: description and forecast examples. *Weather Forecasting*, 9, 265-278.

Bousserez, N., Attié, J.-L., Peuch, V.-H., Michou, M., and Pfister, G. (2007) Evaluation of the MOCAGE chemistry and transport model during the ICARTT/ITOP experiment, *J. Geophys. Res.*, 112, D10S42, doi: 10.1029/2006JD007595.

Briggs G.A. (1985) Analytical parameterization of diffusion: the convective boundary layer. *J. Clim. And Appl. Meteor.*, 24, 1167-1186.

Brode R.W. and Anderson B. (2008) Technical Issues Related to CALPUFF Near-field Applications. US-EPA.

Byun, D. W. and Schere, K. L. (2006) Review of the governing equations, computational algorithms, and other components of the Models3 Community Multiscale Air Quality (CMAQ) Modeling System, *Appl. Mech. Rev.*, 59, 51-77.

Carson D.J. (1973) The development of a dry, inversion-capped, convectively unstable boundary layer. *Quart. J. Roy. Meteor. Soc.*, 99, 450-467.

Flemming J., A. Inness, H. Flentje, V. Huijnen, P. Moinat, M. G. Schultz, and O. Stein (2010). Coupling global chemistry transport models to ECMWF's integrated forecast system

Franzese P., A.K. Luhar and M.S. Borgas (1999) An efficient Lagrangian stochastic model of vertical dispersion in the convective boundary layer. *Atm. Env.*, 33, 2337-2345.

Hanna S.R., Briggs G.A. and Hosker R.P. (1982a) Handbook on atmospheric diffusion. Technical Information Center, U.S. Department of Energy, pp. 102

Hanna, S. R. (1982b) Applications in air pollution modeling, in: *Atmospheric Turbulence and Air Pollution Modelling*, edited by: Nieuwstadt, F. T. M. and van Dop, H., D. Reidel Publishing Company, Dordrecht, Holland.

Hansen, M., R. DeFries, J.R.G. Townshend, and R. Sohlberg (2000), Global land cover classification at 1km resolution using a decision tree classifier, *International Journal of Remote Sensing*. 21: 1331-1365.

Helfand, H. M., M. J. C. Labraga, 1988: Design of non singular level 2.5 second order closure model for the prediction of atmospheric turbulence. *J. Atmos. Sci.*, 45, 113-132.

Hicks B.B. (1985) Behavior of turbulence statistics in the convective boundary layer. *J. Clim. And Appl. Meteor.*, 24, 607-614.

Holtslag, A.A.M., A.P. Van Ulden. 1983. A simple scheme for daytime estimates of the surface fluxes from routine weather data. *J. Climate Applied Meteorology*, 22, 517-529.

Hu Y. and M. T. Odman (2008) A comparison of mass conservation methods for air quality models. *Atmospheric Environment*, 42, 35, 8322-8330.

Hu J., Q. Ying, J. Chen, A. Mahmud, Z. Zhao, S.H. Chen and M.J. Kleeman (2010) Particulate air quality model predictions using prognostic vs. diagnostic meteorology in central California *Atmospheric Environment*, 44 (2), 215-226

Isakov V., A. Venkatram, J. S. Toumaa, D. Koračinc and T. L. Otte (2007). Evaluating the use of outputs from comprehensive meteorological next term models in air quality modeling applications. *Atmospheric Environment*, 41, 8, 1689-1705.

Josse, B., Simon, P., and Peuch, V.-H. (2004) Rn-222 global simulations with the multiscale CTM MOCAGE, *Tellus B*, 56, 339–356.

Kesarkar A.P., M. Dalvi, A. Kaginalkar and A. Ojha (2007) Coupling of the Weather Research and Forecasting Model with AERMOD for pollutant dispersion modeling. A case study for PM10 dispersion over Pune, India. *Atmospheric Environment*, 41, 9, 1976-1988.

Kinnison, D. E., Brasseur, G. P., Walters, S., Garcia, R. R., Marsh, D. R., Sassi, F., Harvey, V. L., Randall, C. E., Emmons, L., Lamarque, J. F., Hess, P., Orlando, J. J., Tie, X. X., Randel, W., Pan, L. L., Gettelman, A., Granier, C., Diehl, T., Niemeier, U., and Simmons, A. J. (2007) Sensitivity of Chemical Tracers to Meteorological Parameters in the MOZART-3 Chemical Transport Model, *J. Geophys. Res.*, 112, D03303, doi: 10.1029/2008JD010739.

Kleeman M.J and G.R. Cass (2001) A 3D Eulerian source-oriented model for externally mixed aerosol. *Environmental Science & Technology*, 35, 4834-4848.

Krol, M., Houweling, S., Bregman, B., van den Broek, M., Segers, A., van Velthoven, P., Peters, W., Dentener, F., and Bergamaschi, P. (2005) The two-way nested global chemistry-transport zoom model TM5: algorithm and applications, *Atmos. Chem. Phys.*, 5, 417–432.
<http://www.atmos-chem-phys.net/5/417/2005/>.

Maul P.R. (1980) Atmospheric transport of sulphur compound pollutants. Central Electricity Generating Bureau MID/SSD/80/0026/R. Nottingham, England.

Mellor, G.L. and T. Yamada, 1974: A hierarchy of turbulence closure models for planetary boundary layers. *J. Atmos. Sci.*, 31, 1791-1806.

Mellor, G. L. and Yamada, T., 1982: Development of a turbulence closure model for geophysical fluid problems. *Rev. Geophys. Space Phys.*, 20, 851-875.

Nieuwstadt F.M.T. (1984) The turbulent structure of the stable, nocturnal boundary layer. *J. Atmos. Sci.*, 41, 2202-2216.

O'Brien J.J. (1970) A note on the vertical structure of the eddy exchange coefficient in the planetary boundary layer. *J. Atmos. Sci.*, 27, 1213-1215.

Otte T. L. and J. E. Pleim (2010) The Meteorology-Chemistry Interface Processor (MCIP) for the CMAQ modeling system: updates through MCIPv3.4.1. *Geosci. Model Dev.*, 3, 243–256.

Panofsky H.A., H. Tennekes, D. H. Lenschow and J.C. Wyngaard (1977). The characteristics of turbulent velocity components in the surface layer under convective conditions. *Boundary Layer Meteorology*, 11, 355-361.

Pleim, J. E., A. Xiu, P. L. Finkelstein, and T. L. Otte, 2001: A coupled land-surface and dry deposition model and comparison to field measurements of surface heat, moisture, and ozone fluxes. *Water Air Soil Pollut. Focus*, 1, 243–252.

Ryall, D. B. and Maryon, R. H.: Validation of the UK Met Office's NAME model against the ETEX dataset, in: ETEX Symposium on Long-Range Atmospheric Transport, Model Verification and Emergency Response, edited by: Nodop, K., European Commission, EUR 17 346, 151–154, 1997.

Scire J.S., Robe F.R., Fernau M.E. and Yamartino R.J. (2000a) A user's guide for the CALMET dispersion model. Earth Tech, Inc.

- Scire J.S., Strimaitis D.G. and Yamartino R.J. (2000b) A user's guide for the CALPUFF dispersion model. Earth Tech, Inc.
- Seaman N.L. (2000) Meteorological modeling for air-quality assessments. *Atmospheric Environment*, 34, 2231-2259.
- Seibert, P., Beyrich, F., Gryning, S.-E., Joffre, S., Rasmussen, A., Tercier, P., 2000. Review and intercomparison of operational methods for the determination of the mixing height. *Atmospheric Environment*, 34, 7, 1001-1027.
- Seinfeld J. And Pandis S. (1998) *Atmospheric Chemistry and Physics, from Air Pollution to Climate Change*. John Wiley, New York, 1326 pp.
- Skamarock, W. C., Klemp, J. B., Dudhia, J., Gill, D. O., Barker, D. M., Duda, M. G., Huang, X.-Y., Wang, W., and Powers, J. G. (2008) A description of the Advanced Research WRF Version 3, National Center for Atmospheric Research, Tech. Note, NCAR/TN-475+STR, 113 pp.
- Stohl A., C. Forster, A. Frank, P. Seibert, and G. Wotawa. Technical note: The Lagrangian particle dispersion model FLEXPART version 6.2. *Atmos. Chem. Phys.*, 5, 2461–2474, 2005
- Stull R.B. (1988) *An introduction to boundary layer meteorology*. Kluwer Press. ISBN 90-277-2768-6
- Turtos Carbonell L.M., M.S. Gacita, J.R. Oliva, L.C. Garea, N.D. Rivero, E. M. Ruiz (2010) Methodological guide for implementation of the AERMOD system with incomplete local data, *Atmospheric Pollution Research*, 1, 102-111
- US-EPA 9th Modeling Conference Presentations.
<http://www.epa.gov/scram001/9thmodconfpres.htm> (visited April 26, 2010)
- Vitali L., F. Monforti, R. Bellasio, R. Bianconi, V. Sacchero, S. Mosca and G. Zanini (2006) Validation of a Lagrangian dispersion model implementing different kernel methods for density reconstruction. *Atmospheric Environment*, 40, 40, 8020-8033.
- Vogelezang, D. H. P. and A. A. M. Holtslag (1996) Evaluation and model impacts of alternative boundary-layer height formulations. *Bound. Layer Meteor.*, 81, 245-269.
- Weil J.C. (1985) Updating applied diffusion models. *J. Clim. And Appl. Meteor.*, 24, 1111-1130.
- Wesely, M. L., 1989: Parameterization of surface resistances to gaseous dry deposition in regional-scale numerical models. *Atmos. Environ.*, 23, 1293–1304.
- Zannetti P. (1990) *Air pollution modeling: theories, computational methods, and available software*. Van Nostrand, New York, 444 pp.
- Zhang Y. Online-coupled meteorology and chemistry models: history, current status, and outlook. *Atmos. Chem. Phys.*, 8, 2895–2932, 2008
- Zilitinkevich S.S. (1972) On the determination of the height of the Ekman boundary layer. *Boundary Layer Meteorology*, 3, 141-145.

Zilitinkevich, S.S., 1989. Velocity profile, the resistance law and the dissipation rate of mean flow kinetic energy in a neutrally and stably stratified planetary boundary layer. *Boundary Layer Meteorology*, 46, 367-387.

BRANK
P
e

Chapter 6

Plume Rise

A comprehensive chapter on “Plume Rise” was presented in Volume I of this book series. The abstract is reprinted below.

Plume rise determination is one of the main processes encountered in air pollution modeling. Therefore, the most commonly used methods for introducing plume rise in dispersion models are presented. They encompass simple but robust and documented semi empirical formulations, easy to be implemented in operative models, and advanced plume rise models. Then, the problem of how to account for plume rise in Lagrangian dispersion particle models is addressed. Finally, special situations of plume rise, like the occurrence of an elevated inversion, or the presence of building and/or stacks features interacting with the plume, are investigated.

For additional information, the reader can visit:

- Atmospheric Dispersion Equation Formulas Calculator
http://www.ajdesigner.com/phpdispersion/effective_stack_height_equation_plume_rise.php
- Logic Diagram for Using The Briggs Equations to Calculate The Rise of Bent-Over Buoyant Plumes
<http://www.air-dispersion.com/briggs.html>
- Development and Evaluation of The Prime Plume Rise and Building Downwash Model
<http://www.epa.gov/scram001/7thconf/iscprime/tekpaper1.pdf>
- Lecture 32 Plume Rise, Area and Line Source Model (YouTube)
<http://www.youtube.com/watch?v=UyG4EL0BBJ0>

BRAND
P
e

Chapter 7

Gaussian Plume Models

An introductory chapter (7A – Introduction to Gaussian Plume Models) was presented in Volume I of this book series. The abstract is reprinted below.

This section describes the development of models used for regulatory applications at scales of the order of ten kilometers. These models are important because they are used extensively to permit industrial sources and assess risk associated with toxic releases in urban areas. AERMOD and ISC are examples of such models. The foundation of these models is the steady-state plume model that assumes that the concentration distributions normal to the direction of the mean flow are Gaussian.

We first discuss the structure of the Gaussian dispersion model as applied to a point source, and then show how this formulation can be used to estimate impact of other types of sources, such as line and area sources. The realism of models for plume spread determines the usefulness of the Gaussian dispersion model. Plume spread, in turn, depends on atmospheric turbulence. Thus, this section provides a brief description of the atmospheric boundary layer before describing models for plume spread.

We describe different approaches to modeling plume spread of surface and elevated releases in the boundary layer. We then show how the Gaussian dispersion model can be modified to incorporate the effects of buildings and complex terrain on dispersion. The section compares the Gaussian approach to other methods being used to model dispersion. We provide a brief description of one such method, the probability density function method that is currently being used in models of dispersion in the convective boundary layer. The section concludes by emphasizing the

usefulness of the Gaussian framework in developing dispersion models for a variety of real world situations.

A comprehensive chapter (7B – Simulation Algorithms in Gaussian Plume Models) was presented in Volume III. The abstract is reprinted below.

This chapter focuses on the development of various Gaussian modeling techniques with an emphasis on the relevant mathematical and numerical details. Beginning with the diffusion equation in one-dimension, we show how one solution of this differential equation for pollutant mixing ratio involves the Gaussian function. The three-dimensional Gaussian plume solution is then constructed via consideration of the advection terms and the use of the separation of variables technique. Influences of the ground and other “reflecting” barriers is then added via the method of images and alternative mathematical formulations of this summation of images is considered, both from theoretical and numerical accuracy viewpoints. The issue of air density varying with height is then discussed as it complicates the solution expressed in terms of mass concentration (e.g., g/m³) versus the more-fundamental mixing ratio (e.g., ppm) formulation. Having an impact on computed results in the 5-15% range, this density complication is presently nearly-universally overlooked. Focus then shifts to extending the point source formulation to various integrated forms that accommodate line and area sources, and including wind shear. Removal processes, particularly dry deposition, are then treated in some detail.

In this Volume IV, additional information on this topic is presented in Chapter 9 (Special Applications of Gaussian Models).

Chapter 8

Gaussian Puff Modeling

A comprehensive chapter on Gaussian Puff Modeling was included in Volume III of this book series. The abstract is reprinted below.

This chapter focuses on the development of various Gaussian puff modeling techniques, with an emphasis on the relevant mathematics. Beginning with the diffusion equation, we first discuss the linkage between the 3D puff and plume formulations and show how the puff approach overcomes many of the limitations associated with plume modeling, including the limit of calm winds. The focus then shifts to consideration of the integral over source emission time and the integral-average over receptor time, both of which must be accomplished in an applied puff model. Puff model enhancements, including consideration of incorporating true puff dispersion coefficients and a detailed evaluation of the effect of wind shears on puff dispersion, conclude the chapter. No attempt has been made to duplicate discussions from Chapter 7B (e.g., summation of images, dry deposition) that are also directly applicable to puffs.

In this Volume IV, additional information on this topic is presented in Chapter 9 (Special Applications of Gaussian Models).

For additional information, the reader can visit:

- The CALPUFF Modeling System
<http://www.src.com/calpuff/calpuff1.htm>
http://www.epa.gov/ttn/scram/dispersion_prefrec.htm#calpuff

BRAND
P
e

Yamartino, R., 2010. *Special Applications of Gaussian Models*. Chapter 9 of *AIR QUALITY MODELING - Theories, Methodologies, Computational Techniques, and Available Databases and Software. Vol. IV – Advances and Updates* (P. Zannetti, Editor). Published by The EnviroComp Institute (www.envirocomp.org) and the Air & Waste Management Association (www.awma.org).

Chapter 9

Special Applications of Gaussian Models

Robert J. Yamartino

Integrals Unlimited, Portland, Maine (USA)
rjy@maine.rr.com

Abstract: This chapter focuses first on the mathematical fundamentals of the Gaussian distribution that bear on its applicability to air quality modeling. These fundamental properties include: that any weighted sum of Gaussian PDFs is itself a Gaussian PDF; that the Fourier transform of a Gaussian is itself a Gaussian; and, that the convolution of a Gaussian with a Gaussian results in a Gaussian. The impact of these fundamentals includes: the connection between the Gaussian velocity PDF and the Gaussian shape of the concentration distribution; the ability to generate mean plumes from an instantaneous plume and a meander envelope; the ability to compute higher-order concentration statistics; and the ability to compute non-linear chemical reactions. Finally, some recent changes to U.S. EPA regulatory Gaussian models are considered.

Key Words: Gaussian methods, atmospheric dispersion modeling.

Given the previous three chapters (i.e., 7A by Venkatram and Thé, 2003, and 7B and 8A by Yamartino, 2008a-b) devoted to Gaussian plume and puff modeling that have appeared in this series, the challenge of this chapter is to avoid repetition and cover areas of application interest that have yet to be covered. While the emphasis will be on applications, one cannot help but first look at some mathematical fundamentals of the Gaussian distribution that bear on its applicability to air quality modeling. The focus will then shift to more specific applications of the Gaussian formulation to air pollution problems and finally to more recent issues with Gaussian-based regulatory models.

1 Some Mathematical Properties of the Gaussian and Their Practical Implications

While the choice of the Gaussian for analytic air pollution modeling applications may seem to have been a somewhat arbitrary choice among suitably peaked and appropriately normalized functions, there are additional mathematical properties of the Gaussian that have proven to be quite advantageous. These fundamental properties include the facts that:

- Any weighted sum of Gaussian probability distribution functions (PDFs) is itself a Gaussian PDF;
- The Fourier transform of a Gaussian is itself a Gaussian; and,
- The convolution of a Gaussian with a Gaussian results in a Gaussian.

It should also be noted that the Gaussian is singled out by the Central Limit Theorem as it states that the mean of a large number of independent random variables, each with finite mean and variance but possessing arbitrary though identical distributional properties, will converge toward being approximately normally distributed.

1.1 Gaussian PDFs Connecting Velocity and Spatial Distribution PDFs

The mathematical property that any weighted sum of Gaussian PDFs is itself a Gaussian PDF can be expressed as:

$$\sum_{i=1}^n a_i \cdot N_i(\mu_i, \sigma_i) = b \cdot N\left(\sum_{i=1}^n (a_i \cdot \mu_i), \sqrt{\sum_{i=1}^n (a_i \cdot \sigma_i)^2}\right) \quad (1)$$

where $N(\mu, \sigma)$ represents a Normal (i.e., or Gaussian) PDF having a mean of μ and a standard deviation of σ , a_i are scalar multipliers, and where b is a multiplier that provides the proper normalization of the composite PDF. Its proof can most easily be found in Lemons (2002, Chapter 2) or online at:

http://en.wikipedia.org/wiki/Sum_of_normally_distributed_random_variables.

This relationship bears on issues such as why Gaussian turbulent velocity distributions are consistent with Gaussian concentration profiles for a point source and why the Gaussian plume/puff solutions permit miniscule concentrations to exist at great distances from a source even just after release.

Consider first the question of why the Gaussian analytic solution to the diffusion equation allows diffused mass to exist at infinite distances from the source in apparent defiance of any reasonable causal linkage. If one instead begins with a Gaussian turbulent velocity distribution, Lemons (2002, Chapter 7) has shown that within the framework of a Langevin stochastic equation for homogeneous flow, the turbulent velocity PDF will always remain Gaussian with a mean of zero and a variance of σ_v^2 . This is because for homogeneous turbulence (i.e., no

turbulence gradient in the dimension of interest), the Langevin equation updates individual particle turbulent velocities via the relation:

$$v(n \cdot \Delta t) = v[(n-1) \cdot \Delta t] \cdot f + \sigma_v \cdot (1 - f^2)^{1/2} \cdot R(0,1), \quad (2)$$

where $R(0,1)$ is a random Gaussian number having a mean of zero and a standard deviation of unity, $f = \exp(-\Delta t/\tau)$, and τ is the Lagrangian time scale. Equation (1) then guarantees that this turbulent velocity PDF will remain normal with constant variance, as $f^2 + (1 - f^2)$ just equals one. As the corresponding particle position, $y(t)$, is computed as a sum over these velocities for various time steps multiplied by the scalar Δt , Equation (1) again provides the guarantee that this distribution of particle positions will remain normal. Durbin (1983), Van Dop et al. (1985), and others have shown that the resulting variance of this normal PDF of particle positions is:

$$\sigma_y^2 = 2 \cdot \sigma_v^2 \cdot \tau^2 \cdot [t/\tau + \exp(-t/\tau) - 1], \quad (3)$$

which for early times (i.e., $t \ll \tau$) provides for a linear-in-time growth of σ_y as $\sigma_y = \sigma_v \cdot t$, and, for late times (i.e., $t \gg \tau$) a $t^{1/2}$ growth as $\sigma_y = 2^{1/2} \cdot \sigma_v \cdot (t \cdot \tau)^{1/2}$. This late time result is consistent with the K-theory solution with $K_y = \sigma_v^2 \cdot \tau$.

Regardless of the initial shape of the turbulent velocity PDF, Pope (2000) has shown that the diffusion term in the underlying differential equation governing the evolution of the turbulent velocity PDF will make it tend towards normal asymptotically. Further, the assumption of a Gaussian PDF for turbulent velocities has been shown by Wilson (2007) to provide a superior fit to Prairie Grass data than three other PDF distributions having attenuated (e.g., $\exp[-v^4/(\gamma \cdot \sigma_v^4)]$, with γ as a fitting constant) or no (e.g., triangular or cosine PDF) high-velocity, v , tails extending out to infinity.

Thus, returning to the Gaussian profile function, $\exp[-y^2/(2 \cdot \sigma_y^2)]$, any concern we might have had over the minute amounts of material at large crosswind distance, y , should now be soothed by knowledge that the corresponding Gaussian turbulent velocity distribution implies a similarly minute amount of material “diffusing” outward at extremely high transverse velocities. Were one to find a well-behaved and superior PDF functional form with such high velocity tails “clipped” away from the distribution, then that would provide a basis for beginning anew; however, the effort involved would likely not prove to be worthwhile, especially now that one understands the relatively benign source of this material found at unlikely transverse distances of many, many σ_y . In the vertical direction, the presence of a gradient in turbulence leads to a skewed velocity PDF, particularly in the case of convective conditions (Luhar and Britter, 1989). One notes that a skewed Gaussian PDF, with its mean shifted by an appropriate area weighted average of updraft and downdraft velocities, can generally accommodate such situations.

1.2 Fourier Transform of a Gaussian is a Gaussian

The Gaussian distribution is also the only functional form for which its Fourier transform is also a Gaussian. To understand this solution characteristic better, we note that the process of taking the Fourier transform of the Gaussian in space (i.e., by multiplying the Gaussian profile shape times the quantity $\exp(-i \cdot k \cdot x)$, where i is the imaginary number, and integrating over all x from $-\infty$ to $+\infty$) yields a Gaussian distribution in k , the conjugate variable to x . Now k , with its units that must be in terms of inverse distance is often referred to as wavenumber, and is usually defined in terms of wavelength as $k \equiv 2 \cdot \pi / \lambda$. Another curious property of this Fourier-transform k -space distribution is that this Gaussian distribution, centered at $k=0$, has a standard deviation inversely proportional to the standard deviation of the original x distribution of the Gaussian solution. More explicitly, one finds that:

$$\sigma_x \cdot \sigma_k = \frac{1}{2} . \quad (4a)$$

One notes that beginning with any other, non-Gaussian distributions results in a different non-Gaussian distribution for the transformed variable, and the subsidiary finding for non-Gaussians that:

$$\sigma_x \cdot \sigma_k > \frac{1}{2} . \quad (4b)$$

Those familiar with quantum mechanics will recall that this mathematical relationship between conjugate variables looks a bit like the Heisenberg Uncertainty Principal. In fact, all we have to do to get there is first recall that at the quantum level, a particle's momentum, p , is simply its wavenumber times the reduced Plank constant, $\hbar \equiv h / (2 \cdot \pi)$, then one obtains the Heisenberg result of:

$$\sigma_x \cdot \sigma_p \geq \hbar / 2 , \text{ or } \Delta x \cdot \Delta p \geq \hbar / 2 \quad (4c)$$

in the more conventional physics notation. Of course, the interpretation of this relation in the Heisenberg Uncertainty Principal case is quite different than the one we consider here, but the Fourier Transform mathematical basis is the same in both cases.

Further analysis of the Gaussian distribution in k -space shows that as the spatial distribution grows, energy is fed into the shorter k values (i.e., $k \cdot \sigma_y < 0.5$) and depleted from k values for which $k \cdot \sigma_y > 0.5$. This increase in the long wave portion (i.e., $\lambda > 4 \cdot \pi \cdot \sigma_y$) indicates that classical diffusion is a smoothing process that would tend to wipe out concentration fluctuations with plume growth. Thus, it is not surprising that the Gaussian plume formulation is considered most appropriate for time-averaged or ensemble-averaged concentration measures.

1.3 Convolution of Gaussians Yields a Gaussian

Another interesting property of the Gaussian is that the convolution of a Gaussian with a Gaussian results in a Gaussian. This property has the important consequence that one can now envision splitting the turbulent velocity spectra into a short-wave component leading to the physical plume's spreading and a long-wave component that causes the entire plume to meander back and forth. While such a division may seem overly-simplistic, it has served as the basis for meandering plume models which represent one of the earliest attempts (e.g., Gifford, 1959) to model concentration fluctuations. The convolution process is defined mathematically as:

$$Y(y, \sigma_T) \equiv \{P, \phi\} \equiv \int_{-\infty}^{+\infty} dy' \cdot P(y - y', \sigma_p) \cdot \phi(y', \sigma_m), \quad (5)$$

where the instantaneous plume is given as:

$$P(y - y', \sigma_p) = \frac{1}{\sqrt{2\pi} \cdot \sigma_p} \cdot \exp\left[-\frac{(y - y')^2}{2 \cdot \sigma_p^2}\right] \quad (6a)$$

and $\sigma_p = \sigma_p(t)$ characterizes the width of the instantaneous plume and the presumed Gaussian envelope defining the plume's meander is given as:

$$\phi(y, \sigma_m) = \frac{1}{\sqrt{2\pi} \cdot \sigma_m} \cdot \exp\left[-\frac{y'^2}{2 \cdot \sigma_m^2}\right] \quad (6b)$$

The result of performing this convolution integration yields a normalized Gaussian distribution, $Y(y, \sigma_T)$,

$$Y(y, \sigma_T) = \frac{1}{\sqrt{2\pi} \cdot \sigma_T} \cdot \exp\left[-\frac{y^2}{2 \cdot \sigma_T^2}\right] \quad (7a)$$

with

$$\sigma_T^2 = \sigma_p^2 + \sigma_m^2. \quad (7b)$$

Performing the integral in Equation (5) requires little more than the technique of "completing the square". Knowing this, it is clear that the process of performing the Equation (5) integration yields a multiplicative factor, β ,¹

¹ Obtaining the correct factor requires knowing that $M \equiv \int_{-\infty}^{+\infty} dx \cdot \exp[-x^2] = \sqrt{\pi}$; however, this is computed by solving for M^2 and then shifting to (r, θ) coordinates.

where

$$\beta = \frac{\sqrt{2\pi} \cdot \sigma_m \cdot \sigma_p}{\sigma_T} . \quad (7c)$$

Implicit in the convolution process is the assumption that the processes of plume growth and plume meander are independent of one another. This independence may also be apparent from the quadrature addition rule for sigmas resulting in the total plume width, σ_T .

Those familiar with the Convolution or Faltung Theorem, which states that:

$$F(\{P, \varphi\}) = k \cdot F(P) \cdot F(\varphi) . \quad (8)$$

where F denotes the Fourier transform process and k is a normalization constant, will note that the idea that the convolution of two Gaussians results in a Gaussian is obvious given the above Convolution Theorem and the fact that the Fourier transform of a Gaussian is a Gaussian.

Thus, beyond the Gaussian representing the simplest K-theory solution to the diffusion equation, there are many mathematical conveniences to be had by choosing the Gaussian, and also there are clear physically-significant linkages (e.g., between observed Gaussian turbulent velocity distributions and the Gaussian concentration profiles obtained from the analytic solution for diffusion) and statistical properties (e.g., the independence of turbulent components of widely different wavelengths) that make the Gaussian the logical distribution of choice for puff and plume modeling.

2 Gaussian Applications

This section will consider applications involving the Gaussian or the Gaussian solution of the diffusion equation, which greatly facilitate obtaining additional results.

2.1 Concentration Fluctuations

As mentioned above, the convolution of an instantaneous Gaussian plume having a spread σ_p with a Gaussian meander envelope of spread σ_m leads to an ensemble-averaged Gaussian plume of width σ_T , where $\sigma_T^2 = \sigma_m^2 + \sigma_p^2$, such that peak-to-mean centerline concentrations are just σ_T / σ_p .

First developed by Gifford (1959) and extended by others, including Hanna (1986) and Sawford and Stapountzis (1986), Equation (5) may be integrated and generalized to yield higher moments of the concentration distribution as:

$$Y^{(n)}(y, \sigma_{Tn}) = \int_{-\infty}^{+\infty} dy' \cdot P^n(y - y', \sigma_p) \cdot \phi(y', \sigma_m) . \quad (9a)$$

By analogy with the Equation (5) integration, we note that performing the Equation (9a) integration will yield the exponential's multiplier, β_n ,

where

$$\beta_n = \frac{\sqrt{2\pi} \cdot \sigma_m \cdot \sigma_p}{\sigma_{Tn} \cdot \sqrt{n}} \quad (9b)$$

and where

$$\sigma_{Tn}^2 = \sigma_m^2 + \sigma_p^2/n . \quad (9c)$$

Thus, $Y^{(2)}$ has centerline (i.e., $y = 0$) value

$$Y^{(2)}(0, \sigma_{T2}) = \frac{1}{\sqrt{2\pi} \cdot \sigma_m \cdot 2\pi \cdot \sigma_p^2} \cdot \beta_2 = \frac{1}{2\pi \cdot \sqrt{2} \cdot \sigma_p \cdot \sigma_{T2}} \quad (10a)$$

with

$$\sigma_{T2}^2 = \sigma_m^2 + 1/2 \cdot \sigma_p^2 ; \quad (10b)$$

whereas,

$$Y^{(1)}(0, \sigma_{T1}) = \frac{1}{\sqrt{2\pi} \cdot \sigma_{T1}} , \quad (11a)$$

with

$$\sigma_{T1}^2 = \sigma_m^2 + \sigma_p^2 . \quad (11b)$$

One may then compute the concentration variance, σ_C^2 , as $\sigma_C^2 \equiv Y^{(2)} - (Y^{(1)})^2$ or that variance normalized by the mean concentration squared as,

$$\frac{\sigma_C^2}{(Y^{(1)})^2} = \left[\frac{\sigma_{T1}^2}{\sqrt{2} \cdot \sigma_p \cdot \sigma_{T2}} - 1 \right] \quad (12)$$

Of course, this concentration variance only reflects plume fluctuations due to meander in y , as $\sigma_C \rightarrow 0$ as $\sigma_m \rightarrow 0$, and ignores any variations in the z direction. It also ignores concentration fluctuations internal to the narrow plume of width σ_p ;

however, now we are beginning to delve into the well-developed specialty of concentration fluctuations, which would require a chapter of its own. The point here was to show the flexibility of the Gaussian and the ease to which one can obtain meaningful results by invoking the convolution theorem.

2.2 Diffusion into Soils

Deposition rates of air pollutants is predicted by a number of regulatory models worldwide, and the results of these surface deposition predictions are then used by other disciplines (e.g., soil scientists interested in watershed acidification, toxicologists assessing lead concentrations in surface soils), but the applications can go much deeper than that -- quite literally. For example, long-lived radioactive isotopes, such as ^{137}Cs deposited over many European countries during the 1986 Chernobyl incident continue to “diffuse” their way deeper into the soils and are readily detectable in core samples (e.g., Rosen et al., 1999; Doering et al., 2006; Kaste et al., 2007).

From Chapter 7B, Vol. 2 of Zannetti (2005), we know that the 1-d time-dependent solution of the diffusion equation is:

$$\phi(y, \sigma) = \frac{1}{2 \cdot \sqrt{\pi \cdot K \cdot t}} \cdot \exp\left[-\frac{z^2}{4 \cdot K \cdot t}\right], \quad (13)$$

where K is now the diffusivity of the soil, with values typically in the range of one cm^2/yr or less (i.e., some 12 orders of magnitude smaller than the rather stable atmospheric diffusivity of $3 \text{ m}^2/\text{s}$), and z is assumed positive in the direction downward into the soil. Carslaw and Jaeger (1959) showed that for a constant surface deposition rate, Q ($\text{g}/\text{cm}^2/\text{yr}$), to the surface (i.e., $z=0$) for all $t \geq 0$, the solution for soil concentration, C_s (gm/cm^3) as a function of depth and time is:

$$C_s(z, t) = \frac{Q}{K} \left[\sqrt{\frac{K \cdot t}{\pi}} \exp\left(\frac{-z^2}{4 \cdot K \cdot t}\right) - \frac{z}{2} \operatorname{erfc}\left(\frac{z}{2 \cdot \sqrt{K \cdot t}}\right) \right] \quad (14)$$

where, as before, $\operatorname{erfc}(x)$ is the complementary error function, $\operatorname{erfc}(x) \equiv 1 - \operatorname{erf}(x)$, and any diffusion upward into the atmosphere is prohibited (i.e., thus accounting for a factor-of-two multiplier) as are all other loss or decay mechanisms. Under such conditions, soil concentrations always increase with total time of deposition.

Now in the more realistic case, deposition occurs up to some cutoff time, $t' = T$, such that for observation times $t > T$, only additional diffusion occurs. Interestingly, there are several ways to formulate this problem. The first is to take the distribution from Equation (14) at time $t = T$ and allow it to diffuse for times $t > T$ via:

$$C_s(z,t) = \left(\frac{2 \cdot Q}{K}\right) \cdot \int_0^\infty dz' \cdot \frac{\left[\sqrt{\frac{K \cdot T}{\pi}} \exp\left(\frac{-z'^2}{4 \cdot K \cdot T}\right) - \frac{z'}{2} \operatorname{erfc}\left(\frac{z'}{2\sqrt{K \cdot T}}\right) \right]}{\sqrt{\pi \cdot K \cdot (t-T)}} \cdot \exp\left(\frac{-(z-z')^2}{4 \cdot K \cdot (t-T)}\right) \quad (15a)$$

however, the part of this integral involving the convolution of the *erfc* with the Gaussian appears rather difficult to solve. Alternatively, one could back up a step from Equation (14) and express the problem as the double-integral:

$$C_s(z,t) = 2 \cdot Q \cdot \int_0^\infty dz' \cdot \int_0^T dt' \cdot \frac{\exp\left(\frac{-z'^2}{4 \cdot K \cdot t'}\right)}{\sqrt{4 \cdot \pi \cdot K \cdot t'}} \cdot \frac{\exp\left(\frac{-(z-z')^2}{4 \cdot K \cdot (t-T)}\right)}{\sqrt{4 \cdot \pi \cdot K \cdot (t-T)}} \quad (15b)$$

Note that in this expression, the $\sqrt{4}$ constant factors have been left in place to show that the overall factor of 2 is needed to account for material at the surface not diffusing upward into the air, but being “reflected” back into the soil. One may then solve this problem by reversing the order of the integrations and performing the spatial convolution first; however, this approach is equivalent to the more direct approach of specifying the diffusion of an emission $Q \cdot dt'$ for all $t > t'$ and then integrating over time t' to yield the concentrations at a specific depth z for $t > T$ as:

$$C_s(z,t) = 2 \cdot \int_0^T \frac{dt' \cdot Q(t')}{\sqrt{4 \cdot \pi \cdot K \cdot (t-t')}} \exp\left(\frac{-z^2}{4 \cdot K \cdot (t-t')}\right); \quad (15c)$$

whereas, the concentration averaged over a depth interval $L \equiv z_2 - z_1$, (i.e., from depth z_1 to depth z_2) can then be written as:

$$C_{s,ave}(t) = \frac{1}{L} \cdot \int_0^T dt' \cdot Q(t') \cdot \left\{ \operatorname{erf}\left(\frac{z_2}{2 \cdot \sqrt{K \cdot (t-t')}}\right) - \operatorname{erf}\left(\frac{z_1}{2 \cdot \sqrt{K \cdot (t-t')}}\right) \right\} \quad (16)$$

Drivas et al. (2010) have shown that these last two integrals can be solved by changing from variable t' to s , where $s = \frac{\lambda}{2 \cdot \sqrt{K \cdot (t-t')}}$, $dt' = \left(\frac{\lambda^2}{2 \cdot K}\right) \cdot \frac{ds}{s^3}$, and, where λ stands for either z , z_2 or z_1 . Their final results for $t > T$ are found to be:

$$C_s(z,t) = \frac{Q \cdot z}{K} \cdot [f(s_L) - f(s_U)], \quad (17)$$

where $f(s) \equiv \left[\frac{\exp(-s^2)}{\sqrt{\pi} \cdot s} + \text{erf}(s) \right]$, $s_L = \frac{z}{2\sqrt{K \cdot t}}$ and $s_U = \frac{z}{2\sqrt{K \cdot (t-T)}}$; and,

$$C_{s,ave}(t) = \frac{Q \cdot L^{-1}}{2 \cdot K} \cdot \left\{ z_2^2 \cdot [g(s_{L2}) - g(s_{U2})] - z_1^2 \cdot [g(s_{L1}) - g(s_{U1})] \right\} \quad (18)$$

where $g(s) \equiv \left[\frac{\exp(-s^2)}{\sqrt{\pi} \cdot s} + \left(1 + \frac{1}{2 \cdot s^2}\right) \cdot \text{erf}(s) \right]$, $s_{L2} = \frac{z_2}{2\sqrt{K \cdot t}}$, $s_{U2} = \frac{z_2}{2\sqrt{K \cdot (t-T)}}$,

$s_{L1} = \frac{z_1}{2\sqrt{K \cdot t}}$ and $s_{U1} = \frac{z_1}{2\sqrt{K \cdot (t-T)}}$.

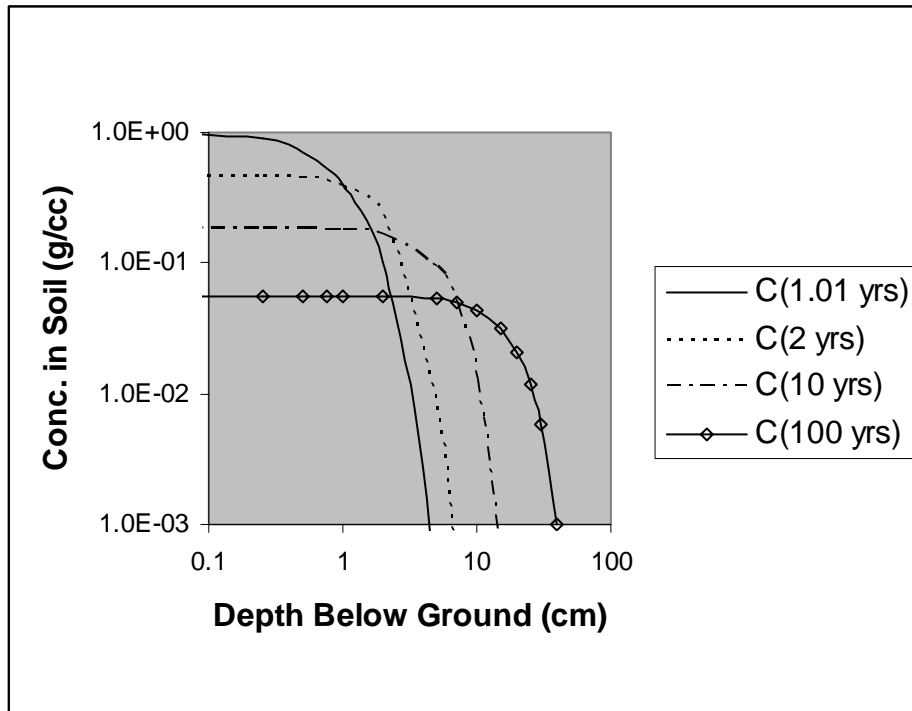


Figure 1. Equation (17) concentrations in soil vs. depth below surface at various times for a unit strength deposition, $Q=1 \text{ g/m}^2/\text{yr}$, beginning at $t=0$ and having a duration of $T = 1 \text{ yr}$. A unit diffusivity of $K=1.0 \text{ cm}^2/\text{yr}$ is also assumed.

Evaluation of these expressions, such as the Equation (17) curves displayed above, show that radioactive, or other non-reactive, species concentrations can show up at some depth, well below the surface, decades after at the deposition at the surface has ceased. This insidious march of hazardous pollutants to deeper depths and eventually to groundwater levels has been the driving force behind many Superfund projects, including the massive cleanup effort in Hanford, WA,

site of many nuclear research activities from the mid-1940s through the late 1980s. Thus, one sees that new and relevant applications of purely Gaussian-based solution formulations continue to be developed and applied.

2.3 Non-Linear Chemistry in Puff Modeling

Photochemical grid models now constitute the major vehicle for addressing ozone and secondary particulate impact issues; however, pure grid models suffer from the shortcoming that point-source emissions are immediately diluted into a grid-cell-sized box of dimensions $dx \cdot dy \cdot dz$. This initial instantaneous dilution ignores near-source, within-plume conversion processes, which can occur very rapidly given the high-concentrations of primary pollutants near the source.

One approach to dealing with this problem is to employ a nested-grid approach, and this approach is often used in regional modeling with horizontal resolutions over source-rich urban or industrial source areas nested down to about 1 km. Nevertheless, initial dilution into a box that is one kilometer squared in area leaves much early chemistry neglected. This early chemistry is now tackled by using various types plume-in-grid (PiG) modules to facilitate reaction of the pollutants close to the source and transport them until the plume's or puff's size is comparable to the grid resolution, whereupon the material is injected into the grid model itself.

Early PiG models involved Gaussian plumes, but it was quickly realized that one needed yet higher, sub-plume scale resolution, so there was a pronounced shift towards using puffs instead. Of course, once starts to think in terms of puffs, the transition to very small puffs or even Lagrangian particles having some finite spatial extent is more a leap of computational intensity than a conceptual one.

To understand the basic challenge of performing non-linear chemistry using puffs, we begin with the basic equation for chemical transformations within an N-species system. In general, the set of N equations describing the time evolution of species mixing ratios², $c(t)_i$, that undergo 1st, 2nd, and pseudo-3rd order chemical reactions can be written as:

$$\frac{dc_i(t)}{dt} = \sum_{j=1}^N \sum_{k=j}^N R_i^{jk} \cdot c_j(t) \cdot c_k(t), \quad i, j, k = 1, 2, 3, \dots, N, \quad (19)$$

where R_i^{jk} is the matrix (i.e., rank-3 tensor) of chemical reaction rates. Now invoking the convention of implied summation over repeated indices (i.e., j and k) and integrating over some agree-upon volume of space one has the equation system:

² A mass concentration, C_i , relates to the dimensionless mixing ratio, c_i via the relation $C_i = \rho \cdot c_i$.

$$\frac{dm_i(t)}{dt} = \iiint_V \rho \cdot \frac{dc_i(t)}{dt} = R_i^{jk} \cdot \iiint_V \rho \cdot c_j(t) \cdot c_k(t), \quad i, j, k = 1, 2, 3, \dots, N, \quad (20)$$

where ρ is the local air density. In the case of grid modeling, the volume, V , to be integrated over is simply the volume of the current cell being considered, and within-cell mixing ratios and masses are related simply by, $m_i = \rho \cdot c_i \cdot V$. However, in the case of dealing with puffs or particles, we have the additional complications that concentrations of each species at any single point can involve the summation over many nearby puffs and that the volumes to be associated with each particle or puff will definitely overlap those volumes associated with other particles or puffs.

Thus, even the definition of species mixing ratios c_i , c_j , and c_k at any point involve sums over all puffs that could possibly contribute to species concentrations at that point. Because any product of sums can always be re-expressed of a sum of products, one sees that the computation of species concentrations involves the spatially-integrated product of the spatial distributions associated with some puff p and any other puff m . Choice of the indices p and m was done partly to avoid confusion with the already used pollutant species indices i , j , and k but also to facilitate bridging back to Equation (5) where our interest was in integrating in one spatial dimension over two Gaussian distributions, displaced from one another by a distance y . Since the three-dimensional Gaussian is nothing more than the product of three one-dimensional Gaussians, the convolution theorem immediately comes to our rescue and enables us to define the integral concentration overlap of puff p with that of puff m as:

$$\iiint_V c_{jp}(t) \cdot c_{km}(t) = \frac{(q_{jp} / \rho_p) \cdot (q_{km} / \rho_m)}{(2\pi)^{3/2} \cdot \sigma_{Tx} \cdot \sigma_{Ty} \cdot \sigma_{Tz}} \cdot \exp \left[-\frac{1}{2} \left(\frac{x^2}{\sigma_{Tx}^2} + \frac{y^2}{\sigma_{Ty}^2} + \frac{z^2}{\sigma_{Tz}^2} \right) \right] \quad (21)$$

where q_{jp} is the mass of species j assigned to puff p , q_{km} is the species k mass of puff m ; (x, y, z) specify the puff center separations; and the puff p - m overlap-sigma quantities σ_{Tx} , σ_{Ty} , and σ_{Tz} are given as:

$$\sigma_{Tx}^2 = \sigma_{px}^2 + \sigma_{mx}^2, \quad \sigma_{Ty}^2 = \sigma_{py}^2 + \sigma_{my}^2, \quad \text{and} \quad \sigma_{Tz}^2 = \sigma_{pz}^2 + \sigma_{mz}^2, \quad \text{respectively.}$$

In practice, the computational tedium of computing many thousands of Gaussians often leads developers to use simpler functions, such as the Epanechnikov kernel estimator (Epanechnikov, 1969) rather than the Gaussian. Like the Gaussian, such a 3-d kernel defines a spatially-diffuse concentration as:

$$c_{jp} = \frac{(q_{jp} / \rho_p)}{\lambda_{px} \cdot \lambda_{py} \cdot \lambda_{pz}} \cdot f \left(\left| \frac{x'}{\lambda_{px}} \right| \right) \cdot f \left(\left| \frac{y'}{\lambda_{py}} \right| \right) \cdot f \left(\left| \frac{z'}{\lambda_{pz}} \right| \right) \quad (22a)$$

where each “bandwidth” λ_p can be related to the corresponding σ_p , (e.g., the relation $\lambda_p = 2.214 \cdot \sigma_p$) and the function $f(\phi)$ is defined as:

$$f(\phi) = \begin{cases} \frac{3}{4}(1-\phi^2) & |\phi| \leq 1 \\ 0 & |\phi| > 1 \end{cases}, \text{ where, for example, } \phi = |x'/\lambda|. \quad (22b)$$

Another advantage of such a finite function which cuts off sharply for $|\phi| > 1$ (e.g., for $|x'/\lambda_{px}| > 1$) is that one has a very clear search window to look for neighboring puffs where the overlap integral is non-zero.

Once all the dm_i/dt quantities are determined, there is the bookkeeping issue of how to assign the mass change dm_i in species i back to the most-appropriate puffs in some proportionate way and without creating nasty problems, such as negative species mass being assigned to any puff/particle. This mass reassignment issue is discussed in Monforti et al. (2006).

3 Gaussian Regulatory Model Improvements

This section will consider recent improvements to U.S. EPA regulatory models that involve changes to the basic way in which the Gaussian solution is applied. Interestingly, some of these changes generally do not involve abandoning the Gaussian, but rather using more of them.

Our first example involves the case of dispersion under convective conditions. AERMOD (U.S. EPA, 2004 and Cimorelli et al., 2005) now treats such convective dispersion by employing two Gaussians: one whose centerline is advected upward by an updraft velocity and another whose centerline is advected downward by a downdraft velocity. These two Gaussians are weighted in proportion to the fractional area of updraft and downdraft zones, respectively. This formulation, developed by Weil and Brower (1984) and Weil (1985), results in asymmetric vertical dispersion that is in better agreement with the Willis and Deardorff (1978) water tank data than that which a single Gaussian could provide, but is completely consistent with the Gaussian approach.

A similar example that appears in AERMOD involves the treatment of flow over complex terrain, in that the final plume is a weighted sum of a plume, which follows terrain and one that does not.

A final AERMOD example involves the treatment of low wind speed conditions. As mentioned by Venkatram and Thé, (2003 - in Chapter 7A, Vol. 1), this issue of providing a proper azimuthal distribution as the mean wind goes to zero is bridged by using the weighted sum of a Gaussian distribution in y and a uniform azimuthal distribution and is given as:

$$H(x, y) = f_r \cdot \frac{1}{2 \cdot \pi \cdot r} + (1 - f_r) \cdot \frac{1}{\sqrt{2 \cdot \pi \cdot \sigma_y}} \exp\left(-\frac{y^2}{2 \cdot \sigma_y^2}\right) \quad (23)$$

where $f_r = \frac{2 \cdot \sigma_v^2}{U_e^2}$, $U_e \equiv (2 \cdot \sigma_v^2 + U_m^2)^{1/2}$, U_m is the vector mean wind speed, and U_e provides the estimate of the total dilutionary wind.

Unfortunately, even this adjustment does not solve the problem of model over-prediction at very low wind speeds. Paine et al. (2010) reported over-predictions by a factor of 2-3 found in several low wind tracer studies, and have found it necessary to use a reformulated expression for the friction velocity, u^* , within the AERMET preprocessor to provide higher u^* at low mean winds, which in turn results in higher levels of vertical and horizontal turbulence and dilutionary wind U_e . Their analysis also suggested the need for imposing a minimum value of 0.4 m/s on σ_v .

For assessments involving mesoscale and longer-range transport (i.e., > 50 km.), CALMET (Scire et al., 1998) and CALPUFF (Scire et al., 2000; Scire, 2008) continues to be EPA's recommended Guideline modeling system; however, the more routine availability of high-resolution prognostic meteorological modeling has called into question some of CALMET's technical options (U.S. EPA et al, 2009) and the wisdom, in general, of filtering self-consistent, prognostic meteorological fields through a diagnostic wind field model with some historical shortcomings (e.g., divergence minimization ignoring air density, formulation in terrain-subtracted coordinates). As an alternative, more direct interface routines between the MM-5 and WRF models and CALPUFF are now being developed (Scire, 2008; Emery et al., 2009). Such more direct interfacing of high-quality meteorological fields, should improve the performance of CALPUFF in mesoscale and long-range tracer study comparisons (e.g., CAPTEX, ETEX) versus its performance using CALMET fields (Anderson and Brode, 2010).

It should also be noted that the wider and more routine availability of high-quality prognostic modeling results incorporating meteorological data assimilation, leads one to question the traditional regulatory dividing line of 50 km between using plume models and puff or particle models. A typical near-surface wind of 5 m/s only carries pollutants 18 km in one hour, and there are often terrain and intervening surface/land-use variations that challenge the assumptions of straight-line flows and uniform turbulence conditions. Low wind speeds represent yet another challenge to traditional plume modeling. Even if one relinquishes the need for specific hour-by-hour predictive power and requires only information about the highest concentration hours within a year or multi-year period, the presence of an intervening land-use shift between source and receptor (e.g., a large lake) could lead to systematic over-/under-predictions.

The CALPUFF model was designed to provide concentration predictions identical to the ISC-3 short-term dispersion model under the assumption of steady-state, uniform flow conditions, and could easily be modified to incorporate the dispersion modeling differences brought about by the transition from ISC to AERMOD (e.g., more realistic treatment of convective conditions), as anything that can be done with plumes can also be done with puffs or slugs (i.e., time-integrated puffs). Puff and particle models also incorporate along-wind dispersion, so that low or calm winds are not problematic.

The traditional objections to switching to puff or particle models, such as computational cost or requisite data base complexity become less relevant each year; however, there are major obstacles that science cannot circumvent, and these appear to arise (i.e., from a modelers perspective) from legal considerations (e.g., precedence, the standing of existing air quality permits, resolution of discrepancies). These same non-scientific considerations also appear to have inhibited regulatory recognition and utilization of uncertainty estimates that arise from predictions of higher concentration moments (i.e., C^2 in addition to C -- as discussed in Section 2.1 and indirectly in Section 2.3). Regulators accepted photochemical grid modeling, not because it was a clever method but because it represented the only way to predict ozone and some secondary aerosol concentrations. A switch in the regulatory approach can only be anticipated when the current approach can be shown to be severely deficient on model performance grounds as opposed to being deficient merely on scientific principle grounds.

Acknowledgments

I would like to thank Professors Steven R. Hanna, Brian Sawford, and John D. Wilson and Dr. Joseph Chang, Gary Moore, and David Strimaitis for their useful comments. I would also like to acknowledge Mr. Robert Paine's providing me with recent AERMOD development manuscripts and helpful comments.

References

- Anderson, B. A. and R. W. Brode, 2010. Evaluation of Four Lagrangian Models Against the Cross-Appalachian and European Tracer Experiments. Presented at the EPA Modeling Workshop, May 13, Portland, OR.
- Bianconi, R., Mosca, S., and Graziani, G., 1999. PDM: a Lagrangian Particle Model for Atmospheric Dispersion. European Communities report 17721 EN, Ispra, Italy.
- Cimorelli, A.J., S.G. Perry, A. Venkatram, J.C. Weil, R.J. Paine, R.B. Wilson, R.F. Lee, W.D. Peters, and R.W. Brode, 2005. AERMOD: A Dispersion Model for Industrial Source Applications. Part I: General Model Formulation and Boundary Layer Characterization. *J. Appl. Met.*, **44**, 682-693. American Meteorological Society, Boston, MA.
- de Haan, P., 1999. On the use of density kernels for concentration estimations within particle and puff dispersion models. *Atmos. Environ.*, **33**, 2007-2021.

- Doering, C. R., Akber, H., Heijnis, 2006. Vertical distributions of ^{210}Pb excess, ^7Be and ^{137}Cs in selected grass covered soils in Southeast Queensland, Australia. *J. Environ. Radioact.*, **87**, 135-147.
- Durbin, P.A., 1983. Stochastic Differential Equations and Turbulent Dispersion, NASA Reference Publication 1103, NASA Lewis Research Center, Cleveland, OH, 73pp.
- Emery, C., B. Brashers, and B. Anderson, 2009. A New Direct MM5/WRF Meteorological Interface Program for CALPUFF. Presented at the AWMA Guideline on Air Quality Models: Next Generation of Models, Oct. 28, Raleigh, NC.
- Epanechnikov, V.K., 1969. Non-parametric estimation of a multivariate probability density. *Theory of Probability and its Applications*, **14**, 153-158.
- Carslaw, H.S. and J.C. Jaeger, 1959. *Conduction of Heat in Solids*, Second Edition. Clarendon Press, Oxford.
- Drivas, P.J., T.S. Bowers, and R. J. Yamartino, 2010. Soil Mixing after Surface Deposition: I. Theory. *Environ. Sci. Technol.*, submitted for publication.
- Gifford, F. A., 1959: Statistical properties of a fluctuation plume dispersion model. *Advances in Geophysics*, **6**, 117–138.
- Hanna, S. R., 1986: Spectra of concentration fluctuations: The two time scales of a meandering plume. *Atmos. Environ.*, **20**, 1131–1137.
- Kaste, J. M., A. M. Heimsath, B. C. Bostick, 2007. Short-term soil mixing quantified with fallout radionuclides. *Geology*, **35**, 243-246.
- Lemons, D. S., 2002. *An Introduction to Stochastic Processes in Physics*. The Johns Hopkins University Press, Baltimore, MD, 124 pp.
- Luhar, A. K., R. E., Britter, 1989. A random walk model for dispersion in inhomogeneous turbulence in a convective boundary layer. *Atmos Environ*, **23**, 1911–1924.
- Monforti, F., L. Vitali, G. Pagnini, R. Lorenzini, L. Delle Monache, and G. Zanini, 2006: Testing kernel density reconstruction for Lagrangian photochemical modelling. *Atmos. Environ.*, **40**, 7770-7785.
- Paine, R. J., J. A. Connors, and C. D. Szembek, 2010: AERMOD Low Wind Speed Evaluation Study: Results and Implementation. AWMA Paper 2010-A-631-AWMA
- Pope, S. B., 2000. *Turbulent Flows*. Cambridge University Press, UK, 806pp.
- Rosen, K, I. Oborn, H. Lonsjo, 1999. Migration of radiocaesium in Swedish soil profiles after the Chernobyl accident, 1987-1995. *J. Environ. Radioact.*, **46**, 45-66.
- Sawford, B. L., 1985: Concentration statistics for surface plumes in the atmospheric boundary layer. *Proc. Seventh Symp. on Turbulence and Diffusion*, Boulder, CO, pp. 323–326.
- Sawford, B. L. and H. Stapountzis, 1986: Concentration fluctuations according to fluctuating plume models in one and two dimensions. *Bound.-Layer Meteor.*, **37**, 89–105.
- Scire, J., 2008. Development, Maintenance and Evaluation of CALPUFF. Presented at the Ninth Conference on Air Quality Modeling, Oct. 9-10, Research Triangle Park, NC.

Scire, J.S., D.G. Strimaitis and R.J. Yamartino, 2000. User's guide for the CALPUFF dispersion model (Version 5). Earth Tech, Inc., Concord, MA.

Scire J.S., F.R. Robe, M.E. Fernau, and R.J. Yamartino, 1998. A User's Guide for the CALMET Meteorological Model (Version 5.0). Earth Tech, Inc., Concord, MA.

U.S. EPA, National Park Service, and U.S. Fish and Wildlife Service, 2009. Reassessment of the Interagency Workgroup on Air Quality Modeling (IWAQM) Phase 2 Summary Report: Revisions to Phase 2 Recommendations. DRAFT Report EPA-454/R-09-xxx.

U.S. EPA, 2004. AERMOD: Description of Model Formulation. EPA-454/R-03-004. Available from <http://www.epa.gov/scram001>.

van Dop, H., F. T. M. Nieuwstadt, and J. C. R. Hunt, 1985. Random walk models for particle displacements in inhomogeneous unsteady turbulent flows. *Phys. Fluids*, **28**, 1639-1653.

Venkatram, A. and J. Thé, 2003. Introduction to Gaussian Plume Models. Chapter 7A in *Air Quality Modeling: Volume I – Fundamentals*. Paolo Zannetti, Ed., EnviroComp Institute and the Air and Waste Management Association.

Weil, J.C., and R. P. Brower, 1984. An updated Gaussian plume model for tall stacks. *J. Air Pollut. Control Assoc.*, **34**, 818–827.

Weil, J.C., 1985, Updating applied diffusion models. *J. Clim. App. Meteor.*, **24**(11), 1111-1130.

Willis, G. E. and J. W. Deardorff, 1978. A laboratory study of dispersion from elevated source within a modeled convection mixed layer. *Atm. Env.*, **12**, 1305-1311.

Wilson, J. D., 2007. Turbulent velocity distributions and implied trajectory models. *Boundary-Layer Meteorol.*, **125**, 39–47.

Yamartino, R.J., 2008a. Gaussian Puff Modeling. Chapter 8A of *AIR QUALITY MODELING - Theories, Methodologies, Computational Techniques, and Available Databases and Software. Vol. III – Advanced Topics*. (P. Zannetti, Editor). Published by The EnviroComp Institute and the Air & Waste Management Association.

Yamartino, R.J., 2008b. Simulation Algorithms in Gaussian Plume Modeling. Chapter 7B of *AIR QUALITY MODELING - Theories, Methodologies, Computational Techniques, and Available Databases and Software. Vol. III – Advanced Topics*. (P. Zannetti, Editor). Published by The EnviroComp Institute and the Air & Waste Management Association.

BRAND
PAPER

Chapter 10

Eulerian Dispersion Models

A comprehensive chapter on Eulerian Dispersion Models was included in Volume I of this book series. The abstract is reprinted below.

The main objectives of this chapter are to introduce the state-of-the-art numerical algorithms for the advection and diffusion used in Eulerian models and to discuss their theoretical and numerical characteristics. The Eulerian approach allows incorporation of different physical and chemical processes involved with the gaseous and particulate constituents in the atmosphere. The governing conservation equation for tracer species dispersion is derived. Approximations in the atmospheric dynamics and fundamental concepts used in the description of turbulence are explained. Some analytical solutions are provided for simplified dispersion conditions to illustrate basic processes in the atmospheric dispersion models. In the Eulerian approach, governing equations can be solved with a fractional time step or an explicit-implicit method to take advantage of numerical efficiency and knowledge of physical parameterizations of atmospheric surface flux exchange, advection, and diffusion processes. This chapter describes numerical solution methods for each physical process component in the Eulerian dispersion model. We provide fundamental steps used in the derivation of numerical advection algorithms, horizontal and vertical eddy diffusivity formulations, and local and non-local vertical diffusion methods. In the Appendix we have compiled vertical eddy diffusivity formulations in the literature, numerical solution methods of the local and non-local vertical diffusion algorithms, and Numerical algorithms with two-level time differencing for constant grid spacing.

For additional information, the reader can visit:

- Models-3/Community Multiscale Air Quality (CMAQ) Modeling System
<http://www.epa.gov/asmdnerl/CMAQ/index.html>
- Comprehensive Air Quality Model with Extensions (CAMx)
<http://www.camx.com/>
- Regional Modeling System for Aerosols and Deposition (REMSAD)
<http://remsad.saintl.com/>
- Urban Airshed Model® (UAM®) Modeling System
<http://uamv.saintl.com/>

Chapter 11

Lagrangian Particle Models

A comprehensive chapter on Lagrangian Particle Models was included in Volume II of this book series. The abstract is reprinted below.

Lagrangian particle dispersion models are being increasingly used to simulate air pollution dispersion at different spatial and temporal scales and in various stability conditions. In this Chapter, a review of the present state of the art of Lagrangian stochastic models for the description of airborne dispersion in the Planetary Boundary Layer is presented. These models are based on the generalized Langevin equation. Their theoretical basis and relevant implementation aspects are reviewed, and examples of main applications are discussed.

For additional information, the reader can visit:

- Online Papers by Marek Uliasz
<http://www.marekulasz.com/modeling/papers.htm>
- The Lagrangian Particle Dispersion Model FLEXPART Version 6.2
<http://www.atmos-chem-phys-discuss.net/5/4739/2005/acpd-5-4739-2005-print.pdf>
- AUSTAL View
<http://www.weblakes.com/products/austal/index.html>
- PARTPUFF Model
<http://journals.ametsoc.org/doi/pdf/10.1175/1520-0450%281994%29033%3C0285%3APLPPAF%3E2.0.CO%3B2>
- FLEXTRA and FLEXPART Models
<http://zardozenilu.no/~andreas/flextra+flexpart.html>
- Puff-Particle Model (PPM)
http://www.epa.gov/scram001/9thmodconf/scire_puff-particle_model.pdf

BRANK
P
e

Chapter 12

Atmospheric Transformations

A comprehensive chapter on Atmospheric Chemistry and Chemical Transformations was included in Volume II of this book series. The abstract is reprinted below.

A typical air quality model tracks the transport and transformation of chemicals in the atmosphere. Transport refers to physical movement (dispersion, emissions, and deposition) of pollutants. Atmospheric transformations encompass both physical and chemical changes of chemicals in the atmosphere. In this chapter, we provide a review of the fundamentals of gas phase chemical reactions, phase transitions, aqueous phase reactions, and an overview of the key processes involved in the formation of ozone, particulate matter, hazardous air pollutants, and halogen chemistry. Modeling air quality entails the mathematical representation of the atmospheric transformations and the numerical solution of the algebraic equations and ordinary differential equations, which are developed in this chapter. The modeling of chemical transformations is discussed, starting with plume models and the gas-phase chemistry at different stages of the plume. We then describe several Eulerian models and their atmospheric mechanisms, including the Carbon Bond Mechanism (CBM)-IV, the Statewide Air Pollution Research Center mechanisms, the Regional Acid Deposition Model mechanism version 2, and others. The modeling of particulate matter and droplets requires a mathematical description of the aqueous-phase and heterogeneous chemistry. Modules that describe the gas/particle partitioning of inorganic species and organic species are discussed. The distribution of the semi-volatile products of gas-phase, aqueous, and heterogeneous reactions onto particles depends on the representation of the particle size distribution. In

one-atmosphere approach, a single model would suffice if it included a comprehensive chemical mechanism containing all gas-phase, heterogeneous, and aqueous-phase reactions for all air pollutants of concern and a phase transition module describing all relevant dynamic processes for different types of particles. In practice, chemical mechanisms have been developed to describe the chemical transformation processes for different air pollutants. Therefore, in addition to models describing ozone and particulate matter (PM), specific models exist for hazardous air pollutants and other models describe the stratosphere. To complete the overview of available models for chemical transformations, plume-in-grid type models that combine plume chemistry with urban/regional chemistry are discussed.

For additional information, the reader can visit:

- Photochemical Air Quality Models
<http://www.epa.gov/ttn/scram/photochemicalindex.htm>
- Photochemical Modeling Applications
http://www.epa.gov/ttn/scram/modelingapps_photo.htm
- Modeled Attainment Test Software (MATS)
http://www.epa.gov/ttn/scram/modelingapps_mats.htm
- Atmospheric Chemistry
<http://www.giss.nasa.gov/research/chemistry/>
http://www.sciencedaily.com/articles/a/atmospheric_chemistry.htm
- Introduction to Atmospheric Chemistry
<http://www.mpch-mainz.mpg.de/~sander/chem-intro.html>
- Information on Atmospheric Chemistry Research
<http://airsite.unc.edu/>
- Harvard Atmospheric Chemistry Modeling Group
<http://acmg.seas.harvard.edu/>

Chapter 13

Deposition Phenomena

A chapter on Atmospheric Deposition Phenomena was included in Volume II of this book series. The abstract is reprinted below.

Deposition phenomena are one of the most important processes occurring in the atmosphere. Deposition phenomena include the exchange of pollutants between the atmosphere and the surface of the earth. This exchange process can be parameterized and modeled by simulating the turbulence characteristics of the atmospheric flow. These turbulence characteristics require specific parameterization procedures to take very different and complex environments such as canopy, water, forest, and others into account. Deposition phenomena are essential processes in atmospheric modeling since they account for all the pollution removal while the atmospheric dispersion and transport are taking place. A correct modeling is needed to address issues such as the “critical load” concept or “surface damage” quantification. In this chapter we will focus on the current approach to describe deposition processes and the modeling techniques needed to simulate, with atmospheric transport models, the boundary conditions at the surface of the earth.

In this Volume IV, we present Chapter 13A on Modeling of Pesticide Application, Deposition and Drift.

BRANK
P
e

Thistle, H.W. et al., 2010. *Modeling of Pesticide Application, Deposition and Drift*. Chapter 13A of *AIR QUALITY MODELING – Theories, Methodologies, Computational Techniques, and Available Databases and Software. Vol. IV – Advances and Updates* (P. Zannetti, Editor). Published by The EnviroComp Institute (<http://www.envirocomp.org/>) and the Air & Waste Management Association (<http://www.awma.org/>).

Chapter 13A

Modeling of Pesticide Application, Deposition and Drift

Harold W. Thistle⁽¹⁾, Milton E. Teske⁽²⁾ and Paul C.H. Miller⁽³⁾

⁽¹⁾ *FHTET, USDA Forest Service, Morgantown, WV (USA)*
hthistle@fs.fed.us

⁽²⁾ *Continuum Dynamics, Inc. Ewing, NJ (USA)*
milt@continuum-dynamics.com

⁽³⁾ *The Arable Group, Silsoe, Bedford (UK)*
paul.miller@thearablegroup.com

Abstract: Applied modeling techniques describing simulation of ground spraying and aerial spraying of pesticides are presented. The state of the art in aerial spraying is somewhat further advanced due to early concerns about off-target drift of aerially applied pesticide sprays. Recent regulatory concern has focused on drift from ground sprayers and has initiated a body of model development work that is currently very active. Modeling of pesticide application generally divides the model domain into regions 1) where the machine and wake effects dominate and 2) where material movement is dominated by ambient environmental conditions. Though well over 30 environmental and mechanical variables have some influence on droplet (or particle) landing position, the primary dependence is with particle size. The existing models have focused on liquid spraying and are generally not atomization models but require a droplet size distribution to be input. The droplet distribution is binned by size and various mathematical schemes are used to transport the released droplets to the position of deposit. Droplet evaporation can be a critical variable in the case of materials with high volatility, so droplet evaporation is described. Models typically will incorporate a scheme to describe the interaction with the target surface (vegetative or otherwise). These schemes must include a description of collection efficiency or ‘likelihood’ that an approaching droplet will deposit. Ground sprayer modeling must also consider droplet plume interaction with horizontal obstacles in an aggregate sense.

Key Words: pesticide deposition, pesticide application modeling, Lagrangian droplet transport, ground spraying, aerial spraying, pesticide spraying, pesticide drift.

1 Introduction

Modeling of pesticide application is undertaken for many of the reasons that most physical modeling is performed. That is, to create a simulation that can be manipulated with respect to the modeled variables at much lower cost than replicating field measurements. Mechanistic models of the type emphasized here can also be used to gain insight to the basic physical phenomena being modeled, test sensitivity to the relevant mechanistic and physical variables, and point out data gaps in our understanding of the underlying relationships.

The models that have developed and evolved (in the sense of having been written and then altered in response to new information and technologies) in the area of pesticide application modeling are mechanistic models but generally do not attempt to be full physics models. For example, though the spray drop size distribution is most often the primary determinant of the landing position of the spray mass, the models described here do not typically tackle the difficult problem of primary atomization. Instead, measured initial droplet spectra are input based on user knowledge of nozzle type, nozzle angle relative to the vehicle movement (the slipstream) etc. The models described below typically use Lagrangian droplet transport schemes but may also incorporate Gaussian elements as well as simple volume dilution approximations (box models).

In the context of this chapter, it is worth noting that pesticide application models can often account for the landing position of a large part of the released mass with an accuracy that might leave some atmospheric dispersion modelers incredulous. It must be remembered that if a slow moving tractor (say 15 km/hr forward speed) is releasing 600 μ m droplets from a boom .6 m above the ground surface, gravity will often put a large majority of the mass in the tractor 'swath' in a relatively predictable manner. Even in this scenario, the various shear forces associated with atomization, wake and atmospheric forces will conspire to produce some fine droplets and move them away from the spray target. It is the challenge of the modern pesticide application modeler to anticipate the fate of smaller and smaller amounts of spray material at greater distances as scrutiny of pesticide application, and concerns about pesticide residue continue to increase.

The development of pesticide application modeling has been driven by regulatory applications. Regulators need relatively simple, consistent tools to determine exposure to pesticides in scenarios ranging from human health to ecotoxicity. In the United States, pesticide use is regulated through label language printed on labels affixed to the pesticide container. Approval of label content and the decision to allow a pesticide on the market for use rests with US EPA and is based on a comprehensive registration process that includes extensive risk assessment. Pesticide application and fate models are used in a formal process as part of pesticide registration. In other countries, pesticide application models are used to set buffers or setbacks that cannot be sprayed into directly. These buffers are often established using pesticide application modeling. In the United States,

pesticide application models are increasingly used by government agencies enforcing the endangered species act. Using ecotoxicity data for specific endangered species and specific chemicals, 'no spray' buffer zones are established around endangered creatures to protect them from deleterious effects due to pesticides. Other regulatory applications of modeling include regulating the types of pesticides that can be used in a given scenario, and the number of times application can occur in a given time period, as well as other application parameters.

This chapter deals with primary drift, which is drift from the sprayer to droplet landing position. A vapor phase exists as liquid droplets evaporate, and this primary vapor drift is not discussed in detail here. Reentrainment, volatilization from surfaces after deposition, etc., known as secondary drift, is not discussed. Formulation chemistry is a field in itself and the chemistry of the spray material is a controlling factor in liquid atomization. Chemicals introduced to improve application efficacy and reduce drift are known as adjuvants and these present a myriad of options to the applicator. Much formulation chemistry is proprietary. To keep modeling manageable, the models generally only need droplet size distribution, volatility and specific gravity specified. If it is believed that the chemistry affecting the position of spray deposition is not adequately described using these properties, wind tunnel droplet sizing must be undertaken with the actual spray mixture used to determine the droplet size spectra. Since the droplet size spectra is the primary determinant of landing position, increasing droplet size is often the goal in drift reduction.

It is difficult to generalize the approaches described here to all spraying scenarios. Two that are recognized by the modeling community as distinct from aerial and ground as described below are orchard air-blast, and public health spraying. Orchard air blast utilizes fine droplets propelled into orchard canopies (often upward) using a strong air stream as the carrier. Though modeling approaches have been proposed for this scenario (see Walklate (1987) and Cross et al. (2001a, 2001b, 2003) for an example of a modeling approach and basic variable interactions) these have not yet been developed into user models and are not discussed here. Public health aerial applications (mosquito control) release ultra-fine droplets either by air or ground with the objective being spray moving through a target volume of air. Moreover, aerial applications are released from high altitudes (30-75m). The aerial modeling techniques described in this chapter have been extensively used by the mosquito adulticiding community, but should be done so with caution as this use requires calculations outside the spatial domain of this model.

Finally, the scope of this short chapter precludes it being a primer on pesticide application. Actual application scenarios range from 1500 μm droplets used for herbicide application from low boom ground sprayers to aerosol droplets being released at a 75m height in an attempt to cause a droplet to encounter a flying mosquito in the air (known as adulticiding). The reader is referred to Matthews

(1992), Picot and Kristmanson (1997) and Kilroy et al., (2003) among many other references for overviews of pesticide application methods and equipment.

2 Sprayer Types

Conventional sprayers for making pesticide applications to ground (field) crops generally consist of a boom that is typically 6.0 to 24.0 m wide (exceptionally up to 42.0 m wide) and constructed of standard steel or aluminum sections in such a way that nozzles can be supported at a constant height above the crop canopy along the length of the boom. Smaller machines are vehicle mounted with tank sizes up to 2000 L also mounted around the vehicle. Larger machines are commonly self-propelled typically with tank sizes from 2000 to 5000 L but exceptionally with tanks larger than this. In Europe, Australia and New Zealand most boom sprayers for use in field crops are fitted with 110° flat fan hydraulic pressure nozzles whereas in the Americas the use of 80° and some hollow cone nozzles is more common. The fan nozzle has the advantage of giving a uniform volume distribution pattern over a wide range of heights and, for 110° nozzles spaced at 0.5 m on the boom (a common configuration), the minimum boom height is between 350 and 500 mm above the crop depending on the design of the nozzle. Machines are typically operated at speeds from 5.0 to 25.0 km/h, the lower speeds being used in some European countries and higher speeds in Australia, Canada and the USA. The machines are used to apply volumes in the range 50 to 400 L/ha with the lower volumes giving advantages in terms of work rate due to the reduced time required to fill the machine.

Aerial spraying can be performed with either fixed or rotary wing aircraft. Fixed wing are often preferred in open terrain where higher speed flying reduces application costs, while helicopters are preferred where maneuverability or slow airspeeds are required. Such scenarios might include mountain spraying or spraying small areas. Though larger airplanes, such as C-130s are used in applications such as mosquito control, typical examples of the larger fixed wing aircraft commonly used in crop and forestry applications are the Air Tractor AT 602 and 802. The 802 has a useful load of over 4000 kg. In some applications, the actual ratio of active ingredient to carrier may be 1% or less but due to the extra cost of carrying additional weight and refilling, more concentrated solutions are used in aerial application when possible. Aerial herbiciding of low canopies may be done with coarse sprays (>350 µm volume median diameter (VMD)) while spraying deep, three-dimensional canopies such as forests with insecticides, might require a very fine spray (100 µm VMD). While most aerial spraying is done with hydraulic nozzles, much insecticide spraying is done with rotary atomizers utilizing a spinning cage to create fine sprays. An AT-802 fixed wing aircraft might work at airspeed of 230 km hr⁻¹ but most aircraft will work at somewhat lower speeds. The Bell 47G helicopter might cruise near 140 km hr⁻¹ but can work at speeds down to hover as is desirable in certain specialty applications.

Two linked videos show a Bell47G3-B2A helicopter spraying a dye to evaluate the role a riparian barrier plays in preventing spray drift to a stream running within the barrier strip. These trials were conducted using electronically driven rotary atomizers producing a droplet Volume Median Diameter (VMD or $D_{V,0.5}$) of $126 \mu\text{m}$ (test details in Thistle et al, 2009). These videos illustrate some of the influences on spray movement discussed in this chapter. The first video ([Trial04.wmv](#)) shows the helicopter flying along the barrier edge releasing spray at a height of 15.2 m, with mean wind velocity toward the barrier at 2.8 ms^{-1} , temperature at $19.5 \text{ }^\circ\text{C}$ and relative humidity of 41%. The Pasquill stability index is D in this trial. Note the spray capture in the vortices and the downward motion of the vortices while the ambient air motion moves the vortices laterally and degrades vortex coherence. Also, note that at low humidities, the droplet VMD is rapidly decreasing after release from the aircraft due to evaporation. In the second video ([Trial13.wmv](#)), release height is 11.3m, the mean wind velocity lacks consistent direction and is at $.7 \text{ ms}^{-1}$, temperature is $.8^\circ\text{C}$ and relative humidity is 88%. Importantly, the Pasquill stability index is F in this trial. The video clearly shows that in this low wind speed, low mixing environment, the vortices descend but linger and a haze of fine droplets remaining aloft can be seen (videos filmed by James Kautz, USDA Forest Service).

3 Ground Application

3.1 Near Field Effects

Prediction of droplet trajectories and spray movement associated with a boom sprayer is dominated by the proximity of the boom and nozzles to the ground. The boom is generally of a relatively aerodynamically porous characteristic but the blockage to the airflow in the region below the boom by the presence of the sprays is considerable. Studies examining the relative magnitude of aerodynamic effects associated with both the boom structure and sprays (Murphy et al. 2000) have shown that changes in boom structure profile had a much smaller effect on the risk of drift than changes to spray nozzle characteristics.

The air entrained within the spray structure is also important in determining droplet trajectories close to the nozzle, particularly when considering the interaction with a cross-flow of air. A combination of the natural wind and the forward motion of the sprayer generate this cross-flow. Initial approaches to the modeling of the dispersion of sprays from ground based boom sprayers ignored the conditions close to the nozzle and assumed that the behavior of droplets detrained from the spray structure would be dispersed by atmospheric turbulence from some arbitrary release condition. This dispersion was then predicted using random walk approaches (Thompson and Ley 1983) or Gaussian plume models (e.g. Schaefer and Allsop 1983). The random walk approach used by Thompson and Ley further developed by assuming that droplets leaving a hydraulic pressure nozzle initially behaved ballistically within the entrained air flow created by the

spray (Miller and Hadfield 1989). Entrained air flow conditions were calculated based on relationships initially proposed by (Briffa and Dombrowski 1966) in which the air velocity along the axis of the fan jet was given by:

$$U_c = U_s \left[\frac{l_c}{h} \right] \delta^2 / 2k \quad (3.1)$$

where U_s is the liquid sheet velocity immediately below the nozzle, l_c is the coherent length of the sheet, h is the distance from the nozzle, δ is a constant which for sprays into air takes a value of 0.4 and k is a dimensionless parameter that is a function of the thickness of the spray structure at right angles to the main spray fan and at a defined distance below the nozzle. Studies reported by Miller and Hadfield measured spray structures from photographs to determine initial values for the $\delta^2/2k$ parameter and then validated the initial predictions by measuring droplet velocities within the spray produced by typical agricultural nozzle conditions. Entrained air velocities within the spray were measured by monitoring droplets in the 40-80 μm size range. A value for $\delta^2/2k$ of 0.95 was shown to give a reasonable prediction of entrained air velocities within the spray and was assumed to be constant across the spray structure. The geometry of the air jet was then modified in studies reported by Hobson et al. (1993) to match that of the spray, although the basic model and predictions of entrained air velocity used methods similar to those of Miller and Hadfield.

The approach to the modeling of spray behavior and drift from boom sprayers reported by Miller and Hadfield was also further developed by Holterman et al. (1997). In this case the definitions of entrained air velocities built on the approaches initially identified by Smith and Miller (1994) and were assumed to vary depending on the position within the spray structure such that entrained air velocities were predicted from:

$$U_e(p, q, h) = U_{e,ax} \cdot \frac{1}{4} \left(\cos\left(\frac{\pi p}{f_h p_o}\right) + 1 \right) \left(\cos\left(\frac{\pi q}{f_h q_o}\right) + 1 \right) \quad (3.2)$$

where p and q represent the two orthogonal distances from the axis parallel and at right angles to the spray fan, p_o and q_o represent the outer limits of the spray fan in the two directions, are proportional to h and dependent on the spray fan angle. f_h is an extension factor for entrained air outside of the spray structure and has taken values of between 1.2 and 1.8 based on empirical assessments of the spray geometry. The entrained air velocity down the axis of the spray jet, $U_{e,ax}$ was calculated using the same relationship as given in Equation 3.1 with the constant $\delta^2/2k$ set as a constant (k_e) with a value of 0.7.

Work reported by Teske et al., (2009) also used the details of the physical structure and entrained air conditions associated with the liquid spray jet to improve upon the predictions of spray dispersion and drift from a ground sprayer using a Gaussian plume model. This work found that a value for the $\delta^2/2k$ parameter in Equation (3.1) of 0.57 gave reasonable predictions for sprays from conventional flat fan nozzles but for air-induction nozzles the value needed to be increased to 2.04 and the agreement between measured and predicted drift deposition was less good than that for the conventional nozzle design. The authors suggested that further laboratory work is needed in order to give model input data for predicting the drift from this nozzle design.

Droplet and entrained air velocities within a spray are major factors influencing behavior both in terms of drift and deposition on target surfaces. The entrained air jet within a spray differs from a turbulent air jet in that the scale of turbulence is much lower in the spray driven air jet (Ghosh et al 1991; Ghosh and Hunt 1994) and the initial rate at which the air velocity decays with increasing distance is a function of $z^{-1/2}$ rather than z^{-1} that is more typical of air jet structures. The velocities of air and droplets in a spray can be expressed as (Miller et al 1996):

$$V_r^2 = V_{r0}^2 \cdot \frac{r_0^2}{r^2} - \frac{K}{r^2} (V_l - V_{l0}) \quad \text{where } K = q_l(\Theta) \frac{\rho_l}{\rho_a} \quad (3.3)$$

for the entrained air, and

$$V_l = V_{l0} \cdot e^{-\lambda(r-r_0)} \quad \text{where } \lambda = \frac{3C_D \cdot \rho_a}{8a \cdot \rho_l} \quad (3.4)$$

for the droplets, and where V_r is the radial component of air velocity from the nozzle, r is the distance from the nozzle, V_l the velocity of droplets, ρ_a and ρ_l are the density of the air and liquid respectively, Θ is half the spray fan angle, C_D is the drag coefficient and a is the radius of the droplet. The subscript 0 relates to the position at the end of the liquid sheet where the droplets are formed. The relationship in Equation 3.3 has a flow rate term (q_l), which is to be expected given that the air jet is driven by the exchange of momentum between the air and the liquid.

The structure of a spray fan below a fixed boom is such that the interaction with a cross-flow that may detrain small droplets that then drift is likely to be directional. Studies reported by Smith and Miller (1994) showed that the quantity of liquid detrained from a spray in wind tunnel conditions was more than eight times greater when the cross-flow was at right angles to the main spray direction compared to when the cross-flow was aligned with the fan. These results were compared with model predictions that included a geometrical description of both the spray and entrained air structures using relationships similar to those included by Holterman et al. (1997) and detailed in Equation (3.2).

The effective component of the cross-wind that can be associated with the forward motion of the sprayer acts at approximately right angles to the main axis of the spray. A fundamental analysis of such a cross-flow interaction by Ghosh and Hunt, (1998) identified up to four areas below a nozzle where the behavior of the flow regime was dependent on the ratios of droplet and entrained air velocities to that of the cross-flow as follows:

- (i) a region immediately below the nozzle where the cross-flow is relatively weak in comparison with droplet and entrained air velocities and where the spray entrains the cross-flow and acts like a line sink for airborne material;
- (ii) an intermediate region where the line sink effect weakens and the cross-flow starts to penetrate the spray structure with some detrainment of small spray droplets;
- (iii) a zone where the cross-flow fully penetrates the spray structure and where substantial detrainment of the small droplet component in the spray occurs but where larger droplets still have a substantial component of their initial release velocity;
- (iv) a final zone where all of the spray has slowed to relatively low velocities and where the action of the cross-flow results in the spray fan being deflected in the direction of the cross-flow.

Regions (i), (ii), and (iii) are those most relevant to the operation of boom sprayers in most conditions. These flow conditions were studied experimentally by Phillips et al. (2000) using both flow visualization techniques and measurements of the droplet size and airborne flux profiles downwind of single and multiple nozzle arrangements using a phase Doppler analyzer in wind tunnel conditions. The work of both Ghosh and Hunt and Phillips et al. show that the interaction of a spray jet with a cross-flow would result in a pair of axial vortices that then move with the cross-flow. It is likely that the presence of these vortex structures will have important implications for the dispersal of detrained small droplets in field conditions and for the characterization of spray nozzles in wind tunnel test conditions. The presence of vortices in the interacting spray jet and cross-flows have also been identified by a number of research teams examining the behavior of sprays with agricultural boom sprayers (e.g. Young 1991, Miller and Smith 1997), but to date little work has been conducted to define the effect that such structures may have on the downwind dispersion of sprays.

3.2 Obstacles to Droplets Moving Laterally

Vegetative boundaries at the edges of a field can provide an effective filter of airborne spray from boom sprayers with reductions in airborne flux of up to 90% (Hewitt 2001, Ucar and Hall 2001, Miller et al 2000, Miller and Lane 1999). The effectiveness of such structures in capturing airborne spray is likely to be a function of many parameters particularly the aerodynamic porosity of the structure. Dense structures will obstruct the flow and scouring of airborne spray will be limited to the front face of the boundary. Greater porosities will enable

flow through the structure and the filtering of the airborne spray. Studies of such systems have been mainly experimental (De Schampheleire et al. 2008a and 2008b, Lazzaro et al. 2007) with some analytical and computational fluid dynamics approaches to support such measurements.

The capture efficiency of a vegetative boundary Δ_b has been defined by (Raupach et al 2001, Connell et al 2010):

$$\Delta_b = \frac{U_b}{U_h}(1 - \tau^{ME}) \quad (3.5)$$

where U_b is the bleed velocity, U_h is the open field wind velocity, τ is the optical porosity, M the meander factor for air flowing through the wind break and E is the capture efficiency that is a function of Stokes Number and is related to leaf dimensions and droplet sizes as:

$$E = \left[\frac{S_t}{(S_t + 0.8)} \right]^2 \quad (3.6)$$

The Stokes Number S_t is given by

$$S_t = \frac{\tau U_0}{d_c} \quad (3.6a)$$

where U_0 is the droplet velocity, d_c is the characteristic dimension of a leaf and τ is the relaxation time that is given by $\tau = \rho d^2 / 18\mu$, where d is the droplet diameter, ρ is the density of the droplet and μ the viscosity of the air. Airborne spray profiles downwind of a boom sprayer do not have a uniform flux distribution with height and therefore Equation 3.5 can be modified (Connell et al 2010) to:

$$\Delta_b = A k_1^{0.5} \cdot \frac{U_b}{U_h} (1 - \tau^{ME}) \quad (3.7)$$

where A and k_1 are factors that account for the wind and airborne flux profiles. Results from predictions based on Equation 3.7 have been shown to approximately agree with field measurements (Connell et al 2010).

4 Aerial Application

Over the last twenty-five years a significant modeling and data collection effort has been undertaken by the USDA Forest Service and its cooperators to develop

accurate, validated models that predict the behavior of pesticides applied by aerial application above forests (Teske et al. 1998b). The model most focused upon is the Lagrangian trajectory model AGDISP (Bilanin et al. 1989). An extensive field study (Hewitt et al. 2002) and model validation effort (Bird et al. 2002) confirmed the predictive capability of the Lagrangian computational engine that drives the model (Teske et al. 2003), to approximately 800 m downwind (Teske and Thistle 2003), and opened the door for improved solution handoff to Gaussian models (Teske and Thistle 2004a) and mesoscale atmospheric transport models (Allwine et al. 2002 and Thistle et al., 2008).

AGDISP is based on a Lagrangian approach to the solution of the spray material equations of motion, and includes simplified models for the effects of the aircraft wake and aircraft-generated and ambient turbulence. Reed (1953) first developed the equations of motion for spray material released from nozzles on an aircraft, exploring the role of the wingtip vortices. Vortex swirling behavior can be quantified by a simple model that, when combined with the local wind speed and with gravity, effectively predicts the motion of spray material released into it. The original AGDISP model included the innovative step of developing ensemble-averaged turbulence equations to predict the growth of the spray cloud during the calculations, eliminating the need for a random component in the solution procedure.



Figure 1. A Bell 47G3-B2A spraying a yellow fluorescent dye in water at a rate of 46.8 L ha^{-1} with a fine (VMD of $126 \mu\text{m}$) droplet size distribution. Note the definite vortices generated at the rotor tips as delineated by the dyed spray (Thistle et al. (2009), photograph by Jim Kautz, USDA Forest Service).

In this same time period other researchers independently developed their own spray drift models, or contributed essential pieces to the modeling process. These authors include Williamson and Threadgill (1974), Bache and Sayer (1975), Trayford and Welch (1977), Frost and Huang (1981), Atias and Weihs (1984), Bragg (1986), Gaidos et al. (1990), Himel et al. (1990), Saputro and Smith (1990), and Wallace et al. (1995).

4.1 Solution Approach

Released spray material can be modeled as a discrete set of droplets, collected into categories, and called a drop size distribution. Each drop size category is defined by its volume average diameter and volume fraction, and is examined sequentially by the model. A Lagrangian approach is used to develop the equations of motion for discrete droplets released from the aircraft, with the resulting set of ordinary differential equations solved exactly from time step to time step. Droplet flight path, as a function of time after release, is computed as the mean droplet locations X_i for all droplets included in the simulation. The positive X direction is taken as the direction the aircraft is flying from; the Y direction is off the right wing as viewed from the pilot's seat; and the Z direction is vertical upward. The interaction of the released material with the turbulence in the environment creates turbulent correlation functions for droplet position and velocity $\langle x_i v_i \rangle$, velocity variance $\langle v_i v_i \rangle$, and position variance $\langle x_i x_i \rangle$, where x_i is the fluctuating droplet position, v_i is the fluctuating droplet velocity, and $\langle \rangle$ denotes ensemble average. The square root of $\langle x_i x_i \rangle$ gives the standard deviation σ of the droplet motion about the mean described by X_i .

The novel feature of the AGDISP methodology is that the dispersion of a group of similarly sized droplets (contained within each drop size category), resulting from turbulent fluid fluctuations in the atmosphere, is quantitatively computed within the wake of the aircraft as the group of droplets descends toward the surface. The Lagrangian equations governing the behavior of a droplet in motion may be ensemble averaged and written

$$\frac{d^2 X_i}{dt^2} = [U_i - V_i] \left[\frac{1}{\tau_p} \right] + g_i \quad (4.1)$$

$$\frac{dX_i}{dt} = V_i \quad (4.2)$$

where t is time, U_i is the mean local velocity, V_i is the mean droplet velocity, and g_i is gravity (0,0,-g). The drag force on the droplet is represented by the droplet relaxation time

$$\tau_p = \frac{4}{3} \frac{D\rho}{C_D\rho_a|U_i - V_i|} \quad (4.3)$$

where D is the droplet diameter, ρ is the droplet density, C_D is the droplet drag coefficient, and ρ_a is the density of air. The term representing the effect of evaporation on droplet acceleration has been removed from Equation (4.1) because its effect is small (droplet evaporation is described in detail in Section 4.2), and its presence significantly complicates the problem (and makes the later analytical solution impossible). C_D is evaluated empirically for spherical droplets (Langmuir and Blodgett 1949) as

$$C_D = \frac{24}{\text{Re}} \left[1 + 0.197 \text{Re}^{0.63} + 0.00026 \text{Re}^{1.38} \right] \quad (4.4)$$

where

$$\text{Re} = \frac{\rho_a D |U_i - V_i|}{\mu_a} \quad (4.5)$$

is the Reynolds number and μ_a is the viscosity of air. The relaxation time τ_p defined in Equation (4.3) has physical significance with regard to dispersion, in that it is the e-folding time required for a droplet to catch up to its local velocity (for V_i to approach U_i).

With a specification of the local velocity field U_i , Equations (4.1) and (4.2) can be solved to obtain the mean trajectory paths for the spray material from each nozzle. Reed (1953) assumed that a counter-rotating pair of vortices, positioned at the aircraft wingtips, generated the local velocity field. This velocity field provides most of the velocity effects close to the aircraft, and will be described later.

Substitution of Equations (4.1) and (4.2) into the full Lagrangian equations results in ensemble-averaged fluctuation equations of the form

$$\frac{d}{dt} \langle x_i x_i \rangle = 2 \langle x_i v_i \rangle \quad (4.6)$$

$$\frac{d}{dt} \langle x_i v_i \rangle = \left[\langle x_i u_i \rangle - \langle x_i v_i \rangle \right] \left[\frac{1}{\tau_p} \right] + \langle v_i v_i \rangle \quad (4.7)$$

$$\frac{d}{dt} \langle v_i v_i \rangle = 2 \left[\langle u_i v_i \rangle - \langle v_i v_i \rangle \right] \left[\frac{1}{\tau_p} \right] \quad (4.8)$$

where u_i is the fluctuating local velocity. Equation (4.6) represents the growth of the spray cloud, as $\langle x_i x_i \rangle$ is the position variance around the mean droplet location X_i . Equations (4.7) and (4.8) require the specification of $\langle x_i u_i \rangle$ and $\langle u_i v_i \rangle$, correlations of the droplet position and velocity with the local background velocity, respectively, before solution is possible. This development is detailed in Teske et al. (2003) and involves use of a Lagrangian spectral density function determined by von Karman and Howarth (1938) and Houbolt et al. (1964).

With the position and velocity information available for the droplet at any time during the simulation, Equations (4.1) and (4.2), and (4.6) to (4.8), may be integrated exactly as an initial value problem for the solution at the next time step, with the assumption that the background conditions U_i , $\langle x_i u_i \rangle$, and $\langle u_i v_i \rangle$ are constant across each time step. The solution may then be advanced one analytical time step at a time for each droplet in the Lagrangian simulation.

4.2 Evaporation

The evaporation model in AGDISP is based on the well-known D-squared law (Trayford and Welch 1977), in which the time rate of change of droplet diameter is taken as

$$\frac{dD}{dt} = -\frac{D}{2\tau_e \left(1 - \frac{t}{\tau_e}\right)} \quad (4.9)$$

where

$$\tau_e = \frac{D^2}{\lambda_\infty \Delta\Theta (1 + 0.27 \text{Re}^{1/2})} \quad (4.10)$$

is the evaporation time scale of the droplet, λ_∞ is the evaporation rate, and $\Delta\Theta$ is the wet bulb temperature depression. For water Trayford and Welch (1977) suggested an evaporation rate of $\lambda_\infty = 84.76 \mu\text{m}^2/(\text{sec}\cdot^\circ\text{C})$. Later tests showed that the evaporation rate could be somewhat lower, down to $\lambda_\infty = 70.24 \mu\text{m}^2/(\text{sec}\cdot^\circ\text{C})$ for deionized water (Riley et al. 1995), and that the evaporation rate is further reduced as the relative velocity $|U_i - V_i|$ approaches zero (Teske et al. 1998a).

In AGDISP the active fraction of an individual droplet changes as the droplet evaporates. Evaporation effects are included from both the active and additive ingredients, as well as the carrier, at a single rate of evaporation, applicable for all three components of the spray mix.

4.3 Flow Field Modeling

The behavior of released droplets is intimately connected to the local background mean velocity U_i and turbulence field q^2 through which the spray material is

transported. In AGDISP, these local effects are approximated by models for the aircraft and the atmosphere.

4.3.1 Fixed-Wing Rolled-Up Tip Vortices

When an aircraft flies at constant altitude and speed, the aerodynamic lift generated by the lifting surfaces of the aircraft equals the aircraft weight. The majority of the lift is carried by the wings, and generates one or more pairs of swirling masses of air (vortices) downstream of the aircraft. If the rollup of this trailing vorticity can be approximated as occurring immediately downstream of the wing, then the local swirl velocity V_s around each vortex (one on each wing tip) may be given by

$$V_s = \frac{\Gamma}{2\pi} \frac{r}{\max(r, r_c)^2} \quad (4.11)$$

where Γ is the vortex circulation strength

$$\Gamma = \frac{2}{\pi} \frac{W}{\rho_a s U_\infty} \quad (4.12)$$

r is the distance from the vortex center to the droplet, r_c is the vortex core radius, W is the aircraft weight, s is the aircraft semispan, and U_∞ is the aircraft speed. For a vortex pair the superimposed effects of four vortices are used to simulate the overall proximity to the ground, with image vortices maintaining the no-flow inviscid ground condition. The vortex strength Γ decays with time because of atmospheric turbulence, following a simple decay model

$$\Gamma = \Gamma_i \exp\left(-\frac{bqt}{s}\right) \quad (4.13)$$

where Γ_i is the initial vortex circulation strength. This functional dependence was validated in a series of aircraft flyovers past instrumented towers (Teske et al. 1993), with an average value of $bq = 0.56$ m/s for in-ground effect. Out of ground effect, the vortical decay may be approximated by $bq = 0.15$ m/s, and smoothly transitioned to the surface (Teske and Thistle 2003).

4.3.2 Helicopter in Forward Flight

The helicopter model partitions the helicopter weight between hover downwash and rotor tip vortices as a function of time. The hover downwash model is taken from actuator disk theory for a propeller (Bramwell 1976) and may be written as

$$w_d = \frac{1}{R} \sqrt{\frac{FW}{2\pi\rho_a}} \quad (4.14)$$

where w_d is the downwash velocity at the helicopter rotor plane and R is the rotor radius of the helicopter. The strength of the vortex pair may be found from

$$\Gamma = \frac{2(1-F)W}{\pi\rho_a R U_\infty} \quad (4.15)$$

where $F = \exp(-x/R)$ found by matching the behavior of this simple model with detailed helicopter models (Wachspress et al. 2003) as a function of the axial distance x . At the beginning of the calculation $x = 0$, $F = 0$, and all of the weight of the helicopter provides downwash through the helicopter rotor blades. As the calculation proceeds, $x > 0$, $F \rightarrow 0$, and all of the weight transitions to provide vortex motion are identical to that of a fixed-wing aircraft. Because of the exponential decay, the transition between downwash and vortex motion occurs within two rotor diameters behind the helicopter.

4.3.3 Mean Crosswind

In a neutral atmospheric surface layer the lateral velocity V is assumed to follow a logarithmic profile

$$V = V_r \frac{\ln((z + z_o)/z_o)}{\ln((z_r + z_o)/z_o)} \quad (4.16)$$

where V_r is the lateral velocity at the reference height z_r , z is vertical distance, and z_o is surface roughness. With a linear integral scale of turbulence ($\Lambda = 0.65z$), the turbulence level (Donaldson 1973; Lewellen 1977) becomes

$$q_{wind}^2 = 0.845 \left[\frac{V_r}{\ln((z_r + z_o)/z_o)} \right]^2 \quad (4.17)$$

Flow effects are additive from all of these contributions to assemble the local velocity U_i and turbulence q^2 . Droplet trajectories are followed from their release points at the nozzle locations until they deposit on the surface or move beyond a downwind location where they are no longer computed.

4.4 Canopy Modeling

AGDISP includes an optical canopy model that can be used to remove spray material by impaction upon its vegetation. The probability that a droplet will penetrate a canopy depends upon the total number and size of vegetative elements encountered on its trajectory through the canopy. If the orientation of these

elements is assumed to be random, then the probability of penetration for a given path length will be the same in all directions. Here, the probability of penetration P_p is defined as the probability that a droplet traveling along its trajectory will penetrate a typical single tree envelope. The value of P_p is determined from optical measurements as a function of sun incidence angle. Since probability of penetration is a “sunlight” feature, it must be corrected for droplet mass through the collection efficiency of a vegetative element of a given size. What this step implies is that, while probability of penetration may only take on values between 0 and 1, a value of 0 does not guarantee that the canopy will capture all of the droplets traveling through it (although a value of 1 does guarantee that the canopy will not capture any droplets).

In AGDISP it is assumed that the Lagrangian trajectory analysis is not affected by the presence of the canopy. While evaporation changes the drop size distribution without changing the amount of active material in the spray, droplet interception with the canopy changes both.

The canopy is divided into layers. It may be argued that the probability that sunlight will penetrate one tree layer can be written as

$$P_k = \exp(-\Delta LAI_k) \quad (4.18)$$

where ΔLAI_k is the incremental Leaf Area Index across the incremental canopy height Δz_k , and only vertical measurement of LAI through the height of the canopy is assumed (Teske and Thistle 2004b). The overall probability of a droplet penetrating a tree layer is then given by

$$P_{Tk} = 1 - E(1 - P_k) \quad (4.19)$$

where E is the collection efficiency of the vegetative elements comprising the trees, and is determined by impaction with various representations of tree vegetative elements (May and Clifford 1967). Probabilities multiply through the canopy layers.

4.5 Deposition Modeling

Deposition begins as released spray material approaches the ground, continuing until all unevaporated material is deposited. Ground deposition is computed by assuming that the concentration of material around the mean may be taken as Gaussian

$$C = \frac{1}{2\pi\sigma^2} \exp\left[-\frac{(y-Y)^2}{2\sigma^2}\right] \exp\left[-\frac{(z-Z)^2}{2\sigma^2}\right] \quad (4.20)$$

where the released spray material is at position (Y, Z) . When the unevaporated material deposits as it approaches the surface, Equation (4.20) is integrated to give

$$M = \frac{1}{2\sqrt{2\pi}\sigma} \exp\left[-\frac{(y-Y)^2}{2\sigma^2}\right] \operatorname{erfc}\left(\frac{Z}{\sqrt{2}\sigma}\right) \quad (4.21)$$

Deposition to the ground is estimated by summing all incremental contributions to M as integration proceeds, then correcting the integrated deposition so that conservation of the released nonvolatile spray material is achieved. It may be seen that for material falling vertically toward the surface, the pattern of chemical deposition to the ground generated by Equation (4.21) will be identical to the traditional Gaussian deposition pattern.

5 Conclusions

Techniques for modeling pesticide spray deposition from a boom ground sprayer and an agricultural spray aircraft have been presented. The models shown are mechanistic, design decisions being generally driven by the desire to have an applied model that can be used in regulatory applications. The assemblages of equations shown above generally have highest accuracy when considering the landing position of large drops near the release point. Accuracy generally decreases when smaller droplets and longer downwind distances are considered, plus the models shown use single point meteorology that limits the downwind domain of these models. Current work is focusing on the incorporation of more realistic meteorological approaches that will allow multiple point meteorology to be used. Of course, these approaches greatly increase the complexity and input requirements of this modeling.

Since much of the model development has been driven by regulatory concerns, the assumption that unintended environmental consequences are greater from aerial spraying drove the aerial spray modeling to a level of sophistication (at least in the regulatory domain) ahead of the ground sprayer modeling. The scrutiny aerial spraying has been put under (including the physical understanding gleaned through the model development process) has led to changes in equipment and practice that have greatly improved the environmental footprint of aerial spraying. Attention is now focusing on advancing the state of the art in modeling ground spraying. This is leading to exciting work in this field that is ongoing. Among current questions relevant to both modeling approaches are such issues as the degree to which droplet cloud effects impact landing position and more sophisticated approaches to the handling of lateral obstacles and canopies.

As food and fiber production need to expand to meet the needs of a growing population, the understanding of the pesticide application process continues to be a critical need. As the increasing human population puts more stress on the

natural environment, minimizing unintended consequences of pesticide application is also crucial. It is hoped that the increased understanding gained from the development of the models described here as well as the availability of these modeling tools, will aid in achieving both of these goals.

References

- Allwine, K. J., H. W. Thistle, M. E. Teske, and J. Anhold. 2002. The agricultural dispersal – valley drift spray drift modeling system compared with pesticide drift data. *Environmental Toxicology and Chemistry* 21(5): 1085-1090.
- Atias, M. and D. Weihs. 1984. Motion of aircraft trailing vortices near the ground. *Journal of Aircraft* 21(10): 783-786.
- Bache, D. H. and W. J. D. Sayer. 1975. Transport of aerial spray I: a model of aerial dispersion. *Agricultural Meteorology* 15: 257-271.
- Bilanin, A. J., M. E. Teske, J. W. Barry, and R. B. Ekblad. 1989. AGDISP: the aircraft spray dispersion model, code development and experimental validation. *Transactions of the ASAE* 32(1): 327-334.
- Bird, S. L., S. G. Perry, S. L. Ray, and M. E. Teske. 2002. Evaluation of the AGDISP aerial spray algorithms in the AgDRIFT model. *Environmental Toxicology and Chemistry* 21(3): 672-681.
- Bragg, M. B. 1986. A numerical simulation of the dispersal of liquid from aircraft. *Transactions of the ASAE* 29(1): 10-15.
- Bramwell, A. R. S. 1976. *Helicopter dynamics*. John Wiley and Sons: New York, NY.
- Briffa, F.E.J. and N. Dombrowski. 1966. Entrainment of air into a liquid spray. *American Institute of Chemical Engineers Journal* 12(4): 708-717.
- Connell, R.R., S.J.R. Woodward, J.A. Zabkiewicz, A.J. Hewitt. 2010 Shelterbelt interception of agrichemicals: Model and field experiments. *Aspects of Applied Biology*, in press.
- Cross J.V., P.J. Walklate, R.A. Murray and G.M. Richardson. 2001a. Spray deposits and losses in different sized apple trees: 1. Effects of spray liquid flow rate. *Crop Protection*, 20 13-30.
- Cross J.V., P.J. Walklate, R.A. Murray and G.M. Richardson. 2001b. Spray deposits and losses in different sized apple trees: 2. Effects of Spray Quality. *Crop Protection*, 20 333-343.
- Cross J.V., P.J. Walklate, R.A. Murray and G.M. Richardson. 2003. Spray deposits and losses in different sized apple trees: 3. Effects of air volumetric flow rate. *Crop Protection*, 22(2) 381-394.
- De Schampheleire, M., D. Nuyttens, D. Dekeyser, P. Verboven, w. Cornelis, D. Gabriels, P. Spanoghe. 2008a. Interception of spray drift by border structures. Part 1. Wind tunnel experiment. *Communications in Agricultural and Applied Biological Sciences*, 73(4), 719 – 722
- De Schampheleire, M. D. Nuyttens, D. Dekeyser, P. Verboven, P. Spanoghe. 2008b. Interception of spray drift by border structures. Part 2. Field experiments. *Communications in Agricultural and Applied Biological Sciences*, 73(4), 723 – 727.
- Donaldson, C. duP. 1973. Atmospheric turbulence and the dispersal of atmospheric pollutants. *AMS Workshop on Micrometeorology* (D. A. Haugen, ed.). Science Press: Boston, MA.

- Frost, W. and K. H. Huang. 1981. Monte Carlo model for aircraft applications of pesticides. Paper No. 81-1507. ASAE: Chicago, IL.
- Gaidos, R. E., M. R. Patel, D. L. Valcore, and R. D. Fears. 1990. Prediction of spray drift deposition from aerial applications of pesticides. Paper No. AA90-007. ASAE/NAAA: Reno, NV.
- Ghosh, S., J.C. Phillips and R.J. Perkins. 1991. Modelling the flow in droplet-driven sprays. *In: Advances in Turbulence 3*. 405-413. Eds. A.V. Johansson and P.H. Alfredsson. Springer-Verlag Berlin, Heidelberg.
- Ghosh, S. and J.C.R. Hunt. 1994. Induced air velocity within droplet driven sprays. *Proceedings Royal Society. London A*. 444: 105-127.
- Ghosh, S. and J.C.R. Hunt. 1998. Spray jets in a cross-flow. *Journal of Fluid Mechanics* 365: 109-136.
- Hewitt, A. J. 2001. Drift filtration by natural and artificial collectors. Stewart Agricultural Research Services Inc.
- Hewitt, A. J., D. R. Johnson, J. D. Fish, C. G. Hermansky, and D. L. Valcore. 2002. Development of the spray drift task force database for aerial applications. *Environmental Toxicology and Chemistry* 21(3): 648-658.
- Himel, C. M., H. Loats, and G. W. Bailey. 1990. Pesticide sources to the soil and principles of spray physics. *Pesticides in the Soil Environment*. SSSA Book Series 2. Soil Science Society of America: Madison, WI.
- Hobson, P.A., P.C.H. Miller, P.J. Walklate, C.R. Tuck, N.M. Western. 1993. Spray drift from hydraulic spray nozzles: the use of a computer simulation model to examine factors influencing drift. *Journal of Agricultural Engineering Research* 54(4): 293-306.
- Holterman, H.J., J.C. van de Zande; H.A.J. Porskamp, J.F.M. Huijsmans. 1997. Modeling drift from boom sprayers. *Computers and Electronics in Agriculture* 19: 1-22.
- Houbolt, J. C., R. Steiner, and K. G. Pratt. 1964. Dynamic response of airplanes to atmospheric turbulence including flight data on input and response. NASA TR R-199: Langley, VA.
- Kilroy B., R. Karsky and H. Thistle. 2003. Aerial Application Equipment Guide. USDA Forest Service, FHTET-0302, Missoula Tech. Dev. Center, Missoula, MT.
- Langmuir, I. and K. B. Blodgett. 1949. A mathematical investigation of water droplet trajectories. Report No. RL225. General Electric Company: Schenectady, NY.
- Lazzaro, L., S. Otto, G. Zanin. 2007. Role of hedgerows in intercepting spray drift: Evaluation and modelling of the effects. *Agriculture, Ecosystems and Environment*, 123(4): 317 – 327.
- Lewellen, W. S. 1977. Use of invariant modeling. *Handbook of Turbulence* (W. Frost and T. H. Moulden, eds.). Plenum Press: Elmsford, NY.
- Matthews G.A. 1992. Pesticide Application Methods. Longman Scientific and Technical, John Wiley and Sons. New York, NY
- May, K. R. and R. Clifford. 1967. The impaction of aerosol particles on cylinders, spheres, ribbons, and discs. *Annals of Occupational Hygiene* 10: 83-95.

- Miller, P.C.H. and D.J. Hadfield. 1989. A simulation model of the spray drift from hydraulic nozzles. *Journal of Agricultural Engineering Research* 42:135-147.
- Miller, P.C.H., M.C. Butler Ellis and C.R.Tuck. 1996. Entrained air and droplet velocities produced by agricultural flat-fan nozzles. *Atomization and Sprays*, 6:693-707.
- Miller, P.C.H., Smith, R.W. 1997. The effects of forward speed on the drift from boom sprayers. Proceedings *Brighton Crop Protection Conference – Weeds*: 399-407.
- Miller, P.C.H. and A.G. Lane. 1999. Relationship between spray characteristics and drift risk into field boundaries of different structure. *Aspects of Applied Biology*, 54, *Field margins and buffer zones: ecology, management and policy*, 45-51.
- Miller, P.C.H., A.G. Lane, P.J. Walklate, G.M. Richardson. 2000. The effect of plant structure on the drift of pesticides at field boundaries. *Aspects of Applied Biology – Pesticide Application*, 57: 75-82.
- Murphy, S.D., P.C.H. Miller, C.S. Parkin. 2000. The effect of boom section and nozzle configuration on the risk of spray drift. *Journal of Agricultural Engineering Research* 75:127-137.
- Phillips, J.C., P.C.H. Miller, N.H. Thomas. 2000. Air flow and droplet motions produced by the interaction of flat-fan sprays and cross-flows. *Atomization and Sprays* 10:83-103.
- Picot J.J.C. and D.D. Kristmanson. 1997. *Forestry Pesticide Aerial Spraying*. Kluwer Academic Publishers, Boston MA.
- Raupach, M.R., Woods, N., Dorr, G., Leys, J.F., Cleugh, H.A. 2001. The entrapment of particles by windbreaks. *Atmospheric Environment* 35: 3373-3383.
- Reed, W. H. 1953. An analytical study of the effect of airplane wake on the lateral dispersion of aerial sprays. Report No. 3032. NACA: Langley, VA.
- Riley, C. M., I. I. Sears, J. J. C. Picot, and T. J. Chapman. 1995. Spray drift task force droplet evaporation studies. *Pesticide formulations and application systems: 14th volume*. STP 1234 (F. R. Hall, P. D. Berger, and H. M. Collins, eds.). ASTM: Philadelphia, PA.
- Saputro, S. and D. B. Smith. 1990. Expert system for aerial spray drift. Paper No. 90-1018. ASAE: Columbus, OH.
- Schaefer, G.W. and K. Allsop. 1983. Spray droplet behavior above and within a crop. Proceedings *10th International Congress of Plant Protection* 3:1057-1065.
- Smith, R.W. and P.C.H. Miller. 1994. Drift predictions in the near nozzle region of a flat fan spray. *Journal of Agricultural Engineering Research* 59: 111-120.
- Teske, M. E., A. J. Bilanin, and J. W. Barry. 1993. Decay of aircraft vortices near the ground. *AIAA Journal* 31(8): 1531-1533.
- Teske, M. E., C. G. Hermansky, and C. M. Riley. 1998a. Evaporation rates of agricultural spray material at low relative wind speeds. *Atomization and Sprays* 8: 471-478.
- Teske, M. E., H. W. Thistle, and B. Eav. 1998b. New ways to predict aerial spray deposition and drift. *Journal of Forestry* 96(6): 25-31.
- Teske, M. E. and H. W. Thistle. 2003. Release height and far-field limits of Lagrangian aerial spray models. *Transactions of the ASAE* 46(4): 977-983.

- Teske, M. E., H. W. Thistle, and G. G. Ice. 2003. Technical advances in modeling aerially applied sprays. *Transactions of the ASAE* 46(4): 985-996.
- Teske, M. E. and H. W. Thistle. 2004a. Aerial application model extension into the far field. *Biosystems Engineering* 89(1): 29-36.
- Teske, M. E. and H. W. Thistle. 2004b. A library of forest canopy structure for use in interception modeling. *Forest Ecology and Management* 198: 341-350.
- Teske, M.E., P.C.H. Miller, H.W. Thistle and N.B. Birchfield. 2009. Initial development and validation of a mechanistic spray drift model for ground boom sprayers. *Transactions of the American Society of Agricultural and Biological Engineers* 52(4): 1089-1097.
- Thistle H.W., D.G. Thompson, B. Richardson, S.L. Bird and R. Karsky. 2008. Deposition of Aerially Released *Bt* over a 2 km sampling grid: Near field model comparison. ASABE Tech. Paper 084124, ASABE, St. Joseph, MI.
- Thistle, H.W., G.G. Ice, R.L. Karsky, A.J. Hewitt and G. Dorr. 2009. Deposition of aerially applied spray to a stream within a vegetative barrier. *Transactions of the ASABE*, 52(5) 1481-1490.
- Thompson, N. and A.J. Ley. 1983. Estimating spray drift using a random-walk model of evaporating drops. *Journal of Agricultural Engineering Research* (28): 419-435.
- Trayford, R. S. and L. W. Welch. 1977. Aerial spraying: a simulation of factors influencing the distribution and recovery of liquid droplets. *Journal of Agricultural Engineering Research* 22: 183-196.
- Ucar, T., and F.R. Hall. 2001. Windbreaks as a pesticide drift mitigation strategy: a review. *Pesticide Management Science*, 57(8), 663 – 675.
- von Karman, T. D. and L. Howarth. 1938. On the statistical theory of isotropic turbulence. *Proceedings of the Royal Society of London* 164A: 192-215.
- Wachspress, D. A., T. R. Quackenbush, and A. H. Boschitsch. 2003. First principles free vortex wake analysis for helicopters and tiltrotors. Proceedings of the 59th Annual Forum of the American Helicopter Society: Phoenix, AZ.
- Walklate P.J. 1987. A random-walk model for dispersion of heavy particles in turbulent airflow. *Boundary Layer Meteorology*, 39, 175-190.
- Wallace, D. J., J. J. C. Picot, and T. J. Chapman. 1995. A numerical model for forestry aerial spraying. *Agricultural and Forest Meteorology* 76: 19-40.
- Williamson, R. B. and E. D. Threadgill. 1974. A simulation of the dynamics of evaporating spray droplets in agricultural spraying. *Transactions of the ASAE* 17: 254-261.
- Young, B.W. 1991. A method for assessing the drift potential of hydraulic spray clouds and the effect of air assistance. BCPC Monograph (46): 77-86.

BRANK
P
e

Chapter 14

Indoor Air Pollution Modeling

A comprehensive chapter on Indoor Air Pollution Modeling was included in Volume II of this book series. The abstract is reprinted below.

Indoor Air Pollution is a major concern to today's engineers, architects, and building occupants. More recent, stringent fire and smoke control ordinances, and concern for building occupants' health, have generated the need to understand the sources of indoor air pollution and predict indoor transport. Heating, ventilation, and air conditioning systems which try to maximize energy efficiency and maintain occupants' comfort and well-being, extensive use of man-made building materials, safety, health and recently encountered security risks have brought the idea of modeling indoor air pollution into the mainstay of building design and operation. Theories of air pollution modeling are presented below. Applicable source terms for indoor air pollution, from the simpler to the complex modeling techniques, are discussed here.

For additional information, the reader can visit:

- US EPA Indoor Environment Management Branch
<http://www.epa.gov/appcdwww/iemb/model.htm>
- Multi-Chamber Indoor Air Quality Model (MIAQ)
<http://www.exposurescience.org/MIAQ>
- Indoor Air Quality Building Education and Assessment Model (I-BEAM)
<http://www.epa.gov/iaq/largebllds/i-beam/index.html>
- Air Pollution Research Reports/Studies - Indoor Air Pollution
<http://www.arb.ca.gov/research/apr/past/indoor.htm>
- Indoor Air Quality Risk Perception Study and Modeling
- Analysis of Factors that Affect Indoor Occupant Exposure
<http://www.lib.ncsu.edu/theses/available/etd-04272006-202522/unrestricted/etd.pdf>

- Indoor Air Pollution (IAP) Updates
<http://iapnews.wordpress.com/>
- Indoor Environment Department
<http://eetd.lbl.gov/ie/>

Chapter 15

Modeling of Adverse Effects

A brief introduction to the topic “Modeling of Adverse Effects” was presented in Volume I of this book series.

A Chapter on this topic (15A – Modeling of Health Risks Associated with Combustion Facility Emissions) was included in Volume II. The abstract is reprinted below.

As part of the Resource Conservation and Recovery Act (RCRA) permitting process, the U.S. EPA regulates emissions from hazardous waste combustion facilities on a site-specific basis. The agency requires that human health and ecological risk assessment be conducted in order to evaluate the impacts of the chemicals emitted. To achieve consistency, the EPA has developed a protocol for estimating both human and ecological risks. In this chapter, the protocol developed by the EPA for human health risk assessment is described and the results of a case study, based on this protocol, are presented. Special attention is given to the uncertainties in risk estimates associated with the methods and default parameter values in the protocol.

Two additional chapters were included in Volume III:

15B – Odor Modeling. The abstract is reprinted below.

Atmospheric dispersion modeling is an invaluable tool in the control and management of air pollution. It has been used for many years in the regulatory arena for the assessment of the air quality impacts from a wide variety of sources of air pollution, such as powerplant stacks, industrial chimneys, and mobile sources. Dispersion models apply mathematical equations, often

modified with empirical factors, to convert a mass emission rate from a source of air pollution to an ambient air concentration at some distance downwind of the source. It has been found that atmospheric dispersion modeling can also be an extremely useful tool in the assessment of offsite impact to evaluate control and better manage odors. However, there can be significant differences between the traditional pollutant-specific modeling and modeling that is performed for odor assessment. Modeling used for air quality compliance purposes, for example, is usually concerned with fixed time-averaged concentrations for direct comparison to ambient air quality standards and criteria (generally 1 hour to 1 year). Odors, on the other hand, can be recognized on the order of seconds or minutes. In addition, unlike air quality standards, which have been quantified, based upon exposure and health related responses, the response to odors can be very subjective and are historically based on nuisance. This chapter discusses the techniques used to model odors, and details the differences that must be addressed from both theoretical and practical points of view when applying dispersion models to odor assessment.

15C – Climate Change - An Introduction to Atmosphere-Ocean General Circulation Modeling. The abstract is reprinted below.

This chapter provides an introduction to the formulation of Atmosphere-Ocean General Circulation Models (AOGCMs), the state-of-the-art tool for attributing and projecting of earth-atmosphere climate change. The formulation topics summarized in this review include gridding, numerical solution and the parameterizations of physical processes used for both atmospheric and oceanic components. A sampling of the results from attribution and projection studies using AOGCMs, presented in the IPCC Fourth Assessment Report (AR4), are then shown. Sources for further reading are listed at the end of the review.

In this Volume IV, we provide:

15E – Ecological Risk Assessment for Air Toxics

15F – Combined Assessment of Health Impacts and Emission Abatement Strategies

Thé, J. et al., 2010. *Ecological Risk Assessment for Air Toxics*. Chapter 15E of *AIR QUALITY MODELING - Theories, Methodologies, Computational Techniques, and Available Databases and Software. Vol. IV – Advances and Updates* (P. Zannetti, Editor). Published by The EnviroComp Institute (<http://www.envirocomp.org/>) and the Air & Waste Management Association (<http://www.awma.org/>).

Chapter 15E

Ecological Risk Assessment for Air Toxics

Jesse Thé⁽¹⁾, Cristiane Thé⁽²⁾, Michael Johnson⁽²⁾, Bryan Matthews⁽²⁾

⁽¹⁾ *Lakes Environmental and University of Waterloo (Canada)*

Jesse.The@weblakes.com

⁽²⁾ *Lakes Environmental Software Inc., Waterloo (Canada)*

info@weblakes.com

Abstract: Ecological Risk Assessment (ERA) has rapidly evolved from an art to a science. Guidances and practices have been developed in the past for groundwater and surface water, but not for air toxics. The authors participated in efforts from the USEPA to define guidances and protocols for conducting ecological risk assessment from exposure to air toxics. One of the results of our efforts was a significant collaboration to develop the USEPA Screening Level Ecological Risk Assessment Protocol (SLERAP) for evaluating risk to ecological receptors including food web interactions resulting from exposure to air toxics. More complex approaches for ecological risk assessment will require more information than is currently available. There are 5 main factors driving the need for advancing state-of-the-science and conducting ecological risk assessments, which are listed below:

1. Improved and expanded regulatory requirements
2. Guidance for personnel conducting risk assessments
3. Accumulated experiences in conducting ecological risk assessments
4. An information resource for permit writers, risk managers, and community relations personnel
5. Species-specific exposure factors and ecological effects

This Chapter will describe existing approaches used to conduct defensible Ecological Risk Assessment studies. Note that the original USEPA SLERAP presents all the air dispersion modeling employing ISCST3, a discontinued model. This Chapter will present the model in a more up-to-date manner employing AERMOD.

Key Words: air toxics, air dispersion modeling, ecological risk assessment.

Disclaimer: This Ecological Air Toxics Risk Assessment Chapter is a summary of many publicly available documents referenced at the end of the Chapter. The main references are based mostly on USEPA publications, which are available at <http://www.epa.gov/chief>. The authors develop some of the approaches presented in this Chapter, while collaborating under contract from the USEPA to develop the Screening Level Risk Assessment Protocol (SLERAP), which applies to air toxics. The authors also produce commercial ecological and human health air toxics risk assessment software packages, which are not mentioned in the Chapter to avoid the perception of conflict of interest or self-promotion.

1 Introduction

Risk assessment is a science used to evaluate the potential hazards to the environment that are attributable to air toxic emissions. There is general guidance available regarding the general ecological risk assessment process including problem formulation, analysis, and risk characterization (U.S. EPA 1997c; 1998c).

This Chapter describes the experience of the authors while developing the USEPA Screening Level Ecological Risk Assessment Protocol (SLERAP) and IT solutions to address implementations of this protocol. SLERAP was developed as national guidance to consolidate information presented in other risk assessment guidance and methodology documents previously prepared by U.S. EPA and state environmental agencies. In addition, this Chapter addresses issues that have been identified while conducting ecological risk assessments for existing hazardous waste combustion units. The overall purpose of this document is to explain how ecological risk assessments should be performed when evaluating the effects of air toxics emitted to the atmosphere. This document is intended as:

1. Guidance for personnel conducting risk assessments
2. An information resource for permit writers, risk managers, and community relations personnel

Regulatory agencies throughout the world have both the authority and the responsibility to establish risk-based permit conditions on a case-by-case basis as necessary to protect human health and the environment. Often, the determination of whether or not a permit is sufficiently protective can be based on its conformance to the technical standards specified in the regulations. Many studies indicate that there can be significant risks from indirect exposure pathways (e.g., pathways other than direct inhalation). Some of these studies are:

1. Draft Health Reassessment of Dioxin-Like Compounds
2. Mercury Study Report to Congress
3. Risk Assessment Support to the Development of Technical Standards for Emissions from Combustion Units Burning Hazardous Wastes: Background Information Document, and the Waste Technologies Industries (WTI) Risk Assessment
4. Air Toxics Risk Assessment (ATRA) Reference Library

For Ecological Risk Assessment (ERA) the food chain pathway is particularly important for bio-accumulative pollutants, which may be emitted from chemical processes or combustion units. In many cases, risks from indirect exposure may constitute the majority of the risk from these sites. This key portion of the risk from air toxic emissions was not directly taken into account when the hazardous emissions standards were developed. In addition, uncertainty remained regarding the types and quantities of non-dioxin products of incomplete combustion emitted from combustion units and the risks posed by these compounds.

The risk manager should consider several factors in its evaluation of the need to perform a risk assessment (human health and ecological). These factors include:

1. Whether any proposed or final regulatory standards exist, which was shown to be protective for site-specific receptors
2. Whether the facility is exceeding any final technical standards
3. The scope of waste minimization efforts and the status of implementation of a facility waste minimization plan
4. Particular site-specific considerations related to the exposure setting, such as physical, land use, presence of threatened or endangered species, and special subpopulation characteristics.
5. The presence of significant ecological considerations (e.g., high background levels of a particular contaminant, proximity to a particular sensitive ecosystem)
6. The presence of nearby off-site sources of pollutants
7. The presence of other on-site sources of pollutants
8. The hazardous constituents most likely to be found and those most likely to pose significant risk
9. The identity, quantity, and toxicity of possible non-dioxin PICs
10. The level of public interest and community involvement attributable to the facility
11. Corporate stewardship and proactive environmental business policies

This list is by no means exhaustive, but is meant only to suggest significant factors that have thus far been identified. Others may be equally or more important.

1.1 Objective and Purpose

This manuscript describes a multi-pathway screening tool based on reasonable, protective assumptions about the potential for ecological receptors to be exposed to, and to be adversely affected by, compounds of potential concern (COPC) emitted from hazardous waste combustion facilities. This ecological risk assessment process is a prescriptive analysis intended to be performed expeditiously using:

1. Measurement receptors representing food web-specific class/guilds and communities
2. Readily available exposure and ecological effects information.

To avoid the time-intensive and resource-consuming process of collecting site-specific information on numerous constituents, this Chapter provides a process to obtain and evaluate various types of technical information that will enable an ecological risk assessor to perform a risk assessment relatively quickly and based on defensible methodologies.

Additionally this Chapter provides:

1. Example food webs for conducting the ERA
2. Example measurement receptor natural history information
3. A comprehensive source of data needed to complete ERA procedures

Implementation of the methodology presented in this Chapter will support defensible estimates of impacts on ecological systems of compound-specific emission rates. Ecological risk assessments should be completed for new and existing facilities as part of the permit application process. This ERA methodology must be a process for evaluating *reasonable*, not theoretical worst-case maximum potential risks to receptors posed by emissions from air toxic emission units. The use of existing and site-specific information early in, and throughout, the ecological risk assessment process is encouraged; protective assumptions should be made only when needed to ensure that emissions from combustion units do not pose unacceptable risks.

Regardless of whether theoretical worst case or more reasonable protective assumptions are used in completing the ecological risk assessment process, every risk assessment is limited by the quantity and quality of:

1. Site-specific environmental data
2. Emission rate information
3. Other assumptions made during the risk estimation process (for example, fate and transport variables, exposure assumptions, and receptor characteristics)

After the initial ecological risk assessment has been completed, it may be used by risk managers and permit writers in several ways:

1. If the initial risk assessment indicates that estimated ecological risks are below regulatory levels of concern, risk managers and permit writers will likely proceed through the permitting process without adding any risk-based unit operating conditions to the permit.
2. If the initial ecological risk assessment indicates potentially unacceptable risks, additional site-specific information demonstrated to be more representative of the exposure setting may be collected and additional iterations of risk assessment calculations can then be performed.
3. If the initial risk assessment or subsequent iterations indicate potentially unacceptable risks, risk managers and permit writers may use the results of the risk assessment to revise tentative permit conditions (for example, waste feed limitations, process operating conditions, and expanded environmental monitoring).

4. If the initial ecological risk assessment, or subsequent iterations, indicates potentially unacceptable risks, risk managers and permit writers may also choose to deny the permit.

As stated earlier, in some instances, a facility or regulatory agency may want to perform a pretrial burn risk assessment following the procedures outlined in this document to ensure that sample collection times during the trial burn or risk burn are sufficient to collect the sample volumes necessary to meet the appropriate detection limits for the risk assessment. This is expected to reduce the need for additional costly trial burn tests or iterations of the risk assessment due to problems caused when detection limits are not low enough to estimate risk with certainty sufficient for regulatory decision making.

2 Site Characterization

This chapter provides guidance on characterizing the nature and magnitude of emissions released from atmospheric sources. This Ecological Risk Assessment Characterization includes:

1. Compiling basic site information
2. Identifying emission sources
3. Estimating emission rates
4. Identifying COPCs
5. Estimating COPC concentrations for non-detect
6. Evaluating contamination in blanks.

2.1 Compiling Basic Facility Information

Basic facility information should be considered in conducting the risk evaluation, and provided to enable reviewers to establish a contextual sense of the facility regarding how it relates to other facilities and other hazardous waste combustion units. At a minimum, the following basic facility information should be considered in the risk evaluation:

1. Principal business and primary production processes
2. Normal and maximum production rates
3. Types of waste storage and treatment facilities
4. Type and quantity of wastes stored and treated
5. Process flow diagrams showing both mass and energy inputs and outputs
6. Type of air pollution control system (APCS) associated with each unit

Risk assessors may want to consult these discussions so that all site-specific information needed to complete the risk assessment can be collected simultaneously, when appropriate, for up front consideration. The risk assessor is also referred to *Briefing the BTAG: Initial Description of Setting, History, and Ecology of a Site* (U.S. EPA 1992a).

2.2 Identifying Emission Sources

Combustion of a hazardous waste generally results in combustion by-products being emitted from a stack. In addition to emissions from the combustion stack, additional types of emissions of concern that may be associated with the combustion of hazardous waste include:

1. Process upsets
2. General fugitive emissions
3. Cement kiln dust (CKD) fugitive emissions
4. Accidental releases.

2.2.1 Emissions from Process Upsets

Uncombusted hazardous waste can be emitted through the stack as a result of various process upsets, such as start-ups, shutdowns, and malfunctions of the combustion unit or APCS. Process upsets occur when the hazardous unit is not being operated as intended, or during periods of startup or shutdown. Emissions can also be caused by operating upsets in other areas of the facility (e.g., an upset in a reactor which vents gases to a boiler burning hazardous waste could trigger a process upset in the boiler, resulting in increased emissions). U.S. EPA (1994d) indicates that upsets are not generally expected to significantly increase stack emissions over the lifetime of the facility.

2.2.2 Fugitive Emissions

Fugitive emission sources that should be evaluated in the risk assessment include waste storage tanks; disposal units (e.g., landfills), process equipment ancillary to the combustion unit; and the handling and disposal of combustion system residues such as ash.

This section contains guidance for quantitatively estimating fugitive emissions on the basis of procedures outlined by emissions inventory guidance and those contained in [Thé, 2008].

2.3 Identifying Compounds of Potential Concern

Compounds of potential concern (COPCs) are those compounds evaluated throughout the risk assessment. The purposes of identifying COPCs are to focus the risk assessment on those compounds that are likely to pose the most risk to ecological receptors exposed to hazardous waste combustion emissions. The COPC identification process is conservative by design to avoid not including compounds that might pose an ecological risk.

There is no one definition of a COPC, because a compound that is a COPC at one hazardous waste combustion unit may not be a COPC at another combustion unit. COPCs in the emissions from hazardous waste combustion units vary widely, depending on:

1. The type of combustion unit
2. The type of hazardous waste feed being burned
3. The type of APCS used
4. Also considered as COPCs are products of incomplete combustion (PICs), which are any organic compounds emitted from a stack, such as:
 - Compounds initially present in the hazardous waste feed stream and not completely destroyed in the combustion process
 - Compounds that are formed during the combustion process. Because PICs may be formed by trace toxic organic compounds in the waste feed stream, these compounds should be evaluated as PIC precursors, in addition to those compounds that constitute most of the hazardous waste feed.

PICs should not be confused with principal organic hazardous constituents (POHC), which are compounds in the waste feed stream used to measure DRE of the combustion unit during a trial burn test. Unburned POHCs and partially destroyed or reacted POHCs are PICs, but PICs are not necessarily related to POHCs.

COPCs previously identified in ecological risk assessments at combustion facilities are as follows:

1. Polychlorinated dibenzo(p)dioxins (PCDD) and polychlorinated dibenzofurans (PCDF)
2. Polynuclear aromatic hydrocarbons (PAH)
3. Polychlorinated biphenyls (PCB)
4. Pesticides
5. Nitroaromatics
6. Phthalates
7. Other organics
8. Metals.

COPCs are identified from the trial burn data based on their potential to pose an increased risk. This identification process should focus on compounds that:

1. Are likely to be emitted, based on the potential presence of the compound or its precursors in the waste feed
2. That are potentially toxic to ecological receptors
3. Have a definite propensity for bio-concentrating in ecological receptors and bio-accumulating in food chains.

As illustrated in Figure 1, the following steps should be used to identify the COPCs that will be evaluated for each facility (U.S. EPA 1994d).

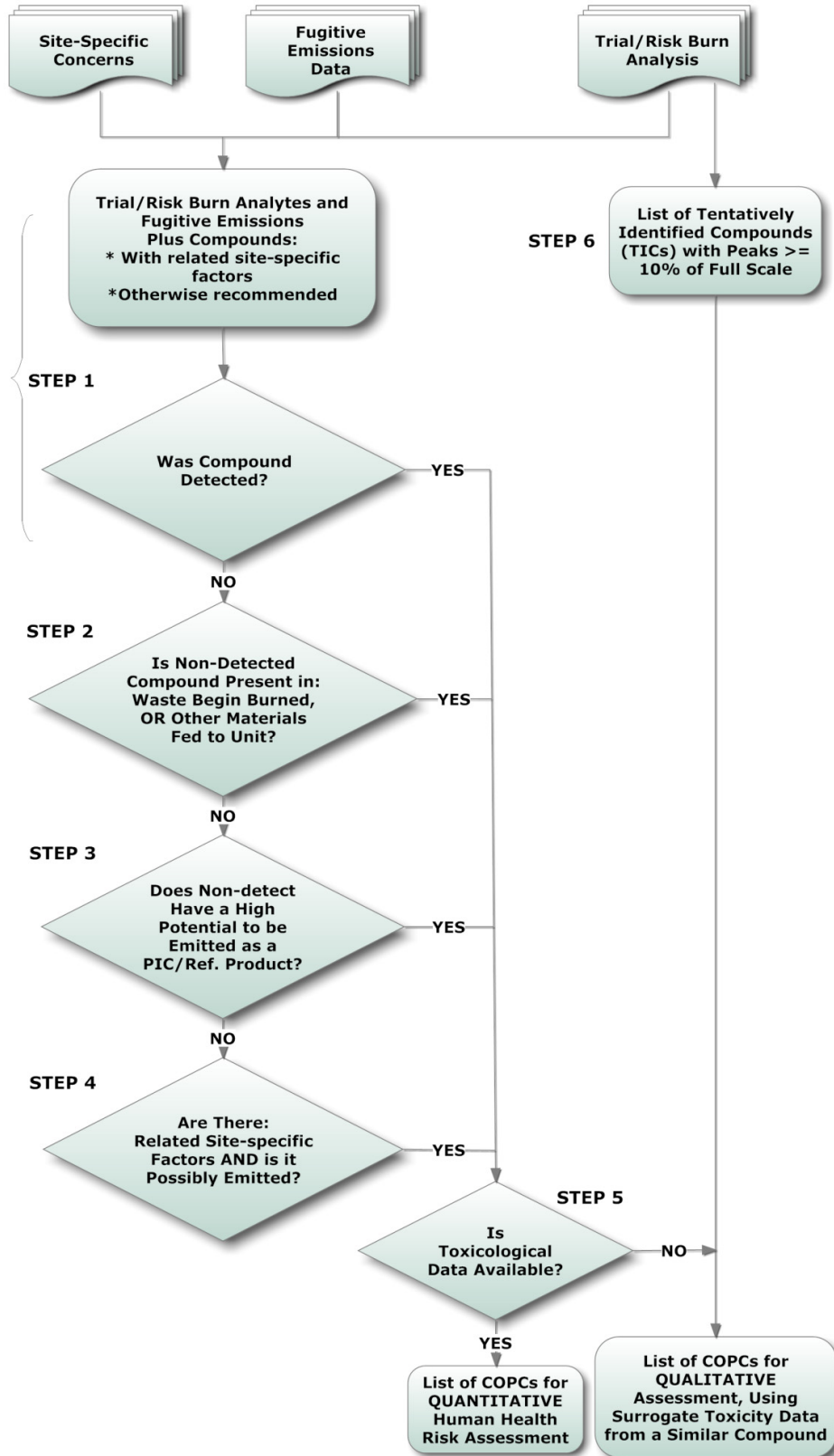


Figure 1. Overview of the Ecological Risk Assessment Process.

If the compound in question does not have a reasonable potential of being present in the stack emissions, the risk assessment report should justify this assertion.

2.3.1 Polychlorinated Dibenzo(p)dioxins and Dibenzofurans

Based on their combustion properties and toxicity PCDDs and PCDFs should be included in every risk assessment. Several PCDDs, PCDFs, and PCBs have been shown to cause toxic responses similar to 2,3,7,8-TCDD, in both laboratory and field situations. Demonstrated toxic effects of 2,3,7,8-TCDD in fish, birds, and mammals include adverse effects on reproduction, development, and endocrine functions; wasting syndrome; immunotoxicity; and mortality (U.S. EPA 2008). Based on increased experience and available data, experts have come to the consensus that the toxicity equivalence methodology for evaluating exposure to PCDDs and PCDFs, can strengthen assessments of ecological risk (U.S. EPA 2008). The general combustion properties and guidance for addressing toxicity of PCDDs and PCDFs are discussed in the following paragraphs and subsections.

PCDDs and PCDFs were first discovered as thermal decomposition products of polychlorinated compounds, including:

1. PCBs
2. Herbicide 2,4,5-T
3. Hexachlorophene
4. Pentachlorophenol
5. Intermediate chemicals used to manufacture these compounds.

Duarte-Davidson et al. (1997) noted that the combustion of chlorine-containing materials in municipal solid waste is responsible for about two-thirds of the total annual emissions of newly formed TCDDs and TCDFs in the United Kingdom. In the United States, U.S. EPA (2006) estimated that emissions of dioxin TEQs from municipal solid waste incinerators accounted for 37 percent of all emissions of dioxins into the environment in 1987, 1995, and 2000.

Procedures specific for **PCDDs and PCDFs** compounds should be followed because congener-specific toxicity and bioaccumulation information is limited. As discussed below, exposure of receptors to PCDDs and PCDFs should be assessed using 2,3,7,8-TCDD toxicity equivalency factors (*TEF*) and 2,3,7,8-TCDD bioaccumulation equivalency factors (*BEF*) to convert the exposure media concentration of individual congeners to a 2,3,7,8-TCDD Toxicity Equivalent (TEQ).

2.3.2 Toxicity Equivalency Factors for PCDDs and PCDFs

There are 210 individual compounds or congeners of PCDDs and PCDFs. Evidence indicates that low levels of PCDD and PCDF congeners adversely affect ecological receptors, especially the 2,3,7,8-substituted congeners (U.S. EPA 2008; Hodson et al. 1992; Walker and Peterson 1992). The 17 congeners containing

chlorine substituents in at least the 2-, 3-, 7-, and 8-ring positions have been found to display dioxin-like toxicity (U.S. EPA 1994i; 2003). Therefore, risk assessment guidances recommend that all risk assessments include all PCDDs and PCDFs with chlorine molecules substituted in the 2, 3, 7, and 8 positions.

The procedure used to assess risk on the basis of the relative toxicity of 2,3,7,8-TCDD, which is assumed the most toxic dioxin (U.S. EPA 1994f), assigns a TEF value to each congener relative to its toxicity in relation to 2,3,7,8-TCDD. For example, 2,3,7,8-TCDD has a TEF of 1.0, and the other PCDDs and PCDFs have TEF values between 0.0 and 1.0. To estimate the exposure media concentration, risk assessments covering PCDDs and PCDFs must be completed using the congener-specific emission rates from the stack and fate and transport properties in the media concentration equations and food web equations. Use of the TEFs allows for the combined risk resulting from exposure to a mixture of the 17 dioxin-like congeners to be computed assuming that the risks are additive.

In June 2005, the WHO held a meeting in Geneva during which the 1998 WHO TEFs for dioxin-like compounds and some PCBs, were reevaluated. As a result, TEF values were updated based on the consensus judgment of experts present at the World Health Organization (WHO) consultations (Van den Berg et al. 1998; 2006).

Table 1. Polychlorinated Dibenzop-dioxin and Polychlorinated Dibenzofuran Congener Toxicity Equivalency Factors (TEFs) for fish, mammals, and birds.

Congener	TEF		
	Mammals ¹	Birds ²	Fish ²
<i>Dioxins</i>			
2,3,7,8-TCDD	1	1	1
1,2,3,7,8-PeCDD	1	1	1
1,2,3,4,7,8-HxCDD	0.1	0.05	0.5
1,2,3,6,7,8-HxCDD	0.1	0.01	0.01
1,2,3,7,8,9-HxCDD	0.1	0.1	0.01
1,2,3,4,6,7,8-HpCDD	0.01	<0.001	0.001
OCDD	0.0003	0.0001	<0.0001
<i>Furans</i>			
2,3,7,8-TCDF	0.1	1	0.05
1,2,3,7,8-PeCDF	0.03	0.1	0.05
2,3,4,7,8-PeCDF	0.3	1	0.5
1,2,3,4,7,8-HxCDF	0.1	0.1	0.1
1,2,3,6,7,8-HxCDF	0.1	0.1	0.1
1,2,3,7,8,9-HxCDF	0.1	0.1	0.1
2,3,4,6,7,8-HxCDF	0.1	0.1	0.1
1,2,3,4,6,7,8-HpCDF	0.01	0.01	0.01
1,2,3,4,7,8,9-HpCDF	0.01	0.01	0.01
OCDF	0.0003	0.0001	<0.0001

Notes: ¹ Van den Berg et al., 2006; ² Van den Berg et al., 1998.

In U.S. EPA 2008 (Table 1), an updated summary is presented of available scientific studies used to evaluate the observed effects in mammals, birds, and fish, resulting from exposure to PCDDs and PCDFs.

2.3.3 Exposure Assessment for Community Measurement Receptors

To evaluate exposure of water, sediment, and soil communities to PCDDs and PCDFs, congener-specific concentrations in the respective media to which the community is exposed should be converted to a 2,3,7,8-TCDD *TEQ*; which allows for direct comparison to 2,3,7,8-TCDD toxicity benchmarks. A media-specific 2,3,7,8-TCDD *TEQ* is calculated and used in the exposure assessment because limited congener-specific toxicity information is available for community receptors (WHO 1997, Van den Berg 1998, 2006). The congener-specific concentrations in the media to which the community being evaluated is exposed, should be calculated consistent with segregated toxic chemical, for assessing exposure of community measurement receptors to other COPCs. The concentration of each PCDD and PCDF congener in the media of exposure should then be multiplied by the congener-specific *TEF* for fish, and summed, to obtain the 2,3,7,8-TCDD *TEQ*.

$$TEQ = \sum (C_{Mi} \times TEF_i)$$

where:

- TEQ = 2,3,7,8-TCDD toxicity equivalence concentration ($\mu\text{g/l}$ [water] or $\mu\text{g/kg}$ [soil or sediment])
- C_{Mi} = Concentration of *i*th congener in abiotic media ($\mu\text{g/L}$ [water] or $\mu\text{g/kg}$ [soil or sediment])
- TEF_i = Toxicity equivalency factor (fish) for *i*th congener (unitless)

The risk assessor should assume that *TEFs* for fish accurately reflect the relative toxicity of PCDD and PCDF congeners to community receptors. Evaluation of all congeners directly as 2,3,7,8-TCDD is assumed overly conservative based on the limited evidence of the aryl hydrocarbon receptor (AhR) or TCDD-like toxicity in invertebrates, and that invertebrates appear to be less sensitive to the toxic effects of dioxin-like compounds (WHO 1997). For the same reasons, *TEF* values specific to invertebrate have not been developed; requiring use of the surrogate *TEF* values for fish.

Use of the *TEFs* allows for the combined risk resulting from exposure to a mixture of the 17 dioxin-like congeners to be computed assuming that the risks are additive. Risk to the water, sediment, or soil community being evaluated is then subsequently estimated by comparing the media-specific 2,3,7,8-TCDD *TEQ* to the corresponding media-specific toxicity benchmark for 2,3,7,8-TCDD.

2.3.4 Exposure Assessment for Class-Specific Guild Measurement Receptors

To evaluate the exposure of class-specific guilds to PCDDs and PCDFs, congener-specific daily doses of all food items (i.e., media, plants, and animals) ingested by a measurement receptor should be converted to a 2,3,7,8-TCDD TEQ daily dose (DD_{TEQ}); which allows for direct comparison to 2,3,7,8-TCDD toxicity benchmarks. The congener-specific daily doses of food items ingested by a measurement receptor should be calculated consistent with the guidance for assessing exposure of class-specific guild measurement receptors to other COPCs. This includes the use of congener-specific media concentrations, congener-specific bio-concentration factors (BCF), and congener-specific food chain multipliers (FCM). The daily dose of each PCDD and PCDF congener ingested by a measurement receptor should then be multiplied by the congener-specific $TEFs$ that correspond to the respective measurement receptor, and summed, to obtain the DD_{TEQ} . Use of the $TEFs$ allows for the combined risk resulting from exposure to a mixture of the 17 dioxin-like congeners to be computed assuming that the risks are additive. The DD_{TEQ} for each measurement receptor should be determined as indicated in the following equation:

$$DD_{TEQ} = \sum [DD_i \times TEF_{(Measurement\ Receptor)}]$$

where:

- DD_{TEQ} = Daily dose of 2,3,7,8-TCDD TEQ ($\mu\text{g}/\text{kg BW}/\text{d}$)
- DD_i = Daily dose of i th congener ($\mu\text{g}/\text{kg BW}/\text{d}$)
- TEF = Toxicity equivalency factor (specific to measurement receptor) (unitless)

These equations include the use of congener-specific BCF and FCM values. The limited availability of congener-specific $BCFs$ requires that media to receptor BCF values for 2,3,7,8-TCDD be utilized in conjunction with congener-specific BEF values to obtain estimated congener-specific BCF values. Calculation of a congener-specific daily dose also requires the use of congener-specific $FCMs$.

2.3.5 Bioaccumulation Equivalency Factors

Modeling the exposure of PCDD and PCDF congeners through the food web requires the quantification of bioaccumulation potential. However, similar to the limited availability of congener-specific toxicity information, measured bioaccumulation data specific to each congener is also limited. Therefore, for use with $TEFs$ in the development of wildlife water quality criteria for the Great Lakes, U.S. EPA (1995c) developed bioaccumulation equivalency factors ($BEFs$) as a measure of a congeners bioaccumulation potential relative to 2,3,7,8-TCDD. U.S. EPA (2008) also provides detailed discussion on deriving PCDD, PCDF and other PCB congener-specific $BEFs$. As indicated in the following equation, $BEFs$

are estimated as a ratio between each PCDD and PCDF congener-specific *BASF* to that of 2,3,7,8-TCDD (Lodge et al. 1994; U.S. EPA 1995c).

$$BEF_i = \frac{BSAF_i}{BSAF_{TCDD}}$$

where:

BEF_i = Bioaccumulation equivalency factor for *i*th congener (unitless)

$BSAF_i$ = Biota-sediment accumulation factor for *i*th congener (unitless)

$BSAF_{TCDD}$ = Biota-sediment accumulation factor for 2,3,7,8-TCDD

BEF values reported by U.S. EPA (1995b and 2008) for the 17 PCDD and PCDF congeners are provided in Table 2. Although developed based on concentration data of PCDDs and PCDFs in sediment and surface water for application of *TEFs* in fish, U.S. EPA OSW assumes that these *BEFs* are applicable to other pathways and receptors. The estimation of PCDD and PCDF congener-specific *BCF* values using *BEFs* is indicated in the following equation:

$$BCF_i = BCF_{TCDD} \times BEF_i$$

where:

BCF_i = Media-to-animal or media-to-plant bioconcentration factor for *i*th congener (L/kg [water], unitless [soil and sediment])

BCF_{TCDD} = Media-to-receptor BCF for 2,3,7,8-TCDD (L/kg [aquatic receptor], unitless [soil and sediment receptor])

BEF_i = Bioaccumulation equivalency factor for *i*th congener (unitless)

Table 2. PCDD and PCDF Bioaccumulation Equivalency Factors (BEFs).

PCDD Congener	Bioaccumulation Equivalency Factor (unitless)	PCDF Congener	Bioaccumulation Equivalency Factor (unitless)
2,3,7,8-TCDD	1.0	2,3,7,8-TCDF	0.80
1,2,3,7,8-PeCDD	0.92	1,2,3,7,8-PeCDF	0.22
1,2,3,4,7,8-HxCDD	0.31	2,3,4,7,8-PeCDF	1.6
1,2,3,6,7,8-HxCDD	0.12	1,2,3,4,7,8-HxCDF	0.076
1,2,3,7,8,9-HxCDD	0.14	1,2,3,6,7,8-HxCDF	0.19
1,2,3,4,6,7,8-HpCDD	0.051	2,3,4,6,7,8-HxCDF	0.67
OCDD	0.012	1,2,3,7,8,9-HxCDF	0.63
		1,2,3,4,6,7,8-HpCDF	0.011
		1,2,3,4,7,8,9-HpCDF	0.39
		OCDF	0.016

Source: U.S. EPA 1995b; 2008

2.3.6 Fluorine, Bromine, and Sulfur PCDD/PCDF Analogs

Available information indicates that fluorinated dioxins and furans are not likely to be formed as PICs; however, the presence of free fluorine in the combustion gases may increase the formation of chlorinated dioxins (U.S. EPA 1996l).

TEF values for brominated dioxins or furans have not been developed (U.S. EPA 1994e; WHO 1997). However, the toxicity of bromo- and chlorobromo-substituted dioxin analogs is comparable to that of chlorinated dioxins in short-term toxicity assays (U.S. EPA 1996m).

1. Description of any combustion unit-specific operating conditions that may contribute to the formation of dioxins
2. Any facility specific sampling information regarding PCDD and PCDF concentrations in air, soil, sediment, water, or biota
3. Information regarding the concentration of sulfur, fluorine, and bromine in the combustion unit feed materials.

2.3.7 Polynuclear Aromatic Hydrocarbons – PAH

Based on their combustion properties and toxicity PAHs should be included in every risk assessment. The following are commonly detected PAHs:

1. Benzo(a)pyrene (BaP)
2. Benzo(a)anthracene
3. Benzo(b)fluoranthene
4. Benzo(k)fluoranthene
5. Chrysene
6. Dibenz(a,h)anthracene
7. Indeno(1,2,3-cd)pyrene.

PAHs are well-known as the principal organic components of emissions from all combustion sources, including coal fires (soot), wood fires, tobacco smoke ("tar"), diesel exhaust, and refuse burning (Sandmeyer 1981). They are generally the only chemicals of concern in particulate matter (Manahan 1991), although the presence of metals and other inorganics in the waste feed can add other contaminants of concern.

2.3.8 Exposure Assessment for PAHs

The risk assessor should model the individual PAH compounds from the emission source to media (i.e., soil, surface water, soil) and plants, using compound-specific emission rates and fate and transport properties, as required in the media concentration equations.

2.3.9 Polychlorinated Biphenyls – PCB

The use and distribution of polychlorinated biphenyls (PCBs) were severely restricted in the late 1970s with additional bans and restrictions taking effect over the next decade (ATSDR 1995d).

PCBs should automatically be included as COPCs for combustion units that burn PCB-contaminated wastes or waste oils, highly variable waste streams such as municipal and commercial wastes for which PCB contamination is reasonable, and highly chlorinated waste streams.

2.3.10 Exposure Assessment for PCBs

WHO (2006) recently convened a conference to discuss and update the derivation of *TEFs* for humans and wildlife. Table 3 lists PCB *TEFs* reported for fish, mammals, and birds (EPA 2008).

Table 3. PCBs Toxicity Equiv. Factors (*TEFs*) For Fish, Mammals and Birds.

Congener	TEF		
	Mammals ¹	Birds ²	Fish ²
Non-ortho PCBs			
3,3',4,4'-TCB (77)	0.0001	0.05	0.0001
3,4,4',5-TCB (81)	0.0003	0.10	0.0005
3,3',4,4',5-PeCB (126)	0.10	0.10	0.005
3,3',4,4',5,5'-HxCB (169)	0.03	0.001	0.00005
Mono-ortho PCBs			
2,3,3',4,4'-PeCB (105)	3E-05	0.0001	< 5E-06
2,3,4,4',5-PeCB (114)	3E-05	0.0001	< 5E-06
2,3',4,4',5-PeCB (118)	3E-05	0.00001	< 5E-06
2',3,4,4',5-PeCB (123)	3E-05	0.00001	< 5E-06
2,3,3',4,4',5-HxCB (156)	3E-05	0.0001	< 5E-06
2,3,3',4,4',5'-HxCB (157)	3E-05	0.0001	< 5E-06
2,3',4,4',5,5'-HxCB (167)	3E-05	0.00001	< 5E-06
2,3,3',4,4',5,5'-HeCB (189)	3E-05	0.00001	< 5E-06

Source: ¹Van den Berg et al., 2006, ²Van den Berg et al., 1998.

2.3.11 Nitroaromatics

Careful consideration should be made before the automatic inclusion of nitroaromatic organic compounds, including 1,3-dinitrobenzene; 2,4-dinitrotoluene; 2,6-dinitrotoluene; nitrobenzene; and penta-chloro-nitrobenzene, in risk assessments.

2.3.12 Phthalates

The main phthalates for risk assessment consideration includes bis (2-ethylhexyl) phthalate (BEHP) and di(n)octyl phthalate (DNOP). DNOP is a plasticizer that is produced in large volumes and is used in the manufacture of plastics and rubber materials. Because plastics have become so widely used in society, phthalate plasticizers such as BEHP and DNOP have become widely distributed in food, water, and the atmosphere (Howard 1990).

2.3.13 Metals

A comprehensive ecological risk assessment should consider the following metals:

1. Aluminum
2. Antimony
3. Arsenic
4. Barium
5. Beryllium
6. Cadmium
7. Hexavalent chromium
8. Copper
9. Lead
10. Mercury (divalent and methyl mercury)
11. Nickel
12. Selenium
13. Silver
14. Thallium
15. Zinc.

2.3.14 Chromium

The oxidation state of chromium is a crucial issue in evaluating the toxicity of this metal and the risks associated with exposure. Hexavalent chromium (Cr^{+6}) is the most toxic valence state of chromium. Trivalent chromium (Cr^{+3}), a commonly found less oxidized and a lower toxic form of chromium, is more commonly found in the environment. Note that media-specific chromium speciation information is often difficult to obtain within the scope of a screening risk assessment.

2.3.15 Mercury

Stack emissions containing mercury include both vapor and particulate forms. Vapor mercury emissions include both elemental (Hg^0) and oxidized (e.g., Hg^{+2}) chemical species, while particulate mercury emissions are thought to be composed primarily of oxidized compounds due to the relatively high vapor pressure of elemental mercury (U.S. EPA 1997b).

The speciation of mercury emissions is thought to depend on the fuel used, flue gas cleaning, and operating temperatures. Most of the total mercury emitted at the stack outlet is found in the vapor phase; although exit streams containing soot or particulate can bind up some fraction of the mercury (U.S. EPA 1997b). Total mercury exiting the stack is assumed to consist of elemental and divalent species, with no emissions of methylmercury assumed. The divalent fraction is split between vapor and particle-bound phases (Lindqvist et al. 1991). Much of the divalent mercury is thought to be mercuric chloride (HgCl_2) as presented in the *Mercury Study Report to Congress* (U.S. EPA 1997b).

2.3.15.1 Phase Allocation and Speciation of Mercury Exiting the Stack

Based on review of mercury emissions data presented for combustion sources in U.S. EPA (1997b) and published literature (Peterson et al. 1995), estimates for the percentage of vapor and particle-bound mercury emissions range widely from 20 to 80 percent. Therefore, at this time, as a screening level ecological risk assessment, a conservative approach should be used. This conservative approach assumes phase allocation of mercury emissions from combustion of 80 percent of the total mercury in the vapor phase and 20 percent of total mercury in the particle-bound phase.

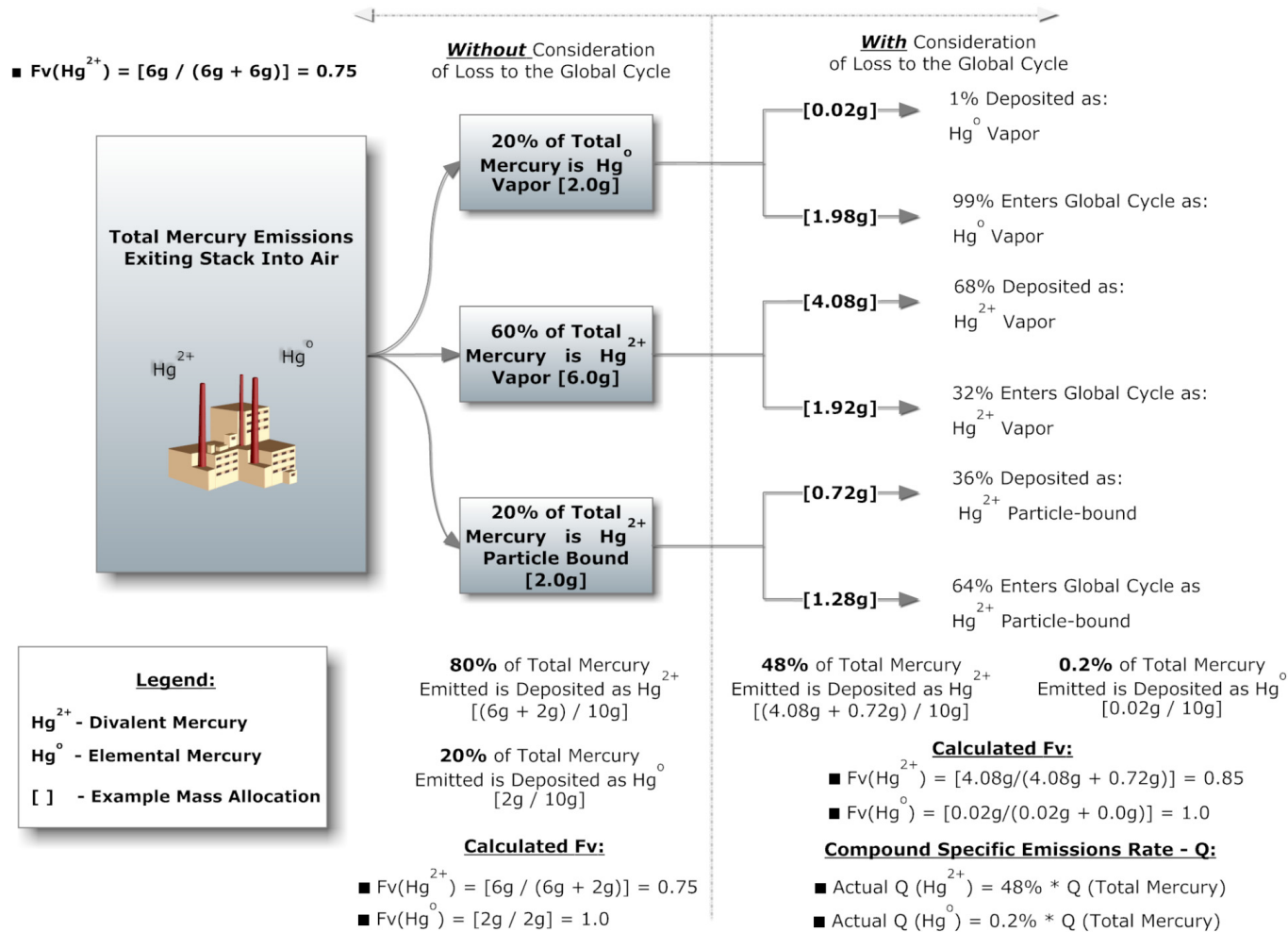


Figure 2. Mercury Speciation.

2.3.15.2 Vapor Phase Mercury

As illustrated in Figure 2, of the 80 percent total mercury in the vapor phase, 20 percent of the total mercury is in the elemental vapor form and 60 percent of the total mercury is in the divalent vapor form (Peterson et al. 1995). A vast majority (assumed to be 99 percent) of the 20 percent vapor phase elemental mercury does not readily deposit and is transported outside of the U.S. or is vertically diffused to the free atmosphere to become part of the global cycle (U.S. EPA 1997b). Only a small fraction (assumed to be one percent) of vapor-phase elemental mercury either is adsorbed to particulates in the air and is deposited or converted to the divalent form to be deposited (assumed to be deposited as elemental mercury, see Figure 2). Of the 60 percent vapor phase divalent mercury, about 68 percent is deposited and about 32 percent is transported outside of the U.S. or is vertically diffused to the free atmosphere to become part of the global cycle (U.S. EPA 1997b).

2.3.15.3 Particle-Bound Mercury

Of the 20 percent of the total mercury that is particle-bound, 99 percent (assumed to be 100 percent in Figure 2) is in the divalent form. U.S. EPA (1997b) indicates that only 36 percent of the particle-bound divalent mercury is deposited, and the rest is either transported outside of the U.S. or is vertically diffused to the free atmosphere to become part of the global cycle.

2.3.15.4 Deposition and Modeling of Mercury

Consistent with U.S. EPA (1997b) and as shown in Figure 2, it is assumed that deposition to the various environmental media is entirely divalent mercury in either the vapor or particle-bound form. Without consideration of the global cycle, mercury speciations will result in 80 percent of the total mercury emitted being deposited as divalent mercury and the remaining 20 percent being deposited as elemental mercury. The risk assessor should employ the percentages provided in U.S. EPA (1997b) to account for the global cycle, the percentage of total mercury deposited is reduced to a total of 48.2 percent (40.8 percent as divalent vapor, 7.2 percent as divalent particle-bound, and 0.2 percent as elemental vapor). These speciation splits result in fraction in vapor phase (F_v) values of 0.85 (40.8/48.2) for divalent mercury, and 1.0 (0.2/0.2) for elemental mercury. Also, to account for the remaining 51.8 percent of the total mercury mass that is not deposited, the deposition and media concentration equations, multiply the compound-specific emission rate (Q) for elemental mercury by a default value of 0.002; and divalent mercury by a default value of 0.48.

Also, only a small fraction (~ 1%) of elemental mercury is in the vapor phase and is assumed to be deposited in its original form. Therefore, any resulting exposure to elemental mercury is considered to be much less significant, and will not be considered in the pathways of the ecological risk assessment.

2.3.15.5 Methylation of Mercury

The net mercury methylation rate, which is the net result of methylation and demethylation, for most soils appears to be quite low; with much of the measured methyl mercury in soils potentially resulting from wet deposition (U.S. EPA 1997b). A fraction of the divalent mercury that is deposited is assumed to speciate to organic mercury (methyl mercury) in soil. In soil, 98 percent of total mercury is assumed to be divalent mercury and the remaining mass as methyl mercury (U.S. EPA 1997b). A significant and important exception to mercury methylation rate being low in soils appears to be wetland soils. Wetlands appear to convert a small but significant fraction of the deposited mercury into methyl mercury; which can be exported to nearby water bodies and potentially bio-accumulated in the aquatic food chain (U.S. EPA 1997b). Therefore, the assumed percentage of methyl mercury in wetland soils may be higher than the 2 percent assumed for non-wetland soils, and may closer approximate the 15 percent assumed for sediments.

There is a great deal of variability in the processing of mercury among water bodies. This variability is primarily a result of the characteristically wide range of chemical and physical properties of water bodies that influence the levels of methylated mercury. In the absence of modeling site-specific water body properties and biotic conditions, 85 percent of total mercury in surface water is assumed to be divalent mercury and the remaining mass as methyl mercury (U.S. EPA 1997b).

2.3.15.6 Exposure Assessment for Mercury

Special consideration is required in evaluating the various forms of mercury modeled to the point of exposure. To evaluate exposure of water, sediment, and soil communities to mercury, species-specific concentrations of divalent mercury and methyl mercury, in the respective media to which the community is exposed, should be directly compared to toxicity benchmarks specific to those compounds. The species-specific media concentrations should be calculated using equations and methods presented in the next sections.

To evaluate the exposure of class-specific guilds to mercury, the media-specific concentrations of both divalent and methyl mercury should be modeled as independent COPCs through the food web, assuming no methylation of divalent mercury to the methyl mercury form within organisms. Therefore, the daily doses of all food items (i.e., media, plants, and animals) ingested by a measurement receptor should be considered for both divalent and methyl mercury, and compared to the respective toxicity benchmarks that are representative of the measurement receptor. The daily doses of food items ingested by a measurement receptor should be calculated using the methodology described in the next sections, for assessing exposure of class-specific guild measurement receptors to other COPCs. This includes the use of species-specific media concentrations, and

methyl mercury bio-concentration factors (*BCF*) and food chain multipliers (*FCM*).

2.3.15.7 Mercury Conclusion

In the event risks associated with mercury exceed target levels based on modeling with equations and initial conservative assumptions presented in this guidance, the permitting authority may approve use of more complex models that utilize more extensive site-specific data to predict transformation of chemical forms and bio-transfer of mercury for evaluation at points of potential exposure. For example, the dry gas algorithm for estimating dry gas deposition in AERMOD or CALPUFF may be utilized. While we do not address what models should be used or how data to support such models should be collected, the decision to use site-specific mercury models in a risk assessment is not precluded just because it is different; nor does this guidance automatically approve the use of such models. A permitting authority that chooses to use complex mercury models should carefully identify and evaluate their associated limitations, and clearly document these limitations in the uncertainty section of the risk assessment report.

Realistic expectations for mercury emission reduction efforts may be established by considering various technology-based mercury emission limits that apply to waste combustors (for example, standards for European combustors, the MACT standards for hazardous waste combustors, or the MACT standards for municipal waste combustors). Site-specific risk assessments as currently conducted may not identify the entire potential risk from mercury emissions. Mercury that does not deposit locally will ultimately enter the global mercury cycle for potential deposition elsewhere.

2.3.16 Particulate Matter

PM is all condensed material suspended in air that has a mean aerodynamic diameter of 10 micrometers or less (PM_{10}). PM can be classified as aerosols, dusts, fogs, fumes, mists, smogs, or smokes, depending on its physical state and origin. Anecdotal evidence suggests that uncontrolled particulate emissions from coal-burning industries have adversely affected local populations of wildlife (U.S. FWS, 1980). For wildlife, PM can adsorb to external surfaces or membranes, for example causing corneal damage. Wildlife exposure can also occur through ingestion of contaminated food, water, and hair (through grooming) (U.S. FWS, 1980). However, PM dose-response information to evaluate risk of particulate matter to ecological receptors is limited. For this reason, PM should not be evaluated as a separate COPC in a risk assessment. However, PM is useful as an indicator parameter for other contaminants because it can be measured in real time and is sensitive to changes in combustion conditions.

2.3.17 Endocrine Disruptors

Endocrine disruptors are chemical compounds that interfere with the endocrine system's normal function and homeostasis in cells, tissues, and organisms. It has been hypothesized by the U.S. that endocrine disruptors adversely affect the reproductive system by interfering with production, release, transport, receptor binding action, or elimination of natural blood-borne hormones and ligands (see: <http://www.epa.gov/raf/publications/pdfs/endocrine-disruptions-factsheet.PDF>).

Several studies have been conducted and serve as the basis for further experimentation to determine whether the hypothesis is correct. These studies include:

1. Wildlife reproduction (feminization of birds, alligators, and certain terrestrial mammals)
2. Wildlife population ecology (population decline)
3. Human reproductive physiology (decreased sperm count in males in industrialized nations)
4. Molecular biology (data on receptor-mediated mode of action)
5. Endocrinology (increased understanding of mechanisms of hormone regulation and impacts of perturbations).

Because the information currently available on endocrine disruptors is inconsistent and limited, U.S. EPA has not yet developed a methodology for quantitative assessments of risk resulting from potential endocrine disruptors (U.S. EPA 1996d). Currently, no quantitative U.S. EPA methods exist to specifically address the effects of endocrine disruptors in a risk assessment. Because the methods for addressing endocrine disruptors are developing at a rapid pace, permits writers and risk assessors should contact the Economics, Methods and Risk Analysis Division (EMRAD) of the Office of Solid Waste for the latest policy on how to deal with endocrine disruptors in site specific risk assessments. Additional information can also be obtained from review of available publications including:

1. USEPA Special Report on Endocrine Disruption
(<http://www.epa.gov/raf/publications/pdfs/endocrine-disruptions-factsheet.PDF>)
2. USEPA Announcement of the Revised Policies and Procedures for the Endocrine Disruptor Screening Program
(http://www.epa.gov/endo/pubs/revised_pandp_frn_041509.pdf)

2.4 Estimates of COPC Concentrations for Non-Detects

The lowest level of an analyte that can be detected using an analytical method is generally termed the detection limit. One particularly difficult issue is the treatment of data in the risk assessment that are reported as below the detection limit.

2.4.1 Definitions of Commonly Reported Detection Limits

U.S. EPAs commonly-used definition for the detection limit for non-isotope dilution methods has been the method detection limit (MDL), as promulgated in 40 CFR Part 136, Appendix B (U.S. EPA 1995d). A level above the MDL is the level at which reliable quantitative measurements can be made; generically termed the quantitation limit or quantitation level. In practice, numerous terms have been created to describe detection and quantitation levels. The significance and applicability of the more widely reported of these detection and quantitation levels by analytical laboratories are summarized below. These levels listed generally from the lowest limit to the highest limit include the following:

1. **Instrument Detection Limit (IDL)** is the smallest signal above background that an instrument can reliably detect, but not quantify. Also, commonly described as a function of the signal-to-noise (S/N) ratio.
2. **Method Detection Limit (MDL)** is the minimum concentration of a substance that can be measured (via non-isotope dilution methods) and reported with 99 percent confidence that the analyte concentration is greater than zero, and is determined from analysis of a sample in a specific matrix type containing the analyte.
3. **Reliable Detection Level (RDL)** is a detection level recommended by the National Environmental Research Laboratory in Cincinnati. It is defined as 2.623 times the MDL (U.S. EPA 1995d). The RDL is a total of 8 standard deviations above the MDL developmental test data (3.14 times 2.623).
4. **Estimated Detection Limit (EDL)** is a quantitation level defined in SW-846 that has been applied to isotope dilution test methods (e.g., SW-846 Method 8290). A variation of the SW-846 defined EDL is also commonly reported by commercial laboratories, however, with the addition of a multiplication factor that generally elevates the EDL value by 3.5 to 5 times that of the SW-846 definition.
5. **Practical Quantitation Limit (PQL)** is a quantitation level that is defined in 50 FR 46908 and 52 FR 25699 as the lowest level that can be reliably achieved with specified limits of precision and accuracy during routine laboratory operating conditions (U.S. EPA 1995d).
6. **Target Detection Limit (TDL)** is a quantitation level constructed similar to the PQL.
7. **Reporting Limit (RL)** is a quantitation level constructed similar to the PQL.
8. **Estimated Quantitation Limit (EQL)** is a quantitation level constructed similar to the PQL.
9. **Sample Quantitation Limit (SQL)** is a quantitation level that is sample-specific and highly matrix-dependent because it accounts for sample volume or weight, aliquot size, moisture content, and dilution. The SQL is generally 5 to 10 times the MDL, however, it is often reported at much higher levels due to matrix interferences.

10. **Contract Required Quantitation Limit (CRQL) / Contract Required Detection Limit (CRDL)** is a quantitation pre-set by contract, which may incorporate U.S. EPA (1986a) SW-846 methods, Office of Water methods, or other methods deemed necessary to meet study objectives. These limits are typically administrative limits and may actually be one or two orders of magnitude above the MDL.

3 Air Dispersion Modeling for Ecological Risk Assessment

Estimation of potential ecological risks associated with air toxic releases requires knowledge of atmospheric pollutant concentrations and annual deposition rates in the areas around the facility at habitat-specific scenario locations. Air concentrations and deposition rates are usually estimated by using air dispersion models.

This Chapter provides guidance on the use of AERMOD, the standard U.S. EPA air dispersion model. AERMOD requires the use of the following information for input into the model, and consideration of output file development:

1. Site-specific characteristics required for air modeling include:
 - Surrounding terrain
 - Surrounding land use
 - Facility building characteristics
2. Unit emission rate
3. Partitioning (i.e., chemical-specific) of emissions
4. Meteorological data
5. Source Characteristics

The USEPA provides extensive information on air dispersion models, meteorological data, data preprocessors, user's guides, and model applicability on the Support Center for Regulatory Air Models (SCRAM) web site at the following address: <http://www.epa.gov/scram001/index.htm> .

3.1 Site-Specific Information Required to Support Air Modeling

Site-specific information for the facility and surrounding area required to support air dispersion modeling includes:

1. Mapped identification of facility information including stack and fugitive source locations
2. Property boundaries of the facility
3. The elevation of the surrounding land surface or terrain
4. Surrounding land uses and land cover (LULC)
5. Characteristics of on-site buildings that may affect the dispersion of chemicals into the surrounding environment.
6. All site-specific maps, photographs, or figures used in developing the air modeling approach

3.2 Use of Unit Emission Rate

The AERMOD model is usually run with a unit emission rate of 1.0 g/s in order to preclude having to run the model for each specific COPC. The unitized concentration and deposition output from AERMOD, using a unit emission rate, are adjusted to the COPC-specific air concentrations and deposition rates in the estimating media concentration equations by using COPC-specific. Concentration and deposition are directly proportional to a unit emission rate used in the AERMOD modeling as described in the following equation:

$$\frac{\text{COPC-Specific Air Concentration}}{\text{COPC-Specific Emissions Rate}} = \frac{\text{Modeled Output Air Concentration}}{\text{Unit Emissions Rate}}$$

For facilities with multiple stacks or emission sources, each source must be modeled separately. The justification for not allowing the inclusion of more than one source in a single run is the requirement to be able to estimate stack-specific risks. If a facility has two or more stacks with identical characteristics (emissions, stack parameters, and nearby locations), agency approval may be requested to represent the stacks with a single set of model runs.

3.3 Partitioning of Emissions

COPC emissions to the environment occur in either vapor or particle phase. In general, most metals and organic COPCs with very low volatility (refer to fraction of COPC in vapor phase [F_v] less than 0.05) are assumed to occur only in the particle phase. Organic COPCs occur as either only vapor phase (refer to F_v of 1.0, or with a portion of the vapor condensed onto the surface of particulates (e.g., particle-bound). COPCs released only as particulates are modeled with different mass fractions allocated to each particle size than the mass fractions for the organics released in both the vapor and particle-bound phases. Due to the limitations of the AERMOD model, estimates of vapor phase COPCs, particle phase COPCs, and particle-bound COPCs cannot be provided in a single pass (run) of the model. Multiple runs are required, one for each phase.

3.3.1 Vapor Phase Modeling

AERMOD output for vapor phase air modeling runs provide vapor phase ambient air concentration and wet vapor deposition at modeled receptor grid nodes based on the unit emission rate.

3.3.2 Particle Phase Modeling (Mass Weighting)

Particle diameter is the main determinant of the fate of particles in air flow, whether dry or wet. The key to dry particle deposition rate is the terminal, or

falling, velocity of a particle. Particle terminal velocity is calculated mainly from the particle size and particle density. Small particles have low terminal velocities, with very small particles remaining suspended in the air flow. Wet particle deposition also depends on particle size as larger particles are more easily removed, or scavenged, by falling liquid (rain) or frozen (snow or sleet) precipitation.

Stack test data will be different from the values presented in Table 4 because of the use of particle cut size for the different cascade impactor filters used during actual stack sampling. The test method will drive the range of particle sizes that are presented in the results of the stack test. However, because AERMOD requires mean particle diameter for each particle size distribution, and the stack test data identifies only the mass (weight) of particles in a range bounded by two specific diameters, stack test data must be converted into a mean particle diameter which approximates the diameter of all the particles within a defined range. The mean particle diameter is calculated by using the following equation:

$$D_{mean} = [0.25 C (D_1^3 + D_1^2 D_2 + D_1 D_2^2 + D_2^3)]^{0.33}$$

where:

- D_{mean} = Mean particle diameter for the particle size category (μm)
- D_1 = Lower bound cut of the particle size category (μm)
- D_2 = Upper bound cut of the particle size category (μm)

For example, the mean particle diameter of 5.5 μm in Table 4 is calculated from a lower bound cut size (assuming a cascade impactor is used to collect the sample) of 5.0 μm to an upper bound cut size of 6.15 μm . In this example, the mean particle diameter is calculated as:

$$D_{mean} = [0.25 (5.0^3 + (5.0)^2 (6.15) + (5.0) (6.15)^2 + (6.15)^3)]^{0.33}$$

Table 4. Default Particle Size Distribution, and Proportion of Surface Area, in Deposition Modeling (When Site Specific Data Unavailable).

1	2	3	4	5	6
Mean Particle Diameter ^a (μm)	Particle Radius (μm)	Surface Area/ Volume (μm^{-1})	Fraction of Total Mass ^b	Proportion Available Surface Area	Fraction of Total Surface Area
> 15.0	7.50	0.400	0.128	0.0512	0.0149
12.5	6.25	0.480	0.105	0.0504	0.0146
8.1	4.05	0.741	0.104	0.0771	0.0224
5.5	2.75	1.091	0.073	0.0796	0.0231
3.6	1.80	1.667	0.103	0.1717	0.0499
2.0	1.00	3.000	0.105	0.3150	0.0915
1.1	0.55	5.455	0.082	0.4473	0.1290
0.7	0.40	7.500	0.076	0.5700	0.1656
< 0.7	0.40	7.500	0.224	1.6800	0.4880

Notes:

a Geometric mean diameter in a distribution from U.S. EPA (1980a)

b The terms mass and weight are used interchangeably when using stack test data

From Table 4, the mean particle diameter is 5.5 μm . The mass of particulate from the 5.0 μm stack test data is then assigned to the 5.5 μm mean particle diameter for the purpose of computing the fraction of total mass.

Typically, eight to ten mean particle diameters are available from stack test results. For facilities with stack test results which indicate mass amounts lower than the detectable limit (or the filter weight is less after sampling than before), a single mean particle size diameter of 1.0 microns should be used to represent all mass (e.g., particle diameter of 1.0 microns or a particle mass fraction of 1.0) in the particle and particle-bound model runs. Because rudimentary methods for stack testing may not detect the very small size or amounts of COPCs in the particle phase, the use of a 1.0 micron particle size will allow these small particles to be included properly as particles in the risk assessment exposure pathways while dispersing and depositing in the air model similar in behavior to a vapor.

The fraction of total mass for each mean particle diameter is calculated by dividing the associated mass of particulate for that diameter by the total mass of particulate in the sample. In many cases, the fractions of total mass will not sum to 1.0 due to rounding errors. In these instances, U.S. EPA OSW advocates that the remaining mass fraction be added into the largest mean particle diameter mass fraction to force the total mass to 1.0.

Direct measurements of particle-size distributions at a proposed new facility may be unavailable, so it will be necessary to provide assumed particle distributions for use in AERMOD. In such instances, a representative distribution may be used. The unit on which the representative distribution is based should be as similar as practicable to the proposed unit.

3.3.3 Particle-Bound Modeling (Surface Area Weighting)

A surface area weighting, instead of mass weighting, of the particles is used in separate particle runs of AERMOD. Surface area weighting approximates the situation where a semi-volatile organic contaminant that has been volatilized in the high temperature environment of a combustion system and then condensed to the surface of particles entrained in the combustion gas after it cools in the stack. Thus, the apportionment of emissions by particle diameter becomes a function of the surface area of the particle that is available for chemical adsorption.

The first step in apportioning COPC emissions by surface area is to calculate the proportion of available surface area of the particles. If particle density is held constant (such as 1 g/m^3), the proportion of available surface area of aerodynamic spherical particles is the ratio of surface area (S) to volume (V), as follows:

1. Assume aerodynamic spherical particles.
2. Specific surface area of a spherical particle with a radius, $r-S = 4 \pi r^2$
3. Volume of a spherical particle with a radius, $r-V = 4/3 \pi r^3$
4. Ratio of S to $V-S/V = 4 \pi r^2 / (4/3 \pi r^3) = 3/r$

After developing the particulate size distribution based on surface area, this distribution is used in AERMOD to apportion mass of particle-bound COPCs (most organics) based on particle size.

3.4 Meteorological Data

The AERMET User's Guide contains detailed information describing file formats and content and including detailed instructions for preparing the required meteorological input files for the AERMOD model (U.S. EPA 2004a and U.S. EPA 2006).

3.5 AERMOD Model Input Files

A thorough instruction of how to prepare the input files for AERMOD is presented in the AERMOD User's Guide, Volume I (U.S. EPA 2004b), which is available for downloading from the SCRAM web site. An example AERMOD input file is provided in Figure 3. This example illustrates a single year run (1990), for particle phase COPC emissions from a single stack, to compute acute (1-hour average) and chronic (annual average) and provide single year results in one hour and annual average plotfiles for post-processing. For ecological risk assessments, only the annual average air parameters are required, not the 1-hour

values. The risk assessment report should document each section of the AERMOD input file to identify consistent methods.

```

CO STARTING
  TITLEONE An input Title
  MODELOPT CONC DDEP WDEP DEPOS FLAT TOXICS
  AVERTIME 1 ANNUAL
  POLLUTID ONEGPS
  RUNORNOT RUN
CO FINISHED
SO STARTING
  LOCATION STACK1 POINT 0.0 0.0 0.0
  SRCPARAM STACK1 500.0 65.00 425. 15.0 5.
  BUILDHGT STACK1 36*50.
  BUILDWID STACK1 62.26 72.64 80.80 86.51 89.59 89.95
  BUILDWID STACK1 87.58 82.54 75.00 82.54 87.58 89.95
  BUILDWID STACK1 89.59 86.51 80.80 72.64 62.26 50.00
  BUILDWID STACK1 62.26 72.64 80.80 86.51 89.59 89.95
  BUILDWID STACK1 87.58 82.54 75.00 82.54 87.58 89.95
  BUILDWID STACK1 89.59 86.51 80.80 72.64 62.26 50.00
  BUILDLEN STACK1 82.54 87.58 89.95 89.59 86.51 80.80
  BUILDLEN STACK1 72.64 62.26 50.00 62.26 72.64 80.80
  BUILDLEN STACK1 86.51 89.59 89.95 87.58 82.54 75.00
  BUILDLEN STACK1 82.54 87.58 89.95 89.59 86.51 80.80
  BUILDLEN STACK1 72.64 62.26 50.00 62.26 72.64 80.80
  BUILDLEN STACK1 86.51 89.59 89.95 87.58 82.54 75.00
  XBADJ STACK1 -47.35 -55.76 -62.48 -67.29 -70.07 -70.71
  XBADJ STACK1 -69.21 -65.60 -60.00 -65.60 -69.21 -70.71
  XBADJ STACK1 -70.07 -67.29 -62.48 -55.76 -47.35 -37.50
  XBADJ STACK1 -35.19 -31.82 -27.48 -22.30 -16.44 -10.09
  XBADJ STACK1 -3.43 3.34 10.00 3.34 -3.43 -10.09
  XBADJ STACK1 -16.44 -22.30 -27.48 -31.82 -35.19 -37.50
  YBADJ STACK1 34.47 32.89 30.31 26.81 22.50 17.50
  YBADJ STACK1 11.97 6.08 0.00 -6.08 -11.97 -17.50
  YBADJ STACK1 -22.50 -26.81 -30.31 -32.89 -34.47 -35.00
  YBADJ STACK1 -34.47 -32.89 -30.31 -26.81 -22.50 -17.50
  YBADJ STACK1 -11.97 -6.08 0.00 6.08 11.97 17.50
  YBADJ STACK1 22.50 26.81 30.31 32.89 34.47 35.00
  SRCGROUP ALL
SO FINISHED
RE STARTING
  GRIDPOLR POL1 STA
  GRIDPOLR POL1 ORIG STACK1
  GRIDPOLR POL1 DIST 175. 350. 500. 1000.
  GRIDPOLR POL1 GDIR 36 10 10
  GRIDPOLR POL1 END
RE FINISHED
ME STARTING
  SURFFILE S0000001.sfc
  PROFFILE S0000001.pfl
  SURFDATA 14913 1990
  UAIRDATA 14918 1990
  PROFBASE 432.00 METERS
ME FINISHED

OU STARTING
  RECTABLE ALLAVE FIRST
  PLOTFILE 1 ALL FIRST S0000001.plp
  PLOTFILE PERIOD ALL S0000001.pap
OU FINISHED

```

Figure 3. Example Input File for Particle Phase.

Three sets of AERMOD runs are required for each COPC emission source. Separate AERMOD runs are required to model vapor phase COPCs, particle phase COPCs, and particle-bound phase COPCs for each source (stack or fugitive) of COPCs. The AERMOD Control Secondary Keywords used for these three runs are:

Vapor Phase:	CONC	DDEP	WDEP	DEPOS
Particle Phase:	CONC	DDEP	WDEP	DEPOS
Particle-Bound Phase:	CONC	DDEP	WDEP	DEPOS

For AERMOD modeling to provide air parameters for ecological risk assessments, only the total deposition (DEPOS) of the particle and particle-bound phases are required. The control secondary keywords for concentration in the air (CONC) and the components of deposition to the ground, dry deposition (DDEP) and wet deposition (WDEP), are not required to be output separately by AERMOD. However, by specifying these control secondary keywords as illustrated, the AERMOD model will compute the needed air parameters for both human health and ecological risk assessments. AERMOD requires site-specific inputs for source parameters, receptor locations, meteorological data, and terrain features.

The AERMOD model utilizes pathways and keyword runstream files to define what functions and model options to initiate during modeling. The pathways used by AERMOD include the following:

1. CO – overall run Control options
2. SO – SOurce location information
3. RE – Receptor information
4. ME – Meteorology information
5. OU – OUtput file information

The following subsections describe how to specify the parameters for each pathway included in the AERMOD input file.

3.5.1 Control Pathway

Model options (MODELOPT) are specified in the Control pathway to direct AERMOD in the types of computations to perform. The regulatory default option in AERMOD includes the use of stack-tip downwash, incorporates the effects of elevated terrain, and includes the calms and missing data processing routines.

The CONC parameter specifies calculation of air concentrations for vapor and particles. The DDEP and WDEP parameters specify dry and wet deposition. The DEPOS specifies computation of total (wet and dry) deposition flux. The following command lines for each of the three runs (these are for rural areas; substitute URBAN for urban areas):

Vapor:	CO	MODELOPT	CONC	DDEP	WDEP	DEPOS	FLAT	TOXICS
Mercury:	CO	MODELOPT	CONC	DDEP	WDEP	DEPOS	FLAT	TOXICS
Particle Phase:	CO	MODELOPT	CONC	DDEP	WDEP	DEPOS	FLAT	TOXICS
Particle-Bound:	CO	MODELOPT	CONC	DDEP	WDEP	DEPOS	FLAT	TOXICS

Note that only the total deposition (DEPOS) air parameter values are required for the ecological risk assessment pathways. The modeler may elect not to include CONC, DDEP and WDEP as separate output components from AERMOD if the air modeling results will not be used for a human health risk assessment.

The averaging times (AVERTIME) should be specified as 'ANNUAL' to compute long-term (annual average) ecological risk. Optionally, the '1' may be specified for convenience in modeling for the maximum 1-hour averages used in computing acute human health risks. Each phase run may be repeated five times (one for each year, or a total of 15 AERMOD runs) to complete a set of 15 runs for the full five years of meteorological data.

Alternatively, the modeler may combine the 5 years of meteorological data into a single meteorological data file and complete only 3 runs for each emission source (one run for each phase). The modeler should select the 'ANNUAL' averaging time for all risk assessment runs, regardless of the number of years in the meteorological data file. The incorrect selection of 'PERIOD' will not compute the correct deposition rates required by the risk assessment equations. No additional AERMOD model execution time is required to obtain 1-year or 5-year air modeling values.

The FLAGPOLE keyword specifies receptor grid nodes above local ground level and is not typically used for ecological risk assessments, which rely on estimates of ground-level impacts.

3.5.2 Source Pathway

For performing unitized modeling a unit emission rate of 1.0 g/s should be entered in AERMOD. Additional source characteristics required by the model include the following:

1. Source type (point source for stack emissions; area or volume for fugitive emissions)
2. Source location (UTM meters)
3. Source base elevation
4. Emission rate (1.0 g/s)
5. Stack height (m)
6. Stack gas temperature (K)
7. Stack gas exit velocity (m/s)
8. Stack inside diameter (m)
9. Building heights and widths (m)
10. Particle size distribution (percent)
11. Particle density (g/cm³)
12. Particle and gas scavenging coefficients (unitless)

3.5.3 Source Parameters – SO

The source parameters keyword of the Source pathway (SO SRCPARAM) identifies the emission rate, stack height, stack temperature, stack velocity, and stack diameter. For unitized modeling a unit emission rate is entered as 1.0 g/s. Stack height is the height above plant base elevation on the SO LOCATION keyword. Stack exit temperature is one of the most critical stack parameter for influencing concentration and deposition. For new or undefined stacks, manufacturer's data for similar equipment should be used. Stack exit velocity should be calculated from actual stack gas flow rates and stack diameter. Actual stack gas flow rates should be determined for existing stacks during stack sampling. Stack diameter is the inside diameter of the stack at the point of exit.

Following is an example of the source parameter input in the SOurce pathway for: source name, emission rate (grams per second), stack height (meters), stack temperature (K), stack velocity (meters per second), and stack diameter (meters):

```
SO SRCPARAM STACK1 1.0 23.0 447.0 14.7 1.9
```

3.5.4 Particle Size Distribution

AERMOD requires particle size distribution for determining deposition velocities. New or undefined sources may use the particle size distribution presented in Table 4.

The following example is the AERMOD input for particle phase run. From Table 4, the distribution for 9 mean diameter sizes includes the data required for the keywords of the SOurce pathway (SO PARTDIAM; SO MASSFRAX). The PARTDIAM is taken from Column 1 (Mean Particle Diameter). The MASSFRAX is taken from Column 4 (Fraction of Total Mass).

```
PARTDIAM STACK1 0.35 0.70 1.10 2.00 3.60 5.50 8.10 12.5 15.0
MASSFRAX STACK1 0.22 0.08 0.08 0.11 0.10 0.07 0.10 0.11 0.13
```

The example for the AERMOD input for the particle-bound run is described below. From Table 4, the PARTDIAM is the same. The MASSFRAX is taken from Column 6 (Fraction of Total Surface Area).

```
PARTDIAM STACK1 0.35 0.70 1.10 2.00 3.60 5.50 8.10 12.5 15.0
MASSFRAX STACK1 0.49 0.17 0.13 0.09 0.05 0.02 0.02 0.01 0.02
```

3.5.5 Particle Density – SO

Particle density is also required for modeling the air concentration and deposition rates of particles. Site-specific measured data on particle density should be determined for all existing sources when possible. For new or undefined sources requiring air modeling, a default value for particle density of 1.0 g/cm³ may be used. Particles from combustion sources, however, may have densities that are

less than 1.0 g/cm^3 (U.S. EPA 1994a), which would reduce the modeled deposition flux.

Following is an example of the particle density input in the Source pathway (SO PARTDENS) for the 9 mean particle size diameters of the previous example:

```
PARTDENS STACK1 1.0 1.0 1.0 1.0 1.0 1.0 1.0 1.0 1.0
```

3.5.6 Scavenging Coefficients – SO

Wet deposition flux is calculated within AERMOD by multiplying a scavenging ratio by the vertically integrated concentration. The scavenging ratio is the product of a scavenging coefficient and a precipitation rate. Studies have shown that best fit values for the scavenging coefficients vary with particle size. For vapors, wet scavenging depends on the properties of the COPCs involved. However, not enough data are now available to adequately develop COPC-specific scavenging coefficients. Therefore, vapors are assumed to be scavenged at the rate of the smallest particles with behavior in the atmosphere that is assumed to be influenced more by the molecular processes that affect vapors than by the physical processes that may dominate the behavior of larger particles (U.S. EPA 2004b).

To use the wet deposition option in AERMOD, users must input scavenging coefficients for each particle size and a file that has hourly precipitation data. For wet deposition of vapors, a scavenging coefficient for a $0.1\text{-}\mu\text{m}$ particle may be input to simulate wet scavenging of very small (molecular) particles.

Research on sulfate and nitrate data has shown that frozen precipitation scavenging coefficients are about one-third of the values of liquid precipitation (Scire, Strimaitis, and Yamartino 1990; Witby 1978).

3.5.7 REceptor Pathway – RE

The REceptor pathway identifies sets or arrays of receptor grid nodes identified by UTM coordinates for which AERMOD generates estimates of air parameters including air concentration, dry and wet deposition, and total deposition.

The following is an example of the REceptor pathway for discrete receptor grid nodes at 500-meter spacing and including terrain elevations (in meters):

```
RE STARTING
ELEVUNIT METERS
DISCCART 630000. 565000. 352.
DISCCART 630500. 565000. 365.
DISCCART 631000. 565000. 402.
DISCCART 635000. 570000. 387.
RE FINISHED
```

Air modeling for air toxic ecological risk assessment should include, at a minimum, an array of receptor grid nodes covering the area within 10 kilometers of the facility with the origin at the centroid of a polygon formed by the locations of the stack emission sources. This receptor grid node array should consist of a Cartesian grid with grid nodes spaced 100 meters apart extending from the centroid of the emission sources out to 3 kilometers from the centroid. For the distances from 3 kilometers out to 10 kilometers, the receptor grid node spacing can be increased to 500 meters. The single grid node array contains both grid node spacings. This same receptor grid node array is included in the REceptor pathway for all AERMOD runs for all years of meteorological data and for all emission sources.

The 1:250,000 scale DEM digital data are available for download free of charge from the following Internet site:

Worldwide Web: <http://www.WebGIS.com>

In addition to the receptor grid node array evaluated for each facility out to 10 kilometers, other grid node arrays may be considered for evaluation of water bodies and their watersheds, ecosystems and special ecological habitats located beyond 10 kilometers.

3.5.8 MEteorological Pathway – ME

The file containing meteorological data is specified in the MEeteorological pathway. The modeler may specify a single year of meteorological data in each AERMOD run, or combine the total period of meteorological data into a single meteorological file for processing by AERMOD in a single 5-year run.

Details of specifying the meteorological data file are provide in the AERMOD and AERMET User's Guide. Each year within the file must be complete with a full year of data (365 days, or 366 days for leap years). The anemometer height must be verified for the surface station from Local Climate Data Summary records, or other sources, such as the state climatologist office.

3.5.9 OUtput Pathway – OU

AERMOD provides numerous output file options in addition to the results in the output summary file specified in receptor tables (RECTABLE). The plotfile is most useful for facilitating post-processing of the air parameter values in the model output. The plotfile lists the x and y coordinates and the concentration or deposition rate values for each averaging period in a format that can be easily pulled into a post-processing program (or spreadsheet). Note that the AERMOD generated >plotfile is not the same format as the AERMOD generated >post= file. The procedures presented here use the plotfile, not the post file.

Following is an example OUtput file specification for single-year run of 1-hour and annual average plotfiles:

```
OU STARTING
RECTABLE ALLAVE FIRST
PLOTFILE 1 ALL FIRST S0000001.plp
PLOTFILE PERIOD ALL S0000001.pap
OU FINISHED
```

For ecological risk assessments, the 1-hour average plotfile is not needed. If the modeler has directed in the AERMOD control pathway for 1-hour averages to be computed for use in a human health acute risk assessment, then the 1-hour average plotfile also should be specified (U.S. EPA 1998b). The second line in the example directs AERMOD to create a table of values for each receptor grid node for all averaging periods in the model run (annual and optionally 1-hour). The third line directs AERMOD to create a separate plotfile of the 1-hour average results, if desired by the modeler. The fourth line directs AERMOD to create another separate plotfile of the annual average results for all sources in the run for each receptor grid node.

3.6 AERMOD Model Execution

Model execution time should be considered for each analysis. A complete air modeling run including air concentration, wet and dry deposition, and plume depletion may require 10 times the run time for the same source and receptor grid nodes for air concentration only.

3.7 Use of Modeled Output

The AERMOD modeled output (air concentrations and deposition rates) is provided on a unit emission rate (1.0 g/s) basis from the combustion unit or emission source, and are not COPC-specific. Table 5 presents the unitized output of concentration and deposition rates. Unitized air modeled output is used in combination with chemical specific emissions rates in the equations to calculate chemical specific results. Procedures for calculating chemical-specific concentration in AERMOD are discussed in detail in the AERMOD Users Guide (U.S. EPA 2004b).

3.7.1 Unit Rate Output vs. COPC-Specific Output

The relationship between the unit emission rate and the unit air parameter values (air concentrations and deposition rates) is linear. Similarly, the relationship between the COPC-specific emission rate (Q) and the COPC-specific air parameter values (air concentrations and deposition rates) would also be linear if the COPC-specific emission rate was used in the air model. This relationship can be expressed by the following equation:

$$\frac{\text{COPC-Specific Air Concentration}}{\text{COPC-Specific Emissions Rate}} = \frac{\text{Modeled Output Air Concentration}}{\text{Unit Emissions Rate}}$$

Table 5. Air Parameters from AERMOD Modeled Output.

Air Parameter	Description	Units
<i>Cyv</i>	Unitized yearly average air concentration from vapor phase	$\mu\text{g-s/g-m}^3$
<i>Cyp</i>	Unitized yearly average air concentration from particle phase	$\mu\text{g-s/g-m}^3$
<i>Dyvw</i>	Unitized yearly average wet deposition from vapor phase	$\text{s/m}^2\text{-yr}$
<i>Dydp</i>	Unitized yearly average dry deposition from particle phase	$\text{s/m}^2\text{-yr}$
<i>Dywp</i>	Unitized yearly average wet deposition from particle phase	$\text{s/m}^2\text{-yr}$
<i>Cyww</i>	Unitized yearly (water body or watershed) average air concentration from vapor phase	$\mu\text{g-s/g-m}^3$
<i>Dywww</i>	Unitized yearly (water body or watershed) average wet deposition from vapor phase	$\text{s/m}^2\text{-yr}$
<i>Dytwp</i>	Unitized yearly (water body or watershed) average total (wet and dry) deposition from particle phase	$\text{s/m}^2\text{-yr}$

Use of this equation requires that three of the variables be known. The modeled output air concentration (or deposition rate) is provided by the air model, the unit emission is 1.0 g/s, and the COPC-specific emission rate; which is obtained directly from stack or source test data.

3.7.2 Determination of the COPC-Specific Emission Rate (*Q*)

The COPC-specific emission rate can usually be determined with information obtained directly from the trial burn report. The COPC-specific emission rate from the stack is a function of the stack gas flow rate and the stack gas concentration of each COPC; which can be calculated from the following equation:

$$Q = SGF \frac{SGC \cdot CFO_2}{10^6}$$

where:

- Q = COPC-specific emission rate (g/s)
 SGF = Stack gas flow rate at dry standard conditions (dscm/s)
 SGC = COPC stack gas concentration at 7 percent O_2 as measured in the trial burn ($\mu\text{g}/\text{dscm}$)
 CFO_2 = Correction factor for conversion to actual stack gas concentration O_2 (unitless)
 1×10^6 = Unit conversion factor ($\mu\text{g}/\text{g}$)

It is sometimes necessary to derive the COPC-specific emission rate from surrogate data, such as for a new facility that has not yet been constructed and trial burned.

3.7.3 Converting Unit Output to COPC-Specific Output

Once the three of the four variables in the equation in section 3.7.2 are known, the COPC-specific air concentrations and deposition rates can be obtained directly by multiplication, as follows:

$$\text{COPC-Specific Air Concentration} = \frac{\text{Modeled Output Air Concentration} \times \text{COPC Specific Emissions Rate}}{\text{Unit Emissions Rate}}$$

For example, if COPC A is emitted at a rate of 0.25 g/s, and the AERMOD modeled concentration at a specific receptor grid node is 0.2 $\mu\text{g}/\text{m}^3$ per the 1.0 g/s unit emission rate, the concentration of COPC A at that receptor grid node is 0.05 $\mu\text{g}/\text{m}^3$ (0.25 multiplied by 0.2). Deposition is calculated similarly, proportional to the emission rate of each COPC.

3.7.4 Output from the AERMOD Model

The AERMOD output is structured and the risk assessor must understand how to read the output in order to ensure accurate use of modeled output in the risk assessment. The output from each AERMOD model run is written to two separate file formats. The output file is specified by name at run time in the execution command. Typical command line nomenclature is:

```
AERMOD inputfile.INP outputfile.OUT
```

where:

- AERMOD: specifies execution of the AERMOD model
 inputfile.INP: is the input file name selected by the modeler
 outputfile.OUT: is the output file name selected by the modeler, typically the same as the input file name

For example, the following AERMOD input line would run the input file (PART84.INP) created by the modeler for particulate emissions using 1984 meteorological data. The output file (PART84.OUT) from the run will automatically be written by AERMOD during model execution.

```
AERMOD PART84.INP PART84.OUT
```

The total deposition is the sum of the dry and wet components of deposition. The single-year values at each receptor grid node being evaluated must be averaged to a 5-year value. The 5-year averaged values at the receptor grid nodes selected for evaluation in the risk assessment, are used in the estimating media concentration equations. This file is usually imported into a post-processing program (or spreadsheet) before entry into the risk assessment computations.

Similar plotfiles are produced for the particle-bound and vapor phase runs. The output for the vapor phase runs will be average concentration and wet deposition. The output for the particle and particle-bound phase runs will be average concentration, dry deposition, wet deposition and total deposition. Again, the 1-year values at each receptor grid node must be averaged to a 5-year value at each node unless a single five-year AERMOD run using a combined meteorological file is used.

3.7.5 Use of Model Output in Estimating Media Equations

The selection of which air modeled air parameter values (air concentrations and deposition rates) to use in the estimating media concentration equations is based on the partitioning theory presented below.

3.7.6 Vapor Phase COPCs

AERMOD output generated from vapor phase air modeling runs are vapor phase air concentrations (unitized C_{yv} and unitized $C_{y\omega v}$) and wet vapor depositions (unitized $D_{y\omega v}$ and unitized $D_{y\omega\omega v}$) for organic COPCs at receptor grid nodes based on the unit emission rate. These values are used in the estimating media concentration equations for all COPC organics except the polycyclic aromatic hydrocarbons dibenzo(a,h)anthracene and indeno(1,2,3-cd)pyrene, which have vapor phase fractions, F_v , less than five percent. The air concentration (unitized C_{yv}) and wet vapor deposition (unitized $D_{y\omega v}$) from the vapor phase run is also used in the estimating media concentration equations for mercury. Values for these COPCs are selected from the vapor phase run because the mass of the COPC emitted by the combustion unit is assumed to have either all or a portion of its mass in the vapor phase.

3.7.7 Particle Phase COPCs

AERMOD output generated from particle phase air modeling runs are air concentration (unitized C_{yp}), dry deposition (unitized D_{ydp}), wet deposition

(unitized $Dywp$), and combined deposition (unitized $Dytwp$) for inorganics and relatively non-volatile organic COPCs at receptor grid nodes based on the unit emission rate. These values are used in the estimating media concentration equations for all COPC inorganics (except mercury) and polycyclic aromatic hydrocarbons with fraction of vapor phase, Fv , less than 0.05, which is the case, for example, of dibenzo(a,h)anthracene and indeno(1,2,3-cd)pyrene. Values for inorganic and relatively non-volatile COPCs are selected from the particle phase run because the mass of the COPC emitted by the combustion unit is assumed to have all of its mass in the particulate phase, apportioned across the particle size distribution based on mass weighting.

3.7.8 Particle-Bound COPCs

AERMOD output generated from particle-bound air modeling runs are air concentration (unitized Cyp), dry deposition (unitized $Dydp$), wet deposition (unitized $Dywp$), and combined deposition (unitized $Dytwp$) for organic COPCs and mercury at receptor grid nodes based on the unit emission rate. These values are used in the estimating media concentration equations for all COPC organics and mercury to account for a portion of the vapor condensed onto the surface of particulates. Values for these COPCs are selected from the particle-bound run because the mass of the COPC emitted by the combustion unit is assumed to have a portion of its mass condensed on particulates, apportioned across the particle size distribution based on surface area weighting.

3.8 Modeling of Fugitive Emissions

Fugitive emissions should be represented in the AERMOD input file SOURCE pathway as either area or volume source types. Fugitive emissions of volatile organics are modeled only in the vapor phase. Fugitive emissions of ash are modeled only in the particle and particle-bound phases, but not vapor phase. The methods in the AERMOD User's Guide should be followed in defining the input parameters to represent the fugitive source.

The following example provided in Figure 4 is for organic fugitive emissions modeled as a volume source type. For a facility, which may have two stack emission sources (B1, B2) and two fugitive emission sources (areas F1, F2); a total of four runs for each year (or 5-year combined file) of meteorological data is required. One run is required for each of the two stacks as point sources. One run is required for each of the two fugitive areas as volume sources (Note: modeler may alternatively model as an area source). Since the emissions are fugitive volatile organics, only the vapor phase is modeled. The vertical extent of the pipes, valves, tanks and flanges associated with each fugitive emission area is 15 feet (about 5 meters) above plant elevation. To define the sources for input to AERMOD, the release height is specified as 2.5 meters (of vertical extent of fugitive emissions). The initial vertical dimension is specified as 1.16 meters

(vertical extent of 5 meters divided by 4.3 as described in the AERMOD User's Guide).

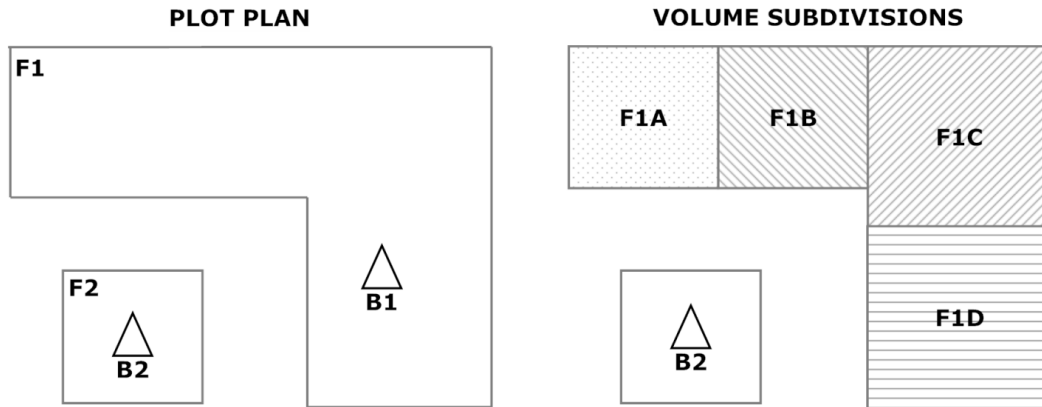


Figure 4. Example Fugitive Area Allocation.

The initial horizontal dimension is the side length of the square fugitive area (footprint) divided by 4.3. If fugitive area F2 has a measured side of 30 meters, the initial horizontal dimension is 6.98 (30 meters divided by 4.3). For fugitive area F1, the area on the plot plan must be subdivided (volume source) to create square areas for input to AERMOD. The four areas depicted represent subdivision into square areas. The resulting four square areas are input into a single AERMOD run for Fugitive source F1 as four separate volume sources (F1A, F1B, F1C, F1D). The initial horizontal dimension for each volume source is the side of the square divided by 4.3.

It is very important to allocate proportionately the unit emission rate (1.0 gram per second) among the subdivided areas. For example, if the areas of the subdivided squares in Figure 4 results in F1A equal to F1B each with 1/8th the total area, the proportion of the unit emissions allocated to each of these volume sources is 0.125 grams per second. The remaining two areas are each 3/8ths of the total area of fugitive F1, so that 0.375 grams per second is specified for the emission rate from each source. The total emissions for the four volume sources sum to the unit emission rate for the F1 fugitive source ($0.125 + 0.125 + 0.375 + 0.375 = 1.0$ g/s). By specifying all sources to be included in the model results from AERMOD (SO SRCGROUP ALL), the AERMOD model will appropriately combine all four volume source subdivisions of fugitive source F1 into combined impact results for fugitive source F1. The resulting air parameter values in the plotfiles may be used directly in the risk assessment equations, the same as if a stack emission were modeled as a single point source. The initial vertical dimension is defined the same as F2, using the vertical extent of 5 meters divided by 4.3 and a release height of 2.5 meters (vertical extent). For volume sources, the location is specified by the x and y coordinates of the center of each square area.

4 Estimation of COPC Concentrations in Media

The air dispersion model output of unitized air parameters (air concentrations and deposition rates) are provided on a unit emission (1.0 g/s) basis from the combustion unit, and are not yet COPC-specific. The estimating media concentration equations, presented in this section, accept these unitized output values directly to calculate COPC-specific media concentrations for use in characterizing ecological risk.

This section presents the estimating media concentration equations used for calculating, from the appropriate AERMOD unitized model output and COPC-specific emission rates, COPC-specific media concentrations in soil, surface water, and sediment. Determining COPC media concentrations is relevant to estimating risks to potentially impacted ecosystems through exposure of ecological receptors to COPCs in air (plant only), soil, surface water, and sediment. This section also includes equations for calculating COPC-specific concentrations in terrestrial plants resulting from foliar and root uptake.

4.1 Calculation of COPC Concentrations in Soil

COPC concentrations in soil are calculated by summing the particle and vapor phase deposition of COPCs to the soil. Wet and dry deposition of particles and vapors are considered, with dry deposition of vapors calculated from the vapor air concentration and the dry deposition velocity. Soil concentrations may require many years to reach steady state. As a result, the equations used to calculate the soil concentration over the period of deposition were derived by integrating the instantaneous soil concentration equation over the period of deposition. The highest 1-year annual average COPC concentration in soil should be used as the soil concentration for estimating ecological risk, which would typically occur at the end of the time period of combustion.

Following deposition, the calculation of soil concentration also considers losses of COPCs by several mechanisms, including leaching, erosion, runoff, degradation (biotic and abiotic), and volatilization. All of these loss mechanisms may lower the soil concentration if included in the soil concentration calculation. Soil conditions such as pH, structure, organic matter content, and moisture content can also affect the distribution and mobility of COPCs in soil.

COPCs may also be physically incorporated into the upper layers of soil through tilling. The concentration in the top 20 centimeters of soil should be computed for estimating a COPC concentration in soils that are physically disturbed or tilled. The COPC concentration in the top 1-centimeter of soil should be computed for estimating a COPC concentration in soils that are not tilled.

4.1.1 Calculating Highest Annual Average COPC Concentration in Soil

The following equation should be used for calculating the highest average annual COPC soil concentration.

Equations for Calculating Highest Annual Average COPC Concentration in Soil (C_s)

$$C_s = \frac{[1 - \exp(-k_s \cdot tD)]}{k_s}$$

where:

- C_s = COPC concentration in soil (mg COPC/kg soil)
- D_s = Deposition term (mg/kg-yr)
- k_s = COPC soil loss constant due to all processes (yr^{-1})
- tD = Total time period over which deposition occurs (time period of combustion) (yr)

This equation calculates the highest annual average soil concentration, which is typically expected to occur at the end of the time period of deposition (U.S. EPA 1994k; 1998c). Derivation of the equation is presented in U.S. EPA (1998c).

4.1.2 Calculating the COPC Soil Loss Constant (k_s)

COPCs may be lost from the soil by several processes that may or may not occur simultaneously. In the equation in section 4.1.1, the soil loss constant, k_s , expresses the rate at which a COPC is lost from soil (U.S. EPA 1998c). The constant k_s is determined by using the soil's physical, chemical, and biological characteristics to consider the losses resulting from:

1. Biotic and abiotic degradation
2. Erosion
3. Surface runoff
4. Leaching
5. Volatilization.

The risk assessor should use the following equation to compute the soil loss constant.

Equation for Calculating COPC Soil Loss Constant (k_s)

$$k_s = k_{sg} + k_{se} + k_{sr} + k_{sl} + k_{sv}$$

where:

- k_s = COPC soil loss constant due to all processes (yr^{-1})
- k_{sg} = COPC loss constant due to degradation (yr^{-1})
- k_{se} = COPC loss constant due to erosion (yr^{-1})
- k_{sr} = COPC loss constant due to runoff (yr^{-1})

$$\begin{aligned}
 k_{sl} &= \text{COPC loss constant due to leaching (yr}^{-1}\text{)} \\
 k_{sv} &= \text{COPC loss constant due to volatilization (yr}^{-1}\text{)}
 \end{aligned}$$

This equation assumes that COPC loss can be defined by using first-order reaction kinetics. At low concentrations, a first-order loss constant may be adequate to describe the loss of the COPC from soil (U.S. EPA 1990a).

The following subsections discuss issues associated with the calculation of the k_{sl} , k_{se} , k_{sr} , k_{sg} , and k_{sv} variables.

4.1.2.1 COPC Loss Constant Due to Biotic and Abiotic Degradation

Soil losses resulting from biotic and abiotic degradation (k_{sg}) are determined empirically from field studies and should be addressed in the literature (U.S. EPA 1990a). Lyman et al. (1990) states that degradation rates can be assumed to follow first order kinetics in a homogenous media. Therefore, the half-life of a compound can be related to the degradation rate constant. Ideally, k_{sg} is the sum of all biotic and abiotic rate constants in the soil media. Therefore, if the half-life of a compound (for all of the mechanisms of transformation) is known, the degradation rate can be calculated. However, literature sources do not provide sufficient data for all such mechanisms, especially for soil.

**Recommended Values for:
COPC Loss Constant Due to Biotic and Abiotic Degradation (k_{sg})**

COPC-Specific
(See the HHRAP Companion Database)

The rate of biological degradation in soils depends on the concentration and activity of the microbial populations in the soil, the soil conditions, and the COPC concentration (Jury and Valentine 1986). First-order loss rates often fail to account for the high variability of these variables in a single soil system. However, the use of simple rate expressions may be appropriate at low chemical concentrations (e.g., nanogram per kilogram soil) at which a first-order dependence on chemical concentration may be reasonable. The rate of biological degradation is COPC-specific, depending on the complexity of the COPC and the usefulness of the COPC to the microorganisms. Some substrates, rather than being used by the organisms as a nutrient or energy source, are simply degraded with other similar COPCs, which can be further utilized. Environmental and COPC-specific factors that may limit the biodegradation of COPCs in the soil environment (Valentine and Schnoor 1986) include:

1. Availability of the COPC
2. Nutrient limitations
3. Toxicity of the COPC
4. Inactivation or nonexistence of enzymes capable of degrading the COPC.

Chemical degradation of organic compounds can be a significant mechanism for removal of COPCs in soil (U.S. EPA 1990a). Hydrolysis and oxidation-reduction reactions are the primary chemical transformation processes occurring in the upper layers of soils (Valentine 1986). General rate expressions describing the transformation of some COPCs by all non-biological processes are available, and these expressions are helpful when division into component reactions is not possible.

4.1.2.2 COPC Loss Constant Due to Soil Erosion (*kse*)

U.S. EPA (1998) recommended the following equation to calculate the constant for soil loss resulting from erosion (*kse*).

$$kse = \frac{0.1 \cdot X_e \cdot SD \cdot ER}{BD \cdot Z_s} \cdot \frac{Kd_s \cdot BD}{\theta_{sw} + (Kd_s \cdot BD)}$$

where:

<i>kse</i>	=	COPC soil loss constant due to soil erosion
0.1	=	Units conversion factor (1,000 g/kg/10,000 cm ² -m ²)
<i>X_e</i>	=	Unit soil loss (kg/m ² -yr)
<i>SD</i>	=	Sediment delivery ratio (unitless)
<i>ER</i>	=	Soil enrichment ratio (unitless)
<i>Kd_s</i>	=	Soil-water partition coefficient (mL/g)
<i>BD</i>	=	Soil bulk density (g/cm ³ soil)
<i>Z_s</i>	=	Soil mixing zone depth (cm)
<i>θ_{sw}</i>	=	Soil volumetric water content (mL/cm ³ soil)

Unit soil loss (*X_e*) is calculated by using the Universal Soil Loss Equation (USLE), as described in this Chapter.

The risk assessor should use the following constant for the loss of soil resulting from erosion (*kse*) - set equal to zero.

**Recommended Value for:
COPC Loss Constant Due to Erosion (*kse*)**

0 (zero)

For additional information on addressing *kse*, consult the methodologies described in U.S. EPA document, *Methodology for Assessing Health Risks Associated with Multiple Exposure Pathways to Combustor Emissions* (U.S. EPA 1998).

4.1.2.3 COPC Loss Constant Due to Runoff (*ksr*)

USEPA recommends the following equation (USEPA 1998c) to calculate the constant for the loss of soil resulting from surface runoff (*ksr*).

Equation for Calculating COPC Loss Constant Due to Runoff (*ksr*)

$$ksr = \frac{RO}{\theta_{sw} \cdot Z_s} \cdot \frac{1.0}{1.0 + (Kd_s \cdot \frac{BD}{\theta_{sw}})}$$

where:

- ksr* = COPC loss constant due to runoff (yr⁻¹)
- RO* = Average annual surface runoff from pervious areas (cm/yr)
- θ_{sw} = Soil volumetric water content (mL/cm³ soil)
- Z_s* = Soil mixing zone depth (cm)
- Kd_s* = Soil-water partition coefficient (mL/g)
- BD* = Soil bulk density (g/cm³ soil)

4.1.2.4 COPC Loss Constant Due to Leaching (*ksl*)

Consistent with U.S. EPA guidance (1994k) and U.S. EPA (1998c), the following equation should be used to calculate the COPC loss constant due to leaching (*ksl*).

Equation for Calculating COPC Loss Constant Due to Leaching (*ksl*)

$$ksl = \frac{P + I - RO - E_v}{\theta_{sw} \cdot Z_s \cdot [1.0 + (Kd_s \cdot \frac{BD}{\theta_{sw}})]}$$

where:

- ksl* = COPC loss constant due to leaching (yr⁻¹)
- P* = Average annual precipitation (cm/yr)
- I* = Average annual irrigation (cm/yr)
- RO* = Average annual surface runoff from pervious areas (cm/yr)
- E_v* = Average annual evapotranspiration (cm/yr)
- θ_{sw} = Soil volumetric water content (mL/cm³ soil)
- Z_s* = Soil mixing zone depth (cm)
- Kd_s* = Soil-water partition coefficient (mL/g)
- BD* = Soil bulk density (g/cm³ soil)

The average annual volume of water (*P + I - RO - E_v*) available to generate leachate is the mass balance of all water inputs and outputs from the area under consideration.

4.1.2.5 COPC Loss Constant Due to Volatilization (*ksv*)

Semi-volatile and volatile COPCs emitted in high concentrations may become adsorbed to soil particles and exhibit volatilization losses from soil. The loss of a

COPC from the soil by volatilization depends on the rate of movement of the COPC to the soil surface, the chemical vapor concentration at the soil surface, and the rate at which vapor is carried away by the atmosphere (Jury 1986).

The soil loss constant due to volatilization (k_{sv}) is based on gas equilibrium coefficients and gas phase mass transfer. The first order decay constant, k_{sv} , is obtained by adapting the Hwang and Falco equation for soil vapor phase diffusion (Hwang and Falco 1986).

Equation for Calculating COPC Loss Constant Due to Volatilization (k_{sv})

$$k_{sv} = \left(\frac{3.1536 \cdot 10^7 \cdot H}{Z_s \cdot Kd_s \cdot R \cdot T_a \cdot BD} \right) \cdot \left(\frac{D_a}{Z_s} \right) \cdot \left[1.0 - \left(\frac{BD}{\rho_{soil}} \right) - \theta_{sw} \right]$$

where:

k_{sv}	=	COPC loss constant due to volatilization (yr^{-1})
$3.1536 \cdot 10^7$	=	Units conversion factor (s/yr)
H	=	Henry's Law constant ($\text{atm} \cdot \text{m}^3 / \text{mol}$)
Z_s	=	Soil mixing zone depth (cm)
Kd_s	=	Soil-water partition coefficient (mL/g)
R	=	Universal gas constant ($\text{atm} \cdot \text{m}^3 / \text{mol} \cdot \text{K}$)
T_a	=	Ambient air temperature (K) = 298.1 K
BD	=	Soil bulk density (g / cm^3 soil)
D_a	=	Diffusivity of COPC in air (cm^2 / s)
θ_{sw}	=	Soil volumetric water content (mL / cm^3 soil)
ρ_{soil}	=	Solids particle density (g / cm^3)

In cases where high concentrations of volatile organic compounds are expected to be present in the soil, consult the methodologies described in U.S. EPA document, *Methodology for Assessing Health Risks Associated with Multiple Exposure Pathways to Combustor Emissions* (U.S. EPA 1998).

4.1.3 Deposition Term (D_s)

The use of the following equation to calculate the deposition term D_s is consistent with earlier U.S. EPA guidance (1994k) and U.S. EPA (1998c).

**Recommended Equation for Calculating:
Deposition Term (D_s)**

$$D_s = \left(\frac{100 \cdot Q}{Z_s \cdot BD} \right) \cdot [F_v \cdot (Dydv + Dywv) + (Dydp + Dywp) \cdot (1 - F_v)]$$

where:

D_s	=	Deposition term (mg COPC/kg soil-yr)
100	=	Units conversion factor ($\text{m}^2 \cdot \text{mg} / \text{cm}^2 \cdot \text{kg}$)

Q	=	COPC-specific emission rate (g/s)
Z_s	=	Soil mixing zone depth (cm)
BD	=	Soil bulk density (g/cm ³ soil)
F_v	=	Fraction of COPC air concentration in vapor phase (unitless)
0.3153	=	Units conversion factor (m-g-s/cm-μg-yr)
V_{dv}	=	Dry deposition velocity (cm/s)
C_{yv}	=	Unitized yearly average air concentration from vapor phase (μg-s/g-m ³)
Dy_{wv}	=	Unitized yearly average wet deposition from vapor phase (s/m ² year)
Dy_{dp}	=	Unitized yearly average dry deposition from particle phase (s/m ² year)
Dy_{wp}	=	Unitized yearly average wet deposition from particle phase (s/m ² year)

4.1.4 Site-Specific Parameters for Calculating Soil Concentration

As discussed in the previous sections, calculating the COPC concentration in soil (C_s) requires some site-specific parameter values, which must be calculated or derived from available literature or site-specific data. These site-specific parameters include the following:

1. Soil mixing zone depth (Z_s)
2. Soil bulk density (BD)
3. Available water ($P + I - RO - E_v$)
4. Soil volumetric water content (θ_{sw})

4.1.5 Soil Mixing Zone Depth (Z_s)

When exposures to COPCs in soils are modeled, the depth of contamination is important in calculating the appropriate soil concentration. Due to leaching and physical disturbance (e.g., tilling) COPCs may migrate deeper in the soil in for some areas. Therefore, the value for the depth of soil contamination, or soil mixing zone depth (Z_s), used in modeling ecological risk should be considered specific to tilled (e.g., large plowed field) or untilled soil areas.

U.S. EPA risk assessment guidance (1990a) estimates that areas under consideration are tilled the soil mixing zone depth is about 10 to 20 centimeters depending on local conditions and the equipment used. If soil is not moved, COPCs are assumed to be retained in the shallower, upper soil layer, with a default value of 1 centimeter. The following are default values for the soil mixing zone depth (Z_s).

**Recommended Values for:
Soil Mixing Zone Depth (Z_s)**

1 cm - untilled
20 cm - tilled

4.1.6 Soil Bulk Density (BD)

BD is the ratio of the mass of soil to its total volume. This variable is affected by the soil structure, type, and moisture content (Hillel 1980). The following is the default value for the soil dry bulk density (BD).

Recommended Value for: Soil Dry Bulk Density (BD)

1.50 g/cm ³ soil

For determination of actual field values specific to a specified location at a site, U.S. EPA (1994k) recommended that wet soil bulk density be determined by weighing a thin-walled, tube soil sample (e.g., a Shelby tube) of known volume and subtracting the tube weight (ASTM Method D2937). Moisture content can then be calculated (ASTM Method 2216) to convert wet soil bulk density to dry soil bulk density.

4.1.7 Available Water ($P + I - RO - E_v$)

The average annual volume of water available ($P + I - RO - E_v$) for generating leachate is the mass balance of all water inputs and outputs from the area under consideration. A wide range of values for these variables may apply in the various U.S. EPA regions.

The average annual precipitation (P), irrigation (I), runoff (RO), and evapotranspiration (E_v) rates and other climatological data may be obtained from either data recorded on site or from the Station Climatic Summary for a nearby airport.

4.1.8 Soil Volumetric Water Content (θ_{sw})

The soil volumetric water content θ_{sw} depends on the available water and the soil structure. A wide range of values for these variables may apply in the various U.S. EPA regions. The following is the default value for θ_{sw} .

Recommended Value for: Soil Volumetric Water Content (θ_{sw})
--

0.2 ml/cm ³ soil

4.2 Calculation of COPC Concentrations in Surface Water and Sediments

COPC concentrations in surface water and sediments are calculated for all water bodies selected for evaluation in the risk assessment. Mechanisms considered for

determination of COPC loading of the water column are illustrated in Figure 5 and Figure 6, which include:

1. Direct deposition,
2. Runoff from impervious surfaces within the watershed
3. Runoff from pervious surfaces within the watershed
4. Soil erosion over the total watershed
5. Direct diffusion of vapor phase COPCs into the surface water
6. Internal transformation of compounds chemically or biologically.

Other potential mechanisms may require consideration on a case-by-case basis (e.g., tidal influences); however, contributions from other potential mechanisms are assumed to be negligible in comparison with those being evaluated.

The USLE and a sediment delivery ratio are used to estimate the rate of soil erosion from the watershed. To evaluate the COPC loading to a water body from its associated watershed, the COPC concentration in watershed soils should be calculated.

Surface water concentration algorithms include a sediment mass balance, in which the amount of sediment assumed to be buried and lost from the water body is equal to the difference between the amount of soil introduced to the water body by erosion and the amount of suspended solids lost in downstream flow. As a result, the assumptions are made that sediments do not accumulate in the water body over time, and equilibrium is maintained between the surficial layer of sediments and the water column. The total water column COPC concentration is the sum of the COPC concentration dissolved in water and the COPC concentration associated with suspended solids. Partitioning between water and sediment varies with the COPC. The total concentration of each COPC is partitioned between the sediment and the water column.

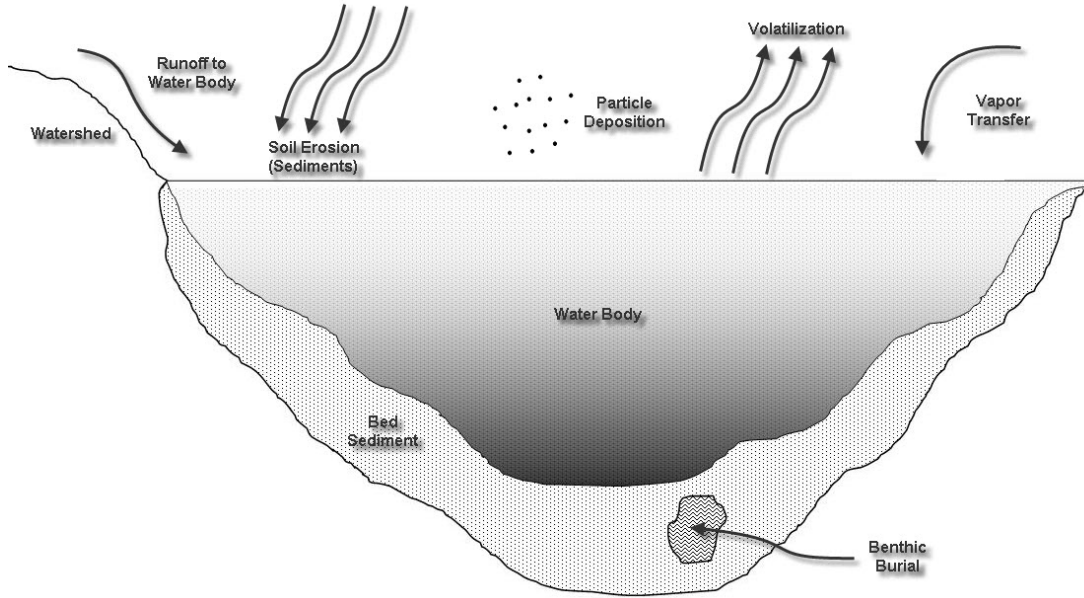


Figure 5. Schematic COPC Loading to Water Body Column.

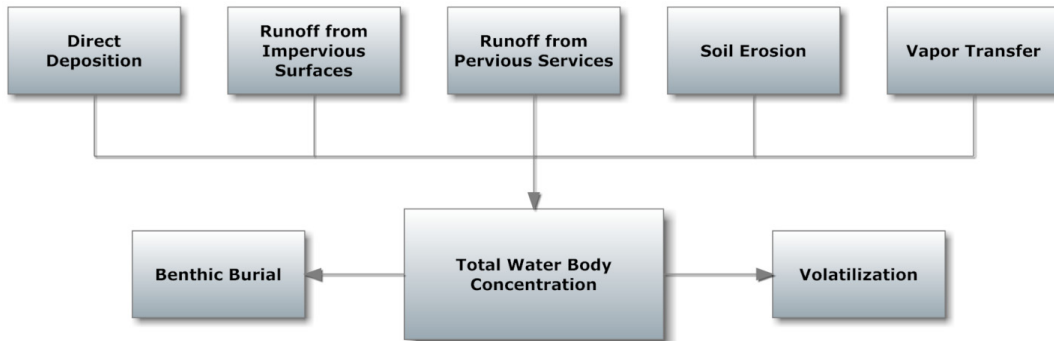


Figure 6. Flowchart COPC Loading to Water Body Column.

4.2.1 Total COPC Loading to a Water Body (L_T)

The risk assessor should use the following equation to calculate the total COPC load to a water body (L_T).

Equation for Calculating Total COPC Load to the Water Body (L_T)

$$L_T = L_{DEP} + L_{dif} + L_{RI} + L_R + L_E + L_I$$

where:

- L_T = Total COPC load to the water body (including deposition, runoff, and erosion) (g/yr)
- L_{DEP} = Total (wet and dry) particle phase and wet vapor phase COPC direct deposition load to water body (g/yr)

L_{dif}	=	Vapor phase COPC diffusion (dry deposition) load to water body (g/yr)
L_{RI}	=	Runoff load from impervious surfaces (g/yr)
L_R	=	Runoff load from pervious surfaces (g/yr)
L_E	=	Soil erosion load (g/yr)
L_I	=	Internal transfer (g/yr)

The default value for L_I , is set to zero, due to the limited data associated with the chemical or biological internal transfer of compounds into daughter products. However, if a permitting authority determines that site-specific conditions indicate calculation of internal transfer should be considered, see the methodologies described in U.S. EPA NCEA document, *Methodology for Assessing Health Risks Associated with Multiple Exposure Pathways to Combustor Emissions* (U.S EPA 1998).

4.2.2 Total (Wet and Dry) Particle Phase and Wet Vapor Phase Contaminant Direct Deposition Load to Water Body (L_{DEP})

The following equation is applied to calculate the load to the water body from the direct deposition of wet and dry particles and wet vapors onto the surface of the water body (L_{DEP}).

**Equation for Calculating:
Total Particle Phase and Wet Vapor Phase Direct Deposition Load to Water Body (L_{DEP})**

$$L_{DEP} = Q \cdot [F_v \cdot Dytwv + (1 - F_v) \cdot Dytwp] \cdot A_W$$

where:

L_{DEP}	=	Total (wet and dry) particle phase and wet vapor phase COPC direct deposition load to water body (g/yr)
Q	=	COPC emission rate (g/s)
F_v	=	Fraction of COPC air concentration in vapor phase (unitless)
$Dytwv$	=	Unitized yearly (water body and watershed) average wet deposition from vapor phase (s/m ² -yr)
$Dytwp$	=	Unitized yearly (water body and watershed) average total (wet and dry) deposition from vapor phase (s/m ² -yr)
A_W	=	Water body surface area (m ²)

4.2.3 Diffusion Load to Water Body (L_{dif})

The following equation is used to calculate the dry vapor phase COPC diffusion load to the water body (L_{dif}).

Vapor Phase COPC Diffusion (Dry Deposition) Load to Water Body (L_{dif})

$$L_{dif} = \frac{K_v \cdot Q \cdot F_v \cdot C_{ywwv} \cdot A_W \cdot 10^{-6}}{H \cdot R \cdot T_{wk}}$$

where:

L_{dif}	= Vapor phase COPC diffusion (dry deposition) load to water body (g/yr)
K_v	= Overall COPC transfer rate coefficient (m/yr)
Q	= COPC emission rate (g/s)
F_v	= Fraction of COPC air concentration in vapor phase (unitless)
C_{ywwv}	= Unitized yearly (water body and watershed) average air concentration from vapor phase ($\mu\text{g}\cdot\text{s}/\text{g}\cdot\text{m}^3$)
A_W	= Water body surface area (m^2)
10^{-6}	= Units conversion factor ($\text{g}/\mu\text{g}$)
H	= Henry's Law constant ($\text{atm}\cdot\text{m}^3/\text{mol}$)
R	= Universal gas constant ($\text{atm}\cdot\text{m}^3/\text{mol}\cdot\text{K}$)
T_{wk}	= Water body temperature (K)

The “overall COPC transfer rate coefficient” (K_v) is obtained from U.S. EPA guidance (1998c). Note that these references recommend a water body temperature (T_{wk}) of 298 K (or 25°C).

4.2.4 Runoff Load from Impervious Surfaces (L_{RI})

In some watershed soils, a fraction of the wet and dry deposition in the watershed will be to impervious surfaces. Dry deposition may accumulate and be washed off during rain events. USEPA guidance recommends (U.S. EPA 1994k and U.S. EPA 1998c) the use of the following equation to calculate impervious runoff load to a water body (L_{RI}).

Equation for Calculating Runoff Load from Impervious Surfaces (L_{RI})

$$L_{RI} = Q \cdot [F_v \cdot D_{ywwv} + (1.0 - F_v) \cdot D_{ytwp}] \cdot A_I$$

where:

L_{RI}	= Runoff load from impervious surfaces (g/yr)
Q	= COPC emission rate (g/s)
F_v	= Fraction of COPC air concentration in vapor phase (unitless)
D_{ywwv}	= Unitized yearly (water body and watershed) average wet deposition from vapor phase ($\text{s}/\text{m}^2\cdot\text{yr}$)
D_{ytwp}	= Unitized yearly (water body and watershed) average total (wet and dry) deposition from vapor phase ($\text{s}/\text{m}^2\cdot\text{yr}$)
A_I	= Impervious watershed area receiving COPC deposition (m^2)

Impervious watershed area receiving COPC deposition (A_I) is the portion of the total effective watershed area that is impervious to rainfall (i.e., roofs, driveways, streets, and parking lots) and drains to the water body.

4.2.5 Runoff Load from Pervious Surfaces (L_R)

U.S. EPA recommends (USEPA 1994k and USEPA 1998c) the use of Equation 3-14 to calculate the runoff dissolved COPC load to the water body from pervious soil surfaces in the watershed (L_R).

Equation for Calculating Runoff Load from Pervious Surfaces (L_R)

$$L_R = RO \cdot (A_L - A_I) \cdot \left(\frac{C_S \cdot BD}{(\theta_{SW} + Kd_S \cdot BD)} \right) \cdot 0.01$$

where:

L_R	=	Runoff load from pervious surfaces (g/yr)
RO	=	Average annual surface runoff from pervious areas (cm/yr)
A_L	=	Total watershed area receiving COPC deposition (m ²)
A_I	=	Impervious watershed area receiving COPC deposition (m ²)
C_S	=	COPC concentration in soil (in watershed soils) (mg COPC/kg soil)
BD	=	Soil bulk density (g soil/cm ³ soil)
θ_{sw}	=	Soil volumetric water content (mL water/cm ³ soil)
Kd_S	=	Soil-water partition coefficient (cm ³ water/g soil)
0.01	=	Units conversion factor (kg-cm ² /mg-m ²)

4.2.6 Soil Erosion Load (L_E)

U.S. EPA recommends (USEPA 1994k and USEPA 1998c) the following equation to calculate soil erosion load (L_E).

Equation for Calculating Soil Erosion Load (L_E)

$$L_E = X_e \cdot SD \cdot ER \cdot Kd_S (A_L - A_I) \cdot \left(\frac{C_S \cdot BD}{(\theta_{SW} + Kd_S \cdot BD)} \right) \cdot 0.001$$

where:

L_E	=	Soil erosion load (g/yr)
X_e	=	Unit soil loss (kg/m ² -yr)
A_L	=	Total watershed area (evaluated) receiving COPC deposition (m ²)
A_I	=	Impervious watershed area receiving COPC deposition (m ²)
SD	=	Sediment delivery ratio (watershed) (unitless)
ER	=	Soil enrichment ratio (unitless)
C_S	=	COPC concentration in soil (in watershed soils) (mg COPC/kg soil)
BD	=	Soil bulk density (g soil/cm ³ soil)
θ_{sw}	=	Soil volumetric water content (mL water/cm ³ soil)

$$Kd_s = \text{Soil-water partition coefficient (mL water/g soil)}$$

$$0.001 = \text{Units conversion factor (k-cm}^2\text{/mg-m}^2\text{)}$$

Unit soil loss (X_e) and watershed sediment delivery ratio (SD) are calculated as described in the following subsections.

4.2.7 Universal Soil Loss Equation - USLE

U.S. EPA recommends (USEPA 1994k and USEPA 1998c) the universal soil loss equation (USLE), be used to calculate the unit soil loss (X_e) specific to each watershed.

Equation for Calculating Unit Soil Loss (X_e)

$$X_e = RF \cdot K \cdot LS \cdot C \cdot PF \cdot \frac{907.18}{4047}$$

where:

$$X_e = \text{Unit soil loss (kg/m}^2\text{-yr)}$$

$$RF = \text{USLE rainfall (or erosivity) factor (yr}^{-1}\text{)}$$

$$K = \text{USLE erodibility factor (ton/acre)}$$

$$LS = \text{USLE length-slope factor (unitless)}$$

$$C = \text{USLE cover management factor (unitless)}$$

$$PF = \text{USLE supporting practice factor (unitless)}$$

$$907.18 = \text{Units conversion factor (kg/ton)}$$

$$4047 = \text{Units conversion factor (m}^2\text{/acre)}$$

The USLE RF variable, which represents the influence of precipitation on erosion, is derived from data on the frequency and intensity of storms. This value is typically derived on a storm-by-storm basis, but average annual values have been compiled (U.S. Department of Agriculture 1982). Information on determining site-specific values for variables used in calculating X_e is provided in U.S. Department of Agriculture (U.S. Department of Agriculture 1997) and U.S. EPA guidance (U.S. EPA 1985).

4.2.8 Sediment Delivery Ratio (SD)

U.S. EPA recommends (USEPA 1994k and USEPA 1998c) the use of the following equation to calculate sediment delivery ratio (SD).

Equation for Calculating Sediment Delivery Ratio (SD)

$$SD = a \cdot (A_L)^{-b}$$

where:

$$SD = \text{Sediment delivery ratio (watershed) (unitless)}$$

$$a = \text{Empirical intercept coefficient (unitless)}$$

- b = Empirical slope coefficient (unitless)
 A_L = Total watershed area (evaluated) receiving COPC deposition (m^2)

The sediment delivery ratio (SD) for a large land area, a watershed or part of a watershed, can be calculated, on the basis of the area of the watershed, by using an approach proposed by Vanoni (1975).

According to Vanoni (1975), sediment delivery ratios vary approximately with the -0.125 power of the drainage area. Therefore, the empirical slope coefficient is assumed to be equal to 0.125. An inspection of the data presented by Vanoni (1975) indicates that the empirical intercept coefficient varies with the size of the watershed.

A_L is the total watershed surface area affected by deposition that drains to the body of water. A watershed includes all of the land area that contributes water to a water body. In assigning values to the watershed surface area affected by deposition, consideration should be given to (1) the distance from the stack, (2) the location of the area affected by deposition fallout with respect to the water body, and (3) in the absence of any deposition considerations, watershed hydrology. Total sediment in a water body may have originated from watershed soils that are (or have the potential to be) both affected and unaffected by deposition of combustion emissions. If a combustor is depositing principally on a land area that feeds a tributary of a larger river system, consideration must be given to an "effective" area. An effective drainage area will almost always be less than the watershed.

4.2.9 Total Water Body COPC Concentration (C_{wtot})

U.S. EPA recommends (USEPA 1994k and USEPA 1998c) the use of the following equation to calculate total water body COPC concentration (C_{wtot}). The total water body concentration includes both the water column and the bed sediment.

Equation for Calculating Total Water Body COPC Concentration (C_{wtot})

$$C_{wtot} = \frac{L_T}{Vf_x \cdot f_{wc} + k_{wt} \cdot A_W \cdot (d_{wc} + d_{bs})}$$

where:

- C_{wtot} = Total water body COPC concentration (including water column and bed sediment) ($g\ COPC/m^3$ water body)
 L_T = Total COPC load to the water body (including deposition, runoff, and erosion) (g/yr)
 Vf_x = Average volumetric flow rate through water body (m^3/yr)
 f_{wc} = Fraction of total water body COPC concentration in the water column (unitless)

k_{wt}	=	Overall total water body COPC dissipation rate constant (yr ⁻¹)
A_W	=	Water body surface area (m ²)
d_{wc}	=	Depth of water column (m)
d_{bs}	=	Depth of upper benthic sediment layer (m)

The depth of the upper benthic layer (d_{bs}), which represents the portion of the bed that is in equilibrium with the water column, cannot be precisely specified; however, U.S. EPA (1998c) recommended values ranging from 0.01 to 0.05. U.S. EPA recommends (1998c) a default value of 0.03, which represents the midpoint of the specified range. Issues related to the remaining parameters are summarized in the following subsections.

4.2.10 Fraction of Total Water Body COPC Concentration in the Water Column (f_{wc}) and Benthic Sediment (f_{bs})

U.S. EPA recommends (1998c) the use of the following equations to calculate fraction of total water body COPC concentration in the water column (f_{wc}), and to calculate the fraction of total water body contaminant concentration in benthic sediment (f_{bs}).

Equation for Calculating Fraction of Total Water Body COPC Concentration in the Water Column (f_{wc}) and Benthic Sediment (f_{bs})

$$f_{wc} = \frac{(1 + Kd_{sw} \cdot TSS \cdot 10^{-6}) \cdot d_{wc} / d_z}{(1 + Kd_{sw} \cdot TSS \cdot 10^{-6}) + d_{wc} / d_z + (\theta_{bs} + Kd_{bs} \cdot C_{BS}) \cdot d_{bs} / d_z}$$

$$f_{bs} = 1 - f_{wc}$$

where:

f_{wc}	=	Fraction of total water body COPC concentration in the water column (unitless)
f_{bs}	=	Fraction of total water body COPC concentration in benthic sediment (unitless)
Kd_{sw}	=	Suspended sediments/surface water partition coefficient (L water/kg suspended sediment)
TSS	=	Total suspended solids concentration (mg/L)
1×10^{-6}	=	Units conversion factor (kg/mg)
d_z	=	Total water body depth (m)
θ_{bs}	=	Bed sediment porosity (L _{water} /L _{sediment})
Kd_{bs}	=	Bed sediment/sediment pore water partition coefficient (L water/kg bottom sediment)
BS	=	Benthic solids concentration (g/cm ³ [equivalent to kg/L])
d_{wc}	=	Depth of water column (m)
d_{bs}	=	Depth of upper benthic sediment layer (m)

The partition coefficient Kd_{sw} describes the partitioning of a contaminant between sorbing material, such as soil, surface water, suspended solids, and bed sediments.

U.S. EPA (1998c) recommends adding the depth of the water column to the depth of the upper benthic layer ($d_{wc} + d_{bs}$) to calculate the total water body depth (d_z).

U.S. EPA (1998c) recommends a default total suspended solids (*TSS*) concentration of 10 mg/L. Average annual values for *TSS* are generally expected to be in the range of 2 to 300 mg/L. If measured data is not available, or of unacceptable quality, a calculated *TSS* value can be obtained for non-flowing water bodies using:

$$TSS = \frac{X_e \cdot (A_L - A_I) \cdot SD \cdot 10^2}{Vf_x + DSS \cdot A_W}$$

where:

<i>TSS</i>	=	Total suspended solids concentration (mg/L)
X_e	=	Unit soil loss (kg/m ² -yr)
A_L	=	Total watershed area (evaluated) receiving COPC deposition (m ²)
A_I	=	Impervious watershed area receiving COPC deposition (m ²)
<i>SD</i>	=	Sediment delivery ratio (watershed) (unitless)
Vf_x	=	Average volumetric flow rate through water body (value should be 0 for quiescent lakes or ponds) (m ³ /yr)
D_{ss}	=	Suspended solids deposition rate (a default value of 1,825 for quiescent lakes or ponds) (m/yr)
A_W	=	Water body surface area (m ²)

The default value of 1,825 m/yr provided for D_{ss} is characteristic of Stoke's settling velocity for the intermediate (fine to medium) silt.

Bed sediment porosity (θ_{bs}) can be calculated from the benthic solids concentration by using the following equation (U.S. EPA 1998c):

$$\theta_{bs} = 1.0 - \frac{C_{BS}}{\rho_s}$$

where:

θ_{bs}	=	Bed sediment porosity (L _{water} /L _{sediment})
ρ_s	=	Bed sediment density (kg/L)
<i>BS</i>	=	Benthic solids concentration (kg/L)

The following default value for bed sediment porosity (θ_{bs}), which was adapted from U.S. EPA (1998c):

Recommended Value for Bed Sediment Porosity (θ_{bs})

$$\theta_{bs} = 0.6 L_{water} / L_{sediment}$$

(assuming $\rho_s = 2.65$ kg/L [bed sediment density] and $C_{BS} = 1$ kg/L [benthic sediment concentration])

Values for the benthic solids concentration (BS) and depth of upper benthic sediment layer (d_{bs}) range from 0.5 to 1.5 kg/L and 0.01 to 0.05 meters, respectively. However, consistent with earlier U.S. EPA guidance (1998c), 1 kg/L is a reasonable default for most applications of the benthic solids concentration (BS), and 0.03 meter is the default depth of the upper benthic layer (d_{bs}). The default depth of 0.03 meters is based on the midpoint of the range presented above.

4.2.11 Overall Total Water Body COPC Dissipation Rate Constant (k_{wt})

U.S. EPA recommends (1998c) the use of the following equation to calculate the overall dissipation rate of COPCs in surface water, resulting from volatilization and benthic burial.

Equation for Calculating Overall Total Water Body COPC Dissipation Rate Constant (k_{wt})

$$k_{wt} = f_{wc} \cdot k_v + f_{bs} \cdot k_b$$

where:

- k_{wt} = Overall total water body dissipation rate constant (yr^{-1})
- f_{wc} = Fraction of total water body COPC concentration in the water column (unitless)
- k_v = Water column volatilization rate constant (yr^{-1})
- f_{bs} = Fraction of total water body COPC concentration in benthic sediment (unitless)
- k_b = Benthic burial rate constant (yr^{-1})

The variables f_{wc} and f_{bs} are discussed in the previous section.

4.2.12 Water Column Volatilization Rate Constant (k_v)

U.S. EPA recommends (1998c) using Equation 3-23 to calculate water column volatilization rate constant.

Equation for Calculating Water Column Volatilization Rate Constant (k_v)

$$k_v = \frac{K_v}{d_z \cdot (1 + Kd_{sw} \cdot TSS \cdot 1 \times 10^{-6})}$$

where:

- k_v = Water column volatilization rate constant (yr^{-1})
- K_v = Overall COPC transfer rate coefficient (m/yr)
- d_z = Total water body depth (m)
- Kd_{sw} = Suspended sediments/surface water partition coefficient (L water/kg suspended sediments)
- TSS = Total suspended solids concentration (mg/L)
- 1×10^{-6} = Units conversion factor (kg/mg)

Total water body depth (d_z), suspended sediment and surface water partition coefficient (Kd_{sw}), and total suspended solids concentration (TSS), are previously described in this section. The overall transfer rate coefficient (K_v) is described in the following subsection.

4.2.13 Overall COPC Transfer Rate Coefficient (K_v)

Volatile organic chemicals can move between the water column and the overlying air. The overall transfer rate K_v , or conductivity, is determined by a two-layer resistance model that assumes that two stagnant films are bounded on either side by well-mixed compartments. Concentration differences serve as the driving force for the water layer diffusion. Pressure differences drive the diffusion for the air layer. From balance considerations, the same mass must pass through both films; the two resistances thereby combine in series, so that the conductivity is the reciprocal of the total resistance.

U.S. EPA recommends (1998c) the use of Equation 3-24 to calculate the overall transfer rate coefficient (K_v).

Equation for Calculating Overall COPC Transfer Rate Coefficient (K_v)

$$K_v = \left[K_L^{-1} + \left(K_G \cdot \frac{H}{R \cdot T_{wk}} \right)^{-1} \right]^{-1} \cdot \theta^{T_{wk} - 293}$$

where:

- K_v = Overall COPC transfer rate coefficient (m/yr)
- K_L = Liquid phase transfer coefficient (m/yr)
- K_G = Gas phase transfer coefficient (m/yr)
- H = Henry's Law constant ($\text{atm} \cdot \text{m}^3/\text{mol}$)
- R = Universal gas constant ($\text{atm} \cdot \text{m}^3/\text{mol} \cdot \text{K}$)
- T_{wk} = Water body temperature (K)
- θ = Temperature correction factor (unitless)

The value of the conductivity K_v depends on the intensity of turbulence in the water body and the overlying atmosphere. As Henry's Law constant increases, the conductivity tends to be increasingly influenced by the intensity of turbulence in water. Conversely, as Henry's Law constant decreases, the value of the

conductivity tends to be increasingly influenced by the intensity of atmospheric turbulence.

The liquid and gas phase transfer coefficients, K_L and K_G , respectively, vary with the type of water body.

The universal ideal gas constant, R , is $8.205 \text{ H } 10^{-5} \text{ atm}\cdot\text{m}^3/\text{mol}\cdot\text{K}$, at 20C. The temperature correction factor (θ), which is equal to 1.026, is used to adjust for the actual water temperature. Volatilization is assumed to occur much less readily in lakes and reservoirs than in moving water bodies.

4.2.14 Liquid Phase Transfer Coefficient (K_L)

Estimations of the liquid phase transfer coefficient (K_L) are obtained by using the following equations:

Equation for Calculating Liquid Phase Transfer Coefficient (K_L)

For flowing streams or rivers:

$$K_L = \sqrt{\frac{10^{-4} \cdot D_w \cdot u}{d_z}} \cdot 3.1536 \times 10^7$$

For quiescent lakes or ponds:

$$K_L = (C_d^{0.5} \cdot W) \cdot \left(\frac{\rho_a}{\rho_w}\right)^{0.5} \cdot \frac{k^{0.33}}{\lambda_z} \cdot \left(\frac{\mu_w}{\rho_w \cdot D_w}\right)^{-0.67} \cdot 3.1536 \times 10^7$$

where:

K_L	=	Liquid phase transfer coefficient (m/yr)
D_w	=	Diffusivity of COPC in water (cm^2/s)
u	=	Current velocity (m/s)
1×10^{-4}	=	Units conversion factor (m^2/cm^2)
d_z	=	Total water body depth (m)
C_d	=	Drag coefficient (unitless)
W	=	Average annual wind speed (m/s)
ρ_a	=	Density of air (g/cm^3)
ρ_w	=	Density of water (g/cm^3)
k	=	von Karman's constant (unitless)
λ_z	=	Dimensionless viscous sublayer thickness (unitless)
μ_w	=	Viscosity of water corresponding to water temperature ($\text{g}/\text{cm}\cdot\text{s}$)
3.1536×10^7	=	Units conversion factor (s/yr)

For a flowing stream or river, the transfer coefficients are controlled by flow-induced turbulence. For a stagnant system (quiescent lake or pond), the transfer coefficient is controlled by wind-induced turbulence.

U.S. EPA recommends (1998c) the use of the following default values.

1. Diffusivity of chemical in water ranging (D_w) from 1.0×10^{-5} to 8.5×10^{-2} cm^2/s ,
2. Dimensionless viscous sublayer thickness (λ_z) of 4
3. von Karman's constant (k) of 0.4
4. Drag coefficient (C_d) of 0.0011 which was adapted from U.S. EPA (1998c)
5. Density of air (ρ_a) of 0.0012 g/cm^3 at standard conditions (temperature = 20°C or 293 K, pressure = 1 atm or 760 millimeters of mercury) (Weast 1986)
6. Density of water (ρ_w) of 1 g/cm^3 (Weast 1986)
7. Viscosity of water (μ_w) of a 0.0169 g/cm-s corresponding to water temperature (Weast 1986).

4.2.15 Gas Phase Transfer Coefficient (K_G)

U.S. EPA recommends (1998c) using the following equations to calculate gas phase transfer coefficient (K_G).

Equation for Calculating Gas Phase Transfer Coefficient (K_G)

For flowing streams or rivers:

$$K_G = 36500 \text{ [m/year]}$$

For quiescent lakes or ponds:

$$K_G = (C_d^{0.5} \cdot W) \cdot \frac{k^{0.33}}{\lambda_z} \cdot \left(\frac{\mu_a}{\rho_a \cdot D_a} \right)^{-0.67} \cdot 3.1536 \times 10^7$$

where:

K_G	=	Gas phase transfer coefficient (m/yr)
C_d	=	Drag coefficient (unitless)
W	=	Average annual wind speed (m/s)
k	=	von Karman's constant (unitless)
λ_z	=	Dimensionless viscous sublayer thickness (unitless)
μ_a	=	Viscosity of air corresponding to air temperature (g/cm-s)
ρ_a	=	Density of air corresponding to water temperature (g/cm^3)
D_a	=	Diffusivity of COPC in air (cm^2/s)
3.1536×10^7	=	Units conversion factor (s/yr)

U.S. EPA (1998c) indicated that the rate of transfer of a COPC from the gas phase for a flowing stream or river is assumed to be constant, in accordance with O'Connor and Dobbins (1958). For a stagnant system (quiescent lake or pond), the transfer coefficients are controlled by wind-induced turbulence. U.S. EPA recommends (USEPA 1994k and USEPA 1998c) $1.81 \times 10^{-4} \text{ g/cm-s}$ for the viscosity of air corresponding to air temperature.

4.2.16 Benthic Burial Rate Constant (k_b)

U.S. EPA recommends (USEPA 1994k and USEPA 1998c) using the following equation to calculate benthic burial rate (k_b).

**Recommended Equation for Calculating:
Benthic Burial Rate Constant (k_b)**

$$k_b = \left(\frac{X_e \cdot A_L \cdot SD \cdot 10^3 - Vf_x \cdot TSS}{A_W \cdot TSS} \right) \cdot \left(\frac{TSS \cdot 10^{-6}}{C_{BS} \cdot d_{bs}} \right)$$

where:

k_b	=	Benthic burial rate constant (yr ⁻¹)
X_e	=	Unit soil loss (kg/m ² -yr)
A_L	=	Total watershed area (evaluated) receiving deposition (m ²)
SD	=	Sediment delivery ratio (watershed) (unitless)
Vf_x	=	Average volumetric flow rate through water body (m ³ /yr)
TSS	=	Total suspended solids concentration (mg/L)
A_W	=	Water body surface area (m ²)
BS	=	Benthic solids concentration (g/cm ³)
d_{bs}	=	Depth of upper benthic sediment layer (m)
1×10^{-6}	=	Units conversion factor (kg/mg)
1×10^3	=	Units conversion factor (g/kg)

The benthic burial rate constant (k_b), which is calculated in the equation above, can also be expressed in terms of the rate of burial (W_b):

$$W_b = k_b \cdot d_{bs}$$

where:

W_b	=	Rate of burial (m/yr)
k_b	=	Benthic burial rate constant (yr ⁻¹)
d_{bs}	=	Depth of upper benthic sediment layer (m)

U.S. EPA (1998c) recommends a benthic solids concentration (BS) value ranging from 0.5 to 1.5 kg/L, which recommends the following default value for benthic solids concentration (BS).

Recommended Default Value for Benthic Solids Concentration (BS)

1.0 kg/L

The calculated value for k_b should range from 0 to 1.0; with low k_b values expected for water bodies characteristic of no or limited sedimentation (rivers and fast flowing streams), and k_b values closer to 1.0 expected for water bodies characteristic of higher sedimentation (lakes). This range of values is based on the relation between the benthic burial rate (k_b) and rate of burial (W_b) expressed

in the two previous equations; with the depth of upper benthic sediment layer (d_{bs}) held constant. For k_b values calculated as a negative (water bodies with high average annual volumetric flow rates in comparison to watershed area evaluated), a k_b value of 0 should be assigned for use in calculating the total water body COPC concentration (C_{wtot}). If the calculated k_b value exceeds 1.0, re-evaluation of the parameter values used in calculating X_e should be conducted.

4.2.17 Total COPC Concentration in Water Column (C_{wctot})

U.S. EPA recommends (1998c) using the following equation to calculate total COPC concentration in water column (C_{wctot}).

**Recommended Equation for Calculating:
Total COPC Concentration in Water Column (C_{wctot})**

$$C_{wctot} = f_{wc} \cdot C_{wtot} \cdot \left(\frac{d_{wc} + d_{bs}}{d_{wc}} \right)$$

where:

- C_{wctot} = Total COPC concentration in water column (mg COPC/L water column)
- f_{wc} = Fraction of total water body COPC concentration in the water column (unitless)
- C_{wtot} = Total water body COPC concentration, including water column and bed sediment (mg COPC/L water body)
- d_{wc} = Depth of water column (m)
- d_{bs} = Depth of upper benthic sediment layer (m)

4.2.18 Dissolved Phase Water Concentration (C_{dw})

U.S. EPA recommends (1998c) the use of the following equation to calculate the concentration of COPC dissolved in the water column (C_{dw}).

Equation for Calculating Dissolved Phase Water Concentration (C_{dw})

$$C_{dw} = \frac{C_{wctot}}{1.0 + Kd_{sw} \cdot TSS \cdot 10^{-6}}$$

where:

- C_{dw} = Dissolved phase water concentration (mg COPC/L water)
- C_{wctot} = Total COPC concentration in water column (mg COPC/L water column)
- Kd_{sw} = Suspended sediments/surface water partition coefficient (L water/kg suspended sediment)
- TSS = Total suspended solids concentration (mg/L)

$1 \times 10^{-6} =$ Units conversion factor (kg/mg)

4.2.19 COPC Concentration in Bed Sediment (C_{sed})

U.S. EPA recommends (1998c) the use of the following equation to calculate COPC concentration in bed sediment (C_{sed}).

Equation for Calculating COPC Concentration in Bed Sediment (C_{sed})

$$C_{sed} = f_{SB} \cdot C_{wtot} \cdot \left(\frac{Kd_{bs}}{\theta_{bs} + Kd_{bs} \cdot C_{BS}} \right) \cdot \left(\frac{d_{wc} + d_{bs}}{d_{bs}} \right)$$

where:

- C_{sed} = COPC concentration in bed sediment (mg COPC/kg sediment)
- f_{bs} = Fraction of total water body COPC concentration in benthic sediment (unitless)
- C_{wtot} = Total water body COPC concentration, including water column and bed sediment (mg COPC/L water body)
- Kd_{bs} = Bed sediment/sediment pore water partition coefficient (L COPC/kg water body)
- θ_{bs} = Bed sediment porosity ($L_{pore\ water} / L_{sediment}$)
- BS = Benthic solids concentration (g/cm^3)
- d_{wc} = Depth of water column (m)
- d_{bs} = Depth of upper benthic sediment layer (m)

The total water body COPC concentration includes water column and bed sediment (C_{wtot}) and the fraction of total water body COPC concentration that occurs in the benthic sediment (f_{bs}). Bed sediment porosity (θ_{bs}), benthic solids concentration (BS), depth of water column (d_{wc}), and depth of upper benthic layer (d_{bs}) are discussed previously.

4.3 Calculation of COPC Concentrations in Plants

As illustrated in Figure 7, the concentration of COPCs in plants is assumed to occur by three possible mechanisms:

1. **Direct deposition of particles** - wet and dry deposition of particle phase COPCs onto the exposed plant surfaces.
2. **Vapor transfer** - uptake of vapor phase COPCs by plants through their foliage.
3. **Root uptake** - root uptake of COPCs available from the soil and their transfer to the aboveground portions of the plant.

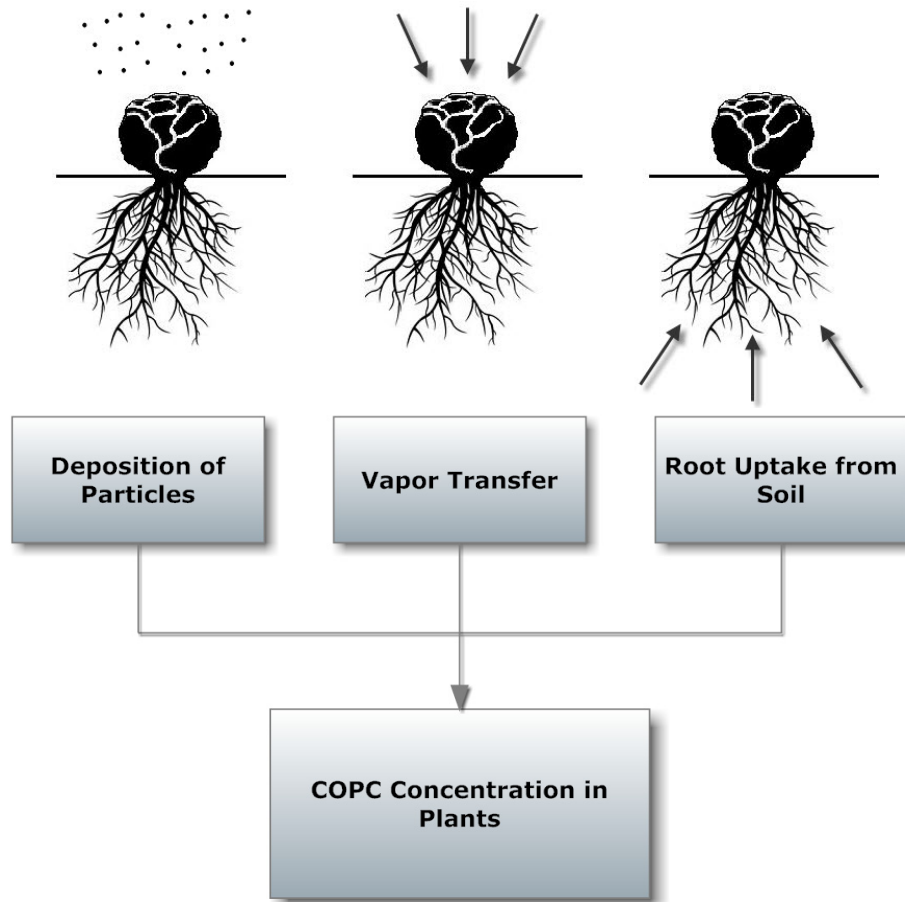


Figure 7. COPC Concentration in Plants.

The total COPC concentration in terrestrial plants, C_{TP} is calculated as a sum of contamination occurring through all three of these mechanisms.

4.3.1 Calculating Plant Concentration Due to Direct Deposition (Pd)

U.S. EPA recommends (1998c) the use of the following equation to calculate COPC concentration in plants due to direct deposition.

Equation for Calculating Plant Concentration Due to Direct Deposition (Pd)

$$Pd = \frac{1000 \cdot Q \cdot (1 - F_v) \cdot [Dydp + (Fw \cdot Dywp)] \cdot Rp \cdot [1.0 - \exp(-kp \cdot Tp)] \cdot 0.12}{Yp \cdot Kp}$$

where:

- Pd = Plant concentration due to direct (wet and dry) deposition (mg COPC/kg WW)
- 1,000 = Units conversion factor (mg/g)
- Q = COPC emission rate (g/s)
- F_v = Fraction of COPC air concentration in vapor phase (unitless)

$Dydp$	=	Unitized yearly average dry deposition from particle phase (s/m ² -yr)
Fw	=	Fraction of COPC wet deposition that adheres to plant surfaces (unitless)
$Dywp$	=	Unitized yearly wet deposition from particle phase (s/m ² -yr)
Rp	=	Interception fraction of the edible portion of plant (unitless)
kp	=	Plant surface loss coefficient (yr ⁻¹)
Tp	=	Length of plant exposure to deposition per harvest of the edible portion of the <i>i</i> th plant group (yr)
0.12	=	Dry weight to wet weight conversion factor (unitless)
Yp	=	Yield or standing crop biomass of the edible portion of the plant (productivity) (kg DW/m ²)

The dry weight to wet weight conversion factor of 0.12 is based on the average rounded value from the range of 80 to 95 percent water content in herbaceous plants and nonwoody plant parts (Taiz et al. 1991).

4.3.2 Calculating Plant Concentration Due to Air-to-Plant Transfer (P_v)

U.S. EPA recommends (USEPA 1994k and USEPA 1998c) the use of the following equation to calculate the plant concentration due to air-to-plant transfer (P_v).

Equation for Calculating Plant Concentration Due to Air-to-Plant Transfer (P_v)

$$P_v = Q \cdot F_v \cdot 0.12 \cdot \frac{C_{yv} \cdot B_v}{\rho_a}$$

where:

P_v	=	Plant concentration due to air-to-plant transfer (mg COPC/kg WW)
Q	=	COPC emission rate (g/s)
F_v	=	Fraction of COPC air concentration in vapor phase (unitless)
C_{yv}	=	Unitized yearly average air concentration from vapor phase (μg-s/g-m ³)
B_v	=	Air-to-plant biotransfer factor ([mg COPC/g DW plant]/[mg COPC/g air]) (unitless)
0.12	=	Dry weight to wet weight conversion factor (unitless)
ρ_a	=	Density of air (g/m ³)

The dry weight to wet weight conversion factor of 0.12 is based on the average rounded value from the range of 80 to 95 percent water content in herbaceous plants and nonwoody plant parts (Taiz et al. 1991).

4.3.3 Calculating Plant Concentration Due to Root Uptake (P_r)

U.S. EPA recommends (USEPA 1994k and USEPA 1998c) the use of the following equation to calculate the plant concentration due to root uptake (P_r).

Equation for Calculating Plant Concentration Due to Root Uptake (Pr)

$$Pr = Cs \cdot BCF_r \cdot 0.12$$

where:

- Pr = Plant concentration due to root uptake (mg COPC/kg WW)
- BCF_r = Plant-soil bio-transfer factor (unitless)
- Cs = COPC concentration in soil (mg COPC/kg soil)
- 0.12 = Dry weight to wet weight conversion factor (unitless)

This equation is based on the soil-to-aboveground plant transfer approach developed by Travis and Arms (1988). The dry weight to wet weight conversion factor of 0.12 is based on the average rounded value from the range of 80 to 95 percent water content in herbaceous plants and non-woody plant parts (Taiz et al. 1991).

4.4 Replacing Default Parameter Values

After completing a risk assessment based on the default parameter values recommended in this guidance, risk assessors may choose to investigate replacing default parameter values with measured or published values if a more representative estimate of site-specific risk can be obtained. Changes to default parameter values must include the following information:

1. An explanation of why the use of a measured or published value other than the default value is warranted.
2. The supporting technical basis of the replacement parameter value, including readable copies (printed in English) of any relevant technical literature or studies
3. The basis of the default parameter value, as understood by the requestor, including readable copies of the referenced literature or studies (if available)
4. A comparison of the weight-of-evidence between the competing studies (e.g., the proposed replacement parameter value is based on a study that is more representative of site conditions, a specific exposure setting being evaluated, or a more scientifically valid study than the default parameter value, the proposed replacement parameter is based on the analysis of 15 samples as opposed to 5 for the default parameter value, or the site-specific study used more stringent quality control/quality assurance procedures than the study upon which the default parameter value is based)
5. A description of other risk assessments or projects where the proposed replacement parameter value has been used, and how such risk assessments or projects are similar to the risk assessment in consideration.

5 Ecological Risk Problem Formulation

Problem formulation, in an Ecological Risk Assessment, establishes the exposure setting used as the basis for exposure analysis and risk characterization. Problem formulation includes:

1. Characterization of the exposure setting for identification of exposed habitats in the assessment area
2. Development of food webs representative of the habitats to be evaluated
3. Selection of assessment endpoints relevant to food web structure and function
4. Identification of measurement receptors.

5.1 Exposure Setting Characterization

Ecological receptors within a potentially impacted habitat can be evaluated through consideration of the combination of exposure pathways to which ecological receptors representing a habitat-specific food web may be exposed to a compound. The habitats identified to be evaluated are selected based on existing habitats surrounding the facility; and also support which habitat-specific food webs are evaluated in risk characterization. Consideration of ecological receptors representative of the habitats also provides the basis for selecting measurement receptors, as well as, it supports demonstration of the presence or absence of federal and state species of special interest.

Resources for characterizing the exposure setting should focus on the areas impacted from emissions as predicted by air dispersion modeling. All habitats (potentially including water bodies and their associated watersheds) both within and outside the facility property boundary should be considered for evaluation.

The following subsections provide information on selection of habitats, and identification of ecological receptors representative of those habitats, to be considered for evaluation in the risk assessment.

5.1.1 Selection of Habitats

Habitats to be considered in the risk assessment are selected by identifying similar habitats surrounding the facility that are potentially impacted by facility emissions, and when overlaid with the air dispersion modeling results, define which habitat-specific food webs should be evaluated in the risk assessment. Habitats can be defined based on their biotic and abiotic characteristics, and are generally divided into two major groups (i.e., terrestrial and aquatic) that can be classified as follows:

- Terrestrial
 1. Forest
 2. Shortgrass prairie
 3. Tallgrass prairie

4. Agricultural/Cropland
 5. Scrub/Shrub
 6. Desert
- Aquatic
 1. Freshwater
 2. Brackish/Intermediate
 3. Marine

Habitat types can typically be identified by reviewing hard copy and/or electronic versions of land use land classification (LULC) maps, topographic maps, and aerial photographs. Sources and general information associated with each of these data types or maps are presented below. Also, the UTM coordinate system format (such as WGS84) for all mapping information should be verified to ensure consistency and prevent erroneous geo-referencing of locations and areas.

Land Use Land Cover (LULC) Maps - These maps provide detailed habitat information based upon the classification system and definitions of Land Use and Land Cover information.

Topographic Maps - Topographic maps are readily available in both hard copy and electronic format directly from USGS or numerous other vendors.

Additional information useful for habitat identification can be obtained from discussions with representatives of private and government organizations which routinely collect and evaluate ecosystem or habitat information including the following:

1. Soil Conservation Service
2. Fish and Wildlife Service (FWS)
3. U.S Department of Agriculture
4. Local, State, and Tribal natural resource agencies

Habitats identified during exposure setting characterization and selected for evaluation in the risk assessment should be clearly mapped and include the following supporting information:

1. Facility emission source location(s) and boundaries
2. Habitat types and boundaries
3. Water bodies and their associated watersheds
4. Special ecological areas

A facility location map, including land-use and land cover data, which allows for identification of habitats to support selection of habitat-specific food webs to be evaluated in the risk assessment.

5.1.2 Selection of Exposure Scenario Locations within Terrestrial Habitats

Exposure scenario locations to be evaluated within the terrestrial habitats identified during the exposure setting characterization are selected at specific receptor grid nodes based on evaluation of the magnitude of air parameter values estimated by AERMOD. The methodology and resulting selection of receptor grid nodes as exposure scenario locations is one of the most critical parts of the risk assessment process, ensuring standardization across all facilities evaluated and reproducibility of results.

The procedures described below should be used in the selection of receptor grid nodes as exposure scenario locations; and that the selected exposure scenario locations correspond to actual AERMOD modeled receptor grid node locations. Exposure scenario locations, at actual receptor grid nodes, should be selected as follows:

Step 1: Define Terrestrial Habitats To Be Evaluated - All habitats, identified during exposure setting characterization for evaluation in the risk assessment, should be defined and habitat boundaries mapped in a format (NAD 27 or NAD 83 UTM) consistent with that used to define locations of facility emission sources and modeled AERMOD receptor grid nodes.

Step 2: Identify Receptor Grid Node(s) Within Each Habitat To Be Evaluated - For each habitat to be evaluated, identify the receptor grid nodes within that area or on the boundary of that area (defined in Step 1) that represent the locations of highest yearly average concentration for each AERMOD modeled air parameter (i.e., air concentration, dry deposition, wet deposition) for each phase (i.e., vapor, particle, particle-bound). This determination should be performed for each emission source (i.e., stacks, fugitives) and all emissions sources at the facility combined. This results in the selection of one or more receptor grid nodes as exposure scenario locations, within a defined habitat area to be evaluated, and that meet one or more of the following criteria, which relates to the “Highest modeled unitized”:

1. Vapor phase air concentration
2. Vapor phase wet deposition rate
3. Particle phase air concentration
4. Particle phase wet deposition rate
5. Particle phase dry deposition rate
6. Particle-bound phase air concentration
7. Particle-bound phase wet deposition rate
8. Particle-bound phase dry deposition rate

Only the air dispersion modeled air parameters corresponding to a single receptor grid node should be used per exposure scenario location as inputs into the media equations, without averaging or statistical manipulation. However, based generally on the number and location of facility emission sources, multiple

exposure scenario locations may be selected to represent the highest potential impact area for a specific habitat being evaluated.

Water bodies and associated watershed in close proximity to the exposure scenario location being evaluated should be identified to represent a drinking water source for applicable receptors. Although the locations and type of sources (i.e., free water, consumption of water as part of food items) of water ingested by an animal through diet are expected to vary depending on the receptor and availability, COPC intake by the receptor through ingestion of water can be estimated by assuming only water intake from a defined water body for which a COPC concentration can be calculated. Therefore, a representative water body should be defined and evaluated, and a COPC concentration in the water column, C_{wctot} , calculated.

If a definable water body is not located within or in close proximity to the terrestrial habitat being evaluated, receptor drinking water intake terms in the exposure equations should be adjusted accordingly (i.e., ingestion of drinking water set equal to zero).

5.1.2.1 Selection of Habitat Exposure Scenario Locations within Aquatic Habitats

Exposure scenario locations to be evaluated within the aquatic habitats identified during the exposure setting characterization may first require differentiating water bodies from land areas within aquatic habitats not typically covered by water (e.g., flood plains or wetland areas transitioning to terrestrial and upland habitats). Exposure scenario locations within land areas of aquatic habitats not characteristic of a standing water body are selected following the same steps as for terrestrial habitats. The associated watershed contributing COPC loading to the water body being evaluated should also be defined.

The following procedures should be used in the selection of exposure scenario locations within defined water body areas of aquatic habitats as follows:

Step 1: Define Aquatic Habitats to be Evaluated - All habitats, identified during exposure setting characterization for evaluation in the risk assessment, should be defined and habitat boundaries mapped in a format consistent with that used to define locations of facility emission sources and modeled AERMOD receptor grid nodes. Water body boundaries should reflect annual average shoreline elevations.

Step 2: Identify Receptor Grid Node(s) Within Each Habitat to be Evaluated - For each water body and associated watershed to be evaluated, the receptor grid nodes within that area and on the boundary of that area (defined in Step 1) should be considered. For water bodies, the risk assessor can select the receptor grid node that represent the locations of highest yearly average concentration for each AERMOD modeled air parameter (i.e., air concentration, dry deposition, wet

deposition) for each phase (i.e., vapor, particle, particle-bound), or average the air parameter values for all receptor grid nodes within the area of the water body. For watersheds, the modeled air parameter values should be averaged for all receptor grid nodes within the area extent or effective area of the watershed (excluding the area of the water body).

For evaluating the COPC loading to the water body from its associated watershed, the area extent of the watershed should be defined and the AERMOD modeled air parameter values at each receptor grid node within the watershed area (excluding the water body) averaged. These averaged air parameter values are then used in the estimating media equations and for calculating the COPC loading to the water body.

The area extent of a watershed is generally defined by topographic highs that result in downslope drainage into the water body. The watershed can be important to determining the overall water body COPC loading, because pervious and impervious areas of the watershed, as well as the soil concentration of COPCs resulting from emissions from facility sources, are also used in the media concentration equations to calculate the water body COPC concentrations resulting from watershed runoff.

Water bodies may also be extensive in size relative to the area that is impacted from facility emissions and exposure point(s) of interest. In such cases, the risk assessor should consider defining and evaluating an “effective” area of the water body that focuses the assessment specific to areas potentially impacted and of most concern when considering potential for exposure.

To address evaluation of habitat areas, water bodies, or watersheds located beyond the coverage provided by the recommended receptor grid node array (greater than 10 km from the facility), the air dispersion model can be conducted with an additional receptor grid node array specified to provide coverage of the area of concern, or the steps above can be executed using the closest receptor grid nodes from the recommended array. However, using the closest receptor grid nodes from the recommended receptor grid node array will in most cases provide a conservative estimate of risk since the magnitude of air parameter values at these receptor grid nodes would most likely be higher than at receptor grid nodes located further from the facility sources and actually within the area of concern.

5.1.2.2 Special Ecological Areas

A special ecological area is a habitat that could require protection or special consideration on a site-specific basis because:

1. Unique and/or rare ecological receptors and natural resources are present
2. Legislatively-conferred protection (e.g., a national monument) has been established. All potentially exposed special ecological areas in the assessment area should be identified for consideration.

The following are examples of special ecological habitats (U.S. EPA 1997c):

1. Marine Sanctuaries
2. National river reaches
3. Spawning areas critical for maintenance of fish/shellfish species
4. Terrestrial areas utilized for breeding by large or dense aggregations of animals
5. Migratory pathways and feeding areas critical for maintenance of anadromous fish species
6. National Preserves
7. Federal lands designated for protection of natural ecosystems
8. National or State Wildlife Refuges
9. Critical areas identified under the Clean Lakes Program
10. Habitats known to be used by Federal or State designated or proposed endangered or threatened species
11. Areas identified under the Coastal Zone Management Act
12. Sensitive areas identified under the National Estuary Program or Near Coastal Waters Program
13. Designated Federal Wilderness Areas
14. State lands designated for wildlife or game management
15. Federal- or State-designated Scenic or Wild Rivers, or Natural Areas
16. Wetlands

5.1.3 Identification of Ecological Receptors

Identification of ecological receptors during exposure setting characterization is used to define food webs specific to potentially impacted habitats to be evaluated in the risk assessment. Ecological receptors for each habitat potentially impacted should be identified to ensure:

1. Plant and animal communities representative of the habitat are represented by the habitat-specific food web
2. Potentially complete exposure pathways are identified.

Examples of sources and general information available for identification of site-specific ecological receptors are presented below:

Government Organizations - U.S. Fish and Wildlife Service (National Wetland Inventory Maps - <http://www.fws.gov/wetlands/data/>) and State Natural Heritage Programs provide maps or lists of species based on geographic location, and are very helpful in identifying threatened or endangered species or areas of special concern.

General Literature (field guides) - Examples of information describing the flora and fauna of North America and useful in the development of habitat-specific food webs include the following:

1. Craig et al. 1987
2. Baker et al. 1991

3. Carr 1994
4. Ehrlich et al. 1988
5. National Geographic Society (1987, 1992)
6. Whitaker 1995
7. Burt and Grossenheider 1980
8. Behler 1995
9. Smith and Brodie 1982
10. Tynning 1990
11. Farrand Jr. 1989.

Private or Local Organizations - Additional private or professional organizations that are examples of sources of information include: National Audubon Society, National Geographic Society, Local Wildlife Clubs, State and National Parks Systems, and Universities.

Ecological receptor identification should include species both known and expected to be present in a specific habitat being evaluated, and include resident and migratory populations. Identification of flora should be based on major taxonomic groups represented in the assessment area. Natural history information may also be useful during food web development in assigning individual receptors to specific habitats and guilds based on feeding behavior.

5.2 Food Web Development

Information obtained during exposure setting characterization should be used to develop one or more habitat-specific food web(s) that represent communities and guilds of receptors potentially exposed to emissions from facility sources. Food webs are interlocking patterns of food chains, which are the straight-line transfer of energy from a food source (e.g., plants) to a series of organisms feeding on the source or on other organisms feeding on the food source (Odum 1971). The importance of a food chain as an exposure pathway primarily depends on receptor dietary habits, the receptors in the food chain, and other factors including bioavailability and depuration of the compound evaluated.

Habitat-specific food webs are developed for use in the risk assessment to:

1. Define direct and indirect exposure pathways
2. Formulate assessment endpoints
3. Develop mathematical relationships between guilds
4. Perform quantitative exposure analysis for ecological receptors

Food webs can be developed using the community approach (Cohen 1978), which includes:

1. Identification of potential receptors in a given habitat for grouping into feeding guilds by class and communities
2. Organizing food web structure by trophic level (e.g., primary producer, secondary consumer)
3. Defining dietary relationships between guilds and communities.

The result of the development of the Community, using this approach, is a complete food web for a defined habitat, which should be developed for each habitat in the assessment area to be evaluated in risk characterization.

5.2.1 Grouping Receptors into Feeding Guilds and Communities

The first step in developing a habitat-specific food web is to identify, based on the dietary habits and feeding strategies of receptors, the major feeding guilds for birds, mammals, reptiles, amphibians, and fish. A guild is a group of species that occupies a particular trophic level and shares similar feeding strategies. Invertebrates and plants are not assigned to guilds, rather these receptors are grouped into their respective community by the environmental media they inhabit. The distinction for grouping upper-trophic-level receptors into class-specific guilds, and invertebrates and plants into communities, is made because the risk to these groups is characterized differently.

Once the major feeding guilds are identified (e.g., herbivore, omnivore, carnivore, insectivore), receptors should be grouped by class (e.g., mammals, birds, amphibians and reptiles, and fish).

5.2.2 Organizing Food Web Structure by Trophic Level

The structure of a food web should be organized by trophic level. A trophic level is one of the successive levels of nourishment in a food web or food chain. The trophic levels are explained below:

1. The first trophic level (TL1) contains the primary producers or the green plants. Members of this trophic level produce their own food from nutrients, sunlight, carbon dioxide, and water. These primary producers are also the source of food for members of the second trophic level (TL2).
2. The second trophic level is often referred to as the primary consumers and is composed of animals that eat plants (herbivores) and animals that subsist on detritus (decaying organic matter) found in sediment and soil (detritivores).
3. The third trophic level (TL3), contains both omnivores and carnivores. Omnivores are animals that eat both plant and animal matter, while carnivores eat primarily animal matter.
4. The fourth trophic level (TL4), contains only carnivores and is sometimes referred to as the dominant carnivores.

Some species can occupy more than one trophic level at a time depending on life stage. For this reason, professional judgment should be used to categorize receptors without making the food web unduly complex.

5.2.3 Defining Dietary Relationships between Guilds and Communities

After species have been grouped into the appropriate guilds and communities, and organized by trophic level, dietary relationships between guilds and communities should be defined. Guilds and communities should be linked together based on dietary relationships by evaluating the dietary composition of the receptors for each guild and community. Although most organisms have a complex diet, it should be assumed that the majority of their diet is composed of a limited number of prey items and, therefore, a limited number of feeding guild interactions occur. Therefore, only those interactions that contribute more than five percent of the total diet should be considered for development of a food web.

In defining the habitat-specific food web the risk assessor should include the identification of (1) media (e.g., soil, sediment, water), (2) trophic levels that include at a minimum producers (TL 1), primary consumers (TL 2), secondary consumers (TL 3), and carnivores (TL 4), (3) guilds divided into classes (e.g., herbivorous mammals, omnivorous birds) and communities, and (4) major dietary interactions.

5.2.4 Example Habitat-Specific Food Webs

To better illustrate food web development as discussed in the previous sections, seven habitat-specific example food webs are presented as Figure 8 through Figure 14. The habitats represented include:

1. Forest
2. Tallgrass prairie
3. Shortgrass prairie
4. Shrub/Scrub
5. Freshwater/Wetland
6. Brackish/Intermediate marsh
7. Salt marsh

The terrestrial and aquatic example food webs are based on information describing the flora and fauna of North America (U.S. FWS 1979; Craig et al. 1987; Baker et al. 1991).

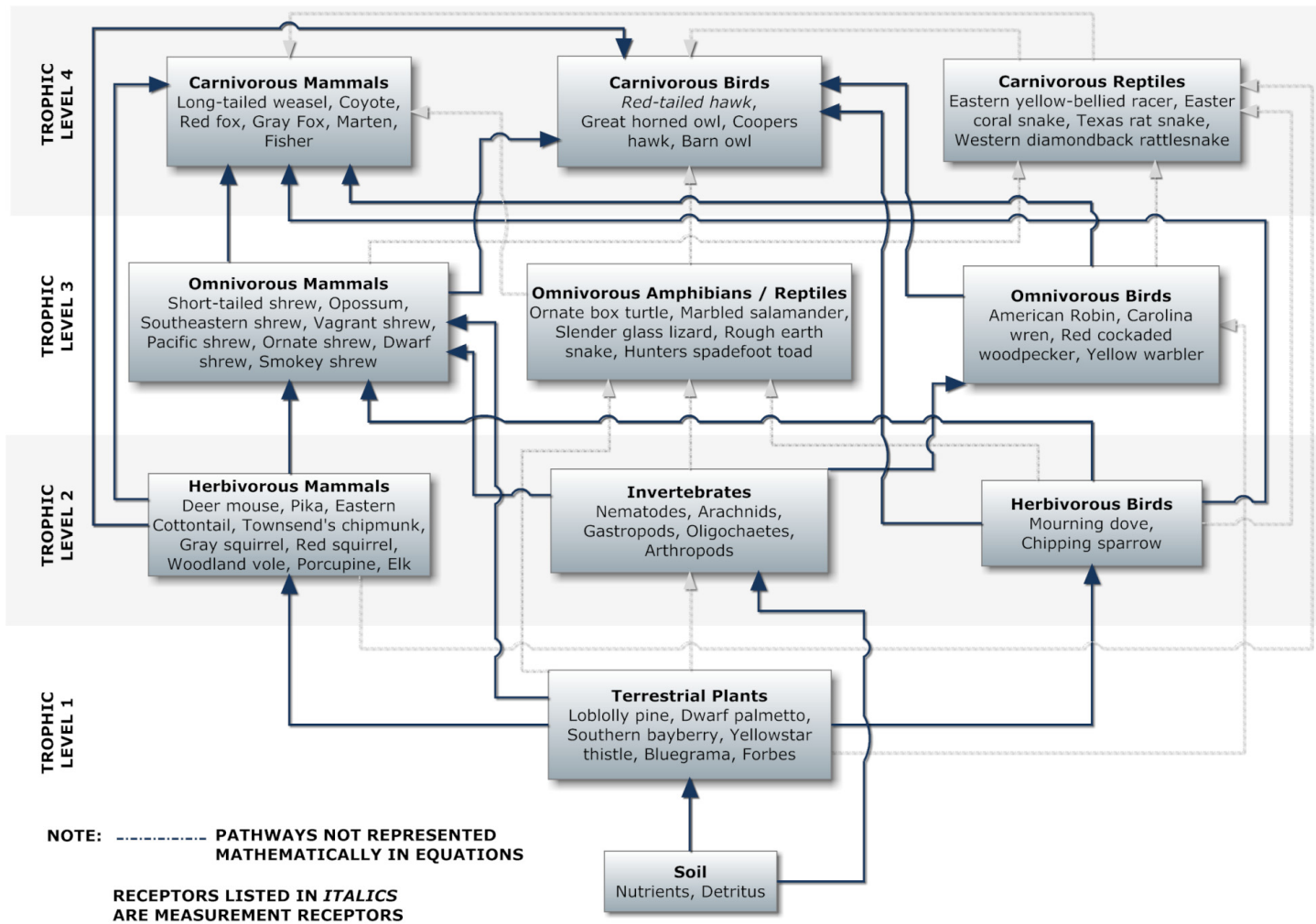


Figure 8. Forest.

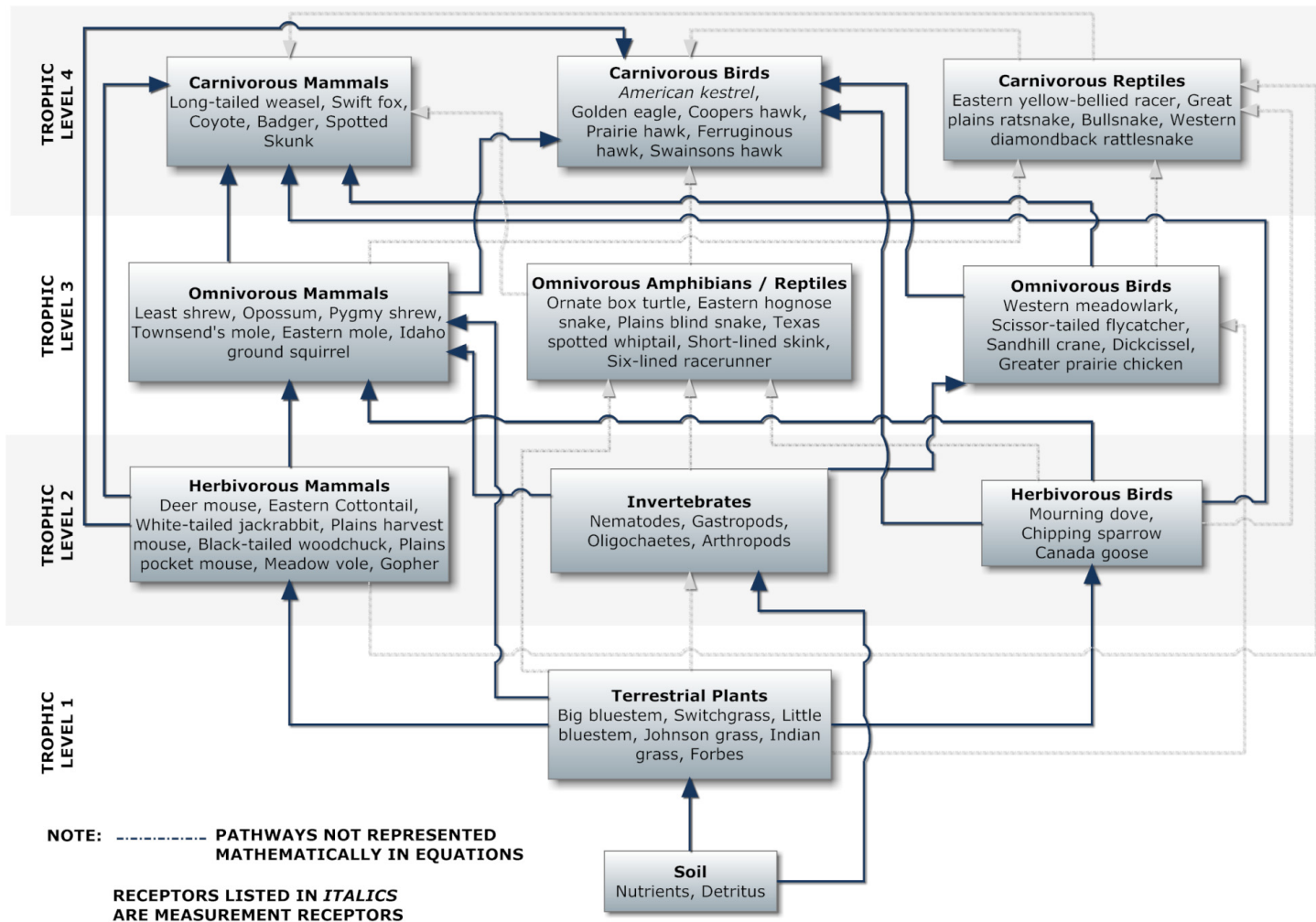


Figure 9. Tallgrass prairie.

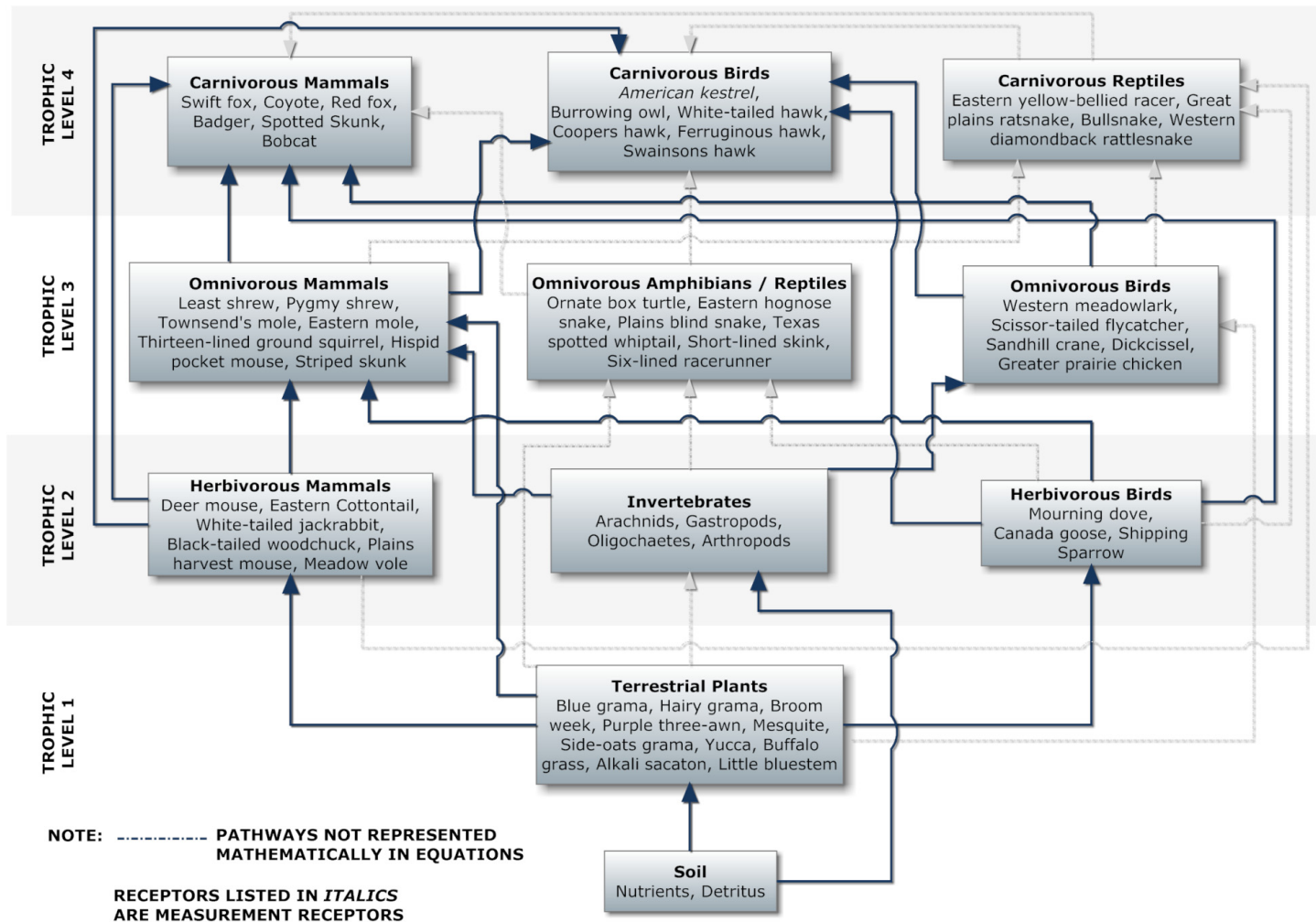


Figure 10. Shortgrass prairie.

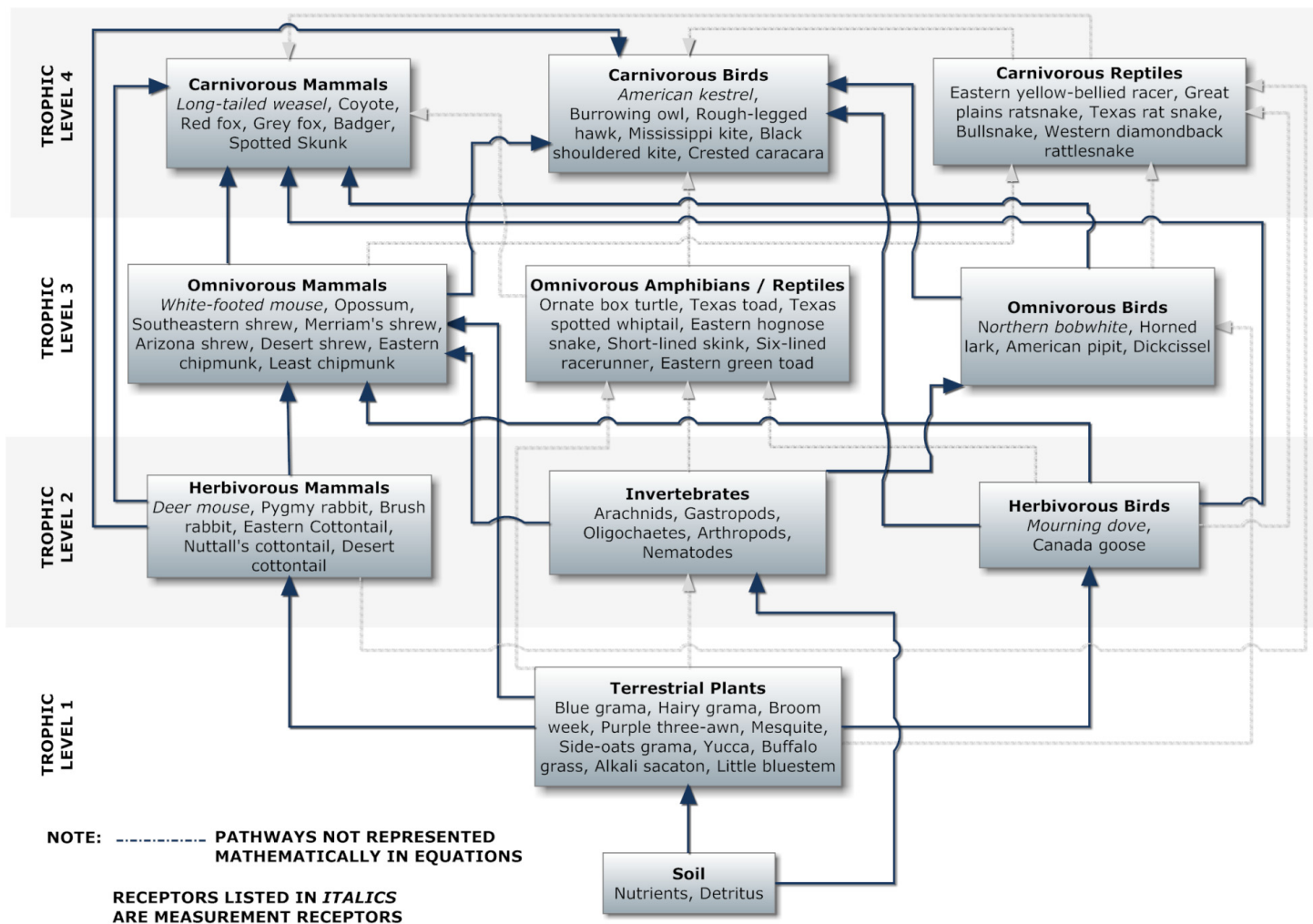


Figure 11. Shrub/Scrub.

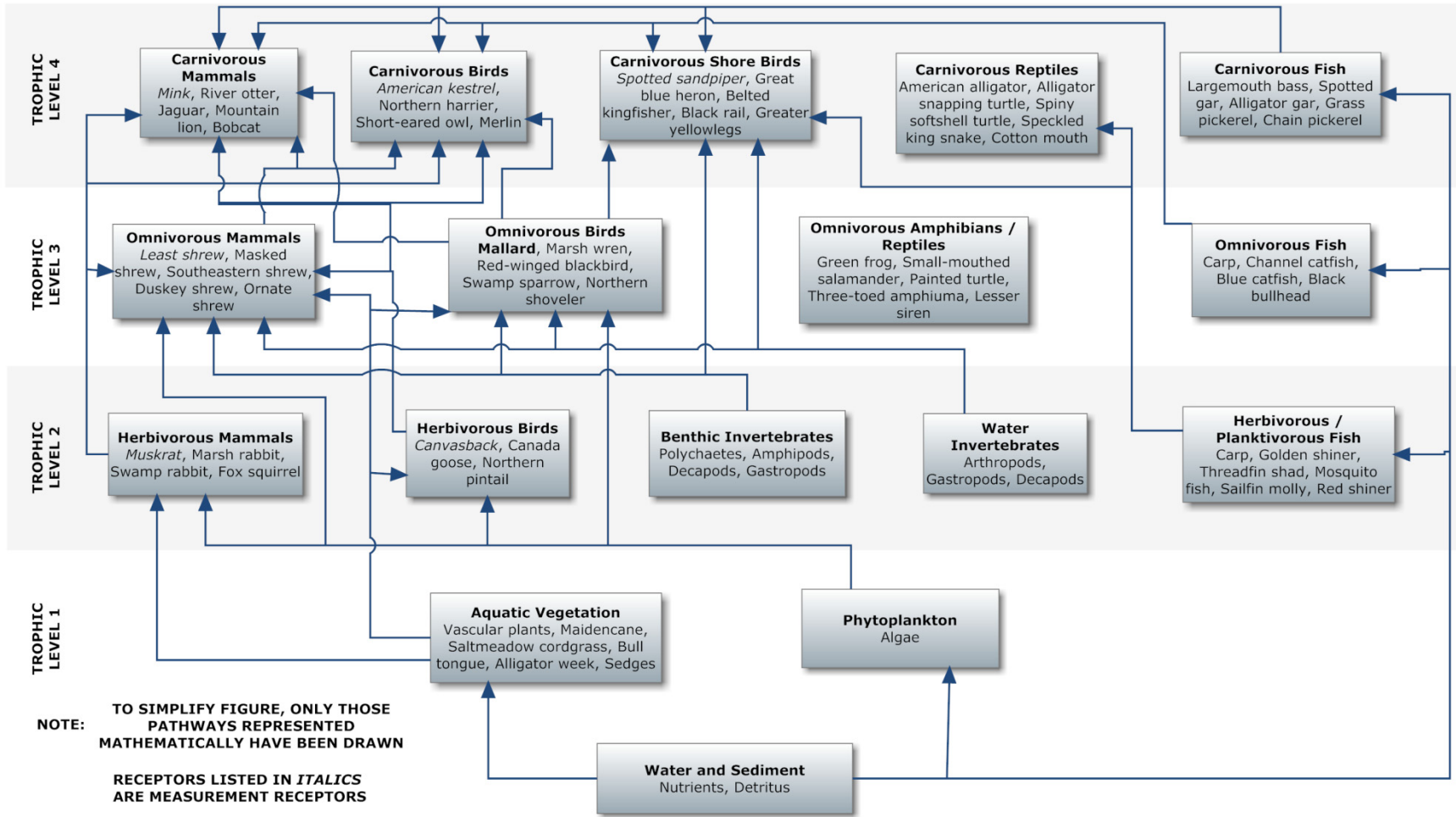


Figure 12. Freshwater/Wetland.

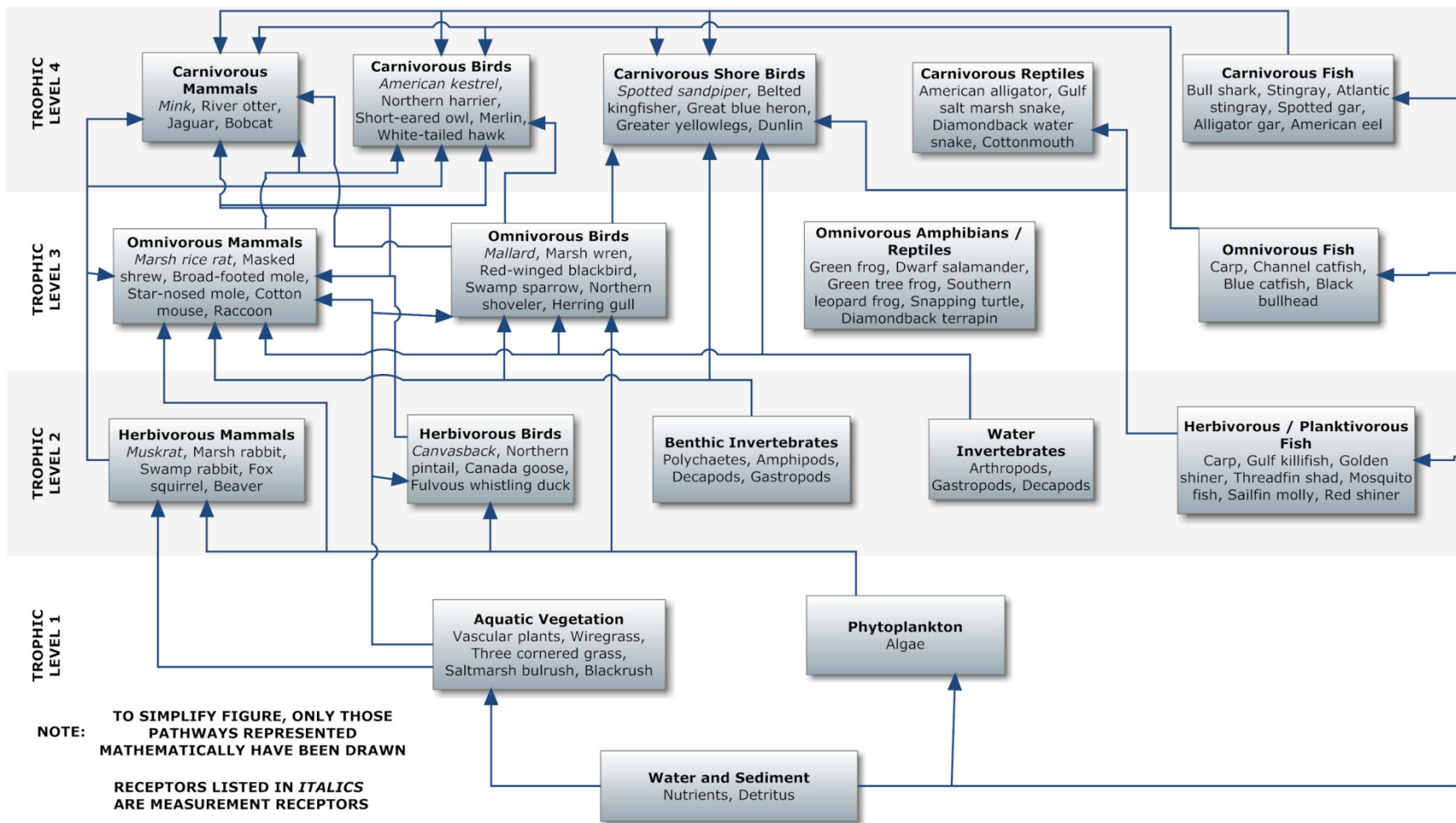


Figure 13. Brackish/Intermediate marsh.

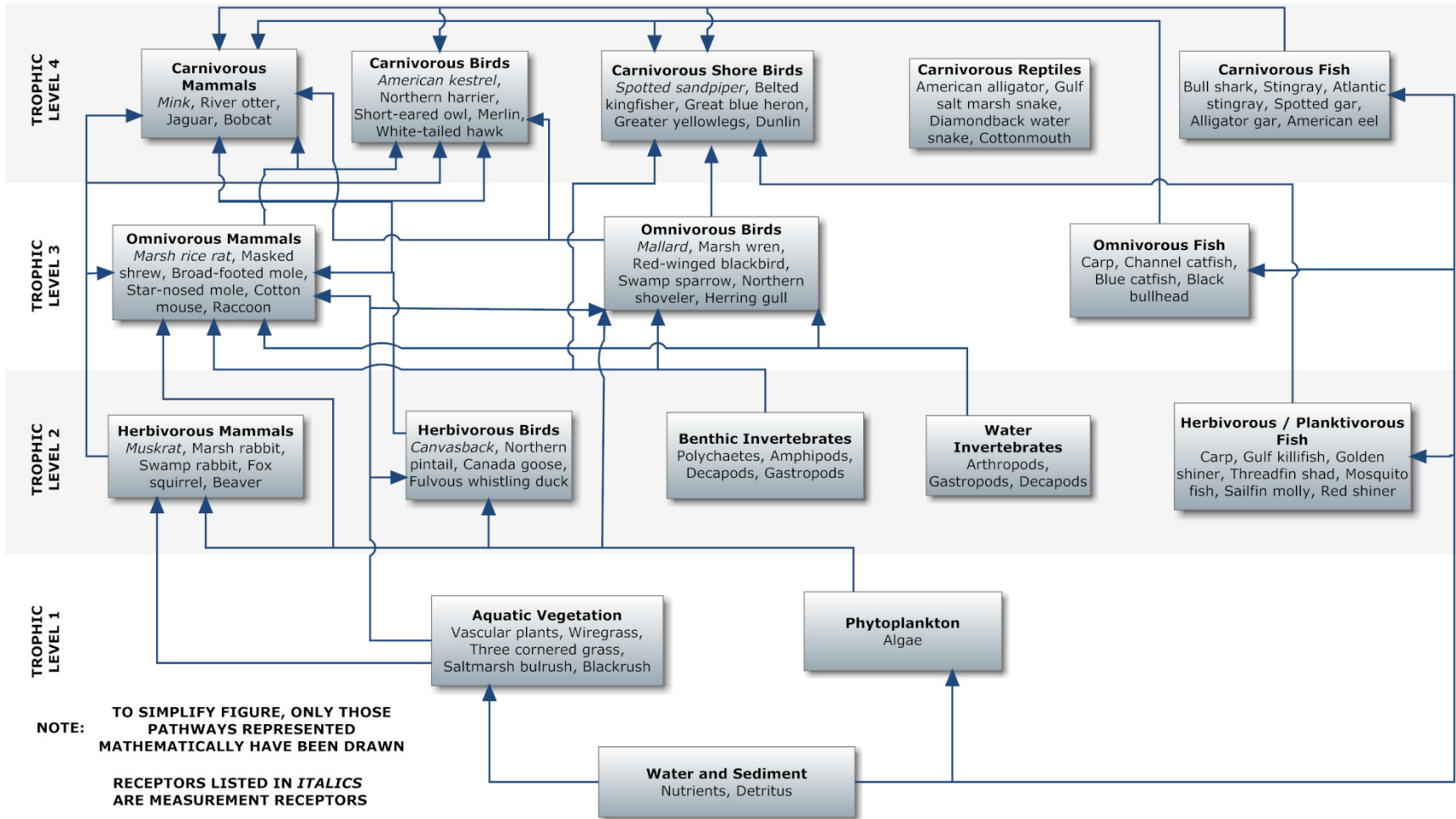


Figure 14. Salt marsh.

5.3 Selecting Assessment Endpoints

An assessment endpoint is an expression of an ecological attribute that is to be protected (U.S. EPA 1997c). A critical ecological attribute of a guild or community is a characteristic that is relevant to ecosystem (food web) structure and function. Protection of the critical ecological attributes of each guild and community is assumed to also ensure the protectiveness of habitat-specific food web structure and function. Therefore, assessment endpoints should be identified specific to each class-specific guild and community within each trophic level of the habitat-specific food web.

Examples of assessment endpoints for guilds include:

1. Seed disperser
2. Major food source for predator
3. Decomposer / detritivore
4. Pollinator
5. Regulate populations of prey (e.g., forage fish, small rodents)

Examples of assessment endpoints for communities include:

1. Diversity or species richness
2. Community composition
3. Productivity
4. Major food source for consumer
5. Habitat for wildlife

Descriptions of ecological attributes to be protected (i.e., assessment endpoints) associated with several guilds and communities in a terrestrial ecosystem are provided as examples below.

1. Herbaceous plant abundance, habitat, and productivity are attributes to be preserved in a terrestrial ecosystem. As food, herbaceous plants provide an important pathway for energy and nutrient transfer from soil to herbivorous (e.g., rabbit) and omnivorous (e.g., mouse) receptors.
2. Woody plant habitat and productivity are critical attributes to be protected. As food, woody plants provide an important pathway for energy and nutrient transfer from soil to herbivorous and omnivorous vertebrates (e.g., white-tailed deer, yellow-bellied sapsucker).
3. Herbivore productivity is an attribute to be protected in the terrestrial ecosystem because herbivores incorporate energy and nutrients from plants and transfer it to higher trophic levels, such as first- and second-order carnivores (e.g., snakes and owls, respectively).
4. Omnivore productivity is an attribute to be protected in the terrestrial ecosystem because omnivores incorporate energy and nutrients from lower trophic levels and transfer it to higher levels, such as first- and second-order carnivores.
5. First-order carnivore productivity is an attribute to be protected in the terrestrial ecosystem because these carnivores provide food to other

carnivores, omnivores, scavengers, and microbial decomposers. They also affect the abundance, reproduction, and recruitment of lower trophic level receptors, such as vertebrate herbivores and omnivores, through predation.

6. Second-order carnivore productivity is an attribute to be protected in the terrestrial ecosystem because carnivores affect the abundance, reproduction, and recruitment of species in lower trophic levels in the food web.
7. Soil invertebrate productivity and function as a decomposer are attributes to be preserved in a terrestrial ecosystem, because they provide a mechanism for the physical breakdown of detritus for microbial decomposition, which is a vital function. Soil invertebrates also function as a major food source for omnivorous birds.

Selection of assessment endpoints represents a scientific and management decision point. Since risk characterization, and subsequently final risk management decisions, is dependent on the selection of assessment endpoints, they should be developed with input from risk managers and other stakeholders. Table 6 lists the assessment endpoints for guilds and communities in the three aquatic and four terrestrial example habitat-specific food webs.

Table 6. Representative Receptors.

Representative Receptors		Example Critical Ecological Attributes
AQUATIC RECEPTORS		
Aquatic Plants	Phytoplankton, Vascular plants	Primary producers convert light energy into biomass, and are the first link in aquatic food chains supporting higher trophic level aquatic consumers and wildlife.
Water Invertebrates	Crustaceans, Rotifers, Amphipods	Aquatic invertebrates are an important food source for many higher trophic level consumers. Zooplankton regulate phytoplankton populations, and are a critical link in energy transfer to higher trophic levels in aquatic ecosystems.
Herbivorous / Planktivorous Fish	Carp, Gulf killifish, Threadfin shad, Molly, Golden Shiner, Goby, Mosquito Fish, Red Shiner	Herbivorous/Planktivorous Fish are an important prey species for higher trophic level predators in the aquatic and terrestrial ecosystems, and provide a critical link for energy transfer from primary producers to higher trophic level consumers.
Omnivorous Fish	Carp, Channel catfish, Gafftopsail fish, Atlantic midshipman, Feather blenny, Gulf toad fish, Bluecat, Bullhead	Omnivorous fish are an important prey item for higher trophic level predators. Through predation, they may also regulate population levels in lower trophic level fish and invertebrates.
Carnivorous Fish	Largemouth bass, Spotted gar, Bull shark, Redfish, Grass pickerel, Alligator gar, Chain pickerel, American eel, Atlantic stingray, Spotted moray eel, Fine toothed shark	Carnivorous fish provide an important function for the aquatic environment by regulating lower trophic populations through predation. They are also an important prey item for many top level mammal and bird carnivores.
SEDIMENT RECEPTORS		
Sediment Invertebrates	Oligochaetes, Pelecypods, Amphipods, Decapods, Polychaetes, Gastropods	Sediment invertebrates are an important food source for many higher trophic level predators. They also provide an important role as decomposers/detritivores in nutrient cycling.

SOIL RECEPTORS		
Terrestrial Plants	Vascular plants, Grasses, Forbs, Lichens	Primary producers provide a critical food source and are the first link in the terrestrial food chain for higher trophic level consumers. In addition, vegetation provides critical habitat for wildlife.
Soil Invertebrates	Nematodes, Gastropods, Oligochaetes, Arthropods	Soil invertebrates provide an important food source for many higher trophic level species. As decomposers/detritivores they play a critical role in nutrient cycling. They also aid in soil aeration and infiltration by increasing macro, and micro porosity.
UPPER TROPHIC LEVEL AVIAN AND MAMMALIAN WILDLIFE		
Herbivorous Mammals	Deer mouse, Nutria, Eastern cottontail, Prairie vole, Fox squirrel, Grey squirrel, Swamp rabbit, Eastern wood rat, White-tailed deer, Fulvous harvest mouse, Black-tailed jackrabbit, Hispid cotton rat, Hispid pocket mouse, Black-tailed prairie dog,	Herbivorous mammals are an important prey item for many higher trophic level predators. They provide an important link for energy transfer between primary producers and higher trophic level consumers. In addition, these organisms generally comprise the majority of the terrestrial tissue biomass, and are important in seed dispersal and pollination for many plant species.
Herbivorous Birds	Mourning dove, Canada goose, Chipping sparrow, Northern pintail	Herbivorous birds are an important prey item for many higher trophic level predators. They are important in seed dispersal for many plants in both terrestrial and aquatic ecosystems. Aquatic herbivorous birds may also play an important role in egg dispersion for fish and invertebrate species.
Omnivorous Mammals	Least shrew, Raccoon, Muskrat, Marsh rice rat, Wild boar, Cotton mouse, Eastern spotted skunk, Coyote, Nine-banded armadillo, Virginia opossum, Elliot=s short-tailed shrew, Striped skunk, Golden mouse, Seminole bat.	Omnivorous mammals are an important prey item for higher trophic level predators, and influence lower trophic level populations through predation. They play an important role in seed dispersal for many types of terrestrial vegetation and aquatic plants.
Omnivorous Birds	American robin, Northern bobwhite, Marsh wren, Carolina wren, Swamp sparrow, Yellow warbler, Lesser prairie chicken, Roadrunner, Mallard, Least sandpiper, Red cockaded wood pecker, Roseate spoonbill, Greater prairie chicken, Scissor-tailed flycatcher, Sandhill crane, Dickcissel, Canada goose, Red-winged blackbird, Hooded merganser, Northern shovler.	Omnivorous birds are an important prey item for higher trophic level predators. They play an important role in seed dispersal and pollination for many types of terrestrial vegetation and aquatic plants. In addition, aquatic species provide egg dispersal for some fish and invertebrate species.

Omnivorous Amphibians and Reptiles	Ornate box turtle, Green frog, Texas toad, Eastern hognose snake, Plains blind snake, Small-mouthed salamander, Diamondback terrapin, Short-lined skink, Six-lined racerunner, Eastern green toad, Marbled salamander, Slender glass lizard,	Omnivorous amphibians and reptiles provide an important food source for predators. They also provide seed dispersal for many plants and regulate lower trophic level populations through predation.
Carnivorous Mammals	Grey fox, Swift fox, River otter, Bobcat, Mountain lion, Long-tailed weasel, American badger, Red fox, American mink, Red wolf	Carnivorous mammals provide an important functional role to the environment by regulating lower trophic level prey populations.
Carnivorous Birds	Red-tailed hawk, American kestrel, Marsh hawk, Great-horned owl, Barn owl, Burrowing owl, White-tailed hawk, Ferruginous hawk, Swansons hawk, Golden eagle, Mississippi kite, Prairie hawk, Merlin	Carnivorous Birds provide an important functional role to the environment by regulating lower trophic level prey populations.
Carnivorous Shore Birds	Great blue heron, Belted kingfisher, Spotted sandpiper, Black rail, Greater yellowlegs, Dunlin,	Carnivorous Shore Birds provide an important functional role to the environment by regulating lower trophic level prey populations, and influencing species composition in terrestrial and aquatic ecosystems. They also provide egg dispersal for some fish and aquatic invertebrates.
Carnivorous Reptiles	Eastern yellowbelly racer, Eastern coral snake, Texas rat snake, Western Diamondback rattlesnake, American alligator, Bullsnake, Alligator snapping turtle, Cotton mouth, Speckled king snake, Spiny softshell turtle, Gulf salt marsh snake,	Carnivorous Reptiles provide an important functional role to the environment by regulating lower trophic level prey and are an important prey item for other upper trophic level predators.

5.4 Identifying Measurement Receptors to Evaluate Measures of Effect

Measures of effect are measures used to evaluate the response of the assessment endpoint when exposed to a stressor (formerly measurement endpoints) (U.S. EPA 1997c). Measures of exposure are measures of how exposure may be occurring, including how a stressor may co-occur with the assessment endpoint (U.S. EPA 1997c). Measures of effect, in conjunction with measures of exposure, are used to make inferences about potential changes in the assessment endpoint.

Measures of effect are selected as:

1. Toxicity values developed and/or adopted by federal or state agencies (e.g., ambient water quality criteria [AWQC], NOAA effects range low [ERL] values) for protection of media-specific communities
2. Receptor-specific chronic no-observed-adverse-effects-levels (NOAELs) or their equivalent for ecologically relevant endpoints for this screening assessment. Measures of exposure are selected as the COPC concentrations in media or dose (e.g., ingestion of contaminated media and/or tissue) to which exposure occurs.

The evaluation of the measure of effect to the assessment endpoint requires identification of a measurement receptor representative of the assessment endpoint. The measurement receptor is selected based on consideration of factors such as:

1. Ecological relevance
2. Exposure potential
3. Sensitivity
4. Social or economic importance
5. Availability of natural history information.

A measurement receptor, specific to each guild, may be selected as a species, population, community, or assemblage of communities. Communities (i.e., soil, surface water, sediment or assemblage of communities) are selected as the measurement receptor. That is, no specific species is selected. For guilds, individual species are selected as measurement receptors. The following sections discuss Community Selection procedures.

5.4.1 Measurement Receptors for Communities

It is inferred that critical ecological attributes of these communities are not adversely affected if a COPC concentration in that respective media does not exceed the toxicity benchmark specific for that community. Representative measurement receptors for soil, surface water, sediment communities include:

1. Soil invertebrate community and terrestrial plant community
2. Surface Water Phytoplankton community, water invertebrate community
3. Sediment Benthic invertebrate community

5.4.2 Measurement Receptor for Guilds

A measurement receptor should be selected for each class-specific guild to model (1) COPC dose ingested, and (2) whole body COPC concentration in prey eaten by predators. The selected measurement receptor should be representative of other species in the guild, with respect to the guild's feeding niche in the ecosystem. The risk assessment should demonstrate that using the measurement receptor ensures that risk to other species in the guild is not underestimated. The following factors should be evaluated to identify a measurement receptor:

1. **Ecological Relevance** - Highly relevant receptors provide an important functional or structural aspect in the ecosystem. Attributes of highly relevant receptors typically fall under the categories of food, habitat, production, seed dispersal, pollination, and decomposition. For example, a sustainable population of forage fish might be critical to the sustainability of a population of carnivorous game fish.
2. **Exposure Potential** - Receptors with high exposure potentials are those that, due to their metabolism, feeding habits, location, or reproductive strategy, tend to have higher potentials for exposure than other receptors. For example, the metabolic rates of small receptors are generally higher than those for large animals. This results in a higher ingestion per body weight (i.e., increased exposure potential).
3. **Sensitivity** - Highly susceptible receptors include those with low tolerances to a COPC as well as receptors with enhanced COPC susceptibility due to other concomitant stressors that may not be related to a COPC, such as reduced habitat availability. For example, raptorial birds are highly sensitive to the effects of chlorinated pesticides that bioaccumulate through the food chain.
4. **Social or Economic Importance** - An assessment endpoint may also be based on socially or economically important receptors. These types of receptors include species valued for economic importance such as crayfish and game fish. For these receptors, critical attributes include those that affect survival, production, and fecundity characteristics.
5. **Availability of Natural History Information** - Natural history information is essential to quantitatively evaluate risk to measurement receptors. If this information such as body weight, food, water, soil, and sediment ingestion rates is unavailable for the desired measurement receptor, a surrogate species should be selected.

Although each of these factors should be evaluated when selecting the measurement receptor, at least one of the measurement receptors selected to represent a class-specific guild should have the highest exposure potential (i.e., ingestion rate on a body weight basis). This ensures that risk to other species in the guild is not underestimated.

U.S. EPA's *Wildlife Exposure Factors Handbook* (U.S. EPA 1993a) is an example of an excellent source of dietary and other natural history information.

5.4.3 Measurement Receptors for Example Food Webs

Consistent with the discussions already presented, measurement receptors were selected for the example food webs. Receptor information documented in *Wildlife Exposure Factors Handbook* (U.S. EPA 1993a) and available literature was evaluated to determine suitable measurement receptors for each class-specific guild represented in the example food webs. These measurement receptors have been provided as examples to facilitate understanding of the previously described selection process, not every assessment endpoint has been represented (e.g., TL3 omnivorous fish, TL3 omnivorous amphibians and reptiles, and TL4 carnivorous fish) as may be expected for a complete ecological risk assessment at a site. Discussions on each of the example measurement receptors follow.

American Kestrel

The American kestrel (*Falco sparverius*), or sparrow hawk, was selected as the measurement receptor for the carnivorous bird guild in the example shortgrass prairie, tallgrass prairie, shrub/scrub, freshwater wetland, and brackish and intermediate marsh food webs.

American Robin

The American robin (*Turdus migratorius*) was selected as the measurement receptor for the omnivorous bird guild in the example forest food web.

Canvasback

The Canvasback (*Aythya valisineria*) was selected as the measurement receptor for the herbivorous bird guild in all three example aquatic food webs.

Deer Mouse

The deer mouse (*Peromyscus maniculatus*) was selected as the measurement receptor for the herbivorous mammal guild in the example forest, shortgrass prairie, tallgrass prairie, and shrub/scrub food webs.

Least Shrew

The least shrew (*Cryptotis parva*) was selected as the measurement receptor for the omnivorous mammal guild in the example tallgrass prairie, shortgrass prairie, and freshwater wetland food webs.

Long-Tailed Weasel

The long-tailed weasel (*Mistily Renata*) was selected as the measurement receptor for the carnivorous mammal guild in the example forest, tallgrass prairie and shrub/scrub food webs.

Mallard Duck

The mallard duck (*Anas platyrhynchos*) was chosen as the measurement receptor for the omnivorous bird guild for the freshwater wetland and brackish/intermediate marsh food webs.

Marsh Rice Rat

The marsh rice rat (*Oryzomys palustris*) was selected as the measurement receptor for the omnivorous mammal guild in the example brackish/intermediate and salt marsh food web.

Marsh Wren

The marsh wren (*Cistothorus palustris*) was selected as the measurement receptor for the omnivorous bird guild in the example salt marsh food web.

Mink

The mink (*Mustela vison*) was selected as the measurement receptor for the carnivorous mammal guild in the example brackish/intermediate marsh and freshwater food webs.

Mourning Dove

The Mourning Dove (*Zenaida macroura*) was selected as the measurement receptor for the herbivorous bird guild in all four example terrestrial food webs.

Muskrat

The muskrat (*Ondrata zibethicus*) was selected as the measurement receptor for the herbivorous mammal guild in the example freshwater wetland and brackish/intermediate marsh food webs.

Northern Bobwhite

The northern bobwhite (*Colinus virginianus*) was selected as the measurement receptor for the omnivorous bird guild in the example shortgrass prairie and shrub and scrub food webs.

Northern Harrier

The Northern harrier (*Circus cyaneus*), also called the Marsh hawk was selected as the measurement receptor for carnivorous bird guild in the example salt marsh food web.

Red Fox

The red fox (*Vulpes vulpes*) was selected as the measurement receptor for the carnivorous mammal guild in the example salt marsh food web.

Red-Tailed Hawk

The red-tailed hawk (*Buteo jamaicensis*) was selected as the measurement receptor in the carnivorous bird guild in the example forest food web.

Salt Marsh Harvest Mouse

The salt marsh harvest mouse (*Reithrodontomys raviventris*) was selected as the measurement receptor for the herbivorous mammal guild in the example salt marsh food web.

Short-Tailed Shrew

The short-tailed shrew (*Blarina brevicauda*) was selected as the measurement receptor for the omnivorous mammal guild in the example forest food web.

Spotted Sandpiper

The spotted sandpiper (*Actitis macularia*) was selected as the measurement receptor for the carnivorous shore bird guild in the example freshwater wetland, brackish/intermediate, and salt marsh food webs.

Swift Fox

The Swift Fox (*Vulpes velox*) was selected as the measurement receptor for the carnivorous mammal guild in the example shortgrass prairie food web.

Western Meadow Lark

The western meadow lark (*Sturnella neglecta*) was selected as the measurement receptor for the omnivorous bird guild in the example tallgrass prairie food web.

White-Footed Mouse

The white-footed mouse (*Peromyscus polionotus*) was selected as the measurement receptor for the omnivorous mammal guild in the example shrub/scrub food web.

6 Risk Analysis

The analysis phase of a risk assessment consists of assessing the exposure of a measurement receptor to a compound of potential concern (COPC), and toxicity of a COPC to a measurement receptor. The exposure assessment and the toxicity assessment are used to characterize ecological risk.

6.1 Exposure Assessment

Exposure is the contact (e.g., ingestion) of a receptor with a COPC. Exposure of ecological receptors to COPCs emitted from facility sources are evaluated through consideration of exposure pathways. All exposure pathways that are potentially complete should be evaluated. The existence of a potentially complete exposure pathway indicates the potential for a receptor to contact a COPC; it does not require that a receptor be adversely affected. Exposure pathways considered in this guidance include all direct uptake pathways of a COPC from media (e.g., soil, sediment, and surface water) for lower trophic level receptors evaluated at the community level, and ingestion of a COPC contaminated organism (plant or animal food item) or media for higher trophic level receptors evaluated as class-specific guilds. It should be noted that exposure pathways currently not addressed in this guidance due to the limitation of data include:

1. Inhalation and dermal exposure pathways for upper trophic level organisms

2. Ingestion via grooming and preening
3. Foliar uptake of dissolved COPCs by aquatic plants.

Exposure assessment consists of quantifying exposure of a measurement receptor to a COPC. As previously noted, exposure to community and class-specific guild measurement receptors is assessed using different approaches. This is because the available toxicity reference values (*TRVs*) used in risk characterization for lower trophic level communities are media specific; whereas *TRVs* for upper trophic level class-specific guilds are provided in terms of dose ingested.

For community measurement receptors (e.g., water, sediment, and soil communities), the exposure assessment consists of determining the COPC concentration in the media that the particular community inhabits. For example, the COPC concentration in soil is determined during the exposure assessment for comparison to the NOAEL for terrestrial plants and soil invertebrates during risk characterization. For class-specific guild measurement receptors, exposure is assessed by quantifying the daily dose ingested of contaminated media and/or organism (expressed as the mass of COPC ingested per kilogram body weight per day).

6.2 Assessing Exposure to Community Measurement Receptors

Since exposure to communities is assumed to be primarily through contact with COPCs within the media they inhabit, the assessment of exposure for community measurement receptors is simply the determination of the COPC concentration in the media that they inhabit. Exposure for water, sediment, and soil community measurement receptors should be determined as follows:

1. **Water Community** - Exposure to the water community as a measurement receptor (e.g., water invertebrates or phytoplankton in the freshwater/wetland food web) is assessed by determining the COPC dissolved water concentration (*C_{dw}*) at the specific location being evaluated.
2. **Sediment Community** - Exposure to the sediment community as a measurement receptor (e.g., sediment invertebrates in the brackish/intermediate food web) is assessed by determining the COPC concentration in bed sediment (*C_{sed}*) at the specific location being evaluated.
3. **Soil Community** - Exposure to the soil community as a measurement receptor (e.g., soil invertebrates or terrestrial plants in the forest food web) is assessed by determining the COPC concentration in soil (*C_s*) at the specific location being evaluated.

6.3 Assessing Exposure to Class-Specific Guild Measurement Receptors

Exposure to measurement receptors of class-specific guilds is assessed by quantifying the daily dose ingested of contaminated food items and media. COPC

daily dose ingested (expressed as the mass of COPC ingested per kilogram body weight per day) depends on the COPC concentration in plant and animal food items and media, the measurement receptor's trophic level (i.e., consumer), the trophic level of animal food items (i.e., prey), and the measurement receptor's ingestion rate of each food item and media.

The daily dose of COPC ingested by a measurement receptor, considering all food items and media ingested, can be calculated from the following generic equation:

$$DD = \sum IR_F \cdot C_i \cdot P_i \cdot F_i + (IR_M \cdot C_M \cdot P_M)$$

where:

DD	=	Daily dose of COPC ingested (mg COPC/kg BW-day)
IR_F	=	Measurement receptor plant or animal food item ingestion rate (kg/kg BW-day)
C_i	=	COPC concentration in i th plant or animal food item (mg COPC/kg)
P_i	=	Proportion of i th food item that is contaminated (unitless)
F_i	=	Fraction of diet consisting of plant or animal food item i
IR_M	=	Measurement receptor media ingestion rate (kg/kg BW-day [soil or bed sediment] or L/kg BW-day [water])
C_M	=	COPC concentration in media (mg/kg [soil or bed sediment] or mg/L [water])
P_M	=	Proportion of ingested media that is contaminated (unitless)

The following sections provide guidance for determining values for the above parameters; including:

1. The determination of measurement receptor food item and media ingestion rates
2. The calculation of COPC concentrations in plant and animal food items.

The daily dose of COPC ingested by a measurement receptor should be determined by summing the contributions from each contaminated plant, animal, and media food item. The equation provided above accounts for 100 percent of the measurement receptor's diet (total daily mass of food items ingested) which can potentially be contaminated. However, if a food item or media at an actual site location is not contaminated (i.e., the COPC concentration in the media or resulting food item is zero), then the daily mass of that food item or media ingested does not contribute to the daily dose of COPC ingested.

For measurement receptors ingesting more than one plant or animal food item, the exposure should be quantified separately assuming that the measurement receptor ingests both "equal" and "exclusive" diets. This constitute the most complete evaluation of exposure potential for a measurement receptor, identifying the pathways that are driving risk specific to a COPC and measurement receptor. It

also allows risk management efforts to be prioritized. Guidance for calculating *DD* assuming “equal diet” and “exclusive diet” is provided below.

Equal Diet - To evaluate exposure to a measurement receptor based on an equal diet, the daily dose of COPC ingested is calculated assuming that the fraction of daily diet consumed by the measurement receptor is equal among food item groups. This is computed by setting the value for fraction of diet consisting of plant and/or animal food items, F_i , equal to 1.0 divided by the total number of plant and animal food item groups ingested. Therefore, F_i values within a specific *DD* equation would be the same numerically.

Exclusive Diet - To evaluate exposure to a measurement receptor based on exclusive diets, the daily dose of COPC ingested is calculated assuming that the fraction of daily diet consumed by the measurement receptor is exclusively (100 percent) one food item group. This is computed by setting the value for F_i equal to 1.0 for each food item group at a time, while the F_i values for the remaining food item groups are set equal to zero. The food item designated as exclusive is alternated to each respective food item represented in the *DD* equation, in this section, to obtain a numeric range of exposure values based on exclusive diets. If the daily diet of a food item (i.e., prey) of a measurement receptor (i.e., consumer) also consists of more than one plant or animal food item, then an equal diet should be assumed for the food item being consumed while evaluating exposure to the measurement receptor.

In addition to quantifying exposure based on equal and exclusive diets for measurement receptors, a screening level risk assessment assumes the following:

1. The COPC concentrations estimated to be in food items and media ingested are bio-available.
2. Only contributions of COPCs from the sources (e.g., combustion stacks, fugitives) included in the risk assessment are considered in estimating COPC concentrations in food items and media.
3. The measurement receptor’s most sensitive life stage is present in the assessment area being evaluated in the risk assessment.
4. The body weights and food ingestion rates for measurement receptors are conservative.
5. Each individual species in a community or class-specific guild is equally exposed.
6. The proportion of ingested food items and ingested media that is contaminated is assumed to be 100 percent (i.e., P_i is assigned a value of 1.0); which assumes that a measurement receptor feeds only in the assessment area.

Any site-specific exposure characterizations that may warrant deviation from these screening level assumptions should be reviewed and approved by the appropriate permitting authority.

6.3.1 Ingestion Rates for Measurement Receptors

Species-specific ingestion rates of food items and media, on a body weight basis, are required for calculating the daily dose of COPC ingested for each measurement receptor. Food and water ingestion rates must be provided on a wet weight basis, and ingestion rates for soil and sediment are on a dry weight basis. Table 7 provides values for ingestion rates for measurement receptors identified in the example food webs presented in this Chapter. These values are primarily obtained from the allometric equations presented in the *Wildlife Exposure Factors Handbook* (U.S. EPA 1993a). Soil ingestion rates were calculated using the percent soil in estimated diets of wildlife as described in Beyer et al. (1994).

Species-specific ingestion rates including food and water have been measured for few wildlife species. Therefore, allometric equations presented in the *Wildlife Exposure Factors Handbook* were used to calculate species-specific food and media ingestion rates. Allometry is defined as the study of the relationship between the growth and size of one body part to the growth and size of the whole organism, including ingestion rates, and can be used to estimate species specific values for ingestion (U.S. EPA 1993a).

Allometric equations should only be used for those taxonomic groups used to develop the allometric relationship. For a detailed discussion on the development and limitations of the allometric equations used to obtain ingestion rate values presented in Table 7 see U.S. EPA (1993a) and Nagy (1987).

If species specific values are not available in U.S. EPA (1993a), or can not be represented by the allometric equations presented, other sources to evaluate include:

1. U.S. Fish and Wildlife Service (FWS) publications (e.g., U.S. FWS 1979)
2. State wildlife resource management agencies
3. Published scientific literature
4. Publications by wildlife conservation organizations (such as The National Audubon Society)

Table 7. Ingestion Rates for Example Measurement Receptors.

Measurement Receptor	Example Food Web ^a	Body Weight (kg)	Reference	Food IR ^e (kg WW/kg BW-day)	Reference	Water IR (L/kg BW-day)	Reference	Soil/Sed IR ^m (kg DW/kg BW-day)	Reference
American Kestrel	SG, TG, SS, FW _s	1.00E-01	U.S. EPA 1993a	4.02E-01 ^f	U.S. EPA 1993a;	1.25E-01 ^k	U.S. EPA 1993a	1.39E-03 ⁿ	Pascoe et al. 1996
American Robin	F	8.00E-02	U.S. EPA 1993a	4.44E-01 ^f	U.S. EPA 1993a;	1.37E-01 ^k	U.S. EPA 1993a	1.43E-02 ^o	Beyer et al. 1994
Canvas Back	FW, BR, SW	7.70E-01 _b	U.S. EPA 1993a	1.99E-01 ^f	U.S. EPA 1993a;	6.43E-02 ^k	U.S. EPA 1993a	1.82E-03 ^p	Beyer et al. 1994
Deer Mouse	TG, F, SG, SS	1.48E-02	U.S. EPA 1993a	5.99E-01 ^g	U.S. EPA 1993a;	1.51E-01 ^l	U.S. EPA 1993a	1.44E-03 ^q	Beyer et al. 1994
Least Shrew	SG, FW, TG	4.00E-03	Audubon 1995	6.20E-01 ^h	U.S. EPA 1993a	1.72E-01 ^l	U.S. EPA 1993a	1.36E-02 ^o	Beyer et al. 1994
Long Tailed Weasel	TG, F, SS	8.50E-02	Audubon 1995	3.33E-01 ⁱ	U.S. EPA 1993a;	1.27E-01 ^l	U.S. EPA 1993a	2.98E-03 ^r	Beyer et al. 1994
Mallard Duck	BR, FW	1.04E+00	U.S. EPA 1993a	1.79E-01 ^f	U.S. EPA 1993a;	5.82E-02 ^k	U.S. EPA 1993a	3.18E-03	Beyer et al. 1994
Marsh Rice Rat	BR, SW	3.00E-02	Audubon 1995	4.40E-01 ^g	U.S. EPA 1993a;	1.41E-01 ^l	U.S. EPA 1993a	2.33E-03 ^s	Beyer et al. 1994
Marsh Wren	SW	1.00E-02	U.S. EPA 1993a	9.26E-01 ^f	U.S. EPA 1993a;	2.75E-01 ^k	U.S. EPA 1993a	1.96E-02 ^o	Beyer et al. 1994
Mink	FW, BR	9.74E-01	U.S. EPA 1993a	2.16E-01 ⁱ	U.S. EPA 1993a;	9.93E-02 ^l	U.S. EPA 1993a	1.93E-03 ^r	Beyer et al. 1994
Mourning Dove	F, SS, TG, SG	1.50E-01 _c	U.S. EPA 1993a	3.49E-01 ^f	U.S. EPA 1993a;	1.09E-01 ^k	U.S. EPA 1993a	7.01E-03 ^o	Beyer et al. 1994

Muskrat	BR, FW	1.09E+00	U.S. EPA 1993a	2.67E-01 ^j	U.S. EPA 1993a;	9.82E-02 ^l	U.S. EPA 1993a	6.41E-04	Beyer et al. 1994
Northern Bobwhite	SG, SS	1.50E-01	U.S. EPA 1993a	3.49E-01 ^f	U.S. EPA 1993a;	1.09E-01 ^k	U.S. EPA 1993a	1.20E-02 ^t	Beyer et al. 1994
Northern Harrier	SW	9.60E-01	U.S. EPA 1993a	1.85E-01 ^f	U.S. EPA 1993a;	5.99E-02 ^k	U.S. EPA 1993a	9.95E-03 ⁿ	Beyer et al. 1994
Red Fox	SW	3.94E+00	U.S. EPA 1993a	1.68E-01 ⁱ	U.S. EPA 1993a;	8.63E-02 ^l	U.S. EPA 1993a	1.51E-03	Beyer et al. 1994
Red-tailed Hawk	F	9.60E-01 _d	U.S. EPA 1993a	1.85E-01 ^f	U.S. EPA 1993a;	5.99E-02 ^k	U.S. EPA 1993a	9.95E-03 ⁿ	Beyer et al. 1994
Salt-marsh Harvest Mouse	SW	9.10E-03	U.S. EPA 1993a	7.41E-01 ^g	U.S. EPA 1993a;	1.58E-01 ^l	U.S. EPA 1993a	1.78E-03 ^q	Beyer et al. 1994
Short-tailed Shrew	F	1.50E-02	U.S. EPA 1993a	6.20E-01 ^h	U.S. EPA 1993a	1.51E-01 ^l	U.S. EPA 1993a	1.36E-02 ^o	Beyer et al. 1994
Spotted Sandpiper	SW, BR, FW	4.00E-02	U.S. EPA 1993a	5.69E-01 ^f	U.S. EPA 1993a;	1.74E-01 ^k	U.S. EPA 1993a	4.15E-02 ^u	Beyer et al. 1994
Swift Fox	SG	1.40E+00	U.S. EPA 1993a	1.93E-01 ⁱ	U.S. EPA 1993a;	9.34E-02 ^l	U.S. EPA 1993a	1.73E-03 ^r	Beyer et al. 1994
Western Meadow Lark	TG	9.00E-02	U.S. EPA 1993a	4.21E-01 ^f	U.S. EPA 1993a;	1.31E-01 ^k	U.S. EPA 1993a	1.39E-02 ^o	Beyer et al. 1994
White-footed Mouse	SS	1.00E-02	U.S. EPA 1993a	6.14E-01 ^g	U.S. EPA 1993a;	1.52E-01 ^l	U.S. EPA 1993a	2.70E-03	Beyer et al. 1994

- Notes: IR- Ingestion Rate; WW- Wet weight; DW-Dry Weight; BW- Body Weight; kg - kilogram; L - Liter
- a = Food Webs: BR - Brackish/Intermediate Marsh; F - Forest; FW - Freshwater/Wetland; SG - Shortgrass Prairie; SS - Shrub/Scrub; SW - Saltwater Marsh; TG - Tallgrass Prairie.
 - b = The body weight reported for the mallard is used as a surrogate value for the canvas back.
 - c = The body weight reported for the northern bobwhite is used as a surrogate value for the morning dove.
 - d = The body weight reported for the red-tailed hawk is used as a surrogate value for the northern harrier.
 - e = Food ingestion rate (IR) values are reported in Table 7 as kg WW/kg BW-day. To convert IR from a dry weight (as calculated using allometric equations) to a wet weight basis, the following general equation is used: $IR_{kg\ WW/kg\ BW-day} = (IR_{kg\ DW/BW-day}) / (1 - \% \text{ moisture}/100)$. Ingestion rate values provided in Table 7 are calculated based on assumed percent moisture content of food items of measurement receptors specified. For herbivores, the moisture content of ingested plant matter is assumed to be 88.0 percent (Taiz et al. 1991). For carnivores, the moisture content of ingested animal matter is assumed to be 68.0 percent (Sample et al. 1997). For omnivores, an equal fraction of plant and animal matter is assumed ingested with an overall average moisture content of 78.0 percent $[(88.0 + 68.0)/2]$.
 - f = Food ingestion rates generated using the following allometric equation for all birds: $IR\ (g/day) = 0.648\ Wt^{0.651}\ (g)$.
 - g = Food ingestion rates generated using the following allometric equation for rodents: $IR\ (g/day) = 0.621\ Wt^{0.564}\ (g)$.
 - h = Allometric equations reported in U.S. EPA (1993a) do not represent intake rates for shrews; therefore, measured field values from the referenced sources are presented.
 - i = Food ingestion rates generated using the following allometric equation for all mammals: $IR\ (g/day) = 0.235\ Wt^{0.822}\ (g)$.
 - j = Food ingestion rates generated using the following allometric equation for herbivores: $IR\ (g/day) = 0.577\ Wt^{0.727}\ (g)$.
 - k = Water ingestion rates generated using the following allometric equation for all birds: $IR\ (L/day) = 0.059\ Wt^{0.670}\ (kg)$.
 - l = Water ingestion rates generated using the following allometric equation for all mammals: $IR\ (L/day) = 0.099\ Wt^{0.900}\ (kg)$.
 - m = Soil and sediment ingestion rates calculated based on percent soil in diet as reported in Beyer et al. 1994.
 - n = Percent soil in diet reported for the bald eagle is used as a surrogate value for the American kestrel, northern harrier, and red-tailed hawk.
 - o = Percent soil in diet is assumed as 10.0 percent of diet based on range presented in Beyer et al. 1994.
 - p = Percent soil in diet reported for the mallard is used as a surrogate value for the canvas back.
 - q = Percent soil in diet reported for the white-footed mouse is used as a surrogate value for the deer mouse and salt-marsh harvest mouse.
 - r = Percent soil in diet reported for the red fox is used as a surrogate value for the long-tailed weasel, mink, and swift fox.
 - s = Percent soil in diet is assumed as 2.0 percent of diet based on range presented for herbivores.
 - t = Percent soil in diet reported for the wild turkey is used as a surrogate value for the northern bobwhite.
 - u = Percent soil in diet reported for the western sandpiper is used as a surrogate value for the spotted sandpiper.

6.3.2 COPC Concentrations in Food Items of Measurement Receptors

Determination of COPC concentrations in food items is required for calculating the daily dose of COPC ingested for each class-specific guild measurement receptor being evaluated. Since the risk assessment considers potential future exposure that may occur as a result of facility emissions over time, these concentrations are generally expected to be estimated mathematically. The following subsections provide guidance for estimating COPC concentrations in the following groups of food items:

1. Invertebrates, phytoplankton, and rooted aquatic plants
2. Terrestrial plants
3. Fish
4. Mammals, birds, reptiles, and amphibians

6.3.3 COPC Concentration in Invertebrates, Phytoplankton, and Rooted Aquatic Plants

COPC concentrations in invertebrate, phytoplankton, and rooted aquatic plants can be calculated by rearranging the mathematical expression for a bio-concentration factor (*BCF*). A *BCF* is the ratio, at steady-state, of the concentration of a compound in a food item to its concentration in a media. The equation can also be expressed in terms of a COPC concentration in a food item.

$$BCF = \frac{C_i}{C_M}$$

where:

- BCF* = Bio-concentration factor (unitless [soil, sediment], or L/kg [water])
- C_i* = COPC concentration in *i*th plant or animal food item (mg COPC/kg)
- C_M* = COPC concentration in media (mg/kg [soil, sediment], or mg/L [water])

The above equation estimates a COPC concentration in an invertebrate, phytoplankton, and rooted aquatic plant to evaluate dose ingested to the measurement receptor.

6.3.4 Equilibrium Partitioning (EqP) Approach

When adequate site-specific characterization data is available, specifically organic carbon fraction data for soil and sediment, the permitting authority may elect in some cases to allow the calculation of COPC concentrations in soil invertebrate (Connell and Markwell 1990) or sediment invertebrate (U.S. EPA 1993a) using the equilibrium partitioning (EqP) approach. However, the EqP approach is not preferred over use of measured *BCF* values multiplied by the COPC

concentration in the media (i.e., sediment or soil), following the approach previously discussed.

The EqP approach utilizes the correlation of the concentrations of nonionic organic compounds in sediment, on an organic carbon basis, to their concentrations in the interstitial water, to determine the observed biological effects on sediment invertebrate (U.S. EPA 1993a). The EqP approach is only applicable for:

1. Hydrophobic nonionic organic compounds
2. Soil- and sediment-invertebrates
3. COPCs with empirical water bio-concentration factors (U.S. EPA 1993a).
4. EqP approach assumes that the partitioning of the compound in sediment organic carbon and interstitial water are in equilibrium, and the sediment-interstitial water equilibrium system provides the same exposure as a water-only exposure (U.S. EPA 1993a).

To calculate the COPC concentration in an invertebrate using the EqP approach, the soil or sediment interstitial water concentration should be multiplied by the BCF_{WI} determined from a water exposure for a benthic invertebrate:

$$C_I = C_{IW} \cdot BCF_{WI}$$

where:

- C_I = COPC concentration in soil or benthic invertebrate (mg/kg)
 C_{IW} = COPC concentration in soil or sediment interstitial water (mg/L)
 BCF_{WI} = Bioconcentration factor for water-to-invertebrate (L/kg)

Equation 5-5 is used to calculate the COPC concentration in soil or sediment interstitial water for this approach:

$$C_{IW} = \frac{C_M}{f_{oc} \cdot K_{oc}}$$

where:

- C_{IW} = COPC concentration in soil or sediment interstitial water (mg/L)
 C_M = COPC concentration in media (mg/kg [soil, sediment])
 f_{oc} = Fraction of organic carbon in soil or sediment (unitless)
 K_{oc} = Organic carbon partitioning coefficient (L/kg)

6.3.5 COPC Concentration in Terrestrial Plants

The COPC concentration in terrestrial plants (C_{TP}) is calculated by summing the plant concentration due to direct deposition (Pd), air-to-plant transfer (Pv), and root uptake (Pr). The concentration in terrestrial plants is calculated as follows:

$$C_{TP} = Pd + Pv + Pr$$

where:

- C_{TP} = COPC concentration in terrestrial plants (mg COPC/kg WW)
- Pd = COPC concentration in plant due to direct deposition (mg/kg WW)
- Pv = COPC concentration in plant due to air-to-plant transfer (mg/kg WW)
- Pr = COPC concentration in plant due to root uptake (mg/kg WW)

6.3.6 COPC Concentration in Fish

The COPC concentration in fish is calculated by multiplying a COPC-specific BCF and trophic level-specific FCM by the dissolved water concentration, as follows:

$$C_F = BCF \cdot FCM \cdot C_{dw}$$

where:

- C_F = COPC concentration in fish (mg/kg)
- BCF = Bio-concentration factor for water-to-fish (L/kg)
- FCM = Food-chain multiplier (unitless)
- C_{dw} = Dissolved phase water concentration (mg/L)

The COPC concentration in fish is calculated using dissolved phase water concentrations, since bio-concentration, or estimated bioaccumulation; values are typically derived from studies based on dissolved phase water concentrations. The FCM used to calculate a COPC concentration in fish should be appropriate for the trophic level of the fish ingested by a measurement receptor. Development of FCM values is discussed in the following subsection, and actual recommended values are provided in Table 8.

6.3.7 Food-Chain Multipliers

$FCMs$ presented in Table 8 were adopted directly from U.S. EPA (1995b), which determined them for K_{ow} values ranging from 3.5 through 9.0. U.S. EPA (1995b) calculated trophic level specific $FCMs$ utilizing BAF values obtained from the Gobas (1993) model and compound specific K_{ow} values.

where:

- FCM = Food-chain multiplier (unitless)
- BAF_l = Bioaccumulation factor reported on a lipid-normalized basis using the freely dissolved concentration of a chemical in the water (L/kg)
- K_{ow} = Octanol-water partition coefficient (L/kg)

U.S. EPA (1995b) determined trophic level-specific *FCMs* by calculating the geometric mean of the *FCM* for each organism in each respective trophic level. The *FCMs* were developed assuming no metabolism of a compound. Thus, for compounds where metabolism may occur (i.e., some PAHs), the COPC concentration in fish ingested by a measurement receptor may be overestimated. This information should be noted as an uncertainty in risk characterization.

U.S. EPA (1995b) assumes that a compound's log K_{ow} value approximates its BCF_l , therefore *FCM* values can also be expressed as follows:

$$FCM = \frac{BAF_l}{BCF_l}$$

where:

- FCM* = Food-chain multiplier (unitless)
- BAF_l* = Bioaccumulation factor reported on a lipid-normalized basis using the freely dissolved concentration of a chemical in the water (L/kg)
- BCF_l* = Bio-concentration factor reported on a lipid-normalized basis using the freely dissolved concentration of a chemical in the water (L/kg)

FCMs are specified for use in this guidance to model a COPC concentration in fish, and also mammalian and bird food items, which are ingested by a measurement receptor. The application of *FCMs* derived from aquatic food web data to terrestrial receptors creates uncertainties. However, the *BCF-FCM* approach is recommended because:

1. Evaluation of multiple food chain exposure pathways is typically required to estimate risk to multiple mammalian and avian guilds in several food webs
2. Screening level risk assessment results are intended to support development of permits and focus risk management efforts, rather than as a final point of departure for further evaluation
3. No other applicable multi-pathway approaches for consistently and estimating COPC concentrations in prey ingested by upper-trophic-level ecological receptors, considering current data limitations.

Currently the *BCF-FCM* approach is the best available quantitative method for estimating COPC concentrations in upper trophic level food items ingested by measurement receptors.

Table 8. Food-Chain Multipliers.

Log K_{ow}	Trophic Level of Consumer		
	2	3	4
2.0	1.0	1.0	1.0
2.5	1.0	1.0	1.0
3.0	1.0	1.0	1.0
3.1	1.0	1.0	1.0
3.2	1.0	1.0	1.0
3.3	1.0	1.1	1.0
3.4	1.0	1.1	1.0
3.5	1.0	1.1	1.0
3.6	1.0	1.1	1.0
3.7	1.0	1.1	1.0
3.8	1.0	1.2	1.0
3.9	1.0	1.2	1.1
4.0	1.0	1.3	1.1
4.1	1.0	1.3	1.1
4.2	1.0	1.4	1.1
4.3	1.0	1.5	1.2
4.4	1.0	1.6	1.2
4.5	1.0	1.8	1.3
4.6	1.0	2.0	1.5
4.7	1.0	2.2	1.6
4.8	1.0	2.5	1.9
4.9	1.0	2.8	2.2
5.0	1.0	3.2	2.6
5.1	1.0	3.6	3.2
5.2	1.0	4.2	3.9
5.3	1.0	4.8	4.7
5.4	1.0	5.5	5.8
5.5	1.0	6.3	7.1
5.6	1.0	7.1	8.6
5.7	1.0	8.0	10
5.8	1.0	8.8	12
5.9	1.0	9.7	14
6.0	1.0	11	16
6.1	1.0	11	18
6.2	1.0	12	20
6.3	1.0	13	22
6.4	1.0	13	23
6.5	1.0	14	25
6.6	1.0	14	26
6.7	1.0	14	26
6.8	1.0	14	27
6.9	1.0	14	27
7.0	1.0	14	26
7.1	1.0	14	25
7.2	1.0	14	24
7.3	1.0	13	23
7.4	1.0	13	21
7.5	1.0	13	19
7.6	1.0	12	17
7.7	1.0	11	14
7.8	1.0	10	12

7.9	1.0	9.2	9.8
8.0	1.0	8.2	7.8
8.1	1.0	7.3	6.0
8.2	1.0	6.4	4.5
8.3	1.0	5.5	3.3
8.4	1.0	4.7	2.4
8.5	1.0	3.9	1.7
8.6	1.0	3.3	1.1
8.7	1.0	2.7	0.78
8.8	1.0	2.2	0.52
8.9	1.0	1.8	0.35
9.0	1.0	1.5	0.23

Source: U.S. EPA. 1995b. "Great Lakes Water Quality Initiative Technical Support Document for the Procedure to Determine Bioaccumulation factors." EPA-820-B-95-005. Office of Water. Washington, D.C. March.

6.3.8 COPC Concentration in Mammals, Birds, Amphibians, and Reptiles

The COPC concentration in mammals and birds, as food items ingested by measurement receptors, are estimated using equations specific to each guild (i.e., herbivores, omnivores, and carnivores), and based on the plant and animal food items, and media ingested. Similar to calculating the COPC concentration in fish, a *BCF-FCM* approach is used to account for bioaccumulation. However, the contribution of COPC concentrations from each food item ingested must be accounted for directly for wildlife, whereas, the derivation of *BCF-FCM* values already accounts for the COPC contributions from all pathways for fish. Also for wildlife, a ratio of *FCMs* is applied to each animal food item ingested to account for the increase in COPC concentration occurring between the trophic level of the prey item (TL_n) and the trophic level of the omnivore (TL₃) or carnivore (TL₄).

General equations for estimating COPC concentrations of food items in each guild, including use of a *FCM* ratio to estimate bio-magnification, are described in the following subsections using mammals and birds as examples. It should be noted that due to limited availability of bio-transfer and toxicity data for reptiles and amphibians, the equations in the following subsections have not been specifically described for use to model exposure to these receptors. .

6.3.9 Herbivorous Mammals and Birds

The COPC concentration in herbivorous mammals and birds is calculated by summing the contribution due to ingestion of contaminated plant food items and media. The general equation for computing COPC concentration in herbivores is as follows:

$$C_H = \sum(C_{Pi} \cdot BCF_{Pi-H} \cdot P_{Pi} \cdot F_{Pi}) + (C_{s/sed} \cdot BCF_{S/BS-H} \cdot P_{S/BS}) + (C_{wctot} \cdot BCF_{W-H} \cdot P_W)$$

where:

$$C_H = \text{COPC concentration in herbivore (mg/kg)}$$

C_{Pi}	=	COPC concentration in i th plant food item (mg/kg)
BCF_{Pi-H}	=	Bioconcentration factor for plant-to-herbivore for i th plant food item (unitless)
P_{Pi}	=	Proportion of i th plant food item in diet that is contaminated (unitless)
F_{Pi}	=	Fraction of diet consisting of i th plant food item (unitless)
$C_{s/sed}$	=	COPC concentration in soil or bed sediment (mg/kg)
$BCF_{S/BS-H}$	=	Bioconcentration factor for soil-to-plant or bed sediment-to-plant (unitless)
$P_{S/BS}$	=	Proportion of soil or bed sediment in diet that is contaminated (unitless)
C_{wctot}	=	Total COPC concentration in water column (mg/L)
BCF_{W-HM}	=	Bioconcentration factor for water-to-herbivore (L/kg)
P_W	=	Proportion of water in diet that is contaminated (unitless)

6.3.10 Omnivorous Mammals and Birds

The COPC concentration in omnivorous mammals and birds is calculated by summing the contribution due to ingestion of contaminated animal and plant food items, and media. However, unlike herbivores, which are TL2 consumers, omnivores are TL3 consumers of animal food items and a ratio of FCMs is applied to each animal food item ingested to account for the increase in COPC concentration occurring between the trophic level of the prey item (TLn) and the trophic level of the omnivore (TL3). In general, the COPC concentration in omnivores depends on the COPC concentration in each food item ingested, and the trophic level of each food item, as follows.

$$C_{OM} = \sum \left(C_{Ai} \cdot \frac{FCM_{TL3}}{FCM_{TLn-Ai}} \cdot P_{Ai} \cdot F_{Ai} \right) + \sum (C_{Pi} \cdot BCF_{Pi-OM} \cdot P_{Pi} \cdot F_{Pi}) + \\ (C_{s/sed} \cdot BCF_{S/BS-OM} \cdot P_{S/BS}) + (C_{wctot} \cdot BCF_{W-OM} \cdot P_W)$$

where:

C_{OM}	=	COPC concentration in omnivore (mg/kg)
C_{Ai}	=	COPC concentration in i th animal food item (mg/kg)
FCM_{TL3}	=	Food chain multiplier for trophic level 3 (unitless)
FCM_{TLn-Ai}	=	Food chain multiplier for trophic level of i th animal food item (unitless)
P_{Ai}	=	Proportion of i th animal food item in diet that is contaminated (unitless)
F_{Ai}	=	Fraction of diet consisting of i th animal food item (unitless)
BCF_{Pi-OM}	=	Bioconcentration factor for plant-to-omnivore for i th plant food item (unitless)
C_{Pi}	=	COPC concentration in i th plant food item (mg/kg)
P_{Pi}	=	Proportion of i th plant food item that is contaminated (unitless)

F_{Pi}	=	Fraction of diet consisting of i th plant food item (unitless)
$C_{s/sed}$	=	COPC concentration in soil or bed sediment (mg/kg)
$BCF_{S/BS-OM}$	=	Bio-concentration factor for soil- or bed sediment-to-omnivore (unitless)
$P_{S/BS}$	=	Proportion of soil or bed sediment in diet that is contaminated (mg/kg)
C_{wctot}	=	Total COPC concentration in water column (mg/L)
BCF_{W-OM}	=	Bio-concentration factor for water-to-omnivore (L/kg)
P_W	=	Proportion of water in diet that is contaminated (unitless)

The use of an FCM ratio to estimate bio-magnification between trophic levels is discussed in a following subsection. Calculation of COPC concentrations in animal and food items is further discussed in this work. The variables representing the diet fraction and proportion of diet contaminated are discussed in later.

6.3.11 Carnivorous Mammals and Birds

COPC concentrations in carnivorous mammals and birds are calculated by summing the contribution due to ingestion of contaminated animal and media food items. In general, the equation for computing a COPC concentration for carnivorous food items is similar to the corresponding equation for omnivores; only without the component accounting for ingestion of plant food items. Similarly, a ratio of $FCMs$ is applied to each animal food item ingested to account for the increase in COPC concentration occurring between the trophic level of the prey item (TL_n) and the trophic level of the carnivore (TL_4). The COPC concentration in carnivores depends on the COPC concentration in media, in each animal food item ingested, their respective trophic level, as follows:

$$C_C = \sum \left(C_{Ai} \cdot \frac{FCM_{TL_4}}{FCM_{TL_n-Ai}} \cdot P_{Ai} \cdot F_{Ai} \right) + (C_{s/sed} \cdot BCF_{S/BS-C} \cdot P_{S/BS}) + (C_{wctot} \cdot BCF_{W-C} \cdot P_W)$$

where:

C_C	=	COPC concentration in carnivore (mg/kg)
C_{Ai}	=	COPC concentration in i th animal food item (mg/kg)
FCM_{TL_4}	=	Food chain multiplier for trophic level 4 (unitless)
FCM_{TL_n-Ai}	=	Food chain multiplier for trophic level of i th animal food item (unitless)
P_{Ai}	=	Proportion of i th animal food item in diet that is contaminated (unitless)
F_{Ai}	=	Fraction of diet consisting of i th animal food item (unitless)
$C_{s/sed}$	=	COPC concentration in soil or bed sediment (mg/kg)
$BCF_{S/BS-C}$	=	Bioconcentration factor for soil- or bed sediment-to-carnivore (unitless)

$P_{S/BS}$	=	Proportion of soil or bed sediment in diet that is contaminated (mg/kg)
C_{wctot}	=	Total COPC concentration in water column (mg/L)
BCF_{W-C}	=	Bio-concentration factor for water-to-carnivore (L/kg)
P_W	=	Proportion of water in diet that is contaminated (unitless)

Media-to-carnivore BCF values are COPC and receptor-specific. The use of an FCM ratio to estimate bio-magnification between trophic levels is discussed in the following subsection.

6.3.12 Use of Food Chain Multiplier Ratio to Estimate Bio-Magnification

Bio-magnification involves the transfer of a chemical in food through successive trophic levels (Hamelink et al. 1971). Chemicals with greatest potential to bio-magnify are highly lipophilic, have low water solubilities, and are resistant to being metabolized (Metcalf et al. 1975). The risk assessor should account for COPC bio-magnification in the food chain by the use of FCM ratios as derived by U.S. EPA (1995b).

FCM ratios are used to estimate the increase in a COPC concentration resulting from the ingestion of TL2 prey (i.e., animal food item) by a TL3 measurement receptor (i.e., omnivore or carnivore), and the ingestion of TL2 and TL3 prey by a TL4 measurement receptor. Bio-magnification, expressed as a bio-magnification factor (BMF), equals the quotient of the FCM of the measurement receptor divided by the FCM of the prey. It is important to note that the basic difference between the FCM and BMF is that the $FCMs$ relate back to trophic level one, whereas $BMFs$ always relate back to the preceding trophic level (U.S. EPA 1995b). This relation is entirely compatible, but confusion can result if the terms specific to trophic level are not used consistently and clearly (U.S. EPA 1995b). As presented in U.S. EPA (1995b), the following relation of FCM to BMF can be expressed as follows:

$$BMF_{TL3} = FCM_{TL3}/FCM_{TL2}$$

where:

BMF_n	=	Bio-magnification factor for n th trophic level
FCM_{TLn}	=	Food chain multiplier for n th trophic level

6.4 Assessment of Toxicity

Toxicity of a COPC is assessed by identifying toxicity reference values ($TRVs$) specific to a COPC and the measurement receptor being evaluated. $TRVs$ are subsequently set as the denominator for computing COPC ecological screening quotients ($ESQs$) during risk characterization. The available $TRVs$ used in risk characterization for lower trophic level communities are media specific; whereas

TRVs for upper trophic level class-specific guilds are provided in terms of dose ingested.

Community (lower trophic level) *TRVs* are media specific and used to screen ecological effects to receptors inhabiting soil, surface water, and sediment. Community *TRVs* are expressed on a concentration basis, such as milligrams of COPC per kilogram of soil, and generally either:

1. A COPC media concentration that, based on its intended use by a regulatory agency, confers a high degree of protection to receptor populations or communities inhabiting the media (these include regulatory values such as federal ambient water quality criteria, state no-effect-level sediment quality guidelines, and sediment screening effect concentrations), or
2. A laboratory-derived toxicity value representing a COPC media concentration that causes, over chronic exposure duration, no adverse effects to a representative ecological receptor (e.g., no-observed-effect-concentration).
3. Class-specific guild (upper trophic level) *TRVs* are used to screen ecological effects to wildlife, and expressed as a COPC daily dose ingested that causes, over a chronic exposure duration, no observed adverse effects to a measurement receptor. Class-specific guild *TRVs* are expressed in units of mass (e.g., milligrams or micrograms) of COPC per kilogram body weight (wet weight) per day.

Guidance for selection of *TRVs* for community and class-specific guild measurement receptors is provided in the following sections.

6.4.1 General Guidance on Selection of Toxicity Reference Values

Compound specific *TRVs* should be identified for each measurement receptor evaluated to characterize risk to a community or class-specific guild. U.S. EPA recommends evaluation of the following sources of toxicity values, listed in order of general preference, in determining *TRVs* for use in a screening level risk assessment:

Toxicity values developed and/or adopted by federal and/or state regulatory agencies; generally provided in the form of standards, criteria, guidance, or benchmarks. Toxicity values developed and/or adopted by federal or state regulatory agencies are generally media specific, and reported only for surface water and sediment. Examples include the federal ambient water quality criteria (AWQC) and the National Oceanic and Atmospheric Administration (NOAA) effects range-low (ERL) values for sediment (Long et al. 1995).

Toxicity values published in scientific literature. Appropriate values should be derived from a laboratory study, which characterizes adverse effects on ecologically-relevant endpoints, such as growth, reproduction, and mortality.

Toxicity values calculated for sediment using equilibrium partitioning (EqP) approach. Calculating sediment toxicity values using the EqP approach requires determination of (1) an organic carbon content of the sediments, and (2) a corresponding surface water toxicity value.

Toxicity values from surrogate compounds. Surrogate compounds are selected through evaluation of parameters such as chemical structure and toxicity mechanisms of action. For example, low molecular weight (i.e. those have two or less rings) polycyclic aromatic hydrocarbons (PAH's) could be grouped together and evaluated using the toxicity data from a PAH congener belonging to this group.

The evaluation of toxicity values published in scientific literature should consider:

1. Ecological relevance of the study
2. Exposure duration (e.g., chronic, acute)
3. Study endpoints (e.g., NOAEL, LOAEL).

The identification of literature toxicity values used to derive *TRVs* should focus on toxicological data characterizing adverse effects on ecologically relevant endpoints, such as growth, seed germination, reproduction, and survival. Study endpoints specified for reported toxicity values generally include the following:

1. Soil, surface water, and sediment measurement receptors
 - No-observed-effect-level (NOEL) or no-observed-effect-concentration (NOEC)
 - Lowest-observed-effect-level (LOEL) or lowest-observed-effect-concentration (LOEC)
 - Median lethal concentration to 50 percent of the test population (LC50) or median effective concentration for 50 percent of the test population (EC50)
2. Wildlife measurement receptors
 - No-observed-adverse-effect-level (NOAEL)
 - Lowest-observed-adverse-effect-level (LOAEL)
 - Median lethal dose to 50 percent of the test population (LD50)

When multiple studies are assessed equally under the criteria above, professional judgment can be applied to determine the most appropriate study and corresponding toxicity value to be selected as the *TRV*. Toxicity values obtained from scientific literature may also require application of an UF to account for extrapolation uncertainty (due to differences in test endpoint and exposure duration) when considering use of the test value as a *TRV* in a screening level risk assessment.

6.4.1.1 Evaluation of Toxicity Test Data

A *TRV* should represent a COPC concentration or dose that causes no observed adverse effects to an ecologically relevant endpoint of a receptor exposed for a chronic (long-term) duration. As noted above, evaluation of test data from ecologically relevant studies should be further assessed based on exposure duration and study endpoint.

The following hierarchy, in terms of decreasing preference, should be followed to assess exposure duration and study endpoint:

1. Chronic NOAEL
2. Sub-chronic NOAEL
3. Chronic LOAEL
4. Sub-chronic LOAEL
5. Acute median lethality point estimate
6. Single dose toxicity value

The following guidelines should be used to generally determine exposure duration:

1. For fish, mammals, and birds:
 - A chronic test lasts for more than 90 days
 - A subchronic test lasts from 14 to 90 days
 - An acute test lasts less than 14 days
2. For other receptors:
 - A chronic test lasts for 7 or more days
 - A subchronic test lasts from 3 to 6 days
 - An acute test lasts less than 3 days

Sources of toxicity values include electronic databases, reference compendia, and technical literature. Toxicity values identified from secondary sources should be verified, wherever possible, by reviewing the original study. If an original study is unavailable, or multiple studies of similar quality are available, best professional judgment should be used to determine an appropriate toxicity value.

6.4.1.2 Best Professional Judgment for Evaluating Toxicity Values

If more than one toxicity study meets a set of qualifying criteria applicable for study endpoint and exposure duration, best professional judgment should be used to identify the most appropriate study and corresponding toxicity value for *TRV* selection. The most appropriate study is the one with the least uncertainty about the accuracy of the value of endpoint (i.e., NOAEL) that, ultimately, provides the greatest degree of protectiveness to the applicable measurement receptor. The most appropriate study should be identified by reviewing the experimental design of each study. Important aspects of experimental design that should be evaluated include:

1. **Number of treatments, spread between treatments, and number of replicates per treatment.** The number of treatments and the spread between exposure concentrations (or dose groups) will affect the accuracy of the test endpoint (such as the NOAEL).
2. **Exposure route.** The exposure route of the test should coincide with the applicable exposure route or pathway under consideration in the risk assessment.
3. **Exposure during sensitive life stage.** Ideally, all toxicity studies would evaluate the effects of a toxicant on the most sensitive life stage, such as neonatal zooplankton and first instar larvae. Therefore, the exposure duration should be receptor - and toxicant-specific.
4. **Nominal or measured test concentrations.** Measured test concentrations more accurately estimate the true concentration of a toxicant presented to a receptor. Nominal, or unmeasured, test concentrations do not account for potential losses of the toxicant (such as toxicant adsorbed to particulate material) or for inaccuracies in preparing test solutions. In addition, samples for measuring test concentrations should be collected from the exposure chamber, not the delivery system.
5. **Use, type, and performance of controls.** A positive control (no toxicant) should be used in each toxicity study. The only difference between a positive control and a treatment is the absence of the toxicant from the control.
6. **Method used to determine endpoint (i.e., NOAEL).** Ideally, an acceptable number of replicates should be used so a test has statistical power. An appropriate statistical test should be performed to identify the NOAEL.

6.4.1.3 Uncertainty Factors for Extrapolation from Toxicity Test Values (TRVs)

Incomplete knowledge of the actual toxicity of a chemical leads to the use of UFs to reduce the likelihood that risk estimates do not underestimate risk. Historically, UFs have been used for various extrapolations, and their applications reflect policy to provide conservative estimates of risk (Chapman et al. 1998). UFs are used in the risk assessment to reduce the probability of underestimating ecological risk from exposures to combustor emissions. This is performed by multiplying a toxicity value by a UF to produce a *TRV* reflecting an NOAEL for a chronic exposure duration.

In most cases, the UFs discussed below should be applicable to available toxicity values. In some cases, however, irregular toxicity data (such as, a sub-chronic LC50) may be the only available information.

Specifically, UFs should be used to account for extrapolation uncertainty due to differences in test endpoint and exposure duration:

1. Test endpoint uncertainty-extrapolation from a non-NOAEL endpoint (e.g., LOAEL, LD50) to an NOAEL endpoint
2. Duration uncertainty-extrapolation from a single dose, acute, or sub-chronic duration to a chronic duration
3. Except as noted above for irregular toxicity data, the following UFs (Calabrese and Baldwin 1993) should be used to convert a toxicity test endpoint to a *TRV* equivalent to a chronic NOAEL:
4. A chronic LOAEL (or LOEL or LOEC) should be multiplied by a UF of 0.1 to convert it to a chronic NOAEL
5. A sub-chronic NOAEL should be multiplied by a UF of 0.1 to convert it to a chronic NOAEL.
6. An acute lethal value (such as an LC50 or LD50) should be multiplied by an UF of 0.01 to convert it to a chronic NOAEL.

7 Risk Characterization

Risk characterization includes risk estimation and risk description (U.S. EPA 1992b). Risk estimation is an integration of the exposure assessment and the toxicity assessment to determine the potential risk to a community or guild from exposure to a COPC. Risk estimation is quantified using the quotient method to calculate an Ecological Screening Quotient (*ESQ*) (Suter 1993). Risk description describes the magnitude and nature of potential risk for each community and guild, based on the quantitative results of the risk estimation and calculated *ESQ* values. Risk assessment reports should discuss the significance of the default assumptions used to assess exposure, because they affect the magnitude and certainty of the calculated *ESQ* value. The resultant risk characterization should consider any major uncertainties and limitations associated with results generated in performing the screening level risk assessment.

7.1 Risk Estimation

To estimate potential ecological risk, an *ESQ* should be calculated specific to each measurement receptor, COPC, and exposure scenario location evaluated in the risk assessment. Also, dietary-variable *ESQ*s should be computed for class-specific guild measurement receptors based on “equal diet” dose and “exclusive diet” dose. An *ESQ* is the quotient of the COPC Estimated Exposure Level (*EEL*) divided by the COPC and measurement receptor specific Toxicity Reference Value (*TRV*), as follows:

$$ESQ = \frac{EEL}{TRV}$$

where:

ESQ = Ecological screening quotient (unitless)

- EEL = COPC estimated exposure level (mass COPC/mass media [communities] or mass daily dose COPC ingested/mass body weight-day [class-specific guilds])
- TRV = COPC toxicity reference value (mass COPC/mass media [communities] or mass daily dose COPC ingested/mass body weight-day [class-specific guilds])

Care should be made to ensure that the units for the EEL value and the TRV are consistent, including correct use of corresponding wet and dry weights. TRV s specific to organic and inorganic compounds are typically expressed in units of $\mu\text{g}/\text{kg}$ and mg/kg , respectively.

ESQ s for community measurement receptors are calculated using EEL s specific to the COPC concentration in the corresponding media. A COPC specific ESQ should be calculated for each community measurement receptor at each location evaluated, as appropriate for the food web being analyzed in the risk assessment. For calculating ESQ s for class-specific guild measurement receptors, the EEL is the daily dose of COPC ingested. A COPC specific ESQ should also be calculated for each class-specific guild measurement receptor at each location evaluated, as appropriate for the food web being analyzed in the risk assessment. For class-specific guild measurement receptors, ESQ s should be calculated specific to equal and exclusive diets.

To evaluate potential risk resulting from exposure of a measurement receptor to multiple COPCs at a specific location, each of the COPC-specific ESQ values should be summed to determine a total ESQ .

$$ESQ_{ReceptorTotal} = \sum ESQ_{COPC\ Specific}$$

where:

- $ESQ_{Receptor\ Total}$ = Total ecological screening quotient for receptor (unitless)
- $ESQ_{COPC\ Specific}$ = COPC specific ecological screening quotient (unitless)

As for COPC-specific ESQ s, total ESQ s for class-specific guild measurement receptors should be calculated specific to equal and exclusive diets.

7.2 Risk Description

Risk description considers the magnitude and nature of potential risk for community and class-specific guild measurement receptors evaluated. Risk descriptions also provide information for the risk manager and permitting authority to evaluate the significance of an ESQ value.

7.3 Magnitude and Nature of Ecological Risk

The magnitude and nature of potential risk should be further considered for each measurement receptor with a COPC-specific *ESQ* value equal to or above risk target levels specified by the appropriate permitting authority. Interaction between the risk assessor and the risk manager and permitting authority has been noted throughout the process. At the risk characterization phase of the risk assessment, most of the interaction between the risk assessor and the risk manager and permitting authority is through description of the certainty of the resulting risk estimates. The risk manager and permitting authority with input from the risk assessor should also consider the need to collect additional information to refine risk estimates and/or implement permit requirements.

The magnitude and nature of potential risk should also be further considered for each measurement receptor with a total *ESQ* value greater than or equal to the target risk levels. The resulting total *ESQ* is determined by summing COPC-specific *ESQs* that will usually be calculated utilizing *TRVs* based on different effects (e.g. growth, reproduction), toxicity endpoints (e.g., NOAEL, LOAEL) and/or exposure durations (e.g., chronic, acute). In considering usability of total *ESQs*, The risk manager and the risk assessor should focus on the highest contributing COPCs, or classes of COPCs, which can appropriately be added across effects, toxicity endpoints and exposure durations, in further evaluating potential risks due to exposure to multiple COPCs.

Potential adverse effects should be described for each community and guild with a COPC-specific or total *ESQ* value equal to or above risk target levels. This should be performed for each selected food web and receptor location evaluated, and specific to equal and exclusive diets for applicable class-specific guilds. The description should characterize potential risk to the selected assessment endpoints, based on the measures of effect and measurement receptors. Risk description specific to a measurement receptor should include, at a minimum:

1. The contributing COPCs
2. The emission sources
3. The Exposure pathways used in the assessment
4. The relevant uncertainties.

7.3.1 Target Levels

Target levels are risk management based and set by the regulatory authority. Target values are not a discrete indicator of observed adverse effect. If a calculated risk falls within target values, a regulatory authority may, without further investigation, conclude that a proposed action does not present an unacceptable risk. A calculated risk that exceeds these targets, however, would not, in and of itself, indicate that the proposed action is not safe or that it presents an unacceptable risk. Rather, a risk calculation that exceeds a target value

triggers further careful consideration of the underlying scientific basis for the calculation.

7.3.2 Fate and Exposure Assumptions

The screening level ecological risk assessment is based on numerous conservative assumptions affecting the potential for a receptor to be exposed to a compound emitted from a facility and the numeric magnitude of the resulting estimated risk. These fate and exposure assumptions are required as a result of current data gaps and uncertainties associated with available scientific information and data required for risk evaluation. Note that the risk assessor should revise default data as more precise information becomes available to address data gaps and reduce uncertainties specific to ecological risks. Some of the fate and exposure assumptions utilized in this guidance to conduct a screening level risk assessment are listed below:

1. The estimated COPC concentration in soil and sediment is 100 percent bio-available. This includes a COPC that is weakly or strongly adsorbed to particles and a COPC that is dissolved in interstitial water.
2. The estimated dissolved COPC concentration in the water column is 100 percent bio-available. For ingestion of water by wildlife, this includes a COPC that is freely dissolved as an ion or compound, and a COPC that may be adsorbed to another matrix, such as dissolved organic carbon.
3. The total COPC mass estimated to be ingested by a measurement receptor is taken up across the gut and reaches the site of toxic action. This includes COPC concentrations in food items and abiotic media. This assumes that no fraction of the COPC mass is metabolized or otherwise depurated by an ecological receptor, and that there is no competition for available sites where the toxic action occurs.
4. The chemical species present is the most toxic form, and is the form represented by the *TRV*.
5. Community measurement receptors inhabiting an abiotic medium take up 100 percent of the COPC concentration to which they are exposed. All COPC mass taken up by a plant or animal food item of a measurement receptor is assimilated into edible biomass.
6. An ecological receptor is continuously exposed during its entire life, including critical life stage(s).
7. A measurement receptor's home range is 100 percent within the assessment area being evaluated in the risk assessment.
8. A measurement receptor's food is 100 percent contaminated.

The relevance of fate and exposure assumptions specific to COPCs at a site, and their numerical bias to resulting *ESQ* values should be considered before application of results.

7.3.3 Uncertainty and Limitations of the Risk Assessment

The discussion of uncertainties in this section was adopted from the U.S. EPA *1996 Risk Assessment Support to the Development of Technical Standards for Emissions from Combustion Units Burning Hazardous Waste*.

Uncertainty can be introduced into a risk assessment at every step of the process outlined in this document. Uncertainty occurs, because risk assessment is a complex process, requiring the integration of the following:

1. Release of pollutants into the environment
2. Fate and transport of pollutants, in a variety of different and variable environments, by processes that are often poorly understood or too complex to quantify accurately
3. Potential for adverse effects in receptors, as extrapolated from studies of differing species
4. Probability of adverse effects in functionality of food web that is made up of species that are highly variable

Uncertainty is inherent in the process even if the most accurate data with the most sophisticated models are used. The methodology outlined in this document relies on a combination of point values—some conservative and some typical—yielding a point estimate of exposure and risk that falls at an unknown percentile of the full distributions of exposure and risk. For this reason, the degree of conservatism in risk estimates cannot be known; instead, it is known that the values combine many conservative factors and are likely to overstate actual risk (Hattis and Burmaster 1994).

It should also be noted, variability is often used interchangeably with the term “uncertainty,” but this is not strictly correct. Variability may be tied to variations in physical and biological processes, and cannot be reduced with additional research or information, although it may be known with greater certainty (for example, the weight distribution of a species may be known and represented by the mean weight and its standard deviation). “Uncertainty” is a description of the imperfect knowledge of the true value of a particular variable or its real variability in an individual or a group. In general, uncertainty is reducible by additional information-gathering or analysis activities (that is, better data or better models), whereas real variability will not change (although it may be more accurately known) as a result of better or more extensive measurements (Hattis and Burmaster 1994).

7.3.4 Types of Uncertainty

Finkel (1990) classified all uncertainty into four types:

1. Variable uncertainty
2. Model uncertainty
3. Decision-rule uncertainty
4. Variability.

Variable uncertainty and model uncertainty are generally recognized by risk assessors as major sources of uncertainty; decision rule is of greatest concern to the risk manager.

7.3.5 Variable Uncertainty

Variable uncertainty occurs when variables appearing in equations cannot be measured precisely or accurately, because of either (1) equipment limitations, or (2) spatial or temporal variances between the quantities being measured. Random, or sample, errors are common sources of variable uncertainty that are especially critical for small sample sizes. It is more difficult to recognize nonrandom, or systematic, errors that result from the basis for sampling, experimental design, or choice of assumptions. True variability is something we can not do much about (except to know that it exists).

7.3.6 Model Uncertainty

Model uncertainty is associated with all models used in all phases of a risk assessment. For example, the use of a single species to represent several will introduce uncertainty into the risk assessment because of the considerable amount of interspecies variability in sensitivity to a COPC. Computer models are simplifications of reality, requiring exclusion of some variables that influence predictions but cannot be included in models because of:

1. Increased complexity
2. A lack of data for these variables.

AERMOD—the air dispersion model recommended for use—has not been widely applied in its present form. Few data are available on atmospheric deposition rates for chemicals other than criteria pollutants, thereby making it difficult to (1) select input variables related to deposition, and (2) validate modeled deposition rates. Because dry deposition of vapor phase materials is evaluated external to the air dispersion model, the plume is not depleted and, as a result, mass balance is not maintained. The effect of this would be to overestimate deposition, but the magnitude of the overestimation is unknown.

In addition to air dispersion modeling, the use of other fate and transport models recommended by the USEPA will also result in some uncertainty.

7.3.7 Decision-Rule Uncertainty

Decision-rule uncertainty is probably of greatest concern to risk managers. This type of uncertainty arises, for example, out of the need to balance different social concerns when determining an acceptable level of risk. The uncertainty associated with risk analysis influences many policy and risk management decisions. Possibly the most important aspect for the risk estimates is the selection of constituents to be included in the analysis.

7.3.8 Description of Qualitative Uncertainty

Often, sources of uncertainty in a risk assessment can be determined but cannot be quantified. For example, this can occur when a factor is known or expected to be variable, but no data are available (e.g., presence of COPCs without toxicity data). Uncertainty also often arises out of a complete lack of data. A process may be so poorly understood that the uncertainty cannot be quantified with any confidence.

7.3.9 Description of Quantitative Uncertainty

Knowledge of experimental or measurement errors can also be used to introduce a degree of quantitative information into a qualitative presentation of uncertainty. For example, standard laboratory procedures or field sampling methods may have a known error level that can be used to quantify uncertainty. In many cases, uncertainty associated with particular variable values or estimated risks can be expressed quantitatively and further evaluated with variations of sensitivity analyses. Finkel (1990) identified a six-step process for producing a quantitative uncertainty estimate:

1. Define the measure of risk (i.e., assessment endpoint). More than one measure of risk may result from a particular risk assessment.
2. Specify “risk equations” that present mathematical relationships that express the risk measure in terms of its components. This step is used to identify the important variables in the risk estimation process.
3. Generate an uncertainty distribution for each variable or equation component. These uncertainty distributions may be generated by using analogy, statistical inference techniques, expert opinion, or a combination of these.
4. Combine the individual distributions into a composite uncertainty distribution.
5. Recalibrate the uncertainty distributions. Inferential analysis could be used to “tighten” or “broaden” particular distributions to account for dependencies among the variables and to truncate the distributions to exclude extreme values.
6. Summarize the output clearly, highlighting the important risk management implications. Address specific critical factors, as for example:
 - a. Implication of supporting a point estimate produced without considering uncertainty
 - b. Balance of the costs of under-or over-estimating risks
 - c. Unresolved scientific controversies, and their implications for research

When a detailed quantitative treatment of uncertainty is required, statistical methods are employed. Two approaches to a statistical treatment of uncertainty with regard to variable values are described here and were used in this analysis where appropriate. The first is to use an appropriate statistic to express all variables for which uncertainty is a major concern. For example, if a value used

is from a sample (such as yearly emissions from a stack), the risk assessor should present the mean and standard deviation. Selection of the appropriate statistic depends on the amount of data available and the degree of detail required. Uncertainties can be propagated by using analytical or numerical methods.

A second approach is to use the probability distributions of major variables to propagate variable value uncertainties through the equations used in a risk analysis. A probability distribution of expected values is then developed for each variable value. These probability distributions are typically expressed as either Probability Density Functions (*PDF*) or Cumulative Density Functions (*CPF*). The *PDF* presents the relative probability for discrete variable values, whereas the *CPF* presents the cumulative probability that a value is less than or equal to a specific value.

A composite uncertainty distribution is created by combining the individual distributions with the equations used to calculate the probability of particular adverse effects and points. Numerical or statistical methods are often used. In Monte Carlo simulations, for example, a computer program is used to repeatedly solve the model equations, under different selections of variable values, to calculate a distribution of exposure (or risk) values. Each time the equations are calculated, values are randomly sampled from the specified distributions for each variable. The end result is a distribution of exposure (or risk). These can again be expressed as *PDFs* or, more appropriately, as *CPFs*.

7.3.10 Risk Assessment Uncertainty Discussion

The science of risk assessment is evolving; where the science base is incomplete and uncertainties exist, science policy assumptions must be made. It is important for risk assessors to fully explain the areas of uncertainty in the assessments and to identify the key assumptions used in conducting the assessments. Toward that end, a table should be added to the end of each section (e.g., stack emissions, air modeling, exposure assessment, risk characterization) that lists the key assumptions in that section, the rationale for those assumptions, their effect on estimates of risk (overestimation, underestimation, neutral), and the magnitude of the effect (high, medium, low). For example, it could explain that using a particular input variable, such as exit gas temperature, will under- or overestimate long-term emissions, and the resulting risks, by a factor of x .

Uncertainties specific to other technical components (e.g., TOE, quantification of non-detects) of the risk assessment process are further described in their respective chapters or sections of this guidance.

7.3.11 Limitations and Uncertainties Specific to a Screening Level Ecological Risk Assessment

As a screening-level tool, the screening level ecological risk assessment has several inherent limitations. After computing the *ESQs* and analyzing the risk assessment results, the risk assessor should evaluate the uncertainty associated with the screening level risk assessment. The following sections provide a list of uncertainties typically evaluated, at least qualitatively, in a screening level risk assessment.

7.3.12 Limitations Typical of a Screening Level Ecological Risk Assessment

The approach used to select the measurement receptors is based, in part, on the premise that if key components of the ecosystem are protected, protection will be conferred to populations and, by extension, communities and the ecosystem. Although this approach is reasonable given the nature of the analysis and the availability of the data, protection of measurement receptors may not always adequately protect all ecologically significant assessment endpoints. Similarly, the selection process for ecological receptors relies on a modified trophic element approach. As a result, representative species may not be the most sensitive to particular compounds, but may have been chosen as a function of their ecological significance and the availability of natural history information.

7.3.13 Uncertainties Typical of a Screening Level Ecological Risk Assessment

A screening level risk assessment is typically performed using at least some default parameter values in place of site-specific measured data, and incorporating assumptions as a result of data gaps. The absence of site-specific information and the need to use these assumptions may result in uncertainty associated with the calculation of *ESQs*. An understanding of the uncertainties associated with the *ESQs* is necessary for understanding the significance of the *ESQs*. After identifying the major uncertainties associated with the risk assessment results, their significance should be evaluated with respect to the computed *ESQs*. Uncertainties that generally should be evaluated in a screening level ecological risk assessment for a combustion facility are listed below:

1. Changes in future COPC emissions compared with modeled emission rates used in the risk assessment.
2. Quantification of emissions and evaluation of non-detects used in the risk assessment.
3. The site-specific representativeness of food web(s) used in the risk assessment.
4. The exposure potential of the measurement receptors.
5. The representativeness of equal and exclusive diet assumptions for measurement receptors.

6. The effect of COPC physicochemical properties on estimates of fate and bioavailability.
7. The effect of site-specific environmental conditions affecting the fate, transport, and bioavailability of the COPCs.
8. The assumption that once exposed, a measurement receptor does not metabolize or eliminate a COPC.
9. The potential risk to measurement receptors of COPCs with no *TRVs*.

References

- Agency for Toxic Substances and Disease Registry (ATSDR). 1989. *Toxicological Profile for 2,4-Dinitrotoluene and 2,6-Dinitrotoluene*. December.
- American Chemical Society. 1980. *Guidelines for Data Acquisition and Data Quality Evaluation in Environmental Chemistry*. Analytical Chemistry. Volume 52. Number 14. Pages 2242-2249. December.
- Baes, C.F., R.D. Sharp, A.L. Sjoreen, and R.W. Shor. 1984. *Review and Analysis of Parameters and Assessing Transport of Environmentally Released Radionuclides through Agriculture*. Oak Ridge National Laboratory. Oak Ridge, Tennessee.
- Beyer, W.N., E.E. Connor, and S. Gerould. 1994. *Estimates of Soil Ingestion by Wildlife*. Journal of Wildlife Management. Volume 58. Pages 375-382.
- Blaylock, B.G., M.L. Frank, and B.R. Shor. 1993. *Methodology for Estimating Dose Rates to Freshwater Biota Exposed to Radionuclides in the Environment* Oak Ridge National Laboratory. Oak Ridge, Tennessee. ES/ER/TM-78.
- Bol, J., M. van den Berg, and W. Seinen. 1989. *Interactive Effects of PCDDs, PCDFs, and PCBs as Assessed by the E.L.S. Bioassay*. Chemosphere. Volume 19. Pages 899-906.
- Calabrese, E.J., and L.A. Baldwin. 1993. *Performing Ecological Risk Assessments*. Lewis Publishers. Chelsea, Michigan. 215 Pages.
- California Air Resources Board. 1990. *Health Risk Assessment Guidelines for Nonhazardous Waste Incinerators*. Prepared by the Stationary Source Division of the Air Resources Board and the California Department of Health Services.
- Carr, A. 1994. *Handbook of Turtles, the Turtles of the United States, Canada and Baja, California*. Comstock Publishing Associates, Ithica, New York.
- Chapman, P.M., A. Fairbrother, and D. Brown. 1998. *A Critical Evaluation of Safety (Uncertainty) Factors for Ecological Risk Assessment*. Environmental Toxicology and Chemistry. Volume 17. Pages 99-108.
- Cohen, M.A., and P.B. Ryan. 1989. *Observations Less than the Analytical Limit of Detection: A New Approach*. Journal of Air Pollution Control Association (JAPCA) Note-Book. Vol. 39, No. 3. Pages 328-329. March.
- Connell, D.W., and R.D. Markwell. 1990. *Bioaccumulation in the Soil to Earthworm System*. Chemosphere. Volume 20. Pages 91-100.

- Duarte-Davidson, R., A. Stewart, R. E. Alcock, I. T. Cousins, and K. C. Jones. 1997. *Exploring the Balance between Sources, Deposition, and the Environmental Burdens of PCDD/Fs in the U. K. Terrestrial Environment: An Aid To Identifying Uncertainties and Research Needs*. Environmental Science and Technology. Volume 31. Pages 1 through 11. January.
- Ehrlich, P.R., D.S. Dobkin, and D. Wheye. 1988. *Birder's Handbook, A Field Guide to the Natural History of North American Birds*. Simon and Schuster, Inc., New York, NY.
- Finkel, A.M. 1990. "Confronting Uncertainty in Risk Management. A Guide for Decision-Makers. Center for Risk Management Resources for the Future. January.
- Gobas, F.A.P.C. 1993. *A Model for Predicting the Bioaccumulation of Hydrophobic Organic Chemicals in Aquatic Food-Webs: Application to Lake Ontario*. Ecological Modeling. Volume 69. Pages 1-17.
- Gobas, F.A.P.C., E.J. McNeil, L. Lovett-Doust, and G.D. Hoffner. 1991. *Bioaccumulation of Chlorinated Aromatic Hydrocarbons in Aquatic Macrophytes*. Environmental Science and Technology. Volume 25. Pages 924-929.
- Hamelink, J.L., R.C. Waybrant, and R.C. Ball. 1971. *A Proposal: Exchange Equilibria Control the Degree Chlorinated Hydrocarbons are Biologically Magnified in Lentic Environments*. Transactions of the American Fisheries Society. Volume 100. Pages 207-214.
- Hattis, D.B., and D.E. Burmaster. 1994. *Assessment of Variability and Uncertainty Distributions for Practical Risk Analyses*. Risk Analysis. 14(5):713-730.
- Hillel, D. 1980. *Fundamentals of Soil Physics*. Academic Press, Inc. New York, New York.
- Hodson, P.V., M. McWhirter, K. Ralph, B. Gray, d. Thiverge, J.H. Carey, G. Van Der Kraak, D. M. Whittle, and M. Levesque. 1992. *Effects of Bleached Kraft Mill Effluent on Fish in the St. Maurice River, Quebec*. Environmental Toxicology and Chemistry. Volume 11. Pages 1635-1651.
- Howard, P.H. 1990. *Handbook of Environmental Fate and Exposure Data For Organic Chemicals*. Lewis Publishers. Chelsea, Michigan. Volume 1. Pages 279-285.
- Hwang S. T. and Falco, J. W. 1986. *Estimation of multimedia exposures related to hazardous waste facilities*. In: Pollutants in a Multimedia Environment. Yoram Cohen, Ed. Plenum Publishing Corp. New York.
- Idaho National Engineering and Environmental Laboratory. 1997. *Idaho National Engineering and Environmental Laboratory Waste Experimental Reduction Facility (WERF) Incinerator Trial Burn, May and July 1997, Volume 1*. U.S. Department of Energy. INEEL/EXT-97-01180. October.
- Jury, W.A., and R.L. Valentine. 1986. *Transport Mechanisms and Loss Pathways for Chemicals in Soil*. Vadose Zone Modeling of Organic Pollutants. S.C. Hern and S.M. Melancorn, Editors. Lewis Publishers, Inc. Chelsea, Michigan.
- Lindqvist, O., K. Johansson, M. Aastrup, A. Andersson, L. Bringmark, G. Hovsenius, L. Hakanson, A. Iverfeldt, M. Meili, and B. Timm. 1991. *Mercury in the Swedish Environment - Recent Research on Causes, Consequences and Corrective Methods*. Water, Air and Poll. 55:(all chapters).

Lodge, K., P.M. Cook, D.R. Marklund, S.W. Kohlbry, J. Libal, C. Harper, B.C. Butterworth, and A.G. Kizlauskas. 1994. *Accumulation of Polychlorinated Dibenzo-p-dioxins (PCDDs) and Dibenzofurans (PCDFs) in Sediments and Fishes of Lake Ontario*.

Long, E.R., and others. 1995. *Incidence of Adverse Biological Effects Within Ranges of Chemical Concentrations in Marine and Estuarine Sediments*. Environmental Management. Volume 19, Pages 81-97.

Lyman, W.J., W.F. Reehl, and D.H. Rosenblatt. 1990. *Handbook of Chemical Property Estimation Methods*. American Chemical Society. Washington, D.C.

Manahan, Stanley E. 1991. *Environmental Chemistry*. Fifth Edition. Chelsea, Michigan. Lewis Publishers.

Metcalf, R.L., J.R. Sanborn, P.Y. Yu, and D. Nye. 1975. *Laboratory Model Ecosystem Studies of the Degradation and Fate of Radiolabeled Tri-, Tetra-, and Pentachlorobiphenyl Compared to DDE*. Archives of Environmental Contamination and Toxicology. Volume 3. Pages 151-165.

Nagy, Kenneth A. 1987. *Field Metabolic Rate and Food Requirement Scaling in Mammals and Birds*. Ecological Monographs. Volume 57, Number 2. Pages 111-128.

New York State Department of Environmental Conservation. 1993. *Technical Guidance for Screening Contaminated Sediments*. Divisions of Fish and Wildlife, and Marine Resources. November 22.

National Institution of Occupational Safety and Health (NIOSH). 1994. *Product Guide to Chemical Hazards*. U.S. Department of Health and Human Services. Cincinnati, Ohio.

Oak Ridge National Laboratory. 1996. *Screening Benchmarks for Ecological Risk Assessments Version 1.5* (database). Environmental Sciences and Health Research Division. Prepared for U.S. Department of Energy.

O'Connor, D.J. and W.E. Dobbins. 1958. *Mechanism of Reaeration in Natural Streams*. ASCE Transactions. Pages 641-684. Paper 2934.

Odum, E.P. 1971. *Fundamentals of Ecology*. Third Edition. W.B. Saunders Company. Philadelphia, Penn. 574 pp.

Pascoe, G.A. and others. 1996. *Food Chain Analysis of Exposures and Risks to Wildlife at a Metals-Contaminated Wetland*. Archives of Environmental Contamination and Toxicology. Volume 30. Pages 306-318.

Research Triangle Institute (RTI). 1996. *Risk Assessment Support to the Development of Technical Standards for Emissions from Combustion Units Burning Hazardous Wastes: Background Information Document*. Final Report. EPA Contract Number 68-W3-0028. February 20.

Root, R.B. 1967. *The Niche Exploitation Pattern of the Blue-Gray Gnatcatcher*. Ecological Monographs. Volume 37, Pages 317-350.

Sample, B.E., M.S. Aplin, R.A. Efrogmson, G.W. Suter II and C.J.E. Welsh. 1997. *Methods and Tools for Estimation of the Exposure of Terrestrial Wildlife to Contaminants*. Prepared for U.S. Department of Energy. Oak Ridge National Laboratory. Oak Ridge, Tennessee. ORNL/TM-13391. October.

- Sandmeyer, E. E. 1981. *Aromatic Hydrocarbons*. In George D. Clayton and Florence E. Clayton, Editors. *Patty's Industrial Hygiene and Toxicology*. Third Revised Edition. Volume 2B. New York. John Wiley & Sons.
- Scire, J.S., D.G. Strimaitis, and R.J. Yamartino. 1990. *Model Formulation and User's Guide for The CALPUFF Dispersion Model*. Sigma Research Corporation. Concord, Massachusetts.
- Suter, G.W. II. 1993. *Ecological Risk Assessment*. Lewis Publishers. Chelsea, Michigan. 538 Pages.
- Suter, G.W. II, and J. Mabrey. 1994. *Toxicological Benchmarks for Screening of Potential Contaminants of Concern for Effects of Aquatic Biota on Oak Ridge Reservation: 1994 Revision*. Oak Ridge National Laboratory. Oak Ridge, Tennessee. ES/ER/TM-86/R2.
- Taiz, L., and E. Geiger. 1991. *Plant Physiology*. Benjamin/Cammius Publishing Co. Redwood City, California. 559 pp.
- Travis, C.C., and A.D. Arms. 1988. *Bioconcentration of Organics in Beef, Milk, and Vegetation*. Environmental Science and Technology. 22:271-274.
- U.S. Congress. 1989. *Clean Air Act Amendments of 1989*. Senate Report No. 228. 101st Congress. First Session. Pages 153-154. December 20.
- U.S. Department of Agriculture (USDA). 1982. *Average Annual Values for the Rainfall Factor, R*. Soil Conservation Service Technical Guide, Section I-C-2. Columbia, Missouri. July.
- USDA. 1997. *Predicting Soil Erosion by Water: A Guide to Conservation Planning With the Revised Universal Soil Loss Equation (RUSLE)*. Agricultural Research Service, Agriculture Handbook Number 703. January.
- U.S. Department of Energy (DOE). 2002. *A Graded Approach for Evaluating Radiation Doses to Aquatic and Terrestrial Biota*. Washington, D.C., DOE-STD-1153-2002. July 2002.
- U.S. EPA. 1980a. *Environmental Assessment of a Waste-to-Energy Process. Braintree Municipal Incinerator*. Office of Research and Development (ORD). Washington, D.C. EPA 600/7-80/149.
- U.S. EPA. 1985. *Water Quality Assessment: A Screening Procedure for Toxic and Conventional Pollutants in Surface and Ground Water Part I (Revised)*. ORD. Athens, Georgia. EPA/600/6-85/002a.
- U.S. EPA. 1986. *Test Methods for Evaluating Solid Waste Physical/Chemical Methods*. SW-846, Third Edition and Update I (July 1992), Update II (September 1994), and Update IIB (January 1995).
- U.S. EPA. 1989a. *Hazardous Waste Treatment, Storage, and Disposal Facilities: Fugitive Particulate Matter Air Emissions Guidance Document*. EPA-450/3-89-019.
- U.S. EPA. 1989b. *Risk Assessment Guidance for Superfund: Volume I. Human Health Evaluation Manual (Part A)*. OERR. Washington, D.C. OERR 9200 6-303-894.
- U.S. EPA. 1989c. *Handbook: Guidance on Setting Permit Conditions and Reporting Trial Burn Results. Volume II of the Hazardous Waste Incineration Guidance Series*. ORD. EPA/625/6-89/019. January.

U.S. EPA. 1989d. *Handbook: Hazardous Waste Incineration Measurement Guidance Manual. Volume III of the Hazardous Waste Incineration Guidance Series.* Office of Solid Waste and Emergency Response (OSWER). EPA/625/6-89/021. June.

U.S. EPA. 1990a. *Interim Final Methodology for Assessing Health Risks Associated with Indirect Exposure to Combustor Emissions.* Environmental Criteria and Assessment Office. ORD. EPA-600-90-003. January.

U.S. EPA. 1990c. *Operations and Research at the U.S. EPA Incineration Research Facility. Annual Report for FY 89.* Risk Reduction Engineering Laboratory. ORD. Cincinnati, Ohio. EPA/600/9-90/012.

U.S. EPA. 1990d. *Standards for Owners and Operators of Hazardous Waste Incinerators and Burning of Hazardous Wastes in Boilers and Industrial Furnaces.* Federal Register. 55:17862-17921.

U.S. EPA. 1990e. *User's Manual for the PM-10 Open Fugitive Dust Source Computer Model Package.* EPA-450/3-90-010.

U.S. EPA. 1991. *Assessment and Control of Bioconcentratable Contaminants in Surface Waters.* Draft. Office of Water. Washington, D.C. March.

U.S. EPA. 1992a. *Briefing the BTAG Initial Description of Setting, History, and Ecology of a Site.* ECO Update. Publication 9345.0-05I. Office of Solid Waste and Emergency Response, Office of Emergency and Remedial Response. August.

U.S. EPA. 1992b. *Framework for Ecological Risk Assessment.* Risk Assessment Forum. Washington, D.C. EPA/630/R-92/001. February.

U.S. EPA. 1992c. *Implementation of Boiler and Industrial Furnace Regulations, New Toxicological Data.* Memorandum from Shiva Garg, OSWER. February 11.

U.S. EPA. 1992d. *National Study of Chemical Residues in Fish.* Office of Science and Technology. September.

U.S. EPA. 1992e. *Technical Implementation Document for EPA's Boiler and Industrial Furnace Regulations.* OSWER. EPA-530-R-92-011. March.

U.S. EPA. 1992f. *Health Reassessment of Dioxin-Like Compounds, Chapters 1 to 8. Workshop Review Draft.* OHEA. Washington, D.C. EPA/600/AP-92/001a through 001h. August.

U.S. EPA. 1993a. *Wildlife Exposure Factors Handbook: Volume I of II.* Office of Research and Development. Washington, D.C. EPA/600/R-93/187a. December.

U.S. EPA. 1994a. *Air/Superfund National Technical Guidance Study Series. Volume V- Procedures For Air Dispersion Modeling At Superfund Sites.* Office of Air Quality Planning and Standards. Research Triangle Park, North Carolina. February.

U.S. EPA. 1994b. *Draft Guidance for Performing Screening Level Risk Analyses at Combustion Facilities Burning Hazardous Wastes. Attachment C, Draft Exposure Assessment Guidance for RCRA Hazardous Waste Combustion Facilities.* April 15.

U.S. EPA. 1994c. *Draft Guidance on Trial Burns. Attachment B, Draft Exposure Assessment Guidance for RCRA Hazardous Waste Combustion Facilities.* May 2.

U.S. EPA. 1994d. *Draft Revision, Implementation Guidance for Conducting Indirect Exposure Analysis at RCRA Combustion Units. Attachment, Draft Exposure Assessment Guidance for RCRA Hazardous Waste Combustion Facilities.* April 22.

U.S. EPA. 1994e. *Estimating Exposure to Dioxin-Like Compounds, Volume I: Executive Summary. External Review Draft.* ORD. Washington, D.C. EPA/600/6-88/005Ca. June.

U.S. EPA. 1994f. *Estimating Exposure to Dioxin-Like Compounds. Volume II: Properties, Sources, Occurrence, and Background Exposures, External Review Draft.* ORD. Washington, D.C. EPA/600/6-88/005Cb. June.

U.S. EPA. 1994g. *Estimating Exposure to Dioxin-Like Compounds. Volume III: Site-Specific Assessment Procedures, External Review Draft.* ORD. Washington, D.C. EPA/600/6-88/005Cc. June.

U.S. EPA. 1994h. *Great Lakes Water Quality Initiative Technical Support Document for the Procedure to Determine Bioaccumulation Factors.* EPA-822-R-94-002. Offices of Water and Science and Technology, Washington, D.C. July.

U.S. EPA. 1994i. *Health Assessment Document for 2,3,7,8-TCDD and Related Compounds. Volume III. Review Draft.* ORD. Washington, D.C. EPA/600/BP-92/001c.

U.S. EPA. 1994j. *Mercury Study Report to Congress, Volume III: An Assessment of Exposure from Anthropogenic Mercury Emissions in the United States.* Draft. Office of Air Quality Planning and Standards and ORD. EPA/600/P-94/002A. December 13.

U.S. EPA. 1994k. *Revised Draft Guidance for Performing Screening Level Risk Analyses at Combustion Facilities Burning Hazardous Wastes: Attachment C, Draft Exposure Assessment Guidance for RCRA Hazardous Waste Combustion Facilities.* Office of Emergency and Remedial Response. Office of Solid Waste. December 14.

U.S. EPA. 1995a. *Compilation of Air Pollutant Emission Factors: Volume I, Stationary Point and Area Sources.* Research Triangle Park, North Carolina. 5th Edition. AP-42. January.

U.S. EPA. 1995b. *Great Lakes Water Quality Initiative Technical Support Document for the Procedure to Determine Bioaccumulation Factors.* EPA-820-B-95-005. Office of Water, Washington, D.C. March.

U.S. EPA. 1995c. *Great Lakes Water Quality Initiative Technical Support Document for Wildlife Criteria.* EPA-820-B-95-009. Office of Water, Washington, D.C. March.

U.S. EPA. 1995d. *Development of Compliance Levels from Analytical Detection and Quantitation Levels.* U.S. EPA, Washington, DC. NTIS PB95-216321.

U.S. EPA. 1996a. *Ecotox Thresholds.* ECO Update. Volume 3. Number 2. Office of Solid Waste and Emergency Response. Washington, D.C. EPA 540/F-95/038. January.

U.S. EPA. 1996b. *Guidance for Total Organics.* EPA/600/R-96/036. NTIS PB97-118533. November.

U.S. EPA. 1996c. *Report on the U.S. EPA Technical Workshop on WTI Incinerator Risk Assessment Issues.* U.S. EPA Office of Research and Development Risk Assessment Forum. Washington, D.C. EPA/630/R-96/001. May

U.S. EPA. 1996d. *PCBs: Cancer Dose-Response Assessment and Application to Environmental Mixtures*. National Center for Environmental Assessment, Office of Research and Development. EPA/600/P-96/001F. September.

U.S. EPA. 1996e. *Review and Comments of EPA's Peer Review Panel on the Risk Assessment in Support of a Proposed Rule for Technical Standards for Emissions from Combustion Units Burning Hazardous Wastes*.

U.S. EPA. 1996f. *Soil Screening Guidance: Technical Background Document Table of Contents*. Office of Solid Waste and Emergency Response. Washington DC. EPA/540/R-95/128. May.

U.S. EPA. 1997a. *Mercury Study Report to Congress, Volumes I through VIII*. Office of Air Quality Planning and Standards and ORD. EPA/452/R-97-001. December.

U.S. EPA. 1997b. *Ecological Risk Assessment Guidance for Superfund: Process for Designing and Conducting Ecological Risk Assessments*. Interim Final. Environmental Response Team. Edison, New Jersey. EPA 540-R-97-006. June 5.

U.S. EPA. 1997c. *Special Report on Environmental Endocrine Disruption: An Effects Assessment and Analysis*. Office of Research and Development and Office of Prevention, Pesticides, and Toxics Substances. Washington, D.C. EPA/630/R-96/012. February 1997.

U.S. EPA. 1998a. *Development of a Hazardous Waste Incinerator Target Analyte List of Products of Incomplete Combustion, Final Report*. National Risk Management Research Laboratory, Air Pollution Prevention and Control Division, U.S. EPA. EPA/600/R-98/076. Research Triangle Park, North Carolina. June 25.

U.S. EPA. 1998b. *Guidance on Collection of Emissions Data to Support Site-Specific Risk Assessments at Hazardous Waste Combustion Facilities*. Peer Review Draft. Office of Solid Waste and Emergency Response. Washington CD. EPA530-D-98-002. August.

U.S. EPA. 1998c. *Human Health Risk Assessment Protocol for Hazardous Waste Combustion Facilities*. External Peer Review Draft. U.S. EPA Region 6 and U.S. EPA OSW. Volumes 1-3. EPA530-D-98-001A. July.

U.S. EPA. 1998d. *Guidelines for Ecological Risk Assessment*. Office of Research and Development. Washington, D.C. EPA/630/R-95/002Fa. Federal Register 63FR26846. Volume 63. May 14.

U.S. EPA. 1999x. *Screening Level Ecological Risk Assessment Protocol*. Office of Solid Waste. EPA 530-D-99-001A. August.

U.S. EPA. 2002. *Supplemental Guidance for Developing Soil Screening Levels for Superfund Sites*. Office of Emergency and Remedial Response. Washington, DC. OSWER 9355.4-24. December.

U.S. EPA. 2003. *Exposure and Human Health Reassessment of 2,3,7,8-Tetrachlorodibenzo-p-Dioxin (TCDD) and Related Compounds*. NAS Review Draft. Exposure Assessment and Risk Characterization Group. Washington DC. EPA/600/P-00/001Cb. December.

U.S. EPA. 2004a. *User's Guide for the AERMOD Meteorological Preprocessor (AERMET)*. Office of Air Quality Planning and Standards. Emissions, Monitoring, and Analysis Division. Research Triangle Park, North Carolina. EPA-454/B-03-002. November 2004.

U.S. EPA. 2004b. *User's Guide for the AMS/EPA Regulatory Model – AERMOD*. Office of Air Quality Planning and Standards. Emissions, Monitoring, and Analysis Division. Research Triangle Park, North Carolina. EPA-454/B-03-001. September.

U.S. EPA. 2004c. *User's Guide to the Building Profile Input Program*. EPA-454/R-93-038. Office of Air Quality Planning and Standards, Technical Support Division. Research Triangle Park, North Carolina. April 21, 2004.

U.S. EPA. 2008. *Framework for Application of the Toxicity Equivalence Methodology for Polychlorinated Dioxins, Furans, and Biphenyls in Ecological Risk Assessment*. Office of the Science Advisor. Risk Assessment Forum. Washington, D.C. 20460. EPA 100/R-08-004 I June 2008.

U.S. Fish and Wildlife Service (FWS). 1979. *An Ecological Characterization Study of the Chenier Plain Coastal Ecosystem of Louisiana and Texas*. FWS/OBS-78/9. National Coastal Ecosystem Team, Office of Biological Services. U.S. DOI, Slidell, Louisiana.

U.S. Fish and Wildlife Service (FWS) (1980). *Evaluating Soil Contamination*. Biological Report 90(2). July.

Valentine, R.L. 1986. *Nonbiological Transformation*. Vadose Zone Modeling of Organic Pollutants. S.C. Hern and S.M. Melacon, Editors. Lewis Publishers, Inc. Chelsea, Michigan.

Valentine, R.L., and J. Schnoor. 1986. *Biotransformation*. Vadose Zone Modeling of Organic Pollutants. S.C. Hern and S.M. Melancon, Editors. Lewis Publishers, Inc. Chelsea, Michigan.

Van den Berg, M; Birnbaum, L; Bosveld, ATC; Brunstrom, B; Cook, P; Feeley, M; Giesy, JP; Hanberg, A; Hasegawa, R; Kennedy, SW; Kubiak, T; Larsen, JC; van Leeuwen, FX; Liem, AK; Nolt, C; Peterson, RE; Poellinger, L; Safe, S; Schrenk, D; Tillitt, D; Tysklind, M; Younes, M; Waern, F; Zacharewski, T. (1998) *Toxic equivalency factors (TEFs) for PCBs, PCDDs, PCDFs for humans and wildlife*. Environ Health Perspect. 106(12):775-792.

Van den Berg, M; Birnbaum, LS; Denison, M, DeVito, M, Farland, W, Feeley, M; Fiedler, H; Hakansson, H; Hanberg, A; Haws, L; Rose, M; Safe, S; Schrenk, D; Tohyama, C; Tritscher, A; Tuomisto, J; Tysklind, M; Walker, N; Peterson, RE. (2006) *The 2005 World Health Organization Reevaluation of Human and Mammalian Toxic Equivalency Factors for Dioxins and Dioxin-Like Compounds*. Toxicol Sci. 93:223-241.

Vanoni, V.A. 1975. *Sediment Engineering*. American Society of Civil Engineers. New York, NY. Pages 460-463.

Walker, M.K., and R.E. Peterson. 1992. *Potencies of Polychlorinated Dibenzo-p-dioxin, Dibenzofuran, and Biphenyl Congeners, Relative to 2,3,7,8-Tetrachlorodibenzo-p-dioxin, for Producing Early Life Stage Mortality in Rainbow Trout (*Oncorhynchus mykiss*)*. Aquatic Toxicology. Volume 21. Pages 219-238.

Weast, R.C. 1986. *Handbook of Chemistry and Physics*. 66nd Edition. Cleveland, Ohio. CRC Press.

Witby, K.T. 1978. *The Physical Characteristics of Sulfur Aerosols*. Atmospheric Environment. 12:135-159.

World Health Organization (WHO). 1997. *Meeting on the Derivation of Toxic Equivalency Factors (TEFs) for PCBs, PCDDs, PCDFs, and Other Dioxin-like Compounds for Humans and Wildlife*. Institute of Environmental Medicine, Karolinska Institute. Stockholm, Sweden. June 15-18. Draft Report, July 30, 1997 version.

Conversion Factors

0.001	=	Units conversion factor (g/mg)
10 ⁶	=	Units conversion factor ($\mu\text{g/g}$)
907.18	=	Units conversion factor (kg/ton)
3.1536 x 10 ⁷	=	Conversion constant (s/year)
4,047	=	Units conversion factor (m ² /acre)
100	=	Units conversion factor (m ² -mg/cm ² -kg)
10 ⁻⁶	=	Units conversion factor (g/ μg)
0.12	=	Dry weight to wet weight (plants) conversion factor (unitless)

List of Acronyms

μg	Microgram
$\mu\text{g/kg}$	Micrograms per kilogram
$\mu\text{g/L}$	Micrograms per liter
$\mu\text{g/s}$	Micrograms per second
μm	Micrometer
$\mu\text{m/s}$	Micrometers per second
μm^2	Square micrometers
°C	Degrees Celsius
°F	Degrees Fahrenheit
°K	Degrees Kelvin
ADOM	Acid Deposition and Oxidant Model
AET	Apparent effects threshold
APCD	Air pollution control device
APCS	Air pollution control system
atm-m ³ /mol-K	Atmosphere-cubic meters per mole-degrees Kelvin
ATSDR	Agency for Toxic Substances and Disease Registry
AWFCO	Automatic waste feed cutoff
AWQC	Ambient water quality criteria
BAF	Bioaccumulation factor
BaP	Benzo(a)pyrene
BCF	Bioconcentration factor
BD	Soil bulk density
BEF	Bioaccumulation equivalency factor
BEHP	Bis(2-ethylhexyl)phthalate
BIF	Boiler and industrial furnace
BPIP	Building profile input program
BS	Benthic solids
BSAF	Sediment bioaccumulation factor
BTAG	Biological Technical Assistance Group
BW	Body weight
CAS	Chemical Abstracts Service
CERM	Conceptual ecological risk model
CKD	Cement kiln dust
COMPDEP	COMPLEX terrain model with DEPosition
COMPLEX I	COMPLEX terrain model, Version 1
COPC	Compound of potential concern
CPF	Cumulative probability density function
CRQL	Contract required quantitation limit
CWA	Clean Water Act
DEM	Digital Elevation Model
DNOP	Di(n)octylphthalate

DOE	U.S. Department of Energy
DQL	Data quality level
DRE	Destruction and removal efficiency
EDQL	Ecological data quality levels
EEL	Estimated exposure level
EPA	U.S. Environmental Protection Agency
EPC	Exposure point concentration
EQL	Estimated quantitation limit
EQP	Equilibrium partitioning
ERA	Ecological risk assessment
ERL	Effects range low
ERT	Environmental Research and Technology
ESP	Electrostatic precipitator
ESI	Ecological screening index
ESQ	Ecological screening quotient
FCM	Food chain multiplier
FWS	U.S. Fish and Wildlife Service
g/s	Grams per second
g/cm ³	Grams per cubic centimeter
g/m ³	Grams per cubic meter
GAQM	Guideline on Air Quality Models
GC	Gas chromatography
GEP	Good engineering practice
HBC	Hexachlorobenzene
HgCl ₂	Mercuric chloride
HQ	Hazard quotient
IDL	Instrument detection limit
IEM	Indirect exposure model
IRIS	Integrated risk information system
ISCST3	Industrial source complex short-term model
ISCSTDF	Industrial Source Complex Short Term Draft
kg	Kilogram
kg/L	Kilograms per liter
L	Liter
LC ₅₀	Lethal concentration to 50 percent of the test population
LCD	Local Climatological Data Annual Summary with Comparative Data
LD ₅₀	Lethal dose to 50 percent of the test population
LEL	Lowest effect level
LFI	Log fill-in
LOAEL	Lowest observed adverse effect level
LOD	Level of detection
LOEL	Lowest observed effect level
m	Meter
m/s	Meters per second
mg	Milligram
mg/kg	Milligrams per kilogram
mg/kg/day	Milligrams per kilogram per day
mg/L	Milligrams per liter
mg/m ³	Milligrams per cubic meter
MACT	Maximum achievable control technology
MDL	Method detection limit
MLE	Maximum likelihood estimation
MPRM	Meteorological Processor for Regulatory Models
NCDC	National Climatic Data Center
NCEA	National Center for Environmental Assessment
NEL	No effect level

NFI	Normal fill-in
NOAA	National Oceanic and Atmospheric Administration
NOAEL	No observed adverse effect level
NOEC	No observed effect concentration
NOEL	No observed effect level
NRC	U.S. Nuclear Regulatory Commission
NTIS	National technical information service
NWS	National weather service
OAQPS	Office of Air Quality Planning and Standards
OAQPS TTN	Office of Air Quality and Planning Standards and Tech Transfer Network
OC	Organic carbon
OCDD	Octachlorodibenzodioxin
ORD	Office of Research and Development
OSW	Office of Solid Waste
PAH	Polycyclic aromatic hydrocarbon
PCB	Polychlorinated biphenyl
PCDD	Polychlorinated dibenzo(p)dioxin
PCDF	Polychlorinated dibenzofuran
PIC	Product of incomplete combustion
PM	Particulate matter
PM10	Particulate matter less than 10 micrometers in diameter
POHC	Principal organic hazardous constituent
PQL	Practical quantitation limit
PU	Polyurethane
QA/QC	Quality assurance/Quality control
QAPjP	Quality assurance project plan
QSAR	Quantitative structure activity relationship
RCRA	Resource Conservation and Recovery Act
RME	Reasonable maximum exposure
SAMSON	Solar and Meteorological Surface Observational Network
SCRAM	Support Center for Regulatory Air Models Bulletin Board System
SFB	San Francisco Bay
SMDP	Scientific management decision point
SO	Source
SQL	Sample quantitation limit
SVOC	Semivolatile organic compound
TAL	Target analyte list
TCDD	Tetrachlorodibenzo(p)dioxin
TDA	Toluene diisocyanate
TEF	Toxicity equivalent factor
TG	Terrain grid
TIC	Tentatively identified compound
TL	Trophic level
TOC	Total organic carbon
TRV	Toxicity reference value
TSS	Total suspended solids
UF	Uncertainty factor
UFI	Uniform fill-in
USGS	U.S. Geological Survey
USLE	Universal soil loss equation
UTM	Universal transverse mercator
VOC	Volatile organic compound
watts/m ²	Watts per square meter
WHO	World Health Organization
WRPLOT	Wind Rose PLOting program

List of Variables

λ_z	=	Dimensionless viscous sublayer thickness (unitless)
μ_a	=	Viscosity of air (g/cm-s)
μ_w	=	Viscosity of water corresponding to water temperature (g/cm-s)
ρ_a	=	Air density (g/cm ³ or g/m ³)
ρ_s	=	Bed sediment density (kg/L)
ρ_w	=	Density of water corresponding to water temperature (g/cm ³)
θ	=	Temperature correction factor (unitless)
θ_{bs}	=	Bed sediment porosity (unitless)
θ_s	=	Soil volumetric water content (mL/cm ³ soil)
a	=	Empirical intercept coefficient (unitless)
A	=	Surface area of affected area (m ²)
AhR	=	Aryl hydrocarbon receptor
b	=	Empirical slope coefficient (unitless)
BAF_l	=	Bioaccumulation factor reported on a lipid-normalized basis using the freely dissolved concentration of a chemical in the water (L/kg)
$BCF_{a/s}$	=	Aquatic-sediment bioconcentration factor (unitless)
BCF_l	=	Bioconcentration factor reported on a lipid-normalized basis using the freely dissolved concentration of a chemical in the water (L/kg)
BCF_{Pi-H}	=	Bioconcentration factor for plant-to-herbivore for i th plant food item (unitless)
BCF_i	=	Soil-to-soil invertebrate bioconcentration factor (unitless)
BCF_{Pi-OM}	=	Bioconcentration factor for plant-to-omnivore for i th plant food item (unitless)
$BCF_{S/BS-C}$	=	Bioconcentration factor for soil- or bed sediment-to-carnivore (unitless)
$BCF_{S/BS-H}$	=	Bioconcentration factor for soil-to-plant (unitless)
BCF_{W-C}	=	Bioconcentration factor for water-to-carnivore (L/kg)
BCF_r	=	Plant-soil biotransfer factor (unitless)
BD	=	Soil bulk density (g soil/cm ³ soil)
BMF_n	=	Biomagnification factor for n th trophic level
BS	=	Benthic solids concentration (kg/L or g/cm ³)
$BSAF$	=	Sediment bioaccumulation factor (unitless)
Bv	=	Air-to-plant biotransfer factor (μ g COPC/g DW plant)/(μ g COPC/g air)
BW	=	Body weight (kg)
C	=	USLE cover management factor (unitless)
C_{Ai}	=	COPC concentration in i th animal food item (mg/kg)
C_C	=	COPC concentration in carnivore (mg/kg)
C_d	=	Drag coefficient (unitless)
C_{dw}	=	Dissolved phase water concentration (mg/L)
C_F	=	COPC concentration in fish (mg/kg)
CFO_2	=	Correction factor for conversion to 4.5 percent O ₂ (unitless)
C_{gen}	=	Generic chemical concentration (mg/kg or mg/L)
C_H	=	COPC concentration in herbivore (mg/kg)
C_i	=	Stack concentration of i th identified COPC (carbon basis) (mg/m ³)
C_i	=	COPC concentration in i th plant or animal food item (mg COPC/kg)
C_I	=	COPC concentration in soil or benthic invertebrate (mg/kg)
C_{IW}	=	COPC concentration in soil or sediment interstitial water (mg/L)
C_M	=	COPC concentration in media (mg COPC/kg [soil, sediment])
C_{OM}	=	COPC concentration in omnivore (mg/kg)
C_{Pi}	=	COPC concentration in i th plant food item (mg/kg)
C_{PREY}	=	Concentration in prey
C_{sed}	=	COPC concentration in bed sediment (mg COPC/kg sediment)
$C_{s/sed}$	=	COPC concentration in soil or bed sediment (mg/kg)
C_{TOC}	=	Stack concentration of TOC, including speciated and unspeciated compounds (mg/m ³)
C_{TP}	=	COPC concentration in terrestrial plants (mg COPC/kg WW)
C_{wctot}	=	Total COPC concentration in water column (mg/L)

C_{wtot}	=	Total water body COPC concentration (g/m^3 or mg/L)
C_{yp}	=	Unitized yearly air concentration from particle phase ($\mu\text{g}\cdot\text{s}/\text{g}\cdot\text{m}^3$)
C_{yv}	=	Unitized yearly air concentration from vapor phase ($\mu\text{g}\cdot\text{s}/\text{g}\cdot\text{m}^3$)
C_{ywv}	=	Unitized yearly watershed air concentration from vapor phase ($\mu\text{g}\cdot\text{s}/\text{g}\cdot\text{m}^3$)
D_a	=	Diffusivity of COPC in air (cm^2/s)
d_{bs}	=	Depth of upper benthic sediment layer (m)
DD_{TEQ}	=	Daily dose of 2,3,7,8-TCDD <i>TEQ</i> ($\mu\text{g}/\text{kg}$ BW/d)
DD_i	=	Daily dose of <i>i</i> th congener ($\mu\text{g}/\text{kg}$ BW/d)
D_{mean}	=	Mean particle size density for a particular filter cut size
D_s	=	Deposition term ($\text{mg}/\text{kg}\cdot\text{yr}$)
D_w	=	Diffusivity of COPC in water (cm^2/s)
d_{wc}	=	Depth of water column (m)
D_{yd}	=	Unitized yearly dry deposition rate of COPC ($\text{g}/\text{m}^2\cdot\text{yr}$)
D_{ydp}	=	Unitized yearly dry deposition from particle phase ($\text{s}/\text{m}^2\cdot\text{yr}$)
D_{ytwp}	=	Unitized yearly watershed total deposition from particle phase ($\text{s}/\text{m}^2\cdot\text{yr}$)
D_{ywp}	=	Unitized yearly wet deposition from particle phase ($\text{s}/\text{m}^2\cdot\text{yr}$)
D_{ywv}	=	Unitized yearly wet deposition from vapor phase ($\text{s}/\text{m}^2\cdot\text{yr}$)
D_{ywwv}	=	Unitized yearly watershed wet deposition from vapor phase ($\text{s}/\text{m}^2\cdot\text{yr}$)
d_z	=	Total water body depth (m)
E_v	=	Average annual evapotranspiration (cm/yr)
ER	=	Soil enrichment ratio (unitless)
F_{Ai}	=	Fraction of diet consisting of <i>i</i> th animal food item (unitless)
f_{bs}	=	Fraction of total water body COPC concentration in benthic sediment (unitless)
FCM	=	Trophic level-specific food-chain multiplier (unitless)
FCM_{TLn}	=	Food chain multiplier for <i>n</i> th trophic level
FCM_{TLn-Ai}	=	Food chain multiplier for trophic level of <i>i</i> th animal food item (unitless)
FCM_{TL3}	=	Food chain multiplier for trophic level 3 (unitless)
f_{wc}	=	Fraction of total water body COPC concentration in the water column (unitless)
F_v	=	Fraction of COPC air concentration in vapor phase (unitless)
F_{OC}	=	Fraction of organic carbon (unitless)
F_{Pi}	=	Fraction of diet consisting of <i>i</i> th plant food item (unitless)
F_w	=	Fraction of COPC wet deposition that adheres to plant surfaces (unitless)
H	=	Henry's law constant ($\text{atm}\cdot\text{m}^3/\text{mol}$)
I_{MEDIUM}	=	Ingestion rate of soil, surface water, or sediment
I	=	Average annual irrigation (cm/yr)
IR	=	Ingestion rate (kg/day)
K	=	USLE erodibility factor (ton/acre)
k_b	=	Benthic burial rate (yr^{-1})
K_G	=	Gas phase transfer coefficient (m/yr)
K_L	=	Liquid phase transfer coefficient (m/yr)
Kd_{bs}	=	Bed sediment/sediment pore water partition coefficient (L/kg or cm^3/g)
Kd_{ij}	=	Partition coefficient for COPC <i>i</i> associated with sorbing material <i>j</i> (unitless)
Kd_s	=	Soil-water partition coefficient (cm^3/g or mg/L)
Kd_{sw}	=	Suspended sediments/surface water partition coefficient (L/kg)
K_{oc}	=	Organic carbon partition coefficient (mg/L)
K_{ocj}	=	Sorbing material-independent organic carbon partition coefficient for COPC <i>j</i>
K_{ow}	=	Octanol-water partition coefficient (unitless)
kp	=	Plant surface loss coefficient (yr^{-1})
ks	=	COPC soil loss constant due to all processes (yr^{-1})
kse	=	COPC loss constant due to soil erosion (yr^{-1})
ksg	=	COPC loss constant due to biotic and abiotic degradation (yr^{-1})
ksl	=	COPC loss constant due to leaching (yr^{-1})
ksr	=	COPC loss constant due to runoff (yr^{-1})
ksv	=	COPC loss constant due to volatilization (yr^{-1})
k_v	=	Water column volatilization rate constant (yr^{-1})
K_v	=	Overall transfer rate coefficient (m/yr)

k_{wt}	=	Overall total water body COPC dissipation rate constant (yr^{-1})
L	=	Monin-Obukhov Length (m)
L_{DEP}	=	Total (wet and dry) particle phase and wet vapor phase direct deposition load to water body (g/yr)
L_{dif}	=	Dry vapor phase diffusion load to water body (g/yr)
L_E	=	Soil erosion load (g/yr)
L_R	=	Runoff load from pervious surfaces (g/yr)
L_{RI}	=	Runoff load from impervious surfaces (g/yr)
L_T	=	Total COPC load to water body (g/yr)
LS	=	USLE length-slope factor (unitless)
MW	=	Molecular weight of COPC (g/mol)
OC_i	=	Organic carbon content of sorbing material I (unitless)
OV	=	Deposition output values
P	=	Average annual precipitation (cm/yr)
P_{Ai}	=	Proportion of i th animal food item in diet that is contaminated (unitless)
P_d	=	COPC concentration in plant due to direct deposition (mg/kg WW)
PF	=	USLE supporting practice factor (unitless)
P_{Pi}	=	Proportion of i th plant food item in diet that is contaminated (unitless)
P_r	=	COPC concentration in plant due to root uptake (mg/kg WW)
$P_{S/BS}$	=	Proportion of soil or bed sediment in diet that is contaminated (unitless)
P_v	=	COPC concentration in plant due to air-to-plant transfer (mg/kg WW)
P_w	=	Proportion of water in diet that is contaminated (unitless)
Q	=	COPC emission rate (g/s)
Q_i	=	Emission rate of COPC (i) (g/s)
$Q_{i(adj)}$	=	Adjusted emission rate of COPC (i) (g/s)
Q_f	=	Anthropogenic heat flux (W/m^2)
Q^*	=	Net radiation absorbed (W/m^2)
r	=	Interception fraction of material in rain intercepted by vegetation and initially retained (unitless)
R	=	Universal gas constant ($\text{atm}\cdot\text{m}^3/\text{mol}\cdot\text{K}$)
RO	=	Average annual runoff (cm/yr)
RF	=	USLE rainfall (or erosivity) factor (yr^{-1})
Sc	=	Average soil concentration over exposure duration (mg/kg)
Sc_{Tc}	=	Soil concentration at time T_c (mg/kg)
SD	=	Sediment delivery ratio (unitless)
SGC	=	COPC stack gas concentration as measured in the trial burn ($\mu\text{g}/\text{dscm}$)
SGF	=	Stack gas flow rate at 7 percent O_2 (dscm/s)
T_a	=	Ambient air temperature (K) = 298.1 K
T_p	=	Plant exposure to deposition per harvest of edible portion of the i th plant group (yr)
tD	=	Total time period over which deposition occurs (time period of combustion) (yr)
TSS	=	Total suspended solids concentration (mg/L)
T_w	=	Water body temperature (K)
u	=	Current velocity (m/s)
V	=	Volume V_{dv} = Dry deposition velocity (cm/s)
V_f^x	=	Average volumetric flow rate through water body (m^3/yr)
VG_{ag}	=	Empirical correction factor for aboveground produce (unitless)
VP	=	Vapor pressure (atm)
W	=	Average annual wind velocity (m/s)
WA_I	=	Area of impervious watershed receiving COPC deposition (m^2)
WA_L	=	Area of watershed receiving COPC deposition (m^2)
WA_w	=	Water body surface area (m^2)
X_e	=	Unit soil loss ($\text{kg}/\text{m}^2\cdot\text{yr}$)
Y_p	=	Standing crop biomass (productivity) (kg/m^2 DW)
Z_s	=	Soil mixing zone depth (cm)

Definitions

The following definitions were adopted from *Superfund: Process for Designing and Conducting Ecological Risk Assessments. Interim Final* (U.S. EPA 1997c) and *Guidelines for Ecological Risk Assessment* (U.S. EPA 1998d), and identify key terms used throughout this guidance.

Area Use Factor: A ratio of an organism's home range, breeding range, or feeding and foraging range to the area of contamination of the assessment area.

Assessment Endpoint: An explicit expression of the environmental value that is to be protected; it includes both an ecological entity and specific attributes of that entity. The assessment endpoint in this protocol is used to link the risk assessment to management concerns and ultimately development of a protective operating permit.

Bioaccumulation: The net accumulation of a substance by an organism as a result of uptake directly from all environmental sources, including food. Bioaccumulation occurs on all exposure routes.

Bioaccumulation Factor (BAF): BAF represents the ratio of the concentration of a chemical to its concentration in a medium. The factor must be measured at steady-state when the rate of uptake is balanced by the rate of excretion. Bioaccumulation factors (BAF) are estimated by multiplying a bioconcentration factor (BCF) by a food chain multiplier (FCM).

Bioconcentration: A process by which there is a net accumulation of a chemical directly from an exposure medium into an organism.

Bioconcentration Factor (BCF): BCF represents the ratio of the concentration of a chemical in an aquatic organism to the concentration of the chemical in surface water, sediment, or soil. BCFs are used to estimate the body burden of a COPC in producers, primary consumers, and fish consumed by mid- or upper-trophic level measurement receptors.

Biomagnification: The process by which the concentration of some chemicals increase with increasing trophic level; that is, the concentration in a predator exceeds the concentration in its prey.

Biotransfer Factor: COPC accumulation factor between a food item and its consumer. Biotransfer factors are used to evaluate transport of contaminants in plants to mammals and birds.

Depuration: The loss of a compound from an ecological receptor as a result of any process.

Direct Uptake: Direct uptake is a term applied to producers, primary consumers, and detritivores. Direct uptake includes all exposure routes for aquatic receptors, benthic receptors, soil invertebrates, and terrestrial plants.

Ecological Effects Assessment: A portion of the analysis phase of the risk assessment that evaluates the ability of a stressor to cause adverse effects under a particular set of circumstances. Toxicity reference values identified in ecological effects assessment are used in risk characterization.

Ecological Risk Assessment: The process that evaluates the likelihood that adverse ecological effects may occur or are occurring as a result of exposure to one or more stressors.

Ecological Screening Quotient (ESQ): A quotient used to assess risk during the risk assessment in which protective assumptions are used. The numerator is the reasonable worst-case COPC concentration at the point of exposure, and the denominator is the no-adverse-effects-based toxicity reference value.

Environmental Attribute: Characteristic of a food web functional group (e.g., herbivorous mammal) that is relevant to the ecosystem. Examples of environmental attributes include seed dispersal, decomposition, pollination, and food source.

Exposure Assessment: A portion of the analysis phase of ERA that evaluates the interaction of the stressor with one or more ecological components. Exposure can be expressed as co-occurrence or contact, depending on the stressor and ecological component involved. Information from the exposure assessment is used in risk characterization.

Exposure Pathway: A pathway by which a compound travels from a combustion facility to an ecological receptor. A complete exposure pathway occurs when a chemical enters or makes contact with an ecological receptor through one or more exposure routes.

Exposure Route: A point of contact or entry of a chemical from the environment into an organism. The exposure routes for terrestrial wildlife are ingestion, dermal absorption, and

inhalation. For example, the exposure routes for aquatic fauna are ingestion, dermal absorption, and respiration.

Food Chain: The transfer of food energy from the source in plants through a series of organisms with repeated eating and being eaten (Odum 1971).

Food Web: The interlocking patterns of food chains (Odum 1971).

Food-Chain Multiplier (FCM): The FCM is used to account for dietary uptake of a compound by an ecological receptor. It supports estimates of *BAF* from a *BCF* in the absence of reliable *BAF* data.

Guild: A group of species occupying a particular trophic level and exploiting a common resource base in a similar fashion (Root 1967).

Habitat: The physical environment in which a species is distributed. Habitat location depends on several factors, such as chemical conditions, physical conditions, vegetation, species eating strategy, and species nesting strategy. By analogy, the habitat is an organism's address.

Measure of Effect: A measurable ecological characteristic that is related to the valued characteristic chosen as the assessment endpoint. It is the measure used to evaluate the response of the assessment endpoint when exposed to a chemical.

Measure of Effect: A measurable ecological characteristic that is related to the valued characteristic chosen as the assessment endpoint.

Measure of Exposure: A measurable stressor characteristic that is used to help quantify exposure.

Measurement Receptor: A species, population, community, or assemblage of communities (such as aquatic life) used to characterize ecological risk to an assessment endpoint.

Problem Formulation: A systematic planning step that identifies the focus and scope of the risk assessment. Problem formulation includes ecosystem characterization, pathway analysis, assessment endpoint development, and measurement endpoint identification.

Special Ecological Area: Habitats and areas for which protection and special consideration has been conferred legislatively (federal or state), such as critical habitat for federally or state-designated endangered or threatened species.

Stressor: Any physical, chemical, or biological entity that can induce an adverse response.

Trophic Level: One of the successive levels of nourishment in a food web or food chain. Plant producers constitute the first (lowest) trophic level, and dominant carnivores constitute the last (highest) trophic level.

Uncertainty Factor: Quantitative values used to adjust toxicity values from laboratory toxicity tests to toxicity values representative of chronic no-observed-adverse-effect-levels (NOAELs).

Uptake: Acquisition by an ecological receptor of a compound from the environment as a result of any active or passive process.

Vlachokostas, C. et al., 2010. *Combined Assessment of Health Impacts and Emission Abatement Strategies*. Chapter 15F of *AIR QUALITY MODELING - Theories, Methodologies, Computational Techniques, and Available Databases and Software. Vol. IV – Advances and Updates* (P. Zannetti, Editor). Published by The EnviroComp Institute (<http://www.envirocomp.org/>) and The Air & Waste Management Association (<http://www.awma.org/>).

Chapter 15F

Combined Assessment of Health Impacts and Emission Abatement Strategies

Christos Vlachokostas ⁽¹⁾, Nicolas Moussiopoulos ⁽²⁾ and Charisios Achillas ⁽³⁾

⁽¹⁾ *Laboratory of Heat Transfer and Environmental Engineering, Aristotle University Thessaloniki, Thessaloniki (Greece)*

vlahoco@aix.meng.auth.gr

⁽²⁾ *Laboratory of Heat Transfer and Environmental Engineering, Aristotle University Thessaloniki, Thessaloniki (Greece)*

moussio@eng.auth.gr

⁽³⁾ *Laboratory of Heat Transfer and Environmental Engineering, Aristotle University Thessaloniki, Thessaloniki (Greece)*

achillas@aix.meng.auth.gr

Abstract: A consensus has been emerging among public health experts that air pollution, even at current ambient levels, aggravates morbidity and leads to premature mortality. In this sense the practicability and success of air pollution control strategies is of critical importance, especially when issues in terms of public health arise. The selection of a bundle of control measures is a complex and multi-disciplinary process involving a wide range of scientists with different expertise and stakeholders. An integrated assessment methodological framework is developed to support optimal decision making especially at urban scale. The approach that is proposed is based on the application of mathematical programming models. In this context, balance between stringent available capital required for emission control strategies and confrontation of urban air pollution problems towards the protection of public health can be successfully realized.

Key Words: air pollution control, health impact assessment, mathematical programming, air quality modeling, cost–benefit analysis, economic benefit/damage, integrated assessment.

1 Introduction

Most economic activities involving the use and conversion of energy are accompanied by emissions of air pollutants (both by stationary and mobile sources), thereby degrading the environment. The problem deteriorates in urban conurbations, considering the fact that human activities are concentrated inevitably in a relatively small area (Moussiopoulos et al., 2009). The adoption of an air pollution control strategy has the ultimate target to reduce sufficiently air pollution levels in the areas of implementation. Forming long-term, efficient air pollution control strategies requires knowledge of the costs associated with their implementation, the emission inventories and emission reductions to be achieved, as well as the concentration variations that represent air quality levels in the area examined. Furthermore, possible benefits (or damages) arising from the adoption of the proposed strategies should additionally be included in the cost-benefit analysis.

The practicability and success of control strategies is of critical importance, since a consensus has been emerging among public health experts that air pollution, even at current ambient levels, aggravates morbidity (especially respiratory and cardiovascular diseases) and leads to premature mortality (e.g. Dockery and Pope, 2006; ExternE, 2005; Holland et al., 2005; Hurley et al., 2005; WHO, 2003; Pope et al., 2002; Hoek et al., 2002; Le Tetre et al., 2002; Katsouyianni et al., 2001; Künzli et al., 2000; Wilson and Spengler, 1996; Armstrong and Tremblay, 1994; Abbey et al., 1993; Schwartz, 1993; Krupnick et al., 1990; Ostro, 1987; Brunekreef, 1984). The consensus is based mainly on the past decade's numerous epidemiological studies worldwide which have measured increases both in mortality and morbidity associated with air pollution (Krzyzanowski et al., 2002).

Development of air pollution control strategies is a complex and multi-disciplinary process involving a wide range of scientists with different expertise and stakeholders with different interests and points of view (Vlachokostas and Moussiopoulos, 2004). Real-life environmental problems link numerous stakeholders with viewpoints, which are usually in conflict, so it is difficult to define an objective optimum. In contrast, the optimization criterion is the strategic parameter that the decision maker is facing in the adopted framework of analysis. Considering the fact that the cost-effectiveness criterion is the "politically preferred" one, the impact of air pollution control strategies is primarily assessed in terms of their influence on the pollution levels compared to the underlying legislative limit values and the respective abatement cost that is to be invested in the area under consideration. In general, the economic impact arising from the application of the proposed strategies is neglected, although mankind incurs an important financial burden caused by the decrement of social prosperity when the latter is not compensated. In this sense, at least, Health Impact Assessment (HIA) and the relevant monetary valuation should be embodied in an integrated assessment analysis.

In regards to the adoption of specific air pollution abatement measures, an integrated assessment methodological framework is presented, developed to support optimal decision making especially at urban scale. The approach that is proposed is based on the application of mathematical programming models. In this context, they are used to balance between stringent available capital required for emission control strategies and the confrontation of urban air pollution problems towards the protection of public health. Such an approach is transparent both to the decision makers of the responsible authorities and to the public. However, it is also important to make clear the assumptions and uncertainties and their impact on the robustness of the results, especially in regards to HIA.

2 Air Quality and Health: The Issue

It is already emphasized that there is a consensus emerged among public health experts that air pollution, even at current ambient levels, aggravates morbidity and leads to premature mortality. State of the art epidemiological research has recently established consistent associations between air pollution and various outcomes such as respiratory symptoms, reduced lung function, chronic bronchitis and premature mortality. Moreover, emission from road traffic has become the most important source of air pollution in many urban conurbations worldwide (Moussiopoulos, 2003). That is to say that traffic related air pollution is considered in many cities as one of the most important environmental pressures.

Some air pollution effects may be related to short-term exposure acute effects or more correctly effects of acute exposure while others have to be considered contributions of long-term exposure chronic effects or more correctly effects of chronic exposure. Although the mechanisms are not fully explained and there is less certainty about specific causes, most recent studies have identified fine particles as a prime culprit. O_3 has also been directly implicated. In addition, there may be significant direct health impacts of SO_2 , but for direct impacts of NO_x the evidence is less convincing (ExternE, 2005). The effects on mortality from long-term exposure to pollution are characterized as chronic mortality. This term, indicates that the total or long-term effects of air pollution on mortality are included, in contrast to acute mortality impacts, which are observed within a few days of exposure to air pollution. It is widely accepted that these are the dominant effects in cost-benefit analysis and HIA (e.g. ExternE, 2005; Hurley et al., 2005).

As evidence of health effects of air pollution has accumulated, governments worldwide, the World Health Organization (WHO), as well as other groups, have begun to use data from these studies to inform environmental decision makers through quantitative estimates of air pollution impacts on public health. Thereupon it is more than evident that assessment of the effects of air pollution on health is an area of the interface of science and policy where quantitative HIA and cost-benefit analysis methods are most strongly developed and used. This would

not have been possible without the vast growth in research on air pollution and health during the last 20 years.

In practice, the decision maker is responsible for the selection of control measures in order to comply with legislation of air quality standards in the area under study. However, the determination of health risks through the inhalation of gases and particles or the setting of air quality standards for protection of human health requires epidemiological input of medical experts. The extent to which such standards are exceeded requires monitoring infrastructure, measurements and relevant data. Careful identification of the emission sources is a precursor to modeling of atmospheric dispersion and validation against available measurements. Data on the available technological options, their cost-effectiveness and quantitative estimations for the social benefits is also required. Combining all the above information is a difficult task. A decision support system is necessary in order to evaluate the control alternatives and provide the optimal solution.

3 Methodological Framework

Figure 1 presents the basic steps for policy-makers, in the framework of multi-pollutant, multi-effect concept. In order to optimize the utilization of the available finite control resources, at least two discernible criteria need to be considered:

- (i) Cost-effectiveness criterion: Minimization of the total control cost subject to compliance with the predefined air quality limit values.
- (ii) Cost-benefit criterion: Estimation of the optimal air quality levels in order to maximize the social benefit objective function. In this case HIA input and the respective social costs (internalization of the external costs) from the adoption of the optimal strategy are considered.

For the formulation of an efficient air quality management scheme, the compilation of an accurate and reliable air pollutant emission inventory is of vital importance since it is a key component of any air pollution control program (Borrego et al., 2000). Reliable emission modeling is crucial since it affects air quality modeling estimations. Moreover, typical local meteorological parameters, land use, orography data, boundary conditions and background concentrations are required in order to imprint the reference year status and predict future concentration fields in accordance with the defined Business as Usual (BAU) scenario.

After having determined the pollutants that pose significant problems in the area under study, it is significant to estimate the “transfer coefficients” matrix. More specifically, the emission sources and sensitive receptors are spatially assigned to the examined geographical grid. Grids with increased emission rates define areas with importance in regards to emission sources. Transfer coefficients relate changes in emission rates of specific grids to changes in the estimated average

concentrations at receptors grids, for typical meteorological conditions. The transfer coefficients matrix elements are calculated with the use of an air quality

model [unit: $\frac{(\mu\text{g}/\text{m}^3)}{t}$]. The use of transfer coefficients is a prerequisite in order to

accomplish least cost solutions, since some sources degrade air quality more than others due to their different location and dispersion parameters (e.g. stack height, stack exit conditions, wind speed and direction etc.). Transfer coefficients, and necessary population data for the receptors affected are inserted in the logical flow presented in Figure 1.

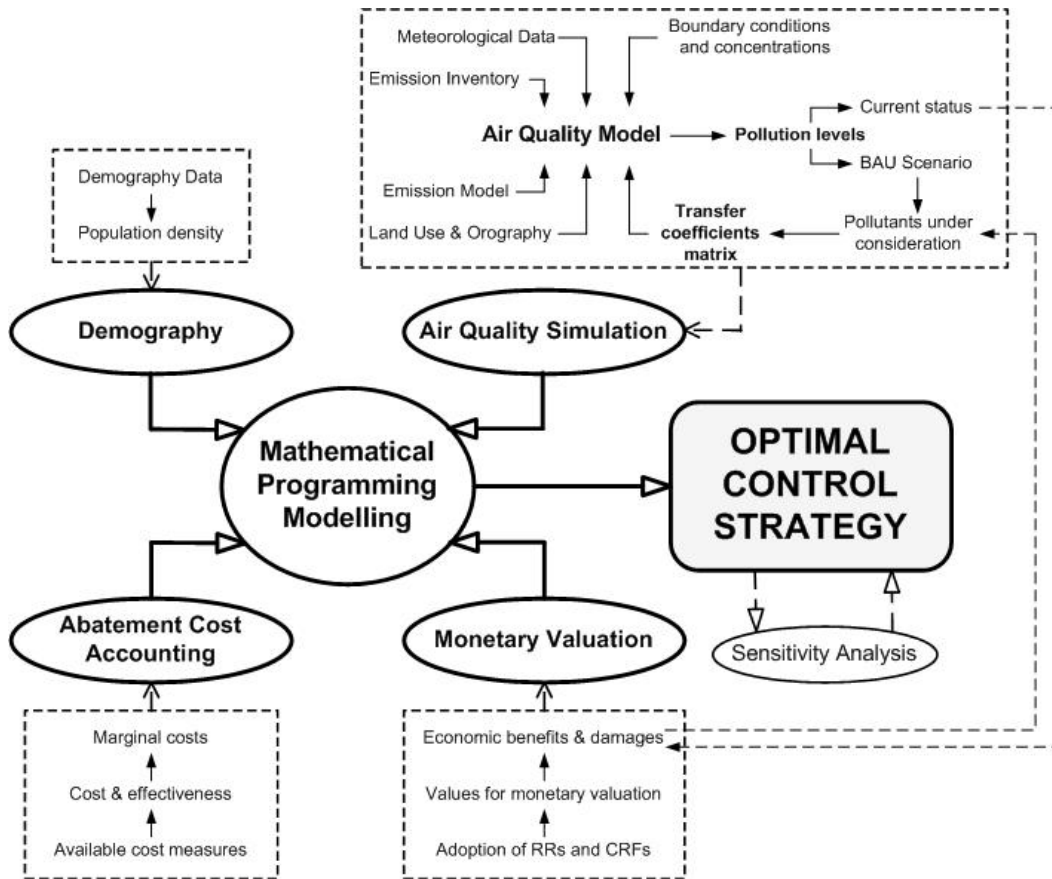


Figure 1. Evaluation of alternative air pollution abatement strategies in urban areas (produced from Vlachokostas et al., 2009).

In parallel to the above, particular features and needs of the area examined define the available control options “pool” that can be selected for air pollution abatement. Estimation of the cost and effectiveness for all available air pollution control measures and pollutants under consideration is a prerequisite in order to estimate marginal costs. The abatement cost accounting system is described analytically elsewhere (e.g. Klimont et al., 2002; Friedrich and Reis, 1999).

HIA and monetary valuation is additionally embodied in the system. A HIA should include only the health endpoints where quantification is based on strong and direct evidence and where a broad scientific consensus regarding evidence of reliable associations are available. This asserts that air pollution causes damage at least as great as quantified in the area under consideration and that reductions in pollution lead to widely, and especially politically accepted quantifiable benefits. Decisions are needed in regards to the Concentration (or Dose or Exposure if available) Response Functions (CRFs) that are adopted, as well as the relevant target population that these are applied to. Introducing monetary valuation of health impacts and the relevant internalization of external costs in this logic sets the problem in its pragmatic sustainable basis. Optimality arises from simultaneous consideration of control costs and economic societal benefits. The cost-benefit criterion exceeds the “polluter’s point of view” that guides the cost-effectiveness analysis. Finally the presented methodological scheme includes sensitivity analysis, since variables and parameter values in practice, originate from an analyst’s estimations, which are sometimes more or less reliable.

4 Health Impact Assessment

The basic steps in HIA include:

- (i) Selection of the set of health outcomes associated with air pollution,
- (ii) Adoption of the risk estimates based on epidemiological studies and
- (iii) Application of the adopted risk estimate to the distribution of exposure experienced by the target population.

There are specific issues of judgment and recommendations required in implementing the basic aforementioned steps of HIA as far as the effects of air pollution are concerned. Most crucial is the hazard identification, and in particular which impact pathways are considered most relevant. Since the pathways for quantification are identified, decisions are needed in regards to the CRFs that will be used as well as the relevant population that this CRF applies to, for example, whether it applies only to specific age groups or to people with a defined chronic disease. Moreover, the background rates or relevant estimates of mortality and morbidity in the target population require clarification. All the above are followed by the monetary valuation of the quantified physical impacts and the estimation of social costs.

Regarding the selection of the set of health outcomes associated with air pollution, it should be noted that the most consistent results globally have been found for particulate air pollution. Multi-pollutant analyses have indicated particulate matter (PM) as the most significant air pollution marker. The largest contribution to total damage cost attributed to air pollution comes from chronic mortality due to PM, calculated on the basis of Pope et al. (2002) risk estimates (ExternE, 2005). Another important contribution is attributed to chronic bronchitis due to PM. Correlations of PM_{10} or $PM_{2.5}$ exposure to chronic

mortality, new cases of chronic bronchitis, Cardiac Hospital Admissions (CHAs), Respiratory Hospital Admissions (RHAs) and Restricted Activity Days (RADs) can at least be included in the combined assessment of health impacts and emission abatement strategies. In addition, RHAs correlation to O₃ has gained a broad epidemiological consensus and it should also be included. One point that is raised here is on the extent to which it is reasonable to aggregate estimated impacts across pollutants. It is considered reasonable to add the estimated health impacts of PM with those attributed to O₃. This viewpoint reflects the issue that SO₂ and NO₂ tend to be more highly correlated with PM and with one another rather than with O₃. Care should be advised in the case that effects in NO₂ and/or SO₂ were to be estimated and added to the effects of PM and O₃ due to the danger of double-counting, especially with the estimated effects of PM (Hurley et al., 2005).

The second step followed is the adoption of risk estimates. Risk estimates are formulated in terms of Relative Risk (RR) or the respective CRF based on epidemiological studies. Most such studies report their results in terms of RR, so “translation” of the RR in terms of a CRF for the cases per exposure increment is needed in order to quantify damages. Quantification of health effects is usually expressed as the linking of two components:

- (i) RR, typically giving the rate of change in health endpoint per unit change in pollutant and
- (ii) The background rate of health effect in the population at risk.

The result of the analysis is the quantification of the expected health burden in the target population, expressed in terms of the number of cases or Years of Life Lost (YOLL) or number of RADs, attributable to the exposure.

The unfavorable implications over the health endpoints that are avoided after a scenario’s adoption are estimated through the following expression:

$$\Delta_{cases,i} = R_{i,p} \cdot \Delta_{conc_p} \cdot Pop \quad (1)$$

where:

- $R_{i,p}$: Correlation coefficient between the pollutant’s p concentration variation and the probability of experiencing or avoiding a specific health implication i (slope of the CRF).
- Δ_{conc_p} : Change in pollutant’s p concentration above the (lowest observed adverse effect level) after the adoption of an emission reduction scenario.
- Pop : Population exposed to pollutant p (target population).

Undoubtedly, mortality issues play a crucial role in health impact assessment issues. Over time, an understanding has emerged of how epidemiological studies of different design can be used to quantify mortality impacts from air pollution. More specifically, the first type is the “time series” studies, available for assessment of the short-term mortality impacts through exposure to specific

pollutants. These studies observe day to day changes in air pollution levels with changes in daily death rates and lead to impact estimates in terms of number of extra deaths brought forward, or lives shortened attributable to changes in air pollution in the immediately preceding days, aggregated over the entire year. In recent years, time series studies extended to provide information on effects on mortality up to several weeks after air pollution changes, rather than just a short period following those changes (APHEIS, 2004).

On the contrary, “cohort” studies examine age-specific death rates (mortality hazards) in study groups of individuals followed up over prolonged periods. Having adjusted for the influence on mortality of other factors measured for individuals (gender, race, smoking habit, educational status, etc.), differences in age-specific death rates are assessed against average pollution concentrations over periods of several years. Cohort studies of chronic exposure give results in terms of changes to mortality hazards per unit change in pollution. Key epidemiological cohort studies are those by Pope et al. (1995, 2002) and Dockery et al. (1993). It is now widely recognized that the strongest chronic mortality associations are with PM, while associations with O₃ are being reviewed. The role of other gaseous pollutants is still unclear.

In addition to the above analysis another issue should be raised at this point. Premature mortality estimations that can be attributed to air pollution can be expressed in two ways. One gives estimates in terms of extra deaths per year attributable to air pollution, while the other gives estimates in terms of YOLL across the whole population at risk. YOLL seems to be the metric that conforms best to the cohort studies from which the risk estimates are taken. On the other hand premature deaths appear easier to understand and sensitize. In order to explore the impact on the results of different valuation approaches, both metrics should be considered in the methodology presented.

5 Cost – Benefit Analysis

There is a growing interest in the internalization of externalities to assist policy and decision-making since it is a way to build the bridge towards sustainable development. Monetary valuation of health impacts attributable to air pollution is important to be included for completeness of any study which combines health impacts and emission abatement strategies. Otherwise there is a deficient picture of the range of adverse effects attributable to air pollution and the benefits to health from reducing it. In order to compare costs and benefits of specific policies to reduce air pollution, it is essential that those be compared on a common basis. That should include monetary valuation of the benefits to health and common accounting time frame for the evaluation of costs and benefits.

It should be emphasized that the Value of a Statistical Life (VSL) is not the most rational economic approach for monetary valuation of the extra deaths brought

forward due to higher air pollution or postponed due to lower air pollution, as it attributes the “full” VSL to what is understood to be only a small portion of a full life expectancy. Air pollution in the days immediately preceding death is one of the many reasons that contribute to life shortening. It is widely understood that higher air pollution in the days before death is a contributory factor to earlier death only for people who already have serious cardio-respiratory diseases or other sensitivities. It seems reasonable to attribute the deaths in greater extent to the underlying disease and, perhaps, to the risk factors (smoking, occupation, diet, poverty etc.) that caused it (Rabl, 2003). YOLL and the relevant Value of Life Year (VOLY) reflects the fact that there is really no such thing as “lives saved” by lower air pollution. However, in order to explore the impact on the results of different valuation approaches, both metrics and their monetary estimates should be considered.

In regards to control cost estimation this can be based on the literature and expert opinions for specific categories of abatement alternatives that can be identified for the main processes in the area under consideration, where there is no available local information (something that usually is the real case). In brief, in order to estimate, for example, the costs of collection devices, the net discounted cash flow of total capital investments and net annual operating costs incurred each year over the useful life of the equipment should be estimated (annual uniform method). To estimate the value of switching to cleaner fuels, the cost of transformation and the cost differential associated with using a different fuel is to be estimated.

6 Uncertainties and Research Needs

The final and most critical issue to address is that there are inherent uncertainties in the combined assessment of health impacts and emission abatement strategies due to specific assumptions that are possibly unavoidable. General sources of individual uncertainties could come from data series uncertainties, emission and atmospheric dispersion and chemistry model uncertainties, uncertainty about the future, synergies and idiosyncrasies of the analyst in the interpretation of ambiguous or incomplete information. Regarding the uncertainties within the core of health impact assessment, these usually apply air pollution effect estimates derived from a study in one population (the evidentiary population), to estimate impacts in another (the target population). Moreover, assumptions about causal links between a pollutant and a health impact, slope of a CRF, assumptions about the form of a CRF (e.g. with or without threshold) contributes to the inherent uncertainties.

Transferring RRs to other countries is rationally questioned due to the fact that the RR differs for populations other than the one in the original epidemiological study. There are uncertainties in applying RRs in a situation where the ambient pollutant mixture is different from the one where the original epidemiological

study was carried out. However, epidemiological results internationally show a remarkable degree of consistency of findings that can be found even from studies with important differences in population, climate and pollution mixture. In any case this should not replace local epidemiological studies.

Furthermore, separating out the roles of SO₂, NO₂ and PM in the CRFs would be particularly problematic, given that they tend to vary together in most locations and studies. In addition, toxicological studies have highlighted that primary, combustion-derived particles have a high toxic potency and that several other components of the PM mixture including sulfates and nitrates are lower in toxic potency. It is not clear to what extent the apparent effects of PM are, in reality a reflection of effects of NO₂ or SO₂ or vice versa, or whether the presence of other pollutants affects the toxicity of PM. Anyhow it is a future challenge to precisely quantify the contributions from different sources and different PM components to health effects, especially in regards to the finer fractions.

Undoubtedly, the current state of knowledge still has gaps and uncertainties. The purpose of ongoing research is to cover more effects and thus reduce gaps and in addition refine the methodology to reduce uncertainties. Clarity in defining these issues is a prerequisite for proper interpretation of the results in the policy arena. Nevertheless, the results are often prone to misinterpretation, even when the assessment is carried out carefully, and its multiple uncertainties are carefully presented and explained to decision makers, the press, and the public (Krzyzanowski et al., 2002). But the important conclusion is that the probable magnitude of the impacts, imposed to public health, avoided would justify the decision to implement policy measures to reduce air pollution in an area with high air pollution levels.

7 Summary and Conclusions

The methodological framework presented supports optimal decision making regarding the adoption of air pollution control options, especially at urban scale, where high air pollution levels are in parallel with high population densities. The incorporation of source-receptor relationships with the respective transfer coefficients and CRFs into mathematical programming models for optimizing urban air pollution control constitutes an important step towards the identification of more sustainable and hopefully, more politically acceptable abatement strategies. The decision maker should not neglect this capability, since it provides an easy to use tool in order to estimate the optimal solutions in crucial environmental problems, as this is urban air pollution.

In our days, the aforementioned need is strengthened considering the fact that during the past years air quality health impact assessment has become a matter of major importance given the increase of scientific proofs that show the impacts of air pollution in public health. Cost-benefit analysis is the sustainable approach

since the optimal levels of air pollution correspond to the point where the net social benefit is maximized and shifts the problem to a **pragmatic sustainable basis**. It passes over the polluter's point of view who simply aims the adequate emission reductions to levels that minimize control cost, with the limitation set by the air quality legislation and gives to public and environmental institutions the possibility of a **real** negotiation regarding air pollution control.

References

- Abbey D.E., Petersen F., Mills P.K. and Beeson W.L., 1993. Long-term ambient concentrations of total suspended particulates, ozone and sulphur dioxide and respiratory symptoms in a non-smoking population. *Archives of Environmental Health* 48: 33-46.
- APHEIS (Air Pollution and Health: A European Information System), 2004. Health impact assessment of air pollution and communication strategy. APHEIS (Medina S., Plasència A., Artazcoz L. Quénel P., Katsouyanni K., Mücke H.-G., De Saeger E., Krzyzanowsky M., Schwartz J. and the contributing members of the APHEIS group), Third Year Report, 2002-2003.
- Armstrong B. and Tremblay C., 1994. Lung cancer mortality and polyaromatic hydrocarbons. *American Journal of Epidemiology* 139 (3), 250-262.
- Borrego C., Tchepel O., Barros N. and Miranda A., 2000. Impact of road traffic emissions on air quality of the Lisbon region. *Atmospheric Environment* 34, 4683-4690.
- Brunekreef B., 1984. The relationship between air lead and blood lead in children: a critical review. *Science of the Total Environment* 38, 79-123.
- Dockery D.W., Pope C.A., Xiping Xu, Spengler J.D., Ware J.H., Fay M.E., Ferris B.G. and Speizer F.E., 1993. An association between air pollution and mortality in six US cities. *New England Journal Medicine* 329, 1753-1759.
- Dockery D.W. and Pope C.A., 2006. Health effects of fine particulate air pollution: lines that connect (2006 critical review), *Journal of the Air & Waste Management Association* 56, 709-742.
- ExternE: Externalities of Energy 2005. *Methodology 2005 Update*. Published by European Commission, Directorate-General for Research, Sustainable Energy Systems, Office of Publications for the European Communities, Luxembourg.
- Friedrich R., Reis S., Voehringer F., Simpson D., Moussiopoulos N., Sahm P., Turlou P.M., Salmons R., Papameletiou D. and Maqueda J.M., 1999. Assessment of policy instruments for efficient ozone abatement strategies in Europe: The INFOS Project, *Proceedings of the EUROTRAC Symposium 98* (P.M. Borrell and P. Borrell, eds.), WITpress, Computational Mechanics Publications, Southampton, Vol. 1, 784-787.
- Hoek G., Brunekreef B., Goldbohm S., Fischer P. and van den Brandt P.A. 2002. Association between mortality and indicators of traffic-related air pollution in the Netherlands: a cohort study. *The Lancet* 360, 1203-1209.
- Holland M., Hunt A., Hurley F., Navrud S. and Watkiss P., 2005. *Methodology for the Cost - Benefit Analysis for CAFE: Volume 1: Overview of Methodology*. Service Contract for Carrying out Cost-Benefit Analysis of Air Quality Related Issues, in particular in the Clean Air for Europe (CAFE) Programme. Didcot UK, AEA Technology Environment.

Hurley F., Hunt A., Cowie H., Holland M., Miller B., Pye S. and Watkiss P., 2005. *Methodology for the Cost-Benefit Analysis for CAFE: Volume 2: Health Impact Assessment*. Service Contract for Carrying out Cost-Benefit Analysis of Air Quality Related Issues, in particular in the Clean Air for Europe (CAFE) Programme. Didcot UK, AEA Technology Environment.

Katsouyanni K., Touloumi G., Samoli E., Gryparis A., Le Tertre A., Monopoli Y., Rossi G., Zmirou D., Ballester F., Boumghar A., Anderson H.R., Wojtyniak B., Paldy A., Braunstein R., Pekkanen J., Schindler C. and Schwartz J. 2001. Confounding and effect modification in the short term effects of ambient particles on total mortality: results from 29 European cities within the APHEA2 project. *Epidemiology* 12(5), 521-31.

Klimont Z., Cofala J., Bertok I., Amann M., Heyes C. and Gyarfas F. 2002. *Modelling Particulate Emissions in Europe - A Framework to Estimate Reduction Potential and Control Costs*. Interim Report IR-02-076, IIASA, Laxenburg, Austria,

Krupnick A.J., Harrington W. and Ostro B., 1990. Ambient ozone and acute health effects: Evidence from daily data. *Journal of Environmental Economics and Management* 18, 1-18.

Krzyzanowski M., Cohen A. and Anderson R., WHO Working Group. 2002. Quantification of health effects of exposure to air pollution. *Journal of Occupational and Environmental Medicine* 59, 791-793.

Kunzli N., Kaiser R., Medina S., Studnicka M., Chanel O., Herry M., Horak F., Puybonnieux-Texier V., Quénel P., Schneider J., Seetaler R., Vergnaud J.C. and Sommer H., 2000. Public health impact of outdoor and traffic-related air pollution: a European assessment. *Lancet* 356, 795-801.

Le Tertre A., Medina S., Samoli E., Forsberg B., Michelozzi P., Boumghar A., Vonk J.M., Bellini A., Atkinson R., Ayres J.G., Sunyer J., Schwartz J. and Katsouyanni K., 2002. Short term effects of particulate air pollution on cardiovascular diseases in eight European cities. *Journal of Epidemiology and Community Health* 56, 773-779.

Moussiopoulos N., ed. (2003). *Air Quality in Cities*. Springer, Heidelberg, 299 pp.

Moussiopoulos N., Vlachokostas Ch., Tsilingiridis G., Douros I., Hourdakis E., Naneris C. and Sidiropoulos C., 2009. Air quality status in Greater Thessaloniki Area and the emission reductions needed for attaining the EU air quality legislation. *Science of the Total Environment* 407, 1268-1285.

Ostro B.D., 1987. Air pollution and morbidity revisited: A specification test. *Journal of Environmental Economics and Management* 14, 87-98.

Pope C.A. 3rd, Thun M.J., Namboodiri M.M., Dockery D.W., Evans J.S., Speizer F.E. and Heath C.W. Jr., 1995. Particulate air pollution as predictor of mortality in a prospective study of US adults. *American Journal of Respiratory and Critical Care Medicine* 151, 669-674.

Pope C.A. 3rd, Burnett R.T., Thun M.J., Calle E.E., Krewski D., Ito K. and Thurston G.D., 2002. Lung cancer, cardiopulmonary mortality, and long-term exposure to fine particulate air pollution. *Journal of the American Medical Association* 287, 1132-1141.

Rabl A., 2003. Interpretation of Air Pollution Mortality: Number of Deaths or Years of Life Lost? *Journal of the Air & Waste Management Association* 53 (1), 41-50.

Schwartz J., 1993. Particulate air pollution and chronic respiratory disease. *Environmental Research* 62, 7-13.

Vlachokostas Ch. and Moussiopoulos N., 2004. The multi-pollutant cost-effectiveness emission reduction problem. *Proceedings of the 7th International Conference on Protection and Restoration of the Environment*, Mykonos, Greece, 28 June - 1 July, CD-ROM edition.

Vlachokostas Ch., Achillas Ch., Moussiopoulos N., Hourdakis E., Tsilingiridis G., Ntziachristos L., Baniyas G., Stavrakakis N. and Sidiropoulos C., 2009. Decision support system for the evaluation of urban air pollution control options: Application for particulate pollution in Thessaloniki, Greece. *Science of the Total Environment* 407, 5937-5948.

Wilson R. and Spengler J., 1996. *Particles in our air: concentrations and health effects*. Boston: Harvard University Press.

World Health Organisation (WHO), 2003. Health aspects of air pollution with particulate matter, ozone and nitrogen dioxide. Report on a WHO Working Group, Bonn, Germany.

BRANKLEY PARK

Chapter 16

Statistical Modeling

A brief introduction to the topic “Statistical Modeling” was presented in Volume I of this book series.

Two chapters on this topic were included in Volume II:

16A – Air Quality Forecast and Alarm Systems. The abstract is reprinted below.

The following chapter reports a review of different stochastic and statistical modeling approaches, and the results obtained by their application to actual case studies both in urban and in industrial areas. The assessment of the results, in terms of daily and hourly forecast performance indexes and statistical indicators, is presented, compared and discussed. The structure of the chapter is the following. After a preliminary section summarizing the most significant stochastic and statistical modeling techniques (Section 1), some literature results are reported in Section 2. A more detailed mathematical description of the main techniques considered for air quality modeling is given in Section 3. Section 4 gives guidelines on how to build a model for air quality forecast and evaluate its performances. Some case studies concerning the modeling of tropospheric ozone concentrations, both in urban and industrial areas, are given in Section 5. In Section 6 the application of the selected techniques to the implementation of an operational decision support system (DSS) is described. Also, the performance of the system for two different metropolitan areas in the Northern part of Italy (namely Brescia and Milan) is evaluated. Finally, a short survey of the available software packages to implement the modeling techniques described is given in Appendix.

16B – Receptor Models. The abstract is reprinted below.

Receptor models complement source models by independently identifying sources and quantifying their contributions using ambient measurements of different observables at different times and locations. Source apportionment is accomplished by solution of the mass balance equations that express concentrations of several measured pollutants as a linear sum of products of pollutant abundances in source emissions and source contributions. These equations can be solved by several methods, including maximum likelihood weighted least squares, singular value decomposition eigenvectors, and positive matrix factorization. A viable solution does not guarantee physical reality, so internal and external validation measures must be evaluated. Receptor models are best used in conjunction with source models to create a “weight of evidence” for justifying emission reduction measures on different source types.

In this Volume IV, we provide:

16C – Ensemble-Based Air Quality Predictions

Delle Monache, L., 2010. *Ensemble-Based Air Quality Predictions*. Chapter 16C of *AIR QUALITY MODELING - Theories, Methodologies, Computational Techniques, and Available Databases and Software. Vol. IV – Advances and Updates* (P. Zannetti, Editor). Published by The EnviroComp Institute (<http://www.envirocomp.org/>) and the Air & Waste Management Association (<http://www.awma.org/>).

Chapter 16C

Ensemble-Based Air Quality Predictions

Luca Delle Monache

*National Center for Atmospheric Research, Research Applications Laboratory,
PO Box 3000, Boulder, CO 80307-3000 (USA)*

lucadm@ucar.edu

Abstract: A review of the current state-of-the-science of ensemble predictions for air quality is presented. Probabilistic predictions are required to better represent the evolution of the atmosphere and its constituents. Ensembles are a practical way to sample the probability density function representing the system state. Proposed ensemble designs are described, and ensemble-based deterministic and probabilistic prediction systems are introduced. The importance of the spread-skill relationship for an ensemble is discussed, along with an analysis of recently proposed methods to postprocess and calibrate deterministic and probabilistic predictions. Finally, the economic value of ensembles is analyzed.

Key Words: air quality forecasting, ensembles, probabilistic predictions, emission control policies.

1 Introduction

High concentration levels of surface ozone and PM_{2.5} cause respiratory and cardiovascular problems leading to premature deaths and high costs associated with health care, school absences, missed work, lost income potential from premature deaths and damages to crops and forests. Moreover, consuming seafood contaminated with high levels of mercury can harm the brain and other organs, especially during in-utero and early childhood development, and acidic and nitrogen compounds deposit onto watersheds and water surfaces can degrade water quality, impair ecosystem health and reduce commercial and recreational use of these areas. It has been estimated that in the U.S. poor air quality causes as

many as 60,000 premature deaths each year with costs between \$100¹ and 150 billion per year².

Accurate air quality predictions can provide individuals and communities with timely information to help them limit exposure and reduce health problems caused by poor air quality, and even save lives. It is difficult to estimate how many lives and costs could be saved with accurate and reliable air quality predictions. Nevertheless, assuming that such predictions reduce by 1% the premature deaths and the costs listed above, about 600 lives and over \$1 billion could be saved each year. It is worth noticing that these are more lives saved than the 500 deaths caused on average each year by all the hydrometeorological threats (including hurricanes, tornados, floods, violent thunderstorms, etc.)³.

The atmosphere is a chaotic system, meaning that its spatio-temporal evolution is sensitive to the initial state from which this evolution is started. Two trajectories of such systems starting from slightly different initial states will eventually diverge one from the other up to a point in which they can be seen as randomly chosen (Lorenz 1963).

Recognizing this intrinsic aspect of the atmosphere behavior has led to the development of probabilistic approaches (rather than purely deterministic) in the field of Numerical Weather Prediction (NWP). Ideally the evolution of the complete probability distribution describing the forecast variable and/or probability for a specific event should be followed in time and space to produce a probabilistic assessment of the future state of the dynamical system under consideration (Epstein 1969). This can be accomplished by solving the Liouville equation, i.e., the continuity equation of the probability density function of the state vector of a dynamical system (Ehrendorfer 2006). However, the latter approach is currently unfeasible due to the prohibitive computational costs associated with solving the Liouville equation when applied to the atmosphere. A Monte Carlo ensemble approach is a practical alternative for large geophysical systems as the atmosphere, where the goal is to create an equitable sample of the probability distribution. An ensemble member is a deterministic model run from a given sample, and the evolution of the probability distribution in space and time is followed by the integrating in time each ensemble member. During the last 20 years or so many NWP operational centers have developed prediction systems based on an ensemble, and in general ensembles have proven to provide better accuracy of any individual ensemble members (e.g., Leith 1974; Toth and Kalnay 1993; Wobus and Kalnay 1995; Molteni et al. 1996; Du et al. 1997, Hamill and Colucci, 1997; Toth and Kalnay 1997; Buizza and Palmer 1998; Stensrud et al., 1998; Krishnamurti et al., 1999; Evans et al., 2000; Kalnay, 2003).

¹ http://www.nrc.noaa.gov/plans_docs/2009/AQSOSFactSheetFinal.pdf

² http://www.weather.gov/ost/air_quality/Fact%20Sheet%200208.pdf

³ <http://www.economics.noaa.gov/?goal=climate&file=users/government/nws>

The US Weather Research Program and its Prospectus Development Team on Air Quality Forecasting (Dabberdt et al., 2004) has recommended a probabilistic approach to air quality forecasting because of the chaotic nature of the atmosphere and chemistry nonlinearity. Recently several efforts have focused on the exploration and development of probabilistic predictions for air quality. Ensembles have been proposed for short-term air quality predictions (e.g., Delle Monache and Stull 2003; McKeen et al. 2005; Pagowski et al. 2005; Delle Monache et al. 2006a,b,c; Pagowski et al. 2006; Pagowski and Grell 2006; Mallet and Sportisse 2006a,b; Vautard et al. 2006; Wilczak et al. 2006; McKeen et al. 2007; Zhang et al. 2007; Delle Monache et al. 2008; Mallet et al. 2009; Pinder et al. 2009; Bei et al. 2010; Djalalova et al. 2010; Garaud and Mallet 2010) and to predict the impact of emission control policies (e.g., Cuvelier et al. 2007; Thunis et al. 2007; van Loon et al. 2007; Vautard et al. 2007; Vautard et al. 2009). Moreover, recent developments have shown that air quality predictions can be improved through the assimilation of chemical data (see Fig. 1 and also Constantinescu et al. 2007b; Carmichael et al. 2008 and references therein). With the increasing availability of observations of atmospheric chemical species, chemical data assimilation will play an important role in air quality forecasting, similar to the role it has already in NWP (with the possibility to be beneficial for weather forecasting as well).

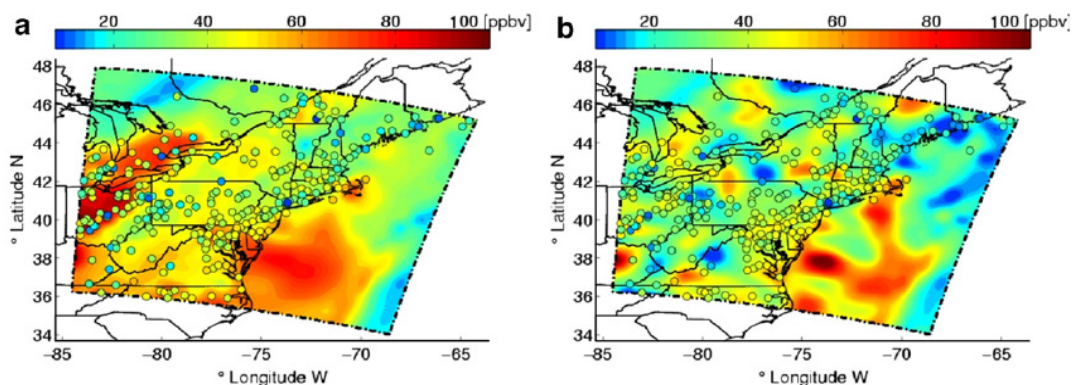


Figure 1. Ground level ozone concentrations in North-Eastern United States at 14:00 EDT on July 20, 2004, before (a) and after data assimilation (b). The ground-level ozone observations used for data assimilation were provided by the AirNow network (<http://www.airnow.gov>) and are shown as circles colored by the measured ozone levels (adapted from Carmichael et al. 2008). Courtesy of Gregory Carmichael.

In air quality, in addition to the uncertainty coming from the driving meteorological fields, other sources of uncertainties have an important contribution to the shape of the probability distribution describing the system state, namely the emissions and the chemistry. Ideally, air quality ensemble designs should be based on perturbations accounting for the uncertainties coming from all these components. Emissions do not exhibit the strong flow-dependency and day-to-day variability of errors as we see in the atmosphere and therefore

different strategies (from what it is done for the weather component) to capture their uncertainties may be more appropriate.

Moreover, also the chemistry may require specific approaches to capture its uncertainties, since it is described by a system of equations that are stiff, i.e., ordinary differential equations representing the evolution of chemical species reacting on very different time scales. These kinds of systems typically are very stable: small perturbations vanish as the system tends to evolve towards a quasi-steady state (Constantinescu et al. 2007a).

The remainder of this chapter will review the benefits of ensemble modeling for air quality that can be summarized as follows:

- The ensemble mean (or median) is the most skillful prediction compared to any individual ensemble member with a variety of metrics computed over a number of cases;
- The ensemble mean reduces random errors by filtering out the unpredictable components of the physical and chemical processes; for this reason, when combined with bias-removal methods that reduce systematic errors, ensemble averaging produce the best deterministic prediction;
- The ensemble mean performance can be further improved by assigning different weights to different ensemble members;
- Ensembles can provide reliable and sharp probabilistic predictions of events of interest (e.g., ozone or particulate matter (PM) above a given concentration threshold); the skill of probabilistic predictions can be largely improve with calibration procedures;
- Ensembles provide an estimate of the uncertainty of the prediction; the spread of a well calibrated ensemble can be used to produce such estimate (the spread can be defined as the standard deviation of the ensemble members' distribution around the ensemble mean). The bigger the spread, the less the confidence in the forecast.

2 Ensemble Designs

A skillful ensemble should be based on a design aiming to capture the main uncertainties along the modeling process that results in prediction uncertainties. For air quality modeling, these uncertainties comes from the driving meteorology, the initial conditions, the boundary conditions in case of limited area models, the emissions, and the chemical modules. Moreover, in this list it should also be included all the model inadequacy resulting from numerical approximations and poor or altogether lacking representations of physical and chemical processes that are not well understood or even known.

2.1 Lagged Ensembles

Hoffman and Kalnay (1983) and Dalcher et al. (1988) introduced and tested the lagged average weather forecast. The forecasts initialized at the current initial time, $\tau = 0$, as well as forecast from the previous times, $\tau = -\tau, -2\tau, \dots, -(N-1)\tau$ are combined at a common valid time to form an ensemble. This simple and efficient procedure allows generating ensembles even when only a deterministic forecast is produced, given a suitable combination of forecast issuing frequency and length.

Delle Monache et al. (2006a) expanded a 12-member ensemble run for 48-h, to an 18-member ensemble available for 24 hours by combining ensembles initialized at two consecutive days, as illustrated in Fig. 2. In their experiments the 18-member ensemble did not exhibit better prediction skills than the 12-member ensemble, probably because the added six lagged forecasts did not span more uncertainty than the original 12-member ensemble, and that no independent information on errors is added with those members. However, the lagged approach could provide skillful predictions when the forecast updates are more frequent than 24 hours (as shown for NWP by Lu et al. 2007; Mittermaier 2007) and it should be considered as a computational economic way to produce an ensemble in cases where resources are limited.

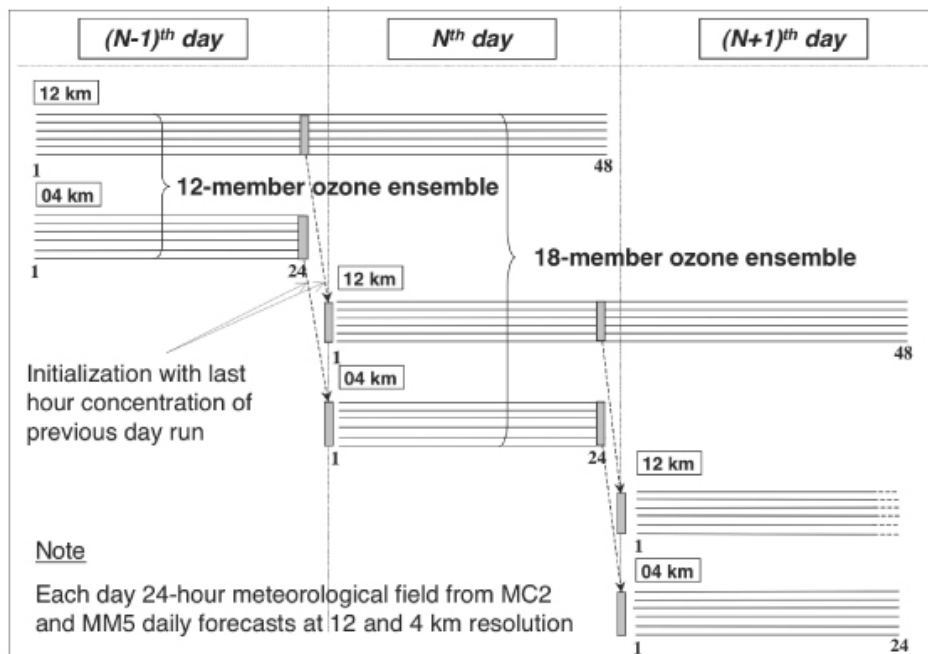


Figure 2. Eighteen-member Ozone Ensemble Forecast System (OEFS). Six 12-km resolution ensemble members are run for 48 hours. The second half of the $(N-1)^{th}$ forecast day can be added to the N^{th} day 12-member OEFS to form a lagged averaged ozone 18-member ensemble (adapted from Delle Monache et al. 2006a).

2.2 An Ensemble Based on Perturbations of Meteorology and Emission

Delle Monache et al. (2006a,c) proposed a new ensemble design where the ensemble members were built upon perturbation of the meteorology and the emissions. The four meteorology fields were provided from two mesoscale weather models each run with 12 and 4 km horizontal grid increments: the Mesoscale Compressible Community (MC2) NWP model (Benoit et al. 1997) and the Penn State/NCAR mesoscale (MM5) model (Grell et al. 1994). In addition seven emission perturbations (Fig. 3) were generated perturbing both VOC and NO_x following the work of Ainslie (2004).

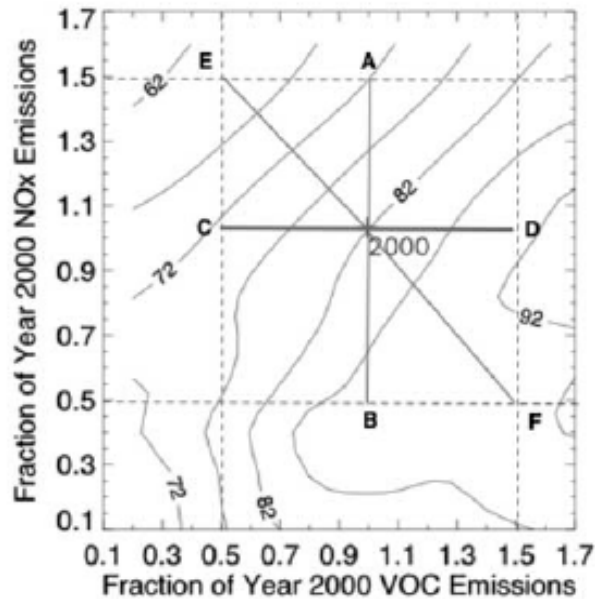


Figure 3. Isopleths of maximum ozone concentration (ppbv) as a function of year 2000 VOC and NO_x emissions over the Lower Fraser Valley (Ainslie 2004). Vertical bar spans plus (point A) and minus (point B) 50% NO_x perturbations. Horizontal bar spans plus (point D) and minus (point C) 50% VOC perturbations. Diagonal bar extends from plus 50% NO_x and minus 50% VOC perturbation (point E) to the minus 50% NO_x and plus 50% VOC perturbation (point F) (adapted from Delle Monache et al. 2006c).

These perturbations allowed generating 28 ensemble members. The authors grouped these members in several ways to study the property of different type of ensembles. These are some of the main findings in Delle Monache et al (2006a,c):

- The ensemble mean is the best forecast when compared to any ensemble member.
- Both meteorology and emission perturbations are needed to have a skillful probabilistic forecast system (PFS), and neither is sufficient alone to form a reliable PFS with a good resolution for the whole range of ozone concentrations.

- Meteorology perturbations are important to capture the ozone temporal and spatial distributions, while emission perturbations are necessary to better predict the ozone concentration magnitude, particularly high concentration levels.
- Nonlinear ozone chemistry and its response to different meteorological forcings play an important role that is not captured by varying the meteorology alone.

2.3 Multi-Physics Ensembles

Mallet and Sportisse (2006a,b), Garaud and Mallet (2010), and Bei et al. (2010) explored the potential of multi-physics ensembles to improve ozone forecasts (Figure 4). The multi-physics approach allows accounting for uncertainties coming from model inadequacies in representing some of the physical and/or chemical processes. Mallet and Sportisse (2006a,b) and Garaud and Mallet (2010) analyzed the performance of ensembles with up to 48 members generated within the modeling system Polyphemus. Members differ in their physical parameterizations, numerics, and initial conditions. The parameterizations used to diversify the ensemble members include the chemical, vertical diffusion, deposition velocities, surface fluxes, cloud attenuation, and critical relative humidity. Moreover, they perturbed among other aspects of the modeling process the emission vertical distribution, the land use coverage, photolysis constants, time step, vertical resolution, first layer height, the boundary layer height, NO and biogenic emissions, and ozone boundary conditions (See Table 1 in Mallet and Sportisse 2006a for details).

The authors found that turbulent closure and the chemical mechanism introduce the highest uncertainty, and the overall uncertainty, was estimated at 17% for the concentration in the interval 40 to 130 ($\mu\text{g m}^{-3}$) and at 11% for the 24-h d maximum ozone concentration. The uncertainty was notably high along the coasts. They concluded that ensemble approaches are necessary in most applications given the uncertainties associated with the modeling process. They also found that the best prediction can be obtained by linear combining the predictions from the different ensemble members, with a decrease of about 10% of the root-mean-square error (RMSE) for 24-h ozone maximum concentration, and larger improvements for hourly concentrations.

Bei et al. (2010) proposed an interesting approach where the ozone ensemble is build on different driving meteorological fields and different parameterizations for the boundary layer (BL). The simulated periods (3, 9, 15, and 29 March 2006), span typical meteorological regimes (“South-Venting”, “ozone-North”, “ozone-South” and “Convection-North”) in the Mexico City basin during the Mexico City Metropolitan Area (MCMA)-2006 / Local And Global Research Observations (MILAGRO) campaign. Their results demonstrate that uncertainties in meteorological initial conditions have significant impacts on the prediction of 24-h ozone maximum concentration, as well as the horizontal and vertical

distributions, and temporal variations of ozone. The magnitude of the ensemble spread varies with different BL schemes and meteorological episodes.

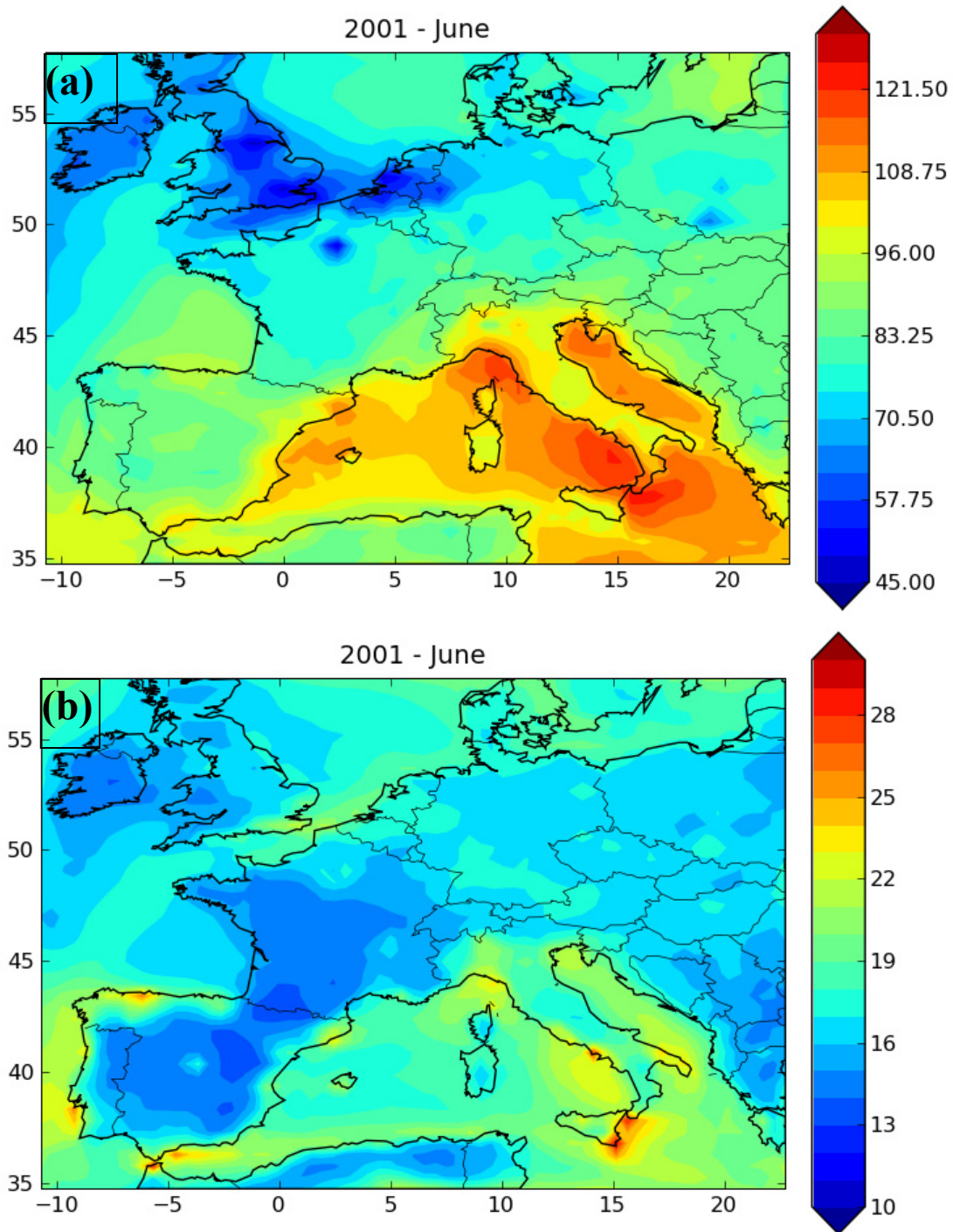


Figure 4. June 2001 monthly averages of ensemble mean (a) and ensemble spread (b) of a 30-member ensemble for ground-level ozone ($\mu\text{g m}^{-3}$) generated with the Polyphemus system (adapted from Garaud and Mallet 2010). Courtesy of Damien Garaud and Vivien Mallet.

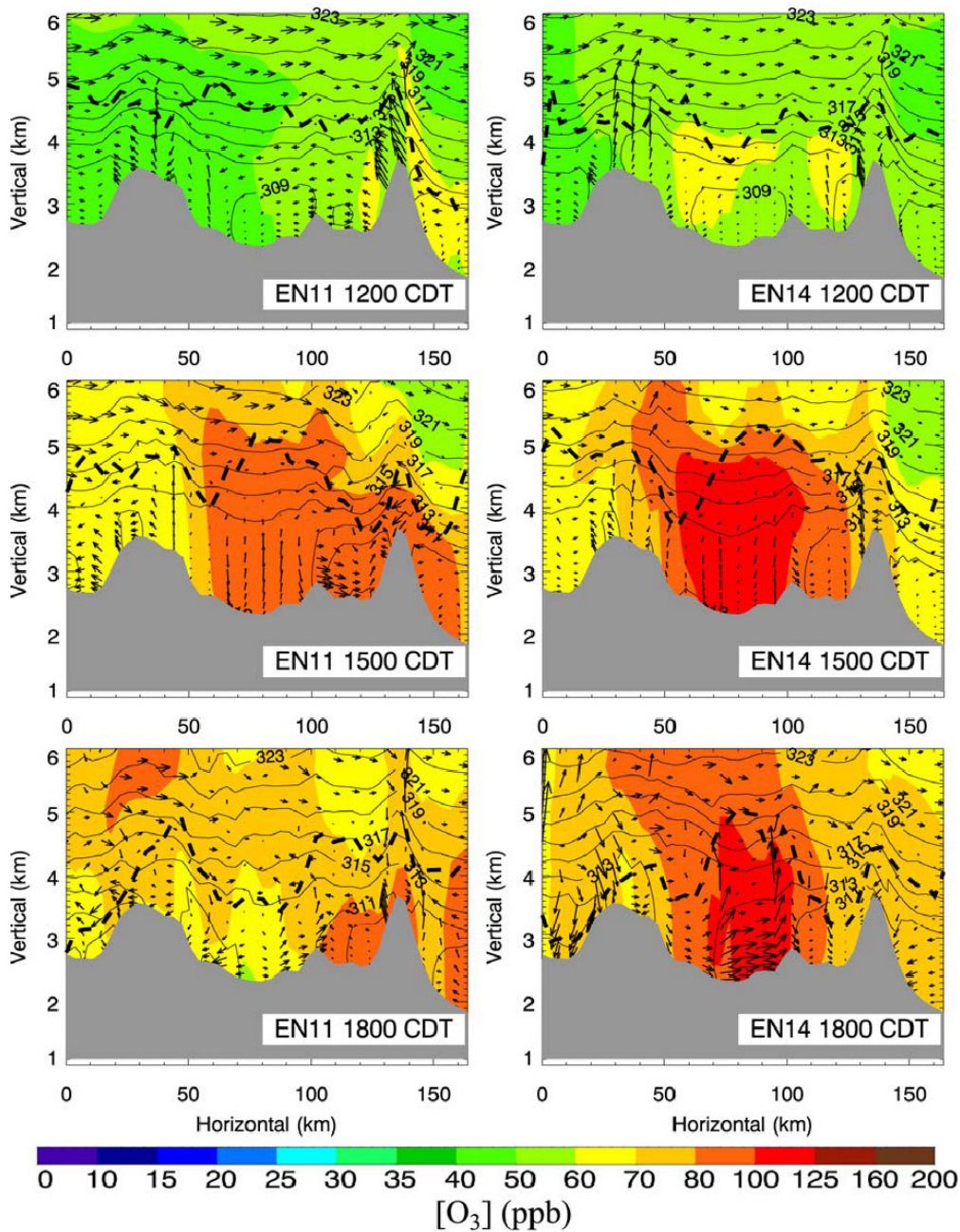


Figure 5. Cross section of ozone concentration (ppb, shading), wind vectors, potential temperatures (K, contours) and BL depth (km, bold dash lines, of two ensemble members (EN-11 and EN-12) valid at 12:00 CDT, 15:00 CDT, and 18:00 CDT on 3 March 2006. EN-11 has lower PBL height, higher wind speed, and lower surface temperature, which act together to lower ozone. EN-14 has higher PBL height, lower wind speed, and higher surface temperature that lead to higher ozone concentrations than with EN-11 (adapted from Bei et al 2010).

BL schemes uncertainties are mainly the results of their ability to represent the BL depth, but overall, these uncertainties are smaller than those generated by the

driving meteorological initial conditions. As an example, Figure 5 shows the large differences between ensemble members predicting the lowest and highest ozone concentration (when averaged over the 19 available sites) for vertical distributions of ozone, potential temperature, wind vectors, and BL depth before (upper), during (middle) and after (bottom) the occurrence of 24-h ozone maximum concentration.

2.4 Multi-Model Ensembles

Interesting discussions on some of theoretical basis supporting the use of multi-model ensembles models for operational long-range transport and dispersion models typically used for real-time simulations of accidental releases can be find in Riccio et al. (2007) and Potempski and Galmarini (2009). Multi-model ensembles have often proven to provide the most skillful prediction system for weather forecasting, when compared to ensembles of different nature or the individual ensemble members (Krishnamurti et al. 1999).

The multi-model approach is the method most widely explored for air quality, the main reason being the fact that it is an affordable effort when several institutions combine the predictions produced by their own modeling systems (e.g., for air quality forecasting see Delle Monache and Stull 2003; McKeen et al. 2005; Pagowski and Grell 2006; Vautard et al. 2006; McKeen et al. 2007; and to predict the impact of emission control policies Cuvelier et al. 2007; Thunis et al. 2007; van Loon et al. 2007; Vautard et al. 2007; Vautard et al. 2009).

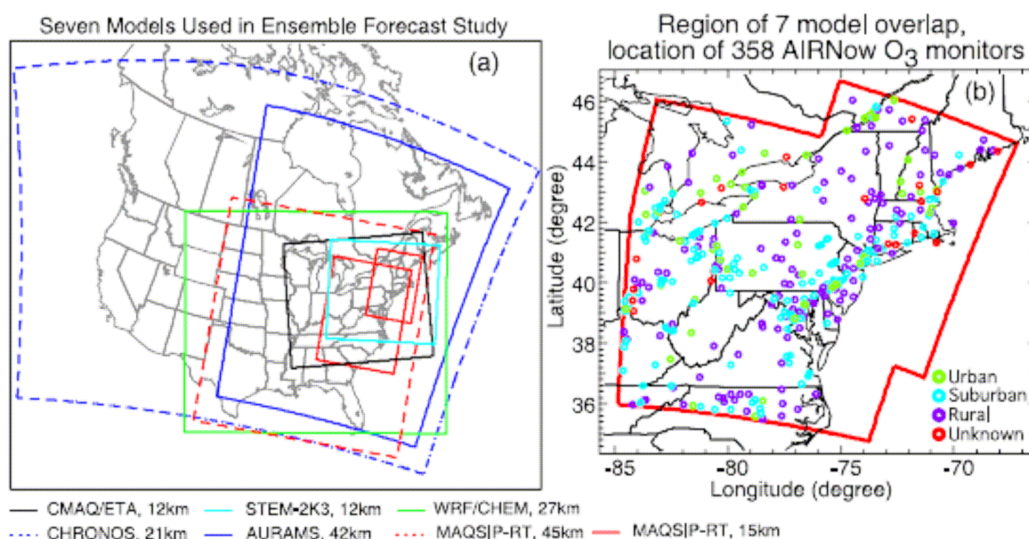


Figure 6. Continental map of North America showing the model boundaries of the eight models used in the analysis and ensemble average (a). Overlap of model domains (red boundary) and the locations of the 358 AIRNow monitors that collected real-time ozone measurements during summer of 2004 (adapted from McKeen et al. 2005). Courtesy of Stuart McKeen.

Multi model ensembles have resulted in improved predictions for ground-level ozone. For instance, Fig. 6 (McKeen et al. 2005) shows the domains and their overlap of eight chemical transport models that were run in the summer of 2004 for 53 days and evaluated at roughly 340 monitoring stations throughout the eastern United States and southern Canada. The ensemble mean and median was found to have significantly more temporal correlation to the observed daily maximum 1-hour average and maximum 8-hour average O₃ concentrations than any individual model. The ensembles performance is superior also for RMSE skill score and threshold statistics when the raw forecasts are corrected with simple bias-correction methods. McKeen et al. (2005) concluded that the higher correlation coefficients, low RMSE, and better threshold statistics for the ensembles compared to any individual model point to their preference as a real-time ozone forecast.

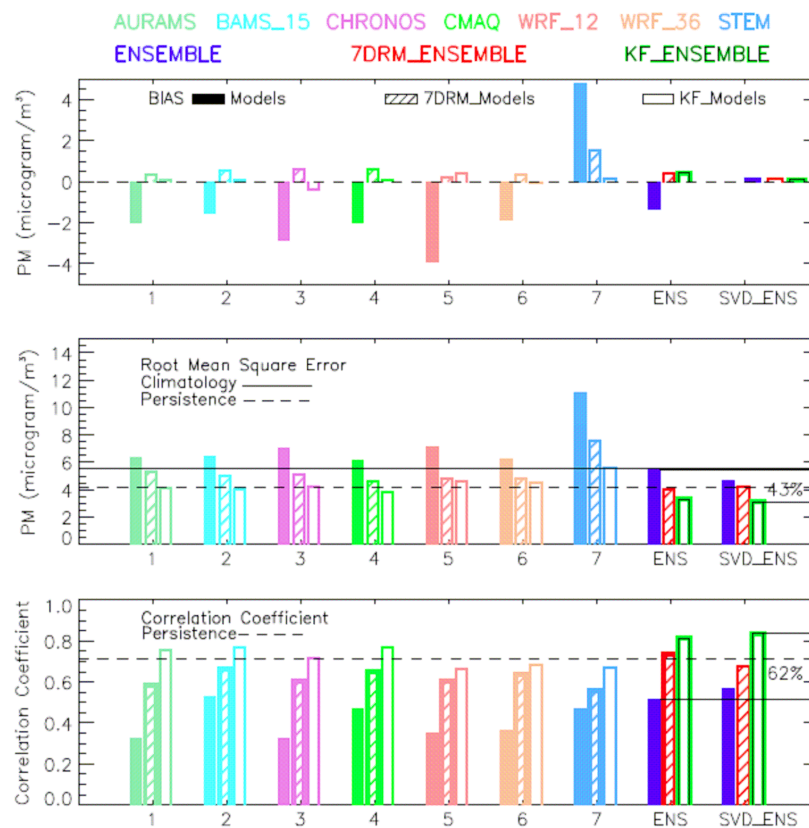


Figure 7, PM_{2.5} bias (top), RMSE (middle) and correlation (bottom) for a 7-member ensemble. Climatology and persistence skills are shown with the solid and dashed lines, respectively. Raw, 7 DRM bias corrected and KF-bias corrected models are depicted, with solid colored, hatched, and open boxes respectively. Also shown is the raw ensemble (blue), the 7-day bias-corrected ensemble (hatched red) and the Kalman Filter bias-corrected ensemble (open green), and their weighted versions, where weights are computed with a Single Value Decomposition (SVD) (Krishnamurti et al. 1999; Pagowski et al. 2005). The improvements of RMSE and correlation of the SVD_KF ensemble compared to the raw ensemble is marked (adapted from Djalalova et al 2010). Courtesy of Irina Djalalova.

Multi-model ensembles also provide the best forecast for PM_{2.5} (e.g., McKeen et al. 2007; Djalalova et al. 2010). Djalalova et al. (2010) tested several air quality forecasting ensembles created from seven models, that were run in real-time during the 2006 Texas Air Quality (TEXAQS-II) experiment. These multi-model ensembles were based on different driving meteorological fields, chemical mechanisms, and emission inventories. The ensembles and the individual models forecasts of surface ozone and PM_{2.5} were evaluated using data from 119 EPA AIRNow ozone sites and 38 PM_{2.5} sites during a 50-day period in August and September of 2006. Fig. 7 (Djalalova et al. 2010) shows an example where for PM_{2.5} forecasts the ensembles reduce bias and RMSE and improve correlation, particularly when combined with two bias correction methods, a 7-day correction (Wilczak et al. 2006) and a Kalman filter (KF) correction (Delle Monache et al. 2006b; Delle Monache et al. 2008) and a weighting procedure (Pagowski et al. 2006).

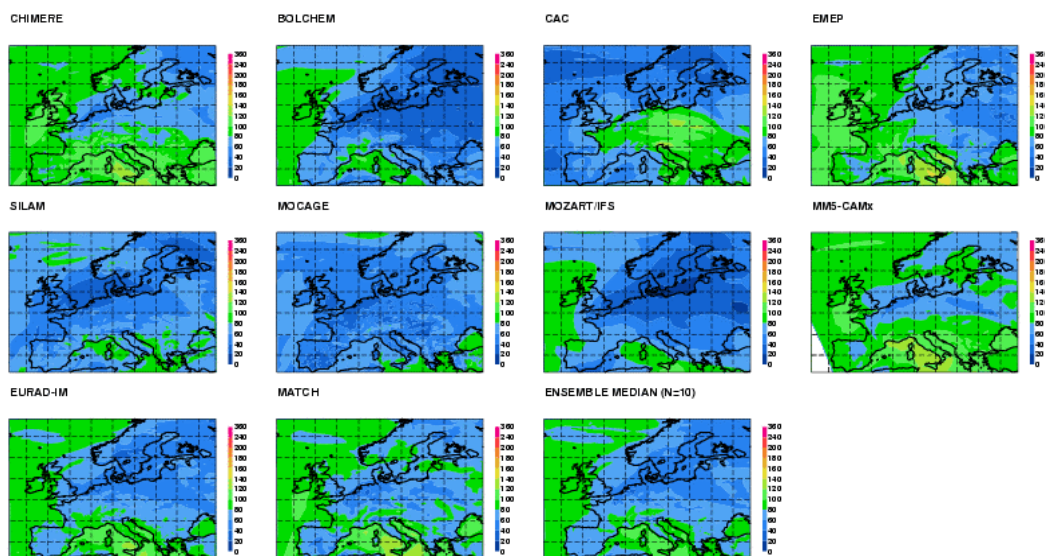


Figure 8. Daily mean of ground-level ozone ($\mu\text{g m}^{-3}$) as predicted by eleven air quality prediction systems, for 18 March 2010. These models are part of the operational air quality ensemble employed by ECMWF over Europe (http://gems.ecmwf.int/d/products/raq/ensemble/epsfields/plot_ensemble_o3/).

Finally, in Europe an operational multi-model air quality ensemble is currently employed by European Centre for Medium-Range Weather Forecasts (ECMWF) under the European Union funded projects Global and regional Earth-system (Atmosphere) Monitoring using Satellite and in-situ data (GEMS) and Monitoring Atmospheric Composition and Climate (MACC) (see http://gems.ecmwf.int/d/products/raq/ensemble/epsfields/plot_ensemble_o3/). Figures 8 and 9 show some of the products available to the public generated with this state-of-the-science prediction capability for regional air quality. Fig. 8 shows the predictions of ground-level ozone over Europe as predicted from eleven different models, while Figure 9 shows predictions of different pollutants at a specific location (Amsterdam, The Netherlands). The boxes show the minimum, median

and maximum value of the ensemble predictions, along with the 10th, 25th, 75th, and 90th percentile of the distribution of predictions, a convenient way to convey clearly the large amount of information provided by an ensemble.

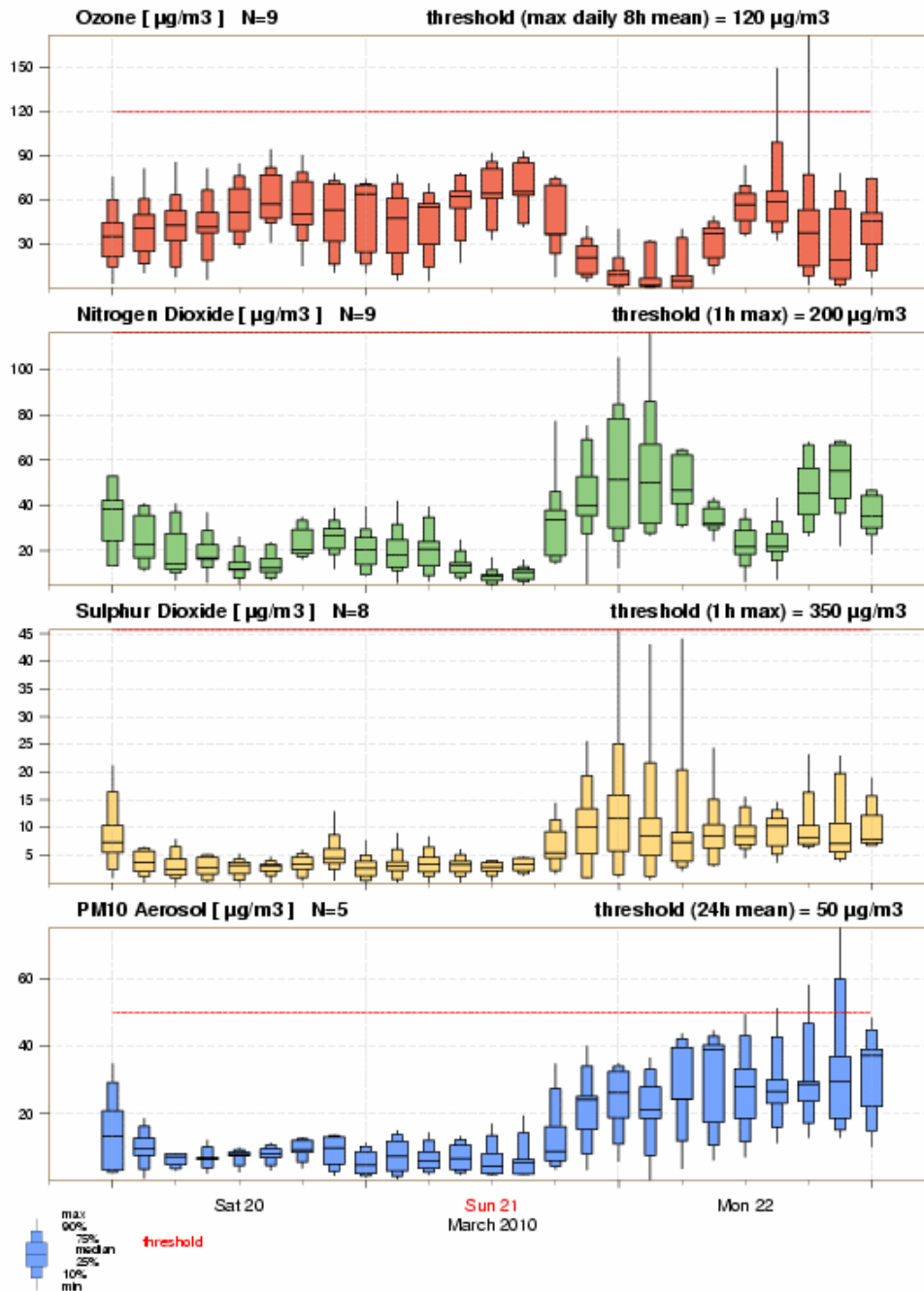


Figure 9. Air quality predictions issued at 00 UTC, 20 March 2010, at Amsterdam, The Netherlands. The boxes show at a give time, the minimum, median, and maximum, as well as the 10th, 25th, 75th, and 90th percentile of the values predicted by the ensemble members (see legend at the bottom left). Red horizontal lines represent the thresholds for each pollutant.

3 Ensemble-Based Deterministic Predictions

Ensembles prediction can provides both high-fidelity deterministic predictions as well as estimates of the probability of an event. In this section the former is discussed, whereas probabilistic predictions are presented in section 4.

Deterministic predictions can be generated from an ensemble of air quality predictions as follows:

- By computing the ensemble linear average at any given time and point in space, often referred to as ensemble mean prediction;
- By computing a weighted ensemble average, where the weights are proportional to the individual ensemble members' skill.
- By selecting a percentile of the ensemble distribution (e.g., the 50th percentile that corresponds to the median of the distribution).

3.1 Ensemble Mean

The ensemble mean has been proven to provide often the best forecast when compared against each individual ensemble member over a range of metrics and for a number of forecasts in several independent studies where different ensemble designs have been exploited (e.g., Delle Monache and Stull 2003; McKeen et al. 2005; Pagowski et al. 2005; Delle Monache et al. 2006a; Pagowski and Grell 2006; Wilczak et al. 2006; McKeen et al. 2007; van Loon et al. 2007; Delle Monache et al. 2008; Mallet et al. 2009; Vautard et al. 2009; Djalalova et al. 2010). For example Figs. 7 (Djalalova et al. 2010) and 10 (McKeen et al. 2005) show the ensemble mean to be superior over a number of metrics for both ozone and PM predictions.

For any given forecast the ensemble average may not be the best performing prediction. However, when the statistical metrics that are used to estimate the prediction skill are computed over a number of forecasts the ensemble mean is indeed the best performing prediction. This is caused by the fact that ensemble averaging filters out the less predictable components of the spatio-temporal evolution of the quantity of interest (e.g., ground-level ozone concentration). For instance, in a 10-member ensemble at a given time and location there may be 8 members providing a skillful prediction, while two may provide an inaccurate prediction. However, at a different time and/or location, the subset of forecasts with less skill may comprise forecasts from the 8 members that were performing well previously, and vice versa the two forecasts that were not skillful previously may now be among the best predictions. If there were an ensemble member that is always the best, than obviously that would be the best deterministic predictions (i.e., better than the ensemble mean). However, the ensemble member that performs the best change often in space and time, and it is not possible to know a priori which ensemble member will perform best for a given location and time. This is due by the nonlinear interaction between uncertainties in the different components of the air quality forecasting process, that lead to less sophisticated

models to outperform better models at times. That is why when averaging all the members the best performing predictions is obtained, when a sufficient number of forecasts are considered.

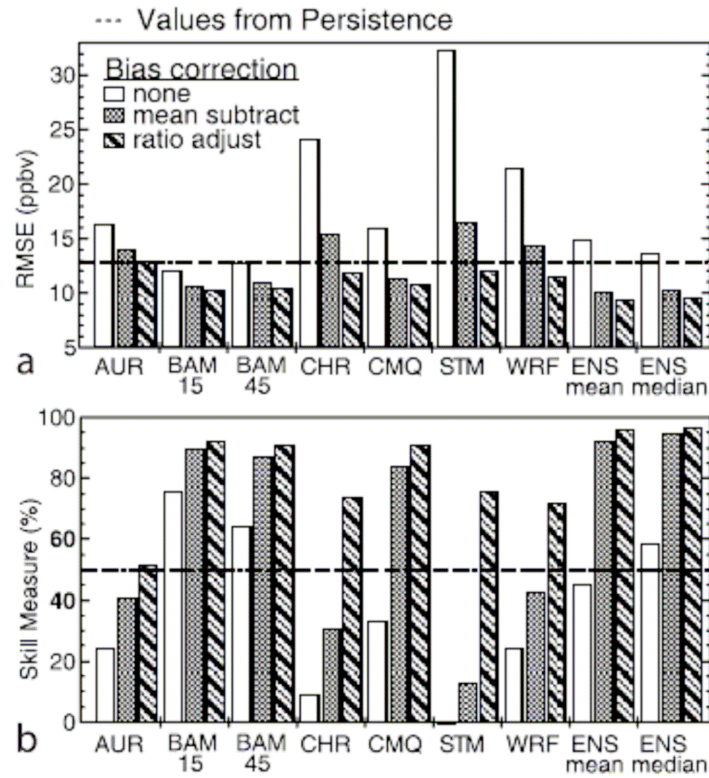


Figure 10. Median RMSE (a) and skill score (b) of maximum 8-hour average ozone for the raw forecast two bias-corrected predictions. The dashed line is the median RMSE of the persistence forecast (a) and the 50% value, or break-even point with the persistence forecast (b) (adapted from McKeen et al. 2005). Courtesy of Stuart McKeen.

3.2 Weighted Ensemble Mean

A further improvement in terms of skill of the ensemble mean can be obtained by considering the relative skills between ensemble members. If an ensemble member is consistently more skillful than another, then weighting this ensemble member more when ensemble averaging should produce a better overall ensemble-based deterministic prediction. The challenging part is that we don't know which member will be the best in the next forecasts, and the weights estimates can be based only on past performances that do not guarantee the same performance for the current prediction.

Nonetheless, several researches have proposed different algorithms to compute the weights to be applied while ensemble averaging, and often the weighted ensemble outperforms the simple linear ensemble mean. Pagowski et al. (2005)

propose a method minimizing the least-square error of the ensemble forecast by weighting accordingly each member. They shown this method to significantly improve the overall statistics (e.g., bias, root mean square error, and index of agreement computed with data from more than 350 AIRNow surface stations) when compared to the ensemble mean or any individual ensemble member. Pagowski et al. (2006) further improved the approach in Pagowski et al. (2005) by proposing a dynamic linear regression (DLR) algorithm to compute the weights. DLR has the additional advantage over the simple linear regression approach of not requiring measurements from multiple stations since it operates on individual time series. Mallet and Sportisse (2006a) explored optimal ways to estimate weights for the ensemble members, and they found that a weighted approach is superior to both the ensemble mean and median. However, in their method they found the weights to be highly unstable. When learning algorithms are applied to compute the weights as in Mallet et al. (2009) the weights values become more stable and the weighted ensemble outperforms the best forecast, resulting in a robust approach more suitable for operational air quality forecasting.

3.3 Ensemble Median

Deterministic predictions can be generated from an ensemble by selecting a percentile of the ensemble distribution. If the 50th percentile is chosen, then the ensemble-based prediction is the median of the distribution. As the mean, the median provides a prediction that is more accurate than any ensemble member as shown for example in McKeen et al. 2005. The median may be more skillful than the mean in cases when the ensemble includes members providing predictions that are outliers of the overall ensemble distribution. It is worth noticing, that if such distribution is Gaussian, with an increasing number of ensemble members the mean and the median get closer and closer, being equal to the limit of an ensemble with infinite size.

4 Ensemble-Based Probabilistic Predictions

The greater advantage of ensemble versus deterministic forecasts is the ability of ensembles to provide probabilistic predictions. The spatio-temporal evolution of the concentration field of a contaminant is chaotic, given the nonlinear dispersion and chemical processes that define such a field. Recognizing this important aspect leads to the natural choice of probabilistic versus deterministic approaches for air quality. Uncertainties in the initial conditions, emissions, meteorology, and in the representation of the chemical processes, interact non-linearly limiting the spatial-temporal predictability of air quality scenarios. These considerations lead to the realization of the necessity of probabilistic predictions also for air quality, whenever they can be afforded computationally. Ensembles (i.e., Monte Carlo methods) provide a practical way to generate probabilistic air quality predictions whose quality can be rigorously assessed by estimating the following important attributes: reliability, resolution and sharpness.

4.1 Reliability

Reliability measures the capability of the probabilistic forecast system to predict unbiased estimates of the observed frequency associated with different forecast frequencies. In a perfectly reliable forecast, the forecasted frequency of the event should be equal to the observed frequency of the event for all the cases when that specific event is forecasted. It can be improved with a forecast calibration such as bias correction; e.g., by reassigning the forecast frequency values on the basis of a long series of past forecasts, or by removing the bias of each individual forecast as shown in Delle Monache et al. (2006b, 2008). Reliability is necessary but not sufficient to establish whether a probabilistic forecast system produces valuable forecasts. For instance, a system that always forecasts the climatological frequency of an event is perfectly reliable, but may not prove valuable for decision makers. Reliability can be measured with rank histograms (Anderson 1996; Hamill and Colucci, 1997; Talagrand and Vautard, 1997) an example of which is shown in Fig. 11.

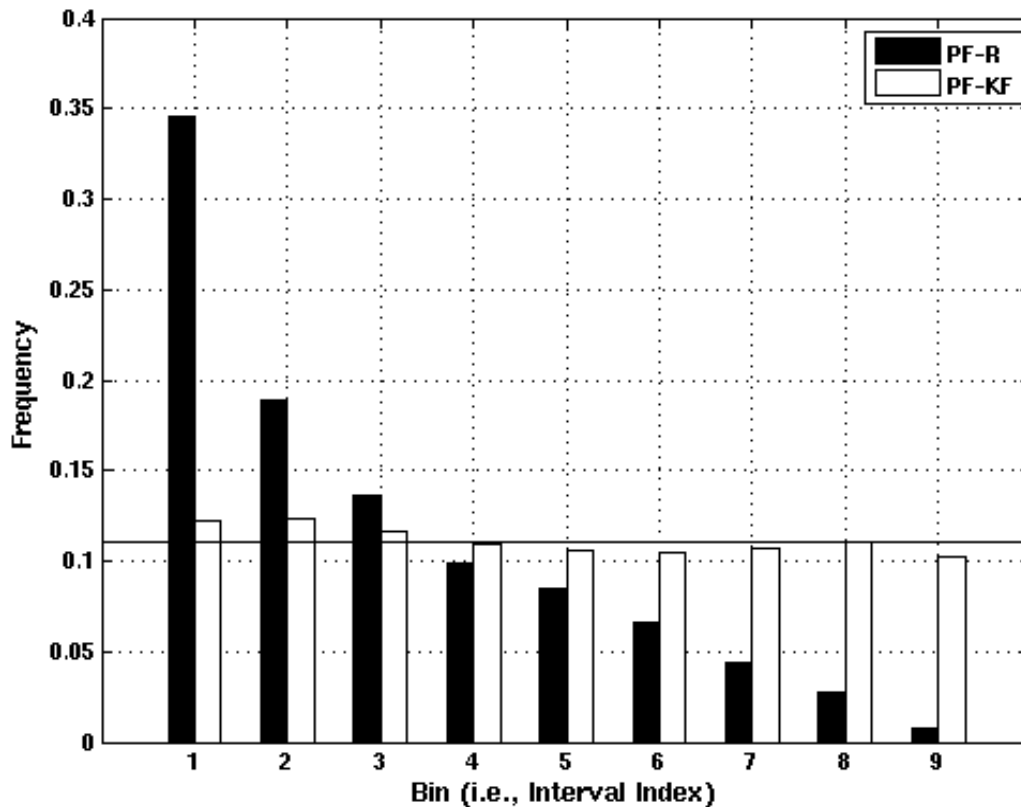


Figure 11. Rank histogram for the probabilistic forecast formed by the raw forecasts (PF-R) (black bars) and the probabilistic forecast formed by the Kalman-filtered corrected forecasts (PF-KF) (white bars) (Delle Monache et al. 2008). The number of bins equals the number of ensemble members plus one. The solid horizontal line represents the perfect rank histogram shape (flat). The closer is the diagram to this horizontal line, the better is the reliability of the probabilistic forecast (adapted from Delle Monache et al. 2008).

First, the ensemble members are ranked for each prediction. Then, the frequency of an event occurrence in each bin of the rank histogram is computed and plotted against the bins. The number of bins equals the number of members plus one. A perfectly reliable probabilistic forecast system shows rank histograms with the same height, where the bins all show the same frequency. If each ensemble member represents an equally likely time evolution and spatial distribution of the ozone concentration, then the ensemble exhibits a perfect spread, and the observations are equally likely to fall between any two members. Reliability can be measured also with the attribute diagram (Wilks 1995), that is, a plot of the forecast probability versus the observed frequency of occurrence. Ideally, the reliability curve should follow the 1:1 line. Examples and discussions of the reliability of probabilistic air quality predictions can be found for example in Delle Monache et al. (2006c), Pagowski and Grell (2006), Wilczak et al. (2006), van Loon et al. (2007), Delle Monache et al. (2008), Vautard et al. (2009) and Djalalova et al. (2010).

4.2 Resolution

Resolution measures the ability of the forecast to sort a priori the observed events into separate groups, when the events considered have a frequency different from the climatological frequency. For an ozone probabilistic forecast system, two different events could be the ozone concentrations above two different thresholds. A probabilistic forecast system with good resolution should be able to separate the observed concentrations when the two different probabilities are forecasted. Resolution can be estimated by the Relative Operating Characteristic (ROC), developed in the field of signal detection theory for discrimination of two alternative outcomes (Mason and Graham 1982). A contingency table of observed versus forecasted event occurrences is built separately for individual forecast probability values. A hit is scored when the ensemble predicts a likelihood of the event greater than or equal to the given probability threshold. The hit rate is computed as the ratio of the number of correct forecasts of the event to the total number of event occurrences, while the false alarm rate is computed as ratio of the number of non-correct event forecasts to the total number of event non-occurrences. Then, hit rates are plotted on the ordinate against the corresponding false alarm rates on the abscissa to generate the ROC curve (see Fig 12). For a probabilistic forecast system with good resolution, the ROC curve is close to the upper left hand corner of the graph. The area under the ROC curve quantifies the ability of an ensemble to discriminate between events, which can be equated to forecast usefulness, and is known also as the ROC score (Mason and Graham 1999). The closer the area is to one, the more useful is the forecast. A value of 0.5 indicates that the forecast system has no skill, relative to a chance forecast from climatology. The ROC curve does not depend on the forecast bias, hence is independent of reliability. It represents the probabilistic forecast system intrinsic value, or the potential value of an unbiased ensemble. Discussion of the resolution of probabilistic predictions for air quality can be found in Delle Monache et al.

(2006c), Pagowski and Grell (2006), Wilczak et al. (2006), Delle Monache et al. (2008), Vautard et al. (2009) and Djalalova et al. (2010).

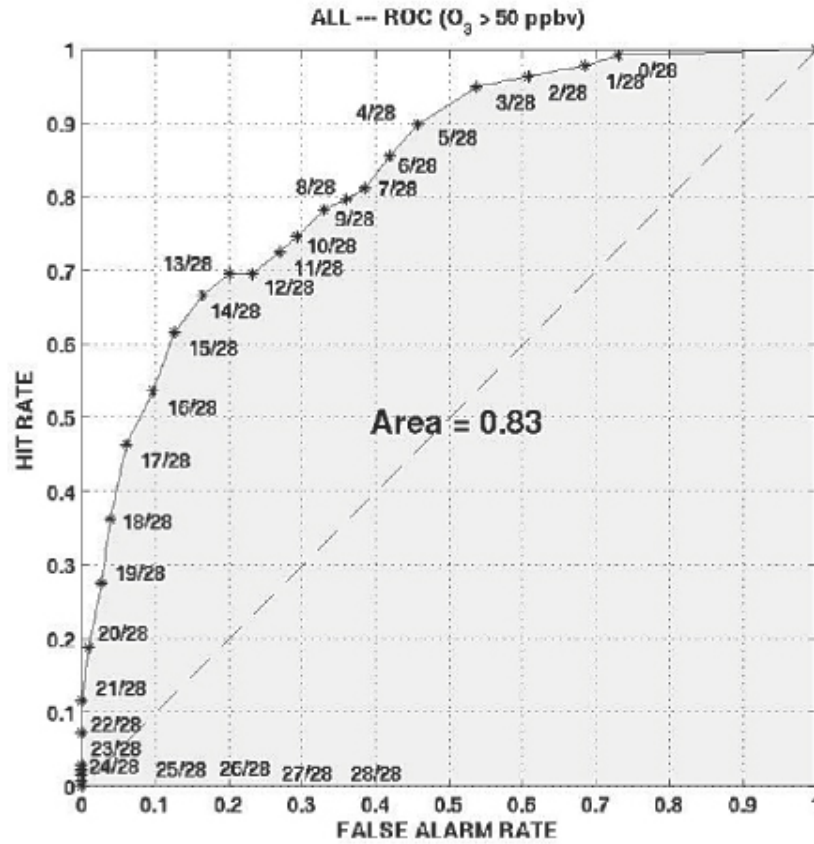


Figure 12. Relative Operating Characteristic (ROC) curve for a 28-member ensemble for observed ozone concentration above 50 ppbv (Delle Monache et al. 2006c). The better the probabilistic forecast, the closer the ROC curve is to the upper left corner. The shaded portion of the plot represents the ROC area (large areas are better) and the dashed line is the ROC curve for a chance forecast. Hit rates are plotted on the ordinate against the corresponding false alarm rates on the abscissa to generate the ROC curve for each frequency threshold (the labels adjacent to the asterisks), where the frequency threshold assumes values from 0/28 to 28/28, with increments of 1/28 (adapted from Delle Monache et al. 2006c).

4.3 Sharpness

Sharpness refers to the concentration of the predictive probability distributions and is a property of the forecasts only; practically is the tendency to estimate probabilities close to either 0 or 1. The more concentrated the predictive distributions, the sharper the forecasts, and the sharper the better, subject to calibration (Gneiting et al. 2007). This means that while trying to calibrate an ensemble the calibration procedure should not degrade the sharpness of the predictive distribution, otherwise the calibrated forecast may result in a less valuable prediction. Calibration algorithms are discussed in section 6. Sharpness

can be assessed with the measure of the width of prediction intervals and graphical devices as boxplots as proposed by Bremnes (2004). Examples of an analysis of sharpness of a probabilistic forecast for AQ can be found in Pinder et al. (2009).

5 Spread-Skill Relationship

Ensemble spread is a measure of the agreement among ensemble members and often is estimated as the standard deviation of the member predictions. A strong relationship between the ensemble spread and the skill of the ensemble mean would be highly desirable, since it would allow a forecast user to have a reliable assessment on the confidence associated with a given forecast. The bigger the error in the forecast, the larger the spread should be, and vice versa. However, the relationship between ensemble spread and forecast error is not yet well defined (Kalnay 2003). Indeed, for short-range weather forecasts some authors have found little correlation between the skill of the ensemble mean and ensemble spread (Hamill and Colucci 1998; Stensrud et al. 1999; Hou et al., 2001), while others have found significant correlations (Kalnay and Dalcher 1987; Grimit and Mass 2002; Stensrud and Yussouf, 2003).

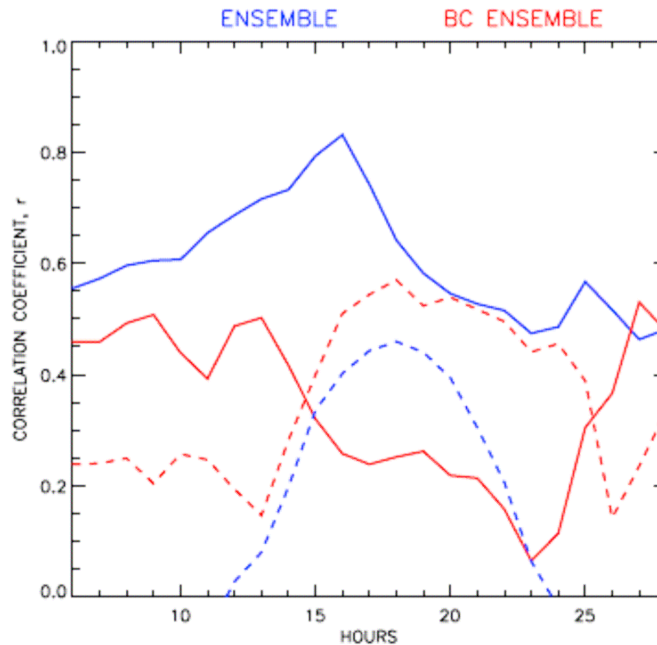


Figure 13. Correlation between standard deviation of the ensemble forecasts (spread) and the absolute error of the ensemble mean (skill), calculated over 49 forecast days and 342 sites at each hour of the forecast cycle. Blue lines are for the raw ensemble, and red lines are for the bias-corrected ensemble. Solid lines indicate that the spread and skill were spatially averaged over all sites and then temporally correlated over the 49 forecast days. Dashed lines indicate that the spread and skill were temporally averaged over the 49 forecast days and then spatially or “pointwise” correlated over the 342 sites (adapted from Wilczak et al. 2006). Courtesy of Jim Wilczak.

In air quality forecasting there have been few attempts to assess the spread-skill relationship of an ensemble system (Delle Monche et al. 2006a,b; Wilczak et al. 2006; Pinder et al. 2009). Fig. 13 (Wilczak et al. 2006) shows the temporal evolution of the correlation between the ensemble spread and the absolute error of the ensemble mean for a multi model ensemble for air quality predictions. The spread-skill correlation is higher for the bias corrected ensemble than the raw ensemble, and also the authors point out the effect of different averaging methods (spatial versus temporal) on the computed correlations.

6 Post-Processing and Calibration

The statistical consistency between the distributions of forecasts and observations, called calibration, can be seen as a property of the set including the predictions and the verifying events (Gneiting et al. 2007).

The goal of calibration methods is to correct the raw predictions so that the updated forecasts have statistical properties similar to the observations. For ensembles exists a number of statistical post-processing methods that try to correct the first moment of the distribution (ensemble mean) and/or the second moment (ensemble spread). Calibration algorithms typically need pairs of observations and predictions, and the success of the procedures typically increase with the length of the historical data available.

Skillful calibration algorithms can reduce the bias (i.e., systematic errors) of both deterministic and probabilistic predictions, improve the quality of the ensemble spread, as well as strengthen the spread-skill relationship of an ensemble system (section 5).

For air quality a number of bias correction methods have been explored to improve both deterministic and probabilistic predictions (e.g., Delle Monache et al. 2006b, 2008; Wilczak et al. 2006; Djalalova et al. 2010). When combining bias correction algorithms with the ensemble averaging often the best forecast is obtained. This is because the two procedures aim at reducing different aspects of the prediction errors and when combined together results in a superior prediction. Bias correction methods reduce the systematic errors, while ensemble averaging filter out the unpredictable components of the forecasted variable, therefore reducing random errors. Fig. 14 shows an example of a simple bias predictor algorithm based on the Kalman filter (KF) applied independently to each member of a multi-model ensemble. The ensemble mean (E) coordinates are the RMSE components of the ensemble mean. The best forecast (i.e., the closest to the origin) is the bias-corrected ensemble mean, and corresponds to the head of the arrow starting from E. Ensemble averaging reduces for the most part the random error, resulting in E with the lowest ordinate value in Fig. 14, while KF mostly reduces the systematic errors as indicated on the plot by the arrows pointing roughly from the right to left. Fig. 11 (Delle Monache et al. 2008) shows the

effects of the application of the same KF bias-correction algorithm to the reliability of a probabilistic prediction of ground-level ozone. The filter is applied to each individual ensemble members resulting in an ensemble with a much improved reliability (section 4.1) after the correction. Delle Monache et al. (2006b, 2008) showed that the KF also provides large improvements for deterministic predictions of surface ozone as measured with a range of metrics. Wilczak et al. (2006) applied a simple 7-day bias correction to a multi-model ensemble for ozone forecasts, and found that this correction improves the forecast skill of all of the individual models across the entire range of observed ozone values. The authors also reported that the ensemble of the bias-corrected models has the highest skill of all forecasts included in their case study, over a variety of skill measures. Fig. 15 (Djalalova et al. 2010) shows that postprocessing procedures can also be beneficial to improve the reliability of probabilistic predictions of PM2.5 (rank histogram and attribute diagram, panels (a) and (b)) and their resolution (section 4.2) (ROC curves, panel (c)).

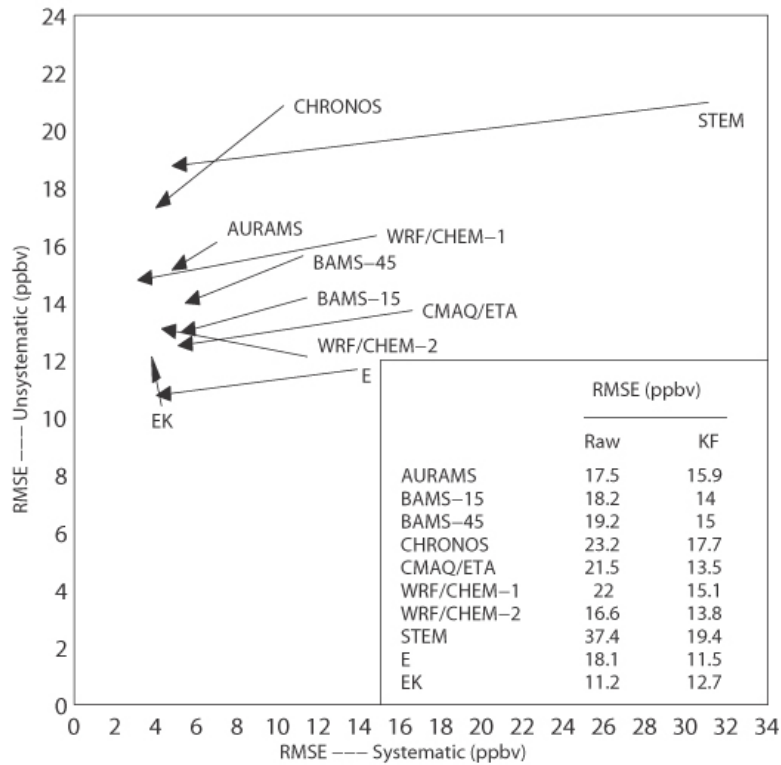


Figure 14. Root mean square error (RMSE) and its systematic ($RMSE_s$) and unsystematic ($RMSE_u$) components (ppbv). Arrow tails have as abscissa the raw forecasts $RMSE_s$ and as ordinate the raw forecasts $RMSE_u$. The distance between the arrow tail and the origin is equal the raw forecast RMSE. Similarly, the arrowhead depicts RMSE and its components for the KF forecasts. RMSE values for both the raw and KF forecasts are reported in the lower left-hand side corner. Values are within the interval $[0, +\infty)$, with a perfect forecast when $RMSE = 0$.

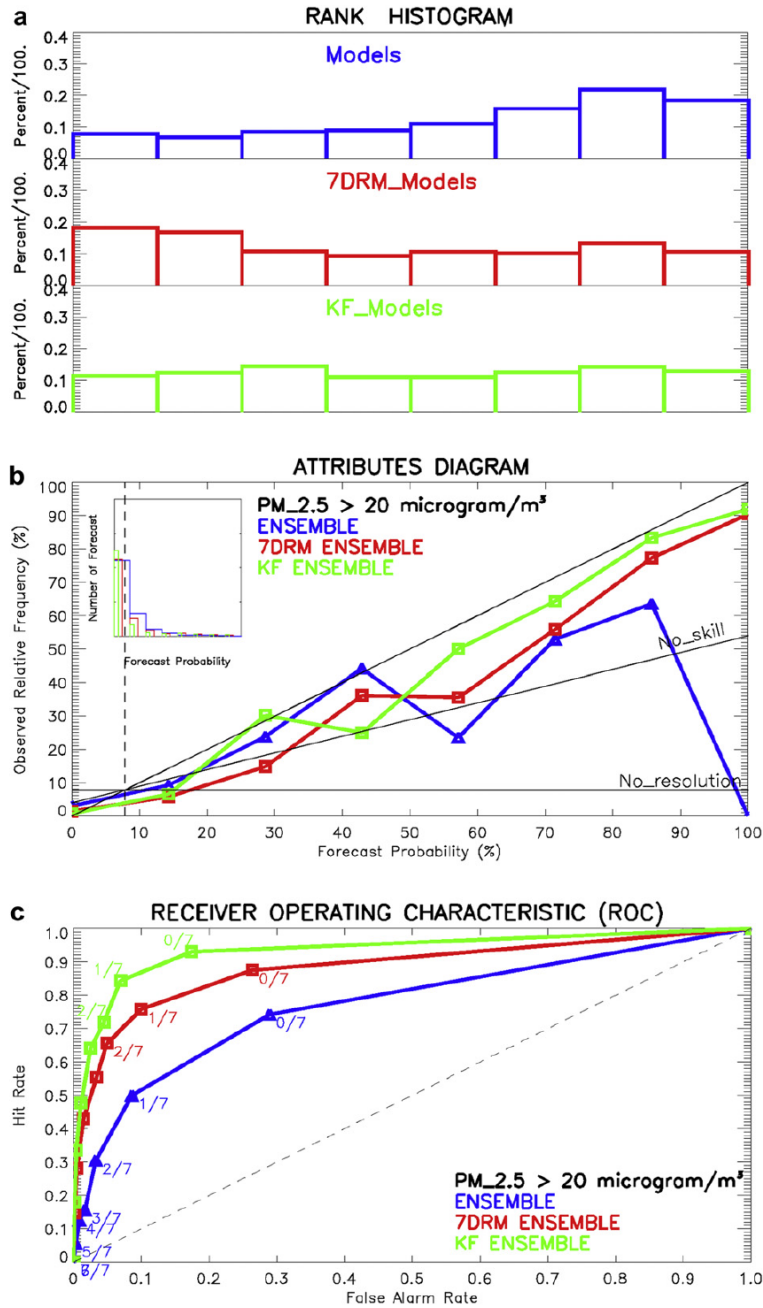


Figure 15. Probabilistic statistics for PM_{2.5} with a threshold of 20 µm m⁻³ including the rank histogram (a), attribute diagram (b) and receiver operating characteristic (ROC) (c). The raw ensemble is shown in light grey lines, the 7DRM ensemble is shown in medium grey lines, and the KF ensemble is shown in black lines in panels (b) and (c).

7 Ensembles Economic Values

Pagowski and Grell (2006) have proposed an interesting approach to assess the economic value of air quality predictions. They argue that although the skill of air

quality forecasts can be assessed with a variety of metrics for both deterministic and probabilistic predictions (as discussed throughout this chapter) the utility of forecasts is most appropriately judged by the benefits they actually provide to users.

Kernan (1975) applied the model proposed by Brier (1955) to maximize the benefits of air quality forecasts in California. The complex relationship between skill and economic value of weather forecasts has been investigated by several authors concluding that by relying only on the forecast may be misleading in terms of the practical value of the forecasts (e.g., Katz and Murphy 1997; Richardson, 2000).

Mylne (1999), Richardson (2000, 2003), and Wilks (2001) recently have applied cost-loss models to assess the potential economic value of weather forecasts. Pagowski and Grell (2006) followed Richardson (2000, 2003) model to assess the skill and potential economic value of probabilistic forecasts of surface ozone, for both deterministic and probabilistic predictions. They based their analysis on the ensemble and calibration procedure presented in Pagowski et al. (2005). As discussed in section 1, air quality predictions can be extremely useful to preserve the public health and the quality of agriculture products. Although a cost-loss analysis may be limited when does not include human health or loss of life, it can be applied to provide guidance to limit exposure to poor air quality for human, animal, and plant.

Although Pagowski and Grell (2006) have not made an attempt to estimate the cost benefit of the ensemble size for air quality predictions (given the limited size of the available ensemble for their analysis) they reached the following interesting conclusions:

- the ensemble average has an higher economic value than any single ensemble member;
- probabilistic forecasts provides a better economic value than the deterministic predictions; and,
- calibration using DLR is beneficial except for rare events.

References

- Ainslie, B., 2004: A photochemical model based on a scaling analysis of ozone photochemistry. *Ph.D. thesis*, 311 pp., Univ. of B. C., Vancouver, B. C., Canada.
- Anderson, J. L., 1996: A method for producing and evaluating probabilistic forecasts from ensemble model integrations. *J. Climate*, **9**, 1518–1530.
- Bei, N., W. Lei, M. Zavala, and L. T. Molina, 2010: Ozone predictabilities due to meteorological uncertainties in Mexico City basin using ensemble forecasts. *Atmos. Chem. Phys. Discuss.*, **10**, 3229–3263.
- Brier, G. W., 1950: Verification of forecasts expressed in terms of probability. *Mon. Wea. Rev.*, **78**, 1–3.

Bremnes, J. B., 2004: Probabilistic forecasts of precipitation in terms of quantiles using NWP. *Mon. Weather Rev.*, **132**, 338–347.

Benoit, R., M. Desgagne, P. Pellerin, S. Pellerin, Y. Chartier, and S. Desjardins, 1997: The Canadian MC2: A semi-Lagrangian, semiimplicit wide band atmospheric model suited for fine scale process studies and simulation. *Mon. Wea. Rev.*, **125**, 2382–2415.

Buizza, R. and T. N. Palmer, 1998: Impact of ensemble size on ensemble prediction. *Mon. Wea. Rev.*, **126**, 2503–2518.

Carmichael, G. R., A. Sandu, T. Chai, D. N. Daescu, E. M. Constantinescu, and Y. Tang, 2008: Predicting air quality: Improvements through advanced methods to integrate models and measurements. *Journal of Computational Physics*, **227**, 3540–3571.

Constantinescu, E. M., A. Sandu, T. Chai, and G. R. Carmichael 2007a: Ensemble-based chemical data assimilation. I: General approach. *Q. J. R. Meteorol. Soc.*, **133**, 1229–1243.

Constantinescu, E. M., A. Sandu, T. Chai, and G. R. Carmichael 2007b: Ensemble-based chemical data assimilation. II: Covariance localization. *Q. J. R. Meteorol. Soc.*, **133**, 1245–1256.

Cuvelier, C., P. Thunis, R. Vautard, and co-author, 2007: CityDelta: A model intercomparison study to explore the impact of emission reductions in European cities in 2010. *Atmos. Environ.*, **41**, 189–207.

Dalcher, A., E. Kalnay, and R.N. Hoffmann, 1988: Medium range lagged average forecasts. *Mon. Wea. Rev.*, **116**, 402–416.

Delle Monache, L. and R. B. Stull, 2003: An ensemble air quality forecast over western Europe during an ozone episode. *Atmos. Environ.*, **37**, 3469–3474.

Delle Monache, L., X. Deng, Y. Zhou, and R. B. Stull, 2006a: Ozone ensemble forecasts: 1. A new ensemble design. *J. Geophys. Res.*, **111**, D05307, doi:10.1029/2005JD006310.

Delle Monache, L., T. Nipen, X. Deng, Y. Zhou, and R. B. Stull, 2006b: Ozone ensemble forecasts: 2. A Kalman-filter predictor bias correction. *J. Geophys. Res.*, **111**, D05308, doi:10.1029/2005JD006311.

Delle Monache, L., J. P. Hacker, Y. Zhou, X. Deng, and R. B. Stull, 2006c: Probabilistic aspects of meteorological and ozone regional ensemble forecasts. *J. Geophys. Res.*, **111**, D24307, doi:10.1029/2005JD006917.

Delle Monache, L., J. Wilczak, S. McKeen, G. Grell, M. Pagowski, S. Peckham, R. Stull, J. McHenry, and J. McQueen, 2008: A Kalman-filter bias correction method applied to deterministic, ensemble averaged and probabilistic forecasts of surface ozone. *Tellus*, **60B**, 238–249.

Djalalova, I., J. Wilczak, S. McKeen, G. Grell, S. Peckham, M. Pagowski, L. Delle Monache, J. McQueen, P. Lee, Y. Tang, J. McHenry, W. Gong, V. Bouchet, R. Marthur, 2010: Ensemble and bias-correction techniques for probabilistic forecast of surface O₃ and PM_{2.5} during the TEXAQS-II experiment of 2006. *Atmos. Environ.*, **44**, 455–467.

Du, J., S. L. Mullen, and F. Sanders, 1997: Short-range ensemble forecasting of quantitative precipitation. *Mon. Wea. Rev.*, **125**, 2427–2459.

Hamill, T. M., S. J. Colucci, 1997: Verification of Eta-RSM shortrange ensemble forecasts. *Mon. Wea. Rev.*, **125**, 1322–1327.

- Epstein, E. S., 1969: Stochastic dynamic prediction. *Tellus*, **21**, 739-759.
- Ehrendorfer, M., 2006: The Liouville equation and atmospheric predictability. In *Predictability of Weather and Climate*, T. Palmer, and R. Hagedorn, Eds., pp. 59-98. Cambridge Univ. Press, Cambridge, UK, 702 pp.
- Evans, R. E., M. S. J. Harrison, and R. Graham, 2000: Joint mediumrange ensembles from the Met. Office and ECMWF systems. *Mon. Wea. Rev.*, **128**, 3104–3127.
- Garaud, D., and V. Mallet, 2010: Automatic generation of large ensembles for air quality forecasting using the Polyphemus system. *Geosci. Model Dev.*, **3**, 69-85, 2010.
- Gneiting, T., F. Balabdaoui, and A. Raftery, 2007: Probabilistic forecasts, calibration and sharpness. *J. R. Statist. Soc. B*, **69**, Part 2, 243–268.
- Grell, G., J. Dudhia, and D. Stouffer, 1994: A description of the fifth generation Penn State/NCAR mesoscale model (MM5). *NCAR Tech. Note*, NCAR/TN-398+STR, Natl. Cent. for Atmos. Res., Boulder, Colorado.
- Grimit, E. P., and C. F. Mass, 2002: Initial results of a mesoscale shortrange ensemble forecasting system over the Pacific Northwest. *Weather Forecasting*, **17**, 192– 205.
- Hamill, T., and S. J. Colucci, 1998: Verification of Eta–RSM shortrange ensemble forecasts. *Mon. Wea. Rev.*, **125**, 1312–1327.
- Hoffman, R. N., and E. Kalnay, 1983: Lagged average forecasting, an alternative to Monte Carlo forecasting. *Tellus*, **35**, 100–118.
- Hou, D., E. Kalnay, and K. K. Droegemeier, 2001: Objective verification of the SAMEX'98 ensemble forecasts *Mon. Weather Rev.*, **129**, 73–91.
- Kalnay, E., and A. Dalcher, 1987: Forecasting forecast skill. *Mon. Weather Rev.*, **115**, 349–356.
- Kalnay, E., 2003: *Atmospheric Modeling, Data Assimilation and Predictability*. Cambridge University Press, New York, 341pp.
- Katz, R. W., and A. H. Murphy (Eds.), 1997: *Economic Value of Weather and Climate Forecasts*. Cambridge Univ. Press, New York, 222 pp.
- Kernan, G. L., 1975: The cost-loss decision model and air pollution forecasting, *J. Appl. Meteorol.*, **14**, 8–16.
- Krishnamurti, T. N., C. M. Kishtawal, T. E. LaRow, D. R. Bachiochi, Z. Zhang, C. E. Willford, S. Gadgil, and S. Surendran, 1999: Improved weather and seasonal climate forecast from multimodel superensemble. *Science*, **285**, 1548–1550.
- Lorenz, E. N., 1963: Deterministic nonperiodic flow. *J. Atmos. Sci.*, **20**, 130-141.
- Lu, C., H. Yuan, B. E. Schwartz, and S. G. Benjamin, 2007: Short-range numerical weather prediction using time-lagged ensembles. *Weather and Forecasting*, **22**, 580-595.
- Mallet, V. and B. Sportisse, 2006a: Ensemble-based air quality forecasts: A multimodel approach applied to ozone. *J. Geophys. Res.*, **111**, D18302, doi:10.1029/2005JD006675.

Mallet, V. and B. Sportisse, 2006b: Uncertainty in a chemistry-transport model due to physical parameterizations and numerical approximations: an ensemble approach applied to ozone modeling. *J. Geophys. Res.*, **111**, D01302, doi:10.1029/2005JD006149.

Mallet, V., G. Stoltz, B. Mauricette, 2009: Ozone ensemble forecast with machine learning algorithms. *J. Geophys. Res.*, **114**, D05307, doi:10.1029/2008JD009978.

Mason, S. J., and N. E. Graham, 1999: Conditional probabilities, relative operating characteristics, and relative operative levels. *Weather Forecasting*, **14**, 713–725.

McKeen, S. A., J. M. Wilczak, G. A. Grell, I. Djalalova, S. Peckham and co-authors, 2005: Assessment of an ensemble of seven real-time ozone forecasts over Eastern North America during the summer of 2004. *J. Geophys. Res.*, **110**, D21307, doi:10.1029/2005JD005858.

McKeen, S., S. H. Chung, J. Wilczak, G. Grell, I. Djalalova, S. Peckham, W. Gong, V. Bouchet, R. Moffet, Y. Tang, G. R. Carmichael, R. Mathur, and S. Yu, 2007: Evaluation of several PM_{2.5} forecast models using data collected during the ICARTT/NEAQS 2004 field study. *J. Geophys. Res.*, **112**, D10S20, doi:10.1029/2006JD007608.

Mylne, K., 1999: The use of forecast value calculations for optimal decision making using probability forecast. *17th Conference on Weather Analysis and Forecasting*, Am. Meteorol. Soc., Denver, Colorado.

Mittermaier, M. P., 2007: Improving short-range high-resolution model precipitation forecast skill using time-lagged ensembles. *Q. J. R. Meteorol. Soc.*, **133**, 1487–1500.

Molteni, F., R. Buizza, T. N. Palmer, and T. Petroliagis, 1996: The new ECMWF ensemble prediction system: methodology and validation. *Quart. J. Roy. Meteor. Soc.*, **122**, 73–119.

Pagowski, M., G. A. Grell, S. A. McKeen, D. Dévényi, J. M. Wilczak, and co-authors, 2005: A simple method to improve ensemble-based ozone forecasts. *Geophys. Res. Lett.*, **32**, L07814, doi:10.1029/2004GL022305.

Pagowski, M. and G.A. Grell, 2006: Ensemble-based ozone forecasts: Skill and economic value. *J. Geophys. Res.*, **111**, D23S30, doi:10.1029/2006JD007124.

Pagowski, M., G. A. Grell, D. Dévényi, S. E. Peckham, S. A. McKeen, W. Gong, L. Delle Monache, J. N. McHenry, J. McQuenn, and P. Lee, 2006: Application of dynamic linear regression to improve skill of ensemble-based deterministic ozone forecasts. *Atmos. Environ.*, **40**, 3240–3250.

Pinder, R. W., R. C. Gilliam, K. W. Appel, S. L. Napelenok, K. M. Foley, And A. B. Gilliland, 2009: Efficient probabilistic estimates of surface ozone concentration using an ensemble of model configurations and direct sensitivity calculations. *Environ. Sci. Technol.*, **43**, 2388–2393.

Potempski, S., and S. Galmarini, 2009: *Est modus in rebus*: analytical properties of multi-model ensembles. *Atmos. Chem. Phys.*, **9**, 9471–9489, 2009.

Riccio, A., G. Giunta, and S. Galmarini, 2007: Seeking for the rational basis of the Median Model: the optimal combination of multi-model ensemble results. *Atmos. Chem. Phys.*, **7**, 6085–6098.

Richardson, D. S., 2000: Skill and relative economic value of the ECMWF ensemble prediction system. *Q. J. R. Meteorol. Soc.*, **126**, 649 – 667.

Richardson, D. S., 2003: Economic value and skill. In *Forecast Verification. A Practitioner's Guide in Atmospheric Science*. Edited by I. T. Joliffe and D. R. Stephenson, John Wiley, Hoboken, N. J., 164 – 187.

- Stensrud, D.J., J.-W. Bao, T. T. Warner, 1998: Ensemble forecasting of mesoscale convective systems. *Proceedings of the 12th Conference on Numerical Weather Prediction*, American Meteorological Society, Phoenix, AZ, Preprints, pp. 265–268.
- Stensrud, D. J., H. E. Brooks, J. Du, M. S. Tracton, and E. Rogers, 1999: Using ensembles for short-range forecasting. *Mon. Weather Rev.*, **127**, 433–446.
- Stensrud, D. J., and N. Yussouf, 2003: Short-range ensemble predictions of 2-m temperature and dewpoint temperature over New England. *Mon. Weather Rev.*, **131**, 2510–2524.
- Talagrand, O., R. Vautard, and B. Strauss, 1998: Evaluation of probabilistic prediction systems. *Proc. ECMWF Workshop on Predictability*, Reading, United Kingdom, ECMWF, 17–28.
- Toth, Z., and E. Kalnay, 1993: Ensemble forecasting at NMC: The generation of perturbations. *Bull. Amer. Meteor. Soc.*, **74**, 2317–2330.
- Toth, Z., and E. Kalnay, 1997: Ensemble forecasting at NCEP: the breeding method. *Mon. Wea. Rev.*, **125**, 3297–3318.
- Thunis, P. and co-authors, 2007: Analysis of model responses to emission-reduction scenarios with in the City Delta project. *Atmos. Environ.*, **41**, 208–220.
- van Loon, M. and co-authors, 2007: Evaluation of long-term ozone simulations from seven regional air quality models and their ensemble. *Atmos. Environ.*, **41**, 2083–2097.
- Vautard, R., M. Van Loon, M. Schaap, R. Bergstrom, B. Bessagnet, J. Brandt, P. J. H. Builtjes, J. H. Christensen, K. Cuvelier, A. Graf, J. E. Jonson, M. Krol, J. Langner, P. Roberts, L. Rouil, R. Stern, L. Tarrason, P. Thunis, E. Vignati, L. White, and P. Wind, 2006: Is regional air quality model diversity representative of uncertainty for ozone simulation? *Geophys. Res. Lett.*, **33**, L24818. doi:10.1029/2006GL027610.
- Vautard, R., P. H. J. Builtjes, P. Thunis, C. Cuvelier, M. Bedogni, B. Bessagnet, C. Honoré, N. Moussiopoulos, G. Pirovano, M. Schaap, R. Stern, L. Tarrason, and P. Wind, 2007: Evaluation and intercomparison of Ozone and PM10 simulations by several chemistry transport models over four European cities within the CityDelta project. *Atmos. Environ.*, **41**, 173–188.
- Vautard R., M. Schaap, R. Bergstrom, B. Bessagnet, J. Brandt, P. J. H. Builtjes, J. H. Christensen, C. Cuvelier, V. Foltescu, A. Graff, A. Kerschbaumer, M. Krol, P. Roberts, L. Rouil, R. Stern, L. Tarrason, P. Thunis, E. Vignati, and P. Wind, 2009: Skill and uncertainty of a regional air quality model ensemble. *Atmos. Environ.*, **43**, 4822–4832.
- Wilczak, J. M., McKeen, S. A., Djalalova, I. and Grell, G., 2006: Bias-corrected ensemble predictions of surface O₃. *J. Geophys. Res.*, **111**, D23S28, doi:10.1029/2006JD007598.
- Wilks, D. S., 1995: *Statistical Methods in The Atmospheric Sciences: An Introduction*. Elsevier, New York, 467 pp.
- Wilks, D. S., 2001: A skill score based on economic value for probability forecasts. *Meteorol. Appl.*, **8**, 209 – 219.
- Wobus, R., and E. Kalnay, 1995: Three years of operational prediction of forecast skill. *Mon. Wea. Rev.*, **123**, 2132–2148.

Zhang, F., N. Bei, J. W. Nielsen-Gammon, G. Li, R. Zhang, A. Stuart, and A. Aksoy, 2007: Impacts of meteorological uncertainties on ozone pollution predictability estimated through meteorological and photochemical ensemble forecasts. *J. Geophys. Res.*, **112**, D04304, doi:10.1029/2006JD007429.

BRANK
P
e

Chapter 17

Evaluation of Air Pollution Models

A comprehensive chapter on “Evaluation of Air Pollution Models” was presented in Volume II of this book series. The abstract is reprinted below.

Information is given about model evaluation, the overall system of procedures designed to measure model performance, and in particular, the process of statistical performance evaluations. Statistical performance evaluation is an assessment of model performance based on the comparison of model outputs with experimental data. Some performance measures, consisting of statistical indices and graphical methodologies, currently used are described. Problems related to uncertainty analysis are highlighted.

For additional information, the reader can visit:

- Validation of a 3-D Hemispheric Nested Air Pollution Model
<http://citeseerx.ist.psu.edu/viewdoc/download?doi=10.1.1.105.4646&rep=rep1&type=pdf>
- Model Validation and Spatial Interpolation by Combining Observations with Outputs from Numerical Models via Bayesian Melding
<http://www.stat.washington.edu/research/reports/2002/tr403.pdf>
- Remote Sensing and GIS as Pollution Model Validation
<http://www.harmo.org/Conferences/Proceedings/Crete/publishedSections/p291.pdf>
- Development and Validation of Tools for the Implementation of European Air Quality Policy in Germany (Project VALIUM)
<http://www.atmos-chem-phys.net/6/3077/2006/acp-6-3077-2006.pdf>
- Performance Evaluation of Air Pollution Models for Delhi City
<http://www.ieindia.org/pdf/87/4n0634c.pdf>
- A Performance Evaluation of MM5/MNEQA/CMAQ Air Quality Modelling System to Forecast Ozone Concentrations in Catalonia
http://cat.tethys.cat/files/tethys2010_02_esborrany.pdf

- Comparison and Performance Evaluation of CFD Based Numerical Model and Gaussian Based Models for Urban Air Quality Prediction
http://www.fluidyn.com/research%20papers/conference_paperawma.pdf
- Comparison and Performance Evaluation of Dispersion Models FDM and ISCST3 for a Gold Mine at Goa
http://www.ismenvis.nic.in/My_Webs/Digital_Library/GSingh/COMPARISON%20AND%20PERFORMANCE%20EVALUATION_Jyoti.pdf

Chapter 18

Regulatory Modeling

A comprehensive chapter “A Historical Look at the Development of Regulatory Air Quality Models for the United States Environmental Protection Agency” was published in Volume II. The abstract is reprinted below.

Information about the development and use of regulatory air quality models, with an emphasis on those whose development was sponsored or promoted by the United States Environmental Protection Agency (EPA), is provided. A broad definition of regulatory is used here to include not only modeling used for setting specific emission limits, but also modeling used in developing EPA’s agenda. The review outlines the major events in U.S. air quality legislation, noting the resulting influence on air quality model development. This partial review is meant to augment critical science reviews available elsewhere.

For additional information, the reader can visit:

- US EPA Support Center for Regulatory Atmospheric Modeling
<http://www.epa.gov/scram001/>
<http://www.epa.gov/scram001/aqmindex.htm>
- Air Quality Models and Documentation
<http://www.arb.ca.gov/html/soft.htm>
- Air Quality Modeling - Resources: Tools and Training
http://www.epa.gov/airquality/aqmportal/management/links/modeling_resources_tool.htm
- Forum for AIR Quality MODelling (FAIRMODE)
<http://fairmode.ew.eea.europa.eu/>
- Air Quality Modeling Guidance for Permits
<http://www.colorado.gov/airquality/permits.aspx>

- Air Dispersion Modeling - Minnesota Pollution Control Agency
<http://www.pca.state.mn.us/index.php/air/air-monitoring-and-reporting/air-emissions-and-monitoring/air-dispersion-modeling/air-dispersion-modeling.html>
- Air Quality Modeling Program - NH Department of Environmental Services
<http://des.nh.gov/organization/divisions/air/pehb/apps/aqm/index.htm>
- Air Dispersion Modeling Guidelines for Oklahoma Air Quality Permits
<http://www.deq.state.ok.us/aqdnew/permitting/modelguide.pdf>

Chapter 19

Case Studies

A chapter dedicated to the topic “Case Studies - Air Pollution Modeling at Local, Regional, Continental, and Global Scales” was presented in Volume I of this book series. The abstract is reprinted below.

In this chapter various case studies are presented, which are relevant to air pollution modeling/simulation and pollution control/abatement issues. Several groups active in air pollution modeling (see also chapter 21) submitted pre-defined information on individual cases, thus providing insight to a variety of details with regard to the scientific objectives of the particular study. This includes information on the physico-chemical processes analyzed, the origin of the data used, the main results and their application potential, the collaborating groups/scientists and publications that have resulted from the study. The inclusion of several case studies had the purpose of presenting in detail the research areas and activities that were lately or are currently being elaborated by the scientific community, thus underlying various issues and outstanding problems of particular interest with regard to air pollution simulation and prevention. A thorough examination of these case studies allows for detecting those research fields that are still open for further elaboration and exploitation.

In this Volume IV, we present:

19A – Case Studies: Multi-Scale Air Pollution and Meteorological Modeling

BRANKLEY PARK

Moussiopoulos, N. et al., 2010. *Case Studies: Multi-Scale Air Pollution and Meteorological Modeling*. Chapter 19A of *AIR QUALITY MODELING - Theories, Methodologies, Computational Techniques, and Available Databases and Software. Vol. IV – Advances and Updates* (P. Zannetti, Editor). Published by The EnviroComp Institute (<http://www.envirocomp.org/>) and The Air & Waste Management Association (<http://www.awma.org/>).

Chapter 19A

Case Studies: Multi-Scale Air Pollution and Meteorological Modeling

Nicolas Moussiopoulos, Evangelia Fragkou and John Douros

Aristotle University of Thessaloniki, Laboratory of Heat Transfer and Environmental Engineering, Thessaloniki (Greece)
moussio@eng.auth.gr

Abstract: In the U.S., air quality models have been systematically used for over two decades for regulatory purposes, while the current European Directive on Ambient Air Quality (2008/50/EC) promotes the use of modeling tools for air quality assessment and management. In this chapter, the role of scale interaction processes in air quality modeling and assessment is demonstrated through a number of relevant case studies. The case studies represent recent examples from around the world of using a multi-scale modeling approach for different assessment purposes, including urban and hot-spot air quality assessment, source apportionment, dispersion of ozone and particles, accidental releases and forecasting and warning systems. These examples describe the most important methods currently used for introducing the concept of scale interaction in meteorological and air quality modeling.

Key Words: multi-scale modeling, atmospheric modeling, air quality assessment, atmospheric dispersion processes, model coupling, nesting.

1 Introduction

The atmospheric processes exhibit a multi-scale character. This is because the atmosphere is a dynamic system where various energy transfer mechanisms act simultaneously at different scales. In general, atmospheric pollutant transport, dispersion and transformation depend on the accurate representation of the dynamics and physics across a wide range of scales. For example, dispersion and transformation of urban air pollution are governed by processes that occur

between the local and urban scales, while long-term transport mainly concerns urban and regional scales. Scale interaction depends on the degree of relative strength of flow motions involved and how those affect the evolution of chemical processes in the atmosphere. Thus, in the case of a very weak disturbance embedded in a slowly varying mean flow, the flow is predominately controlled by the mean flow rather than by the disturbance. If this disturbance, however, becomes stronger, then it may exert an increasing influence on the mean flow, which may lead to the development of other scales of motion. Scaling of atmospheric motions is generally based on observational and theoretical methods.

Table 1. Atmospheric scale classifications [adapted from Thunis and Bornstein 1996].

Horizontal Scale Length	Lifetime	Pielke (1984)	Orlanski (1975)	Present	Atmospheric Phenomena
10000 km	1 month	Synoptic Regional	Macro- α	Macro- α	General circulation, long waves
2000 km	1 week		Macro- β	Macro- β	Synoptic cyclones
			Meso- α	Macro- γ	Fronts, hurricanes
200 km	1 day	Meso	Meso- β	Meso- β	Low-level jets, thunderstorm groups, mountain winds and waves, sea breeze, urban circulations
20 km	1 h	Micro	Meso- γ	Meso- γ	Thunderstorm, clear- air turbulence
2 km			Micro- α	Meso- δ	Cumulus, tornadoes, katabatic jumps
200 m	30 min		Micro- β	Micro- β	Plumes, wakes, waterspouts, dust devils
20 m	1 min		Micro- γ	Micro- γ	Turbulence, sound waves
2 m	1 s			Micro- δ	

Efforts to understand the interaction dynamics in atmospheric processes mainly involve numerical model simulations. This is due to the understanding of the complexity characterizing scale interaction, as well as to the requirement for predicting air pollutant transfer and dispersion influenced by this interaction. Accurate pollution transport and dispersion forecasting is required for efficient air quality assessment in order to apply appropriate and effective air quality management strategies. Therefore, the correct representation of atmospheric and chemical scale interaction processes controlling pollutant transfer is necessary. The complex interaction of pollutants with atmospheric species under the influence of specific meteorological conditions may result to the generation, destruction and dispersion processes taking place in considerable distances from the emission source. However, the pollution source itself may be represented in a

very small scale. In order to understand the dynamical and physical properties characteristic of the atmospheric processes at each scale, different approximations of the governing equations have been developed. Mathematical modeling deals with all these processes and numerical codes have been developed and applied in order to describe phenomena taking place at any of the aforementioned scales, as well as processes resulting from interactions of phenomena between those scales. Because of this multi-scale behavior of the polluted plume, particular modeling techniques have to be developed and applied that will allow resolving concentration profiles over the whole range of dispersion. These methods include mainly model coupling, nesting and variable grid resolution, although there is a general tendency to use several methods simultaneously, usually model coupling and nesting.

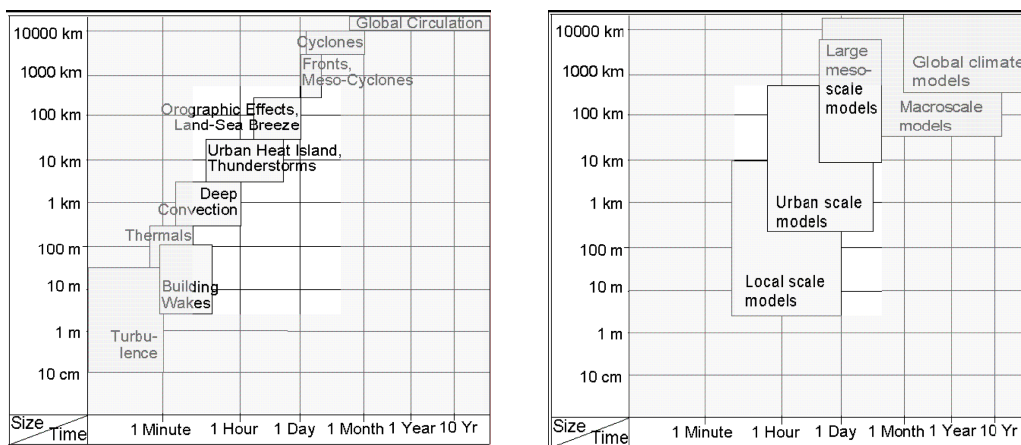


Figure 1. Characteristic time scale (abscissa) and characteristic horizontal scale (ordinate) of common atmospheric phenomena (left) and of atmospheric models (right) (based on Schlünzen, 1996).

As shown in Figure 1, atmospheric phenomena at any specific scale are influenced by the ensemble of interacting atmospheric processes occurring at various scales (Figure 1, left), which is of great importance to the characteristics of predicting pollutant transport in urban areas (non-shaded scales in Figure 1). Urban areas are the main focus of air quality assessment and management efforts, as large population numbers are exposed to and suffering from urban air pollution. The phenomena at the local and urban scales have a horizontal extension of several meters to 500 km and a characteristic time scale of several minutes to several days.

The case studies that follow examine the use of multi-scale modeling tools for the assessment and prediction of air pollution levels in urban areas, as well as at a regional scale. The case studies are categorized according to the corresponding air quality assessment needs, which involve:

- Assessment in urban areas
- Assessment in hot-spot areas and source apportionment
- Dispersion of ozone and particles

- Accidental releases and emergency planning and
- Forecasting and warning systems

2 Case Studies

2.1 Assessment in Urban Areas

Rapidly increasing urbanization will be a major environmental driving force in the 21st century, affecting air quality on all scales—local, regional, and global, through complex mechanisms of pollutant transport and dispersion. Integrated modeling systems that are able to describe multi-scale physical and chemical processes and estimate the contribution of transported polluted air masses to the local and regional air quality are thus receiving particular scientific attention. The complexity of the terrain induces difficulties in accurately simulating the fate of air pollutants in the overlying air, by affecting wind flow patterns. Wind fields are closely associated with pollutant dispersion and they are strongly influenced by atmospheric processes occurring at the next larger scale. Therefore, although the microscale flow in street canyons in urban areas is largely dependent on the canyon and surrounding building geometry, it is also greatly affected by the mesoscale wind. For example, mesoscale wind circulations associated with horizontal temperature gradients, e.g., mountain-valley wind systems and sea/land breezes, particularly affect microscale flow, and subsequently, air quality in cities. In addition, atmospheric circulations created by the city itself, notably the so-called urban heat island, directly influence the dispersion of pollutants. The following case studies are recent examples of urban assessment with the use of multi-scale modeling, where the characteristic features and processes of the urban environment described above are taken into account.

2.1.1 A Metamodeling Implementation of a Two-Way Coupled Mesoscale-Microscale Flow Model for Urban Area Simulations

A two-way coupled modeling system, consisting of the prognostic mesoscale model MEMO and the microscale model MIMO, has been applied for the city of Athens during two multi-day periods (Tsegas et al. 2008). The microscale feedback on the mesoscale domain was simulated using a metamodeling approach, where the effect of local flows on the vertical profiles was estimated for representative urban areas of sizes up to a few hundred meters and used as calibration input for a set of interpolating metamodels. Using this approach, shown in the following Figure, the effect of the microscale feedback on the mesoscale flow was evident in the simulation, both as a reduction of lower-level wind speeds in urban cells as well as an overall increase in turbulent kinetic energy production over densely-built areas.

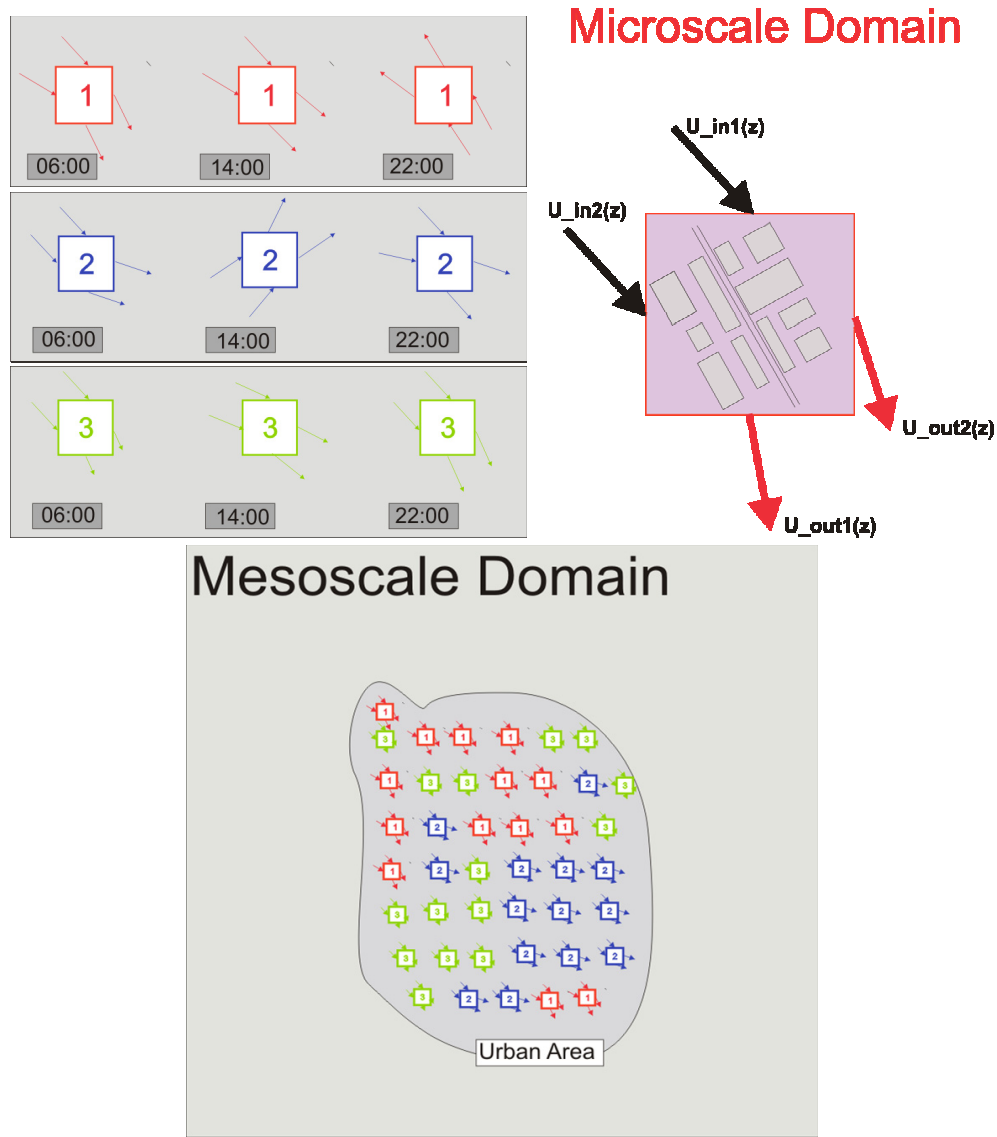


Figure 2. Spatial and temporal sampling of microscale cases inside the urban area.

2.1.2 Characterizations of Chemical Oxidants in Mexico City: A Regional Chemical Dynamical Model (WRF-Chem) Study

The weather research and forecasting (WRF) model is a mesoscale numerical weather prediction system designed to serve both operational forecasting and atmospheric research needs. A chemical model was fully (on-line) coupled with the WRF model, and the resulting integrated WRF-Chem modeling system was used to simulate small-scale and regional circulations and to describe pollutant transport and diffusion of pollutants influenced by the complex terrain over Mexico City (Tie et al. 2007). Diurnal cycles and distribution patterns of ozone, NO and CO were examined. In general, the model results were in good agreement with observations, however some discrepancies occurred mainly associated with

the model simulation of meteorological parameters, such as boundary layer height, and the inaccurate representation of emission sources and magnitude. More difficulties occurred in the prediction of meteorological parameters in areas with strong topographical features, such as mountains.

2.1.3 An Integrated ARPS-MM5-CMAQ Modeling Approach for Predicting PM₁₀ Concentration in the Metropolitan Region of Beijing in Winter

The capabilities of multi-scale modeling tools are particularly explored in assessing and predicting air pollution concentrations in complex terrain areas, where air quality is largely controlled by local-scale circulation systems. In this case, one of the most important parameters to realistically simulate pollutant dispersion processes is an accurate representation of local wind field patterns, along with larger scale meteorological conditions. In a relevant study (Chen et al. 2005), two meteorological models treating physical processes at different scales were combined with CMAQ to study the PM₁₀ concentrations in winter periods in Beijing. Due to the complex topography of Beijing, its air quality is affected by meteorological and environmental conditions both locally and regionally. Therefore, in order to simulate air pollution dispersion and concentrations in this area it is necessary to develop an advanced and comprehensive modeling system which will examine small-scale characteristics, while also considering the mesoscale background conditions. The Fifth-Generation NCAR/Penn State Mesoscale Model (MM5) and the Advanced Regional Prediction (ARPS) with considerable performance for small-scale simulations were combined to provide the necessary input data for the innermost domain of the atmospheric model CMAQ. The Community Multi-scale Air Quality (CMAQ) system was developed by the USEPA to incorporate various state-of-the-art techniques within a general framework, allowing for the simulation of all atmospheric and land processes that affect the transport and transformation of atmospheric pollutants at both regional and urban scales. The ARPS is a three-dimensional, non-hydrostatic compressible model in terrain-following coordinates designed for the explicit representation of convective and cold-season storms, with good performance on calculating high-resolution wind fields over steep terrain. Model calculated PM₁₀ values showed reasonable agreement with observed concentrations, with most key features in the observation being captured by the modeling system. Furthermore, examination of the PM₁₀ episode in Beijing revealed that both local emissions as well as regional atmospheric transport contributed to the increased pollution load.

In a later study (Cheng et al. 2007), the coupled MM5-ARPS-CMAQ air quality modeling system was applied to assess and quantify the contributions of various emission sources to the ambient concentrations of PM₁₀ in the Beijing metropolitan region of China, and to explore possible future emission reduction strategies. A three-level nested simulation domain was used for the purpose of the study. The analysis of the results showed the usefulness of multi-scale modeling

systems for providing the scientific basis for developing effective air quality management strategies.

2.1.4 Coupling of the Weather Research and Forecasting Model with AERMOD for Pollutant Dispersion Modeling. A Case Study for PM₁₀ Dispersion Over Pune, India

AERMOD, the Gaussian air pollutant dispersion model of the United States Environmental Protection Agency (USEPA) was coupled to the Weather Research and Forecasting (WRF) Model developed by the National Center for Atmospheric Research (NCAR). WRF is a next generation, fully compressible, Eulerian non-hydrostatic mesoscale forecast model with a run-time hydrostatic option. This model is useful for downscaling of weather and climate ranging from a kilometer to thousands of kilometers and, thus it is useful for deriving meteorological parameters required for air quality models. AERMOD is a steady-state Gaussian plume model that simulates pollutant dispersion in a range of applications, from rural to urban areas, in flat and complex terrain, for surface and elevated pollutant releases and from multiple sources (point, area and volume) of emissions. As AERMOD requires steady hourly surface and upper air meteorological observations, the use of information on meteorological parameters derived from regional meteorological models, such as WRF is an appropriate solution in the absence of meteorological observations at an hourly interval. The system was applied to simulate the dispersion of respirable particulate matter over Pune, India (Kesarkar et al. 2007). The comparison of model results with observations indicated that the model generally underestimated the concentrations at selected sites over the city.

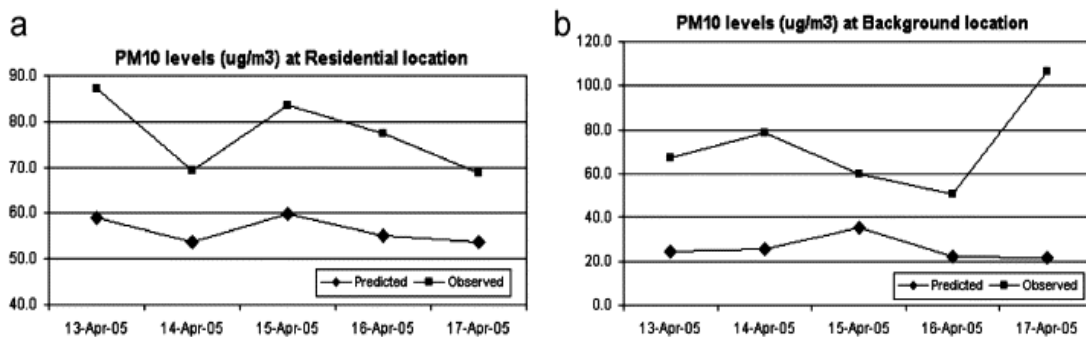


Figure 3. PM₁₀ values predicted by the coupled WRF/AERMOD modeling system compared with observations at different stations over Pune, India.

This was mainly attributed to the overestimation of WRF predicted wind speeds compared to those observed. Further applications using different WRF parameterizations are required in order to derive reliable conclusions on the suitability of regionally averaged meteorological parameters for driving Gaussian models. In conclusion, the methodology of coupling a prognostic regional weather model with a Gaussian air pollution model for simulating pollutant dispersion showed encouraging results, which is particularly important in cases

where the availability of frequent and continuous local meteorological observations is limited.

2.2 Assessment in Hot-Spot Areas and Source Apportionment

Urban air quality assessment requires the representation of the contribution of hot spots and major roads to the ambient air concentrations in different areas in the city. In this context, multi-scale modeling has recently emerged as a particularly relevant tool and has been successfully applied to estimate local contribution in urban air pollution levels in several cities in Europe.

2.2.1 Integrated Air Quality Modeling for a Designated Air Quality Management Area in Glasgow

Several urban air quality models have been coupled with higher resolution street canyon modules or CFD modules in order to account for these local contributions. For this purpose, within the frame of the local air quality management in Glasgow, a Gaussian urban air quality model was enhanced by integrating traffic flow data for urban road networks using the SATURN software, traffic pollutant emission data and a three-dimensional CFD dispersion model (PHOENICS) to account for the effect of turbulence in a complex configuration of street canyons (Mumovic, Crowther and Stevanovic 2006). Model simulation results were in good agreement with measurements taken during an accompanying continuous monitoring campaign, showing that a general CFD code has the potential for regulatory use.

2.2.2 Air Pollution Levels at Hot-Spot Areas of Selected European Cities

In this case study a complete regional–urban–local scale modeling sequence was used in order to estimate the increased pollution levels at traffic hot spot areas in 20 European cities, compared to the urban background concentrations (Kalognomou et al. 2009). As ambient concentrations of certain pollutants, such as NO_x , PM_{10} and $\text{PM}_{2.5}$, show strong variability at the urban and local scales, this analysis aimed to support future pollution abatement decisions by considering the increased pollution load at urban hot spots induced by local traffic sources. The urban scale OFIS model was applied, driven by results of the regional scale model EMEP. As a final step, the local scale OSPM model was applied using OFIS results to derive the urban background conditions required. The current air quality was estimated at the selected traffic sites, along with two future emission scenarios based on Current Legislation and Maximum Feasible Reductions respectively.

2.3 Multi-Scale Simulations of Pollutant Dispersion for Ozone and Aerosols

The assessment and dispersion simulation of particular pollutants, such as ozone, requires the treatment of physical and chemical processes at different scales, due to the governing complex and nonlinear transport and transformation mechanisms that take place. Multi-scale modeling is applied in the following case studies

2.3.1 Evaluation of the Models-3 Community Multi-Scale Air Quality (CMAQ) Modeling System with Observations Obtained During the TRACE-P Experiment: Comparison of Ozone and Its Related Species

As mentioned in an earlier example, the Models-3 Community Multi-scale Air Quality (CMAQ) modeling system is a Eulerian modeling tool developed by the US Environmental Protection Agency to address tropospheric ozone, acid deposition, visibility, particulate matter and other pollutant issues in the context of a “one atmosphere” perspective, where complex interactions between atmospheric pollutants and regional and urban scales are considered. Models-3/CMAQ was applied using meteorological fields provided by the Regional Atmospheric Modeling System (RAMS) to examine spatial distributions of tropospheric ozone over East Asia (Zhang et al. 2006). RAMS is a 3D, Eulerian, non-hydrostatic, regional mesoscale model, and it is widely used to drive air quality models. Model performance was evaluated by comparing modeled concentrations of ozone and its closely related chemical species with observations obtained during the Transport and Chemical Evolution over the Pacific (TRACE-P) field campaign from the end of February to early April of 2001. The results revealed that the model reproduced the temporal and spatial distributions of ozone and its related chemical species reasonably well, and most model results were within a factor of 2 of the observations.

2.3.2 Vertically Nested Non-Hydrostatic Model for Multi-Scale Resolution of Flows in the Upper Troposphere and Lower Stratosphere

Scale interaction processes are influencing the transport and dispersion of pollutants not only in the horizontal but also in the vertical dimension, particularly over areas with topographical features such as mountains. For highly reactive pollutants, such as ozone, that participate in complex chemical processes, transport and transformation in the vertical dimension should be adequately represented, as they partly control surface concentrations. For ozone, convective activity often serves as a sink in the lower troposphere due to the redistribution of pollutants by vertical mixing in a deep column.

A limited number of studies examine the effect of improved vertical resolution of atmospheric flows near the tropopause and in the lower stratosphere on model simulation results. In a relevant study (Mahalov and Moustouai 2009), the microscale domains of the high resolution coupled WRF-ARW/microscale

system were nested both in the horizontal and the vertical, and all microscale fields were relaxed towards the WRF finest nest. Model simulations were produced by conducting mesoscale simulations with several nests interacting in a two way mode, with a finest WRF nest of a horizontal grid spacing of 1 km. Vertical nesting was implemented by coupling the finest resolution nest of WRF with a sequence of microscale nests, constructed with increased resolution in both the horizontal and the vertical, with refined vertical gridding to resolve small-scale processes near the tropopause and in the lower stratosphere. The application of microscale vertical nesting was assessed in real case simulations of the TREX campaign of measurements where observations have indicated extreme events taking place near the tropopause and in the lower stratosphere. Model performance was evaluated under several conditions including mountain wave generation and moist deep convection. The ability of vertical nesting to improve the numerical solution was demonstrated by conducting a large domain simulation with coarse resolution, a simulation nested only in the horizontal dimension, and a simulation nested in both the horizontal and the vertical dimensions. Horizontal nesting alone was not sufficient to achieve a converged solution, but keeping the same horizontal gridding and refining the vertical resolution computed a converged solution. The results confirmed that refined microscale nests allowed the model to fully resolve sharp adiabatic layers.

2.3.3 GEM-AQ, An On-line Global Multi-Scale Chemical Weather System: Model Description and Evaluation of Gas Phase Chemistry Processes

The meteorological Global Environmental Multi-scale model (GEM) can be configured to simulate atmospheric processes over a broad range of scales, from the global scale down to the mesoscale (2–20 km). GEM was augmented by implementing air quality chemistry, including the gas phase, aerosol and cloud particles, limited wet chemistry, emission, deposition and transport processes. The resulting GEM-AQ model has been run in a number of configurations ranging from a global uniform domain, global variable resolution for regional scenarios, to high-resolution studies. The on-line implementation of environmental processes in the GEM model allows for multi-scale chemical weather modeling with simulations in global uniform, global variable, and limited area configurations. This approach ensures that all required dynamics and physics fields are considered for chemistry at every time step. The on-line implementation of chemistry and aerosol processes provides feedback on model dynamics and physics. The implemented air quality modules include 35 advected and 15 non-advected gas phase species. Transport of the chemically active tracers by the resolved circulation is calculated using the semi-Lagrangian advection scheme native to GEM.

In this study (Kaminski et al. 2007), GEM-AQ was applied and evaluated for a 5-year simulation (2001–2005) on a global uniform $1.5^{\circ} \times 1.5^{\circ}$ resolution domain. The objectives of this simulation were to derive a multi-year model climatology, to examine seasonal variation and regional distribution of ozone, NO_2 and CO

concentrations, evaluate global emissions, and provide chemical initial and boundary conditions for high resolution model simulations. The comparison with surface observations revealed that the meteorological conditions and the transport patterns of ozone were adequately captured, but the climatological emissions used for this simulation could not capture any specific emission event, which deviated from the general background values.

2.3.4 Development of a Comprehensive, Multi-Scale “One-Atmosphere” Modeling System: Application to the Southern Appalachian Mountains

The urban-to-regional multi-scale (URM) model has been widely used for simulating photochemical air pollutant dispersion. It is a three-dimensional Eulerian photochemical model that uses a finite element, variable mesh transport scheme along with the SAPRC chemical mechanism for simulating the gas-phase reaction kinetics in order to predict concentration distributions of ozone and precursors at different scales. It has been enhanced to include aerosol dynamics, wet deposition scavenging processes and heterogeneous sulfate chemistry to account for aerosol transport and transformation processes. This integrated, multipollutant, “one-atmosphere” modeling system also features variable size grids in its horizontal domain, allowing for the use of fine grids over the source and/or receptor areas, thus providing more satisfactory predictions of both urban and regional pollutant levels. This enhanced version of URM was applied using meteorological data from the RAMS Eulerian mesoscale model to simulate the fate of atmospheric pollutants over the Eastern US for the July 11th–19th, 1995 episode (Boylan et al. 2002). The model generally under predicted the daytime ozone peaks but the diurnal variations and the timing of the peaks did conform well with observations. In the case of fine PM (sulfate, ammonium, and organic carbon) predictions generally had high-normalized mean errors of less than 40 percent. Spatial distribution was not accurately described, mainly due to errors in simulating the magnitude and patterns of precipitation.

2.4 Multi-Scale Model Simulations of Accidental Releases and Emergency Planning

In response to legislation requirements, recent research effort focuses on developing models that can describe the chemical and physical processes affecting concentrations of dangerous air pollutants in the atmosphere, at spatial scales ranging from local (<1 km) to regional (~36 km). The advantage of these multi-scale modeling tools is that they will be able to combine information from a number of sources in order to more accurately describe the temporal and spatial variability of ground-level concentrations of dangerous air pollutants. By developing improved regional and local scale modeling tools and linking them to human exposure models, assessments of the exposure of humans and ecosystems to hazardous releases will be improved. This can be achieved by incorporating improved chemical mechanisms to predict the concentrations of toxic chemicals

and application of these models at a variety of scales. In this context, EPA is planning to extend the capabilities of the Community Multi-scale Air Quality (CMAQ) to include prediction of high-priority toxic air pollutants at different scales. Methods and tools for incorporating sources of information on concentrations at scales finer than CMAQ current grid resolutions will be examined and tested, including Gaussian plume dispersion models, computational fluid dynamics (CFD) models, large eddy simulation (LES) techniques, and computational methods for determining sub-grid variability.

2.4.1 krX System: Multi-Scale Modeling of Atmospheric Dispersion and Consequences Assessments for Radiological Emergencies

Downscaling is of particular importance in case of accidental releases, as the impact on receptors both in the vicinity of the site as well as in surrounding areas has to be assessed. The multi-scale krX modeling system simulates the plume behavior and examines consequences of releases in case of a nuclear emergency. The krX system consists of a suite of meteorological and atmospheric dispersion models. The meteorological module is essentially the Eulerian, non-hydrostatic, terrain-following atmospheric model, MM5. Different dispersion models have been coupled with MM5 in order to simulate dispersion at different spatial scales. For the local scale, the atmospheric dispersion modeling is using the multi-module PX model. PX provides an option to choose between 3 dispersion models: a pure Gaussian Puff, a Lagrangian model and a mixed Eulerian-Lagrangian one. For the regional to continental scale, the krX system uses a special adaptation of the POLAIR3D/POLYPHEMUS model, a flexible system that handles a wide range of applications from passive tracers to complex chemical mechanisms (Isnard et al. 2006).

2.4.2 A Dynamically Adapting Weather and Dispersion Model: The Operational Multi-Scale Environment Model with Grid Adaptivity (OMEGA)

For cases where accurate and fast real-time flow predictions are required, such as the release of hazardous materials in accidents and emergency situations, the capability of flexible grid structure becomes important in model simulations of the pollutant fate. In response to this need, the Operational Multi-scale Environmental Model with Grid Adaptivity (OMEGA) was developed (Bacon et al. 2000). OMEGA is a multi-scale, non-hydrostatic, three-dimensional prognostic atmospheric simulation model operating on the basis of an adaptive grid that permits a spatial resolution ranging from roughly 100 km to less than 1 km without the need for nested grids. To improve the prediction skill of hazardous dispersion models, it is essential that the atmospheric transport and diffusion processes be realistically described both at local as well as at larger scales. This can be achieved by placing the nest where calculations are performed over all areas of concern. For this purpose, OMEGA applies an unstructured mesh numerical technique to atmospheric simulation to increase local resolution to

better capture topography or the important physical features of the atmospheric circulation and cloud dynamics.

2.4.3 Impact of Transboundary Transport of Carbonaceous Aerosols on the Regional Air Quality in the United States: A Case Study of the South American Wildland Fire of May 1998

The local concentration levels are also in many cases influenced by regional scale processes such as the atmospheric transport of pollutants emitted in surrounding cities and industrialized areas, which provide the background for the local scale. As an adequate description of scale interactions is a prerequisite for reliable air quality assessments, multi-scale modeling is particularly important for these cases where transboundary air pollution is responsible for poor regional and local air quality. In the context of global climate change, natural or human induced large-scale events and accidents, including wildfires, dust transfer from desert areas etc. will increase in frequency and intensity. Therefore, transboundary transfer of pollutants is an important source that should be accurately estimated. One approach towards this direction is to improve the performance of regional air quality models by linking them with larger scale models, such as global chemistry transport models for providing initial and lateral boundary conditions. In a related study (In et al. 2007), the pollution load due to a severe biomass-burning event during May 1998 in Mexico and Central America was assessed by incorporating the GEOS-Chem global model output into the CMAQ modeling system, in the form of lateral boundary and initial values. An interpolation method reconciling the differences in the vertical and horizontal coordinates and the chemical species representations of the two models was applied. The comparison of model predicted daily and monthly mean aerosol concentrations against observational data from the Interagency Monitoring of Protected Visual Environments (IMPROVE) surface network suggested that the combined modeling system improved model simulation of carbonaceous aerosols, such as the elemental carbon (EC) and organic carbon (OC), demonstrating successful simulations of transboundary transport of aerosols.

2.5 Forecasting and Warning Systems: the Need for a Multi-Scale Approach

Modeling activities increase the knowledge on transport and dynamics of pollutants to assess compliance with air quality standards and to inform the population about air quality levels. Therefore, models are recognized as useful tools for analyzing and forecasting air quality and for evaluating the efficiency of alternative scenarios of emission reduction measures. Furthermore, numerical atmospheric modeling constitutes an essential and strategic tool to inform the population in advance of the potential exceedances of thresholds (information, alert or protection of human health thresholds), for example when pollution episodes occur.

2.5.1 Enhancing High-Resolution Air Quality Forecasting in Marenstrum Supercomputer

An example of applying multi-scale modeling for forecasting purposes is the Barcelona Supercomputing Center, which currently operates air quality forecasts in Europe and the Iberian Peninsula with the MM5-EMEP-CMAQ-DREAM modeling system on a daily basis. The operational system provides 48-hr forecasts of O₃, NO_x, SO₂, CO and PM, as well as chemograms in selected cities. CMAQ was coupled with Eta-DREAM in order to include the influence of Saharan dust in the operational daily forecasts of particle pollution load. As a first approach, the natural dust contribution from Eta/DREAM was added on-line to the output of CMAQ (Jiménez-Guerrero et al. 2007). The model was used to calculate the concentration of desert dust is the Dust Regional Atmospheric Model (DREAM), which is an operative tool extensively tested and validated by the scientific community. DREAM is fully inserted as one of the governing equations in the atmospheric NCEP/Eta model and simulates all major processes of the atmospheric dust cycle. The air quality forecasting system is currently being upgraded, in order to be implemented using variable resolution grids with increased horizontal and vertical resolution for selected cities in Spain (for example 1 km resolution for Madrid and Barcelona) and other hot-spot areas.

2.5.2 Linking the Eta Model with the Community Multi-Scale Air Quality (CMAQ) Modeling System to Build a National Air Quality Forecasting System

Much of the poor air quality during the summer in the northeast United States is linked to high ozone concentrations. The spatial variation observed in surface ozone concentrations dictates the need for multi-scale analysis of the physical and chemical processes governing its distribution patterns. Harmful concentrations of near-surface O₃ typically originate in and most often affect urban areas, but rural areas in substantial distances from the city area can be impacted because of long-range pollutant transport. Thus, in order for national authorities to estimate the differences in health burden induced by spatial variations in ozone concentrations in a country or region, information on ozone levels at different horizontal scales has to be provided by relevant modeling tools.

In order to improve the communication of daily air quality information to the public and to use a consistent system nationwide, NOAA and the United States Environmental Protection Agency (EPA) have developed a national air quality forecasting (AQF) system (Otte et al. 2004). The AQF system generates gridded model forecasts of ground-level ozone and provides warnings for the public of the onset, severity, and duration of poor air quality conditions. The results can be further used by state and local agencies to produce local air quality forecasts. The AQF system is based on the mesoscale meteorological NCEP's Eta Model and the EPA's Community Multi-scale Air Quality (CMAQ) Modeling System. The system meets the necessary NOAA requirements to achieve full operational

status, namely performance standards for accuracy ($\geq 90\%$ exceedances and non-exceedances forecast correctly) and product availability ($\geq 95\%$ on time delivery of guidance) and was implemented into operations in September 2004 for ozone predictions in the northeast United States.

References

- Bacon, D. P., N. N. Ahmad, Z. Boybeyi, T. J. Dunn, M. S. Hall, P. C. S. Lee, R. A. Sarma, M. D. Turner, K. T. Waight, S. H. Young and J. W. Zack. 2000. A Dynamically Adapting Weather and Dispersion Model: The Operational Multiscale Environment Model with Grid Adaptivity (OMEGA). *Mon. Weather Rev.* (128): 2044-2076.
- Boylan, J. W., M. T. Odman, J. G. Wilkinson, A. G. Russell, K. G. Doty, W. B. Norris and R. T. McNider. 2002. Development of a comprehensive, multiscale “one-atmosphere” modelling system: application to the Southern Appalachian Mountains. *Atmos. Environ.* (36) N.23: 3721-3734.
- Chen, D. S., S. Y. Cheng, X. R. Guo, T. Lei, X. Y. Zhao, Z. H. Chen and Z. H. Ren. 2005. An Integrated ARPS-MM5-CMAQ Modelling Approach for Predicting PM₁₀ Concentration in the Metropolitan Region of Beijing in winter. *Environmental Informatics Archives.* (3): 439 – 448.
- Cheng, S., D. Chen, J. Li, H. Wang and X. Guo. 2007. The assessment of emission-source contributions to air quality by using a coupled MM5-ARPS-CMAQ modelling system: A case study in the Beijing metropolitan region, China. *Environ. Model. Softw.* (22) N.11: 1601-1616.
- In, H.J., D. W. Byun, R. J. Park, N.K. Moon, S. Kim and S. Zhong. 2007. Impact of transboundary transport of carbonaceous aerosols on the regional air quality in the United States: A case study of the South American wildland fire of May 1998. *J. Geophys. Res.* (112): D07201, doi: 10.1029/2006JD007544.
- Isnard, O., J. P. Benoit, D. Didier, P. Dubiau, D. Quelo, E. Quentric, S. Masset, A. Mathieu, Y. Minier, L. Soulhac and B. Sportisse. 2006. krX system: multiscale modelling of atmospheric dispersion and consequences assessments for radiological emergencies. *Geophysical Research Abstracts.* (8): 07249.
- Jiménez-Guerrero, P., O. Jorba, C. Pérez, S. Gassó and J. M. Baldasano. 2007. Enhancing high-resolution air quality forecasting in marenstrum supercomputer. *In the Proceedings of the 11th International Conference on Harmonisation within Atmospheric Dispersion Modelling for Regulatory Purposes.*
- Kalognomou E.A., Mellios G., Moussiopoulos N., Larssen St., Samaras Z., van den Hout D., de Leeuw F., Kukkonen J. and Fiala J. 2009. The study of traffic hotspot air quality and street scale modelling in the Street Emission Ceilings (SEC) Project, *International Journal of Environment and Waste Management* (4): 156-178.
- Kaminski, J. W., L. Neary, J. Struzewska, J. C. McConnell, A. Lupu, J. Jarosz, K. Toyota, S. L. Gong, J. C'ot'e, X. Liu, K. Chance and A. Richter. 2007. GEM-AQ, an on-line global multiscale chemical weather system: model description and evaluation of gas phase chemistry processes. *Atmos. Chem. Phys. Discuss.* (7): 14895–14937.
- Kesarkar, A. P., M. Dalvi, A. Kaginalkar and A. Ojha. 2007. Coupling of the Weather Research and Forecasting Model with AERMOD for pollutant dispersion modelling. A case study for PM₁₀ dispersion over Pune, India. *Atmos. Environ.* (41) N.9: 1976-1988.

- Mahalov, A. and M. Moustouli. 2009. Vertically nested non-hydrostatic model for multiscale resolution of flows in the upper troposphere and lower stratosphere. *J. Comput. Phys.* (228) N.4: 1294-1311.
- Mumovic, D., J.M. Crowther and Z. Stevanovic. 2006. Integrated air quality modelling for a designated air quality management area in Glasgow. *Build. Environ.* (41): 1703–1712.
- Otte, T. L., G. Pouliot, J. E. Pleim, J. O. Young, K. L. Schere, D. C. Wong, P. C. S. Lee, M. Tsidulko, J. T. McQueen, P. Davidson, R. Mathur, H.-Y. Chuang, G. DiMego and N. L. Seaman. 2004. Linking the Eta Model with the Community Multiscale Air Quality (CMAQ) Modelling System to Build a National Air Quality Forecasting System. Final Draft for *Weather Forecast*.
- Schlünzen, K. H. 1996. Validierung hochauflösender Regionalmodelle. Ber. aus dem Zentrum f. Meeres- und Klimaforschung, Meteorologisches Institut, Universität Hamburg, A23, pp 184.
- Thunis, P. and R. Bornstein. 1996. Hierarchy of mesoscale flow assumptions and equations. *J. Atmos. Sci.* (53): 380-397.
- Tie, X., S. Madronich, G.-H. Li, Z. Ying, R. Zhang, A. R. Garcia, J. Lee-Taylor and Y. Liu. 2007. Characterisations of chemical oxidants in Mexico City: A regional chemical dynamical model (WRF-Chem) study. *Atmos. Environ.* (41) N.9: 1989-2008.
- Tsegas, G., Ph. Barmpas, I. Douros and N. Moussiopoulos. 2008. A metamodelling implementation of a two-way coupled mesoscale-microscale flow model for urban area simulations. *In the Proceedings of the 12th International Conference on Harmonisation within Atmospheric Dispersion Modelling for Regulatory Purposes V*. Đuričić, ed., Cavtat, Croatia, 6-9 October, 181-186.
- Zhang, M., I. Uno, R. Zhang, Z. Han, Z. Wang and Y. Pu. 2006. Evaluation of the Models-3 Community Multiscale Air Quality (CMAQ) modelling system with observations obtained during the TRACE-P experiment: Comparison of ozone and its related species. *Atmos. Environ.* (40) N.26: 4874-4882. Special issue on Model Evaluation: Evaluation of Urban and Regional Eulerian Air Quality Models.

Chapter 20

The Future of Air Pollution Modeling

A chapter dedicated to the topic “The Future of Air Pollution Modeling” was presented in Volume I of this book series. The abstract is reprinted below.

In the following chapter a discussion is presented about some future trends and developments regarding air pollution modeling. The main emphasis of the chapter deals with the progress of Internet technologies for future air pollution modeling systems. Comprehensive modeling systems are also discussed and the basic needs and structures explained. Some future activities regarding advanced remote sensing techniques from space are also examined, together with future research needs in air pollution modeling. Model evaluation issues – an area of major concern - are also discussed.

For additional information, the reader can visit:

- Atmospheric Modeling and Analysis Division (AMAD)
<http://www.epa.gov/AMD/>
<http://www.epa.gov/AMD/ModelDevelopment/>
- GIS Applications in Air Pollution Modeling
<http://www.gisdevelopment.net/application/environment/air/mi03220.htm>
- Understanding Air Quality
http://www.oar.noaa.gov/weather/t_understanding.html
- Dispersion Modeling Futures
http://www.cleanairinfo.com/modelingworkshop/presentations/Future_Modeling_Peters.pdf
- AIRNow-International: The Future of the United States Real-Time Air Quality Reporting and Forecasting Program with GEOSS Participation
<http://www.earthzine.org/2010/01/25/airnow-international-the-future-of-the-united-states-real-time-air-quality-reporting-and-forecasting-program-with-geoss-participation/>

- ESRL Model Development Activities on Regional and Local-Scale
<http://www.esrl.noaa.gov/research/themes/regional/RegionalModeling.pdf>
- Numerical Air Quality Modelling: Past, Present and Future
<http://www.cawcr.gov.au/bmrc/basic/wksp16/papers/Cope.pdf>
- Integrating GIS with Models: A Bibliography
<http://gisandscience.com/resources/linking-gis-with-models-a-bibliography/>
- The Application of MM5/WRF Models to Air Quality Assessments
<http://www.mmm.ucar.edu/mm5/workshop/ws03/sessionJ1/Klausmann.pdf>
- Development and Applications of CFD Simulations Supporting Urban Air Quality and Homeland Security
<http://ams.confex.com/ams/pdfpapers/105308.pdf>
- Research Projects in Air Quality
<http://www.smhi.se/en/Research/Research-departments/Air-quality/research-projects-in-air-quality-1.5413>

Georgieva E. and S. Trini Castelli 2010. *Active Groups in Air Pollution Modeling*. Chapter 21 of *AIR QUALITY MODELING - Theories, Methodologies, Computational Techniques, and Available Databases and Software. Vol. IV – Advances and Updates* (P. Zannetti, Editor). Published by The EnviroComp Institute (<http://www.envirocomp.org/>) and the Air & Waste Management Association (<http://www.awma.org/>).

Chapter 21

Active Groups in Air Pollution Modeling³

Emilia Georgieva ⁽¹⁾ and Silvia Trini Castelli ⁽²⁾

⁽¹⁾ *Institute for Environment and Sustainability, EC Joint Research Centre, Ispra (Italy)*

emilia.georgieva@jrc.ec.europa.eu

⁽²⁾ *Institute of Atmospheric Sciences and Climate, National Council of Research (CNR-ISAC), Torino (Italy)*

S.TriniCastelli@isac.cnr.it

Abstract: The air pollution modeling community is continuously growing and the activities and different approaches related to air quality studies and applications are diversifying more and more, facing all relevant issues and covering all spatial and temporal ranges of interest. Therefore, to identify all groups working in air pollution modeling, and to summarize all the theoretical and computational approaches to simulate the dispersion and transformation of pollutants in the atmosphere, is surely a challenge. The database provided here was built up following a two-step procedure. First, active groups in air pollution modeling have been identified examining recent specialized scientific literature and looking at participants to the main international conferences on air pollution modeling. The groups have then been contacted and invited to provide specific information using a web-based template. The template was designed with the aim to provide insight in the groups' main objectives, tools, skills and competences. A short version of the template is used in the printed book, while a longer one is prepared for the electronic version of the book, where submitted animations could be also found. The database contains the templates from 80 modeling groups coming from 28 countries. Of course, the list does not have any pretensions of being complete, however it provides a picture of the currently active air pollution modeling groups and of the modeling tools developed or used by them.

Key Words: air pollution, modeling, template, model developer, model user, research projects, type of model, type of application, link to animation, service provided.

³ This chapter replaces the original Chapters 21 and 22 presented in Volume I of this book series.

1 Introduction

Air quality, and the problems related to atmospheric pollution, is an issue of high and growing relevance and a topical interest for the society. Scientists are more and more requested to provide knowledge, tools and answers to investigate and tackle the impact on the environment and public health of the harmful substances released in the atmosphere. In this frame, the air pollution modeling community is widening and new subjects are continuously joining it worldwide. This leads also to a growth and diversification of the approaches related to air quality studies, of the modeling tools and of their applications. In the field of air pollution modeling, all relevant purposes are treated and any kind of models are developed, at all spatial and temporal scales of interest. The main goal of this contribution is to provide a picture of active air pollution modeling groups and of the model tools either developed or used in different parts of the world. To identify the groups working in air pollution modeling worldwide, to summarize all the various theoretical and computational approaches for simulating the dispersion and transformation of pollutants in the atmosphere, has been the main challenge to pursue this goal.

In order to provide a database containing as much as possible group's information, a two-step procedure was applied. First, a survey of air pollution modeling groups based on the specialized scientific literature and on the participation to the main air pollution modeling international conferences was performed, collecting the contacts. Then, a template was prepared with a two-fold aim. The first aim was to get insight into group's main objectives, competences and skills, modeling tools developed and used, recent research projects and services provided. The second aim, related to the organization of the content of this chapter, was to have a possibility to extract a short or longer version of the template. The short version contains some basic information for the group and is included in the printed version of the book, the longer version of the template, more detailed and providing information also on research projects and services supplied on a regular basis, is included only in the electronic version of the book. Some groups submitted examples of their models applications as animations; these files also are available in the electronic version of the book.

The template was made available to all contacted researchers on a web facility and the database presented in this chapter was elaborated using the information given directly by the groups.

The database contains the templates provided by 80 air quality modeling groups from 28 countries worldwide. We decided to collect the information and present it in this chapter with reference to two categories, "model developer group" or "model user group", depending on the kind of activity performed by the group and on how a group identifies itself. This classification was aimed at giving space to all the different kind of contributions, delivered by both academic and research institutions and also by consultancy firms. The final aims of the group's activity

can be focused both on fundamental research and on applications, like environmental impact studies, air quality assessment and emergency response. Of course, model developers are in general also model users. The motivation for proposing these two main groups was thus to highlight groups that make efforts in developing air pollution models and, at the same time, to give the chance to groups using models developed elsewhere to present their own activity.

Inside each category the modeling teams are presented by Countries (in alphabetical order) and for each Country different groups are ordered by their name (also in alphabetical order).

In the attempt to provide useful information to the reader, we decided to include in the printed version of the book not only the names of the groups, but also some basic information on the models (either developed or used), regarding the type of the model, the spatial-temporal scales and the type of application. It is not our goal here to put emphasis on the characteristics of the models, for these the reader could consult other existing web databases (for instance, some of them are the Model Documentation System⁴, the Model Inventory⁵ of COST728/732, and the Wiki list⁶ of atmospheric dispersion models. Rather, this chapter is finalized to provide information on the main group's activities, tools and software, and thus to facilitate collaboration between groups as well as to help third parties in orientating to select a model/group according to their specifications.

Hereafter a brief summary of the information provided in this Chapter is reported.

For model developers:

- Institution and its URL; name and contacts of the group leader;
- Brief description of the developed models: model acronym, model extended name, type of model, type of scales, type of applications;
- Brief description of other models used by the group: model acronym, type of model, and type of applications.

For model users:

- Institution and its URL; name and contacts of the group leader;
- Brief description of the models used by the group: model acronym, type of model, and type of applications.

In the long-version of this chapter, available on the CD electronic support, more details and additional fields are included. A hyperlink to submitted or web-available animations, provided by the participants, is highlighted in the text.

⁴ <http://pandora.meng.auth.gr/mds/mds.php>

⁵ http://www.mi.uni-hamburg.de/Model_Inventory.504.0.html and
<http://www.mi.uni-hamburg.de/Model-Inventory.5554.0.html>

⁶ http://en.wikipedia.org/wiki/List_of_atmospheric_dispersion_models

For model developers:

- Institution and its URL; name and contacts of the group leader; name and contacts of key group members;
- Main objectives related to the group's activity;
- Brief description of the developed models: model acronym; type of model; type of scales; type of application; extended name; objectives of the model use; type of emissions; availability of the model to third parties; partners in model development; group's own contribution in the model development;
- Brief description of other models used by the group: model acronym and URL, type of model, type of applications;
- Brief description of Related Projects: name of the project; objectives; partners; group's own contribution; source of funding; project URL.
- Services Provided and Additional Remarks.

For model users:

- Institution and its URL; name and contacts of the group leader; name and contacts of key group members;
- Main objectives related to the group's activity;
- Brief description of the models used by the group: model acronym and URL, type of model, type of applications;
- Brief description of Related Projects: name of the project; objectives; partners; group's own contribution; source of funding; project URL;
- Services Provided and Additional Remarks.

The database is surely not complete for many reasons, such as incomplete list of contacted groups, limited time to complete the template, no motivation in participating etc. However, the final goal of this work was to provide a picture of the state-of-the-art in air pollution modeling and of the tools applied and available worldwide. Considering the large participation to this initiative, we think this goal was achieved.

2 Model Developers' Groups ⁷

Country	ARGENTINA
GROUP NAME	Air Pollution Modeling Group
Institution	National Technological University. Faculty Regional Avellaneda.
Inst. URL	www.utn.edu.ar

⁷ This symbol is an active hyperlink to additional information in the CD-ROM version of this book.

Group Leader Nicolas A. Mazzeo, nmazzeo@fra.utn.edu.ar

MODEL TOOLS DEVELOPED BY THE GROUP

Model Acronym RGSONDE
Extended Name Rotating Grid Screening Model
Type of Model Gaussian plume dispersion model
Scales Distances less than 10km and short term concentrations
Applications Screening evaluation of point source emissions impact

Model Acronym DAUMOD
Extended Name Urban area dispersion model
Type of Model Analytical non-Gaussian model
Scales Distances less than 50km, from 1h to annual concentrations
Applications To estimate urban background air pollutant concentrations.

Model Acronym DAUMOD-RD
Extended Name Urban area dispersion model with chemical reactions and deposition
Type of Model Analytical non-Gaussian model
Scales Distances less than 50km, from 1h to annual.
Applications Urban background concentrations and deposition over water.

OTHER MODEL TOOLS USED BY THE GROUP

Model Acronym WinOSPM
URL www.dmu.dk/International/Air/Models/OSPM
Type of Model Semi empirical model
Applications Street canyon model

Model Acronym AERMOD
URL www.epa.gov/ttn/scram
Type of Model Eulerian model
Applications Point, area and volume source impact assessment

Model Acronym CALPUFF
URL www.src.com/calpuff/calpuff1.htm
Type of Model Lagrangian puff model
Applications Point, area and volume source impact assessment

Country **AUSTRIA**

GROUP NAME Air Quality Department Styria and Graz University of Technology
URL <http://www.umwelt.steiermark.at/cms/ziel/2054533/DE/>
Institution Air Quality Department of Styria and Graz University of Technology
Inst. URL <http://vkm-thd.tugraz.at/>
Group Leader Dietmar Oettl, dietmar.oettl@stmk.gv.at

MODEL TOOLS DEVELOPED BY THE GROUP

Model Acronym GRAL
Extended Name Graz Lagrangian Model
Type of Model Lagrangian Particle Model
Scales Local - regional; hours - years
Applications Urban air pollution with high spatial resolution

Model Acronym GRAMM
Extended Name Graz Mesoscale Model
Type of Model Prognostic wind field model
Scales Local - regional; hours - weeks
Applications Regional - urban - microscale flow field simulations

GROUP NAME **BOKU-Met Environmental Meteorology**
URL <http://www.boku.ac.at/met/envmet/>
Institution Institute of Meteorology (BOKU-Met), University of Natural Resources & Appl. Life Sci. Vienna
Inst. URL <http://met.boku.ac.at/>
Group Leader Petra Seibert, petra.seibert@boku.ac.at

MODEL TOOLS DEVELOPED BY THE GROUP

Model Acronym FLEXTRA
Extended Name Flexible Trajectory Model
Type of Model Trajectory model
Scales Regional to global
Applications Scientific research, AQ assessment, emergency, risk assessment
Link to Animation: <http://www.nilu.no/trajectories/index.cfm>

Model Acronym FLEXPART
Type of Model Lagrangian particle dispersion model
Scales Regional to global
Applications Scientific research, AQ assessment, emergency, risk assessment
Link to Animation: <http://transport.nilu.no/products>

Model Acronym FLEXPART-6.2_MM5-3.7
Extended Name FLEXPART Version 6.2 for MM5 (V3.7) Beta version
Type of Model Lagrangian particle dispersion model
Scales Mesoscale (gamma to alpha)
Applications Scientific research, AQ assessment, emergency, risk assessment

OTHER MODEL TOOLS USED BY THE GROUP

Model Acronym CAMx
URL <http://www.camx.com/>
Type of Model Eulerian chemistry-transport model with source apportionment
Applications Scientific research, AQ assessment, operational AQ forecasts

Model Acronym SMOKE
URL <http://www.smoke-model.org/>
Type of Model Emission model for creating input to CAMx (or other AQ models)
Applications Scientific research, AQ assessment, operational AQ forecasts

GROUP NAME Department of Environmental Meteorology
URL www.zamg.ac.at
Institution Central Institute for Meteorology and Geodynamics (ZAMG)
Inst. URL www.zamg.ac.at

Group Leader Martin Piringer, m.piringer@zamg.ac.at

MODEL TOOLS DEVELOPED BY THE GROUP

Model Acronym AQA
Extended Name Air Quality Model for Austria
Type of Model Eulerian grid

Scales	Mesoscale
Applications	Air quality forecasts, environmental assessment studies
Model Acronym	TAMOS
Extended Name	TAWES Modeling System
Type of Model	Lagrangian particle (FLEXPART), trajectory model (FLEXTRA)
Scales	Mesoscale
Applications	Nuclear emergency response, long range transport studies
Model Acronym	AODM
Extended Name	Austrian Odor Dispersion Model
Type of Model	Gaussian
Scales	Local
Applications	Odor pollution

OTHER MODEL TOOLS USED BY THE GROUP

Model Acronym	TRACE (Toxic Release Analysis of Chemical Emissions)
URL	www.safersystem.com
Type of Model	Lagrangian puff model
Applications	Emergency response modeling of explosive, or flammable gas
Model Acronym	MISKAM
URL	www.lohmeyer.de
Type of Model	CFD model
Applications	Air pollutants in the vicinity of building structures
Model Acronym	LASAT (Lagrange-Simulation of Aerosol-Transport)
URL	www.janicke.de/de/lasat.html
Type of Model	Lagrangian particle
Applications	Air pollutants influenced by orography, simple buildings

Country **BELGIUM**

GROUP NAME	Atmospheric Modeling Unit
URL	http://www.vito.be/VITO/EN/HomepageAdmin/Home/WetenschappelijkOnderzoek/RuimtelijkeMilieuaspecten/
Institution	VITO - Flemish Institute for Technological Research
Inst. URL	www.vito.be
Group Leader	Stijn Janssen, stijn.janssen@vito.be

MODEL TOOLS DEVELOPED BY THE GROUP

Model Acronym AURORA
Extended Name Air Quality Modeling in Urban Regions using an Optimal Resolution Approach
Type of Model Eulerian
Scales Urban, regional
Applications Scientific research, Air Quality Assessment

Model Acronym SMOGSTOP
Extended Name Statistical Model Of Ground level Short Term Ozone Pollution
Type of Model Stochastic model
Scales Local, regional
Applications Air quality forecasting

Model Acronym IFDM
Extended Name Immission Frequency Distribution Model
Type of Model Gaussian, Plume-rise
Scales Local
Applications Scientific research, Air Quality Assessment, Regulatory purposes & compliance

Model Acronym RIO
Extended Name Residual Interpolation optimized for Ozone
Type of Model Statistical interpolation model
Scales Local, regional
Applications Interpolation of air quality measurements

Model Acronym E-MAP
Extended Name Emission Mapper
Type of Model Emission Top Down Disaggregation Model
Scales Local, regional
Applications Conversion of low resolution emissions to high resolution gridded emissions

OTHER MODEL TOOLS USED BY THE GROUP

Model Acronym BeIEUROS
URL <http://www.vito.be/VITO/EN/HomepageAdmin/Home>
Type of Model Eulerian
Applications Scientific research, Air Quality Assessment, Policy support

Model Acronym ENVI-met
URL <http://www.envi-met.com/>
Type of Model CFD-based micro-climate and local air quality model

Applications Scientific research, Air Quality Assessment

Country **BRAZIL**

GROUP NAME **Gervasio Annes Degrazia**
URL <http://www.gruma.ufsm.br>
Institution Universidade Federal de Santa Maria
Inst. URL <http://www.ufsm.br>

Group Leader Gervasio Annes Degrazia,
gervasiodegrazia@gmail.com

MODEL TOOLS DEVELOPED BY THE GROUP

Model Acronym LES
Extended Name Large Eddy Simulation Model
Type of Model Eulerian grid
Scales Microscale
Applications Scientific research and air quality assessment

Country **BULGARIA**

GROUP NAME **GPhI group**
URL <http://www.geophys.bas.bg/atmos/atmo.htm>
Institution Geophysical Institute, Bulgarian Academy of Sciences
Inst. URL www.geophys.bas.bg

Group Leader Kostadin Ganev, kganev@geophys.bas.bg

MODEL TOOLS DEVELOPED BY THE GROUP

Model Acronym PLUME
Type of Model Gaussian
Scales Regional, local
Applications Scientific research, air quality assessment, emergency and risk assessment

Model Acronym TRAFFIC ORACLE
Type of Model Gaussian
Scales Mesoscale, regional, local, urban, microscale
Applications Scientific research, air quality assessment, emergency and risk assessment

GROUP NAME NIMH group
Institution National Institute of Meteorology and Hydrology
Inst. URL www.meteo.bg

Group Leader Dimiter Syrakov, dimiter.syrakov@meteo.bg

MODEL TOOLS DEVELOPED BY THE GROUP

Model Acronym EMAP
Extended Name Eulerian Model for Air Pollution
Type of Model 3D Eulerian grid
Scales Long-range, mesoscale, regional, local
Applications Scientific research, air quality assessment, emergency response
Link to Animation: NIMH_EMAP_KurskNPP.gif 

Model Acronym PLUM
Extended Name PLUme Model
Type of Model Gaussian plume
Scales Local (up to 100 km area)
Applications Environmental impact assessment, regulatory purposes

Model Acronym LED
Extended Name Lagrangian-Gaussian Diffusion
Type of Model Gaussian puff
Scales Long-range, mesoscale, regional, local
Applications Scientific research, air quality assessment, emergency response

OTHER MODEL TOOLS USED BY THE GROUP

Model Acronym US EPA Models-3 System (MM5, CMAQ, SMOKE)
URL <http://www.cmascenter.org/>
Type of Model Eulerian grid
Applications Scientific research, air quality assessment, emergency response

Model Acronym WRF ARW
URL <http://www.mmm.ucar.edu/wrf/users/>
Type of Model Non-hydrostatic
Applications Scientific research, air quality assessment, emergency response

Model Acronym ALADIN-Bulgaria, ALADIN-CLIMAT
URL <http://www.cnrm.meteo.fr/aladin/>
Type of Model Hydrostatic
Applications Operational weather forecast, climate change

Country **CHINA**

GROUP NAME	Nested Air Quality Prediction Modeling System Group
URL	http://naqpms.iap.ac.cn/
Institution	Institute of Atmospheric Physics, Chinese Academy of Sciences
Inst. URL	http://www.iap.ac.cn/
Group Leader	Zifa WANG, zifawang@mail.iap.ac.cn

MODEL TOOLS DEVELOPED BY THE GROUP

Model Acronym	NAQPMS
Extended Name	Nested air quality prediction modeling system
Type of Model	Chemical transport model
Scales	From intercontinental scale to urban scale, 72-96h forecast
Applications	Research and real time forecast

EU **EUROPEAN COMMISSION - JRC**

GROUP NAME	AIRMODE (Air Quality and Transport Modeling)
URL	http://ies.jrc.ec.europa.eu/index.php?page=action-13206
Institution	European Commission-Joint Research Centre, Ispra (Italy), Institute for Environment and Sustainability
Inst. URL	http://ies.jrc.ec.europa.eu
Group Leader	Panagiota Dilara, panagiota.dilara@jrc.ec.europa.eu

MODEL TOOLS DEVELOPED BY THE GROUP

Model Acronym	Sub-grid scale model for the treatment of emission heterogeneity
Type of Model	Second-order closure
Scales	Sub-grid
Applications	Improvement of the definition of emission representation below grid size

OTHER MODEL TOOLS USED BY THE GROUP

Model Acronym	MM5
URL	http://www.mmm.ucar.edu/mm5/
Type of Model	Meteorological model
Applications	Meteorological fields for dispersion simulations

Model Acronym WRF
URL <http://www.wrf-model.org/index.php>
Type of Model Weather research and forecast model
Applications Meteorological fields for dispersion simulations

Model Acronym CHIMERE
URL <http://www.lmd.polytechnique.fr/chimere/>
Type of Model Eulerian chemistry transport model
Applications Scientific research, air quality assessment

GROUP NAME **REM (Radioactivity Environmental Monitoring)**
URL <http://rem.jrc.ec.europa.eu>
Institution European Commission-Joint Research Centre, Ispra (Italy), Institute for Environment and Sustainability
Inst. URL <http://ies.jrc.ec.europa.eu/>
Group Leader Marc de Cort, marc.de-cort@jrc.ec.europa.eu

MODEL TOOLS DEVELOPED BY THE GROUP

Model Acronym ENSEMBLE system
URL <http://ensemble.jrc.ec.europa.eu/>
Type of Model ENSEMBLE system for the real-time inter-comparison of multi model simulations and ensemble treatment (web based)
Scales Any scale
Applications Model validation and ensemble treatment
Link to Animation: http://ensemble.jrc.ec.europa.eu/Ensemble_files/et1.gif

Country **FINLAND**

GROUP NAME **FMI-Dispersion modeling**
URL http://www.fmi.fi/research_air/air_2.html
Institution Finnish Meteorological Institute
Inst. URL <http://www.fmi.fi/>
Group Leader Ari Karppinen, ari.karppinen@fmi.fi

MODEL TOOLS DEVELOPED BY THE GROUP

Model Acronym SILAM
Extended Name Air Quality and Emergency Modeling System

Type of Model Eulerian grid & Lagrangian particle
Scales Regional
Applications Scientific research, operational forecasts, risk assessment

Model Acronym CAR-FMI
Extended Name Contaminants in the Air from a Road
Type of Model Gaussian line-source model
Scales Urban/local scale
Applications Research and AQ assessment

Model Acronym ESCAPE
Extended Name Expert System for Consequence Analysis using a Personal computer
Type of Model Gaussian
Scales Local scale
Applications Emergency and risk assessment, research

Model Acronym HILATAR
Extended Name A Regional Scale Grid Model for the Transport of Sulphur and Nitrogen Compounds
Type of Model Eulerian grid
Scales Regional scale
Applications Scientific research, air quality assessment

Model Acronym UDM-FMI
Extended Name Urban Dispersion Modeling System
Type of Model Gaussian
Scales Urban/local
Applications Air quality assessment

OTHER MODEL TOOLS USED BY THE GROUP

Model Acronym OSPM
URL <http://www.dmu.dk/International/Air/Models/OSPM>
Type of Model Street Canyon model (parametric)
Applications Scientific research, AQ assessment

Model Acronym FLUENT
URL <http://www.fluent.com/>
Type of Model CFD
Applications Research, air quality assessment
GROUP NAME **SILAM modeling team**
URL <http://silam.fmi.fi>
Institution Finnish Meteorological Institute
Inst. URL <http://www.fmi.fi>

Group Leader Sofiev Mikhail, mikhail.sofiev@fmi.fi

MODEL TOOLS DEVELOPED BY THE GROUP

Model Acronym SILAM
Extended Name Air Quality and Emergency Modeling System
Type of Model Chemical transport model
Scales From global to beta-mesoscale
Applications Standard dispersion and source apportionment applications

Country FRANCE

GROUP NAME Atmospheric fluid mechanics and short-range air quality modeling

URL <http://cerea.enpc.fr/en/axes.html>

Institution Centre d'Enseignement et de Recherche en Environnement Atmosphérique

Inst. URL <http://cerea.enpc.fr/en/index.html>

Group Leader Bertrand Carissimo, carissim@cerea.enpc.fr

MODEL TOOLS DEVELOPED BY THE GROUP

Model Acronym Code_Saturne
Extended Name Code_Saturne (formerly Mercure_Saturne)
Type of Model Eulerian (unstructured mesh) + Lagrangian module
Scales < 100km and < 24h
Applications Local scale atmospheric environmental applications
Link to Animation: Code_Saturne_mov5.avi 

GROUP NAME Atmospheric Modeling and Environmental Mapping

Institution INERIS

Inst. URL www.ineris.fr

Group Leader Bessagnet Bertrand, bertrand.bessagnet@ineris.fr

MODEL TOOLS DEVELOPED BY THE GROUP

Model Acronym CHIMERE
Type of Model Air quality model

Scales Regional
Applications Air quality assessment, scientific research

GROUP NAME **Chemical Transport Modeling of Air Quality**
URL <http://cerea.enpc.fr/en/index.html>
Institution CEREА (Centre d'Enseignement et de Recherche en Environnement Atmosphérique)
Inst. URL <http://cerea.enpc.fr/en/index.html>
Group Leader Christian Seigneur, seigneur@cerea.enpc.fr

MODEL TOOLS DEVELOPED BY THE GROUP

Model Acronym Polair3D
Extended Name Polair3D of the air-quality platform Polyphemus
Type of Model Eulerian with plume-in-grid
Scales Regional, mesoscale
Applications Scientific research, impact studies, data assimilation

Model Acronym Stationary Gaussian model and puff Gaussian model
Extended Name Gaussian of the air-quality platform Polyphemus
Type of Model Stationary Gaussian model and puff Gaussian model
Scales Local
Applications Scientific research, impact studies

OTHER MODEL TOOLS USED BY THE GROUP

Model Acronym MM5
URL www.mmm.ucar.edu/mm5
Type of Model Limited-area, nonhydrostatic model
Applications Simulation of mesoscale atmospheric circulation

Model Acronym Weather Research and Forecasting (WRF)
URL <http://www.wrf-model.org/index.php>
Type of Model Mesoscale numerical weather prediction system
Applications Simulation of mesoscale atmospheric circulation

Model Acronym ISORROPIA
URL <http://nenes.eas.gatech.edu/ISORROPIA/>
Type of Model Inorganic aerosol thermodynamic model
Applications Compute the phase state of aerosols.

GROUP NAME CHIMERE
URL <http://www.lmd.polytechnique.fr/chimere/>
Institution Laboratoire de Meteorologie Dynamique, IPSL, CNRS, Ecole Polytechnique
Inst. URL <http://www.lmd.jussieu.fr/>
Group Leader Laurent Menut, menut@lmd.polytechnique.fr

MODEL TOOLS DEVELOPED BY THE GROUP

Model Acronym CHIMERE
Extended Name Chemistry-transport model CHIMERE
Type of Model Eulerian
Scales From urban to mesoscale
Applications Scientific research, air quality, risk

GROUP NAME CNRM-GAME
URL <http://www.cnrm.meteo.fr/>
Institution Meteo-France and CNRS URA 1357
Inst. URL <http://www.meteo.fr>, <http://www.insu.cnrs.fr/>
Group Leader Vincent-Henri Peuch, Vincent-Henri.Peuch@meteo.fr

MODEL TOOLS DEVELOPED BY THE GROUP

Model Acronym MOCAGE
Extended Name MODèle de Chimie Atmosphérique À Grande Echelle
Type of Model Eulerian grid
Scales Regional to global (zoom in option with up to 3 sub-domains)
Applications Scientific research, AQ and emergency risk assessment

GROUP NAME Dynamics of Inhabited Atmosphere
URL www.ec-nantes.fr
Institution Ecole Centrale de Nantes
Inst. URL www.ec-nantes.fr
Group Leader Isabelle CALMET, Isabelle.Calmet@ec-nantes.fr

MODEL TOOLS DEVELOPED BY THE GROUP

Model Acronym CHENSI
Type of Model Eulerian micrometeorological CFD model - building resolving
Scales Microscale
Applications Scientific research

Model Acronym SUBMESO
Type of Model Eulerian - LES
Scales Meso to local scale
Applications Passive scalar, points/linear/area time-varying emissions

GROUP NAME FLUIDYN
URL <http://www.fluidyn.com>
Institution TRANSOFT International / FLUIDYN
Inst. URL <http://www.fluidyn.com>
Group Leader Claude Souprayen, contact@fluidyn.com

MODEL TOOLS DEVELOPED BY THE GROUP

Model Acronym PANACHE
Extended Name fluidyn-PANACHE
Type of Model CFD (flow, dispersion), Lagrangian particles and puffs
Scales Regional, local, urban, microscale
Applications Air quality and risk assessment, research
Link to Animation: dispersion_panache.gif 

Model Acronym PANEPR
Type of Model CFD (flow, dispersion), Lagrangian particles and puffs
Scales Local, urban, microscale
Applications Emergency and risk assessment
Link to Animation: dispersion_panepr.gif 

Model Acronym PANEIA
Type of Model CFD (flow, dispersion), Lagrangian particles and puffs
Scales Local, urban, microscale
Applications Industrial impact assessment
Link to Animation: dispersion_paneia.gif 

Model Acronym PANROAD
Type of Model CFD (flow, dispersion)

Scales	Local, urban, microscale
Applications	Road and transport infrastructure impact
Link to Animation:	dispersion_panroad.gif 
Model Acronym	PANAIR
Type of Model	CFD (flow, dispersion), Lagrangian particles and puffs
Scales	Regional, local, urban, microscale
Applications	Air quality, pollution episodes, radionuclide's transport
Link to Animation:	dispersion_panair.gif 

Country **GERMANY**

GROUP NAME	Bernhard Vogel
URL	http://www.imk-tro.kit.edu/3487.php
Institution	IMK, Karlsruhe Institute of Technology
Inst. URL	http://www.imk-tro.kit.edu
Group Leader	Bernhard Vogel, bernhard.vogel@kit.edu

MODEL TOOLS DEVELOPED BY THE GROUP

Model Acronym	COSMO-ART
Type of Model	Eulerian
Scales	Regional to continental, days to decades
Extended Name	COSMO = Consortium for Small-scale Modeling, ART= Aerosols and Reactive Trace

GROUP NAME	EURAD-IM Data Assimilation Group
URL	http://www.eurad.uni-koeln.de
Institution	Rhenish Institute of Environmental Research at the University of Cologne
Inst. URL	http://www.eurad.uni-koeln.de
Group Leader	Hendrik Elbern, he@eurad.uni-koeln.de

MODEL TOOLS DEVELOPED BY THE GROUP

Model Acronym	EURAD-IM
Extended Name	EUROpean Air pollution Dispersion-Inverse Model
Type of Model	Eulerian grid
Scales	Regional to local, short-range to long-range
Applications	Scientific research, air quality forecast and assessment

OTHER MODEL TOOLS USED BY THE GROUP

Model Acronym	MM5-V3
URL	http://www.mmm.ucar.edu/mm5/mm5-home.html
Type of Model	Eulerian mesoscale meteorological model
Applications	Provision of meteorological fields driving the EURAD-IM

GROUP NAME	IVU Umwelt GmbH
URL	www.ivu-umwelt.de/e
Institution	IVU Umwelt GmbH
Inst. URL	www.ivu-umwelt.de/e

Group Leader	Volker Diegmann, vd@ivu-umwelt.de
---------------------	---

MODEL TOOLS DEVELOPED BY THE GROUP

Model Acronym	IMMISnet
Type of Model	Gaussian
Scales	Regional, urban, local; hourly up to one year
Applications	Air quality assessment

Model Acronym	IMMISluft
Type of Model	Gaussian, parametric
Scales	Local (street canyon); yearly mean and EU short term values
Applications	Air quality assessment

Model Acronym	IMMIScpb
Type of Model	Gaussian, Box model
Scales	Local (street canyon); hourly up to one year
Applications	Air quality assessment

Model Acronym	IMMISmt
Type of Model	Gaussian, Box model
Scales	Urban (street network); hourly up to one year
Applications	Air quality assessment and monitoring, traffic management

OTHER MODEL TOOLS USED BY THE GROUP

Model Acronym	LASAT
URL	http://www.janicke.de/en/lasat.html
Type of Model	Lagrangian particle model

Applications	Air quality assessment, scientific research
Model Acronym	MISKAM
Type of Model	Eulerian grid, CFD
Applications	Air quality assessment
Model Acronym	RCG
URL	http://www.geo.fu-berlin.de/met/ag/trumpf/RCG/index.html
Type of Model	Eulerian, 3D-Aerosol-Photochemistry-Transport-Model
Applications	Air quality on various scales, scientific research

GROUP NAME	Janicke Consulting
URL	www.janicke.de
Institution	Janicke Consulting
Inst. URL	www.janicke.de

Group Leader Ulf Janicke, uj@janicke.de

MODEL TOOLS DEVELOPED BY THE GROUP

Model Acronym	LASAT
Extended Name	Lagrangian Simulation of Aerosol Transport
Type of Model	Lagrangian particle model (conforming with VDI 3945/3)
Scales	Regional, local, urban, microscale; seconds to years
Applications	Research, air quality and risk assessment, monitoring

Model Acronym	AUSTAL2000
Extended Name	Ausbreitungsrechnung nach TA Luft 2000
Type of Model	Lagrangian particle model (conforming with VDI 3945/3)
Scales	Local, urban, microscale; hour to year
Applications	Assessments according to the German Regulation TA Luft

Model Acronym	LASAIR
Extended Name	Lagrange-Simulation der Ausbreitung und Inhalation von Radionukliden
Type of Model	Lagrangian particle model (conforming with VDI 3945/3)
Scales	Local, urban, microscale; minutes to day

Applications Decision support system for nuclear hazards

Model Acronym LASPORT

Extended Name LASAT for Airports

Type of Model Lagrangian particle model (conforming with VDI 3945/3)

Scales Local, regional; hour to year

Applications Assessment of airport-related emissions and concentrations

Model Acronym SMOD

Extended Name Screening Model of Odor Dispersion

Type of Model Hybrid Euler-Gaussian

Scales Local, urban; year

Applications Screening model for odor dispersion

GROUP NAME TrUmF (Troposphaerische Umweltforschung - Tropospheric Environmental Research)

URL www.trumf.de

Institution Institute of Meteorology - Freie Universitaet Berlin

Inst. URL <http://www.geo.fu-berlin.de/met/>

Group Leader Rainer Stern, rstern@zedat.fu-berlin.de

MODEL TOOLS DEVELOPED BY THE GROUP

Model Acronym REM_Calgrid

Extended Name Regional Eulerian Model - California Grid Model

Type of Model Eulerian grid

Scales Regional, local

Applications Air quality assessment, scientific research

Link to Animation: <http://wekuw.met.fu-berlin.de/trumf/analyzer/10/01/26/ozon.htm>

Country **GREECE**

GROUP NAME Laboratory of Atmospheric Physics

URL <http://lap.phys.auth.gr/>

Institution Aristotle University of Thessaloniki

Inst. URL <http://www.auth.gr/home/>

Group Leader Dimitrios Melas, melas@auth.gr

MODEL TOOLS DEVELOPED BY THE GROUP

Model Acronym	NEMO
Extended Name	Natural Emissions MModel
Type of Model	Emission model
Scales	Sub-urban to continental, Hourly to annual
Applications	Air quality assessment, Scientific research

OTHER MODEL TOOLS USED BY THE GROUP

Model Acronym	CAMx
URL	http://www.camx.com/
Type of Model	3-D Eulerian photochemical dispersion model
Applications	Air quality forecasting and assessment, Scientific research

Model Acronym	MM5
URL	http://www.mmm.ucar.edu/mm5/
Type of Model	Mesoscale meteorological model
Applications	Operational forecasting, Atmospheric research

Model Acronym	WRF
URL	http://www.wrf-model.org/index.php
Type of Model	Mesoscale meteorological model
Applications	Operational forecasting, Atmospheric research

GROUP NAME	Laboratory of Heat Transfer and Environmental Engineering (LHTEE)
URL	http://aix.meng.auth.gr/lhtee/index.html
Institution	Aristotle University Thessaloniki
Inst. URL	http://www.auth.gr/home/

Group Leader	Nicolas Moussiopoulos, moussio@eng.auth.gr
---------------------	---

MODEL TOOLS DEVELOPED BY THE GROUP

Model Acronym	MEMO
Extended Name	Mesoscale Model
Type of Model	Eulerian grid, 3D meteorological prognostic model
Scales	Mesoscale
Applications	Scientific research, air quality assessment, policy support

Model Acronym	MIMO
----------------------	------

Extended Name	Microscale Model
Type of Model	Eulerian, 3D prognostic model
Scales	Microscale
Applications	Air quality assessment, policy support, emergency planning
Model Acronym	MARS
Extended Name	Model for the Atmospheric Dispersion of Reactive Species
Type of Model	3D Eulerian dispersion model
Scales	Local-to-regional
Applications	Air quality assessment, policy support, scientific research
Model Acronym	OFIS
Extended Name	Ozone Fine Structure Model
Type of Model	Two-layer 2D Eulerian photochemical dispersion model
Scales	Urban (local, local-to-regional)
Applications	Air quality assessment, regulation, public information

OTHER MODEL TOOLS USED BY THE GROUP

Model Acronym	MM5
URL	http://www.mmm.ucar.edu/mm5/
Type of Model	3D meteorological prognostic Eulerian model
Applications	Policy support, air quality assessment, scientific research
Model Acronym	PAL
URL	http://www.ess.co.at/GAIA/models/pal.htm
Type of Model	Gaussian plume model
Applications	Urban air quality simulations, emergency planning
Model Acronym	AUSTAL2000
URL	http://www.austal2000.de
Type of Model	3D Lagrangian particle model
Applications	Air quality assessment, regulatory purposes and compliance

Country

HUNGARY

GROUP NAME	ELU-TREX
URL	http://nimbus.elte.hu/~cuda/
Institution	Eötvös Loránd University, Department of Meteorology

Inst. URL <http://nimbus.elte.hu/>
Group Leader Róbert Mészáros, mrobi@nimbus.elte.hu

MODEL TOOLS DEVELOPED BY THE GROUP

Model Acronym	TREX-Euler
Extended Name	TRansport-EXchange-Eulerian
Type of Model	Eulerian
Scales	Regional
Applications	Scientific research
Model Acronym	TREX-Lagrange
Extended Name	TRansport-EXchange-Lagrangian
Type of Model	Lagrangian particle
Scales	Mesoscale
Applications	Scientific research, emergency and risk assessment

Country **INDIA**

GROUP NAME **Atmospheric dispersion modeling**
Institution Indian Institute of Technology Delhi;
 Centre for Atmospheric Sciences.
Inst. URL <http://www.iitd.ac.in/center/cas/>
Group Leader Maithili Sharan, mathilis@cas.iitd.ac.in

MODEL TOOLS DEVELOPED BY THE GROUP

Model Acronym	Low wind
Type of Model	Analytical with constant eddy diffusivity- plume and puff
Scales	Local scales
Applications	EIA; Industry etc
Model Acronym	Variable K model
Type of Model	Analytical
Scales	Local
Applications	Impact assessment studies
Model Acronym	Cross-wind
Type of Model	Analytical
Scales	Local
Applications	Vehicular: research applications

OTHER MODEL TOOLS USED BY THE GROUP

Model Acronym Pielke's model
Type of Model Mesoscale model
Applications Boundary layer: Meteorological fields for dispersion model

Model Acronym WRF
Type of Model Weather and research forecasting model
Applications Regional and local meteorological fields for dispersion

Model Acronym LPD
Type of Model Particle dispersion model
Applications Dispersion

Country**ITALY**

GROUP NAME **Arianet**
URL www.aria-net.it
Institution Arianet S.r.l.
Inst. URL www.aria-net.it

Group Leader Giuseppe Brusasca, g.brusasca@aria-net.it

MODEL TOOLS DEVELOPED BY THE GROUP

Model Acronym FARM
Extended Name Flexible Air Quality Regional Model
Type of Model Eulerian chemical grid
Scales Mesoscale
Applications Air quality assessment, scenarios analysis
Link to Animation: [Arianet_Farm_1.pps](#) 

Model Acronym SPRAY5
Extended Name Spray 5.0
Type of Model Microscale, local scale, mesoscale
Scales Microscale, local scale, mesoscale, real-time applications
Applications Microscale, local scale, mesoscale, real-time applications
Link to Animation: [Arianet_Spray5_2.pps](#) 

OTHER MODEL TOOLS USED BY THE GROUP

Model Acronym Aria Impact
URL www.aria.fr
Type of Model Gaussian standard and Gaussian hybrid model

Applications Air quality assessment

GROUP NAME **Complex System Laboratory - Turbulence and Dispersion**

URL <http://www.mfn.unipmn.it/Informazioni/ricerca/complexsystems/index.html>

Institution Department of Science and Advanced Technologies
University of East Piedmont

Inst. URL <http://dista.unipmn.it/>

Group Leader Enrico Ferrero, enrico.ferrero@mfn.unipmn.it

MODEL TOOLS DEVELOPED BY THE GROUP

Model Acronym RANS model
Type of Model Turbulence higher order model
Scales PBL scale

Model Acronym
Type of Model Lagrangian particle model with chemical reaction
Scales Short term local scale
Applications Short term dispersion of reactive pollutants

OTHER MODEL TOOLS USED BY THE GROUP

Model Acronym CAMx
Type of Model Photochemical Eulerian dispersion model
Applications Air quality assessment

Model Acronym RAMS
Type of Model Regional circulation model
Applications Modeling chain for dispersion
GROUP NAME **Environment and Industrial Accidental Release Modeling Group**

URL http://www.ispesl.it/urp/schedeTecniche/dipia/9.DIPIA_Modellistica.pdf

Institution ISPESL

Inst. URL <http://www.ispesl.it>

Group Leader Armando Pelliccioni, armando.pelliccioni@ispesl.it

MODEL TOOLS DEVELOPED BY THE GROUP

Model acronym CLPDMNN
Extended Name Concentration Levels Predicted by Dispersion Model and Neural Net

Type of Model	Eulerian, statistical, Neural Network and Air Dispersion Model
Scales	Urban scale
Application	Scientific research, Air Quality Assessment, Risk Assessment

OTHER MODEL TOOLS USED BY THE GROUP

Model Acronym	FARM
URL	www.aria-net.it
Type of Model	Chemical transport model
Applications	Mesoscale Gas and Aerosol dispersion

Model Acronym	SPRAY
URL	www.aria-net.it
Type of Model	Lagrangian Model
Applications	Continuous and Accidental release on local scale

Model Acronym	EFFECTS
URL	www.tno.nl/effects
Type of Model	Accidental Release model
Applications	Evaluation of consequences analysis

GROUP NAME	ENVIROWARE
URL	http://www.enviroware.com
Institution	ENVIROWARE
Inst. URL	http://www.enviroware.com

Group Leader	Sonia Mosca, info@enviroware.com
---------------------	---

MODEL TOOLS DEVELOPED BY THE GROUP

Model Acronym	LAPMOD
Extended Name	LAgrangian Particle Model
Type of Model	Lagrangian particle model
Scales	Local to mesoscale, from less than one hour to many years
Applications	Research, air quality, emergency including nuclear

Model Acronym	TOXFLAM
Type of Model	Analytical
Scales	From 50 m to 20 km, few minutes and up
Applications	Research, emergency

Model Acronym TUNNEL
Type of Model Eulerian finite volumes
Scales Microscale

Applications Research, air quality assessment

Model Acronym EXPFIRE
Extended Name EXPlosions and FIREs risk assessment
Type of Model Parametric
Scales Microscale
Applications Risk assessment

OTHER MODEL TOOLS USED BY THE GROUP

Model Acronym CALMET/CALPUFF
URL http://www.epa.gov/scram001/dispersion_prefrec.htm#calpuff
Type of Model Lagrangian puff
Applications Air quality assessment

Model Acronym AERMOD
URL http://www.epa.gov/scram001/dispersion_prefrec.htm#aermod
Type of Model Gaussian
Applications Air quality assessment

Model Acronym ISC3
URL http://www.epa.gov/scram001/dispersion_alt.htm#isc3
Type of Model Gaussian
Applications Air quality assessment

GROUP NAME ESMA (Environmental Systems Modeling and Assessment) research group
URL <http://automatica.ing.unibs.it/esma/esma.html>
Institution Department of Information Engineering - University of Brescia
Inst. URL <http://www.unibs.it/on-line/ing/Home.html>
Group Leader Giovanna Finzi, finzi@ing.unibs.it

MODEL TOOLS DEVELOPED BY THE GROUP

Model Acronym TCAM
Extended Name Transport and Chemical Aerosol Model
Type of Model Eulerian Grid

Scales	1km to 10km grid cell size. Daily to yearly simulations.
Applications	Air quality assessment, Scientific research
Model Acronym	AQUIS
Extended Name	Air Quality Urban Integrated System
Type of Model	Integrated stochastic models system
Scales	Urban scale (up to 100 km); short-term forecasting
Applications	Short-term forecasting, scientific research
Model Acronym	MODICA
Extended Name	Multi Objective Decision support system for Integrated Control of Air quality
Type of Model	Integrated assessment model
Scales	Regional scale, long-term applications
Applications	Decisions support system, scientific research

GROUP NAME	Gabriele Curci
URL	http://pumpkin.aquila.infn.it/gabri/
Institution	CETEMPS, Dept. Physics, University of Aquila
Inst. URL	http://cetemps.aquila.infn.it/Cetemps/it/
Group Leader	Gabriele Curci, gabriele.curci@aquila.infn.it

MODEL TOOLS DEVELOPED BY THE GROUP

Model Acronym	CHIMERE
Type of Model	Eulerian grid
Scales	Regional (50 km) to local (2 km), days to years
Applications	Scientific research, air quality monitoring and forecasting

OTHER MODEL TOOLS USED BY THE GROUP

Model Acronym	GEOS-Chem
URL	http://acmg.seas.harvard.edu/geos/
Type of Model	Eulerian grid global scale
Applications	Tropospheric chemistry simulation of gases and aerosol
Model Acronym	WRF/Chem
URL	http://ruc.noaa.gov/wrf/WG11/
Type of Model	Eulerian grid regional scale, online meteorology
Applications	Air quality research and forecasting

GROUP NAME	ISAC-TO Environmental Physics Group
URL	www.isac.cnr.it/~turboto
Institution	Institute of Atmospheric Sciences and Climate - National Research Council
Inst. URL	www.isac.cnr.it , www.cnr.it
Group Leader	Domenico Anfossi, D.Anfossi@isac.cnr.it

MODEL TOOLS DEVELOPED BY THE GROUP

Model Acronym	MILORD
Extended Name	Method for the Investigation of LOng Range Dispersion
Type of Model	3D Lagrangian particle dispersion model
Scales	Long range
Applications	Scientific research

Model Acronym	LAMBDA
Extended Name	Lagrangian Model for Buoyant Dispersion in the Atmosphere
Type of Model	3D Lagrangian particle dispersion model for flat terrain
Scales	Regional and local
Applications	Scientific research

Model Acronym	SPRAY and MicroSPRAY
Extended Name	SPRAY5.0
Type of Model	3D Lagrangian particle dispersion model
Scales	SPRAY regional & local scale; MicroSPRAY urban & microscale
Applications	Scientific research, air quality assessment, emergency response

Model Acronym	RMS and MicroRMS
Type of Model	Integrated modeling system, meteorology and Lagrangian dispersion
Scales	RMS mesoscale-regional- local; MicroRMS urban-microscale
Applications	Scientific research, air quality and environmental assessment

OTHER MODEL TOOLS USED BY THE GROUP

Model Acronym	RAMS
URL	www.atmet.com
Type of Model	Atmospheric model: meteorological preprocessor for Lagrangian models

Applications	Scientific research, air quality and environmental assessment
Extended Name	RAMS-MIRS-SPRAY modeling system
Model Acronym	MSS - MicroSwiftSpray
URL	www.aria-net.it
Type of Model	Integrated modeling system diagnostic meteo + Lagrangian
Applications	Scientific research, air quality and environmental assessment

GROUP NAME	Meteorology and Climatology for Energy application
URL	www.erse-web.it
Institution	ERSE (ENEA Ricerca per il settore Elettrico)
Inst. URL	www.erse-web.it
Group Leader	Paolo Bonelli, paolo.bonelli@erse-web.it

MODEL TOOLS DEVELOPED BY THE GROUP

Model Acronym	SPRAY (ERSE version)
Type of Model	Lagrangian particle model
Scales	Regional, urban, microscale
Application	Scientific research, air quality assessment

OTHER MODEL TOOLS USED BY THE GROUP

Model Acronym	RAMS
URL	www.atmet.com
Type of Model	Meteorological model
Model Acronym	CAMx
Type of Model	Chemical Eulerian model
Applications	Regional air pollution evaluations

GROUP NAME	Turbulence and Dispersion
URL	http://bolchem.isac.cnr.it
Institution	cnr-isac
Inst. URL	www.isac.cnr.it

Group Leader Alberto Maurizi, a.maurizi@isac.cnr.it

MODEL TOOLS DEVELOPED BY THE GROUP

Model Acronym BOLCHEM
Extended Name BOlogna Limited area model for CHEMistry
Type of Model Mesoscale atmospheric dynamics and composition model
Scales Limited by hydrostatic approximation
Applications Regional air quality

Country JAPAN

GROUP NAME Mitsubishi Heavy Industries (MHI)
URL www.mhi.co.jp
Institution Nagasaki R&D Center
Inst. URL <http://www.mhi.co.jp/ngsrdc/index.html>

Group Leader R. Ohba, ryohji_ohba@mhi.co.jp

MODEL TOOLS DEVELOPED BY THE GROUP

Model Acronym MEASURES
Extended Name Multiple Radiological Emergency Assistance System for Urgent Response
Type of Model Meteorological diffusion model
Scales A few km to 1000 km for space and a few minutes to one year
Applications Emergency response system and environmental planning

OTHER MODEL TOOLS USED BY THE GROUP

Model Acronym RAMS and HYPACT
URL www.atmet.com
Type of Model Mesoscale meteorological model and gas diffusion model
Applications Weather forecast and environmental assessment

Country KOREA

GROUP NAME Aerosol Modeling
URL www.caem.re.kr
Institution Center for Atmospheric and Environmental Modeling, Seoul

Inst. URL www.caem.re.kr
Group Leader Soon-Ung Park, supark@snu.ac.kr

MODEL TOOLS DEVELOPED BY THE GROUP

Model Acronym ADAM2 (Asian Dust Aerosol Model 2)
Extended Name Asian Dust Aerosol Model, 1, 2
Type of Model Operational Asian dust forecast model
Scales Domain of 70-160E, 5-60N. 30*30 km, 3 days forecast
Applications Operational forecast model
Link to Animation: Asian_Dust.gif 

Model Acronym Aerosol Dynamic Modeling System (ADMS)
Type of Model Aerosol impact assessment system
Scales The same domain in ADAM2 but aerosol simulation
Applications Impact assessment of aerosols (dust and anthropogenic aero.)

Country **NETHERLANDS**

GROUP NAME **HSM (Health, Safety and Modeling)**
URL <http://www.kema.com/services/consulting/hse/airquality/Default.aspx>
Institution KEMA
Inst. URL <http://www.kema.com>

Group Leader René van Egmond

MODEL TOOLS DEVELOPED BY THE GROUP

Model Acronym STACKS+
Type of Model Physical & chemical model
Scales Hour-to-hour model; up to 30 kilometers
Applications Industry, traffic, airports, shipping, cattle ranches

GROUP NAME **LOTOS-EUROS Modeling group**
URL www.lotos-euros.nl
Institution TNO, Environment and Geosciences
Inst. URL www.tno.nl

Group Leader Martijn Schaap, martijn.schaap@tno.nl

MODEL TOOLS DEVELOPED BY THE GROUP

Model Acronym LOTOS-EUROS
Extended Name Long term ozone simulation
Type of Model Eulerian
Scales Long-range, regional and urban
Applications Scientific research and AQ assessment

Country **POLAND**

GROUP NAME **APC-WUT; Air Pollution Control Group at Warsaw University of Technology, Poland**

URL <http://eng.pw.edu.pl/>

Institution Faculty of Environmental Engineering, Warsaw University of Technology

Inst. URL <http://eng.pw.edu.pl/Faculties/Faculty-of-Environmental-Engineering>

Group Leader Katarzyna Juda-Rezler, katarzyna.juda-rezler@is.pw.edu.pl

MODEL TOOLS DEVELOPED BY THE GROUP

Model Acronym MOD3
Type of Model Eulerian three-level grid model with a Lagrangian module for subgrid dispersion from point sources
Scales Urban; short-term
Applications Scientific research, air quality assessment

Model Acronym URFOR-2
Extended Name URban air pollution FORecasting model
Type of Model Gaussian plume model
Scales Urban; short-term
Applications Simulation of the air pollution in the urban area

Model Acronym SPM
Extended Name Segmented Plume Model
Type of Model Segmented Gaussian plume model, variable input parameters
Scales Local to regional scale; short term
Applications Simulation of the air pollution from the point sources

Model Acronym MRPM
Extended Name Multibox Reactive Plume Model

Type of Model	Multibox Reactive plume model
Scales	Local to regional scale; short term
Applications	Simulation of the reactive plumes from point source
Model Acronym	SOXNOX
Extended Name	Sulphur and Nitrogen Species Eulerian Grid Model for Poland
Type of Model	2D Eulerian grid model
Scales	Regional scale, long-term
Applications	Scientific research, air quality and deposition assessment

OTHER MODEL TOOLS USED BY THE GROUP

Model Acronym	CALMET-CALPUFF
URL	http://www.src.com/calpuff/calpuff1.htm
Type of Model	Non-steady-state Gaussian Puff Model
Applications	Scientific research, air quality assessment
Model Acronym	CAMx
URL	http://www.camx.com/
Type of Model	3D Eulerian Grid Photochemical Model
Applications	Scientific research, air quality & deposition assessment
Model Acronym	RegCM
URL	http://users.ictp.it/~pubregcm/
Type of Model	Hydrostatic Regional Climate Model
Applications	Scientific research, climate change impacts on air quality

Country PORTUGAL

GROUP NAME	GEMAC - Group on Emissions, Modeling and Climate Change
URL	http://www.dao.ua.pt/gemac/
Institution	University of Aveiro
Inst. URL	http://www.ua.pt/
Group Leader	Carlos Borrego, cborrego@ua.pt

MODEL TOOLS DEVELOPED BY THE GROUP

Model Acronym	VADIS
Extended Name	Pollutant dispersion in the atmosphere under variable wind conditions

Type of Model CFD RANS with a Lagrangian module for pollutants dispersion
Scales Local/urban and microscale
Applications Scientific research; air quality assessment
Link to Animation: UAVR_GEMAC_VADIS.avi 

Model Acronym DISPERFIRE
Type of Model Lagrangian particle
Scales Local scale
Applications Air quality assessment in forest fires and experimental burn

Model Acronym RISCAV
Type of Model Gaussian model coupled with a box model
Scales Local/urban
Applications Scientific research, emergency and risk assessment

Model Acronym AIRFIRE
Type of Model Eulerian
Scales Mesoscale, regional, episodic (2-3 days)
Applications Scientific research, forest fires impact on air quality

OTHER MODEL TOOLS USED BY THE GROUP

Model Acronym CHIMERE
URL <http://www.lmd.polytechnique.fr/chimere/>
Type of Model Eulerian
Applications Air quality assessment and forecast and scientific research

Model Acronym CAMx
URL <http://www.camx.com/>
Type of Model Eulerian
Applications Air quality assessment and scientific research

Model Acronym LOTOS-EUROS
URL <http://www.lotos-euros.nl/>
Type of Model Eulerian chemistry transport model (CTM)
Applications Air quality assessment, forest fire impacts on air quality

Country

RUSSIAN FEDERATION

GROUP NAME Air Pollution Modeling and Forecasting Lab
Institution Voeikov Main Geophysical Observatory, St. Petersburg

Inst. URL www.mgo.rssi.ru
Group Leader Eugene Genikhovich, ego@main.mgo.rssi.ru

MODEL TOOLS DEVELOPED BY THE GROUP

Model Acronym OND-86
Type of Model Analytical approximation of CFD results
Scales Urban (up to 100 km), 20 - 30 min averaged concentration
Applications Air quality and risk assessment

Model Acronym MEAN
Extended Name Model for calculation of long-term MEAN concentrations
Type of Model Source-receptor, analyt. approx
Scales Up to 100 km, long-term (e.g., mean annual) concentration
Applications Air quality and risk assessment

Model Acronym RD 52.04.253-90
Extended Name Model for estimating of scales of the contamination
Type of Model Inversed source-receptor
Scales Urban
Applications Emergency and risk assessment

OTHER MODEL TOOLS USED BY THE GROUP

Model Acronym SILAM
Type of Model Eulerian grid
Applications Air quality, emergency and risk assessment

Country **SPAIN**

GROUP NAME **Barcelona Supercomputing Centre - Centro Nacional de Supercomputación**
URL www.bsc.es/caliope
Institution Barcelona Supercomputing Centre - Centro Nacional de Supercomputación
Inst. URL www.bsc.es
Group Leader Jose Maria Baldasano, jose.baldasano@bsc.es

MODEL TOOLS DEVELOPED BY THE GROUP

Model Acronym BSC-HERMES

Extended Name The High-Elective Resolution Modeling Emission System
Type of Model Emission model
Scales Regional; 1km x 1km; 1 hour
Applications Air quality assessment; top-down and bottom-up approaches

Model Acronym BSC-DREAM8b
Extended Name Dust Regional Atmospheric Model
Type of Model Mineral dust forecast model
Scales 0.3°x0.3°; 6 hours
Applications Air quality assessment

OTHER MODEL TOOLS USED BY THE GROUP

Model Acronym WRF
URL www.wrf-model.org
Type of Model Meteorological model
Applications Weather research and forecasting

Model Acronym CMAQ
URL www.cmaq-model.org
Type of Model Air quality model
Applications Air quality assessment

GROUP NAME Environmental Software and Modeling Group
URL <http://artico.lma.fi.upm.es>
Institution Technical University of Madrid (UPM)
Inst. URL <http://www.upm.es>

Group Leader Roberto San José, roberto@fi.upm.es

MODEL TOOLS DEVELOPED BY THE GROUP

Model Acronym MICROSYS
Extended Name MICROscale air quality modeling SYStem
Type of Model Eulerian CFD
Scales Microscale (a few meters spatial resolution)
Applications Scientific research, air quality assessment, emergency, risk assessment

Model Acronym CAMO
Extended Name Cellular Automata MOdel
Type of Model Cellular automata model

Scales Microscale
Applications Scientific research, air quality assessment, emergency, risk assessment

Model Acronym EMIMO
Extended Name EMIssion MOdel
Type of Model Model to estimate by downscaling the emissions for air quality models
Scales All (global to microscale)
Applications Scientific research, air quality assessment, emergency, risk assessment

Model Acronym OPANA
Extended Name Operational Air Quality Numerical Modeling System
Type of Model Eulerian Air Quality Model (on-line model; no feedbacks)
Scales Mesoscale up to 1 km spatial resolution
Applications Scientific research, air quality assessment, emergency, risk assessment

Model Acronym TEAP
Extended Name A Tool to evaluate the Air Quality Impact by industrial plants
Type of Model Eulerian Air Quality Modeling System for industrial plants
Scales Mesoscale
Applications Operational for emergencies and risk assessment

OTHER MODEL TOOLS USED BY THE GROUP

Model Acronym WRF/chem
URL <http://www.acd.ucar.edu/wrf-chem/>
Type of Model Eulerian numerical model
Applications Scientific research

Model Acronym CMAQ
URL <http://www.cmaq-model.org/>
Type of Model Eulerian mesoscale model
Applications Air Quality Impact studies, Operational real-time forecasting systems, process analysis, etc.

Model Acronym CCSM3
URL <http://www.cesm.ucar.edu/>
Type of Model Eulerian global model
Applications Climate Change, global modeling, paleontology

GROUP NAME Grupo de Modelización Atmosférica (Atmospheric Modeling Group)
URL <http://www.ciemat.es/>
Institution CIEMAT
Inst. URL <http://www.ciemat.es/>

Group Leader Fernando Martin, fernando.martin@ciemat.es

MODEL TOOLS DEVELOPED BY THE GROUP

Model Acronym MELPUFF
Extended Name Mesoscale Lagrangian Puff Model
Type of Model Lagrangian Puff model
Scales Local and mesoscale. Minutes, hours, days.
Applications Air quality assessment, control and forecasting

Model Acronym SLP-2D
Extended Name Street Lagrangian Particles Model in 2D
Type of Model Particle Lagrangian Puff Model for street canyons
Scales Microscale seconds and minutes.
Applications Air quality assessment and research

OTHER MODEL TOOLS USED BY THE GROUP

Model Acronym CHIMERE
URL <http://www.lmd.polytechnique.fr/chimere/>
Type of Model Photochemical Eulerian model
Applications Air quality assessment and forecasting

Model Acronym WRF
URL <http://www.wrf-model.org/index.php>
Type of Model Meteorological model
Applications Meteorological simulations for inputs to air quality models

Model Acronym CALMET-CALPUFF
URL <http://www.src.com/calpuff/calpuff1.htm>
Type of Model Diagnostic meteorological model and Lagrangian Puff model
Applications Air quality assessment and training in AQ modeling

Country SWITZERLAND

GROUP NAME	Gasphase and Aerosol Chemistry Group
URL	http://lac.web.psi.ch/LAC_Groups/GPC/GPC_main.html
Institution	Laboratory of Atmospheric Chemistry (LAC), Paul Scherrer Institut (PSI)
Inst. URL	http://lac.web.psi.ch/ , http://www.psi.ch/
Group Leader	André S. H. Prévôt, andre.prevot@psi.ch

MODEL TOOLS DEVELOPED BY THE GROUP

Model Acronym	mm5prep
Extended Name	MM5 Pre-processing
Type of Model	Pre-processor for MM5 (IDL)
Scales	Mesoscale, days to several months
Applications	Scientific research, air quality assessment
Model Acronym	wrfprep
Extended Name	WRF/WPS Pre-processing
Type of Model	Pre-processor for WRF-ARW and WPS (IDL)
Scales	Mesoscale, days to several months
Applications	Scientific research, air quality assessment
Model Acronym	emCAMx
Extended Name	Emissions for CAMx
Type of Model	Emission generator for CAMx
Scales	Mesoscale, days to several months
Applications	Scientific research, air quality assessment
Model Acronym	CAMxRunner
Type of Model	Runtime environment for CAMx
Scales	Only limited by CAMx (mesoscale, days to several months)
Applications	Scientific research, air quality assessment
Model Acronym	AQM
Extended Name	Air quality model plot software
Type of Model	Plot software
Applications	Scientific research, air quality assessment

OTHER MODEL TOOLS USED BY THE GROUP

Model Acronym	MM5
URL	http://www.mmm.ucar.edu/mm5/
Type of Model	Eulerian grid meteorological model

Applications	Scientific research, air quality assessment
Model Acronym	WRF-ARW
URL	http://box.mmm.ucar.edu/wrf/users/
Type of Model	Eulerian grid meteorological model
Applications	Scientific research, air quality assessment
Model Acronym	CAMx
URL	http://www.camx.com/
Type of Model	Eulerian grid photochemical dispersion model
Applications	Scientific research, air quality assessment

Country **TURKEY**

GROUP NAME	Fatih University Air Quality Research Group
URL	http://airpol.fatih.edu.tr/aboutus.php
Institution	Fatih University
Inst. URL	www.fatih.edu.tr
Group Leader	Omar Alagha, oyalagha@fatih.edu.tr

MODEL TOOLS DEVELOPED BY THE GROUP

Model Acronym	NN-Airpol
Type of Model	Neural network based air quality prediction model
Scales	Local scale, dynamic
Applications	Prediction of PM ₁₀ , and gaseous pollutants
Model Acronym	airpol tool

Country **UNITED KINGDOM**

GROUP NAME	Air Quality & Composition
URL	http://www.metoffice.gov.uk/
Institution	Met Office
Inst. URL	http://www.metoffice.gov.uk/
Group Leader	Paul Agnew, paul.agnew@metoffice.gov.uk

MODEL TOOLS DEVELOPED BY THE GROUP

Model Acronym	MetUM
Extended Name	Met Office Unified Model
Type of Model	Eulerian Grid, online meteorology

Scales Global to local scales
Applications AQ Forecasting, AQ scenarios, climate, NWP

GROUP NAME Cambridge Environmental Research Consultants' developers

URL www.cerc.co.uk

Institution Cambridge Environmental Research Consultants

Inst. URL www.cerc.co.uk

Group Leader David Carruthers, David.Carruthers@cerc.co.uk

MODEL TOOLS DEVELOPED BY THE GROUP

Model Acronym ADMS 4
Extended Name Atmospheric Dispersion Modeling System 4
Type of Model Advanced 3-D quasi-Gaussian model
Scales Local scale. From annual to instantaneous.
Applications Air quality permits, emergency, flow fields, research.

Model Acronym ADMS-Urban
Extended Name Atmospheric Dispersion Modeling System Urban
Type of Model Advanced 3-D quasi-Gaussian nested in a trajectory model
Scales Local and urban scale. From annual to 15 minutes
Applications Air quality management, policy development, and research.

Model Acronym ADMS-Airport
Extended Name Atmospheric Dispersion Modeling System Airport
Type of Model Advanced 3-D quasi-Gaussian nested in a trajectory model
Scales Local and urban scale. From annual to 15 minutes
Applications Air quality management, policy development, and research.

Model Acronym ADMS-Roads
Extended Name Atmospheric Dispersion Modeling System Roads
Type of Model Advanced 3-D quasi-Gaussian model
Scales Local scale. From annual to 15 minutes.
Applications Air quality management for towns and rural road networks

Model Acronym EMIT
Extended Name Emissions Inventory Toolkit

Type of Model Database for storing, editing and managing emissions.
Scales Local and urban up to regional scale. Annual.
Applications Greenhouse gas and local emissions inventories

GROUP NAME **Environmental Health Sciences**
URL <http://www.gees.bham.ac.uk/research/clusters/health/index.shtml>
Institution University of Birmingham, UK
Inst. URL <http://www.gees.bham.ac.uk>

Group Leader Roy Harrison, r.m.harrison@bham.ac.uk

MODEL TOOLS DEVELOPED BY THE GROUP

Model Acronym RAMS-CANYON
Extended Name Birmingham Urban Street Canyon LES
Type of Model Large-eddy simulation model of street canyon flows
Scales dx=0.3 m, dt=0.03 sec; Lx=20 m, Ly=40 m, Lz=100 m
Applications Dispersion of passive scalars and photochemical species

Model Acronym FLUENT
Type of Model Commercial CFD model
Scales Unstructured grid
Applications Dispersion of traffic related pollutants in urban canyons

Country UNITED STATES

GROUP NAME **Atmospheric Chemistry and Meteorology Group**
URL <http://www.pnl.gov/atmospheric>
Institution Pacific Northwest National Laboratory
Inst. URL <http://www.pnl.gov/>

Group Leader William Shaw, will.shaw@pnl.gov

MODEL TOOLS DEVELOPED BY THE GROUP

Model Acronym WRF-Chem
Extended Name Chemistry version of the Weather Research and Forecasting (WRF) model
Type of Model Eulerian chemical transport model
Scales 1 - 100 km, days to months

Applications Research on evolution of particulates and their precursors

Model Acronym FLEXPART-WRF
Extended Name WRF version of the FLEXPART model
Type of Model Lagrangian particle dispersion model
Scales Meters to hundreds of kilometers
Applications Scientific research

Model Acronym MOSAIC
Extended Name Model for Simulating Aerosol Interactions and Chemistry (MOSAIC)
Type of Model Aerosol model
Scales Urban to global scale
Applications Scientific research on particulate evolution

GROUP NAME **Baron Advanced Meteorological Systems**
URL <http://www.baronservices.com>

Group Leader John N. McHenry, john.mchenry@baronams.com

MODEL TOOLS DEVELOPED BY THE GROUP

Model Acronym CMAQ
Extended Name Community Multi-scale Air Quality Model
Type of Model Photochemical, Particulate
Scales Regional-to-Local
Applications Forecast and Assessment

Model Acronym MAQSIP-RT
Extended Name Multi-Scale Air Quality Simulation Platform
Type of Model Photochemical
Scales Regional-to-Local
Applications Forecast

Model Acronym SMOKE
Extended Name Sparse-Matrix Kernel Operator Emissions System
Type of Model Emissions processing and modeling
Scales Regional to local
Applications Forecast and Assessment

Model Acronym WRF-Chem
Extended Name Weather Research and Forecasting Chemistry Model

Type of Model Coupled meteorological-air quality
Scales Regional to local
Applications Forecast

GROUP NAME **EnviroComp Consulting, Inc.**
URL www.envirocomp.com
Institution EnviroComp Consulting, Inc.
Inst. URL www.envirocomp.com

Group Leader Paolo Zannetti, zannetti@envirocomp.com

MODEL TOOLS DEVELOPED BY THE GROUP

Model Acronym MONTECARLO
Type of Model Lagrangian particle model
Scales Short-range applications (a few km)
Applications Non-reactive chemicals
Link to Animation: EnviroComp_MONTECARLO_Monsanto.wmv 

OTHER MODEL TOOLS USED BY THE GROUP

Model Acronym AERMOD and CALPUFF
URL http://www.epa.gov/scram001/dispersion_prefrec.htm
Type of Model US EPA Gaussian models
Applications Short range (AERMOD) and long range (CALPUFF)

Model Acronym FLUENT
URL <http://www.fluent.com/>
Type of Model CFD
Applications Indoor air pollution at computer industrial sites (e.g. IBM)

Model Acronym ALOFT-FT
URL <http://www.fire.nist.gov/aloft/>
Type of Model CFD
Applications Fire plume model

GROUP NAME **ENVIRON Air Sciences Group**
URL www.camx.com
Institution ENVIRON International Corporation
Inst. URL www.environmentcorp.com

Group Leader Ralph E. Morris, rmorris@environcorp.com

MODEL TOOLS DEVELOPED BY THE GROUP

Model Acronym CAMx
Extended Name Comprehensive Air-quality Model with extensions
Type of Model Eulerian photochemical grid model
Scales Plume to continental and minutes to years
Applications Air pollution including ozone, PM, toxics, mercury

Model Acronym CONCEPT
Extended Name CONSolidated Community Emissions Processing Tool
Type of Model Emissions modeling system for photochemical grid models
Scales User selected (point sources to continental scale)
Applications Air pollution including ozone, PM, toxics, mercury

OTHER MODEL TOOLS USED BY THE GROUP

Model Acronym CMAQ
URL www.cmascenter.org
Type of Model Eulerian photochemical grid model
Applications Air pollution

Model Acronym WRF
URL www.wrf-model.org
Type of Model Prognostic meteorological model
Applications Meteorology

Model Acronym CALPUFF
URL www.src.com
Type of Model Lagrangian puff model
Applications Inert or linear chemical plume modeling

Group Name **Computational Chemodynamics Laboratory**
URL <http://www.ccl.rutgers.edu>
Institution Environmental and Occupational Health Sciences Institute
Inst. URL <http://www.eohsi.rutgers.edu>

Group Leader Panos G. Georgopoulos, panosg@ccl.rutgers.edu

MODEL TOOLS DEVELOPED BY THE GROUP

Model acronym MENTOR-1A
Extended Name Modeling ENvironment for TOtal Risk studies (MENTOR) in a "One Atmosphere" (1A) setting
Type of Model Stochastic Agent-Based Model for Human Exposures
Scales Meso scale to urban
Application Scientific Research

Model acronym MENTOR-2E
Extended Name Modeling ENvironment for TOtal Risk studies (MENTOR) for Emergency Events
Type of Model Stochastic Agent-Based Model for Human Exposures
Scales Urban scale
Application Scientific Research; Emergency and Risk Assessment

Model acronym RPM-3DAERO
Extended Name Three Dimensional Reactive Plume Model with Aerosol processes
Type of Model Hybrid Lagrangian/Eulerian
Scales Urban to local scale
Application Scientific Research

Model acronym Indoor-AERO
Extended Name Indoor Air Quality Model with explicit Aerosol Treatment
Type of Model Compartmental model/Parametric
Scales Microenvironmental Scale/Minutes
Application Scientific Research, Risk Assessment

OTHER MODELS USED BY THE GROUP

Model acronym CMAQ
URL: <http://www.cmascenter.org>
Type of Model Eulerian grid
Application Scientific Research, Air Quality and Risk Assessment

Model acronym CALPUFF
URL: <http://www.src.com/calpuff>
Type of Model Lagrangian puff model
Application Scientific Research, Risk Assessment

Model acronym HYPACT
URL: <http://www.atmet.com/>
Type of Model Lagrangian particle transport
Application Scientific Research, Risk Assessment

GROUP NAME	National Atmospheric Release Advisory Center (NARAC)
URL	https://narac.llnl.gov
Institution	Lawrence Livermore National Laboratory
Inst. URL	www.llnl.gov
Group Leader	Gayle Sugiyama, sugiyama@llnl.gov

MODEL TOOLS DEVELOPED BY THE GROUP

Model Acronym	ADAPT
Extended Name	Atmospheric Data Assimilation and Parameterization Techniques
Type of Model	Atmospheric data assimilation
Scales	10 to 10,000 km; 1 hr to 1 yr typical
Applications	For initialization of 3-D dispersion model
Model Acronym	LODI
Extended Name	Lagrangian Operational Dispersion Integrator
Type of Model	Lagrangian particle dispersion
Scales	10 to 10,000 km; 1 hr to 1 yr typical
Applications	Emergency response
Model Acronym	FEM3MP
Extended Name	Finite Element Model Version 3 Multi-Processor
Type of Model	Lagrangian particle CFD dispersion model
Scales	100 m to 10 km; 1 hr to 24 hr typical
Applications	Dense gas and explicit building dispersion
Model Acronym	HotSpot
Extended Name	HotSpot Health Physics Codes
Type of Model	Gaussian
Scales	1-100 km; 1 hr to 1 year
Applications	Nuclear and radiological incident modeling

GROUP NAME	Yuhang Wang's Tropospheric Chemistry Group
URL	http://apollo.eas.gatech.edu
Institution	Georgia Institute of Technology
Inst. URL	http://www.gatech.edu/

Group Leader Yuhang Wang, ywang@eas.gatech.edu

MODEL TOOLS DEVELOPED BY THE GROUP

Model Acronym REAM
Extended model name REgional chemical trAnsport Model
Type of Model Regional chemical transport model
Scales Regional
Applications Scientific research and air quality assessment

OTHER MODEL TOOLS USED BY THE GROUP

Model Acronym GEOS-Chem
URL <http://acmg.seas.harvard.edu/geos/>
Type of Model Global chemical transport model
Applications Scientific research and air quality assessment

Model Acronym CMAQ
URL <http://www.cmaq-model.org/>
Type of Model Regional multi-scale air quality modeling system
Applications Air quality assessment

Model Acronym WRF
URL <http://www.wrf-model.org/index.php>
Type of Model Mesoscale numerical weather prediction system
Applications Generate the meteorological data for air quality modeling

3 Model Users' Groups

Country	AUSTRIA
GROUP NAME	Environmental Software & Services GmbH
URL	http://www.ess.co.at
Institution	Environmental Software & Services GmbH
Inst. URL	http://www.ess.co.at
Group Leader	Kurt Fedra, kurt@ess.co.at
MODEL TOOLS USED BY THE GROUP	
Model Acronym	CAMx
URL	www.camx.com
Type of Model	Eulerian, nested grid, photochemical
Applications	Real time forecast, scenario analysis, emission control
Model Acronym	AERMOD
URL	www.epa.gov/scram001/dispersion_prefrec.htm
Type of Model	Gaussian, regulatory
Applications	High-resolution convolution (traffic), regulatory long-time
Country	BRAZIL
GROUP NAME	Maria de Fatima Andrade
Institution	Instituto de Astronomia, Geofísica e Ciências Atmosféricas, Universidade de São Paulo
Inst. URL	www.dca.iag.usp.br
Group Leader	Maria de Fatima Andrade, mftandra@model.iag.usp.br
MODEL TOOLS USED BY THE GROUP	
Model Acronym	WRF-Chem
Type of Model	Eulerian Mesoscale modeling with chemistry on line
Applications	Air quality assessment, air quality research
Model Acronym	BRAMS
Type of Model	Eulerian Grid Mesoscale model
Applications	Weather forecast, air quality studies

Country **CHILE**

GROUP NAME	Air Quality Modeling
URL	www.solucionesambientales.cl
Institution	Pontificia Universidad Catolica de Chile
Inst. URL	www.ing.puc.cl
Group Leader	Hector Jorquera, jorquera@ing.puc.cl
MODEL TOOLS USED BY THE GROUP	
Model Acronym	CAMx
URL	www.camx.com
Type of Model	Eulerian Grid
Applications	Air quality assessment in urban and regional zones in Chile
Model Acronym	CALPUFF
URL	http://www.src.com/calpuff/calpuff1.htm
Type of Model	Lagrangian puff model
Applications	Assessment of air quality impacts near industrial sources
Model Acronym	AIRVIRO
URL	http://www.smhi.se/airviro
Type of Model	Eulerian model
Applications	Air quality management at Santiago, Chile

Country **CROATIA**

GROUP NAME	AQCT group
URL	http://www.gfz.hr/eng/meteorologija/AQCT/project_team.htm
Institution	Department of Geophysics, Faculty of Science, University of Zagreb
Inst. URL	http://www.gfz.hr/eng/index.html
Group Leader	Zvezdana Bencetic Klaic, zklaic@rudjer.irb.hr
MODEL TOOLS USED BY THE GROUP	
Model Acronym	CAMx
URL	http://www.camx.com/
Type of Model	Eulerian grid model
Applications	Scientific research
Model Acronym	WRF
URL	http://www.wrf-model.org/index.php
Type of Model	Eulerian grid model

Applications	Regional climate change studies
Model Acronym	CAMx
URL	http://www.camx.com/
Type of Model	Chemistry-transport model
Applications	Air quality modeling

EU**EUROPEAN COMMISSION - JRC**

GROUP NAME	GAPCC
URL:	http://ies.jrc.ec.europa.eu/index.php?page=action-24001
Institution	European Commission -Joint Research Centre, Ispra (Italy), Institute for Environment and Sustainability
Inst. URL	http://ec.europa.eu/dgs/jrc/index.cfm
Group Leader	Rita Van Dingenen, rita.van-dingenen@jrc.ec.europa.eu

MODELS USED BY THE GROUP

Model Acronym	TM5
URL	http://www.phys.uu.nl/~tm5/
Type of Model	Eulerian, global model, CTM
Applications	AQ assessment, Policy applications

Model Acronym	ECHAM5-HAMMOIZ
URL	http://www.mpimet.mpg.de/en/wissenschaft/modelle/echam/echam5.html
Type of Model	Eulerian, global model, GCM
Applications	Climate effects, Policy applications

Country**GERMANY**

GROUP NAME	Air Quality
URL	http://imk-ifu.fzk.de/87.php
Institution	Institute for Meteorology and Climate Research (IMK-IFU)
Inst. URL	http://imk-ifu.fzk.de/index.php
Group Leader	Peter Suppan, peter.suppan@kit.edu

MODEL TOOLS USED BY THE GROUP

Model Acronym	WRF/Chem
----------------------	----------

Type of Model	Eulerian grid
Applications	Air quality assessment
Model Acronym	MCCM
Type of Model	Eulerian grid
Applications	Air quality assessment
Model Acronym	GRAL
Type of Model	Lagrangian
Applications	Street Canyon Dispersion; Air Quality Assessment

Country **GREECE**

GROUP NAME	Numerical applications in the atmosphere
URL	
Institution	National and Kapodistrian University of Athens, Environ. Phys.& Meteo. Division
Inst. URL	http://en.uoa.gr/
Group Leader	Maria Tombrou – Tzella, mtombrou@phys.uoa.gr

MODEL TOOLS USED BY THE GROUP

Model Acronym	CAMx
URL	http://www.camx.com/
Type of Model	Eulerian, 3D, air quality model
Applications	Local to regional gaseous and aerosol pollution
Model Acronym	GEOS-Chem
URL	http://acmg.seas.harvard.edu/geos/
Type of Model	Global 3-D chemical transport model (CTM)
Applications	Global atmospheric composition
Model Acronym	MM5
URL	http://www.mmm.ucar.edu/mm5/
Type of Model	Eulerian, 3D meteorological model
Applications	Meteorological, local to regional

Country **ITALY**

GROUP NAME	Atmospheric Environment Group
Institution	ISMES Environment and Territory Division of CESI
Inst. URL	www.cesi.it
Group Leader	Gabriele Carboni, gabriele.carboni@cesi.it

MODEL TOOLS USED BY THE GROUP

Model Acronym CALMET-CALPUFF
URL www.src.com
Type of Model Lagrangian puff model
Applications Short & long term AQ monitoring, forecasting, assessment

Model Acronym RAMS/MM5-SPRAY
URL www.atmet.com , www.mmm.ucar.edu, www.cesi.it
Type of Model Lagrangian particle model
Applications Short & long term AQ monitoring, forecasting, assessment

Model Acronym RAMS/MM5-CAMx
URL www.atmet.com , www.mmm.ucar.edu , www.camx.it
Type of Model Eulerian grid CTM
Applications Source apportionment, AQ assessment, forecasting

GROUP NAME AQMODISACLE1
URL www.le.isac.cnr.it/aqmodisacle1
Institution Institute of Atmospheric Sciences and Climate CNR
Inst. URL www.isac.cnr.it

Group Leader Cristina Mangia, c.mangia@isac.cnr.it

MODEL TOOLS USED BY THE GROUP

Model Acronym CALPUFF
URL www.src.com/calpuff/calpuff1.htm
Type of Model Lagrangian puff model
Applications Air quality assessment

Model Acronym WRF-CHEM
URL <http://cprm.acd.ucar.edu/Models/WRF-Chem/>
Type of Model Eulerian grid model
Applications Scientific research -air quality assessment

Model Acronym CALGRID
URL www.arb.ca.gov/eos/soft.htm
Type of Model Eulerian grid model
Applications Air quality assessment scientific research

GROUP NAME ESASAS
URL <http://www.esasas.com/>
Institution Joint venture "Environmental System Analysis s.r.l." and "Take Air s.r.l."

Group Leader Maria Chiara Metallo, c.metallo@esasas.com

MODEL TOOLS USED BY THE GROUP

Model Acronym CMAQ
URL <http://www.cmaq-model.org/>
Type of Model Eulerian Grid
Applications Air quality assessment

Model Acronym WRF
URL <http://www.wrf-model.org/index.php>
Type of Model Eulerian Grid
Applications Air quality assessment

Model Acronym CALPUFF
URL <http://www.src.com/calpuff/calpuff1.htm>
Type of Model Lagrangian puff
Applications Air quality assessment

Country JAPAN

GROUP NAME **Regional Atmospheric Modeling Section, Asian Environment Research Group**
Institution National Institute for Environmental Studies
Inst. URL <http://www.nies.go.jp/index.html>

Group Leader Toshimasa Ohara, tohara@nies.go.jp

MODEL TOOLS USED BY THE GROUP

Model Acronym CMAQ
URL <http://www.cmaq-model.org/>
Type of Model Eulerian grid
Applications Scientific research, air quality assessment

Model Acronym CHASER
URL <http://chaser.env.nagoya-u.ac.jp/index.html>
Type of Model Eulerian grid
Applications Scientific research, air quality assessment

Model Acronym GEOS/Chem
URL <http://acmg.seas.harvard.edu/geos/>

Type of Model Eulerian grid
Applications Scientific research, air quality assessment

Country POLAND

GROUP NAME Air Protection Unit of EKOMETRIA
URL www.ekometria.com.pl
Institution EKOMETRIA Ltd.
Inst. URL www.ekometria.com.pl

Group Leader Wojciech Trapp, wojtek.trapp@ekometria.com.pl

MODEL TOOLS USED BY THE GROUP

Model Acronym CALMET-CALPUFF
URL <http://www.src.com/>
Type of Model Gaussian puff model with chemical removal and other effects
Applications Air quality assessment, regulatory purposes and other

Model Acronym CAMx
URL <http://www.camx.com/>
Type of Model 3D Eulerian tropospheric photochemical model
Applications Air quality assessment, regulatory purposes and other

Model Acronym CALINE-4
URL <http://www.dot.ca.gov/hq/InfoSvcs/EngApps/>
Type of Model Gaussian model
Applications Air quality assessment near roadways

GROUP NAME ENVIRO Group - Faculty of Energy and Fuels
URL <http://www.wpie.agh.edu.pl/>
Institution AGH University of Science and Technology
Inst. URL <http://www.agh.edu.pl/>

Group Leader Artur Wyrwa, awyrwa@agh.edu.pl

MODEL TOOLS USED BY THE GROUP

Model Acronym POLYPHEMUS
URL <http://cerea.enpc.fr/polyphemus/>
Type of Model Several models: Gaussian, Eulerian, Lagrangian

GROUP NAME MANHAZ
URL <http://manhaz.cyf.gov.pl>
Institution Institute of Atomic Energy POLATOM
Inst. URL www.iea.cyf.gov.pl

Group Leader Mieczyslaw Borysiewicz, manhaz@cyf.gov.pl

MODEL TOOLS USED BY THE GROUP

Model Acronym CMAQ
URL www.cmaq-model.org
Type of Model Eulerian
Applications Scientific research

GROUP NAME Meteorology Group
URL <http://meteo.is.pw.edu.pl>
Institution Faculty of Environmental Engineering, Warsaw University of Technology
Inst. URL www.is.pw.edu.pl

Group Leader Lech Loboeki, Lech.Loboeki@is.pw.edu.pl

MODEL TOOLS USED BY THE GROUP

Model Acronym GEM-AQ
URL <http://collaboration.cmc.ec.gc.ca/science/rpn.comm> ,
<http://maqnet.ca>
Type of Model Eulerian grid, global tropospheric chem. non-hydrostatic
Applications Weather prediction, research, AQ studies, chemical climate

Model Acronym MC2-AQ
URL <http://collaboration.cmc.ec.gc.ca/science/rpn.comm> ,
<http://maqnet.ca>
Type of Model Eulerian grid, regional, non-hydrostatic
Applications Research, wind energy, AQ studies

Country SPAIN

GROUP NAME Environmental Modeling
URL www.usc.es/enxqu/?q=gl/node/184
Institution University of Santiago de Compostela
Inst. URL www.usc.es

Group Leader Juan J. Casares-Long, juanjose.casares@usc.es

MODEL TOOLS USED BY THE GROUP

Model Acronym CAMx
URL www.camx.com/
Type of Model Air quality model - Eulerian
Applications Simulation of tropospheric ozone episodes

Model Acronym WRF
URL www.wrf-model.org/
Type of Model Meteorological model
Applications Meteorological input of air quality simulation

Model Acronym CHIMERE
URL www.lmd.polytechnique.fr/chimere/
Type of Model Air quality model - Eulerian
Applications Simulation of tropospheric photochemistry

GROUP NAME EOLO
URL www.ehu.es/eolo
Institution University of the Basque Country
Inst. URL www.ehu.es

Group Leader Gabriel Ibarra-Berastegi, gabriel.ibarra@ehu.es

MODEL TOOLS USED BY THE GROUP

Model acronym WRF
URL <http://www.wrf-model.org/index.php>
Type of Model Meteorological model
Application Operational, downscaling of IPCC climate models

Country UNITED STATES

GROUP NAME NYSDEC/SUNY - Albany/SUNY - Stony Brook
Multi-Model Air Quality Forecasting Group
URL <http://www.asrc.albany.edu/research/aqf/aqvis/>
Institution Atmospheric Sciences Research Center, SUNY-Albany
Inst. URL <http://www.asrc.albany.edu/>
Group Leader Christian Hogrefe, chogrefe@dec.state.ny.us

MODEL TOOLS USED BY THE GROUP

Model Acronym CMAQ
URL <http://www.cmaq-model.org/>
Type of Model Multiscale air quality model
Applications Forecasting, planning, climate change impact assessment

Model Acronym CAMx
URL <http://www.camx.com/>
Type of Model Multiscale air quality model
Applications Forecasting, planning, climate change impact assessment

Acknowledgements

We would like to thank Fabrizio Roccatò, web master at ISAC-C.N.R., Seat of Bologna, who built and handled on the ISAC server facilities the web template for the collection of the databases for the model developers and users. He actively collaborated to the elaboration of the data and his contribution was fundamental for the preparation of this chapter.

Chapter 22

Available Software

A chapter on Available Software was presented in Volume I of this book series. The abstract is reprinted below.

This chapter identifies a variety of air quality models and model-related products and services that have been developed by government environmental and meteorological agencies, universities, non-profit groups and for-profit companies. Many of the models are available free of charge. Others are available for a fee. Model-related products and services include preprocessors, visualization software, emission factor methodologies, meteorological data, terrain data and training programs. These models, products and services are available from a variety of sources including the World Wide Web.

Additional information on modeling software and other computer programs can be found in Chapter 21 of this Volume IV and Chapter 27 (Pre-Processing) of Volume III.

BRANK
P
e

Chapter 23

Available Databases

A chapter on Available Databases was presented in Volume I of this book series. The abstract is reprinted below.

There have been significant enhancements in the sophistication of regulatory dispersion models being developed for use in the United States, including those for local impacts from point sources (AERMOD) and multiple source impacts at ranges of 50 km and beyond (CALPUFF). Less well known, however, are the implications for modelers of the \$5 billion investment by the National Weather Service over the last decade in the national meteorological infrastructure. There have been dramatic enhancements in the quantity and quality of meteorological data and analyses, such as those generated by the National Centers for Environmental Prediction (NCEP). As an example, the Rapid Update Cycle (RUC2) generates nationwide, hourly, physically consistent mesoscale analyses on a 20 km mesh with 50 vertical layers. RUC2 produces gridded meteorological fields suitable as direct input into CALMET for simulations using a relatively coarse horizontal mesh. Alternately, RUC2 would serve as ideal initializing fields for finer mesh prognostic model runs to be used as CALPUFF input. The options now becoming available to the air quality community to employ greatly enhanced meteorological inputs to regulatory models are presented.

Additional material can be found in Chapter 27 (Pre-Processing) of Volume III and Chapter 21 of this Volume IV.

For additional information, the reader can visit:

- Human Exposure Modeling Databases to Support Exposure Modeling
http://www.epa.gov/ttn/fera/human_data.html

- The GAIA Model Base Air Quality Simulation Models
<http://www.ess.co.at/GAIA/models/aria.htm>
- Database Tools for Modeling Emissions and Control of Air Pollutants from Consumer Products, Cooking, and Combustion
<http://www.bfrl.nist.gov/IAQanalysis/docs/NISTIR%207364.pdf>
- Databases in Europe
<http://air-climate.eionet.europa.eu/databases>
- Databases and Software
<http://www.epa.gov/epahome/data.html>
- Using GIS for Air Quality Management and Air Pollution Assessment: A Bibliography
<http://gisandscience.com/2009/10/29/using-gis-for-air-quality-management-and-air-pollution-assessment-a-bibliography/>
- SPECIATE - EPA's Database of Speciated Emission Profiles
http://www.cmascenter.org/conference/2009/abstracts/mobley_whats_new_2009.pdf
- Data Finder Provides an Initial Collection of EPA's Data Sources
<http://www.epa.gov/data/>
- Global Indoor Air Pollution Database
http://www.who.int/indoorair/health_impacts/databases_iap/en/index.html
- AirBase: Public Air Quality Database
<http://www.eea.europa.eu/themes/air/airbase>
- Search Engines / Databases
<http://www.arb.ca.gov/html/databases.htm>
- Climate and Atmosphere - Searchable Database
http://earthtrends.wri.org/searchable_db/index.php?theme=3
- UK National Air Quality Archive
<http://www.airquality.co.uk/>

Chapter 24

Physical Modeling of Air Pollution

A chapter titled “Wind Tunnel Modeling of Pollutant Dispersion” was enclosed as Chapter 24A Volume III of this book series. The abstract is reprinted below.

This chapter provides a brief historical overview of wind tunnel modeling of pollutant dispersion. The theoretical basis behind wind tunnel modeling and why it can provide an accurate simulation of atmospheric flows and dispersion is discussed. In addition, typical methods used for setting up wind tunnel simulations are also discussed. Some example applications of wind tunnel modeling are discussed, such as, determining “Equivalent Building Dimensions” for input into EPA dispersion models; determining “Good Engineering Practice” stack height, numerical modeling testing and validation; and site specific concentration estimates.

For additional information, the reader can visit:

- Numerical and Physical Modeling of Bluff Body Flow and Dispersion in Urban Street Canyons
<http://www.engr.colostate.edu/~meroney/PapersPDF/CEP99-00-3.pdf>
- Air Pollution Dispersion Studies through Environmental Wind Tunnel
<http://nopr.niscair.res.in/bitstream/123456789/5146/1/JSIR%2064%288%29%20549-559.pdf>
- Wind Tunnel and Numerical Simulation of Pollution Dispersion: A Hybrid Approach
<http://www.engr.colostate.edu/~meroney/projects/ASI%20Crocher%20Paper%20Final.pdf>
- Evaluation of Air Quality for Residential Area by Means of Wind Tunnel Tests
http://www.peutz.de/pdf/ITM_Leipzig_MISKAM.pdf

- Meteorological Wind Tunnel
http://www.epa.gov/facilities_network/windtunnel.html
- Smog Chambers Experiments of Urban Mixtures
<http://www.unc.edu/~doylem/documents/AAAR-PM/AAAR%20poster%20rev.pdf>
- Paul Scherrer Institut - Laboratory of Atmospheric Chemistry
http://lac.web.psi.ch/LAC_Tools/smogchamber/smogchamber.html
- Secondary Organic Aerosol Formation in a Smog Chamber
<http://iccpa.lbl.gov/presentations/iccpa-08-baltensperger.pdf>
- Dispersion in Atmospheric Convective Boundary Layer with Wind Shears: from Laboratory Models to Complex Simulation Studies
<http://ams.confex.com/ams/pdfpapers/79999.pdf>

Rappolt, T.J. and S.L. Kerrin 2010. *Measurement of Atmospheric Dispersion Using Gaseous Tracers*. Chapter 25 of *AIR QUALITY MODELING – Theories, Methodologies, Computational Techniques, and Available Databases and Software. Vol. IV – Advances and Updates* (P. Zannetti, Editor). Published by The EnviroComp Institute (<http://www.envirocomp.org/>) and The Air and Waste Management Association (<http://www.awma.org/>).

Chapter 25

Measurement of Atmospheric Dispersion Using Gaseous Tracers

Thomas J. Rappolt ⁽¹⁾ and Stephen L. Kerrin ⁽²⁾

⁽¹⁾ *SCS Tracer Environmental*³, San Marcos, CA (USA)
trappolt@scsengineers.com

⁽²⁾ *SCS Tracer Environmental*, San Marcos, CA (USA)
skerrin@scsengineers.com

Abstract: The use of tracer studies can be a very valuable tool when establishing a model for atmospheric dispersion assessment. Tracer studies are the best and most accurate way to validate and/or verify existing models as well as support the design of a new model. Therefore, the basic components of a tracer study are presented. They touch on equipment as well as certain techniques for performing tracer studies. Then, the dissemination methods of various tracers are addressed along with the collection and analysis for the various tracers. Finally, issues regarding quality control and quality assurance, such as random sampling, are investigated.

Key Words: atmospheric tracers, electron capture detector (ECD), sulfur hexafluoride (SF₆), Perfluorocarbon (PFC), dissemination, Fickian diffusion, quality assurance, quality control, model validation, dispersion modeling, calibration, surrogate, chromatograph.

1 Introduction to Atmospheric Tracer Studies

In the modern industrialized world, thorough study of the transport and fate of airborne chemical vapors has become necessary to fully understand the effects of these chemicals on human health and the environment, both acutely and with prolonged exposure. In circumstances where chemical species of interest cannot

³ SCS Tracer Environmental is a separate operating group within Sterns, Conrad, and Schmidt Consulting Engineers, Inc. (SCS Engineers, Inc.) as a result of a merger between Tracer Environmental Sciences and Technologies, Inc. (Tracer ES&T) and SCS Engineers on 9/30/2009.

be directly measured (such as when the source no longer exists or has been substantially modified) or must be simulated (prior to constructing an industrial facility, for example) chemical surrogates known as tracers are employed to simulate emissions. Tracers are also utilized to determine the impacts of a single existing emission source where multiple sources may exist. Sample gathering at various receptors in the area of interest followed by quantitative analysis of samples for the selected tracer provides direct measurement of dispersive dilution of emissions from a subject source. Additionally, quantitative tracer dispersion data provides a valuable tool with which to validate and “fine tune” both diagnostic and prognostic atmospheric dispersion models. The scope of application for tracers ranges from microscale, such as characterizing building ventilation systems, to documenting atmospheric transport of pollutants across continents.

Ideally, a suitable tracer would be a chemical species that does not normally occur or is minimally present in the environment to be characterized. It should exhibit physical characteristics similar enough to the chemical(s) of interest to behave as a faithful transport surrogate. Further, an ideal tracer would possess no negative health or environmental characteristics. In addition to its uniqueness in the environment, it should be amenable to unequivocal identification and quantification by accepted analytical practice.

2 Historical Perspective and Application of Atmospheric Tracers⁴

As a result of early above-ground nuclear weapons testing, the long-range effects of atmospheric transport and diffusion of airborne particles became of interest to the federal government as early as the 1940's. In the 1950's it was realized that radioactive fallout was an exceedingly complex issue, involving extremely long range transport through the atmosphere and affecting all aspects of the environment (NOAA, 2004). Investigations into the physics of atmospheric transport began to appear in the literature in the late 1950s (Cramer, et al., 1958; Haugen, 1959).

The invention of the electron capture detector (ECD) (Lovelock and Lipsky, 1960) arguably helped usher in the age of environmentalism with its selective sensitivity to pesticides and CFCs (Simmonds et al., 1973). This invention also opened the door to the use of sulfur hexafluoride as a conservative gaseous tracer with limits of detectability in the previously unattainable parts-per-trillion by volume (pptv) range (Turk et al., 1968; Dietz and Cote, 1973). Increasing background levels of SF₆ (Maiss and Levin, 1994) and its identification as a greenhouse gas have prompted the development of methods to utilize fully

⁴ Additional data and information on past tracer studies can be found at http://www.jsirwin.com/Tracer_Data.html

perfluorinated alkyl-substituted cycloalkanes (perfluorocarbons or PFCs) as atmospheric tracers (Lovelock and Ferber, 1982; Dietz, 1987; D'Ottavio et al., 1986; Lagomarsino, 1996). It is likely that the use of SF₆ as an atmospheric tracer will be phased out in the near future due to environmental concerns arising from its high global warming potential (GWP). PFCs exhibit extremely low global background and are detectable at concentrations of parts per quadrillion (ppqv) by volume. Additionally they are chemically inert, thermally stable and non-toxic to the extent that they have been investigated as blood plasma substitutes. (Dagani, 1982).

Perfluorocarbons are the tracer of choice for most atmospheric dispersion studies where a combination of sensitivity and/or the need to simultaneously tag multiple sources is required. Sulfur hexafluoride is still employed for studies over short distances or inside buildings where multiple sources are not required. Short-range tracer experiments (such as for nuisance odor complaint resolution) are frequently performed to define local source-receptor relationships as well as to characterize building ventilation systems. Additionally, PFC tracers have been used to locate leaks in underground storage tanks and underground cabling (Dietz, 1992; Ghafurian et al., 1999). Longer-range transport studies have been carried out in urban areas (Draxler, 1989; Britter et al., 2000; Cooke et al., 2001), within geographical regions (Ferber et al., 1986; Green, 1999; Kim et al., 2002) and across continents (Draxler et al., 1991; Nodop et al., 1998). While the global background of PFCs is extremely low, their global warming potential is extremely high (10^3 to 10^4 times that of CO₂). Their long estimated atmospheric lifetimes of 3,000 to 50,000 years (WMO, 1999) have led to their being called the “immortal molecules.” Thus, the future may see the imposition of limitations on their use.

3 Typical Components of a Tracer Study

As with any field project, attention to details, adequate planning, and competent personnel provide for successful execution. To best plan, manage and execute an atmospheric tracer study, it is advantageous to divide the effort into logical technical components. These technical components include:

- Dissemination Methods
- Sampling Systems
- Analytical Laboratory Equipment and Procedures
- Data Processing
- Quality Assurance
- Support Meteorological Measurements

Integrated into these basic technical components are the management steps necessary to properly implement a study. The underlining aspects contributing to the management of tracer studies include:

- Technical Study Design
- Logistical Considerations

- Preparation Phases
- Field Operations
- Quality Control and Quality Assurance
- Budget Control and Project Timeline

Tracer studies require a somewhat different approach than most ambient air monitoring exercises. The challenge begins with the design, such that one properly estimates the correct mass of tracer to be released. This determination may need the assistance of a model, but if the environment in which the test is to be conducted is not easily represented by a model, then other intuitive methods must be used to properly specify the tracer release. Hence, experience plays a substantial role in the proper planning of a tracer experiment. A second challenge arises in designing a receptor network that adequately intercepts the tracer plume to provide appropriate data density within the targeted concentration range. Frequently, scientists with good instrumentation and monitoring skills fail at executing tracer studies because they are inexperienced in mentally visualizing the simulated plume and do not fully understand the limits of their analytical capability. In such instances, the downwind receptor network of samplers is inadequate to capture the plume structure with sufficient data density to provide meaningful and useful results. Additionally, the same inexperience can result in over estimating the tracer release rate, which frequently proves to be a very costly mistake both in terms of tracer released, and difficulty analyzing field samples.

It cannot be over-emphasized that exceptional attention is required to the subject of maintaining separation between dissemination equipment and/or personnel and sampling equipment and/or personnel. When dealing with picoliter and femtoliter range analytical sensitivity it takes little contamination to render samples useless. Contamination of samples is the most common mistake made by those who are inexperienced in conducting tracer studies.

3.1 Tracer Dissemination

Dissemination of tracers consists of two aspects. First, a dissemination rate must be estimated that will provide a concentration at the center of the sampling grid that will be within the sensitivity range of the analytical method used to quantify field samples. This aspect of program design also has economic implications as the release of excessive amounts of tracer equates to higher than necessary program cost.

Second, a means must be provided to ensure that the dissemination rate is accurately controlled and constant throughout the dissemination period. The measurement and recording of actual dissemination rate of tracer chemicals is vital to a successful tracer study and adequate attention needs to be given to these aspects.

Third, it is highly recommend that any equipment, tools, personnel and other test related items that are involved with the dissemination of the tracer chemicals must not come near the sampling and analytical systems of the same experiment.

3.1.1 Dissemination Rate Estimation

Determining the rate at which gaseous tracers will be released in a specific test, generally requires the application of a dispersion model. Using a model to estimate results that will be used to validate that model may seem contradictory. However, model results allow determination of an approximate release rate of the tracer gas such that the expected downwind impacts (from the closest receptor to the most distant) will lie within a targeted concentration range appropriate for the analytical method used. For example, if the analytical detection range is 1 part per trillion to 10 parts per billion, a tracer release rate that provides an approximate 100 pptv concentration at the center of the receptor grid is recommended. This level provides 2 decades of latitude (higher or lower) in the actual concentration measurement, which is generally ample to capture any variability in model prediction.

It is also helpful to work in X/Q space since it is well known that most ambient dispersion situations resides between 1×10^{-4} to 1×10^{-8} sec/m². In very near-field dispersion experiments, X/Q values greater than 1×10^{-4} sec/m² will need to be considered and very long range studies likely involve X/Q values less than 1×10^{-8} sec/m². The ability to successfully quantify this entire spectrum of dispersion ranges depends upon the ability to expand the active range of detection in the tracer analytical capability. Additionally, the ability to reach very low detection levels, enables one to release less tracer chemicals, which provides not only a cost benefit to the study budget, it limits any seen and unforeseen environmental impact.

3.1.2 Dissemination Methods

It is important that tracer vapor be thoroughly mixed either into the ambient air or into an air stream for delivery to a point source such as a vent or a stack. The methods employed for SF₆ differ from those used for the PFCs due to their physical characteristics.

Sulfur hexafluoride is a liquid under pressure as it is normally encountered in steel cylinders. The pressure of gaseous SF₆ above the liquid varies with ambient temperature but is generally between 100 psig and 180 psig. The typical method for dissemination of SF₆ is to control the release of the pressurized vapor by means of a suitably calibrated mass flow controller. This works well with a single cylinder for release rates up to about 5 kg/hour in ambient temperatures warmer than approximately 5-10 degrees Celsius. At higher flows or lower temperatures, the cooling of the cylinder caused by the rapid vaporization of the liquid reduces cylinder pressure, often to a point below that at which the mass flow controller

will operate properly. For release rates greater than 5 kg/hour, multiple cylinders are frequently connected to a manifold to reduce cooling in individual cylinders. In extreme cases, electric heating jackets may be required to warm the cylinder contents and maintain cylinder pressure.

The PFCs are generally high vapor pressure liquids. As such, different dissemination techniques are required than are used for SF₆. Dissemination of PFCs requires that the liquid material be vaporized either through direct heating of the liquid or mechanically by the creation of rapidly evaporating micro-droplets. A peristaltic pump is typically used in both approaches to deliver a constant volumetric flow of PFC.

The liquid flow can be thermally vaporized by introducing it to a heated plenum where the vapor is entrained in an air stream that is piped to the desired release location. Alternately, if an ambient release is required, simply dripping the liquid on a heated surface is generally sufficient.

Mechanical means may also be utilized, in ambient releases, to create micro-droplets of the liquid that rapidly evaporate. This can be accomplished by several methods including sonic nebulization or by dripping the liquid PF onto a rapidly rotating serrated disk.

A mechanical balance or strain gauge device is frequently paired with data recording equipment to provide a backup record of dissemination rate and flow history.

3.2 Sampling Techniques

Analyzers that provide realtime concentration data for SF₆ have appeared over the years based on a design by Simmonds and Lovelock (Simmonds 1976). At least one commercial version (Sciencetech TGA-4000) was available. In their various incarnations these analyzers were expensive and had a reputation for being somewhat temperamental in operation. Since they relied on a stoichiometric reduction of atmospheric oxygen, variations in ambient O₂ concentration with altitude or within confined spaces, for example, resulted in considerable signal drift. Careful attention to flow control and electronic signal processing yielded individual instruments that performed nearer expectations but still possessed unique operating characteristics and performance.

Most atmospheric dispersion studies utilize a fixed network of sampling equipment to acquire time-averaged samples over averaging periods ranging from minutes to several hours. Selection of the averaging period is generally based on the downwind distance at which samples are to be obtained with longer averaging times being employed at greater distances. Shorter averaging times may be advantageous with shorter plume fetches or where it is desirable to characterize plume characteristics such as meander.

For field sampling of SF₆ or PFC, sufficient testing should be conducted to ensure that the sampling systems do not retain a history of past contact of tracer laden air and/or are unable to retain a valid sample over the storage time between sampling and analysis. It is extremely important that the components (tubing, valves, pumps, etc.) of the sampling system not have the inherent capability of adsorbing the tracer chemicals. It is equally important that the materials selected for sample containers not allow permeation of the tracer molecules, thus affecting the tracer concentration over time. Prior to deployment in to the field, all sample containers should be flushed with ultra-zero air to ensure that no contamination is present in any sample containers. Ideally, the final flush of each sample container would be analyzed for contamination but, practically, random analysis is generally sufficient.

3.2.1 Sulfur Hexafluoride Sampling

SF₆ samples are generally collected in inert bags made of Tedlar[®]. While available in capacities ranging from less than one liter to more than 10 liters, sample analysis requires less than 1 ml of sample (Section 3.3). Thus, the capacity used will be dictated by the characteristics of the sample acquisition apparatus.

The most common portable sampler for SF₆ contains an air pump, valves, and control electronics to obtain multiple samples in a single container. These samplers are generally battery-operated portable devices capable of being programmed for start time, sample duration and sample volume. Samples represent time-averaged concentration over the selected sample duration. Managing the duty cycle of a fixed flow rate pump generally controls sample volume.

A second type of sampler (commonly called a “lung” sampler) consists of a single sample bag mounted in a sealed enclosure whose inlet is connected to ambient air. A pump draws a vacuum on the sealed chamber expanding the sample bag and drawing sample in. The evacuation flow rate can be quite rapid making this method most useful when obtaining nearly instantaneous samples such as those required in nuisance odor studies.

Variations on these methods have appeared over the years and, for example, have utilized disposable hypodermic syringes instead of Tedlar[®] bags.

3.2.2 Perfluorocarbon Sampling

The extreme sensitivity that PFCs offer is due to their ability to be adsorbed onto suitable sorbent material such as carbonaceous molecular sieve. Thus, several liters of sample can be captured either as a field sample directly on sorbent tubes or in Tedlar[®] bags whose contents are concentrated onto a specially designed enrichment “trap” connected to the inlet of the laboratory gas chromatograph. The

large volume of sample provides an effective increase in sensitivity of a thousand fold or more.

Bag sampling utilizes the same equipment and procedures as for SF₆ described above. Sorbent tube samplers can be either active where a pump draws air through the tube or passive where Fickian diffusion provides the “pumping.” In either approach, the amount of air sampled must be known in order to calculate the concentration of PFC. This can be done in the mechanically pumped version by controlling the flow rate. In the passive sampling approach, a naturally occurring universally distributed chemical species may be used as a marker to calculate sample volume.

3.3 Analytical Methods

Analysis of samples returned from the field is performed by gas chromatography using an electron capture detector (ECD). The ECD exhibits extreme sensitivity and selectivity to halogenated and perfluorinated compounds. Two different sample introduction methods and gas chromatographic configurations are used for analysis of SF₆ and perfluorocarbon tracers. Both methods employ digital data systems to both record and quantify the chromatographic peaks. There are many such systems available commercially both as integral parts of a chromatography system or as after-market devices able to be used with many different gas chromatographs.

3.3.1 Sulfur Hexafluoride Analysis

Analysis of samples containing SF₆ is performed using a fixed-volume sample valve to introduce the sample to the chromatographic column where the SF₆ is separated from oxygen and (depending on the carrier gas used) nitrogen. As the separated components emerge from the column, they enter the ECD where they cause a change in its operating current. This change is amplified and conditioned and the resulting electronic signal processed by a chromatographic data system. A typical chromatogram for SF₆ is presented in Figure 1.

3.3.2 Perfluorocarbon Analysis

The successful use of PFCs as atmospheric tracers is due to both their low atmospheric background concentrations and their amenability to detection at low concentrations by electron capture gas chromatography (Simmonds et al., 1976; DeBortoli and Pecchio, 1985; Lagomarsino, 1996). Direct injection of a sample, as previously described for SF₆, would realize detectability in the low pptv range. Detection limits may be significantly enhanced by utilizing sample enrichment (D’Ottavio et al., 1986; Lagomarsino, 1996).

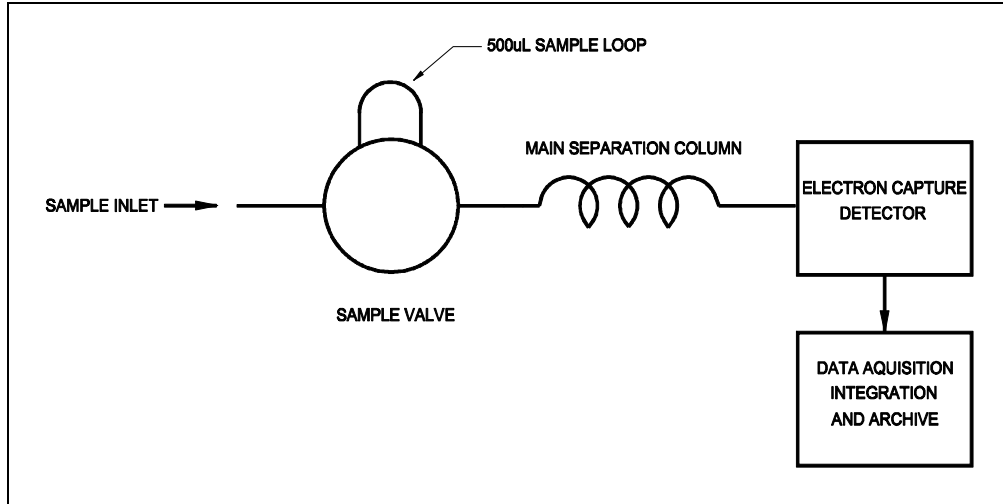
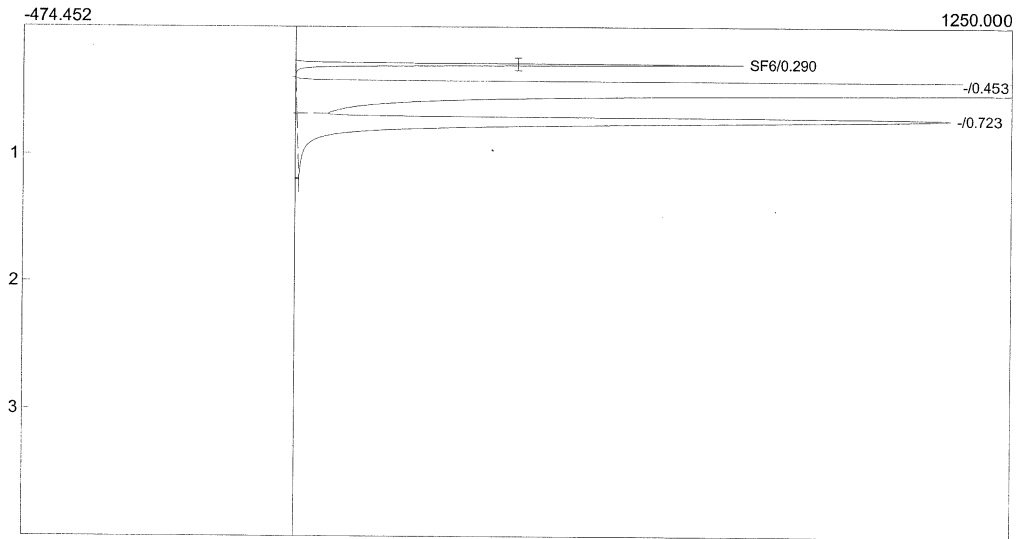


Figure 1. SF₆ Gas Chromatograph Configuration.

Lab name: Tracer ES&T
 Analysis date: 03/31/2005 13:43:32
 Method: 500 uL sample loop
 Description: CHANNEL 1
 Column: 5A MS
 Carrier: P5 @ 35 ml/min
 Data file: SF6-504-1.CHR (c:\BHHS_DATA\sf6\)
 Sample: SF6
 Comments:
 Temperature program:

Init temp	Hold	Ramp	Final temp
-----------	------	------	------------



Component	Retention	Area	Height	External	Units
SF6	0.290	880.9749	780.748	727.8875	
		880.9749		727.8875	

Figure 2. SF₆ Chromatogram.

A recently developed technique allows detection at the sub-ppqv level (Simmonds et al., 2002). Most perfluorocarbon based tracer studies employ sample enrichment techniques in order to optimize the amount of tracer materials needed to perform the study. This enhancement technique can result in substantial savings in project costs. Figure 3 presents a block diagram of a basic perfluorocarbon gas chromatograph. For analysis of samples taken in, for instance, Tedlar[®] bags, a controlled volume of sampled air is drawn through an adsorbent trap by a vacuum pump. The total volume sampled is determined by the setpoint of a mass flow controller and a fixed time interval. Perfluorocarbons (as well as other compounds) are adsorbed onto the trap. Several liters of sample may be concentrated in this manner. Returning air to the laboratory for concentration has the advantage of allowing replicate analysis of a sample either for quality assurance purposes or if the need to re-analyze a sample occurs for any reason.

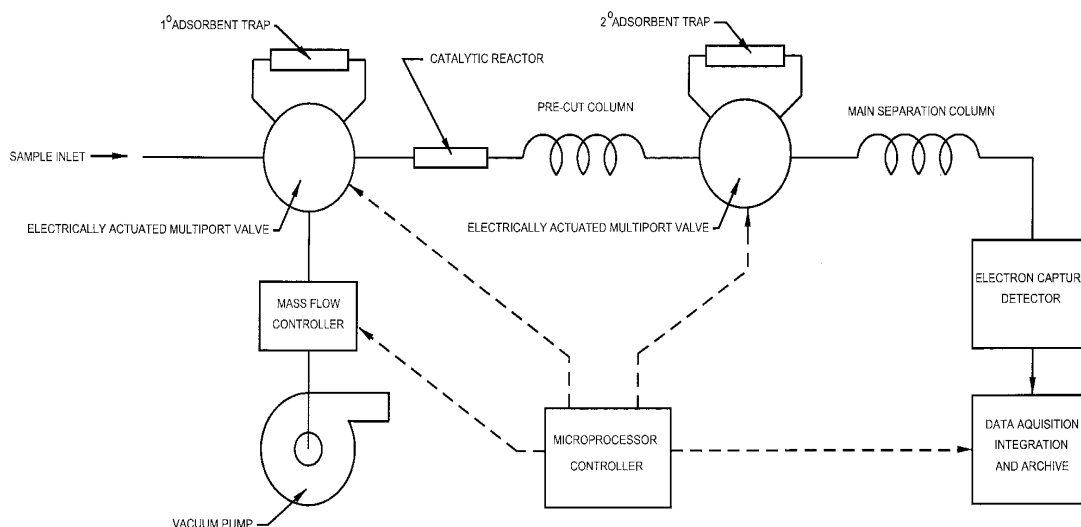


Figure 3. Basic Perfluorocarbon Gas Chromatograph Block Diagram

In the case of samples that have been obtained on sorbent tubes, the chromatograph is configured to allow the sorbent tubes to be connected in the primary trap loop. Sampling devices are available for the inlet of the gas chromatograph that allows several sorbent tubes to be loaded and analyzed under automatic control.

In either method, the primary trap now contains both the desired PFCs and other potentially interfering compounds such as chlorofluorocarbons (CFCs). The trap is rapidly heated to desorb the adsorbed material and the resultant mixture of chemical species is swept by carrier gas through a catalytic reactor where all compounds other than the stable PFCs are destroyed. To provide further isolation of the desired components, the sample passes through a short chromatographic column to a secondary adsorbent trap. The timing of valve switching is such that

the flow to the secondary trap ceases after the last tracer of interest emerges from the pre-column. Since all interfering species have been destroyed the secondary trap now contains only the PFCs of interest. This trap is then thermally desorbed onto the analytical column and finally to the ECD.

Figure 4 provides an example of a chromatogram for selected PFCs. It should be noted that this chromatogram was generated using a packed column and provides incomplete resolution of the isomers of perfluorodimethylcyclohexane (PDCH) and perfluorotrimethylcyclohexane (PTCH). This was acceptable for this study and provided high sample throughput. Separation of the individual isomers of PDCH requires an appropriate capillary column.

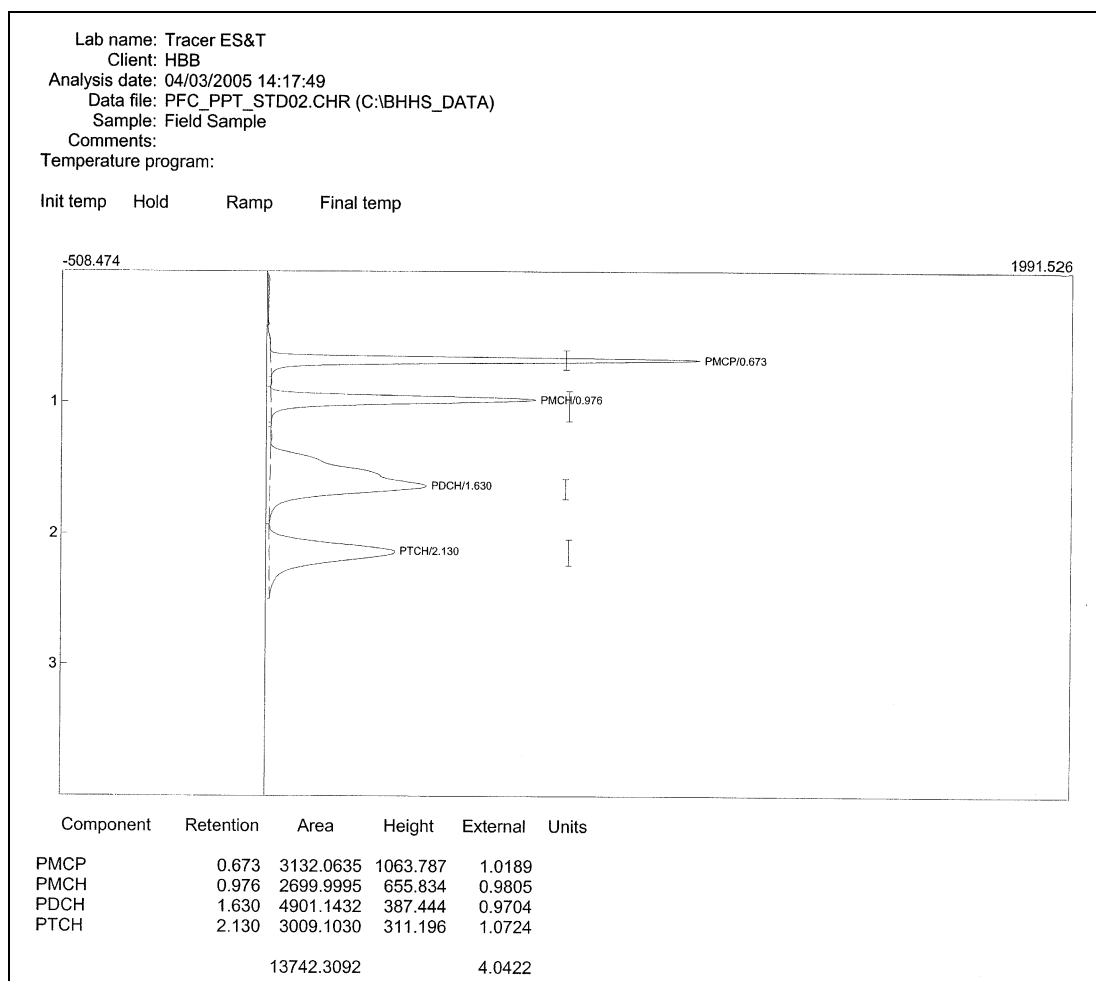


Figure 4. PFC Chromatogram

3.4 Meteorological Measurements

Most tracer dissemination studies, especially those in support of numerical modeling, can require a large base of field meteorological data for interpretation of results. Depending upon the specific model being validated and/or confirmed

by way of a tracer study, several meteorological parameters must be measured and recorded. The underlying requirement is to obtain enough meteorological data to reasonably enable the reconstruction of wind field conditions coincident with each test trial on a time scale that is at least equivalent to the time averaging used to define the tracer concentration measurements. For example, if the tracer measurements are reported on a 1-hour averaging period, then valid meteorological measurements should have similar 1-hour averages or less. Meteorological sensors should meet EPA-PSD monitoring guidelines. This generally requires that all support wind and temperature sensors must be operated at a minimum of 1 Hz sampling frequency to obtain valid and comparable time averages. Depending upon the complexity of the environment in which testing is conducted, multiple wind and stability sensors may be required to better define test condition micro-meteorology. At minimum, one system at the point of dissemination (if at a fixed position) and one or more systems situated at downwind tracer sampling locations are recommended. In highly complex terrain situations, vertical profiling of wind and temperature is desirable to gain a better understanding of the complex physical parameters affecting the transport mechanisms that drive the tracer plume.

4 Quality Assurance

As with any field measurement program, stringent quality assurance and quality control is required to ensure that the data collected is valid, defensible and accurate. All measurement methods should follow protocols that will ensure traceability to National Institute of Standards and Technology (NIST) standards and/or good engineering practices as called for by ASTM (D-4844, D-3614-07, E-741-00, E-2029-99, D-6196-03, for example). Additional standards and protocols would include Class 4 Protocol for weights and measures. Quality Control procedures should be applied to every aspect of field operations and laboratory analysis. This effort should include the obvious components such as tracer purity and calibration of release and sampling systems. Special attention is not lost on assuring that analytical results meet the highest degree of accuracy and precision attainable. Ample documentation must be collected to ensure the traceability of every data point collected. All samples must have complete chain of custody records and be analyzed in observance of regulatory accepted protocols to ensure precision and accuracy as well as reproducibility.

In addition to chain of custody, quality control efforts for sampling operations should include a sufficient number of duplicate field samples to ensure that the samples collected are accurate and reflective of local conditions. Additional blanks and spiked samples should be introduced into the sample queue as defined in the program QA plan. Replicate analysis of calibration standards during periodic performance checks will provide a measure of system variability. However, random replicate analysis of samples should be performed as a check on the entire analytical process for field samples.

Bulk calibration standards in pressurized cylinders should be produced to NIST traceable standards by a third party. The equipment and techniques required for production of precise dilutions of gases and liquid vapor to the low concentrations used in tracer studies are best left to specialty gas vendors. Certified mixtures obtained from these sources are used in-house to generate a response curve for the laboratory gas chromatograph. The frequency of calibration curve generation and periodic response checks will depend on the analytical backlog. For instance, a continual flow or samples from the field may require the laboratory to operate around the clock for extended periods. In this case, initial calibration curve generation with response check samples every 4 hours will indicate when calibration curve regeneration is required as set forth in the program plan. If samples are returned infrequently, once a week for example, it is advisable to develop a new calibration curve even if the GC had been operational but idle in the intervening period.

The organization that conducts the tracer field study should employ its own QA/QC Program for air measurement systems in general and for tracer projects specifically. Such a program must be designed to maintaining adequate Quality Control (QC) (routine internal checks) and Quality Assurance (QA) (external QC) to assure the provisions of data, which adheres to predefined requirements for completeness, precision, accuracy, representativeness, reproducibility, and comparability. Generally such a QA/QC program, whether it is authored specifically for tracer studies or generally for an ambient air monitoring program, must be tailored from principals found the US EPA's Quality Assurance Handbook for Air Pollution Measurements and define minimum criteria upon which acceptable data will be generated. Program components that are addressed by a QA/QC program include:

- Document Control
- Organization and Personnel Qualifications
- Quality Planning
- Personnel Training
- Pre-Test Preparations
- Material and Supplies Procurement
- Equipment Performance
- Preventative Maintenance
- Calibrations
- Configuration and Inventory Control
- Corrective Action
- Sample Collections and Chain of Custody
- Data Handling and Analysis
- Data Validation
- Audit Procedures (in field and in lab)
- Quality Reporting

5 Data Management Techniques for Tracer Studies

Accurate and accountable data management is essential to the success of any tracer study. Typically, a tracer study will generate thousands of data records that require verification and validation. Therefore a system of keeping track of every data point regarding a field sample is very important. When conducting a tracer study the following parameters are important relative to each air sample collected:

- Date and time
- Exact location
- Type of Tracer
- Tracer Concentration value
- Analytical and sampling support data (calibrations, etc.)
- Confirmed units of measure

Generally, there are also several accompanying data sets that merge with tracer data. These include tracer release rates (confirmed measured values) and coincident meteorological data. The common aspect of all these data sets is the time/date when the data was generated.

Spreadsheets are very useful in organizing data sets as we have found that database programs are somewhat overkill. Spreadsheets are highly transportable, flexible and allow for a variety of presentations and applications.

6 Applying Tracer Data to Validation of Model Performance

One of the primary purposes in conducting tracer field studies is to generate a unique database of field measurement data that can be applied to gauge the performance of candidate atmospheric dispersion models. It is well known that models, both proprietary and public domain, may not be capable of addressing all dispersion scenarios with similar accuracy and precision metrics. Often times, models are applied to situations and settings for which they were not designed and under such circumstances performance is unknown. Under such circumstances, scenario specific tracer data can be used to evaluate the performance of candidate models to enable the selection or validation of the appropriate model. When such evaluation is necessary, it is recommended that the analyst follow ASTM D6589-05 (Standard Guide for Statistical Evaluation of Atmospheric Dispersion Model Performance) (ASTM, 2005). Additional validation and calibration techniques are discussed by Canepa and Irwin (Canepa and Irwin 2005).

While there are many components to a model evaluation effort (ASTM, 2005), an important step is statistical evaluation with field data (usually defined to be tracer data). The basic approach is to compare field observations or measured data of selected chemicals (tracers) with modeled values of the same parameters under an identical scenario. The model that depicts the smallest bias and deviation with regard to field data is usually the best candidate. But other issues come into play,

such as comparisons with other models, particularly those models that are more widely accepted in the peer review process, scientific peer reviews, software reviews and sensitivity analysis. Information for all these evaluations provides for a good understanding on the limitations and applicability of the model of choice.

Conducting field studies in support of meaningful model evaluations, much uncertainty exists in defining how much data should be generated. Sampling or Estimation Theory (Walpole, 1972) is a useful tool in determining a valid sample size with which to represent a situation or scenario within a predefined confidence interval. We have found that to achieve the equivalent of a measured annual average within a 90% confidence interval for a selected meteorological scenario (wind-speed, stability, etc.) nearly 800 to 1,000 parameter-hours of tracer data may be required. Hence, with 30 samplers, this would mean approximately 25 to 30 hours of data (hourly averages) would be required. With lower confidence level requirements, such as 80% or less, substantially less data is needed (Larsen, 1971).

Sampling array design is another critical aspect of a tracer study design. Generally, a test is conducted with downwind arrays comprised of fixed arcs at select radial distances. In such test designs, there is uncertainty in defining how densely to place the samplers on each arc. We have found success in using a simple Gaussian model to determine the expected width of an instantaneous plume at each arc position under neutral to slightly stable conditions. It is then recommended to design the sampler spacing density such that at least 3 samplers will always be in the modeled plume, simultaneously. Furthermore, the angular range of the array on each arc should match the expected angular range of wind direction anticipated during the field-testing plus the angular width of the previously modeled plume. This will ensure that all samplers will probably be able to sample the tracer plume within the design sampling time interval.

References

ASTM, Designation: D 6589-05, 2005

Britter, R., Caton, F., DiSabatino, S., Cooke, K.M., Simmonds, P.G. Nickless, G., 2000. Proceeding of the Third Symposium on the Urban Environment, American Meteorological Society, pp. 30-31.

Cooke, K.M., Simmonds, P.G., Nickless, G., Caton, F., DiSabatino, S. Britter, R., 2001. Tracers and dispersion of gaseous pollutants within an urban canopy. Proceedings of the EUROTRAC-2-Symposium, 27-31 March 2000, Garmisch-Partenkirchen, DE.

Canepa, E. and J. Irwin. *Evaluation of Air Pollution Models*. Chapter 17 of AIR QUALITY MODELING –Theories, Methodologies, Computational Techniques and Available Databases and Software. Vol II – Advanced Topics (P. Zannetti, Editor). Published by the EnviroComp Institute (<http://www.envirocomp.org>) and the Air and Waste Management Association (<http://www.awma.org/>).

Cramer, H.E., Record, F.A., Vaughan, H.C., 1958. The study of the diffusion of bases or aerosols in the lower atmosphere. ARCRL-TR-58-239, The MIT Press, 133 pp.

Dagani, R., 1982. Synthetic blood research progressing. Chemical and Engineering News 60, 31-33.

DeBortoli, M., Pecchio, E.J., 1985. Sensitive determination of perfluorocarbon tracers in air by intermediate trapping and GC-ECD analysis. High Resolution Chromatographic Communications 8, 422-425.

Dietz, R.N., Cote, E.A., 1973. Tracing atmospheric pollutants by gas chromatographic determination of sulfur hexafluoride. Environmental Science and Technology 7, 338-342.

Dietz, R.N., 1987. Perfluorocarbon tracer technology. BNL 38847 Presented at the Ispra Courses Regional and Long-Range Transport of Air Pollution, Ispra, Italy.

Dietz, R. N. 1992. Tracer technology pinpoints underground cable leak. Brookhaven Bulletin 46, 47:1 – 47:2.

D'Ottavio, T.W., Goodrich, R. W., Dietz, R. N., 1986. Perfluorocarbon measurement using an automated dual-trap analyzer. Environmental Science and Technology 20, 100-104.

Draxler, R. R. Metropolitan Tracer Experiment (METREX) 1989. NOAA Technical Memoranda ERL ARL-140. Air Resources Laboratory, US Department of Commerce, Silver Spring, MD.

Draxler, R. R., Dietz, R. N., Lagomarsino, R. J., Start, G., 1991. Across North America tracer experiment (ANATEX): Sampling and analysis. Atmospheric Environment 12, 2815-2836.

EPA, *Ambient Monitoring Guidelines for Prevention of Significant Deterioration (PSD)*, EPA-450/4-87-007, 1987.

EPA, *Quality Assurance Handbook for Air Pollution Measurement Systems, Volume IV: Meteorological Measurements*, EPA-600/R-94/038d, March 1995.

Ferber, G.J., Heffter, J.L., Draxler, R.R., Lagomarsino, R.J., Dietz, R.N., Thomas, F.L., Benkovitz, C.L., 1986. Cross-Appalachian tracer experiment (CAPTEX'83) Final Report, NOAA Technical Memorandum, Environmental Research Laboratory, ARL-142.

Ghafurian, R., Dietz, R.N., Rodenbaugh, T., Dominguez, J., Tai, N., 1999. IEEE Transactions on Power Delivery 14, 18-22.

Green, M.C., 1999. The project mohave tracer study: study design, data quality, and overview of results. Atmospheric Environment 33, 1955-1968.

Haugen, D.A. (ed.) 1959. Project Prairie Grass, a field program in diffusion. Geophysical Research Papers 59, 673.

Kim, H., Yea, S., Ro, C. Lee, C. Jang, M., Lee, G., Yoo, E., Han, J., 2002. Determination of atmospheric perfluorocarbon background concentrations at the western coastal area of Korea. Bulletin of the Korean Chemical Society 23, 301-308.

Lagomarsino, R.L., 1996. An improved gas chromatographic method for the determination of perfluorocarbon tracers in the atmosphere. Journal of Chromatographic Science 34, 405-412.

Larsen, Ph.D., Ralph I., 1971. A Mathematical Model for Relating Air Quality Measurements to Air Quality Standards. Environmental Protection Agency, Research Triangle Park, NC.

Lovelock, J.E., Ferber, G.J., 1982. Exotic tracers for atmospheric studies. *Atmospheric Environment* 16 1467-1471.

Lovelock, J.E., Lipsky, S.R., 1960. *Journal of the American Chemical Society* 82, 431-433.

Maiss, M., Levin, I., 1994. Global increase of SF₆ observed in the atmosphere. *Geophysical Research Letters* 21, 569-572.

NOAA, 2004. History of the Air Resources Laboratory <http://www.arl.noaa.gov/history.html>.

Nodop, K., Connoly, R., Girardi, F., 1998. The field campaigns of the European tracer experiment (ETEX): overview and results. *Atmospheric Environment* 32, 4095-4108.

Simmonds, P.G., Kerrin, S.L. Lovelock, J.E., Shair, F.H., 1973. Distribution of atmospheric halocarbons in the air over the Los Angeles Basin. *Atmospheric Environment* 8, 209-216.

Simmonds, P.G., Lovelock, A.J., Lovelock, J.E., 1976. Continuous and ultrasensitive apparatus for the measurement of air-borne tracer substances. *Journal of Chromatography* 126, 3-9.

Simmonds, P.G., Grealley, B.R., Olivier, S., Nikless, G., Cooke, K.M., Dietz, R.N. 2002. The background atmospheric concentrations of cyclic perfluorocarbon tracers determined by negative ion-chemical ionization mass spectrometry. *Atmospheric Environment* 36, 2147-2156.

Turk, A., Edmonds, S.M., Mark, H.L., Collins, G.F., 1968. Sulfur hexafluoride as a gas-air tracer. *Environmental Science and Technology* 2, 44-48.

Walpole, Ronald E., Myers, Raymond H., 1972. *Probability and Statistics for Engineers and Scientists*. The Macmillan Company, New York, NY 10022.

World Meteorological Organization (WMO), Scientific assessment of ozone depletion, 1988.

Report 44, Global Ozone Research and Monitoring Project, Geneva, 1999.

BRANK
P
2000

Chapter 26

Air Quality Modeling: Pre-Processing and Post-Processing – An Update

A chapter on “Air Quality Modeling: Pre-Processing and Post-Processing” was enclosed as Chapter 26 in Volume III of this book series. The abstract is reprinted below.

Environmental scientists now have an abundance of tools and data readily available to conduct and visualize air quality modeling simulations. Examples of using current tools for preprocessing and post-processing in air quality modeling are discussed, along with sources of data and the increasingly important role of Geographic Information Systems (GIS) in post-processing and visualization of modeling results.

We enclose below a short update to this chapter prepared by the author.

1-minute and 5-minute ASOS data

Most major airports have an Automated Surface Observing System (ASOS)¹ that records weather conditions every minute. ASOS data from stations in the continental United States, Alaska, Hawaii, and Puerto Rico are available for downloading from year 2000 to present, and it is reported as 1-minute data² and 5-minute data³. One needs to know the call sign of a station to locate the correct files (e.g. "KSFO" for San Francisco). The availability of this high-resolution ASOS data means that air modelers now have an additional resource to

¹ <http://www.weather.gov/ost/asostech.html>

² <ftp://ftp.ncdc.noaa.gov/pub/data/asos-onemin/>

³ <ftp://ftp.ncdc.noaa.gov/pub/data/asos-fivemin/>

characterize winds for an entire hour. Documentation is available for the 1-minute⁴ and 5-minute⁵ ASOS data.

Updated Links

The following links have been updated in reference to Chapter 26 in Volume III:

- Footnote 18: change <http://www.worldgeodata.com/home.aspx> to <http://www.breeze-software.com/data/>
- Footnote 26: change <http://www.lsuagcenter.com/weather/> to <http://weather.lsuagcenter.com/>
- Footnote 28: change http://raob.fsl.noaa.gov/intl/fsl_format-new.cgi to http://www.esrl.noaa.gov/raobs/intl/fsl_format-new.cgi
- Footnote 29: change <http://raob.fsl.noaa.gov/> to <http://www.esrl.noaa.gov/>
- Footnote 31: change <http://www.worldgeodata.com/home.aspx> to <http://www.breeze-software.com/data/>
- Footnote 54: change http://edc.usgs.gov/guides/landsat_tm.html to http://eros.usgs.gov/#/Guides/landsat_tm
- Footnote 56: change <http://coweb.ecn.purdue.edu/~biehl/MultiSpec/> to <https://engineering.purdue.edu/~biehl/MultiSpec/>

⁴ <http://www1.ncdc.noaa.gov/pub/data/documentlibrary/tddoc/td6405.pdf>

⁵ <http://www1.ncdc.noaa.gov/pub/data/documentlibrary/tddoc/td6401.pdf>

Zannetti, P., 2010. *Air Quality Modeling Resources on the Web – An Update*. Chapter 27 of *AIR QUALITY MODELING - Theories, Methodologies, Computational Techniques, and Available Databases and Software. Vol. IV – Advances and Updates* (P. Zannetti, Editor). Published by The EnviroComp Institute (<http://www.envirocomp.org/>) and the Air & Waste Management Association (<http://www.awma.org/>).

Chapter 27

Air Quality Modeling Resources on the Web – An Update¹

Paolo Zannetti ⁽²⁾

⁽²⁾ *The EnviroComp Institute, Fremont, CA (USA)*
zannetti@envirocomp.org

Abstract: This chapter presents a list of web addresses of useful sites for scientists, engineers, and managers using or developing air quality models.

Key Words: Air quality modeling, Internet sites, regulatory models, available software, courses online.

1 Introduction

The Internet revolution during the last 15 years has caused enormous progress in sharing data and information worldwide. The resources available on the Web today are enormous, and it is practically unthinkable, for a scientist, to work without this tool. However, some problems still remain. For example, 1) it is not always easy to identify the best and most reliable sources of information; 2) important sites often change address; and 3) the enormous amount of information on the web sometimes provides a distraction more than a solid scientific support.

Nevertheless, the Internet revolution has changed scientists' lives - ways of operating, performing research and development studies. This has been particularly true for environmental sciences, in general, and air quality modeling, in particular.

¹ This chapter is an update of Chapter 27 in Volume III.

This chapter presents an update of a similar chapter presented in Volume III of this book series. It contains a semi-organized list of topics and Internet addresses that may be particularly useful to scientists, engineers, and managers using or developing air quality models. The list is certainly incomplete and should be regarded like a collection of examples, more than a comprehensive catalog; but in spite of its limitation, it represents a good starting point, especially for a researcher at the beginning or intermediate stage of his exploration of the world of air quality modeling.

Readers are encouraged to provide new Hyperlinks by contacting the author via email. All valuable suggestions will be included in possible future publications.

2 Regulatory Issues

Title: Air Dispersion Modeling

Owner: Minnesota Pollution Control Agency (MPCA)

Summary: Air quality dispersion modeling is a computer simulation that predicts air quality concentrations from various types of emission sources. For pollutants emitted through a stack, it considers the emission rate, stack height, stack diameter, and stack gas temperature and velocity, as well as the effect of nearby buildings and terrain. Other emission sources like vehicle traffic or wind erosion from storage piles are represented as 2-dimensional area sources or 3-dimensional volume sources.

Hyperlink:

<http://www.pca.state.mn.us/index.php/air/air-monitoring-and-reporting/air-emissions-and-monitoring/air-dispersion-modeling/air-dispersion-modeling.html?menuid=&missing=0&redirect=1>

Title: Dispersion Modeling

Owner: The Virginia Department of Environmental Quality

Summary: Dispersion modeling is generally associated with the construction permit application process and is used to predict the air quality impact of new or modified emission sources. Other uses of dispersion modeling include: analysis of monitored violations of the National Ambient Air Quality Standards (NAAQS), assistance in planning and the development of rules. The following information is provided as general guidance to help you through the air quality modeling process.

Hyperlink:

<http://www.deq.state.va.us/air/assessments/dispersion.html>

Title: Air Quality Modeling Guidelines

Owner: Utah Division of Air Quality (UDAQ)

Summary: Industry and control agencies have long expressed a need for consistency in the application of air quality models for regulatory purposes. This Utah Division of Air Quality (UDAQ) guideline document provides a common

basis for estimating the air quality concentrations used in assessing control strategies and developing emission limits.

Hyperlink:

http://www.airquality.utah.gov/Planning/Modeling/NSR_Permit_Modeling/Modguint.htm

Title: State of Montana Modeling Guideline for Air Quality Permit Applications

Owner: State of Montana

Summary: This Montana Modeling Guideline for Air Quality Permits (Guideline) presents current MDEQ modeling guidance for estimating impacts from stationary sources of air pollution. This document addresses modeling requirements for all sources requiring an Montana Air Quality Permit including: minor sources, major sources subject to the Prevention of Significant Deterioration (PSD) regulations, and sources located in non-attainment areas.

Hyperlink:

[http://deq.mt.gov/AirQuality/docs/MontanaModelingGuidelineForAirQualityPermits\(3\).pdf](http://deq.mt.gov/AirQuality/docs/MontanaModelingGuidelineForAirQualityPermits(3).pdf)

3 Books

Title: List of available books in Air Quality Modeling

Author(s): Several

Summary: Book list

Hyperlink:

<http://www.environmental-expert.com/publications.aspx?word=air%20quality%20modeling>

Title: Atmospheric dispersion modeling

Author(s): Several

Summary: Book list (bottom of web page)

Hyperlink:

http://en.wikipedia.org/wiki/Atmospheric_dispersion_modeling

4 Available Software

Title: BREEZE Software

Owner: Trinity Consultants

Summary: Environmental professionals use BREEZE software products worldwide to analyze the effects of air pollutant emissions and explosions. BREEZE is easy to learn and use because it adheres to Microsoft® standards for intuitive, uniform graphical user interfaces, and features standardized toolbars, views, menus, commands, and dialog boxes.

Hyperlink:

<http://www.breeze-software.com/default.aspx>

Title: Lakes Environmental Software

Owner: Lakes Environmental

Summary: Lakes Environmental is committed to supplying robust and easy-to-use software, training, and services to consulting companies, industry, governmental agencies, and academia. Since 1995, Lakes Environmental has been recognized internationally for its technologically advanced software and its exceptional expertise in the area of environmental science.

Hyperlink:

<http://www.weblakes.com/>

5 Dispersion Models

Title: Atmospheric dispersion modeling

Owner: Wikipedia

Summary: Atmospheric dispersion modeling is the mathematical simulation of how air pollutants disperse in the ambient atmosphere. It is performed with computer programs that solve the mathematical equations and algorithms, which simulate the pollutant dispersion. The dispersion models are used to estimate or to predict the downwind concentration of air pollutants or toxins emitted from sources such as industrial plants, vehicular traffic or accidental chemical releases.

Such models are important to governmental agencies tasked with protecting and managing the ambient air quality. The models are typically employed to determine whether existing or proposed new industrial facilities are or will be in compliance with the National Ambient Air Quality Standards (NAAQS) in the United States and other nations. The models also serve to assist in the design of effective control strategies to reduce emissions of harmful air pollutants.

Hyperlink:

http://en.wikipedia.org/wiki/Atmospheric_dispersion_modeling

Title: Air Dispersion Modeling

Owner: Google Directory

Summary: Directory

Hyperlink:

http://www.google.com/Top/Science/Environment/Air_Quality/Air_Dispersion_Modeling/

6 Photochemical Models

Title: CMAQ Science Documentation

Owner: US Environmental Protection Agency

Summary: Science Algorithms of the EPA Models-3 Community Multiscale Air Quality (CMAQ) Modeling System

Hyperlink:

<http://www.epa.gov/AMD/CMAQ/CMAQscienceDoc.html>

7 Receptor Models

Title: Receptor Modeling

Owner: US Environmental Protection Agency

Summary: Receptor models are mathematical or statistical procedures for identifying and quantifying the sources of air pollutants at a receptor location. Unlike photochemical and dispersion air quality models, receptor models do not use pollutant emissions, meteorological data and chemical transformation mechanisms to estimate the contribution of sources to receptor concentrations. Instead, receptor models use the chemical and physical characteristics of gases and particles measured at source and receptor to both identify the presence of and to quantify source contributions to receptor concentrations. These models are therefore a natural complement to other air quality models and are used as part of State Implementation Plans (SIPs) for identifying sources contributing to air quality problems. The EPA has developed the Chemical Mass Balance (CMB) and UNMIX models as well as the Positive Matrix Factorization (PMF) method for use in air quality management. CMB fully apportions receptor concentrations to chemically distinct source-types depending upon the source profile database, while UNMIX and PMF internally generate source profiles from the ambient data.

Hyperlink:

<http://www.epa.gov/scram001/receptorindex.htm>

8 Air Quality Forecast and Resources

Title: NOAA's National Weather Service Air Quality Forecast Guidance

Owner: National Oceanic and Atmospheric Administration

Summary: Maps show NOAA's National Weather Service Air Quality Forecast Guidance. Ozone is shown as 1-hour and 8-hour concentrations (in parts per billion or ppb), updated twice daily. Official Air Quality point forecasts, issued by state and local air quality forecasters, along with additional information on air quality can be found under EPA's AIRNow site. Surface and column-average concentrations of predicted smoke for large fires are displayed as 1-hour averages (in micrograms per cubic meter), updated each day. Fire locations are provided by NOAA / NESDIS' Hazard Mapping System. For further information, please visit NOAA's Air Resources Laboratory web site.

Hyperlink:

<http://www.nws.noaa.gov/aq/>

Title: Air Quality & Pollution by The Weather Channel

Owner: The Weather Channel

Summary: Your daily forecast for better health

Hyperlink:

<http://www.weather.com/activities/health/airquality/>

9 Visibility Modeling

Title: WRAP Regional Haze Air Quality and Visibility Modeling Results

Owner: WRAP Regional Modeling Center

Summary: Air quality and visibility modeling results are organized into 3 tables. Table 1 includes CMAQ results for the 2002 model performance evaluation (MPE) case and results for the 2002 Planning Case and the 2018 Base Case. Table 2 includes results for the CAMx MPE case and the PSAT source apportionment simulations. Table 3 includes other model sensitivity studies. Older model results (e.g., preliminary evaluation and test cases) are listed in the archive section.

Hyperlink:

<http://pah.cert.ucr.edu/aqm/308/cmaq.shtml>

Title: CALPUFF Visibility Modeling Protocol: MDU Heskett Unit 2 BART Analysis

Owner: Montana-Dakota Utilities Co. AECOM, Bismarck, North Dakota

Summary: The North Dakota Department of Health (NDDH) has conducted CALPUFF modeling for emission sources for all BART-eligible facilities in North Dakota. This study updates and refines the CALPUFF modeling for one of these facilities, Heskett Unit 2, which is owned and operated by Montana-Dakota Utilities Co. (MDU). Heskett Unit 1, operational in 1954, has a capacity of 40 MW and is not BART eligible since it was put into service before 1962. Unit 2, operational in 1963, has a capacity of 75 MW. Unit 2 was retrofitted to a fluidized-bed combustor in 1987, thus making it BART eligible.

Hyperlink:

http://www.ndhealth.gov/AQ/RegionalHaze/Regional%20Haze%20Link%20Documents/Appendix%20A/MDU%20BART%20Modeling%20Protocol_AECOM.PDF

10 Courses Online

Title: Lecture Series on Environmental Air Pollution by Prof. Mukesh Sharma, Department of Civil Engineering IIT Kanpur. (For more details on NPTEL visit <http://nptel.iitm.ac.in>)

Author(s): Prof. Mukesh Sharma

Summary: Several lessons available on YouTube, e.g.:

Hyperlink:

<http://www.youtube.com/watch?v=UyG4EL0BBJ0>

Table of Contents – Volume I¹

	Preface	xi
	About the Editor	xiii
	About the Publishers	xv
	About the Chapter Authors	xvii
1	The Problem – Air Pollution	1
	1 Our Natural Environment	1
	2 Air Pollution, Some Definitions	3
	3 Primary and Secondary Pollutants	4
	4 A Short History of Air Pollution Modeling	5
	5 Air Pollution Regulations	8
2	The Tool – Mathematical Modeling	13
	1 Why Air Quality Modeling	13
	2 Modeling Categorized	14
	3 Modeling the Atmosphere	19
	4 Modeling Alternatives	20
	5 Spatial and Temporal Scales	22
	6 Spatial and Temporal Resolution	23
	7 Uncertainty: Bias, Imprecision, and Variability	24
	8 Evaluation of Model Performance	25
	9 Data Needs	27
	10 Uses of Models	29
3	<i>Emission Modeling</i>	33
4	Air Pollution Meteorology	37
	1 Synoptic Meteorology	38
	2 Boundary-Layer Meteorology	61
5	<i>Meteorological Modeling</i>	101
6	Plume Rise	103
	1 Introduction	108
	2 Semi-Empirical Formulations	112
	3 Advanced Plume Rise Models	131
	4 Particle Models for Plume Rise	137
	5 Special Cases	157
7	<i>Gaussian Plume Models</i>	183

¹ Chapters in italics will be provided in subsequent volumes.

7A	Introduction to Gaussian Plume Models	185
1	Introduction	186
2	The Point Source in the Atmospheric Boundary Layer	186
3	The Atmospheric Boundary Layer	190
4	Dispersion in the Atmospheric Boundary Layer	193
5	Building Downwash	197
6	Terrain Treatment	199
7	Modifications to the Gaussian Framework	202
8	Concluding Remarks	206
8	<i>Gaussian Puff Models</i>	209
9	<i>Special Applications of Gaussian Models</i>	211
10	Eulerian Dispersion Models	213
1	Air Quality Modeling Methods	214
2	Eulerian Formulations	218
3	Analytical Solutions for Ideal Atmospheric Conditions	232
4	Numerical Solution Methods	237
5	Numerical Algorithms for Advection	244
6	Horizontal Diffusion Algorithm	251
7	Vertical Diffusion Algorithm	258
8	Simplified Eulerian Models	268
	Appendix A	272
	Appendix B	276
	Appendix C	279
11	<i>Lagrangian Particle Models</i>	293
12	<i>Atmospheric Transformations</i>	297
13	<i>Deposition Phenomena</i>	301
14	<i>Indoor Air Pollution Modeling</i>	303
15	<i>Modeling of Adverse Effects</i>	305
16	<i>Statistical Modeling</i>	307
17	<i>Evaluation of Air Pollution Models</i>	309
18	<i>Regulatory Air Quality Models</i>	311
19	Case Studies – Air Pollution Modeling at Local, Regional, Continental, and Global Scales	313
1	List of Case Studies	314
2	Additional Information on Case Studies Relevant to Air Pollution Modeling/Simulation	323

20	The Future of Air Pollution Modeling	325
	1 Processor Technology and Air Pollution Modeling	325
	2 Comprehensive Modeling Systems (CMS)	330
21	Active Groups in Air Pollution Modeling	355
	1 List of Active Groups	356
	2 Additional Information on Groups Working on Air Pollution Modeling Issues	360
22	Available Software	363
	1 Short-Range Models	366
	2 Urban and Regional Photochemical Models	380
	3 Long-Range Transport Models for Acid Deposition, Visibility Impairment and Complex Terrain	387
	4 Emergency Release and Dense Gas Models	394
	5 Meteorological Models	406
23	Available Databases	409
	1 Overview	409
	2 The Challenges	411
	3 Characteristics of Weather Data Sets	413
	4 NCEP Gridded Data Products	414
	5 Data Archival	416
	6 Reanalysis Techniques	418
	7 Mesoscale Prognostic Models	421
	8 Future Developments	423
	Authors' Index	427
	Subject Index	429

Blank Page

Table of Contents – Volume II¹

	Preface	xi
	About the Editor	xiii
	About the Publishers	xv
	About the Chapter Authors/Contributors for Volumes I and II	xvii
1	The Problem – Air Pollution	1
2	The Tool – Mathematical Modeling	3
3	<i>Emission Modeling</i>	5
4	Air Pollution Meteorology	7
5	Meteorological Modeling	9
	<i>5A Mesoscale Meteorological Modeling</i>	
	5B Large-Eddy Simulations of the Atmospheric Boundary Layer	11
	1 Introduction	11
	2 Theoretical Background	14
	3 The ABL Simulations	35
	4 Final Remarks	74
	<i>5C Computational Fluid Dynamics of Microscale Meteorological Flows</i>	
6	Plume Rise	83
7	Gaussian Plume Models	85
	7A Introduction to Gaussian Plume Models	
	<i>7B Simulation Algorithms in Gaussian Plume Models</i>	
8	<i>Gaussian Puff Models</i>	87
9	<i>Special Applications of Gaussian Models</i>	89

¹ Chapters in italics will be provided in subsequent volumes.

10	Eulerian Dispersion Models	91
11	Lagrangian Particle Models	93
1	The Lagrangian Approach	94
2	Lagrangian Stochastic Models (LSM)	95
3	LSM Applications	128
12	Atmospheric Transformations	163
1	Introduction	164
2	Gas-Phase Transformations	165
3	Heterogeneous and Aqueous Processes	172
4	Chemical Transformations Involved in the Formation of Air Toxics	179
5	Chemistry of the Upper Atmosphere: Stratospheric Ozone	183
6	Modeling of Gas-Phase Chemistry	193
7	Modeling of Heterogeneous and Aqueous Processes	199
8	Modeling of Reactive Plumes	207
9	Eulerian Models	212
13	Deposition Phenomena	233
1	Introduction	234
2	Different Deposition Parameterizations	240
3	Examples of Deposition Monitoring Programs	248
4	Examples of Air Quality Models	251
5	Sensitivity Analysis by Using the OPANA Model	257
14	Indoor Air Pollution Modeling	267
1	Introduction	270
2	Fluid Flow Fundamentals	274
3	Contaminant Sources	284
4	Design Criteria	293
5	Simple Modeling Techniques	297
6	Dynamics of Particles and Gases/Vapors	310
7	Numerical Modeling – CFD	322
15	Modeling of Adverse Effects	349
15A	Modeling of Health Risks Associated with Combustion Facility Emissions	351
1	Introduction	351
2	Case Study	354
	<i>15B Odor Modeling</i>	
	<i>15C Visibility Modeling</i>	
	<i>15D Ecological Adverse Effects</i>	
	<i>15E Global Issues</i>	

16	Statistical Modeling	395
16A	Air Quality Forecast and Alarm Systems	397
1	Introduction	398
2	Some Literature Results	401
3	Time Series Modelling	405
4	Building a Model for Air Quality Forecast	419
5	Identification of Statistical Air Quality Models	426
6	An Operational Decision Support System	437
7	Conclusions	445
	Appendix	453
16B	Receptor Models	455
1	Introduction	455
2	Receptor Model Types	457
3	Multivariate Receptor Model Mathematics	465
4	Model Input Measurements	469
5	Receptor Model Assumptions, Performance Measures, and Validation Procedures	482
6	Summary and Conclusions	491
17	Evaluation of Air Pollution Models	503
1	Introduction	503
2	Terminology	504
3	Background	507
4	Framework	510
5	Performance Measures	516
6	Model Evaluation	526
7	Statistical Model Evaluation	528
8	Model Quality Assurance	543
9	Guidelines for Model Evaluation: Towards Harmonization in Model Evaluation Methodology	547
18	A Historical Look at the Development of Regulatory Air Quality Models for the United States Environmental Protection Agency	557
1	Introduction	557
2	Legislative History of Air Pollution Modeling	561
3	Air Quality Models for Individual Industrial Facilities	566
4	The Development of Urban-Scale Long-Term Air Quality Models	575
5	Development of Tropospheric Chemistry Models	579
6	Current Issues and Trends in Model Development	598
19	Case Studies – Air Pollution Modeling at Local, Regional, Continental, and Global Scales	623
20	The Future of Air Pollution Modeling	625
21	Active Groups in Air Pollution Modeling	627
22	Available Software	629

23	Available Databases	631
24	<i>Physical Modeling of Air Pollution</i>	633
	Table of Contents – Volume I	635
	In Memoriam – Philip M. Roth	639
	Authors’/Contributors’ Index for Volumes I and II	641
	Subject Index for Volumes I and II	643

Table of Contents – Volume III¹

	Preface	xi
	About the Editor	xiii
	About the Publishers	xv
	About the Chapter Authors/Contributors	xvii
1	The Problem – Air Pollution	1
2	The Tool – Mathematical Modeling	3
3	Emissions Modeling and Inventory	5
1	Introduction to Emissions Inventory and Emissions Modeling	6
2	Overview of Inventories	10
3	Process-Level Codes Used in Emissions Inventories	18
4	Emissions Estimation Techniques	21
5	Characterization of Emissions	28
6	Characterization of Point Sources	37
7	Area Sources	66
8	Fire Emissions	90
9	Biogenic and Geogenic	92
10	Available Emissions Models	93
11	Estimating Emissions for Use in Air Quality Modeling	95
12	Estimating Emissions for Air Toxic Human Health Risk Assessment	97
13	Emissions Inventory Quality Control	100
14	Greenhouse Gases	102
15	Data Quality Objectives (DQO)	107
16	Data Gap Filling	108
17	Rule Effectiveness, Rule Penetration, and Control Efficiency	108
18	Pollutant Monitoring and Fuel Analysis Methodologies	110
19	Emissions Inventory Terms	116
4	Air Pollution Meteorology	127
5	Meteorological Modeling	129

¹ Chapters in italics will be provided in subsequent volumes.

5A	Meteorological Modeling for Air Quality Applications	131
1	Introduction	131
2	Modeling Approaches	137
3	Modeling Framework	142
4	Dynamical and Thermodynamical Processes	145
5	Physics Parameterizations	146
6	Model Numerics	160
7	Data Ingest	162
8	Model Verification and Validation	163
9	Symbols	164
10	List of Acronyms	165
5B	Large-Eddy Simulations of the Atmospheric Boundary Layer	
5C	Computational Fluid Dynamics of Microscale Meteorological Flows for Air Quality Applications	169
1	Introduction	170
2	Synopsis of CFD: the Math, Assumptions, and Availability	171
3	Simulating the Atmosphere in CFD	189
4	Industry Opinion and Guidelines	207
5	Validation and Verification	215
6	Conclusion	229
6	Plume Rise	235
7	Gaussian Plume Models	237
7A	Introduction to Gaussian Plume Models	
7B	Simulation Algorithms in Gaussian Plume Modeling	239
1	Introduction	239
2	Theoretical Background	241
3	Extending the Plume Formulation Beyond Point Sources	253
4	Removal Processes in Gaussian Plume Modeling	268
8	Gaussian Puff Modeling	281
1	Introduction	281
2	Theoretical Background	285
3	Puff Model Enhancements	301
9	<i>Special Applications of Gaussian Models</i>	315
10	Eulerian Dispersion Models	317
11	Lagrangian Particle Models	319
12	Atmospheric Transformations	321
13	Deposition Phenomena	323

14	Indoor Air Pollution Modeling	325
15	Modeling of Adverse Effects	327
15A	Modeling of Health Risks Associated with Combustion Facility Emissions	
15B	Odor Modeling	329
1	Modeling for Odors in the Atmosphere	329
2	Odor Measurement	330
3	Odor Modeling-Related Issues	333
4	Odor Criteria	338
5	Odor Models and Modeling Techniques	340
6	Summary	349
15C	Climate Change - An Introduction to Atmosphere-Ocean General Circulation Modeling	353
1	Introduction	353
2	AOGCM Formulation	355
3	Applications of AOGCMs	365
4	Future Development Needs and Further Readings	370
16	Statistical Modeling	379
16A	Air Quality Forecast and Alarm Systems	
16B	Receptor Models	
17	Evaluation of Air Pollution Models	381
18	Regulatory Modeling	383
18A	A Historical Look at the Development of Regulatory Air Quality Models for the United States Environmental Protection Agency	
19	Case Studies – Air Pollution Modeling at Local, Regional, Continental, and Global Scales	385
20	The Future of Air Pollution Modeling	387
21	Active Groups in Air Pollution Modeling	389
22	Available Software	391
23	Available Databases	393
24	Physical Modeling of Air Pollution	395

24A	Wind Tunnel Modeling of Pollutant Dispersion	397
1	Introduction	397
2	Theoretical Basis	399
3	Experimental Methods and Instrumentation	406
4	Typical Applications	418
25	<i>Tracer Studies</i>	433
26	Air Quality Modeling: Pre-Processing and Post-Processing	435
1	Introduction	435
2	Pre-Processing	436
3	Post-Processing	440
4	GIS in Air Quality Modeling	449
5	Summary	452
27	Air Quality Modeling Resources on the Web	453
1	Introduction	453
2	Regulatory Issues	454
3	Books	456
4	Available Software	456
5	Dispersion Models	459
6	Photochemical Models	460
7	Receptor Models	462
8	Air Quality Forecast and Resources	463
9	Visibility Modeling	464
10	Publications and Information Online	465
11	Courses Online	467
12	Case Studies	468
13	Resources and lists of References	470
14	Calculation Sites	471
	Table of Contents – Volume I	473
	Table of Contents – Volume II	477
	Authors’/Contributors’ Index for Volumes I, II and III	481
	Subject Index for Volumes I, II and III	485

Authors'/Contributors' Index¹ for Volumes I – IV

Achillas, Charisios	IV – p 303
Anfossi, Domenico.....	I – p 103 II – p 93
Bellasio, Roberto.....	IV – p 73
Bianconi, Roberto	IV – p 73
Builtjes, Peter J.H.....	I – p 1 IV – p 1
Buono, Maureen E.	III – p 329
Byun, Daewon W.....	I – p 213
Canepa, Elisa.....	I – p 103 II – p 503
Carrington, David B.	II – p 267
Chow, Judith C.....	II – p 455
Cochran, Brad	III – p397
Daly, Aaron.....	III – p 435
Degrazia, Gervásio.....	II – p 93
Delle Monache, Luca	IV – p 319
Diosey, Phyllis G.	III – p 329
Douros, John	IV – p 355
Eastman, Joseph L.....	I – p 409
Ferrero, Enrico	II – p 93
Finzi, Giovanna.....	II – p 397
Fragkou, Evangelia	IV – p 355
Freedman, Frank R.....	III – p 353
Georgieva, Emilia.....	IV – p 373
González Barras, Rosa M.....	II – p 233
Hibberd, Mark	II – p 93

¹ Readers are encouraged to use the CD-ROM version of the book for text searching.

Hurley, Peter	II – p 93
Irwin, John S.	II – p 503, 557
Johnson, Michael	IV – p 165
Keen, Cecil S.....	I – p 409
Kerrin, Stephen L.	IV – p 441
Lacser, Avraham	I – p 213
Lee, Russell	I – p 363
Luhar, Ashok.....	II – p 93
Lyons, Walter A.	I – p 409
Matthews, Bryan	IV – p 165
McAlpine, J.D.	III – p 169
Michelsen, Hope	II – p 163
Miller, Paul C.H.	IV – p 139
Moon, Dennis A.	I – p 409
Moussiopoulos, Nicolas	I – p 313, 355 IV – p 303 , 355
Nelson, Thomas E.	I – p 409
Nunnari, Giuseppe.....	II – p 397
Oetl, Dietmar.....	I – p 325
Paine, Robert	IV – p 1 , 21
Pepper, Darrell W.....	II – p 267
Pérez, Juan L.	II – p 233
Petersen, Ronald L.	III – p 397
Physick, William	II – p 93
Pun, Betty K.	II – p 163
Rappolt, Thomas J.....	IV – p 441
Reynolds, Steven D.....	I – p 13 IV – p 21
Richter, Richard O.	II – p 351

Roth, Philip M.....	I – p 13
Ruby, Michael.....	III – p 169
San José, Roberto.....	I – p 325 II – p 233
Sarma, Ananthakrishna.....	III – p 131
Seigneur, Christian.....	II – p 163
Sheehan, Patrick J.....	II – p 351
Solomon, Douglas.....	III – p 5
Sorbjan, Zbigniew.....	I – p 37 II – p 11 IV – p 53
Teske, Milton E.....	IV – p 139
Thé, Cristiane.....	IV – p 165
Thé, Jesse.....	I – p 185, 363 III – p 5 IV – p 165
Tourlou, Paraskevi-Maria.....	I – p 313, 355
Thistle, Harold W.....	IV – p 139
Trini Castelli, Silvia.....	II – p 93 IV – p 373
Vlachokostas, Christos.....	IV – p 303
van Dop, Han.....	I – p 103 II – p 93
Venkatram, Akula.....	I – p 185
Watson, John G.....	II – p 455
Yamartino, Robert J.....	I – p 213 III – p 239, 281 IV – p 113
Zannetti, Paolo.....	I – p 213 II – p. 93 III – p 453 IV – p 461

Blank Page

Subject Index¹ for Volumes I – IV

2D visualization	III – p 435
3D visualization	III – p 435
Abatement	I – p 313, 355
Acid deposition	I – p 363
Advection	I – p 213
Aerial photography.....	III – p 435
Aerial spraying.....	IV – p 139
AERMOD	I – p 185, 409
Aerodynamic resistance	II – p 233
Air dispersion modeling.....	IV – p 165
Air dispersion models.....	I – p 363
Air pollution.....	I – p 1, 185, 313, 355
	IV – p 1 , 373
Air pollution control.....	IV – p 303
Air pollution episode.....	I – p 313, 355
Air pollution model(s).....	I – p 185, 409
Air pollution modeling	I – p 1, 325
Air pollution modeling.....	IV – p 1
Air pollution regulations	I – p 1
Air pollution regulations	IV – p 1
Air quality	I – p 185
	II – p 55
	III – p 169
Air quality assessment.....	IV – p 355
Air quality forecasting.....	I – p 313, 355
	II – p 397
	IV – p 319
Air quality modeling	I – p 13, 213
	II – p 233
	III – p 329, 453
	IV – p 21 , 303 , 461
Air quality models.....	I – p 363
	IV – p 73
Air toxics.....	IV – p 165
Air-conditioning.....	II – p 267
Airflow	III – p 169
Algorithms.....	III – p 131
Ambient measurement.....	II – p 455
Ambient turbulence.....	I – p 103
Aqueous reactions	II – p 164
ArcExplorer.....	III – p 435
ArcGIS	III – p 435
Atmosphere	III – p 169
Atmosphere-Ocean General Circulation Models	III – p 353
Atmospheric boundary layer	I – p 37, 185
	II – p 11
Atmospheric chemistry.....	II – p 164
Atmospheric dispersion.....	III – p 397
Atmospheric dispersion modeling.....	III – p 239, 281
	IV – p 113

¹ Readers are encouraged to use the CD-ROM version of the book for text searching.

Atmospheric dispersion processes	IV – p 355
Atmospheric modeling	IV – p 355
Atmospheric motions	I – p 37
Atmospheric tracers.....	IV – p 441
Available software	III – p 453
	IV – p 461
Building and terrain wakes.....	III – p 397
Building contamination	II – p 267
Building effects	I – p 185
Building safety	II – p 267
Buildings	III – p 169
Bulk resistance	II – p 233
Buoyant plumes.....	I – p 103
Calibration.....	IV – p 441
CALMET	I – p 409
CALPUFF	I – p 409
Canopy resistance.....	II – p 233
CFD	III – p 169
Chemical mass balance (CMB).....	II – p 455
Chemical mechanisms	II – p 164
Chemical transformation	I – p 13
	IV – p 21
Chemical transport models.....	II – p 164
Chen-Kim	III – p 169
Chromatograph.....	IV – p 441
Clean Air Act	II – p 557
Clean Air Act Amendments	II – p 557
Climate change.....	III – p 353
Cloud-free boundary layer	II – p 11
Cloud-topped boundary layer.....	II – p 11
Combustion facilities.....	II – p 351
Compensation point.....	II – p 233
Complex terrain.....	I – p 363
Complex terrain dispersion	I – p 185
Computational fluid dynamics	III – p 169
Computational wind engineering	III – p 169
Constant flux layer	II – p 233
Convection	I – p 37
	II – p 11
Convective boundary layer.....	I – p 185
Cost-benefit analysis.....	IV – p 303
Coupled general circulation models	III – p 353
Courses online.....	III – p 453
	IV – p 461
Data needs	I – p 13
	IV – p 21
Decision support system.....	II – p 397
Dense gas models	I – p 363
Deposition	II – p 233
Deposition of air pollutants	I – p 313, 355
Diagnostic models.....	I – p 363
Diffusion	I – p 37, 213
Direct chemical exposures	II – p 351
Dispersion	I – p 185, 313, 355
	III – p 169

Dispersion modeling	I – p 13, 103
	IV – p 21 , 441
Dissemination.....	IV – p 441
Ecological risk assessment.....	IV – p 165
Economic benefit/damage	IV – p 303
Eddy diffusivity.....	I – p 213
Effective plume heights.....	I – p 103
Electron capture detector (ECD).....	IV – p 441
Emergency releases	I – p 363
Emission control policies	IV – p 319
Emission data	III – p 435
Emissions inventory	III – p 5
Emissions modeling	I – p 13
	III – p. 5
	IV – p 21
Emissions tools.....	III – p 5
Ensembles	IV – p 319
ERCOFTAC.....	III – p 169
ESRI.....	III – p 435
Eulerian modeling	I – p 213
Fate modeling.....	II – p 351
Fickian diffusion	IV – p 441
Fluid dynamics	II – p 267
Footprint analysis	II – p 94
Four-dimensional data assimilation.....	I – p 363
Future modeling	I – p 325
Gaussian dispersion model.....	I – p 185
Gaussian methods.....	III – p 239
	IV – p 113
Gaussian model	IV – p 21
Gaussian model(s).....	I – p 13, 363
Gaussian puff methods.....	III – p 281
Geocoding	III – p 435
Georeferencing.....	III – p 435
GIS	III – p 435
Global Mapper	III – p 435
Google Earth	III – p 435
Gradient-based scaling.....	IV – p 53
Grid-based models	I – p 13
	IV – p 21
Ground spraying.....	IV – p 139
GUI.....	III – p 435
Guidelines	III – p 169
Hazardous air pollutants.....	II – p 164
Hazardous waste incinerators.....	II – p 351
Health impact assessment.....	IV – p 303
Heterogeneous reactions	II – p 164
Human health	II – p 351
Indirect chemical exposures	II – p 351
Indoor air quality	II – p 267
Integrated assessment.....	IV – p 303
Internet	I – p 325
Internet sites	III – p 453
	IV – p 461
Inventory preparation plan	III – p 5
ISC	I – p 185

Jet plumes.....	I – p 103
K-epsilon.....	III – p 169
Kinetics	II – p 164
Lab hood	III – p 169
Lagrangian air pollution modeling.....	II – p 94
Lagrangian droplet transport.....	IV – p 139
Lagrangian models.....	I – p 363
Lagrangian puff model.....	IV – p 21
Land use/land cover data.....	III – p 435
Langevin equation.....	II – p 94
Large-eddy simulations.....	II – p 11
Link to animation.....	IV – p 373
Local and non-local closure.....	I – p 213
Long-range transport.....	I – p 363
	II – p 94
Mathematical programming.....	IV – p 303
Mesoscale dispersion.....	II – p 94
Meteorological data.....	I – p 363, 409
	III – p 435
Meteorological input.....	IV – p 73
Meteorological models.....	IV – p 73
Micrometeorology.....	III – p 169
Mixed layers.....	I – p 37
	II – p 11
Mixing.....	I – p 37
	II – p 11
Model coupling.....	IV – p 355
Model developer.....	IV – p 373
Model development.....	II – p 557
Model evaluation.....	II – p 503
Model performance evaluation.....	I – p 13
	IV – p 21
Model quality assurance.....	II – p 503
Model user.....	IV – p 373
Model validation.....	IV – p 441
Modeling.....	I – p 313, 355
	III – p 169
	IV – p 373
Monin-Obukhov theory.....	II – p 233
Multi-scale modeling.....	IV – p 355
Nesting.....	IV – p 355
Numerical algorithms.....	I – p 213
Numerical modeling.....	II – p 267
	III – p 131, 353
Odor dispersion modeling.....	III – p 329
Odor impacts.....	III – p 329
Odor modeling.....	III – p 329
Odors.....	III – p 329
Offline coupling.....	IV – p 73
Ozone formation.....	I – p 313, 355
Parameterizations.....	III – p 131
Particle models.....	I – p 363
Particulate matter (PM).....	II – p 164, 455
Particulate transport.....	II – p 267
Perflourocarbon (PFC).....	IV – p 441
Performance measures.....	II – p 503

Pesticide application modeling.....	IV – p 139
Pesticide deposition.....	IV – p 139
Pesticide drift	IV – p 139
Pesticide spraying.....	IV – p 139
Photochemical models.....	I – p 13, 363
	IV – p 21
Physical modeling	III – p 397
Plume.....	III – p 169
Plume-in-grid	II – p 164
Plume models	I – p 363
Pollution	III – p 169
Pollution control.....	I – p 313, 355
Pollution roses.....	III – p 435
Probabilistic predictions.....	IV – p 319
Prognostic models	I – p 363
Project EMU.....	III – p 169
Puff models	I – p 363
QNET-CFD.....	III – p 169
Quality assurance	IV – p 441
Quality control	IV – p 441
Radicals	II – p 164
Receptor model	II – p 455
Regional models.....	I – p 363
Regulatory application	I – p 13
	IV – p 21
Regulatory model	I – p 185
Regulatory models.....	III – p 453
	IV – p 461
Remote sensing	III – p 435
Research projects	IV – p 373
Resolution	I – p 13
	IV – p 21
Resuspension.....	II – p 267
Risk assessment.....	II – p 351
RNG	III – p 169
RUC2	I – p 409
Satellite imagery.....	III – p 435
Secondary air pollutants	II – p 164
Second-hand smoke	II – p 267
Self-induced turbulence	I – p 103
Service provided.....	IV – p 373
SHEBA data	IV – p 53
Short-range models	I – p 363
Similarity theories	I – p 37
Similarity theory.....	IV – p 53
Simulation	I – p 313, 355
Simulation models.....	I – p 13
	IV – p 21
SketchUp.....	III – p 435
Source apportionment	II – p 455
Source profile.....	II – p 455
Stability conditions.....	I – p 103
Stable boundary layer.....	I – p 185
	IV – p 53
Stacks	III – p 169
Statistical indices.....	II – p 503

Statistical model evaluation.....	II – p 503
Steady state flow	III – p 169
Stochastic models	II – p 94, 397
Stratospheric ozone	II – p 164
Street canyon.....	I – p 313, 355
Sulfur hexafluoride (SF6)	IV – p 441
Surface fluxes.....	II – p 233
Surface layer.....	III – p 169
Surrogate	IV – p 441
Template.....	IV – p 373
Terrain data	I – p 363
	III – p 435
Thermodynamics	II – p 164
Transport	I – p 313, 355
Transport modeling	II – p 351
Tropospheric ozone.....	II – p 397
Turbulence.....	I – p 37
	II – p 11
	III – p 169
Turbulence modeling.....	II – p 267
Type of application	IV – p 373
Type of model	IV – p 373
Uncertainty	I – p 13
	IV – p 21
Uncertainty analysis	II – p 503
Urban models	I – p 363
Urban ozone	II – p 164
Urban plume.....	I – p 313, 355
Urban.....	III – p 169
Validation	III – p 169
Ventilation.....	II – p 267
Visibility.....	I – p 363
Volatile organic compound (VOC).....	II – p 455
Weather systems.....	I – p 37
Wind tunnel modeling.....	III – p 397

Additional Information About the Chapter Authors/ Contributors for Volumes I – IV

Achillas, Charisios

-  [CV](#)
-  [Picture](#)

Anfossi, Domenico

-  [CV](#)
-  [Picture](#)

Bellasio, Roberto

-  [CV](#)
-  [Picture](#)

Bianconi, Roberto

-  [CV](#)
-  [Picture](#)

Buono, Maureen E.

Builtjes, Peter J.H.

-  [CV](#)
-  [Picture](#)

Byun, Daewon W.

-  [Bio](#)
-  [Picture](#)

Canepa, Elisa

-  [CV](#)
-  [CV-short](#)
-  [Picture](#)

Carrington, David B.

-  [CV](#)
-  [Picture](#)

Chow, Judith C.

-  [CV](#)
-  [Picture](#)

Cochran, Brad

-  [Bio](#)
-  [Picture](#)

Daly, Aaron

-  [CV](#)
-  [Picture](#)

Degrazia, Gervásio

-  [CV](#)
-  [Picture](#)

Delle Monache, Luca

-  [CV](#)
-  [Picture](#)

Diosey, Phyllis G.

-  [Resume](#)
-  [Picture](#)

Douros, John

-  [CV](#)
-  [Picture](#)

Ferrero, Enrico

-  [Bio](#)
-  [Picture](#)

Finzi, Giovanna

-  [CV](#)
-  [Picture](#)

Fragkou, Evangelia

-  [CV](#)
-  [Picture](#)

Freedman, Frank R.

-  [Resume](#)
-  [Picture](#)

Georgieva, Emilia

-  [CV](#)
-  [Picture](#)

González Barras, Rosa M.

-  [CV](#)

Hibberd, Mark

-  [Bio](#)
-  [Picture](#)

Hurley, Peter

-  [Bio](#)
-  [Picture](#)

Irwin, John S.

-  [CV](#)

Johnson, Michael

-  [CV](#)

Kerrin, Stephen L.

-  [Resume](#)

Lacser, Avraham

-  [CV](#)

Lee, Russell

-  [CV](#)

Luhar, Ashok

-  [Bio](#)
-  [Picture](#)

Lyons, Walter A.

-  [CV](#)
-  [Bio](#)
-  [Picture](#)

Matthews, Bryan

McAlpine, J.D.

-  [Resume](#)
-  [Picture](#)

Michelsen, Hope

-  [CV](#)
-  [Picture](#)

Miller, Paul C.H.

-  [CV](#)
-  [Picture](#)

Moussiopoulos, Nicolas

-  [CV](#)
-  [Picture](#)

Nunnari, Giuseppe

-  [CV](#)
-  [Picture](#)

Öetl, Dietmar

-  [CV](#)
-  [Picture](#)

Paine, Robert

-  [CV](#)
-  [Picture](#)

Pepper, Darrell W.

-  [CV](#)
-  [Picture](#)

Pérez, Juan L.

-  [CV](#)
-  [Picture](#)

Petersen, Ronald L.

-  [Bio](#)
-  [Picture](#)

Physick, William

-  [Bio](#)
-  [Picture](#)

Pun, Betty K.

-  [CV](#)
-  [Picture](#)

Rappolt, Thomas J.

-  [Resume](#)

Reynolds, Steven D.

-  [CV](#)

Richter, Richard O.

-  [CV](#)
-  [Picture](#)

Roth, Philip M.

-  [In Memoriam](#)

Ruby, Michael

-  [Resume](#)
-  [Picture](#)

San José, Roberto

-  [CV](#)
-  [Picture](#)

Sarma, Ananthakrishna

-  [CV](#)
-  [Picture](#)

Seigneur, Christian

-  [CV](#)
-  [Picture](#)

Sheehan, Patrick J.

-  [CV](#)
-  [Picture](#)

Solomon, Douglas

-  [Email](#)

Sorbjan, Zbigniew

-  [CV](#)
-  [Picture](#)

Teske, Milton E.

-  [CV](#)
-  [Picture](#)

Thé, Cristiane

Thé, Jesse

-  [CV](#)

Thistle, Harold W.

-  [CV](#)
-  [Picture](#)

Trini Castelli, Silvia

-  [CV](#)
-  [Picture](#)

van Dop, Han

-  [CV](#)
-  [Picture](#)

Venkatram, Akula

-  [Picture](#)

Vlachokostas, Christos

-  [CV](#)
-  [Picture](#)

Watson, John G.

-  [CV](#)
-  [Picture](#)

Yamartino, Robert J.

-  [CV](#)
-  [Picture](#)

Zannetti, Paolo

-  [CV](#)
-  [Picture](#)